Development and Characterisation of an *in vitro* Human Gut Model to Study the Biofilm Mode of Growth of *Clostridium difficile* and the Indigenous Gut Microbiota

by

Grace Samantha Crowther

Submitted in accordance with the requirements for the degree of

Doctor of Philosophy

The University of Leeds

Leeds Institute of Biomedical and Clinical Sciences

School of Medicine

August, 2013

The candidate confirms that the work submitted is her own and that appropriate credit has been given where reference has been made to the work of others.

Acknowledgements

I wish to thank my supervisor Professor Mark Wilcox for his continued advice, support and guidance and providing me with the opportunity to complete this research.

I would also like to thank Dr Caroline Chilton for her technical advice and encouraging words. Your contributions to our lengthy discussions were vital to the success of this project and my professional development.

Many thanks to all my colleagues in Professor Wilcox's research group, particularly Dr Jane Freeman and Dr Warren Fawley for their invaluable source of ideas and guidance and Miss Sharie Todhunter for her technical support and friendship. Additionally, I would like to thank Dr Simon Baines for his continued support and input.

Finally, I would like to express my gratitude to my family and friends for their unwavering patience, help and emotional support. I am forever grateful to my parents for all they have done for me, especially throughout the difficult times. Without your love and support none of this would have been possible.

Abstract

Clostridium difficile infection (CDI) is associated with significant patient morbidity, mortality and financial burden. Until recently, antimicrobial treatment options were limited to metronidazole and vancomycin, but both agents are associated with recurrence rates of approximately 20%.

The human gastrointestinal tract harbours a complex microbial community which exist in planktonic and sessile form. Sessile organisms are known to cause chronic infection such as cystic fibrosis. Mucosal biofilms exist on surfaces of the gastrointestinal tract, but the existence and role of *C. difficile* in these structures remains unknown.

The present study describes the process undertaken to adapt and validate an *in vitro* human gut model to study the planktonic and biofilm mode of growth of *C. difficile* and the indigenous gut microbiota. A triple stage chemostat gut model, primed with a human faecal emulsion was used to induce and treat simulated CDI. A glass rod system was incorporated into the third vessel to facilitate the formation and subsequent analysis of mixed-species biofilms.

Sessile and planktonic gut microbiota and *C. difficile* populations within an *in vitro* gut model are similar in the absence of antimicrobial intervention. Differences in behaviours of the two modes of growth are evident upon antimicrobial administration, with a delayed response in sessile populations. The sessile mode of growth of *C. difficile* within mature biofilm structures is complex and variable. Within the redesigned biofilm gut model, sessile *C. difficile* remained in spore form for the duration of the experiment, despite

induction of simulated CDI, treatment of CDI and recurrence of disease evident within planktonic communities.

Recalcitrant spores within biofilms may be seeded into the planktonic fluid of the gut model after apparent successful initial treatment and contribute to recurrence of CDI. The role of sessile *C. difficile* in recurrent CDI should be further investigated.

Table of Contents

List of Tables

List of Figures

1.0 Introduction

1.1 *Clostridium difficile*

1.1.1 History

In 1935 Hall and O'Toole first isolated *Clostridium difficile* from the stool of neonates[1]. They referred to this isolate as '*Bacillus difficilis*' due to the difficulty encountered whilst culturing the organism. Snyder carried out further work and described this organism as a Gram-positive, anaerobic bacillus with lethal toxigenic properties when injected subcutaneously or intra-peritoneally into animals[2]. However, he also noted that the bacterium was commensal in the gut of infants; hence, colonised infants were asymptomatic.

Pseudomembranous colitis (PMC) was first reported in 1893 by Finney, who noted diphtheritic colitis in a surgical patient[3]. The incidence of PMC increased greatly with the widespread use of antimicrobial agents[4]. Early work linked the use of clindamycin to the development of the disease, stimulating interest in this area[5]. It was known that stool samples from patients with PMC contained high levels of cytotoxic activity[6, 7]; but it was not known which agent produced this toxin. Reports from several laboratories noted that the cytotoxic activity was neutralized by gas gangrene antiserum[4, 5], which led investigators to research the neutralizing effect of the antiserum of several clostridial species, *C. sordellii* being the most effective[8, 9]. As a result, it was believed that *C. sordellii* was the aetiological agent in PMC, but the organism was almost never isolated from the stool of patients. It was subsequently demonstrated that *C. difficile* could be isolated in high numbers from the stool of patients with PMC and that it produced toxins that could be neutralized by the antiserum of *C. sordellii*[10, 11].

The prevalence of this anaerobic, Gram-positive, spore-forming bacterium within the hospital setting has increased with the use of antimicrobial

agents. The highly resistant characteristic of *C. difficile* spores gives rise to their persistence in close proximity to vulnerable patients which facilitates CDI and allows infection to spread in healthcare institutions leading to epidemics[12-14].

1.1.2 Clinical Manifestations

Clostridium difficile infection (CDI) symptoms range from mild, self-limiting diarrhoea to fulminant colitis with megacolon or perforation[15, 16]. The wide spectrum of disease is a consequence of both host-specific (immune status, age, comorbidities, level of colonisation resistance) and pathogen-specific (virulence of infecting strain) factors. Interestingly, a high percentage of infants are carriers of *C. difficile* and harbour high levels of toxin in their faeces without showing any signs or symptoms of infection[17]. Asymptomatic carriers may act as a reservoir for *C. difficile* and facilitate the spread of spores and subsequent infection of at-risk patients[13].

Mild diarrhoea is common with antimicrobial therapy, and is often associated with an osmotic imbalance within the colon[18]. Approximately 20% of antibiotic-associated diarrhoea cases are due to *C. difficile*. Disease is usually mild and in 15-25% of all cases symptoms cease when antimicrobial therapy is discontinued[19]. Colitis with the formation of a pseudomembrane produces more serious illness with abdominal pain, nausea, fever and malaise often present[20]. PMC is the characteristic manifestation of CDI and may be fatal[21]. Fulminant colitis infection occurs in a small proportion of patients and manifestations include toxic megacolon, marked leukocystitis, colonic perforation and death[22].

1.1.3 Pathophysiology and Disease Risk factors

The intestinal tract is home to a diverse microbial population. Conservation of this microbiota is necessary to maintain a healthy gut, and its disruption can lead to the colonisation and proliferation of intestinal pathogens, including *C. difficile*[23]. *C. difficile* can form part of the microbiome of approximately 50% of neonates and 6% of adults without causing disease[17, 24-27]. This asymptomatic carriage may be due to the maintenance of a healthy gut microbiota so that the level of *C. difficile* present is not sufficient to cause disease[23]; the strain of *C. difficile* present may not be toxigenic[28]; or the patient may have mounted as sufficient (antitoxin) antibody response to prevent disease[29].

C. difficile often persist within hospital environments as spores[30, 31]. These spores can survive the acidic environment of the stomach and once exposed to certain conditions in the small bowel, can germinate and form vegetative cells[32]. If there has been disruption to the commensal gut microbiota, and conditions are favourable, vegetative *C. difficile* proliferate in the colon where flagella may assist them to translocate to the mucous membrane[33, 34].

Bacteria must then gain access to the underlying epithelial cells where receptors bind to toxins, causing cytoskeleton changes that result in disruption of tight junctions[35] and loosening of the epithelial barrier, resulting in cell death or the production of inflammatory mediators that attract neutrophils and monocytes. The release of immunomodulatory mediators from the epithelial cells, phagocytes and mast cells is induced by the cytotoxic effects of toxin, resulting in inflammation and the accumulation of neutrophils[36].

Colonisation resistance is the mechanism whereby the intestinal microbiota protects itself against incursion by new and often harmful microorganisms. The barrier effect of these microbes against *C. difficile* is very effective and

disease will only occur once this barrier has been disrupted, usually by antibiotics. Larson *et al* [37] have validated this hypothesis when hamsters challenged with *C. difficile* only showed signs of disease when they had been pre-treated with antibiotics. Further to this, they also showed that hamsters pre-treated with antibiotics remained healthy until they were exposed to *C. difficile*, indicating that disruption of the microbiota and colonisation are both prerequisites to the onset of CDI[37].

Antibiotics can be inactivated in the gut by metabolism or adsorption[38, 39]. Any active antimicrobial agent present in the gut may affect the commensal microbiota of the intestine. If the concentration of antibiotic in the gut is sufficient to inhibit the growth of commensal microbiota, this provides potentially pathogenic microorganisms (PPMO) with greater nutrient and spatial availability, potentially allowing the colonisation and proliferation of *C. difficile*. *C. difficile* spores are able to survive the passage through the stomach and duodenum and into the jejunum, where the concentration of primary bile salts and nutrients are high[40]. It is postulated that the availability of cholate derivatives and glycine enable spores to germinate and pass through the ileum into the colon, where anaerobic bacteria are able to metabolise the cholate derivatives into deoxycholate. Bile acid, deoxyxcholate, potentially prevents outgrowth of the vegetative cell from the germinated spore and the host remains uncolonised. If the commensal anaerobic bacteria have been inhibited by antimicrobial agents and are unable to metabolise the cholate derivatives, vegetative growth may be possible[32].

One to the most significant risk factors associated within the onset of CDI is antibiotic exposure[41]. Most antimicrobial agents have been linked to the onset of CDI but those most commonly associated are broad-spectrum antibiotics, particularly clindamycin, third-generation cephalosporins and fluoroquinolones[42-44]. In the past, clindamycin has been associated with a

high propensity to induce CDI, but clindamycin use has since been severely reducued and other antibiotics with widespread use have become the main causative agents for CDI. Antibiotics that are rarely associated with CDI include aminoglycosides, glycopeptides and tetracyclines. A recent report published by the Health Protection Agency (HPA) highlighted that the most commonly reported antimicrobial agents associated with CDI onset were co-amoxiclav and piperacillin-tazobactam, both of which are in common use. Caution should be taken when analysing such data as these may reflect trends in prescribing practices (including the use of multiple antibiotics)[45].

As well as the use of antibiotics, other risk factors for the development of CDI have been identified. McFarland *et al* [46] carried out a prospective cohort study of 399 patients on a single ward over 11 months in an endemic situation. They identified older age, severe underlying illness, use of cephalosporins or penicillins, gastrointestinal stimulants, stool softeners and enemas as risk factors for the development of CDI. Other researchers have also identified gastric acid-suppressive therapy such as proton pump inhibitors; increased length of hospitalisation, abdominal surgery, intensive care unit admission, contact with healthcare institutions and severe underlying disease as other contributions to the onset of disease[47-52].

1.1.4 Virulence Factors

1.1.4.1 Toxins A and B

The major virulence factors for *C. difficile* are the two highly related toxins, toxin A (TcdA); a 308 kDA enterotoxin and toxin B (TcdB); a 250 kDA cytotoxin[53, 54], which share 63% amino acid similarity[55]. Toxin yield varies amongst *C. difficile* strains and is influenced by environmental conditions. Toxin synthesis increases as cells enter stationary phase and is controlled by growth temperature, cellular growth phase, nutrient levels of butyric acid,

certain amino acids, carbohydrate sources, growth-limiting levels of biotin and certain antibiotics[56, 57,58, 59,60].

Both toxins comprise four domains with distinct functional properties; the catalytic domain, the cysteine protease domain, the translocation domain and the receptor binding domain[55, 61, 62]. The translocation domain facilitates the delivery of the N-terminal catalytic domain across the membrane of the host cell where it is then cleaved and released into the cytosol by autoproteolysis[63, 64]. Rho, Ras and Cdc42 are GTPases which regulate tight junctions and the actin cytoskeleton[65]. Once inside the cytosol, the catalytic domain inactivate GTPases by glucosylation of threonine residue leading to disruption of the actin cytoskeleton and tight junctions, causing cell rounding[66, 67].

1.1.4.1.1 Toxicity of Toxin A and B

The exact roles and contributions of toxin A and B in causing disease remain unclear. Animal models such as the rabbit and rat ileal loop models, and golden Syrian hamster model have been used to demonstrate the inflammatory response that occurs in PMC and can be used to assess the relative role of the two toxins. However, inter-species differences in clinical manifestations are evident, therefore extrapolation of data from one to the other should be tentative[68]. Originally, the major role in disease was attributed to toxin A. Lyerly *et al*[69] reported that intragastric administration of toxin A to hamsters and mice caused haemorrhagic secretion in the small intestine, but toxin B only caused damage if the bowel was damaged prior to toxin B exposure. Whilst toxin B lacks enterotoxic effects in experimental animals, it is extremely cytotoxic to cultured mammalian cells, including those from the human intestine[70], and is reported to be ~1000 times more potent than toxin A in most cells lines. This led to the hypothesis that

toxin A is required to bind to its receptor on the lateral surface of the epithelial cells causing initial damage to the tight junction and allowing the subsequent passage of toxin B through the epithelial cells to its receptor on the basal surface of the cell. However, the existence of toxinA$^-$ toxinB$^+$ strains, which are able to cause disease in hamsters[71] and are present in up to 10% of clinical human specimens[72,73-76], contradicted the hypothesis that toxin A was required for pathogenicity.

Lyras *et al*[77] developed mutated strains of *C. difficile* to provide evidence that toxin B (not A) is essential for virulence. Hamsters challenged with a toxin A-inactivated mutant were as likely to die as those challenged with the wild-type strain, whereas hamsters challenged with a toxin B-inactivated mutant were much more likely to survive. More recently Steele *et al* showed that the administration of anti-toxinB antibodies protected 100% of piglets from *C. difficile* challenge from morbidity and mortality whilst the administration of anti-toxinA antibodies resulted in 100% of piglets displaying signs of severe gastrointestinal and systemic disease, with 67 - 83% fatality[78].

1.1.4.1.2 Receptors for Toxins A and B

In order to elicit cytotoxic effects toxins must first be internalised into the host cell via endocytosis, which requires the binding of the C-terminal domain of the toxin to a receptor. Several potential carbohydrate receptors for toxin A have previously been identified. The glycan sequence αGal(1,3)βGal(1,4)βGlcNAc, which is present on rabbit erythrocytes and hamster brush border membranes was first identified as a potential receptor for toxin A[79]. However, this carbohydrate is not present in humans[80]. Later, carbohydrates Galβ(1,4)Fuα(1,3) GlcNAc (Lewis X),

Galβ(1,4)GlcNAcβ1 (Lewis Y) and Galβ(1,14)GlcNacβ(1,3)Galβ(1,4)(Glc) (Lewis I) which are present in human intestinal epithelial cells were suggested as possible receptors for toxins A[81]. The receptor for toxin B has been less well characterised. Due to the cytotoxic effects on a wide range of intestinal cells lines it is thought that the toxin B receptor is ubiquitous[63, 82].

1.1.4.1.3 The Pathogenicity Locus

The genes encoding toxin A and B are situated within a chromosomal region designated as the pathogenicity locus (PaLoc)[83]. The PaLoc (figure 1.1) is 19.6-kb in length and contains five genes that regulate toxin expression. In non-toxigenic strains ($tcdA^-tcdB^-$) the PaLoc is replaced by a 115 bp region of non-coding sequence[84]. Variation in the PaLoc gives rise to *C. difficile* strains with varied toxigenicity.

The pathogenicity locus contain genes t*cdA* and *tcdB* which encode toxins A and B respectively; along with three other genes, *tcdR, tcdC, tcdE*. The open reading frames encoding *tcdR, tcdB, tcdE* and *tcdA* are transcribed in one direction with *tcdC* oriented in the opposite direction[83] (depicted by arrow direction in figure 1.1).

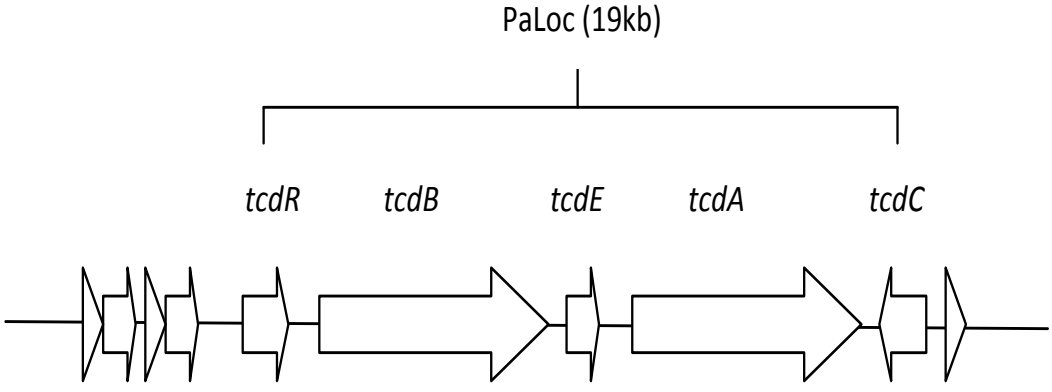

Figure 1.1: Pathogenicity locus of toxigenic *C. difficile* strains[83].

The *tcdR* sequence encodes a positive regulator of *tcdA* and *tcdB;* and *tcdC* encodes a putative negative regulator of *tcdA* and *tcdB*[85, 86]. *TcdR* initiates toxin gene expression as an alternative RNA polymerase sigma factor, directing RNA polymerase to transcribe the toxin genes as well as its own encoding gene, resulting in a rapid increase in toxin production[87]. As is the case for the toxin genes, *tcdR* expression is controlled by cellular growth phase, growth medium and temperature[59, 86].

The mechanism of TcdC action has not been fully elucidated. TcdC is divergently transcribed from the toxin genes and is expressed during rapid exponential phase growth and displays reduced expression during stationary phase growth[88]. The converse is true for TcdR and the toxin genes, indicating the putative negative role of tcdC in toxin expression. Evidence suggests that *tcdC* negatively regulates *C. difficile* toxin gene expression by destabilising the formation of a *tcdR*-containing RNA polymerase holoenzyme, thereby hampering its ability to recognize the *tcdA* and *tcdB* promoters rather than by directly interacting with the target promoters[89]. Some strains, (PCR ribotype 027) have a mutated negative regulator gene *tcdC* which potentially leads to increased toxin yield and has contributed to these strains being classified as 'hypervirulent'. However, recently the role of TcdC has been disputed[90, 91]. *In vivo* and *in vitro* studies on the importance of TcdC on toxin production show conflicting results[92, 93]. Mutation and subsequent restoration of *tcdC* of *C. difficile* PCR ribotype 027 strains found no association between *tcdC* genotype and toxin production[92]. Conversely, *tcdC* complementation in a *C. difficile* PCR ribotype 027 strain resulted in reduced toxin production and virulence within a hamster model[93].

TcdE is a small, hydrophobic protein of 166 amino acids which contains structural features similar to those of the class I holins of which phage λ S protein is a member[94]. Dupuy *et al* demonstrated that TcdE has a holin-like activity and is required for efficient secretion of toxins into the extracellular environment without inducing cellular lysis[95].

1.1.4.1.4 PaLoc Variation Amongst *C. difficile* Strains

Toxin production varies amongst *C. difficile* isolates. Patients infected with *C. difficile* PCR ribotype 027 often suffer from increased morbidity and mortality[96], which is hypothesised to be due to an increase in toxin production. Ribotype 027 has an 18 base pair deletion in the *tcdC* gene which is a putative negative regulator of toxin gene expression[97]. This deletion causes a frame shift mutation and the formation of a truncated protein. It is speculated that this therefore inhibits or reduces the expression of the *tcdC* gene during exponential growth, allowing the transcription of *tcdA* and *tcdB* earlier, or for longer, than in other strains.

Warny *et al*[97] have compared ribotype 027 toxin yields to that of a non-027 strain in batch culture and reported a 16 and 23 times increased toxin yield in toxin A and B respectively. However, Baines *et al* utilised an *in vitro* continuous culture model of simulated CDI to demonstrate an equal level of maximum toxin production compared with a PCR ribotype 001 strain. By contrast, the duration of toxin production by the 027 strain was greater than the 001 strain[98].

1.1.4.2 Binary Toxin

An additional binary toxin, CDT (*C. difficile* transferase), is found in approximately 6% of *C. difficile* strains[99, 100]. PCR ribotype 027 strains carry

the gene for CDT, and it has been postulated that the toxin could be associated with increased virulence[97]. It consists of a binding and an enzymatic component displaying an actin ribosyl transferase activity. The *cdtA* and *cdtB* sequences encode the binding and enzymatic component of the toxin respectively. These genes along with a gene encoding a 30 kDa regulatory protein (CdtR) are located on the *cdT* locus[101].

The binding domain of the toxin is involved in binding and transporting the enzymatic domain into the cytosol of the target cell. Once inside the cell, the enzymatic domain catalyses the ADP-ribosylation of the G-actin monomers at Arginine-117[102]. This inhibits actin polymerisation by acting as a capping protein at barbed ends of the actin filament preventing incorporation of further actin monomers. ADP-ribosylating toxins also induce the formation of microtubule-based protrusions on the surface of epithelial cells, potentially leading to increased adherence of these *C. difficile* strains[103]. Whilst the effects of ADP-ribosylating toxins on actin are well understood, their role as virulence factors is less clear.

Barbut *et al*[104] showed no statistically significant increase in the severity of CDI caused by CDT^+ strains compared with CDT^- strains and Geric *et al*[105] demonstrated no disease in hamsters with $TcdA^-TcdB^-CDT^+$ strains. Whilst, Bacci *et al* found that patients infected with strains possessing $tcdA^+tcdB^+CDT^+$ genes displayed higher 30-day case-fatality rates, compared with strains possessing toxin A and B genes only[106]. In addition, $TcdA^-TcdB^-CDT^+$ strains have been isolated from both symptomatic and asymptomatic patients[107], indicating that CDT may provide an adjunctive role to toxins A and B during the disease causing processes.

1.1.4.3 Hydrolytic Enzymes

Anaerobic bacteria produce a variety of hydrolytic enzymes which are thought to play a role in the aetiology of infection, causing connective tissue degradation, leading to colitis and pseudomembrane formation[108]. *C. difficile* produces hyaluronidase, chronditin-4-sulphatase, gelatinase and collagenase[109]. The precise role in pathogenicity is unknown but it has been postulated that the enzymes may be involved in the degradation of host proteins, releasing nutrients beneficial to *C. difficile*. Proteolytic enzyme production is associated with increased virulence within the hamster model[108,110]. Cwp84 is a protease of *C. difficile* which is associated with the S-layer proteins and shows degrading activity against fibronectin, laminin and vibronectin[111].

1.1.4.4 Flagella

Flagellar mediated motility is an important trait required for survival, colonisation and virulence in some organisms[112-115]. Flagella expression by *C. difficile* is variable with conflicting evidence regarding the correlation between flagella presence and virulence[116]. Flagella allow the chemostatic movement of organisms. Borriello *et al*[117] demonstrated that human gut mucus acts as a chemo-attractant for *C. difficile* and the degree of chemotaxis is positively correlated with the virulence of the strain.

Flagellin FliC is a major structural component of the flagellar filament (encoded by *fliC)*, and FliD is a hook-associated component of the filament cap (encoded by *fliD*). Evidence suggests that the presence of the flagellar proteins FliC and FliD increase the adherence of *C. difficile* strains; Tasteyre *et al*[118] reported a 10-fold increase in tissue association in flagellated strains when compared with non-flagellated strains. Conversely, Dingle *et al*[119]

have demonstrated the increased colonisation of Caco-2 intestinal epithelial cells by *C. difficile fliC- fliD-* mutants compared with the wild-type stain. Moreover, this mutant strain displayed increased virulence in hamster compared with the wild-type, indicating that the presence of FliC and FliD reduce virulence.

1.1.4.5 Adhesins

Association and persistence of *C. difficile* in the gastrointestinal tract is an important precursor to disease manifestation. Several putative adhesins of *C. difficile* vegetative cells have been identified including S-layer proteins, Cwp66 and heat-shock proteins.

Borriello first reported the association of *C. difficile* to the gut mucosa following recovery of *C. difficile* from a washed colonic biopsy specimen from a patient with PMC[120]. Borriello *et al*[121] later compared the efficacy of the adherence of poorly virulent and highly virulent strains to the mucosal surface, demonstrating that a poorly virulent, toxigenic strain colonised less efficiently than a highly virulent strain. The co-administration of crude preparations of *C. difficile* toxins with a non-toxigenic strain resulted in a significantly greater adherence to the small bowel mucosa comparable with that of the toxigenic strain. It was hypothesised that *C. difficile* toxins A and B may be involved in the promotion of mucosal association[121]. Waligora *et al*[122] compared the adherence of toxigenic and non-toxigenic strains, demonstrating that *C. difficile* adherence to Vero cells (as opposed to mucosal association), was not promoted by toxigenic status.

Vegetative *C. difficile* have been shown to bind to intestinal cell lines such as Caco-2, HT29-MTX and Vero cells[122, 123], with binding mediated by a proteinaceous component[123-126]. This allows vegetative cells to persist within

close proximity to the epithelial cells, hence in close proximity to toxin receptors.

The structures on the surface of the vegetative cell responsible for mediating adherence to the gut epithelium were until recently poorly characterised. Surface layer proteins have been shown to be required for virulence of some bacteria. Unlike most bacterial species, *C. difficile* expresses two distinct S-layer proteins, P36 a low molecular weight protein and P47 a high molecular weight protein[127]. Both proteins are derived from a common precursor and mediate cellular adherence, with P47 showing strong and specific binding to gastrointestinal tissues and some extracellular matrix proteins. P47 is highly conserved amongst strains whilst P36 displays high sequence diversity[128]. *C. difficile* surface layer proteins bind to collagen I, vibronectin and thromospondin, but not to collagen IV, fibronectin or laminin[129].

*C. difficile c*ell surface protein, Cwp66, mediates *in vitro* adherence to Vero cells[126]. The Cwp66 protein possesses a cell-wall anchoring N-terminal domain and a cell surface exposed C-terminal domain with adhesive properties[126]. Cwp66 displays homology to S-layer proteins and the genes encoding these proteins are located near each other in a 37-kb DNA cluster in the *C. difficile* genome [130].

The heat shock proteins GroEL[131], Hsp60, Hsp70 and the fibronectin-binding protein Fbp68[132] have also been reported to play a role in the adhesion of *C. difficile* to the gut mucosa.

Attachment of *C. difficile* spores to gut mucosa may be an important factor in colonisation and relapse of CDI. The ability of a spore to adhere to a surface is governed by factors such as its hydrophobicity, the formation of

appendages and the presence of an exosporium. Panessa-Warren *et al*[133] have shown that the endospores of *C. difficile* develop a thickened exosporial extension from one end of the spore in the early stages of germination, which facilitates attachment to agar surfaces. Further studies have shown that spores are able to rapidly attach to Caco-2 cells[133, 134].

1.1.4.6 Other Putative Virulence Factors

C. difficile can persist on the mucosal surface of the gastrointestinal tract despite the presence of large numbers of polymorphonuclear leukocytes (PMN). Dailey *et al*[135] determined that antibody-mediated opsonisation was required for phagocytosis and that toxigenic strains of *C. difficile* are more resistant to phagocytosis than non-toxigenic strains. It was speculated that toxigenic strains may possess an antiphagotic capsule. Davies and Borriello later confirmed the presence of this capsule using ruthenium red dye to stain the capsular glycocalyx[136]. Correlation between capsule expression and virulence status of *C. difficile* strains with a hamster model of CDI proved unrelated[136].

Another factor that may contribute to the virulence of *C. difficile* is its ability to produce a phenolic compound, *para*-cresol. *C. difficile* can withstand concentrations of up to 0.5% of this compound whilst the growth of other anaerobic bacteria is inhibited by this product[137, 138]. The increased tolerance of *C. difficile* to this compound may potentially provide a competitive advantage over other gut microbiota, thus allowing *C. difficile* to proliferate.

1.1.5 *C. difficile* spores

1.1.5.1 Spore Durability

Some Gram-positive bacteria have evolved to form spores, which are resistant to adverse environmental conditions such as extreme heat, radiation and acidity, adverse atmospheric conditions, desiccation and chemical substances, and have been recovered from numerous surfaces in the nosocomial environment[139-142].

The ability of *C. difficile* strains to sporulate and their subsequent ability to adhere and persist in the hospital setting, on surfaces and on the hands of healthcare workers[143] may affect virulence, explaining why some strains persist in the nosocomial environment to a greater extent than others. Spores are resistant to many hospital cleaning agents[144, 145]. Wilcox *et al*[144] compared the sporulation levels of an epidemic *C. difficile* strain (P24), a clinical isolate (B31), both of which produce toxin A and B, and a non-toxigenic environmental strain *C. difficile* (E4). They showed that the epidemic strain produced significantly more spores than the non-prevalent strains and that sporulation was further enhanced when the strain was exposed to non-chlorine based cleaning agents. Other research groups have reported the apparent increased sporulation capacity of *C. difficile* PCR ribotype 027[146 147], which may contribute to its increased infection rate, outbreaks and disease severity. However, a more recent study reported that sporulation rates amongst a diverse range of clinical isolates, including 28 separate PCR ribotype 027 isolates, did not display increased sporulation characteristics for the 027 strain compared with strains of other ribotypes[148]. Moreover, sporulation rates differed amongst different 027 isolates[148].

1.1.5.2 Spore Structure

C. difficile spores have a complex outer structure, with one or more spore coats, a cortex and core (protoplast)[149]. The core of the spore contains DNA, RNA, ribosomes, enzymes and calcium, manganese, potassium and phosphorus[150, 151]. The cortex, which is involved in the maintenance, but not creation of the dormant state consists largely of peptidoglycan. The coats are largely protein, of which five proteins, CotA, CotB, CotC, CotD and CotE are produced by *C. difficile*[152]. The main function of the coat is to protect the spore and regulate the conversion from dormant to vegetative state, a process known as germination. The outer most structure of *C. difficile* spores is the exosporium[153, 154], a multi-layered shell surrounding the coat, present in some but not all strains. Studies based on *Bacillus subtilis* have identified the exosporium composition as protein, lipids and carbohydrate. The role of this structure is largely unknown, but it is postulated that it may allow the colonisation of specific niches[149, 155].

1.1.5.3 Sporulation and Transmission

The process of sporulation begins with a vegetative cell, which undergoes asymmetric cell division forming two cell compartments, the smaller of which is referred to as a prespore. The mother cell then engulfs the prespore, forming a distinct cell termed the forespore. The peptidoglycan-composed spore cortex is then synthesized, followed by spore coat formation[156]. The spore becomes dehydrated as it matures, becoming increasingly refractile, before being eliminated from the mother cell[154, 157, 158]. The spore is protected from adverse conditions until the environment becomes more favourable.

Spo0A is a master regulator that controls the signal transduction pathway of sporulation initiation. This pathway has been most extensively studied in the genus *Bacillus*[159]. Within *Bacillus subtilis* five sensory histidine kinase molecules (KinA – KinE) respond to environmental and cellular signals, which indicate when vegetative cell growth is no longer viable[160]. These kinases initiate sporulation by modulating the activity of Spo0A through an autophosphorelay. Phosphorylation of the active site aspartate of Spo0A promotes binding to a specific target sequence (0A box) in or near to the promoters of genes under Spo0A control, resulting in gene expression or repression[161, 162]. Orthologues of Spo0A encoded by *C. difficile* are similar to that of *B. subtilis,* and are essential for initiation of sporulation in *C. difficile*[163].

It has been suggested that the sporulation master regulator Spo0A may directly or indirectly affect toxin production[164, 165], but conflicting reports have also been published. Underwood *et al* published further data confounding the role of Spo0A in toxin production, where they utilised ClosTron technology to inactivate the *spo0A* gene, which resulted in a marked defect in toxin production[166].

Conversely, recent work demonstrated that supernatant derived from a *spo0A* mutant displayed no less cytotoxicity towards Vero cells than the wild-type strain[167]. In addition, *spo0A* mutants gene in 027 ribotype *C. difficile* caused increased morbidity within murine model of CDI, with increased level of toxin A and B produced during stationary phase growth of the mutant 027 strain compared to the wild-type[163]. Other conclusions reached from similar experiments suggested that *spo0A* mutants exhibited retarded colonisation, persistence and relapse compared to the wild-type[163]. The ability of *C. difficile* to transmit infection from human-human and persist within the environment is highlighted by this data.

1.1.5.4 Spore Germination

Bacterial endospores undergo a complex series of events termed germination to form vegetative cells. This process occurs in three stages; activation, germination and outgrowth. The activation of germination is triggered by external stimuli such as appropriate pH, heat and atmosphere. This process is reversible and an activated spore, whilst still retaining its protective properties can revert back to its dormant state. Germination is initiated by various stimuli termed germinants. Once the spore has committed to germination this process is irreversible. During this stage the hydrolysis of the spore peptidoglycan cortex takes place allowing enzymatic activity and metabolism. The spore can then swell and sheds its outer layers before the new cell can outgrow[168].

The conditions causing *C. difficile* to germinate remain unclear, although a study by Sorg and Sonenshein *et al* demonstrated that the bile salts taurocholate and glycine may act together as co-germinants of *C. difficile* spores[32]. The bile salts deoxycholate and chenodeoxycholate have been identified as germination suppressors with increased concentrations of these bile salts inhibiting the germination effect of taurocholate[32, 169].

C. difficile germination capacity has been shown to display considerable isolate variation. Heeg *et al*[170] have demonstrated a diverse rate of germination amongst different strains (ribotype 027 versus non-027) in response to a rich medium containing taurocholate and glycine. Whilst some studies report the inhibitory germination properties of chenodeoxycholate, this group reported the varied response of its inhibitory properties amongst different *C. difficile* isolates[170]. These conflicting data highlight the complexity of germination of *C. difficile* spores, and indicates

that further work is required to gain a more comprehensive understanding of this process.

1.1.6 Epidemiology

1.1.6.1 Surveillance in the Nosocomial Setting

In order to monitor the incidence of CDI within UK healthcare institutions comprehensively, a voluntary reporting initiative was introduced in 1990. Mandatory surveillance of *C. difficile*, initially in patients ≥65 years (and then all those >2 years old, from 2007) for acute Trusts in England was introduced in 2004. This scheme is coordinated by Public Health England (PHE) (formerly the HPA) on behalf of the Department of Health.

The establishment of the mandatory surveillance initiative corresponded with a dramatic decrease in disease incidence, with the number of reports of CDI in patients > 2 years declining from 40,705 in 2008 to 14,987 in 2012 (figure 1.2)[171]. Prior to this, the total number of reported cases of *C. difficile* increased steadily from 1,194 in 1990 to 57,255 in 2007[172]. Reports of *C. difficile*-associated mortality rates have also decreased, with the number of death certificates which mention *C. difficile* declining from 8.324 in 2007 to 2,053 in 2011[173].

The incidence of CDI causes a significant clinical and financial burden on healthcare settings with the European Centre for Disease Prevention and Control estimating costs between €5,000 – 15,000 per case in England[174] and a European wide systematic review by Wiegand *et al* reported incremental costs of each CDI case in Germany, Ireland and UK (costs adjusted to 2010 price levels for comparison) as £8843, £4577 and £6986, respectively[175].

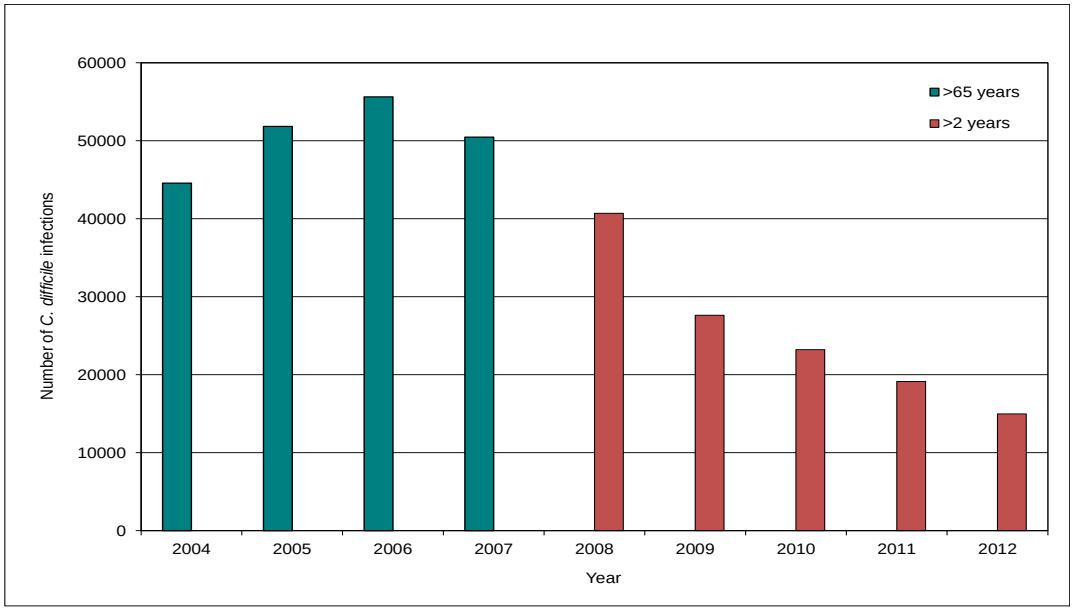

Figure 1.2: Total number of *C. difficile* infections in patients aged 65 years and over (2004-2007)[176] and over 2 years (2008-2012)[171].

1.1.6.2 *Clostridium difficile* in the Community

Whilst CDI is primarily viewed as a nosocomial infection, the number of community-onset cases is becoming increasingly apparent. The definition of community-acquired CDI is unclear and not universally used. The Centers for Disease Control and Prevention defines a patient with symptomatic onset 48 hours before hospitalisation as having community-onset, healthcare facility-associated CDI. Patients discharged from hospital within 4 weeks of onset would be classified as having intermediate disease. Patients with no history of hospitalisation 4-12 weeks prior to onset would be classified as having community-associated CDI[177].

CDI in the community was first reported in the late 1980s. Historically, rates of CDI in the community have been low, with cases ranging from 3.2 to 16.2/100,000 individuals[178-180]. Although rates of CDI in the community are lower than hospital-acquired rates, these numbers are continuing to rise, with one study reporting an increase from less than 1 case per 100,000 in 1994 to 22 cases per 100,000 in 2004[181]. A recent report

highlighted that up to 41% of all CDI cases within one county in the US are community acquired[182], with other studies also reporting large proportion of CDI cases being acquired in the community[52, 180, 182, 183]. Community-acquired CDI is associated with a younger mean age, lower comorbidity scores, less severe disease and decrease antibiotic use compared with hospital-acquired disease[182, 184].

The persistence of *C. difficile* spores within the hospital setting may lead to increased colonisation of patients recently discharged, therefore Bauer *et al*[185] postulated that this increase in asymptomatic carriage may increase community exposure and hence cause the observed increase in community-acquired CDI cases.

C. difficile has been increasingly isolated from animals[186-189] and retail meat products[190, 191] highlighting the role of animals as potential reservoirs for *C. difficile* and leading to concerns of a possible zoonotic transmission of the pathogen.

C. difficile is recognised as an important causative agent of enteritis in neonatal pigs, with positive *C. difficile* recovery from diarrhoeic and non-diarrhoeic newborns animals, but not from animals between 1-2 month-old[186]. PCR ribotype 078 strains are predominately isolated from swine and calves[192] in the US and Europe and isolated with increasing frequency in humans[193]. In the Netherlands, one study reported the distribution of humans infected with PCR ribotype 027 strains were localised in rural areas where potential contact with livestock is higher[193]. A recent study of CDI prevalence in cattle at slaughter (< 7 days old) in Australia identified an average *C. difficile* carriage rate of 53.4%, with 100% of strains possessing at least one toxin gene[189]. Reported carriage rates from studies in

other countries are lower and may reflect differences in slaughter ages between countries[194-196].

1.1.6.3 *C. difficile* Molecular Typing Methods

The increase in incidence of CDI observed in recent years has been concurrent with the increased prevalence of an apparently hypervirulent *C. difficile* strain. In 2004 it was noted by Pepin *et al* that the incidence and morbidity of CDI in Quebec, Canada had increased between 1991 and 2003, particularly amongst the over 65 year olds[96]. The predominant strain responsible for a large number of infections during this increase in incidence of CDI was identified by restriction endonuclease analysis (REA) as type BI, as North American pulse-field gel electrophoresis (PFGE) type NAP1 and as PCR ribotype 027 (BI/NAP1/027)[97, 197, 198]. The emergence of this apparently hypervirulent strain was also concurrent with an increase in CDI incidence throughout North America and Europe[199-201].

In order to provide a more comprehensive study of CDI epidemiology typing methods have been employed to monitor patterns of *C. difficile* types prevalent within regions, as well as providing information on environment and patient-patient transmission within outbreaks. An increasing number of *C. difficile* molecular typing methods have been developed including REA, PFGE, toxinotyping, multilocus variable repeat analysis (MLVA), multilocus sequence typing (MLST), whole genome sequencing and PCR ribotyping. Reproducibility, stability and discriminatory power are attributes required for typing methods.

PCR ribotyping is the most common technique employed in Europe and the UK for molecular epidemiological analysis of *C. difficile*[202]. The *Clostridium difficile* Ribotyping Network (CDRN) Service is a PHE funded initiative

offering ribotyping assistance to hospitals in England. PCR ribotyping examines polymorphisms in the 16S-23S intergenic spacer region of the ribosomal RNA gene complex. In 1999 Stubbs *et al* constructed a reference library consisting of 116 distinct PCR ribotypes from various clinical, environmental and veterinary sources, ribotype 001 being the most prevalent (55%; n= 682)[202]. From 1999 until 2003/04 *C. difficile* PCR ribotype 001 was responsible for approximately 60% of cases of CDI in England. In 2005 PCR ribotypes 001, 106 and 027 were equally prevalent. In 2007 Brazier *et al* carried out a surveillance study of strains causing CDI in England and determined that PCR ribotype 027 was the most prevalent (41.3%), with 106 the second most common (20.2%) and 001, which was once the most common reduced to 7.8% of the total[203]. Recently the proportion of CDI cases due to PCR ribotype 027 has begun to decrease with compensatory increases seen in other ribotypes[204]. Preliminary results from the CDRN for 2012 indicate that 027 is no longer the most prevalent strain in England (figure 1.3) (report in progress), and it is worth noting that this decrease in the hypervirulent 027 ribotype is concurrent with a decrease in CDI mortality rates in the UK. With increasing typing of *C. difficile*, approximately 500 ribotpyes have now been identified (pers comm. MH Wilcox & WN Fawley).

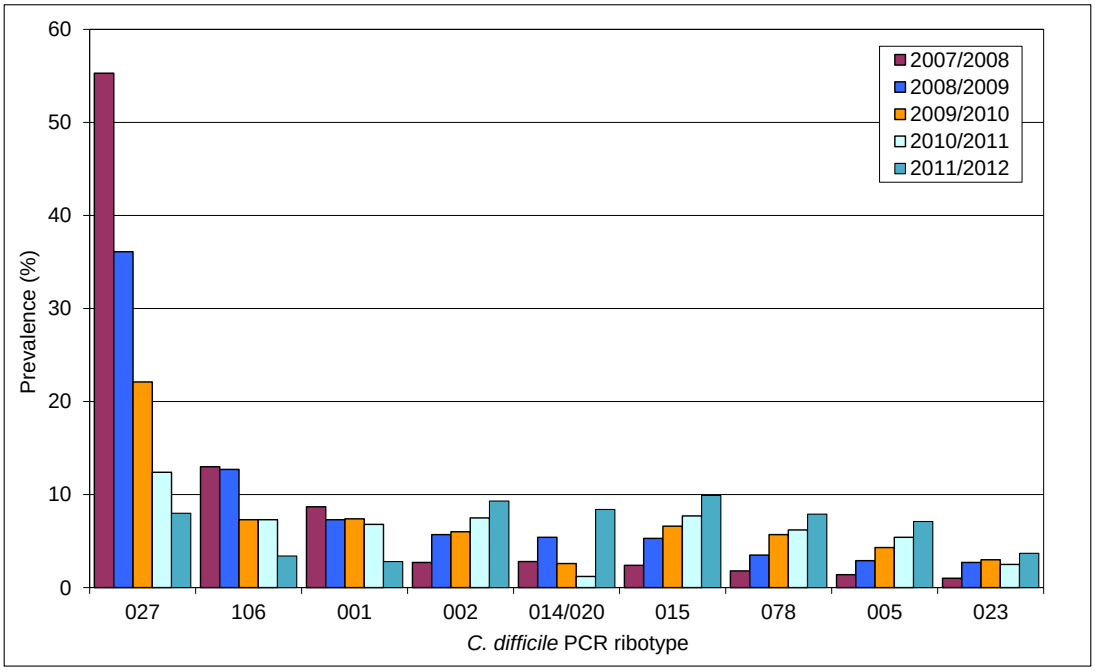

Figure 1.3: Prevalence of *C. difficile* PCR ribotypes in the UK from 2007-2012[205].

1.1.7 Antimicrobial Resistance

In 2005/06 the HPA (now PHE) carried out susceptibility testing on 881 isolates of *C. difficile* and revealed universal susceptibility to metronidazole, vancomycin, co-amoxiclav and piperacillin/tazobactam. Resistance to erythromycin and moxifloxacin was noted but appeared to be related to PCR ribotype, with the strains 001, 106 and 027 virtually always resistant[206].

One of the first reports of *C. difficile* resistance to metronidazole was published in 2002, detailing 6.3% of 415 isolates with minimum inhibitory concentrations (MIC) ≥ 16 mg/L[207], but these observations have not been verified.

More recently, 1010 *C. difficile* isolates from CDRN received during 2008/09 were screened for susceptibility to metronidazole and vancomycin[208]. Overall geometric mean (GM) MICs for vancomycin and

metronidazole were 0.9 mg/L and 0.7 mg/L, respectively, with epidemic PCR ribotypes 027, 106 and 017 displaying significantly higher metronidazole MICs (GM = 1.73, 1.56, 1.15 mg/L respectively; $p \leq 0.0001$). Metronidazole MICs of 8 mg/L were also observed in PCR ribotypes 027, 016, 015, 118[208]. Further isolation of strains showing reduced susceptibility to metronidazole have been reported, although MIC values appear to be method-dependant[209, 210]. Vancomycin MICs varied little amongst the top 10 most common PCR ribotypes (GM= 0.62-0.81 mg/L). However, 12 isolates with MICs of 4 mg/L were identified[208]. The CDRN continues to monitor reduced susceptibility to metronidazole and vancomycin and utilise MLVA to identify the possible clustering of reduced susceptibility isolates[204]. This apparent reduced susceptibility of *C. difficile* isolates to the two main-line treatment options currently available for CDI could have implications in increased treatment failure and disease recurrence. Reported mean metronidazole concentrations in the faeces of patients receiving metronidazole were 9.5 mg/kg[211-213]. *C. difficile* strains displaying elevated MICs levels (8 to 16 mg/L) may not be inhibited by metronidazole therapy and therefore may be attributable to treatment failure. Faecal vancomycin concentrations of 520 to 2200 mg/L were reported in patients following vancomycin instillation[214]. MICs of vancomycin to clinically-relevant strains, including those displaying reduced susceptibility to vancomcyin (≤ 4 mg/L), are considerably lower than faecal concentrations. Therefore, any apparent reduced susceptibility to vancomycin may have little or no clinical significance.

1.1.8 Diagnosis

With the incidence of CDI increasing in many countries, prompt and accurate diagnosis is vital to commence correct and timely treatment of the

disease, and also to reduce the risk of transmission of *C. difficile* spores to patients and/or the surrounding environment.

Symptomatic CDI patients usually present with unformed stool or watery diarrhoea with a distinctive foul-smelling odour[215]. There are many diagnostic platforms available to identify *C. difficile* as the causative agent of these symptoms and much debate exists as to which diagnostic method is the most specific, sensitive, and least time consuming and labour-intensive.

1.1.8.1 Reference Methods

The 'gold standard' reference methods for CDI diagnosis are cytotoxin assay (CTA) and cytotoxigenic culture (CC)[216-218]. CTA detects the presence of toxin in faecal samples by monitoring action of faecal sample on cell cultures. CC involves the culture of *C. difficile* from stool, and subsequent CTA from the culture rather than directly from stool sample. However, these reference methods are time consuming, labour intensive and require specific laboratory facilities and staff expertise.

1.1.8.2 Toxin Enzyme Immunoassay

Many healthcare trusts in the UK have abandoned the use of 'gold standard' methods in favour of rapid enzyme immunoassays (EIA). A recent report highlighted that up to 70% of hospital trusts in England and Wales use toxin EIA as a standalone diagnostic test[219]. EIA kits detect the antigens of toxins A and B, are relatively simple to use, inexpensive and provide rapid results. There are concerns over the performance of this diagnostic method, with sensitivity rates sometimes reported to be less than 50%[218, 220-222]. However, a systematic review of these tests reported sensitivity values of 75-95% and specificity values of 83-98% compared with CTA[223]. Whilst CTA was considered as the reference method in this study, its sensitivity

rates compared to CC have been reported to range from 67.2% to 98%[218, 224-226].

1.1.8.3 Glutamate Dehydrogenase

EIA tests are also available to detect the surface-associated enzyme, GDH. However, GDH is produced by both toxigenic and non-toxigenic strains, therefore it can only confirm the presence/absence of *C. difficile*, but will not give any information on the ability of the bacteria to cause symptomatic disease. The sensitivity and specificity of this diagnostic test has been reported to range from 89.1% to 100%, and 82.7% to 98.7%, respectively, when compared with CTA[227].

1.1.8.4 PCR Amplification

Commercial PCR amplification/nucleic acid amplification tests (NAAT) are available to detect the presence of *tcdB*. These tests are highly sensitive for the detection of *tcdB*, with reported sensitivity rates of 92% and specificity rates of 94-96% compared with CTA[228,218]. One of the limitations of these tests is that it can only detect the presence of the *tcdB* gene, not toxin B, and gives no information on *tcdA*.

1.1.8.5 Algorithm

Current diagnostic tests exhibit suboptimal sensitivity and specificity values, or relevance to symptomatic disease when performed as standalone tests for the diagnosis of CDI. Therefore, the use of multiple step algorithms to improve diagnosis of has been investigated. In the UK, the Department of Health recently published new *C. difficile* testing guidelines, which outline the use of a two-test algorithm comprising an initial GDH EIA or

NAAT/PCR test to determine whether *C. difficile* is present, and whether further testing is required[229]. If a positive GDH/NAAT is obtained then a sensitive toxin EIA should be carried out to determine whether or not toxin is being produced. Only GDH/NAAT and EIA positive patients should be reported as part of the mandatory reporting scheme.

Pseudomembranous colitis can be diagnosed using colonoscopy or sigmoidoscopy to identify the presence of raised, yellow plaques or lesions[230].

1.1.9 Treatment

Once CDI has been diagnosed, the administration of antimicrobial agents or other pre-disposing medications should be discontinued where possible and alternatives therapies sourced. First-line treatment for CDI in the UK is oral metronidazole (400mg TD for 7-10 days), with vancomycin (125mg QD for 7-12 days)[231] generally reserved for patients with severe disease. Early reports suggested that these antimicrobial agents have a similar effectiveness, although more recent reports provide evidence that vancomycin is more effective for severe cases, with rates of cure for severe disease for vancomycin and metronidazole 97% and 76% respectively[232]. The cost of a metronidazole course is less than vancomycin, therefore metronidazole is the preferred antimicrobial in the UK for mild to moderate disease with vancomycin reserved for more severe cases[97,98]. Fidaxomicin, a new macrocyclic antimicrobial agent has been approved by the FDA from May 2011 in the USA, and June 2012 in the UK for the treatment of CDI. Data from two licensing trials show that fidaxomicin can reduce the rate of CDI recurrence compared with vancomycin[233].

Alternative treatments currently available or in development include rifaximin[234], nitazoxanide[235], daptomycin derivative CB_183,315[236, 237], toxoid A/B vaccine[238, 239], monoclonal antibodies[240], faecal transplant[241] and probiotics[242]. Efficacy and suitability of these alternative treatment agents should be considered before use.

1.1.10 Recurrence of Disease

One of the most difficult situations facing clinicians in CDI treatment is the management of recurrence of infection seen in approximately 5% - 30% of CDI patients[243-245]. There is evidence to suggest that this proportion of patients suffering from disease recurrence is increasing and the emergence of the apparently hypervirulent 027 strain may be a contributory factor[246, 247]. Studies highlight that increased age (>65 years), the administration of concomitant antimicrobial therapy, poor immune response, gastric acid suppression medicine, increased underlying disease severity and increased hospitalisation are more likely to predispose recurrent CDI[46, 246, 248].

A treatment response is considered successful when the frequency and/or consistency of stool decreases or improves. Recurrent infection is manifested by the increased frequency of stool for at least two consecutive days, or other new signs of disease development, and microbiological evidence of toxin-producing *C. difficile* in the stool after successful treatment[249].

Recurrence of disease can occur either because of the persistence of the original infecting *C. difficile* strain within the gastrointestinal tract, which germinates within the colon when antimicrobial therapy has ceased (relapse), or re-infection by a new organism[250]. Little is known about the persistence of *C. difficile* in the gut but recurrent bacterial infections have been associated with the presence of biofilms[251]. Therefore, it is possible that

the existence of mucosal biofilms within the gut may harbour and protect a population of *C. difficile* spores, vegetative cells or toxin, leading to a recurrence of symptoms. The onset of initial CDI is associated with the disruption of the gut microbiota by antimicrobial agents. Hence, prolonged antimicrobial therapy (including the use of anti-CDI therapy) may continue this disruption, providing conditions that allow the subsequent re-establishment of *C. difficile* populations through relapse or re-infection[252, 253].

The European Society of Clinical Microbiology and Infectious Diseases (ESCMID) recommend treatment of a first case of recurrent infection by continuing with the initial treatment therapy unless disease has developed from mild to severe. If a second episode of recurrence, or subsequent recurrences have occurred then the use of tapered vancomycin dosing where the frequency of dosing is gradually decreased and then pulsed is recommended where possible[249].

Faecal transplant, or faecal biotherapy, is a novel treatment option available for patients with multiple episodes of recurrent disease. It involves the instillation of a faecal emulsion from a healthy donor into the upper gastrointestinal tract of the patients via a nasogastric tube, or into the colon via a colonoscopy, or distal colon via enema. A faecal transplant reintroduces healthy microbiota into the patient's gastrointestinal tract which can re-establish a population and provide a colonisation resistance to *C. difficile* re-infection. A systematic review of faecal biotherapy in 2011 identified disease resolution of 92% (89% after single treatment; 95% after retreatment) amongst 317 patients treated across 27 case series and reports[241]. Standard protocols for the administration of this therapy are not currently in place and randomized controlled trials have not yet been reported. As a result different health care facilities adopt varying protocols regarding its route of administration, quantity of donor stool, and other

treatment options. The review highlighted above identifies that variations in method procedures may affect resolution rates although other groups have reported that faecal transplant is an effective treatment option for recurrent CDI regardless of the instillation route[254]. A randomized controlled study is required to draw conclusions about these variations.

This therapy is generally considered as a last resort option and is not widely adopted in health-care facilities, although the reported high cure rates are resulting in increased interest.

1.1.11 Current CDI Models

1.1.11.1 *In vivo*

CDI has been studied in a number of animal species including hamsters, mice, guinea pigs, rabbits and rats[255-258], with the Golden Syrian hamster model most widely used to investigate host-pathogen interactions[68]. Identification of *C. difficile* as the causative agent of CDI was determined within a hamster model[5] and has proven to be a reliable model of the pathogenesis of CDI. Hamsters pre-treated with clindamycin, and challenged with *C. difficile* spores manifest fulminant disease, correlating with clinical observations in humans[259, 260], although the full spectrum of disease in humans is not represented within the hamster model.

Mouse models, including conventional and gnotobiotic models, have also been used extensively to study CDI[261-263]. Normal mice are not as readily susceptible to disease of hamsters, although Chen *et al*[261] have developed a 'conventional' mouse model of CDI that appears to resemble disease in humans, and disease severity correlates with challenge dose. Germ-free murine models are widely used as they reliably develop *C. difficile* colonisation and intestinal pathology[264]. Lawley *et al*[265] demonstrated that virulent *C. difficile* strains can asymptomatically colonise immunocompetent

mice and establish a long-term carrier state, with antibiotic treatment triggering a supershedder state, and later used the same mouse model to evaluate the role of microbiota dysbiosis and restoration in CDI[266].

1.1.11.2 *In vitro*

Early studies of *C. difficile* pathogenesis involved simple batch/continuous culture experimental systems or *in vivo* hamster models; both of which may be considered poorly reflective of the human colonic environment[105, 267, 268]. Ethical and practical issues have led to the development of more complex *in vitro* systems. Macfarlane *et al* developed and validated a triple stage chemostat model of the human gut, designed to reflect the physicochemical and microbiological environment of the colon from proximal to distal, and validated it against the intestinal contents from sudden death victims[269]. Baines *et al* have utilised the same triple stage chemostat gut model as an *in vitro* system in which to study the effects of antimicrobial administration on human gut microbiota and *C. difficile*[270]. This has proven to be a reliable and reproducible model in which to study the response of *C. difficile* to antimicrobial administration. Thus, antimicrobials with a recognised propensity to induce CDI *in vivo* facilitated *C. difficile* spore germination, proliferation and high-level cytotoxin production in the gut model, *e.g.* clindamycin and moxifloxacin[271, 272]. Conversely, the absence of antimicrobial administration, and agents considered low-risk for CDI induction, did not induce simulated CDI[273]. The gut model has proven useful in the evaluation of the propensity of existing and novel antimicrobials to induce and treat CDI. Gut model studies have also indicated the importance of gut antimicrobial concentrations in the development of CDI, and allowed the comparative evaluation of epidemic *C. difficile* strains. While this current system has proven a successful *in vitro*

model of CDI, it is unable to reflect accurately the extensive and complex bacterial communities that colonise intestinal mucosal surfaces in biofilm structures. There is increasing interest in the development of novel therapies for CDI, noting the paucity of current options, and their associated high recurrence/relapse rates[244]. There is therefore a fundamental need to understand the interplay between antimicrobial agents and *C. difficile* at the gut mucosal surface, since this is where toxins bind to receptors.

1.2 Gastrointestinal Tract

1.2.1 Gut Microbiota

The human colon is a highly complex and diverse ecosystem consisting of over 500 bacterial species with a total concentration of approximately 10^{12} cfu/g of faeces[274]. The digestive tract of the human foetus is sterile. After natural birth the tract is colonised by a variety of microorganisms originating from the birth canal and surrounding environment[275, 276]. During childhood the commensal microbiota is established and remains relatively stable throughout life[277].

It is estimated that the human microbiota is distributed over 1,000 bacterial species[278], the composition of which is highly variable amongst individuals. Firmicutes and Bacteriodetes[279] are most often reported as predominant families, with Actinobacteria[280] and Proteobacteria[281] also representing high populations within gut microbiota communities.

Before the use of metagenomic techniques, much of our existing knowledge of the intestinal microbiota relied on culturing planktonic faecal bacteria onto selective and non-selective agars. Whilst these methods provided preliminary information on these bacterial communities they were unable to

provide information on the extent and complexity of the intestinal ecosystem. Faecal culture studies provide evidence that anaerobic bacteria outnumber facultative anaerobic bacteria by a factor of 100-1000, with bacteroides, bifidobacteria, eubacteria and clostridia the predominant genera in humans[282]. However, it is believed that only a minority of the intestinal microbiota species can be consistently cultured[283-285].

The initial introduction of culture-independent techniques was largely based on targeted sequencing of 5S and 16S ribosomal RNA genes. Reports suggested that only 20-24% of molecular species recovered from faecal samples correspond to organisms described in culture-dependant sampling, the remaining represent previously unknown species[279,283,280].

The Human Microbiome Project and the European Metagenomics of the Human Intestinal Tract were initiated to provide more in-depth information on the bacterial populations that colonise human hosts, and address the relationship between health and disease. These studies utilise molecular methods in order to gain greater insight into the gut microbiota.

The introduction of next generation sequencing technologies (including pyrosequencing Roche-454[286, 287] and Illumina[278, 288, 289]) allows the timely and relatively cheap generation of large volumes of sequence data necessary for the comprehensive characterisation of microbiota population dynamics[290,291]. Sequence determination of microbial communities can be approached using whole genome sequencing or targeted 16S rRNA sequencing. Whole genome shotgun sequence determination provides a minimally biased view of microbial communities which is absent from 16S rRNA sequencing methods. The depth of the reference library governs the identification of rare bacterial species within complex microbial communities.

Bacterial populations within the gastrointestinal tract exist in two forms; planktonic free-floating communities within the lumen, and sessile bacteria within mucosal-associated biofilm communities[292]. Many intestinal microbiota studies are derived from faecal samples and only provide information on planktonic populations, therefore may not accurately represent colonic microbiota communities. Sessile bacterial populations have been visualised on the mucosal surface and in the mucus layer of the colon[293]. These communities are difficult to identify and enumerate due to the physical inaccessibility of this region. Bacteroides and fusobacteria predominate on the mucosal layer, with other groups including eubacteria, clostridia and anaerobic Gram-positive cocci also present[293, 294]. Another study identified the predominant bacterial groups from mucosal biopsies as Bacteroides, and the lactic acid bacteria Leuconostoc and Weisella, with microbial communities displaying some homogeneity[281]. The degree to which composition and function of faecal and mucosal microbiota differ remains unclear, although some reports suggest a distinct difference in microbial composition at the two sites[292].

1.2.2 The Role of Gut Microbiota

Diversity of bacterial species found in the human colon is mediated by the availability of nutrients such as indigestible starches, the ability to compete for limited resources and adhesion sites on food particles and the mucosal layer, with unsuccessful species being rapidly eliminated from the gut.

Despite the presence of complex, antigenically and metabolically distinct microbial communities within the gastrointestinal tract, a largely mutualistic relationship exists between the host and indigenous gut microbiota. Evidence obtained through the use of germ-free animals suggested that the intestinal microbiota has important metabolic, trophic and protective

functions[295]. Non-digestible dietary products, particularly carbohydrates, and endogenous mucus are fermented by colonic microbiota to provide energy and nutrients for bacterial growth[128]. Bacteria possess enzymes that are lacking in human hosts, which are required for degradation of specific proteins, peptides and carbohydrates into short-chain fatty acids (SCFAs). These substances in turn provide the host with energy and nutritional resources, and increase its ability to absorb nutrients such as calcium, magnesium and iron. SCFAs also increase the growth of intestinal epithelial cells and control their proliferation and differentiation[129]. The benefits that these intestinal microorganisms provide the host with are largely greater than the possible pathogenic threat, and indeed the host and microorganism establish a long-term cooperative and stable relationship. However, imbalance in bacterial populations, for instance through antimicrobial administration, may result in detrimental outcomes for the host.

1.2.3 Mucous Membrane

Mucous membranes line bodily cavities, including the gastrointestinal tract. At least four microhabitats of the gastrointestinal tract have been described: the intestinal lumen, the unstirred mucus layer (gel that covers the epithelium), the deep mucus layer, and the surface of the intestinal epithelial cells.

In order for bacteria and host to maintain a symbiotic relationship the penetration of bacteria across the epithelial barrier is limited, minimising activation of the host immune system. The mucus layer protects the underlying epithelium from the external environment, including pathogens. Abnormalities in the mucosal composition have been implicated in diseases such as ulcerative colitis[296,297].

1.2.3.1 Mucin

Goblet cells within the epithelium produce a mucus gel composed primarily of mucin glycoproteins, which are synthesised and secreted from the apical surface of goblet cells. Mucins can be classified into acidic or neutral subgroups[298]. The former predominate in the colonic epithelium and the latter in the gastric mucosa[299]. The physiological relevance of mucin subgroups is not well understood, although it is speculated that acidic mucins protect against bacterial translocation[300, 301].

Intestinal mucus is a viscous gel with a high negative charge and a large hydration capacity, and is composed primarily of high molecular weight glycoproteins[302, 303]. These glycoproteins are composed of a peptide core, rich in serine and threonine residues, which are protected from proteases by oligosaccharides linked via *O*- or *N*-glycosidic bonds[304, 305]. Carbohydrate monosaccharides such as frucose, galactose, *N*-acetylglucosamine, *N*-acetylgalactosamine and sialic acid account for up to 80% of the dry weight of mucins[306, 307]. Mucins act as the main structural component of the mucus layer, giving rise to its polymeric, viscoelastic and protective properties. The attachment of sulphate and *O*-acetyl substituted sialic acids to terminal mucin oligosaccharides confers resistance to digestion by glycosidases[308]. Intestinal mucins undergo *O*-linked glycosylation where the attachment of a group of oligosaccharides occurs directly to proteins through the hydroxyl group of threonine or serine. In order for bacteria to degrade these carbohydrate structures they must synthesise deglycosylating enzymes[309]. Miller *et al* suggested that a sub-population of faecal bacteria produce extracellular glycosidases with high specificities for certain oligosaccharides of colonic mucins[310]. It is the sequential breakdown of these mucins by a population of diverse bacterial species which leads to the destruction of the mucus layer[309].

1.2.3.2 Mucus Layer

The mucus layer is composed of an outer layer which harbours symbiotic bacteria and a protected inner layer which is largely resistant to bacterial penetration[311-313]. A study of healthy ileal and colonic biopsy samples identified bacterial populations predominantly associated with the outer mucus layer, with no bacteria detected in association with epithelial cells[313]. The mucus gel is constantly exposed to acids and irritants and is often sloughed off due to peristaltic movements of the gastrointestinal tract. In the stomach, the mucus layer can reach a thickness of 450 μm, gradually decreasing through the intestine to 285 μm in the rectum[306, 312]. Under normal conditions goblet cells continuously synthesise and secrete mucins to replenish the mucus layer and to maintain its thickness. When goblet cells are exposed to potent secretagogues (substances which increase the rate of mucin production) [314, 315], such as bacterial toxin[316], mucin is released in an accelerated fashion.

The ability of the intestinal gut microbiota to metabolise mucus offers ecological advantages including the provision of a source of carbohydrates, peptides, vitamins and minerals[317]. Bacteria capable of colonising mucus may avoid expulsion from the intestine via peristalsis.

Both commensal and pathogenic bacteria may derive significant benefits from their ability to chemically regulate mucin synthesis or secretion from host goblet cells. However, some enteric pathogenic bacteria have the ability to degrade the inner and outer mucus layer, providing access to the underlying epithelia cells and enabling attachment to receptors, thus causing disease. Sub-populations of faecal microbiota have been shown to degrade the oligosaccharide side chains of hog gastric mucin, which structurally resembles human epithelial mucin[310]. Once bacteria have gained entry to the

epithelial cells, many intestinal pathogens actively down-regulate microbicidal mechanisms of macrophages, allowing survival and replication in host tissues[318].

1.2.3.3 Mucosal Epithelium

The intestinal epithelium comprises simple columnar, immune and goblet cells. In order for pathogens to cause disease they must traverse the inner mucus layer to gain entry to the underlying epithelial cells and evade or overcome the immune response of the host (*i.e.* inhibiting chemotaxis; negating opsonisation; avoiding phagocytosis). Epithelial cells such as Paneth cells secrete antimicrobial peptides which contribute to the destruction of bacteria that have gained entry to the inner layer[319]. If bacteria are detected within close proximity to the epithelia, B lymphocytes induce the production and secretion of bacteria-specific IgA which reduce the number of epithelial-adherent bacteria [320, 321]. Bacteria that cross the epithelial barriers often succumb to rapid phagocytosis and elimination by macrophages[322].

1.3 Biofilms

1.3.1 Discovery of Biofilms

Biofilms were first observed by Antonie Van Leeuwenhoek in the 17th century when he used an early microscope to view 'animalcules' in the dental plaque on teeth. In the 1940s, researchers began to publish reports on the adherence of marine bacteria to surfaces[323]. It is now the general consensus amongst microbiologists that, in their natural state, most bacteria exist within biofilms and possess unique characteristics, which distinguish them from their planktonic counterparts.

1.3.2 Ubiquity of Biofilms

A biofilm is traditionally defined as a community of microbial cells irreversibly bound to a surface and embedded in a self-produced exopolysaccharide matrix.

Biofilms are ubiquitous in nature and almost any surface may facilitate biofilm formation, including contact lenses, ship hulls, teeth, rocks in streams, indwelling medical devices and industrial water systems[324, 325,326-328]. Whilst biofilms are associated with beneficial functions such as nutrient recycling, bioremediation and colonisation resistance, adverse effects such as infection, recalcitrance to antimicrobial mechanisms and contamination have led to biofilms becoming a topic of focus for researchers.

It is becoming increasingly clear that biofilms elicit a major impact on healthcare, owing to their formation on medical devices and role in persistent infections. It has been estimated that biofilms are associated within the US 65% of nosocomial infections with treatment of such infections costing over $1 billion annually[329, 330]. Within industry, biofilms prove problematic, leading to corrosion of pipes, reduced heat transfer in cooling water systems and biofouling of ship hulls[331-333].

1.3.3 Biofilm Development

Biofilm formation is a highly complex and diverse process, which has been studied extensively. Although every biofilm forms under a unique set of conditions, the biofilm life cycle is typically divided into four steps; initial reversible adhesion, irreversible adhesion, maturation and dispersal.

1.3.3.1 Initial Reversible Adherence

The solid-liquid interface between a surface and an aqueous medium provides an ideal environment for the attachment and growth of bacteria. In order for these bacteria to translocate to a conditioned surface they do so in a directed (*i.e.* via chemotaxis and motility) or random fashion (*i.e.* propelled to the surface by the natural movement of the liquid in which they are suspended). Once the organism reaches close proximity to a surface, factors such as the level of attractive and repulsive forces, temperature, substratum composition, environmental conditioning factors and hydrodynamics of the liquid determine whether or not attachment will commence.

1.3.3.1.1 Substratum and Fluid Properties

The composition of a surface material determines the extent, rate and type of species colonising the surface. Biotic surfaces may contain specific ligands and receptors which aid the adhesion of specific organisms. Abiotic surfaces lack these specific adhesion sites and colonisation relies on non-specific factors, such as substratum material hydrophobicity and roughness, or conditioning of the surface with an organic film[334].

Increased roughness of an abiotic material provides an increased surface area and reduces the shear forces surrounding the area, encouraging the attachment of microbes to the surface. There is also evidence to suggest that hydrophobic, non-polar surfaces facilitate greater adherence of microbial organisms[335-337].

A substratum material surface submerged within a liquid environment becomes colonised by organic compounds such as polysaccharides or glycoproteins. Within an *in vivo* environment a surface may be conditioned by tears, saliva, and other secretions, often within minutes[338 339]. This conditioning film develops on a surface over time, and may mask the

properties of the surface underneath, enhancing the attachment of a greater diversity of bacterial species. Temperature, pH, nutrient availability and ionic strength of the aqueous medium in which the substratum material is submerged may influence the extent of colonisation[340-343].

Biofilm formation is not limited to association with a solid surface. Certain organism form pellicles at the liquid-air interface[344, 345], allowing sessile bacteria access to aqueous and gaseous phases.

1.3.3.1.2 Cell Properties

Once bacterial cells come into contact with a surface they must overcome repulsive forces to adhere to that surface. Properties of the bacterial cell, such as cell surface hydrophobicity and charge, presence of fimbriae, pili, flagella and adhesins all influence the rate of colonisation[342, 346-348]. Most bacteria are negatively charged but still contain hydrophobic surface components. Fimbriae contribute to this hydrophobicity and play a role in overcoming the initial electrostatic repulsion that exists between cell and substratum material[349]. Similarly, flagella help bacteria overcome electrostatic repulsive forces, allowing translocation of bacteria to the substratum material. Pratt and Kolter demonstrated that *E. coli* require flagellum-mediated motility to initiate initial attachment for biofilm development[347]. Whilst O'Toole and Kolter[350] utilised *Pseudomonas aeruginosa* mutants to demonstrate that flagella mutant strains exhibit diminished adherence to plastic surfaces compared to the wild-type. Furthermore, *P. aeruginosa* strains displaying type IV pili mutants were able to form a monolayer of attached cells but subsequent formation of microcolonies was retarded[350].

1.3.3.2 Irreversible Adhesion

Once initial interaction between a bacterial cell and surface has been initiated, if not immediately separated, bacteria can anchor themselves to the surface using strong cellular surface-adhesins and host- or tissue- specific interactions. Once committed to adhesion, certain species may upregulate specific adhesion genes and/or begin to synthesise extra polymeric substance (EPS) material which contributes to the irreversible attachment and transition to the sessile mode of growth of these organisms. This theory is supported by the observation that *P. aeruginosa* organisms that have recently attached to a surface upregulate *algC* , which is required for EPS alginate synthesis[351].

Once this second stage of attachment is complete, adherent bacteria can only be removed from the surface by physical or chemical intervention. These first colonists facilitate the arrival of other bacterial species by providing more diverse adhesion sites and beginning construction of the extracellular matrix that holds the biofilm together.

1.3.3.3 Co-aggregation

Many bacterial species possess multiple adhesion sites that facilitate adhesion to a substratum surface and also inter-bacterial adhesin-receptor interactions. The adherence of an initial coloniser to another genetically distinct species is known as co-aggregation, and allows increased diversity amongst multi-species sessile communities.

There are an abundance of studies focusing on co-aggregation in oral microbiology, with reports of co-aggregation of over 1000 oral bacteria strains[352]. The utilisation of FISH technology identified that initial colonisation of oral biofilms *in vivo* involved the co-aggregation of *Streptococcus* spp. and *Actinomyces* spp., and that as the biofilms matured

Streptococcus populations were replaced by an increase in *Fusobacterium nucleatum* populations[353, 354].

Donelli *et al* have recently outlined evidence that mono- and dual- species biofilms exist *in vitro* between selected intestinal strains. More specifically *Finegoldia magna* and *Clostridium difficile*, *Fusobacterium necrophorum* and *Veillonella* spp., and *Finegoldia magna* and *Bacteroides fragilis* pairs appeared to enhance biofilm growth when grown in mixed cultures as opposed to single species cultures[355]. Ledder *et al*[356] have also demonstrated that *C. perfringens* appears to co-aggregate with *B. adolescentis* and *B. fragilis* but weakly co-aggregates with other enteric and oral bacterial species.

1.3.3.4 Maturation

Once bacteria have successfully completed the second, irreversible stage of attachment, proliferation and maturation of the biofilm can commence.

During maturation, density and complexity of the biofilm increases as existing bacteria proliferate, and new bacterial species are recruited. The biofilm begins to change shape and size, and water channels form, providing nutrients to cells deep within the structure[357]. Certain unique characteristics of a biofilm such as antibiotic resistance are often conferred once the biofilm has developed in maturity[358].

The maturation and lifecycle of the biofilm is dependent on the availability of nutrients in the immediate vicinity of the biofilm, the transportation of nutrients into all areas of the biofilm, and the removal of any waste or toxic products into the surrounding environment[359]. Other factors such as hydrodynamic forces, pH, availability of gaseous substances, carbon sources and osmolarity all influence the maturation of a biofilm. Once a biofilm has formed on a surface *in vivo,* it typically remains relatively stable and is often beneficial to the host.

There is evidence to suggest that biofilm maturation is dependent on quorum sensing molecules known as acyl-homoserine lactones (AHL)[360]. *P. aeruginosa* strains with mutated genes encoding an enzyme for the synthesis of an acyl-AHL undergo the early stages of biofilm formation, but maturation, and the typical architecture of the biofilm is absent.

1.3.3.5 Dispersal

Once a biofilm has reached a defined biomass the outermost layer of the biofilm begins to detach from the main structure, generating planktonic organisms. This can be a passive or active process and is caused by factors such as increased fluid shear, response to changes in nutrient levels, enzymatic degradation, quorum sensing, or by the release of EPS or surface-binding proteins[361-364]. In some species detachment seems to be a strategy by which bacteria actively colonise new niches. Within a clinical setting this has implications in the dissemination of infection.

The enzymatic degradation of the biofilm matrix is a mechanism of biofilm dispersal where bacteria produce extracellular enzymes that degrade specific targets of the biofilm matrix[365-367]. Dispersin B is a matrix-degrading glycosidase enzyme produced by *Aggregatibacter actinomycetemcomitans*. Mutant bacterial strains deficient in dispersin B production were able to form mature biofilms but unable to release and disperse cells[368].

There are numerous mechanisms for biofilm dispersal: swarming/seeding dispersal[369]; clumping dispersal and surface dispersal. Swarming dispersal involves the release of individual cells (often motile) in to the bulk fluid or surrounding environment from within hollow cavities of the biofilm structure[370, 371]. Clumping dispersal occurs when aggregates of cells are shed as clumps or emboli[361]. These aggregates are still surrounded by EPS and

constitute a form which is physiologically similar to sessile bacteria, potentially retaining their protective properties[372]. Cell aggregates released in this manner often contain high cell densities, in some cases exceeding the infective dose for pathogenic bacteria[361]. The active movement of self-propelled single cells across a surface away from a biofilm through swimming, sliding or twitching motility is known as surface dispersal[373]. These individual cells no longer possess the protected biofilm phenotypes, although surface motility of whole biofilm structures has been identified, causing a major problem in medical devices such as endotracheal tubes, which may lead to dissemination into the lungs[374].

1.3.4 Biofilm Structure

1.3.4.1 Biofilm Architecture

Biofilms form under a unique set of conditions which facilitates the formation of unique, complex structures, although some structural components can be considered universal[375]. Most mature biofilms comprise sessile bacteria within matrix-enclosed, heterogeneous microcolonies, which form a three-dimensional structure interspersed with open water channels. The architecture of the biofilm alters over time and space in response to external and internal processes and conditions.

Developments in digital imaging techniques allow researchers to study biofilm structure in greater definition. Confocal Scanning Laser Microscopy (CSLM) has proven particularly suitable for the study of microbial biofilms as it allows non-destructive imaging of these hydrated structures with depth selectivity *in situ*. Coupling the use of this digital imaging technique with fluorescent probes allows the visualisation of specific or non-specific structures within the biofilm[376].

The structural visualisation of *P. aeruginosa* microcolonies within biofilms demonstrates a mushroom like structure, with the majority of cells localised in the 'crown' of the mushroom shape with fewer present in the 'stalk'. The former display motility and the latter non-motility[377].

1.3.4.2 Extracellular Matrix

Once bacteria have irreversibly attached to a surface they produce extra cellular material which is often referred to as the biofilm matrix.

This matrix accounts for over 90% of the dry mass of a biofilm, with microorganisms accounting for only 10%[378]. The matrix itself is highly hydrated with reports suggesting that 97% of its structure comprises water[379]. The remaining components, EPS, are hydrated biopolymers including polysaccharides, nucleic acids and lipids, which are mostly secreted by cells within the biofilm[380-382]. Biofilm matrix also retains the components of lysed cells, including DNA, which may represent a reservoir of genes for horizontal gene transfer[383]. The presence of uronic acids or ketal-linked pyruvates gives the biofilm anionic properties, allowing cross-linking of polymer strands to provide greater integrity[384]. The matrix can also protect organisms against desiccation, host immune responses, and some antimicrobial agents.

The biopolymers within the matrix are responsible for the macroscopic appearance of biofilms. Although the ability to produce an extracellular matrix appears to be a common feature of some biofilm bacteria, the structure of biofilms produced is remarkably diverse. Matrix structures form the scaffold for the three-dimensional architecture of the biofilm and are responsible for cohesion. EPS immobilises biofilm cells, keeping them in close proximity, allowing for cell-cell communication and the formation of

synergistic micro-consortia. Bacteria deficient in EPS synthesis produce biofilms with altered morphology. For example, alginate is a well characterised EPS expressed by mucoid strains of *P. aeruginosa*[382]. Whilst alginate is not essential for the formation of a biofilm, overexpression produces a structurally mature biofilm, with similar reports pertaining to the role of colonic acid in *E. coli* biofilms *in vitro*[385, 386]. Mutations in *Vibrio cholera*[387] and *Staphylococcus epidermidis*[388], which elicit defective EPS production, render these strains defective in the initial stages of biofilm formation.

1.3.5 Biofilm Properties

1.3.5.1 Cell-Cell Communication

Quorum sensing is the regulation of gene expression in response to fluctuations in cell-population density, occurring both within and between bacterial species. Quorum sensing bacteria produce small chemical signalling molecules known as autoinducers[389]. These autoinducers increase in concentration as a function of cell density, with an increase in bacterial density resulting in AHL accumulation until a threshold concentration is reached, thereby inducing altered gene expression[390].

Gram-positive and Gram-negative bacteria use quorum sensing communication circuits to regulate a diverse array of physiological activities, including surface attachment, extracellular polymer production, virulence factor production, conjugation, antibiotic susceptibility, motility, sporulation and biofilm formation[391-394]. It has been demonstrated that many species, including *P. aeruginosa* activate EPS production at high cell densities, and organisms with mutated AHL genes produce densely packed cells which are only a few layers thick[360], rather than mature biofilm. Other species, such as

Vibrio cholerae populations terminate EPS production once cell densities levels reach a threshold level[395].

1.3.5.2 Antimicrobial Resistance

Biofilm infections pose a major problem to healthcare facilities worldwide and cause chronic infections due, in part, to their recalcitrance to antimicrobial therapy. Furthermore, biofilm infections are often able to evade host defences, even in individuals with competent immune systems[396-398], although tissues adjacent to biofilms may undergo collateral damage by immune complexes and invading neutrophils.

In vitro biofilm models have shown the survival of sessile bacteria at antimicrobial concentrations up to 100 - 1000 times the MIC of planktonic cultures[399-401]. *In vivo* antimicrobial agents suppress the initial symptoms of infection, but once therapy has ceased symptoms can return, which can lead chronic infections and often surgical intervention is required to eradicate the infection[402-405].

Several theories exist to explain the mechanisms which confer resistance of biofilm bacteria to antimicrobial agents exist, and these are summarised below.

1.3.5.2.1 Barrier Effect

The highly hydrated biofilm matrix has many functions and it has been suggested that one of its roles is to protect bacterial cells within the biofilm from the action of antimicrobial agents. Initially it was postulated that this matrix structure may prevent the penetration of antimicrobial agents to the bacterial cells within. However, mathematical models have since demonstrated that the diffusion of molecules the size of antibiotics through

the biofilm matrix should not be retarded. It has since been hypothesised that antibiotic deactivation, binding or reaction within the biofilm matrix may occur faster than diffusion of the molecule through the matrix.

There have been many conflicting reports pertaining to the biofilm barrier effect, with Hatch and Schiller[406] demonstrating that a 2% suspension of alginate isolated from *P. aeruginosa* inhibited diffusion of gentamicin and tobramycin, and that this effect was reversed when alginate lyase was used. Other groups have demonstrated that, because of their positive charge, aminoglycosides bind to negatively charged polymers within the biofilm matrix, thus retarding penetration[407, 408].

Furthermore, it was observed that ampicillin demonstrated reduced penetration and antimicrobial activity against wild-type *Klebsiella pneumonia* biofilms, but β-lactamase-deficient *Klebsiella pneumoniae* biofilms allowed the penetration of ampicillin but remained resistant to this agent[409].

Whilst there is increasing evidence to suggest that the presence of the matrix alone does not prevent the penetration of antimicrobial agents, the penetration of larger immune response objects may well be retarded by the matrix of some biofilm structures[410].

1.3.5.2.2 Slow Growth Rate

It is well established amongst microbiologists that non-dividing bacteria are less susceptible to many antimicrobial agents. Biofilm communities experience nutrient limitation, therefore a subpopulation of sessile bacteria often referred to as 'persisters', exist in a slow-growing/dormant state[411]. These bacterial cells exhibit a distinct phenotype which is associated with the chronic nature of biofilm infections and their inherent resistance to antimicrobial chemotherapy. Once antimicrobial therapy has ceased it is

postulated that persister cells within the biofilm repopulate the site and lead to disease recurrence.

Research into this particular area is limited because the measurement of divisional activity is difficult. Certain antibiotics are able to exert an effect on non-growing cells and these antibiotics have demonstrated an enhanced activity against sessile bacteria compared with those antibiotics whose mechanism of action require an actively growing cell for activity[412-414].

The use of acridine orange stain identified that inner areas of biofilm structures display low relative RNA content, indicating slow growing bacterial growth, whilst the outer edge of the biofilm display relative high RNA content, indicating high bacterial growth[415]. Furthermore, there is evidence to suggest that oxygen levels and potentially nutrients are depleted in the centre of microcolonies[411].

1.3.5.2.3 Induction of Biofilm Phenotype

There is an abundance of data detailing the physiological diversity of sessile bacteria from their planktonic counterparts[416-418]. Sessile bacteria display unique gene expression patterns some of which are not observed in planktonic bacteria[371, 382, 419].

The increasing availability of complete genome sequences coupled with microarray technologies allows researchers to compare the genomic expression of biofilm and planktonic organisms. Data from several reports revealed genomic up- or down-regulation is apparent in sessile compared to planktonic organisms, although no common expression patterns were identified. Stanley *et al* showed that in *B. subtilis*, 519 genes were differentially expressed during the time-course of biofilm formation, with more than 55% expressed at only one of three time points investigated, indicating temporal control of gene expression[420]. DNA microarray analysis

of *P. aeruginosa* identified 1% of genes with altered expression in the biofilm structures compared to planktonic cells[421]. These were assigned as proteins encoding motility, adherence, translation, metabolism, transport and regulation functions. Temperate 'phage genes were the most highly activated[421].

1.3.5.2.4 Heterogeneity

The biofilm is a diverse and heterogenetic structure, with distinct microcolonies with separate nutrient availabilities, signalling systems and waste products. Therefore bacteria within biofilms exist within distinct environments and thus may express different phenotypes. This increases the chances of a subpopulation of bacteria evading the mechanism of antimicrobial action.

Studies utilising a fluorescent probe specific for respiratory activity have shown that after challenge with a biocide, the outer most edge of a biofilm incurred the greatest loss of respiratory activity whilst the inner portion of the biofilm maintained the greatest respiratory activity[422].

1.3.5.2.5 General Stress Response

More recently is has been postulated that the slow growth rate of cells within a biofilm may be a consequence of a general stress response where cells undergo physiological changes in response to environmental stresses such as pH, temperature and chemical agents[423]. The master regulator of this stress response in *E. coli* is the alternate sigma factor, RpoS. RpoS is typically expressed by cells under conditions of nutrient deprivation or stress, or as cells enter the stationary phase of growth. Studies have indicated that RpoS may also be expressed at high cell densities[424,425]. King *et al* have demonstrated that certain *E. coli* strains with attenuated RpoS levels display

lower levels of resistance to external stress[426]. Furthermore, environmental *E. coli* strains with functioning RpoS genes possessed a greater capability for long-term survival than those with RpoS disrupting mutations[427].

1.3.6 Biofilms in Medicine

Biofilms have been implicated in numerous chronic infections such as urinary tract infections, middle ear infections, cystic fibrosis and dental caries, as well an association with indwelling medical devices[327, 428-430]. Some of these infections are exacerbated by their recalcitrance to antimicrobial therapy.

A biofilm-associated feature which may confer disease persistence is the ability of a biofilm to shed individual cells or slough off sections of its structure into surrounding areas. This may cause recurrent acute disease and allow reseeding of distinct biofilm structures at a different site. Identification of a biofilm-associated infection is important to help clinicians manage treatment options. However, biofilm infections are often difficult to identify. Parsek and Singh[431] have composed a four point criterion to help define a biofilm-associated infection and these are: the pathogenic bacteria are surface-associated; examination reveals bacteria in clumps and encased in a matrix material; the infection is localised; and it is resistant to relevant antibiotics.

The gastrointestinal tract harbours a diverse and complex microbial community which provides protection from colonisation by numerous opportunistic pathogens. The characterisation of the biofilm forming properties of these species remains largely unexplored due to the difficulties in accessing the colon of healthy adults. However, the adhesive and biofilm forming properties of an enteroaggregative *E. coli* strain within the gastrointestinal tract have been well studied[432, 433]. Due to the abundance of

evidence regarding the role of biofilms in chronic infections in other parts of the body, and additional evidence pertaining to the existence of pathogenic bacteria within mucosal biofilm structures in the gastrointestinal tract, it is postulated that other pathogenic bacteria such as *C. difficile* could cause infection when associated with gastrointestinal biofilms.

1.3.7 Biofilm Models

1.3.7.1 Model Organisms for Biofilm Study

Biofilm formation and behaviour of *P. aeruginosa* has been extensively studied, and much of our current knowledge on the biofilm mode of growth is based on work using this organism. *P. aeruginosa* is a common causative agent of chronic lung infection in cystic fibrosis patients, and which is widely regarded as a biofilm-based infection[430]. Cystic fibrosis patients are commonly colonised by both the mucoid and non-mucoid *P. aeruginosa* phenotypes, the former of which is recognised as causing morbidity, with the infection persisting despite prolonged and aggressive antimicrobial therapy.

The biofilm-forming properties of *B. subtilis* have also been well documented, and since this Gram-positive, spore forming organism shares common properties inherent to *Clostridium* species, it is often used as a model organism for clostridial investigations. Observations of the behaviour of *B. subtilis* may be extrapolated to gain insights into the biofilm mode of growth of C. *difficile,* which remains largely uncharacterised.

Spo0A is a master regulator which controls cellular function. As described previously, this regulator controls sporulation in many Gram-positive bacilli including *B. subtilis* and *C. difficile*. Differential phosphorylation of Spo0A in response to environmental conditions such as nutrient limitation can directly

or indirectly regulate the transcription of genes involved in matrix production, cannibalism and motility as well as sporulation[434-436].

Biofilms are composed of heterogeneous bacterial populations and gene expression is spatio-temporally regulated. Cell types which exist within biofilms can be classified as motile, matrix-producing or sporulating. Within *B. subtilis*, high level phosphorylation of Spo0A (Spo0A-P) induces the irreversible induction of the sporulation cascade, whilst low levels of Spo0A-P induce the expression of a regulator and its agonist SinR/SinI, thereby regulating genes involved in the production of extracellular matrix and sporulation. Whilst less well understood, there is also evidence to suggest that Spo0A is involved in the repression of a flagellin motility gene (hag)[434] and cannibalism[435].

Vlamakis *et al*[434] demonstrated that *B. subtilis* gene expression is dynamic throughout biofilm development. They highlighted that during early biofilm formation (12 hours) the majority of cells express the motility gene *hag* promoter but this declined as the biofilm matured. After 24 hours, biofilm expressed peak levels of matrix-production gene *yqxM* promoter, whilst expression of the sporulation gene *sspB* promoter commenced after 48 hours. Furthermore, motile cells began to localise on the edge and base of biofilm structures as time progressed, whilst matrix-producing cells remained distributed throughout the biofilm, and sporulated cells were localised at the upper aerial structures. These results indicate that sporulation, motility and extracellular matrix production are all related and are necessary to construct an architecturally mature biofilm.

1.3.7.2 *In vitro* Models

The use of *in vitro* models allows researchers to manipulate and control certain factors and/or conditions, thus providing a valuable tool for many

areas of research including biofilms. Many *in vitro* biofilm model systems have been utilised and can provide a reproducible and defined system to study the biofilm mode of growth of pure or mixed cultures. Some of these models are been highlighted below.

1.3.7.2.1 Microtiter Tray-Based Models

One of the simplest forms of biofilm models are those based on microtiter plates. Bacterial cultures are inoculated into the microtiter plate (most commonly 96-well) where biofilms grow on the bottom or walls of the wells. Whilst this format is useful due to its ease of use and low cost, the batch-culture like nature can be a limitation. As there is no flow in or out of the system, waste products will increase and nutrient levels will decrease unless fluid is regularly replaced, making the environment inconsistent with *in vivo* conditions.

Microtiter-based models are often used to screen large numbers of samples simultaneously and have also been adapted by Ceri *et al* to analyse antimicrobial susceptibility to biofilms[399]. This system is known as the Calgary Biofilm Device (CBD) or Minimum Biofilm Eradication Concentration assay (MBEC). The system utilises pegs which are attached to the lid of a microtiter plate and immersed in a bacterial culture, allowing biofilm formation on the pegs. The lid and peg system is then transferred to a second plate and immersed in a serial antimicrobial dilution. After a certain period the lid can be removed and biomass/sessile bacterial population enumerated using viable counting or microscopic techniques.

1.3.7.2.2 Flow Displacement Model

Unlike the microtiter-based model, flow displacement models are continuous culture systems in which growth medium and nutrients are supplied into the system as waste products are removed.

The Modified Robbins Device (MRD), which was developed at the University of Calgary, allows the formation of biofilm on a variety of substratum materials at a controlled flow rate[437]. The MRD is usually constructed out of plastic or stainless steel and contains ports in which to insert numerous coupons, which can be composed of a variety of material types. The model is typically inoculated with a suspension of microorganisms and the flow rate, temperature and nutrient input can be controlled. This device allows biofilm formation and removal from a variety of substratum materials, and under differing conditions to be monitored relatively cheaply and has widespread use in biofilm research.

The Centers for Disease Control group designed a biofilm reactor which comprises a glass vessel with removable polypropylene rods inserted into the lid. Each rod supports biofilm formation. In this biofilm reactor, identical biofilms can be formed simultaneously and easily removed over time for analysis[438]. This model has also been utilised to evaluate the efficacy of antimicrobial agents against *Staphylococcus aureus* biofilms[439].

The constant depth film fermenter is often used to study the long-term formation of oral biofilms[440]. The biofilm depth can be manipulated by mechanically removing excess biofilm, a process designed to reflect the movement of the tongue over the teeth.

Other continuous flow fermentation models have been employed by many research groups with various adaptations[441-443]. Bowden *et al* utilised a modified chemostat with ports to accept rods, which provided a surface for bacterial adhesion. The accumulation of oral bacteria onto glass surfaces has

been characterised using this model[444]. The Sorbarod biofilm fermenter employs cellulose acetate filter plugs which provide a large surface area for the adherence of bacterial populations under a continuous flow system[443]. The growth rate, expression of target proteins and effect of antibiotics over extended periods on bacteria in the biofilm mode of growth can be studied with this model[443, 445]. MacFarlane *et al* investigated the colonization and degradation of mucin by faecal bacteria utilising a pH-controlled fermentation system for the growth of planktonic and sessile intestinal bacterial ecosystems[446]. Probert and Gibson utilised a similar model system coupled with fluorescence *in situ* hybridization (FISH) to compare sessile and planktonic populations in a simulated human colon environment[447].

1.3.7.2.3 Cell-Culture Model Systems

Whilst the majority of model systems described previously have been based on biofilm formation on abiotic surfaces, formation on biotic surfaces has also been studied. A reconstituted human epithelia model[448] has been utilised to form a *Candida albicans* dimorphic fungus biofilm on the epithelial-like structure, and can be used to study the interaction between microorganisms and epithelial tissue, although the simulation of the commensal microbiota is absent from this system. Similar model systems are in place for other cell lines, including human microvascular endothelial cells[449] and HeLa cells[450]. These models allow the biofilm formation on clinically relevant tissues to be monitored, and the damage caused to these tissues by their exposure to certain microorganisms.

1.3.8 Gastrointestinal Tract Biofilms

The microorganisms present in the gastrointestinal tract often form multispecies sessile communities attached to the mucosal layer[292-294].

Mucosal populations are difficult to investigate in healthy individuals due to the physical inaccessibility of the gut; thus, there has been restricted study of these communities.

MacFarlane *et al* have shown that bacterial populations strongly adhere to particulate matter in stools with bacteroides and bifidobacteria predominating[451]. Confocal laser microscopy revealed a mixture of living and dead bacteria existing in microcolonies at the interface with the substratum. Bacteroides, eubacteria, bifidobacteria, clostridia and Gram-positive cocci have been detected in human mucosal surfaces[293, 294]. Microscopic investigation of the 3D structure of colonic biofilms has shown that microbial mucosal bacteria are distributed throughout the mucus layer, although they are not usually found in healthy crypts[452]. Live/dead staining and 16S rRNA FISH probes show that most of the bacteria are alive, particularly those that are close to the mucosal surface[451]. These finding suggest that the bacteria were actively growing in the mucus layer and that their presence was not due to the passive transference of the cells from faecal material in the gut lumen.

Zoetendal *et al*[292] utilised 16S rRNA to evaluate the mucosa-associated bacterial communities in different areas of the colonic biopsies. They identified that mucosa-associated bacterial populations were host-specific and uniformly distributed along the colon, but differed significantly from faecal communities.

Examination of mucosal-associated microorganisms from the healthy colon wall of sudden death victims identified that predominant bacterial populations were *Bacteroides* and *Fusobacterium* spp., although species isolated varied between individuals. Microscopy revealed that microorganisms were present with the mucus and displayed complex microbial structures, but major variation along the colon was not evident[294].

In vitro continuous culture flow systems have been used to mimic the conditions of the gastrointestinal tract and to investigate the formation of biofilms on mucins. MacFarlane *et al* developed a two-stage continuous flow model which reflects the proximal and distal colon, and uses a faecal emulsion to provide the indigenous microbiota of the human colon[446]. Porcine mucin gels were used to provide an interface similar to the mucus layer covering the gastrointestinal tract. Rapid colonisation of mucin gels by faecal bacteria occurred in both culture vessels. However, bifidobacteria grew slowly on the mucin and only under the nutrient-limited conditions of vessel 2, where they achieved high cell numbers. In general, anaerobic bacteria in the mucin biofilms did not reach the cell population densities seen in the planktonic phase. It was also evident that mucin biofilm communities contained proportionally higher numbers of enterobacteria than the planktonic phase within the chemostats. FISH, with a mixture of three genus-specific 16S rRNA oligonucleotide probes, showed that the predominant biofilm bacteria bacteroides and enterobacteria grew in close juxtaposition to each other in the mucus, and bacteroides often formed microcolonies[446].

Probert and Gibson designed an *in vitro* fermentation system to model the human colonic microbiota[447], utilising a framework of mucin alginate beads to facilitate the adhesion of bacteria. These beads were encased in a dialysis membrane and inoculated with a faecal emulsion. Populations from this biofilm system were compared to those from a conventional single-stage chemostat. FISH was used to enumerate the bacterial populations and demonstrated that the biofilm fermentation vessel supported a greater cell density than the conventional culture chemostat, notably supporting a greater population of clostridia and *E. coli*.

1.4 *Clostridium difficile* Biofilm Research

CDI is primarily a nosocomial disease associated with high levels of morbidity. Despite most patients responding well to initial medical therapy, ~20% of patients suffer clinical recurrence following withdrawal of antimicrobial therapy[243]. Many patients enter a repetitive cycle of recurrent disease, which introduce difficulties in treatment management. The pathophysiological mechanisms of recurrent CDI are not fully understood, but likely involve continued disruption of the host gut microbiota, persistence of *C. difficile* spores and inadequate host immune response.

First-line CDI treatment options in the UK are predominantly metronidazole or vancomycin therapy[231]. Whilst clinical cure of these two agents is often successful, recurrence of disease is sometimes evident. These agents demonstrate good activity against *C. difficile* vegetative cells. However, they do not possess anti-spore activity, potentially allowing spores to germinate within the disrupted post-antibiotic colonic environment, once antimicrobial therapy has been withdrawn.

Chronic infection is often associated with persistence of microbial organisms within a protected biofilm structure. The gastrointestinal tract is covered by a complex biofilm community adherent to the colonic mucous membrane. *C. difficile* is known to adhere to colonic cells and mucus[124, 453]; however, there is a paucity of information regarding its existence and behaviour within colonic biofilms. Since persistent spores likely mediate recurrent disease it is important to understand the role of biofilms in CDI.

Current understanding of the role of biofilms in CDI remains rudimentary. Whilst in recent years several research groups have begun to focus on this particular hypothesis[454, 455], much of this work utilises basic *in vitro* systems which are poorly reflective of conditions *in vivo*. There is therefore a

fundamental need to carry out more complex experiments which more accurately reflect conditions *in vivo*.

Studies of human gut biofilms indicate distinct differences between sessile and planktonic bacterial populations and metabolic activities within the gut lumen[452, 456]. It is unknown whether these differences affect responses by gut microbiota and/or *C. difficile* to antimicrobial exposure.

Whilst work regarding the existence and behaviour of *C. difficile* within a mixed-species mucosal biofilm remains largely unexplored, recent work has begun evaluating the ability of *C. difficile* to form pure culture biofilms *in vitro.* Laning *et al*[457] successfully grew vegetative *C. difficile* pure culture biofilms on polycarbonate membranes and colony architecture was monitored from 24 hours to 6 days using CLSM and phase contrast microscopy. Results indicated that 24-hour biofilms comprised mainly vegetative cells but, 6-day-old biofilm contained very few vegetative cells limited to the outer edge of the biofilm with an abundance of spores within the inner biofilm structure.

Western immunoblot analysis was performed to identify the presence of toxin antibodies within biofilm structures. Biofilms were cultured for five days using toxigenic and non-toxigenic strains and western blot analysis identified signals at around 300kDa, suggesting the presence of toxin, within the toxigenic strain biofilm whereas no signal was evident in the non-toxigenic strain biofilm. As this author previously identified that vegetative *C. difficile* within 3-day-old biofilms had begun sporulation and at 6 days, *C. difficile* were comprised entirely of spores; they therefore expected to find greater amounts of toxin within younger biofilms. However, western blot analysis indicated that toxin concentration actually increased over time from 1-day-old biofilm to 6-day-old biofilms even though sporulation began at day 3. This may be due to the increased cell mass of older biofilms which have undergone increased cellular division.

These results remain unclear and further work is required to help clarify these observations.

Key surface and regulatory proteins required for biofilm formation in *C. difficile* have been identified using isogenic mutations[454]. Cysteine protease, Cwp84, flagellin protein FliC, putative quorum sensing modulator enzyme, LuxS, and sporulation and matrix production master regulator Spo0A mutants all resulted in defective biofilm formation when compared with the wild-type strains, indicating that individually these genes all play a role in the formation of biofilm structures. SleC (a germination protein) mutants form biofilm-like structures although they are thinner and uneven. Binary toxin components CdtA and CdtB mutations did not adversely affect biofilm formation.

Within the same study, exposure of 1- and 3-day-old biofilms to 10x MIC of vancomycin resulted in 5- and 12-fold increased survival of sessile cells compared with planktonic cultures. This resistance appeared to be mediated by the matrix or other mechanism rather than a genetic change in the biofilm bacteria. Furthermore, sub-inhibitory concentrations of vancomycin did not significantly induce biofilm formation whereas inhibitory levels did increase biofilm formation. These results indicate that *C. difficile* form complex biofilm structures *in vitro* and that biofilm formation is a multifactorial process which remains to be fully elucidated.

Furthermore, recent work has outlined the presence of *C. difficile* within dual species biofilms. *C. difficile* formed moderately adherent mono-species biofilms *in vitro*, however, when grown in the presence of another intestinal strain *Finegoldia magna* a thick, dense biofilm formed indicating a synergy between the two species[355].

Dawson *et al*[455] have recently characterised the biofilm-forming properties of *C. difficile* and the role of Spo0A. They provide evidence that sporulation

master regulator Spo0A may play a key role in biofilm formation. Mutations in the *spo0A* gene resulted in decreased biofilm formation and increased sensitivity to oxygen stress. Six day old biofilm grown on abiotic surfaces possessed greater levels of spores and decreased populations of vegetative cells compared with 3-day-old biofilms. Intact 3-day-old biofilms when exposed to oxygen stress for 24 hours resulted in 45% vegetative cell survival with increased populations of spores. Three-day-old biofilm structures disrupted by vortex when exposed to oxygen stress displayed vegetative cells below the level of detection, with spore survival. The authors concluded that the protected environment of an intact biofilm protects *C. difficile* from oxygen stress[455].

Cyclic diguanylate (3', 5'-cyclic diguanylic acid) (c-di-GMP) is a second messenger which has been well characterised in Gram-negative bacteria and has been shown to mediate the transition from planktonic to the biofilm mode of growth. C-di-GMP facilitates biofilm formation by increasing adhesin and EPS production[458-460], whilst reducing the transcription of flagellar genes[461, 462] and disrupting pilus assembly[463, 464]. C-di-GMP has also been shown to coordinate responses to the entry of cells into stationary phase[465], expression of virulence genes[466, 467], resistance to antibiotics and host immune responses[468, 469].

The sequenced genome of *C. difficile* 630 identifies 37 proteins thought to be involved in c-di-GMP metabolism[470]. Purcell *et al*[471] identified that elevated levels of c-di-GMP represses *C. difficile* motility and induces the formation of *C. difficile* cell aggregates, a function often related to biofilm formation, thereby providing additional evidence of the potential biofilm forming properties of *C. difficile.*

The recent surge in projects pertaining to the biofilm forming properties of *C. difficile* and the role of biofilms in CDI highlights the importance of further investigation of this area.

1.4.1 Project Aims

It is proposed to develop and validate a human gut model system as a model in which to study biofilm-forming behaviour of *C. difficile* and indigenous gut microbiota. It is anticipated that this new model will provide valuable data regarding the interplay between antibiotics, *C. difficile* biofilms and gut microbial biofilms and further our understanding of CDI. Importantly, such developments can contribute significantly to the development of therapeutic agents for CDI.

2.0 Materials and Methodology

2.1 *Clostridium difficile* Isolation, Culture and Identification

Brazier's cycloserine cefoxitin egg-yolk agar (LabM, Leeds, UK) supplemented with 5 mg/L lysozyme (LabM), 2% lysed horse blood (E & O, Bonnybridge, Scotland), 250 mg/L cycloserine and 8 mg/L cefoxitin (LabM) (CCEYL) was routinely used throughout these experiments for the isolation of *C. difficile* vegetative cells and spores. CCEYL supplemented with 2 mg/L moxifloxacin (Bayer, Berkshire, UK) (CCEYLM) was used for the isolation of *C. difficile* vegetative cells during use of the gut model system (chapters 4.0-8.0).

CCEYL and CCEYLM plates were pre-reduced for 24 hours at 37° C in an anaerobic cabinet (Mk III Anaerobic Workstation, Don Whitley Scientific, Shipley, UK) prior to use. *C. difficile* colonies isolated on CCEYL and CCEYLM were identified based on the typical characteristics described by Brazier & Borriello[472]; colonies are 3-5 mm in diameter, irregularly edged, opaque and brown/grey in colour with a distinct odour of *para*-cresol.

2.2 Enumeration and Identification of Gut Microbiota

Selective and non-selective agars were used to identify cultivable gut microbiota species, as described previously for a human gut model system[270, 473, 474], these agars are detailed in table 2.1 and appendix A3.

Planktonic and sessile cultures were serially diluted 10-fold in pre-reduced peptone water (Oxoid, Basingstoke, UK) to 10^{-7}. Twenty microlitres of four appropriate dilutions were inoculated to quarter plates of each culture medium in triplicate (figure 2.1). All sample manipulations were performed anaerobically. Culture media selective for anaerobic organisms were

pre-reduced for 24 hours prior to use. Inoculated plates were incubated anaerobically (obligate anaerobes) or aerobically (facultative anaerobes) at 37° C for 48 hours.

C. difficile spores were enumerated by exposing planktonic and biofilm cultures to 1:1 v/v 100% ethanol (VWR) for at least 1 hour, after which the ethanol:culture mixture was enumerated by serial dilution as described above.

Bacterial colonies were identified on the basis of medium selection, colony morphology, Gram staining, biochemical activity, antimicrobial selectivity and UV fluorescence. Bacterial populations were converted to $\log_{10}$cfu/g (sessile) or $\log_{10}$cfu/mL (planktonic) using the following equations:

mean colony forming units (cfu) per 20 μL x 50 = cfu/mL

cfu/mL x 10^Z = actual cfu/mL (Z = dilution factor)

viable counts expressed as $\log_{10}$cfu/mL

actual cfu/mL*(1/Y) = cfu/g (Y = weight of pellet of 1 mL of culture)

Viable counts expressed as $\log_{10}$cfu/g

Standard errors of mean bacteria counts ($\log_{10}$cfu/mL or $\log_{10}$cfu/g) were determined.

2.3 *Clostridium difficile* Spore Preparation

C. difficile was inoculated onto a single CCEYL plate and incubated anaerobically at 37° C for 48 hours. All growth was removed and sub-cultured onto 10 Columbia blood agar plates (FBA) (Leeds Teaching Hospitals, Leeds, UK) and incubated anaerobically at 37° C for 7-10 days. All growth was removed and emulsified into 1 mL of sterile saline (Sigma-Aldrich, Poole, UK), to which 1mL of 99.6% ethanol (VWR International, Lutterworth, UK) was added. The suspension was vortexed

for 30 seconds and stored aerobically at room temperature. The total viable count of this suspension was determined by 10-fold serial dilution in pre-reduced peptone water under anaerobic conditions to a dilution of 10^{-7}. Twenty microlitres of the appropriate dilution was inoculated in triplicate onto CCEYL and converted to cfu/mL (figure 2.2).

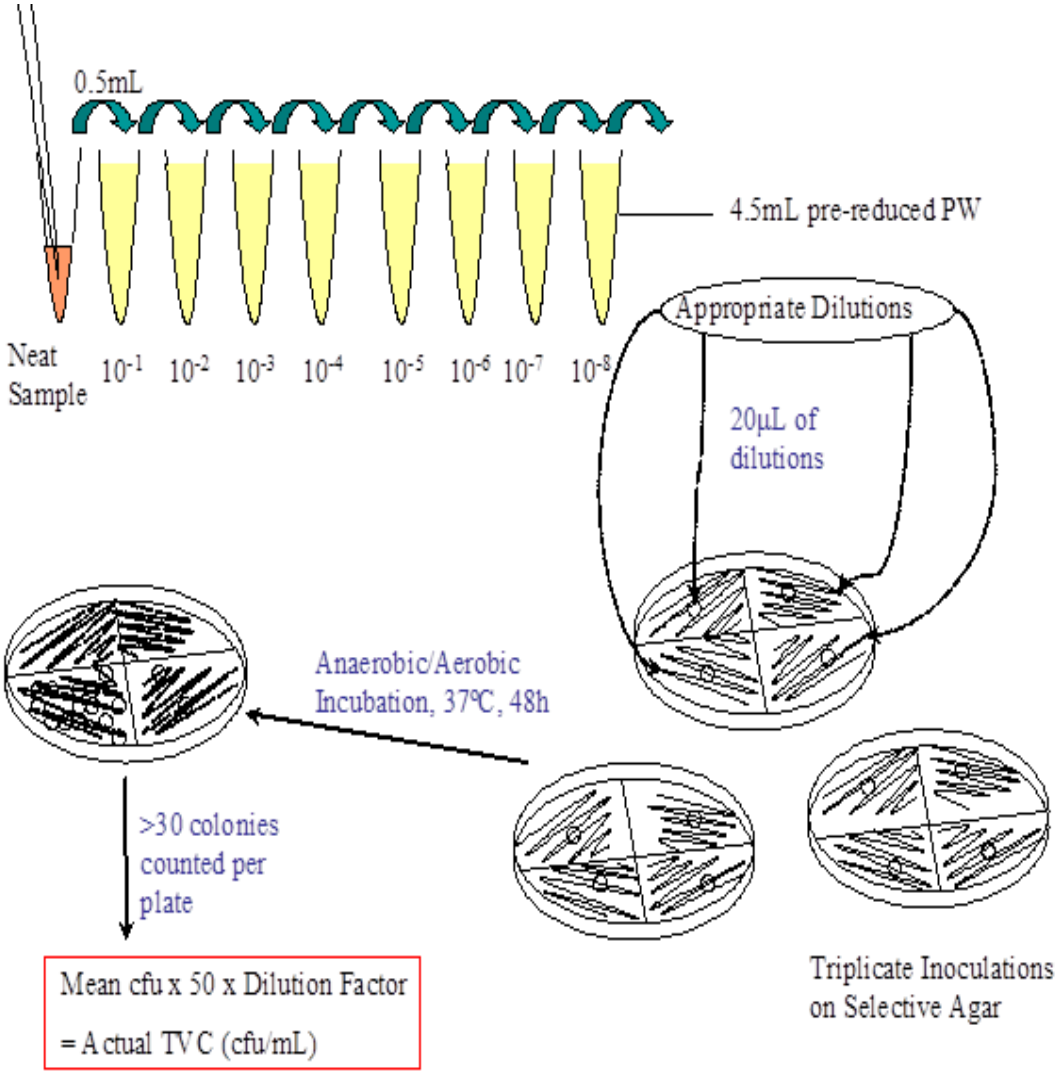

Figure 2.1: Schematic representation of the serial dilution procedure used for bacterial enumeration. (TVC, Total viable counts; PW, peptone water).

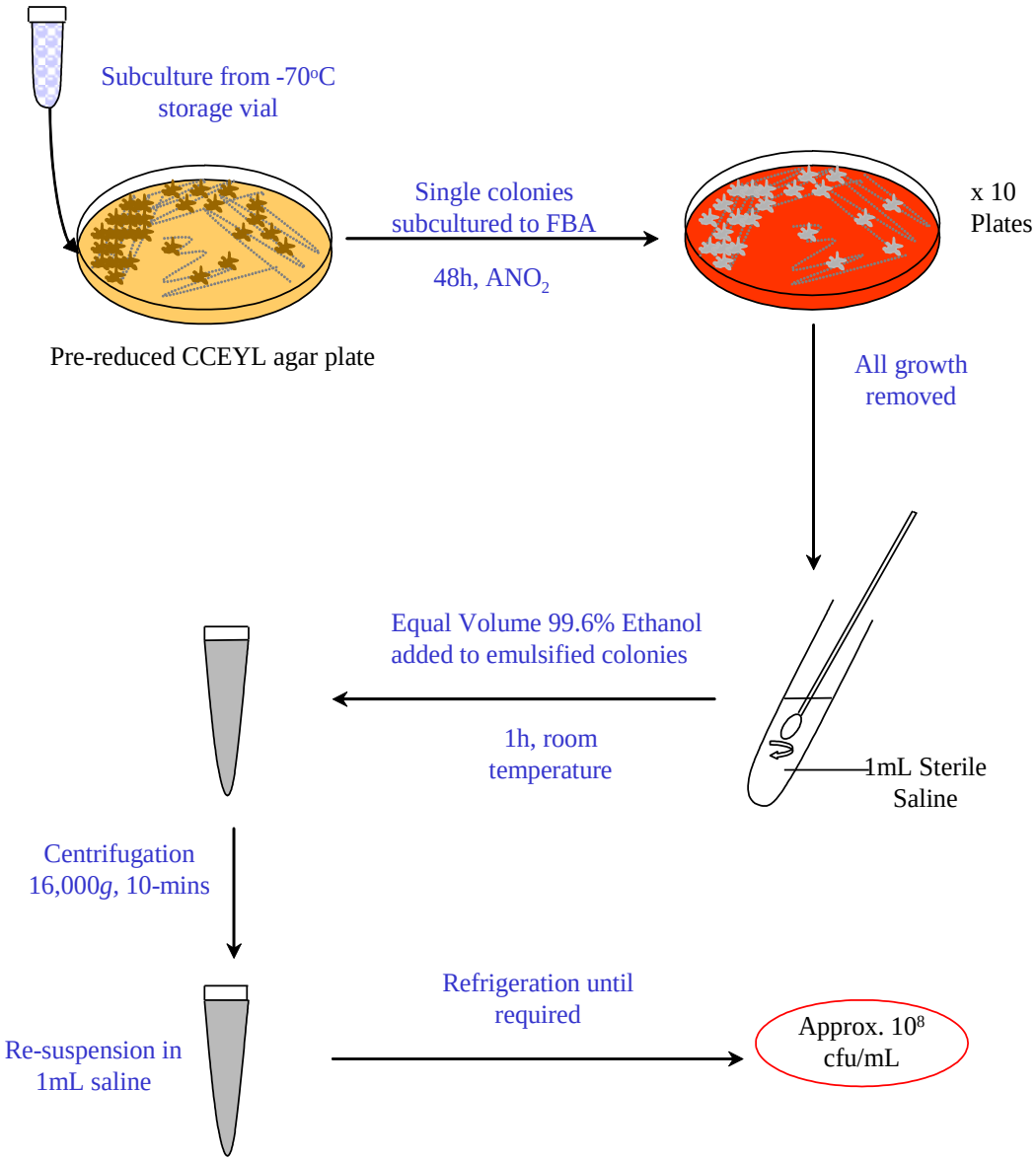

Figure 2.2: Schematic representation of the preparation of *C. difficile* spores.

Medium	**Target species**
Fastidious anaerobe agar (FAA) [475]	Total anaerobes and total clostridia
Bacteroides Bile Aesculin agar (BBE)	*B. fragilis* group.
LAMVAB[476]	*Lactobacillus* spp.
Beerens agar[477]	*Bifidobacterium* spp.
Nutrient agar	Total facultative anaerobes
MacConkey agar	Lactose-fermenting Enterobacteriaceae
Kanamycin Aesculin Azide agar	*Enterococcus* spp.

Table 2.1: Solid culture medium used for the isolation and identification of indigenous gut microbiota. (Manufacturer's details and supplements Appendix A3).

2.4 Cytotoxin Assay

Vero cells (African Green Monkey Kidney Cells, ECACC 84113001) were cultured in flat bottom tissue culture flasks (Nunc, Rochester, USA) containing 20 mL of Dulbecco's Modified Eagles Medium (DMEM) (Sigma) supplemented with 50 mL newborn calf serum (Gibco, Paisley, UK), 5mL antibiotic/antimycotic solution (Sigma) and 5 mL L-glutamine (Sigma) and incubated in 5% CO_2 at 37° C (Sanyo, Watford, UK) until Vero cell monolayers were confluent upon examination under an inverted microscope (Olympus UK Ltd, Middlesex, UK).

Upon satisfactory growth the monolayer of Vero cells was harvested by discarding the DMEM and rinsing the flask with 1 mL of Hanks Balanced Salt Solution (Sigma) containing 0.25 g/L trypsin-EDTA (Sigma) (HBSS-EDTA) and discarding. A further 6 mL of HBSS-EDTA was inoculated into the flask and incubated in 5% CO_2 at 37° C for 10 minutes or until the monolayer of cells were no longer adherent to the flask. The HBSS-EDTA cell mixture was then diluted 1:20 in fresh DMEM for further passage or seeding into a 96F microtiter tray (Nunc). One hundred and sixty microlitres of the harvested Vero cells were inoculated into the wells to which antitoxin would be added and 180 μL of trypsinsed Vero cells were added to all other wells and incubated in 5% CO_2 at 37° C for 2 days or until Vero cell monolayers were confluent upon examination under an inverted microscope. The Vero cells were continuously passaged for the duration of each experiment (figure 2.3).

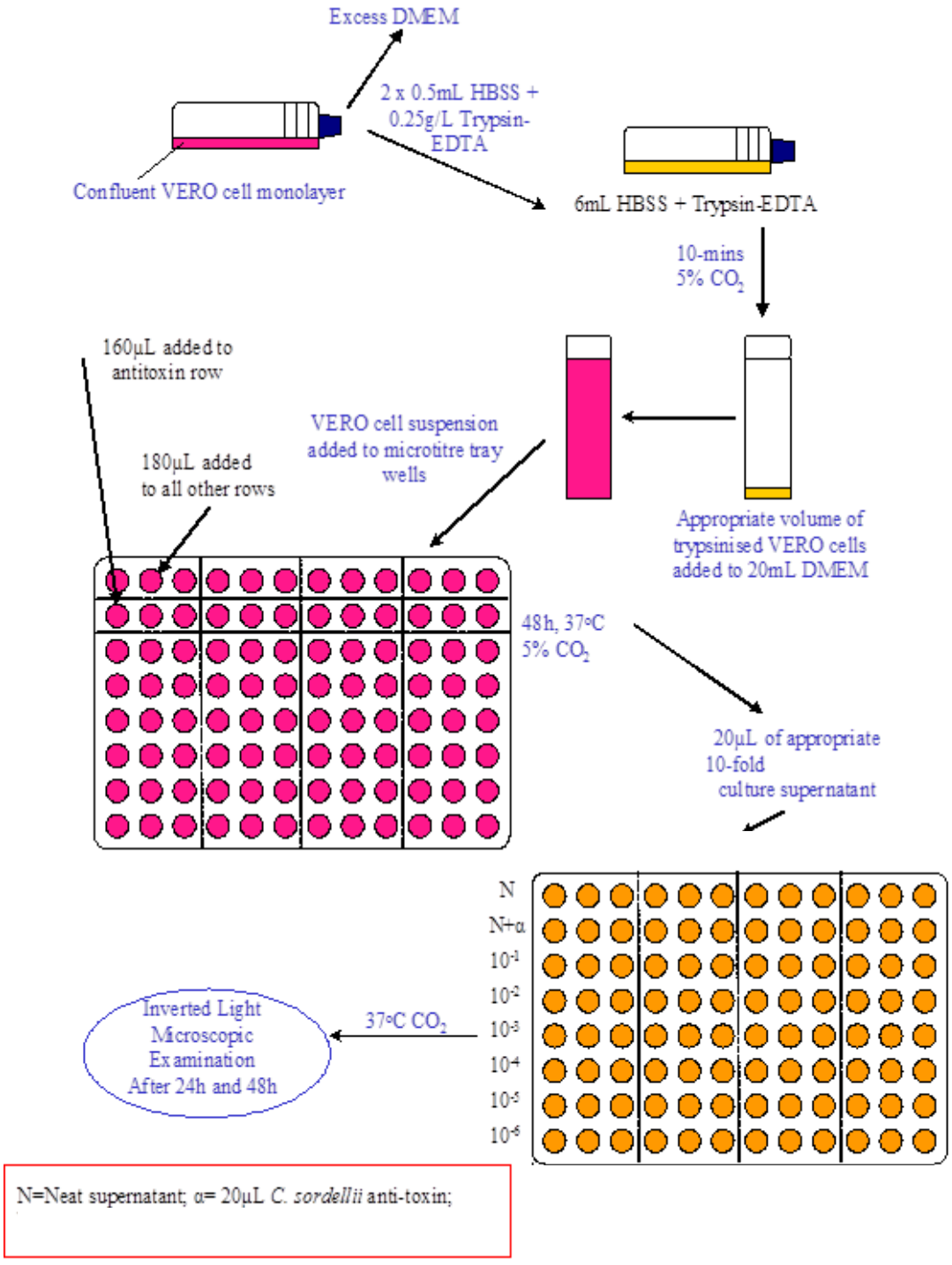

Figure 2.3: Vero cell cytotoxin assay.

One millilitre samples for toxin enumeration were centrifuged at 16000 *g* for 15 minutes and the supernatant stored at 4° C. Sample supernatant and positive cytotoxin controls (48 hour culture of *C. difficile* in Brain Heart Infusion broth (BHI) (Oxoid) were serially diluted 10-fold in sterile phosphate buffered saline (PBS-pH7) to 10^{-5}. Serial dilutions were aseptically transferred into microtiter trays containing Vero cell monolayers. Twenty microlitres of *C. sordellii* antitoxin (Prolab Diagnostics, Neston, UK) was used to neutralise any cytotoxic effect and ensure that cell rounding observed was specific to *C. difficile*. A sample was designated as positive if ~80% of the Vero cell monolayer was rounded (figure 2.4). A relative unit was used to quantify the level of cytotoxin present by assigning a titre to the sample based on the greatest dilution of which a positive cytotoxic effect was observed (*i.e.* if toxin was present in the neat only dilution this was assigned a titre of 1; if a positive cytotoxin effect was observed in the 10^{-1} dilution then it was assigned a titre of 2, *etc*.).

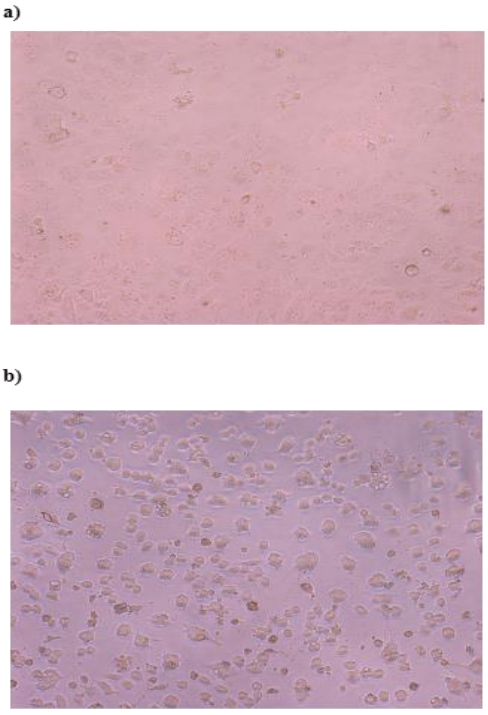

Figure 2.4: Vero cell monolayer a) intact monolayer, b) *C. difficile* cytotoxic effect.

2.5 Collection of Human Faecal Material

Faecal material was donated by at least 3 healthy elderly (>60 years) volunteers with no history of antimicrobial therapy for at least 2 months prior to donation. Samples were stored in sealed anaerobic zip lock bags (Becton Dickinson, Sparks, MD, USA) for no longer than 12 hours during transportation and transfer to an anaerobic cabinet.

2.6 Screening of Faecal Material

To ensure the absence of *C. difficile* populations within the faecal material, samples were plated directly onto CCEYL agar in duplicate and incubated anaerobically at 37° C for 48 hours. Faecal material from any donor testing positive for *C. difficile* was eliminated from the study.

2.7 Preparation of Faecal Emulsion

Faecal emulsion was prepared by suspending 10% w/v *C. difficile*-negative faeces in pre-reduced PBS (Sigma), and the suspension emulsified in a stomacher (Stomacher Lab-Blender 400, Borolabs, Aldermaston, UK) until a smooth slurry was formed. Any large material was removed by filtration through a sterile muslin cloth (Bigger Trading Limited, Watford, UK).

3.0 Batch Culture Experiments

3.1 Background

It is generally accepted within the *C. difficile* research community that the use of batch culture experiments for this organism has limited use due to the lack of reliable and consistent data. Batch culture experiments do not reflect the continuous removal and replacement of nutrients and waste products observed *in vivo.* Nutrient availability is known to affect the physiology of *C. difficile* and numerous studies have highlighted that results obtained using batch culture methods are inconsistent and sometimes contradictory to clinical observations[478,56, 57, 479,479], whilst other results demonstrated some similarity with observations *in vivo*[480, 481].

Borriello and Barclay[23] devised an *in vitro* batch culture model of colonisation resistance to *C. difficile,* demonstrating the inhibition of proliferation and toxin production in the presence of human faecal material. This inhibitory capacity was absent from heat or filter sterilised faecal emulsions, thus implicating the importance of an as yet unidentified component/s of the faecal microbiota in providing this resistance. This research also identified the varying degree of colonisation resistance. Faecal emulsions from healthy adult volunteers (age range 21-57 years) elicited a greater resistance to *C. difficile* germination and toxin production than the emulsions from geriatric volunteers (age range 71-92 years)[23].

Whilst it is important to consider these limitations, batch culture systems can still provide useful preliminary information, so these systems were used to investigate the ability of different *C. difficile* strains to form pure culture biofilms *in vitro.*

3.2 Materials and Methodology

3.2.1 Microtiter Tray Assay

3.2.1.1 Rationale

Microtiter tray assays are often used in biofilm research as they allow researchers to screen a large number of organisms/strains quickly and with ease. This format has been widely used in biofilm research to assess the biofilm forming capabilities of organisms such as *P. aeruginosa*, *Staphylococcus aureus*[482], *Listeria monocytogenes*[483] and *B. subtilis*[484] whilst *C. difficile* research using this method remains rudimentary[355,454, 455].

The microtiter tray model uses batch growth conditions, therefore potentially limiting the formation of mature biofilms, which require increased time frames for some organisms. However, it has provided researchers with valuable information regarding the initial stages of biofilm formation[485]. In addition, microtiter trays are commercially available in a variety of materials, allowing the investigation of substratum material on biofilm growth.

Our group hoped to identify strong biofilm forming *C. difficile* strains, allowing us to focus our research accordingly.

3.2.1.2 Organisms

An initial panel of 7 *C. difficile* clinical isolates were studied for their ability to adhere to inanimate surfaces (table 3.1). These *C. difficile* strains were chosen as a representative selection of UK epidemic ribotypes[205].
*S. aureus 8*325-4[486], a known biofilm-producing stain supplied courtesy of Dr Alex O'Neil, University of Leeds, UK and *Clostridium perfringens* ATCC 13124[346] served as positive controls.

3.2.1.3 Culture Media

Brain heart infusion broth (BHI), cooked meat medium (CM), Tryptic soy broth (TSB) were prepared according to the manufacturer's instructions.

All laboratory media were purchased from Oxoid, Basingstoke, UK and prepared according to the manufacturers' instructions unless otherwise stated.

3.2.1.4 Substrata

Polystyrene (Nunc), glass (Porvair, Leatherhead, UK) and polyethylene (Nunc) 96F-well microtiter trays were used in these assays.

3.2.1.5 Experimental Assay

C. difficile strains were cultured onto CCEYL and *C. perfringens* was cultured onto Columbia Blood Agar (FBA) and incubated anaerobically at 37° C for 48 hours. *S. aureus* was cultured onto FBA and incubated aerobically at 37° C for 24 hours.

A 0.5 McFarland suspension (approximately $1.5x10^8$ cfu/mL) of each strain was prepared in each growth medium and incubated anaerobically at 37° C overnight. The overnight culture was diluted 1:10 in pre-reduced growth medium within the microtiter tray. Two wells of each tray were inoculated with growth medium only and served as a negative control.
*S. aureus 8*325-4 and *C. perfringens* served as positive controls. Each assay was performed in duplicate using the same bacterial cultures and growth conditions and the plates were placed in a plastic box containing air holes and a moist paper towel and incubated anaerobically at 37° C for 24 or 48 hours.

Contents from each well were discarded and wells washed three times with sterile PBS (Sigma) before 200 μL of crystal violet solution (0.1% w/v) was added into each well and allowed to stand for 15-20mins. Excess stain was discarded and wells washed three times with sterile water before 200 μL of ethanol (96%) (VWR) was added to solubilise the stain bound to adherent cells.

The optical density (OD) of the contents of each well was determined at 570 nm using a microplate spectrophotometer (Spectra Max 250, Molecular Devices). Positive biofilm growth was classified as an OD of three standard deviations above the mean for the negative control.

PCR ribotype	Isolate designation	Isolate origin
027	SM	Outbreak of CDI Stoke-Mandeville Hospital, 2005
027	210	Outbreak at Maine Medical Centre, Portland, MA, 2005
106	36/64	Clinical isolate from LGI
078	BM	Clinical isolate from Beaumont Hospital, Ireland
001	P24	Clinical isolate from LGI
153	153	Clinical isolate
010	E4	Non-toxigenic strain isolated from LGI

Table 3.1: List of *C. difficile* isolates used in the microtiter tray assay. (LGI; Leeds General Infirmary).

3.2.2 Mucin Alginate Batch Culture Experiments

3.2.2.1 Rationale

Microtiter tray experiments provide information regarding the ability of organisms to adhere to inanimate surfaces, but conditions *in vivo* will provide a vastly different environment. The colon is covered in a layer of mucus which provides the epithelial cells with a protective barrier from the harsh conditions of the intestinal lumen[312]. In order to provide a more realistic substratum material, mucin alginate (MA) beads were used in a batch culture system to investigate the ability of *C. difficile* to form pure culture biofilms on a biotic surface. Gibson *et al* previously utilised MA beads to provide a framework for complex intestinal microbiota biofilms *in vitro*[447].

3.2.2.2 *C. difficile* Strains

Four *C. difficile* strains associated with human infection (027 (210), 106 (36/64), 078 (BM) and 001 (P24)), which are epidemiologically representative of prevalent strains in the UK were selected for this study (table 3.1).

3.2.2.3 Culture Media

BHI (Oxoid) and saline (Sigma) were prepared according to the manufacturer's instructions. Biofilm gut model growth medium (Appendix A1) was prepared as described by Gibson *et al*[447].

3.2.2.4 Mucin-Alginate Bead Preparation

MA beads were produced based on the method described by Probert and Gibson[447]. Hog gastric mucin (2 % w/v: Sigma) and sodium alginate (2 %

w/v: Sigma) were added to warm sterile water, stirring continuously until a smooth paste was formed. The MA mixture was fed into peristaltic pump through E1000 tubing (Fisher Scientific, Loughborough, UK) which was suspended from a height of approximately 40 cm and allowed to fall into stirred, 0.3 M $CaCl_2$ (Sigma), to give each bead a mean diameter of 2.9 mm. The beads were allowed to cure overnight and stored at 4° C. MA bead preparation was carried out within a sheltered structure where possible to reduce the likelihood of environmental contamination.

3.2.2.5 Experimental Assay

Fifty percent (w/v) MA beads were added to each culture medium and inoculated with 300 μL of *C. difficile* spore suspension (section 2.3). Cultures were incubated anaerobically at 37° C for 72 hours.

3.2.2.6 Sampling of Planktonic Bacteria

Planktonic bacteria were sampled immediately upon addition of MA beads and *C. difficile* spores to the media and then daily for 3 days.
Approximately 5 mL of culture media and beads were removed for analysis. MA beads were isolated for bead-associated analysis (section 3.2.2.7). The planktonic culture fluid was inoculated in triplicate onto CCEYL and *C. difficile* spores and TVCs enumerated as described in sections 2.1 and 2.2. Viable counts were expressed as $\log_{10}$cfu/mL.

3.2.2.7 Sampling of Bead-Associated Bacteria

MA beads were transferred to pre-weighed tubes and the weight of beads determined. Beads were re-suspended in 5 mL pre-reduced peptone water, gently agitated to remove loosely adherent bacteria, and peptone water

discarded. Two millilitres of 0.001% (w/v) cetyltrimethlyammonium bromide (CTAB)[447], diluted in sterile water, was added to the beads to dissociate adherent bacterial cells and shaken intermittently for 30 mins. The CTAB and bead-associated mixture was serially diluted 10-fold under anaerobic conditions in pre-reduced peptone water to 10^{-7} and the bead-associated culture inoculated in triplicate onto CCEYL and *C. difficile* spores and TVCs enumerated as described in sections 2.1 and 2.2. Viable counts were expressed as $\log_{10}$cfu/g of beads.

3.2.3 CTAB Inhibition Assay

3.2.3.1 Rationale

CTAB is a cationic surfactant which can be utilised to dissociate bacteria from MA beads as described by Probert and Gibson[447]. Salton *et al*[487] highlighted potential bactericidal properties of CTAB. Therefore it was necessary to determine the effect of CTAB exposure on faecal and *C. difficile* populations.

3.2.3.2 Organisms

C. difficile strain 027 (210) (table 3.1) was used for this study.

3.2.3.3 Preparation of Faecal Emulsion

A 10% faecal emulsion was prepared from faecal samples donated from healthy adult volunteers as described in sections 2.5-2.7.

3.2.3.4 Experimental Assay

One millilitre of an overnight Schaedler's broth culture (Oxoid) of *C. difficile* PCR ribotype 027 (210) (~ 10^8 cfu/mL) was inoculated into the 10% faecal

emulsion. Two *C. difficile*-positive faecal emulsion samples were centrifuged at 16000 *g* for 5 mins before being transferred to anaerobic conditions. The supernatants were discarded. One pellet was re-suspended in 2 mL of pre-reduced 0.001% CTAB and the other pellet was re-suspended in 2 mL pre-reduced sterile water. Bacterial populations were enumerated 30 mins, 120 mins and 240 mins after exposure to CTAB using the selective and non-selective agars as described in sections 2.1 and 2.2. The faecal suspension was enumerated and used as a non-CTAB exposed control.

3.2.4 Mucin Degradation Assay

3.2.4.1 Rationale

Certain bacteria are able to utilise mucin as a source of nutrition when substrate availability is low (such as in the distal colon). The exposure of MA beads within a model of the human gut resulted in the gradual degradation of these beads (see chapter 5.0). An assay was designed to establish the source of this degradation. A minimal growth medium was used so that the glycoproteins present represented the only major carbon source available for bacterial growth.

3.2.4.2 Organisms

Indigenous gut microbiota strains evaluated were: *Lactobacillus plantarum, Bacteroides thetaiotaomicron, Bifidobacterium adolescentis, Clostridium innocuum, Enterococcus faecium, Proteus mirabilis, Klebsiella oxytoca* and *C. difficile* PCR ribotype 027 (210) (table 3.1). All bacterial strains (except *C. difficile*) were isolated from the human gut model, providing a mixture of Gram positive, obligate and facultative anaerobes, and were identified using 16S-rRNA PCR.

3.2.4.3 Culture Medium

Mucin or MA (0.5% w/v) with or without 1% glucose (w/v) was incorporated into minimal growth medium B consisting of tryptone (Oxoid, 7.5 g/L); casitone (Beckton Dickinson, 7.5 g/L); yeast extract (Oxoid, 3.0 g/L); meat extract (Fluka, 5.0 g/L); NaCl (Sigma, 5.0 g/L); $K_2HPO_4.3H_2O$ (AnalR, 3.0 g/L); KH_2PO_4 (AnalR, 0.5 g/L); $MgSO_4.7H_2O$ (Sigma, 0.5 g/L); cysteine HCl (Sigma, 0.5 g/L); resazurin (Sigma, 0.002 g/L); D-(+)-glucose (Sigma, 10 g/L); porcine gastric mucin (type III) (Sigma), 5; agar technical number 3 (Oxoid), 15. The media was adjusted to pH 7.2±0.2 with 2M NaOH[488, 489].

Molten medium B, with or without glucose (1% w/v) was poured into Petri dishes and allowed to set.

3.2.4.4 Experimental Assay

A 0.5 McFarland suspension (~ 10^8 cfu/mL) of each bacterial isolate was prepared in fastidious anaerobe broth (BioConnections, Leeds, UK) and incubated, anaerobically overnight at 37° C, except for *E. faecium*, *K. oxytoca* and *P. mirabilis* which were incubated aerobically. A 10% (w/v) faecal emulsion prepared from a healthy adult volunteer, as described in sections 2.5-2.7 was used as a positive control. The same faecal emulsion was autoclaved and used as a negative control. Agar plates were dried prior to inoculation. Bacterial species were inoculated onto the surface of the agar using a multipoint inoculator to achieve a final inoculum of 10^4 cfu/spot. All agars were then incubated anaerobically at 37° C for 72 hours. Agar plates were subsequently stained with 0.1% amido black (Sigma), dissolved in 3.5M acetic acid for 30 min, and then washed with 1.2M acetic acid. The formation of a mucinolytic zone around the colony was measured using callipers accurate to 0.1mm. This method was modified from that of Zhou *et al*[490].

3.2.5 Adherence Assay

3.2.5.1 Rationale

The unbound/planktonic indigenous gut microbiota populations were monitored in this experiment so that the inverse binding relationship could be used in order to estimate the levels of adherence of bacteria to different bead materials. Rather than directly enumerating adherent populations, decreases in planktonic populations can be used to reflect the transition from planktonic to bead-adherent states. Total planktonic populations of bacterial groups at t = 0 mins were enumerated and recorded as 100% of the faecal emulsion populations. The relative decrease in this baseline population could be calculated when exposed to MA or glass beads over time. A greater decrease in percentage of faecal baseline population would indicate a greater number of bacteria which were bound to the beads, rather than remaining in the enumerated planktonic form.

3.2.5.2 Organisms

C. difficile strain 027 (210) (table 3.1) was used for this study.

3.2.5.3 Experimental Assay

A 10 % faecal emulsion was prepared as described previously (sections 2.5-2.7). Fifty percent (w/v) MA (section 3.2.2.4) and glass beads (2 mm diameter) (VWR) were added to separate 30 mL faecal emulsions along with 200 μL of an overnight Schaedler's broth culture of *C. difficile* (~ 10^8 cfu/mL). Planktonic samples were taken at time (t) = 0 (faecal emulsion prior to exposure to beads as a control), 1, 2, 4, 24 and 48 hours after the addition of the beads. Planktonic bacterial populations were enumerated as described previously (sections 2.1 and 2.2). The bacterial counts were converted to a percentage of the t = 0 mins control and plotted

against time. All experimental procedures were carried out anaerobically at 37° C.

3.2.6 Biofilm Removal Assay

3.2.6.1 Rationale

One of first stages of biofilm formation is the irreversible attachment of bacteria to a substratum material. Once a bacterium has committed itself to attachment to a surface and begun the process of biofilm formation its subsequent removal may be difficult. In order to enumerate the bacterial populations associated with surfaces accurately it is necessary to remove adherent bacteria.

One of the greatest problems facing clinicians and industrial workers is the effective removal of these biofilm structures. Numerous techniques and technologies have been utilised to maximise the removal of the adherent bacteria, although many require direct interaction with the site which can be problematic. Various techniques to remove the biofilms in research settings include sonication[491], vortexing[492], disinfectants[493], scraping[494] and shaking with beads[493]. Not all of these methods are suitable for this study as bacterial removal need to be non-destructive of the substratum material and allow the subsequent enumeration of adherent bacterial populations. Three techniques (CTAB, sonication and vortexing) were selected for this assay due to their ease of use and non-destructive nature and are described below.

3.2.6.2 Organisms

C. difficile strain 027 (210) (table 3.1) was used for this study.

3.2.6.3 Experimental Assay

Fifty percent (w/v) glass or MA beads (section 3.2.2.4) were added to 3 x 20 mL BHI broths and inoculated with 100 μL of an overnight Schaedler's broth culture of *C. difficile* (~ 10^8 cfu/mL). After 24 hours, culture medium was removed and discarded, and the beads re-suspended in 5 mL pre-reduced peptone water to remove loosely adherent bacteria. One set of each bead type was either re-suspended in 20 mL pre-reduced 0.001% CTAB and shaken for 30 mins; re-suspended in 20 mL pre-reduced saline and placed into a sonicating water bath for 30 mins; or re-suspended in 20 mL pre-reduced saline and vortexed intermittently for 30 mins.

From this point on the samples were treated the same and sessile *C. difficile* populations were enumerated as previously described (sections 2.1 and 2.2).

Positive bacterial adherence in each growth medium was defined as an OD_{570} value of 3 standard deviations above the mean for the negative control. This value was subtracted from each adherence assay absorbance reading and displayed in figures 3.3.1a and 3.3.1b.

3.3 Results

3.3.1 Microtiter Tray Assay

A microtiter tray format was used to screen seven *C. difficile* clinical isolates for their ability to adhere to inanimate surfaces.

Growth medium choice and incubation time appeared to affect the adherence of *C. difficile* to inanimate surfaces. Substratum material did not provide any affect on biofilm formation, therefore only polystyrene results are presented here. In general, BHI elicited the greatest level of bacterial adherence, with maximum absorbance readings amongst *C. difficile* isolates 300% greater when grown in BHI compared with the minimum absorbance value for that strain. CM elicited only minimal adherence by most strains. Adherence was substantially decreased after 48 hours incubation compared with 24 hours incubation. Maximal adherence was observed for *S. aureus* in BHI incubated for 24 hours. Amongst strains of *C. difficile,* PCR ribotype 078 exhibited the greatest level of adherence when grown in BHI for 24 hours, with maximum absorbance values 17.7 % greater than other strains. All *C. difficile* and positive control strains were deemed to provide positive biofilm growth when grown in CM and TSB for 24 hours. All *C. difficile* strains (with the exception of P24) and positive control strains produced positive biofilm growth when grown in BHI for 24 hours. Biofilm growth appeared more variable with greater standard error values after 24 hour incubation compared with 48 hour growth.

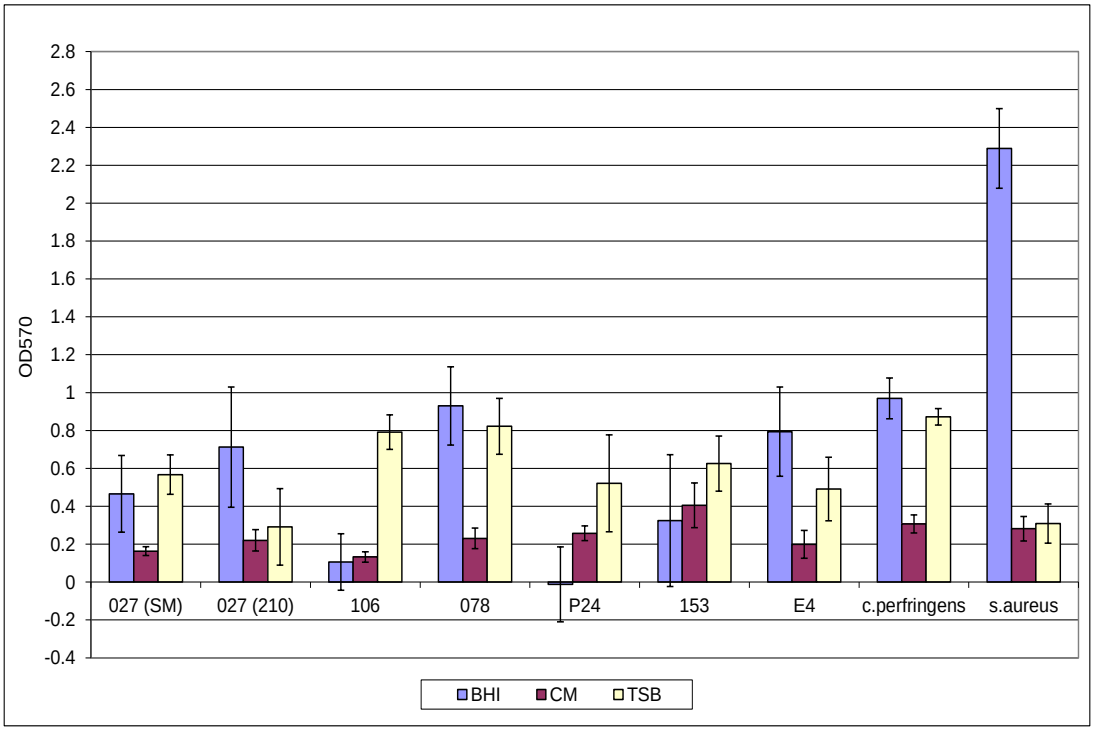

Figure 3.3.1a:

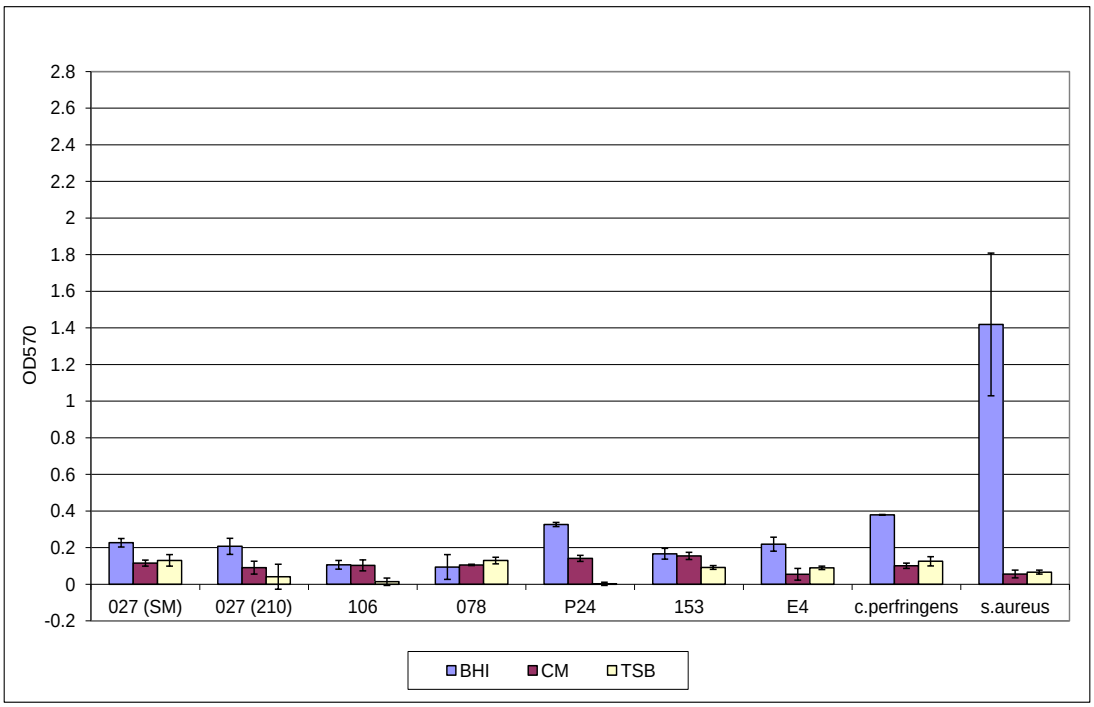

Figure 3.3.1b: Absorbance values at 570 nm (±SE) of adherence by a panel of *C. difficile* isolates to polystyrene microtiter trays when incubated in different growth media for 24 (figure 3.3.1a) and 48 (figure 3.3.1b) hours. (BHI, brain heart infusion; CM, cooked meat medium; TSB, tryptic soy broth).

3.3.2 Mucin Alginate Batch Culture Assay

Incubation of *C. difficile* PCR ribotype 106, 078, 001 and 027 spores in biofilm gut model growth medium elicited spore germination and vegetative cell proliferation, detected within the planktonic culture fluid within 1-2 days, whilst spore populations decreased to around the limit of detection (LOD) for the remainder of the experiment (figures 3.3.2.1-3.3.2.2; appendix D1 an D2). Due to the low levels of spores present in this medium the association of spores with the MA beads could not be analysed. Vegetative *C. difficile* populations associated with MA beads reached populations of ~3 $\log_{10}$cfu/g beads for PCR ribotypes 106, 078 and 027. There was no bead-associated *C. difficile* detected for PCR ribotype 001 in biofilm gut model growth medium.

When *C. difficile* PCR ribotype 106, 078, 027 and 001 spores were exposed to MA beads in BHI broth, TVC of *C. difficile* detected within the planktonic culture fluid were up to ~2.5 $\log_{10}$cfu/mL greater than spore counts, indicating that germination and proliferation had occurred, but the majority of the *C. difficile* population remained as spores. Bead attachment occurred at levels of ~2-5 $\log_{10}$cfu/g and comprised predominantly spores (figures 3.3.2.3-3.3.2.4; appendix D3 and D4).

C. difficile PCR ribotype 001, 106, 078 and 027 spores incubated in saline remained quiescent for the duration of the experiment (figures 3.3.2.5-3.3.2.6; appendix D5 and D6). *C. difficile* spore association with MA beads was present at a population of ~3-5 $\log_{10}$cfu/g.

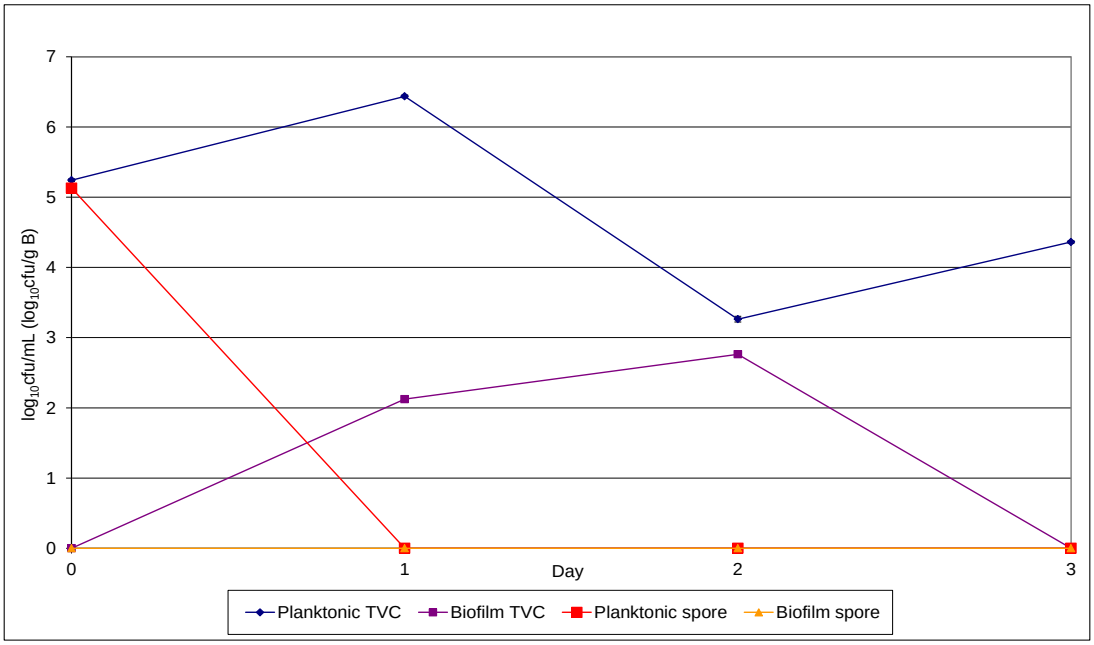

Figure 3.3.2.1: Mean populations (±SE) of *C. difficile* PCR ribotype 027 (210) in planktonic (log_{10}cfu/mL) and biofilm (log_{10}cfu/g) form when grown in biofilm gut model growth medium. (TVC, total viable counts; limit of detection (LOD, ~ 2 log_{10}cfu/g, ~ 1.5 log_{10}cfu/mL).

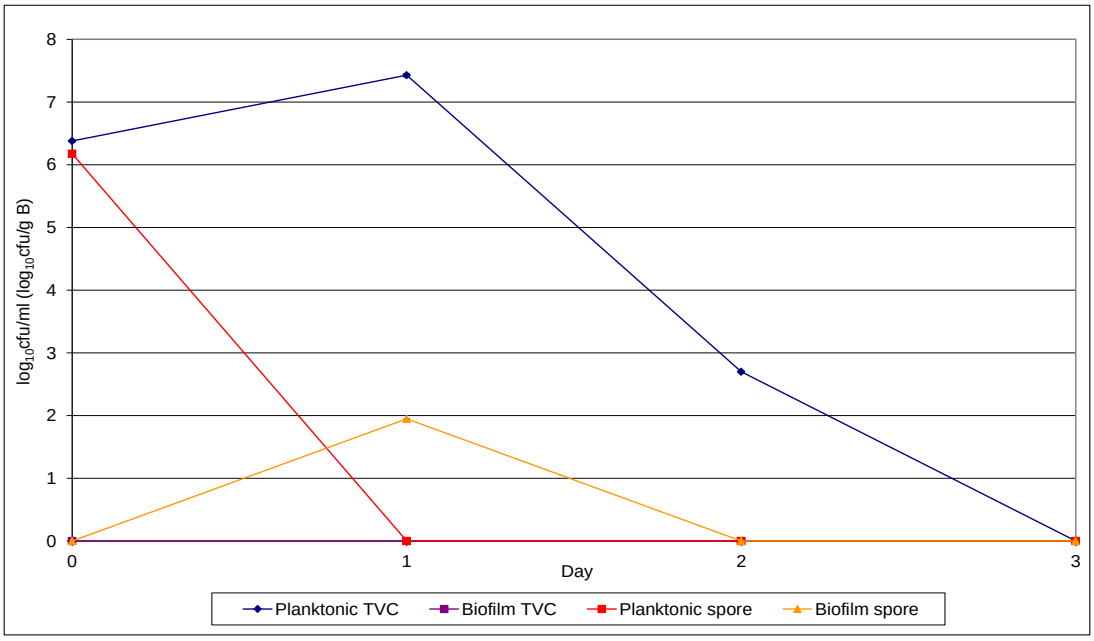

Figure 3.3.2.2: Mean populations (±SE) of *C. difficile* PCR ribotype 001 (P24) in planktonic (log_{10}cfu/mL) and biofilm (log_{10}cfu/g) form when grown in biofilm gut model growth medium. (TVC, total viable counts; LOD, ~ 2 log_{10}cfu/g, ~ 1.5 log_{10}cfu/mL).

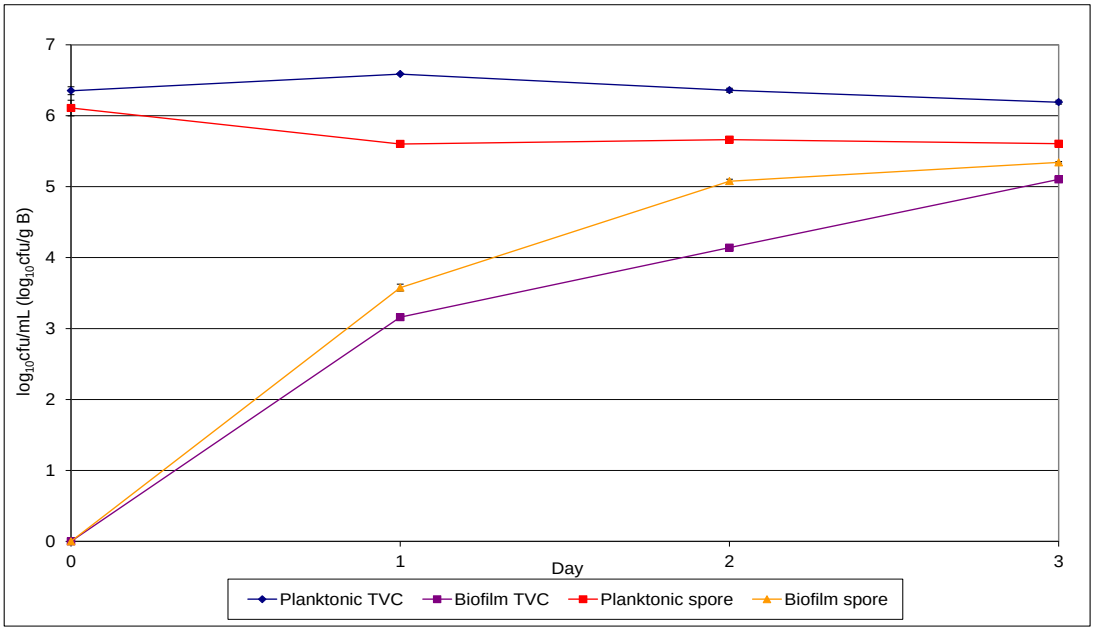

Figure 3.3.2.3: Mean populations (±SE) of *C. difficile* PCR ribotype 027 (210) in planktonic (log_{10}cfu/mL) and biofilm (log_{10}cfu/g) form when grown in brain heart infusion broth. (TVC, total viable counts; LOD, ~ 2 log_{10}cfu/g, ~ 1.5 log_{10}cfu/mL).

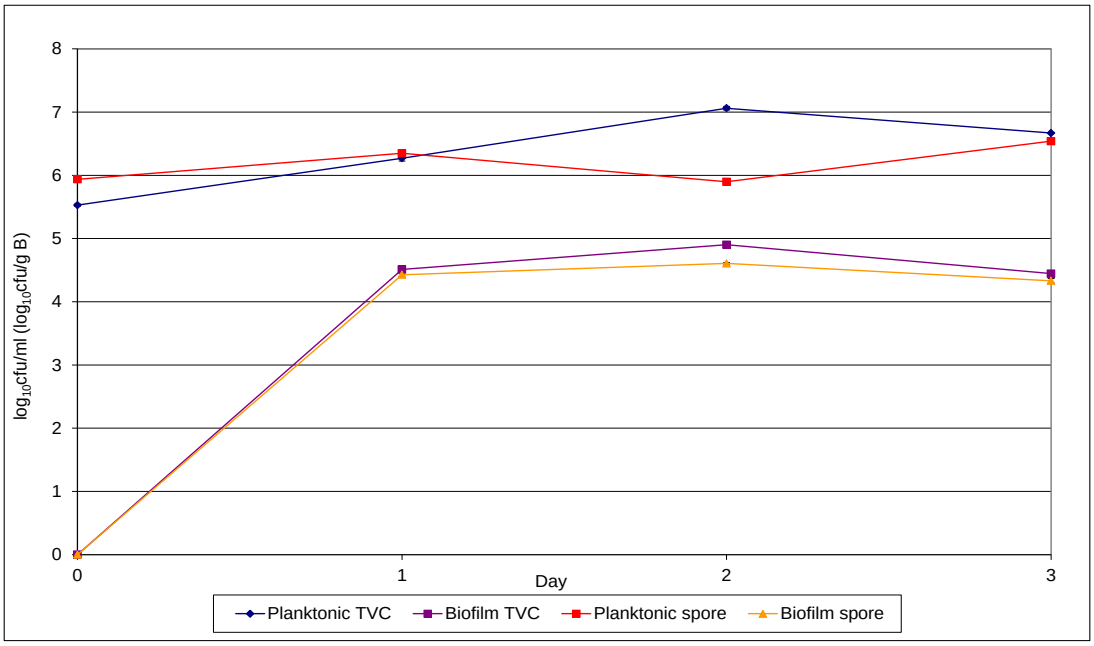

Figure 3.3.2.4: Mean populations (±SE) of *C. difficile* PCR ribotype 001 (P24) in planktonic (log_{10}cfu/mL) and biofilm (log_{10}cfu/g) form when grown in brain heart infusion broth. (TVC, total viable counts; LOD, ~ 2 log_{10}cfu/g, ~ 1.5 log_{10}cfu/mL).

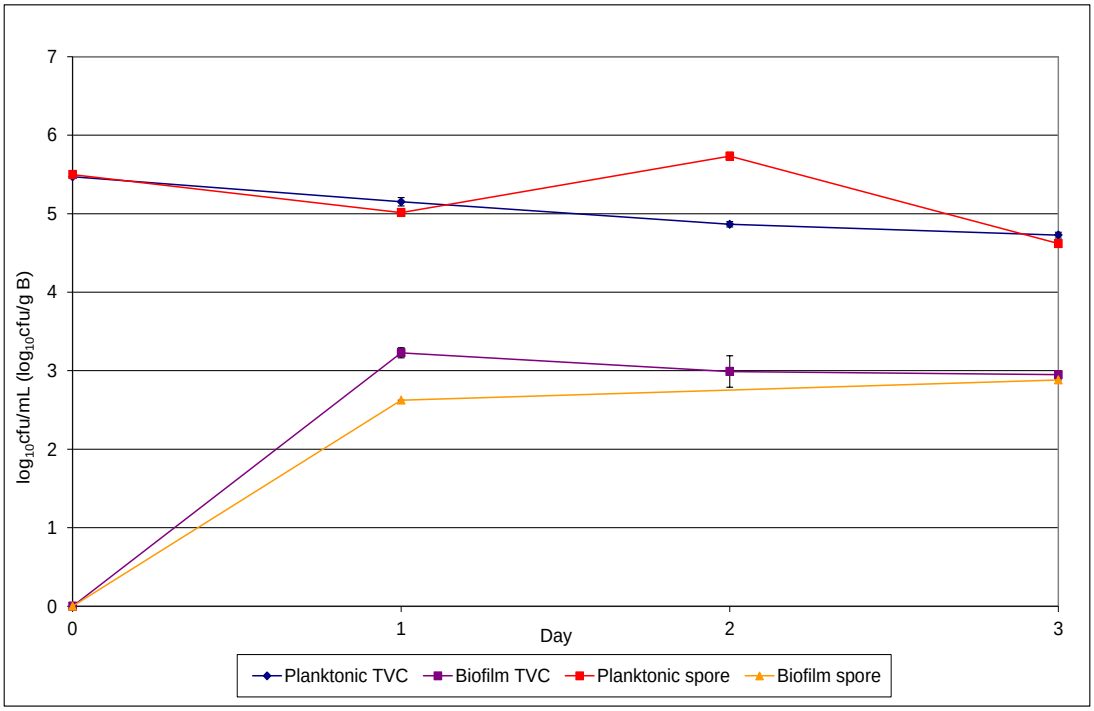

Figure 3.3.2.5: Mean populations (±SE) of *C. difficile* PCR ribotype 027 (210) in planktonic (log_{10}cfu/mL) and biofilm (log_{10}cfu/g) form when grown in saline. (TVC, total viable counts; LOD, ~ 2 log_{10}cfu/g, ~ 1.5 log_{10}cfu/mL).

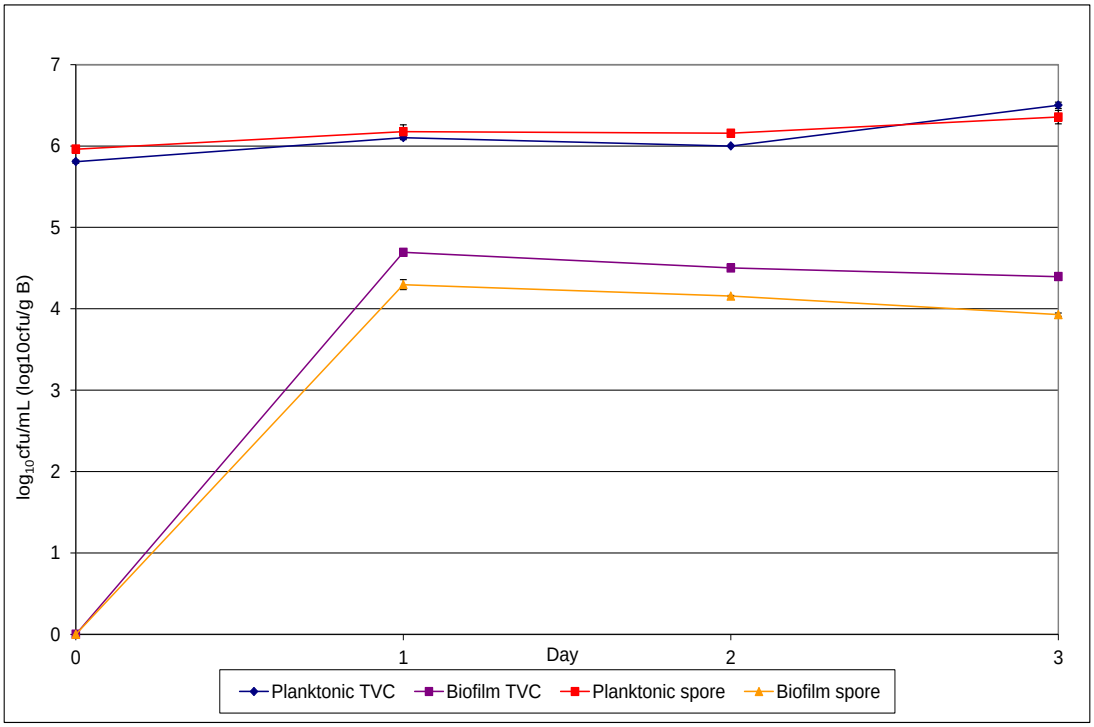

Figure 3.3.2.6: Mean populations (±SE) of *C. difficile* PCR ribotype 001 (P24) in planktonic (log_{10}cfu/mL) and biofilm (log_{10}cfu/g) form when grown in saline. (TVC, total viable counts; LOD, ~ 2 log_{10}cfu/g, ~ 1.5 log_{10}cfu/mL).

3.3.3 CTAB Inhibition Assay

CTAB (0.001%) did not have a deleterious effect on the indigenous gut microbiota analysed in this study after exposure for 240 mins (figure 3.3.3.1).

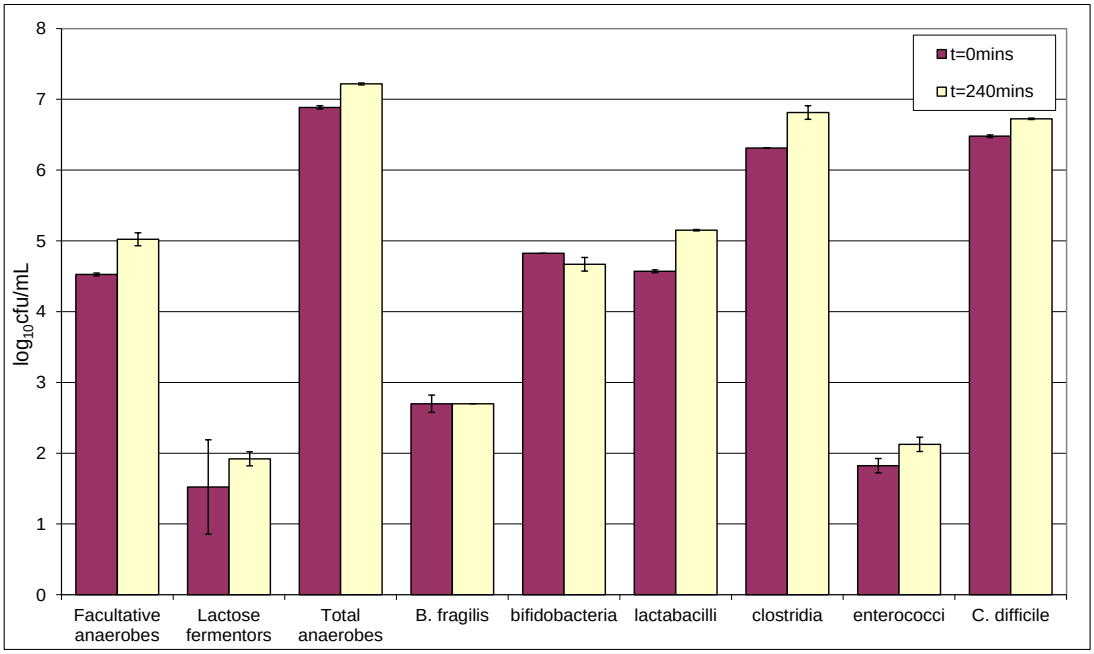

Figure 3.3.3.1: Mean (±SE) populations (log_{10}cfu/mL) of members of indigenous gut microbiota after 0 (no exposure) and 240 minutes of exposure to 0.001% CTAB.

3.3.4 Mucin Degradation Assay

Faecal emulsion inoculation onto mucin and MA-containing medium B agar elicited the formation of a mucinolytic halo around inoculation spots. The asymmetrical shape of the mucinolytic halo made accurate measurement difficult; therefore maximum halo sizes were estimated. Approximate zone sizes on mucin-containing agar were larger than on MA-containing agar. The heat-inactivated faecal emulsion and all other test strains produced no mucinolytic halo on any agar. When 1% glucose was incorporated into the agar, faecal emulsion produced a small, weak mucinolytic halo on 33.3% of technical replicates on mucin agar, and 16% of technical replicates on MA agar.

3.3.5 Adherence Assay

At early stages of incubation (up to 4 hours), less than 10% of all viable bacterial populations were associated with MA beads.

After 48 hours, *Enterococcus* spp., *C. difficile*, *Lactobacillus* spp. and lactose-fermenting Enterobacteriaceae bound readily to MA beads. Less than half (~30-55%) of bacterial populations remained in planktonic form (figure 3.3.5.1), indicating that ~45-70% of bacteria were adherent to the beads. However, even at 48 hours there was no increase in the percentage of viable *Clostridium* spp., *Bacteroides* spp. and *Bifidobacterium* spp. bound to the MA beads.

Indigenous gut microbiota bound to glass beads less readily than to MA beads; only *C. difficile* and *Lactobacillus* spp. were bound to glass beads at greater than 10% of the population after 48 hours (figure 3.3.5.2).

3.3.6 Biofilm Removal Assay

C. difficile bound to MA beads more readily than glass beads, with the number of vegetative cells recovered from MA beads using CTAB, vortex and sonication methods 1.2-, 2.9- and 2.2-$\log_{10}$cfu/g greater than glass beads respectively (figures 3.3.6.1 and 3.3.6.2). The vortex removal method provided 11.5-20.1% greater biofilm retrieval for both vegetative cells and spores from each bead type. Sonication provided the second greatest biofilm retrieval and CTAB the least. Spores were not removed from glass beads using the sonication method (figure 3.3.6.2). If the LOD (~1.5 $\log_{10}$cfu/g) for this assay is considered then it is evident that *C. difficile* spore populations for other methods are at LOD.

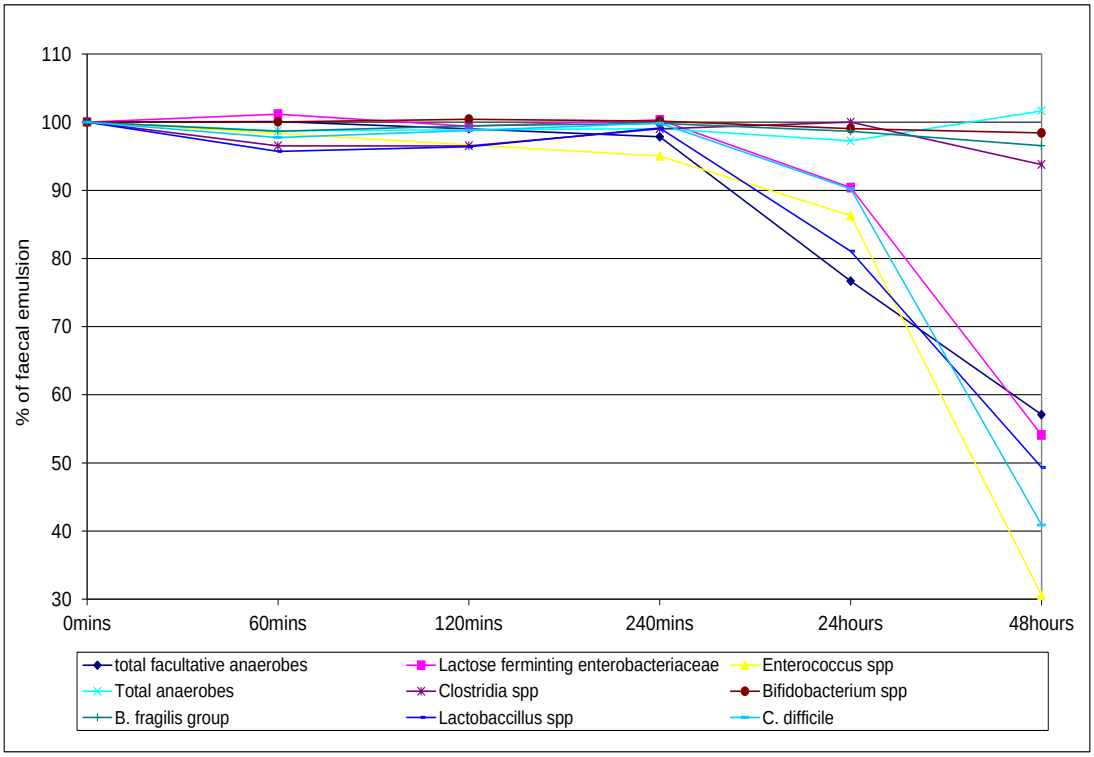

Figure 3.3.5.1: Populations of indigenous gut microbiota in planktonic form when exposed to mucin alginate beads.

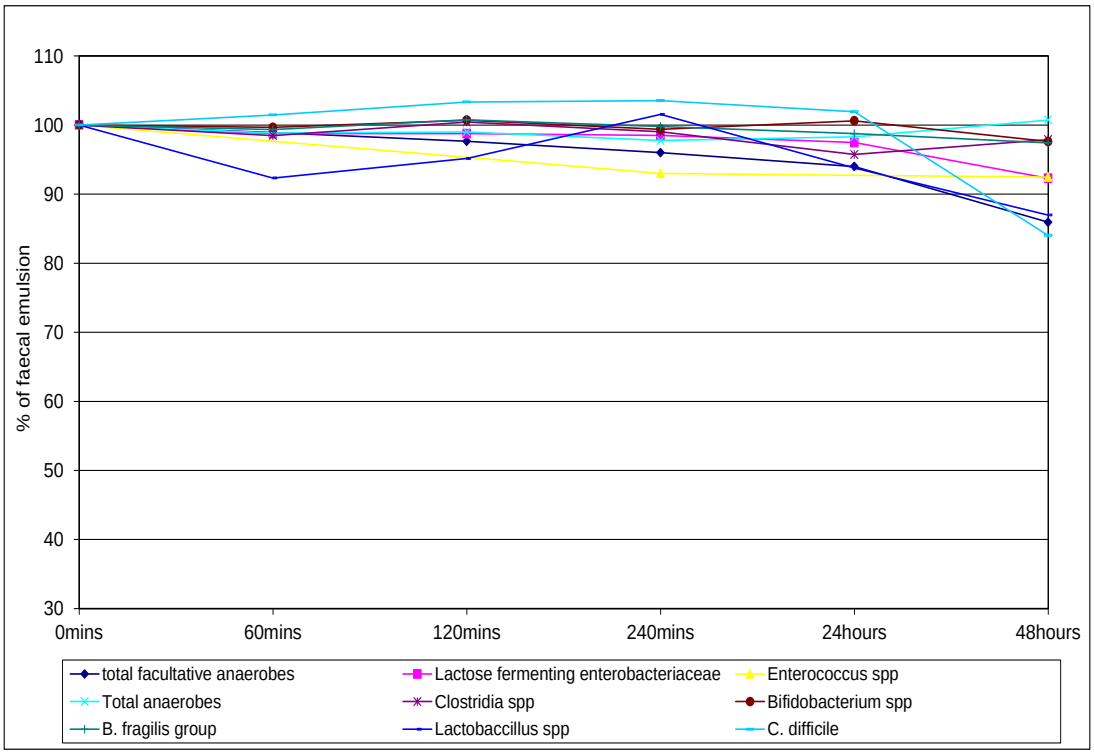

Figure 3.3.5.2: Populations of indigenous gut microbiota in planktonic form when exposed to glass beads.

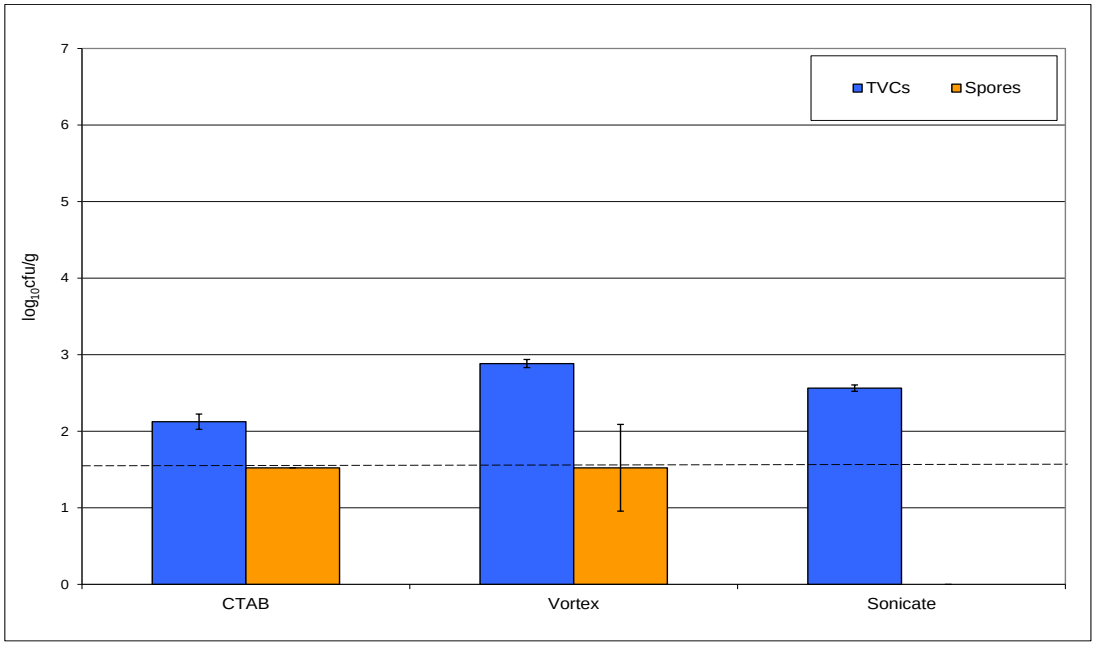

Figure 3.3.6.1: Mean populations (log_{10}cfu/g) (±SE) of *C. difficile* total viable counts (TVCs) and spores recovered from glass beads using three different biofilm removal techniques. Dotted line represents the approximate limit of detection for this assay.

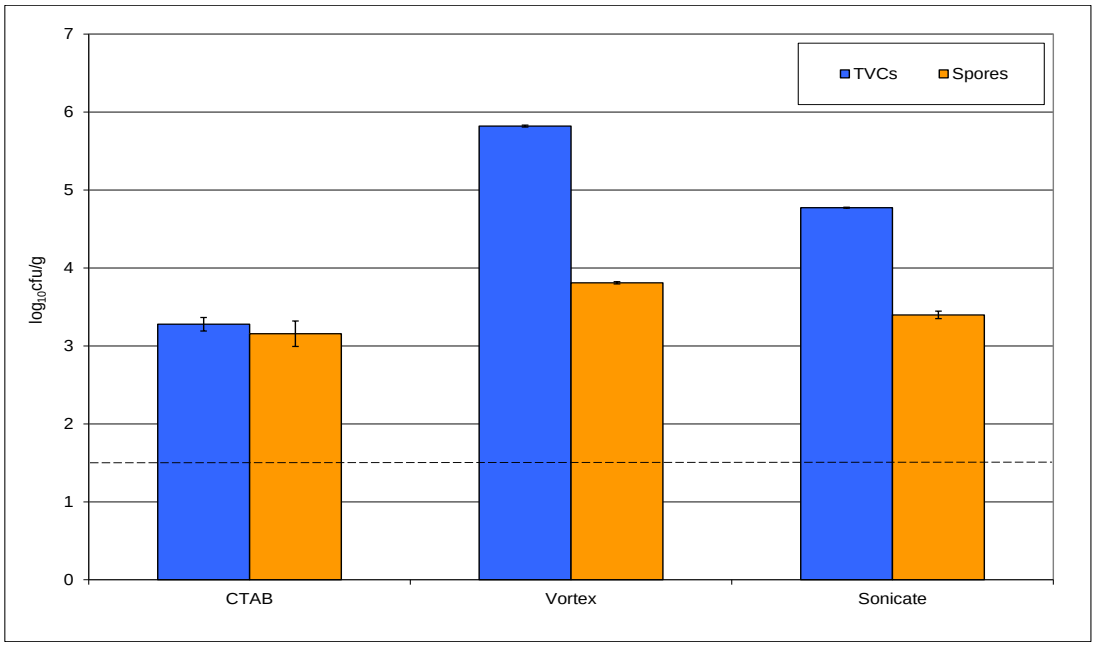

Figure 3.3.6.2: Mean populations (log_{10}cfu/g) (±SE) of *C. difficile* total viable counts (TVCs) and spores recovered from mucin-alginate beads using three different biofilm removal techniques. The dotted line represents the approximate limit of detection for this assay.

3.4 Discussion

Whilst the possible sequestration of *C. difficile* within biofilm structures in the human colon has been hypothesised to be associated with recurrent CDI, there has been a paucity of research investigating this hypothesis. Studies examining *C. difficile* pure culture biofilms were recently reported (*i.e.* since the onset of the present PhD studies)[355, 454, 455], yet our understanding of the existence and behaviour of these biofilms both *in vitro* and *in vivo* remains elementary.

In the present study results obtained when growing pure culture *C. difficile* biofilms in microtiter trays were inconsistent, with large variations in absorbance values between biological replicates. Attempts to increase consistency by investigating other growth media and substratum materials were unsuccessful. Even though the results presented here demonstrate that pure culture *C. difficile* biofilm biomass is largely inconsistent, positive results were obtained. This study also provides evidence that *C. difficile* adherence within microtiter trays decreases from 24 to 48 hours. This increased incubation time may elicit increased yield of *C. difficile* cultures, although increased adherence was not evident. This may be due to increased levels of sporulation after increased time frames. *C. difficile* spores may display a reduced ability to adhere to microtiter trays than their vegetative counterparts, possibly due to reduced expression of surface adhesins.

The use of microtiter trays to assay the adherence of *C. difficile* to inanimate surfaces has been carried out by a number of research groups[455,355, 454]. *C. difficile* pure culture biofilms were measured as moderately adherent whilst strains of other *Clostridium* spp. and anaerobic bacteria were measured as strongly adherent in a microtiter tray assay[355]. *Finegoldia magna* strain FmBs21 produced a thick, dense biofilm. When this strain was grown

in the presence of *C. difficile* they formed a homogenous biofilm with a dense and thick appearance which appeared visually distinct (visualized using scanning electron microscopy) from that of the *F. magna* biofilm alone; whilst only a thin, sparse biofilm was produced when *C. difficile* was grown as a monospecies biofilm. The authors postulated that either *C. difficile* when grown in close proximity to *Finegoldia magna* developed the ability to form thick, mature biofilms; or that *C. difficile* can co-exist within a mature biofilm produced by another bacterial species. Either theory has strong implications for the existence of *C. difficile* in complex biofilm communities within the gastrointestinal tract and provides evidence that *C. difficile* may have the ability to exist within mature biofilms *in vivo.*

Dawson *et al* encountered similar difficulties when growing pure culture *C. difficile* biofilms in microtiter trays (L. Dawson, personal communication). Greater success was achieved when growing *C. difficile* biofilms in larger vessel sizes[455]. A biofilm can be defined as a consortium of bacteria adherent to a substratum material or other bacterial cells and encased in a self-produced extracellular matrix. These results only provide evidence of the ability of *C. difficile* to adhere to inanimate surfaces *in vitro*, the existence of extracellular matrix and a true biofilm mode of growth has not been explored in these preliminary experiments.

Ethapa *et al* utilised 24-well microtiter plates, describing the medium-dependent nature of *C. difficile* pure culture biofilm formation, with glucose promoting biofilm formation in strain 630, but not R20291[454]. In addition, maximal biofilm formation of strains 630 and R20921 was evident after five and one day's incubation, respectively.

Whilst the data presented here and from other groups provides strong evidence that *C. difficile* is able to adhere to inanimate surfaces, there is

uncertainty as to whether or not a mature biofilm, encased in extra cellular material is produced.

Dawson *et al* visualised EPS matrix providing a scaffold for 3-day-old pure culture *C. difficile* biofilms[455] and Ethapa *et al*[454] utilised multiple staining procedures to identify the presence of a complex biofilm matrix comprising bacterial proteins, DNA and surface polysaccharides. However, Donelli *et al* observed a thin, sparse monolayer of adherent *C. difficile* cells after 48 hour incubation, although co-culture of *C. difficile* with *F. magna* elicited increased levels of EPS production[355]. The production of this extracellular material is a definitive feature of a biofilm and may be responsible for the unique characteristics associated with sessile communities. However, evidence suggests that when *C. difficile* is grown in the presence of other biofilm producers or for increased periods, it can exist within this protected environment, and may develop into the sessile mode of growth which provides further survival advantages.

The inanimate surfaces investigated in the microtiter tray experiments are not structurally or biologically representative of the human gastrointestinal tract. Therefore, other biofilm models with greater biological significance were explored.

Hog porcine gastric mucin is structurally similar to human epithelial mucin therefore this was combined with alginate to provide a framework for the beads[304], which more accurately reflects the colonic environment. Four clinically important *C. difficile* strains (001, 106, 078 and 027) were able to associate with MA beads in spore and/or vegetative cell forms. This suggests that these *C. difficile* strains may have adherence factors enabling cells to bind to the mucosal surface, the first step necessary for biofilm formation. This experiment was conducted without the use of biological repeats therefore data should be interpreted with caution. Results from the

microtiter tray experiments suggested that *C. difficile* PCR ribotype 001 was unable to produce a positive biofilm result after 24 hours although all other ribotypes tested did. These results coupled with the inability of PCR ribotype 001 to adhere to MA beads when grown in biofilm human gut model media may provide evidence that this ribotype has an inherent reduced ability to adhere to surfaces in mono-culture when compared with other ribotypes tested in this study.

The association of *C. difficile* to mucus *ex vivo* and *in vivo* in mice models, and to mucosal surfaces in hamsters and human has previously been demonstrated[120, 121, 495]. However, *in vivo, C. difficile* spores or vegetative cells migrating toward the colonic mucosa will firstly encounter biofilm communities, covering the colonic mucus. Therefore, recruitment of *C. difficile* into these multispecies consortia is vital for their persistence within the colon. Subsequent translocation of *C. difficile* or their toxins through the mucus to the epithelium is a potential pathogenetic pathway.

The adherence of intestinal microbiota to MA substratum material was superior to that of glass beads. MA-facilitated adherence of *Enterococcus* spp. *C. difficile, Lactobacillus* spp. and LFE, but not *Clostridium* spp., *Bifidobacterium* spp. or *B. fragilis* group. Adherence of other intestinal bacterial species, including clostridia, bacteroides and enterobacteria[446, 447], to mucin/MA and glass surfaces has also been characterised, although *Lactobacillus* populations were not always detected. The association of bifidobacteria with mucin within continuous culture systems has only been reported within nutrient-limited conditions[446]. Some of these results provide a level of disagreement with results from batch culture experiments in this study. Other researchers utilised a continuous culture system, which potentially mediates adherence of distinct bacterial groups from batch culture systems due to differences in nutrient availability. Other groups have reported rapid bacterial colonisation of mucus, typically occurring

within 15 mins of exposure to bacterial cells[496, 497]. However, only minimal bacterial association of MA beads described here was evident two hours after exposure.

Despite minimal levels of adherence of gut microbiota to glass beads, *C. difficile* spore adherence to glass beads was demonstrated within the biofilm removal experiment (section 3.3.6), although a greater level of adherence was observed to MA. Other groups have also demonstrated the adherence of spores to glass and stainless steel surfaces[133, 498].

The adherence assay was designed to compare the adherence of faecal bacterial groups to MA and glass beads and also the relative proportion of binding of each bacterial group. However, these results must be interpreted with caution, because the control was not monitored throughout the duration of the experiment. Therefore, it is not known whether or not bacterial population fluctuations (*i.e.* cell death or proliferation) occurred naturally. Moreover, settling of planktonic bacteria to the bottom of the culture vessel due to gravity may be evident, thus preventing adherence. It is unlikely that the decrease in planktonic bacteria observed in the MA experiment is due to cell death, because this was not observed in the presence of glass beads to the same degree. Degradation or utilisation of mucin as a carbon source elicit may changes in culture conditions, such as increased levels of fermentation products[499] and pH, thereby potentially promoting cell death within MA, but not glass-exposed populations.

The main virulence factor of *C. difficile* is the production of toxins A and B, which bind to receptors on the epithelial cells of the gastrointestinal tract. The human gastrointestinal tract is covered by a layer of mucus which must be translocated in order for pathogenic bacteria (such as *C. difficile*) and/or their toxins in order to access underlying epithelial cells and cause infection.

Binding to mucin provides bacteria with an ecological advantage, preventing expulsion from the gastrointestinal tract via the peristaltic motion of the bowel. However, certain bacteria are also able to utilise mucin as a carbon source when substrate availability is low (such as in the distal bowel)[500]. Mucins are large complex molecules composed of protein backbones and branched oligosaccharides[304]. Before they can be assimilated by intestinal microorganisms, mucins need to be degraded by glycosidases with appropriate specificities for each of the glycoside linkages within the oligosaccharide side chains, as well as proteases that act on the protein core[302]. Prizont and Konigsberg demonstrated that these degradative enzymes are bacterial in origin[501] and Hoskins and Boulding demonstrated that an unidentified sub-population of human faecal bacteria degrade oligosaccharide side chains of hog gastric mucin[309]. Several bacterial groups have been shown to produce these glycoprotein hydrolyses including *Bifidobacterium bifidum*[502], *Clostridium perfringens*[503], *Clostridium cocleatum*[504] and *Bacteroides fragilis*[505], demonstrating their ability to contribute to mucin degradation. Certain bacterial species may be able to degrade the oligosaccharide side chains of mucins but not posses the proteases necessary fully to degrade the mucin including the core. This would produce no mucinolytic zone. Bacteria capable of fully degrading hog gastric mucin may be able to translocate through human gastrointestinal mucins and gain entry to the underlying epithelial cells or allow the passage of other potentially pathogenic organisms.

A mucinolytic zone was visible around a faecal emulsion inoculum when grown on a minimal medium agar, with mucin representing the major carbon source. However, heat inactivated faecal emulsion and the individual indigenous gut microbiota species tested were unable to produce a mucinolytic zone when grown on this agar. This suggests that the faecal microbiota present within the faecal emulsion used in these studies

contained an unidentified population of mucin-degrading bacteria, which upon autoclaving were inactivated. These results indicate that faecal emulsion contains additional organisms with the ability to degrade mucin, or allow the sequential breakdown of distinct regions of the mucin glycoproteins. In order to determine further whether extracellular enzymes were responsible for this degradation it would be necessary to include filtered faecal emulsion samples into the investigation.

The mucinolytic zone around a faecal inoculum on MA agar was smaller than that on mucin only agar, suggesting that the incorporation of alginate may reduce mucin degradation. The incorporation of glucose into the minimal medium was intended to provide an easily utilised nutrient source rather than the complex mucin structures[506-508]. A small, weak mucinolytic zone was produced by 16 - 33% of the faecal emulsions on glucose-containing media suggesting that faecal bacteria may utilise a small amount of mucus in addition to glucose as a carbon source. These results should perhaps be interpreted with caution due to this unexpected result. Whilst this result is unexpected, other results suggest that individual bacterial groups are unable to degrade mucin, whilst full mucin degradation is possible by complex microbial communities present in the faecal emulsion. Stanley *et al* demonstrated that the degradation of gastric mucin was not affected by the presence of glucose in growth medium[509].

C. difficile is known to adhere to mucus[121], although the mucin degradation properties of this organism have not been evaluated in appropriately designed studies. The mucin degradation experiment presented here suggests that *C. difficile* is unable to degrade mucus. However, it is possible that during antimicrobial therapy the decrease in commensal faecal bacteria may allow for a subpopulation of mucin degrading bacterial species to thrive and hence increase the degradation of the mucus layer. In healthy adults this subpopulation of bacteria may be maintained at numbers low

enough so that the synthesis of mucus by the goblet cells is equal to the bacterial degradation and natural shedding of the mucus layer. If the integrity of this layer is reduced by disease this could lead to the passage of *C. difficile* into the epithelial cells. Kindon *et al* have presented evidence that the presence of colonic mucin glycoproteins at the time of addition of *C. difficile* toxin A to a human colonic cancer-derived T84 cell line significantly prevented disruption of the monolayer barrier[510]. These results suggest that the integrity of the mucosal barrier is important for the prevention of CDI.

CTAB is a cationic surfactant which was used to dissociate bacteria from MA beads[447]. It alters the surface properties of objects to which bacteria are attached, which facilitates the dissociation of bacteria from these objects hence it is often used as a biofilm removal chemical. Salton has published data concerning the possible bactericidal properties of CTAB against bacteria[487] at concentrations of 45 μg/mL (0.0045% w/v). For biofilm removal in this experiment CTAB was used at the lower concentration of 0.001%, which was not inhibitory to faecal bacteria. Comparison of surfactants (CTAB), vortexing and sonication for bacterial dissociation from beads showed vortexing to be the most efficient and suitable method and was therefore used in subsequent studies. However, only one *C. difficile* strain was utilised in this study, therefore the removal of indigenous gut microbiota and other *C. difficile* strains using different techniques could not be determined from this experiment.

As well as the negligible binding of bacterial populations to glass beads, the sampling procedures also proved difficult due to the density of the beads. Since the gastrointestinal mucosal layer is composed of mucin, porcine gastric mucin offers the most realistic substratum surface and in all likelihood, the most accurate results therefore, the use of MA beads will be investigated further. Furthermore, the most effective biofilm removal

techniques and an explanation for the degradation of MA beads observed in mucin alginate investigational gut model experiments (chapter 5) allowed more informed decisions to be made in subsequent experiments.

4.0 Triple Stage Biofilm Analysis

4.1 Background

Bacterial growth dynamics within continuous culture systems vary greatly from those within batch cultures, with the former more accurately reflecting conditions *in vivo.* As a result, continuous culture models are becoming increasingly utilised. Macfarlane *et al*[511] developed and validated a triple stage chemostat model of the human gut which Baines *et al* later utilised to study the effects of antimicrobial administration on the human gut microbiota and *C. difficile*[512]. One of the limitations of the current model is it can only be used to monitor the planktonic mode of growth. Adaptations to this model system will be investigated to analyse its potential to study the biofilm mode of growth.

The macroscopic formation of biofilm is consistently observed on the inner walls of the original triple stage human gut model vessels[270]. The removal of this biofilm provides an opportunity to investigate the *in vitro* biofilm mode of growth of the indigenous gut microbiota and *C. difficile*. However, removal of the biofilm is a destructive process, requiring dismantling of the model, therefore sampling could only take place upon the completion of each experiment.

Experimental protocols on the planktonic mode of growth of the original gut model were carried out by research staff as a separate study and not presented here. Upon completion of 10 separate gut model experiments with distinct experimental designs biofilm was removed and analysed as part of this study. The indigenous gut microbiota, *C. difficile* vegetative cells, spores, cytotoxin and antimicrobial activity were all analysed in each biofilm analysis experiment.

4.2 Materials and Methodology

4.2.1 Triple Stage Chemostat Gut Model

The triple stage gut model consists of three glass fermentation vessels (Soham Scientific, Ely, UK) connected in a weir cascade system (figure 4.2.1). The working volumes are 280 mL, 300 mL and 300 mL, for vessel 1, 2 and 3 respectively. Vessels were maintained at 37° C via a water jacketed system connected to a circulating heated water bath (Grant Instruments, Cambridgeshire, UK). The pH values of the vessels were maintained at 5.5 (±0.2), 6.2 (±0.2), 6.8 (±0.2) for vessel 1, 2 and 3, respectively and were monitored by pH probes (P200 chemotrode, Hamilton, Reno, NV, USA) and controlled by delivering 0.5M NaOH/HCl into the vessels using a pH controller unit (Biosolo 3, Brighton Systems, UK). The anaerobiosis of the system was maintained by the continuous sparging of oxygen free nitrogen into each vessel. Vessels were magnetically stirred to allow even distribution of constituents. The system was top fed with a complex growth medium (section 4.2.2; Appendix A1) through Tygon E1000 tubing (Fisher) at a controlled rate (flow rate; 13.2 mL/h) using a peristaltic pump. Excessive foaming was prevented by the addition of 0.5 mL of 10% (w/v) polyethylene glycol (Sigma) *ad libitum*.

4.2.2 Preparation of Gut Model Growth Medium

The model was top fed with a complex growth medium which was prepared in 2L volumes. The constituents of this medium are listed in Appendix A1. Growth medium was prepared in Büchner flasks plugged with a bung adapted to incorporate media delivery ports. Sterilisation of the growth media was achieved by autoclaving at 123° C for 15 minutes (Priorclave, London, UK) after which resazurin (Sigma; 0.005 g/L) and glucose

(Sigma; 0.4 g/L) were filter sterilised into the medium through 0.22 μm syringe filters (Millipore Corporation, Billerica, MA, USA).

4.2.3 Preparation of the Gut Model

Each vessel of the gut model was inoculated with approximately 150 mL of pooled faecal emulsion (prepared as described in sections 2.5-2.7).
Vessel 1 was topped up to approximately 280 mL with growth medium and the media pumped started.

4.2.4 *Clostridium difficile* Strains

The strain used throughout the biofilm gut model experiments unless otherwise stated was the *C. difficile* PCR ribotype 027 (table 3.0) which was isolated during an outbreak of CDI at the Maine Medical Centre, Portland, MA, USA.

4.2.5 Planktonic Sampling Protocol and Bacterial Enumeration

Planktonic culture samples were removed from each vessel of the gut model via a sample outlet port which is secured via a glass stopper. One millilitre volumes of planktonic culture fluid were centrifuged (10 mins, 16,000 *g*), supernatants removed and weight of remaining pellet determined.
Planktonic *C. difficile* TVC, spores (vessels 1-3), and indigenous gut microbiota (vessels 2 and 3 only) populations were enumerated and expressed as $\log_{10}$cfu/g as described in sections 2.1 and 2.2.

4.2.6 Sessile Sampling Protocol and Bacterial Enumeration

Once the original human gut model experiment had been completed and no further interventions were necessary macroscopic biofilm was scraped from the vessel walls and glass ports of each vessel of the gut model using a sterile spatula and transferred to a pre-weighed universal tube. The weight of biofilm was determined before re-suspending in pre-reduced sterile saline (Sigma) and vortexed for 1 minute. One millilitre volumes of biofilm culture fluid were centrifuged (10 mins, 16,000 *g*), supernatants removed and pellet weight determined. Sessile indigenous gut microbiota (vessels 2 and 3 only), *C. difficile* TVC and spore populations (vessels 1-3) were enumerated and converted to $\log_{10}$cfu/g (as described in sections 2.1 and 2.2).

4.2.7 Detection and Enumeration of Cytotoxin

One millilitre samples of biofilm and planktonic cultures fluid from each vessel of the gut model were centrifuged (15 mins, 16,000 *g*) and the supernatants stored at 4° C for cytotoxin assay (as described in section 2.4).

4.2.8 Detection and Quantification of Antimicrobial Activity

One millilitre planktonic and sessile samples from each vessel of the gut model were centrifuged (15 min, 16,000 *g*) and the supernatants sterilised by filtration through 0.22 μm syringe filters and stored at -20° C. The concentration of active antimicrobial agent was determined by an in-house, large plate bioassay. See table 4.1 for assay specificities.

Indicator organisms were inoculated onto fresh FBA and incubated aerobically (37° C) overnight. A 0.5 McFarland suspension (~10^8 cfu/mL) of indicator organism was prepared in sterile saline and 1 mL added to 100 mL molten (50° C) agar. Inoculated agars were mixed by inversion, poured into 245 mm x 245 mm bioassay plates (Nunc) and allowed to set.

Inoculated agars were dried (37° C) for 10 min and 25 wells (each 9 mm diameter) removed from the agar using a cork borer. Twenty microliters of target agent calibrator (doubling dilution calibration series) or each filter-sterilised sample from the gut model were randomly assigned to bioassay wells in triplicate. Bioassay plates remained at ambient temperature for 4 h prior to overnight aerobic incubation at 37° C. Zone diameters were measured using callipers accurate to 0.1 mm. Calibration lines were plotted from squared zone diameters and unknown concentrations from culture supernatants determined. Coefficient of variation values were typically 10% and R^2 values for calibration lines were all ≥0.97.

Quantification of biofilm-associated antimicrobial activity was determined using the assumption that 1 g of biofilm was equal to 1 mL of planktonic culture fluid.

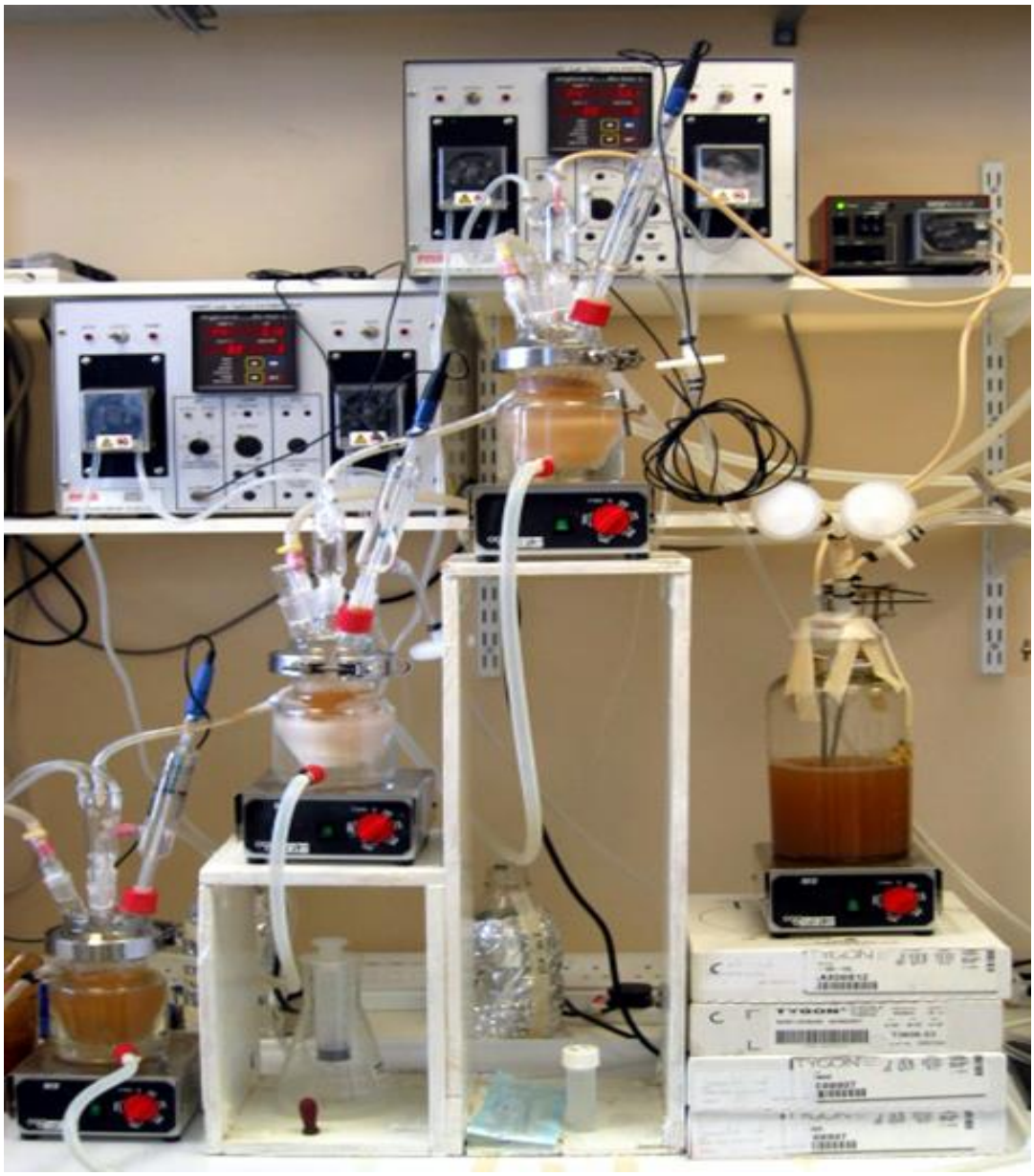

Figure 4.2.1: Triple stage human gut model.

Target antimicrobial agent	Indicator organism	Agar	Range of concentration evaluated
Clindamycin	*K. rhizophila*	Wilkins-Chalgren (Sigma)	4 – 256 mg/L
Oritavancin	*S. aureus* ATCC 29213	Mueller-Hinton	8 – 256 mg/L
Vancomycin	*S. aureus* ATCC 29213	Mueller-Hinton	8 – 512 mg/L
Co-amoxiclav	Assay A: *K. rhizophila* Assay B: *S. aureus*	Wilkins-Chalgren Mueller-Hinton	0.06 mg/L – 4 mg/L < 4 mg/L
Drug Z [a]	*K. rhizophila*	Antibiotic medium number 1	1 – 256 mg/L
Fidaxomicin	*K. rhizophila*	Wilkins-Chalgren	1 – 64 mg/L
Metronidazole [b]	*C. sporogenes* (0.5 McFarland in Schaedler's broth)	Wilkins-Chalgren	1 – 16 mg/L

Table 4.1: Indicator organism and media used for triple stage biofilm analysis antimicrobial bioassays. ([a] a potential CDI therapeutic agent under development; [b] Assay carried out under anaerobic conditions).

4.3 Biofilm Analysis 1

4.3.1 Experimental Design

The triple stage human gut model experimental design is outlined in figure 4.3.1. After the gut model was inoculated with faecal emulsion no further interventions were made for 14 days to allow the system to equilibrate (period A). On day 14 an inoculum of approximately 10^7 cfu *C. difficile* PCR ribotype 027 spores were added to vessel 1 of the gut model (period B). This serves as an internal control period. After 7 days a further inoculum of approximately 10^7 cfu *C. difficile* PCR ribotype 027 spores were added to vessel 1 of the gut model along with a dosing regimen of clindamycin (33.9mg/L QD 7 days – period C). Both clinical observations[513] and previous use of the gut model [272] have demonstrated the high risk of CDI associated with clindamycin therapy. Clindamycin was instilled to achieve levels equivalent to those in bile[514]. Biofilm was sampled on day 55.

Planktonic indigenous gut microbiota (periods A-D, vessels 2 and 3 only), *C. difficile* TVC, spores, cytotoxin (periods B-D, all vessels) and antimicrobial activity (periods C-D, all vessels) were monitored during the experiment.

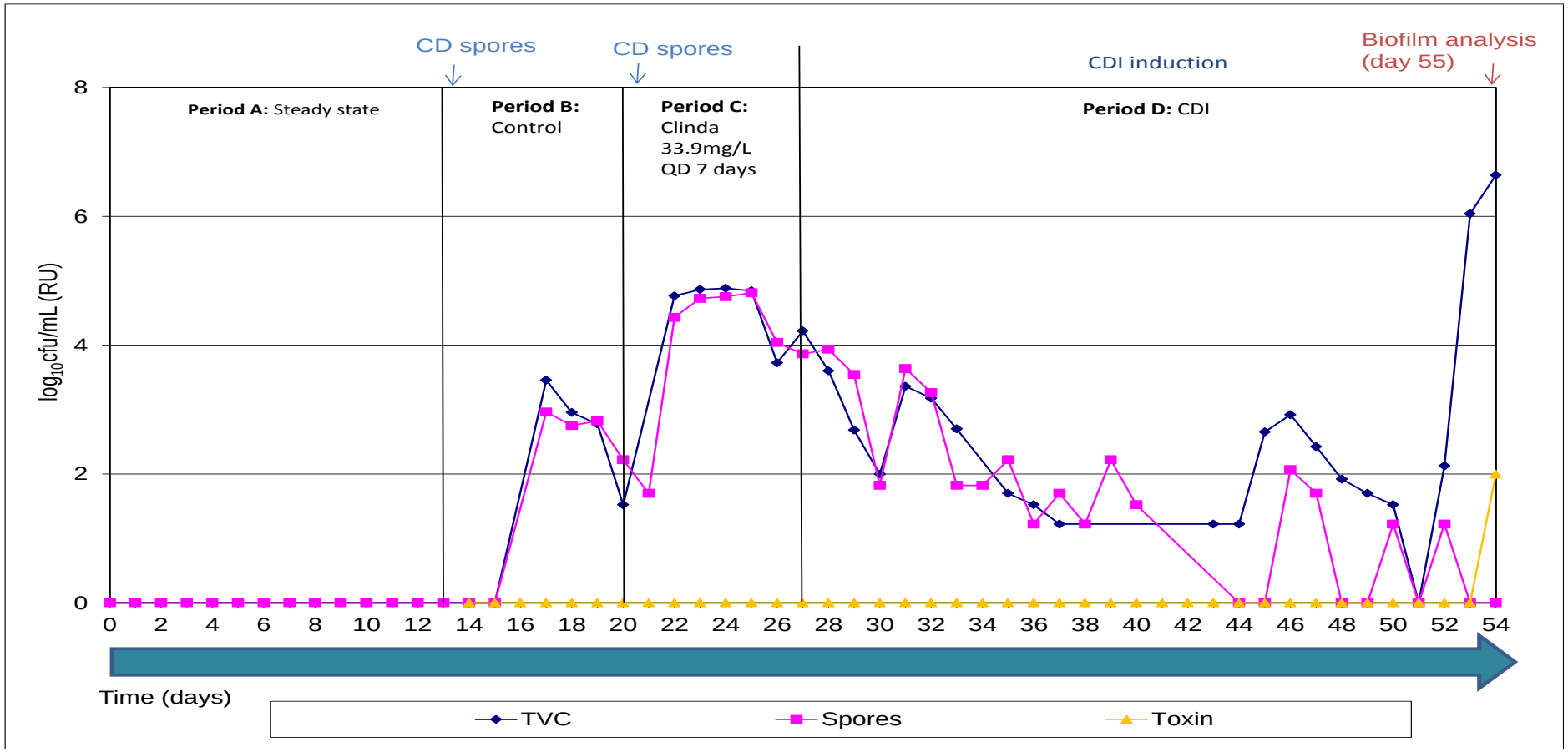

Figure 4.3.1: *C. difficile* results from vessel 3 of the original gut model and experimental design of human gut model prior to biofilm sampling. Vertical line indicates last day of period. (CD: *C. difficile* PCR ribotype 027 (~10^7cfu); Clinda: clindamycin).

4.3.2 Results

Results presented in this section detail findings from the biofilm analysis experiments only. Results obtained from the planktonic gut model cultures (days 0-53) are not shown. Vessel 3 is of most physiological relevance for CDI, therefore only indigenous gut microbiota from this vessel are presented in this chapter.

4.3.2.1 Indigenous Gut Microbiota Populations

Bacterial populations within the human gut model were dominated by lactose-fermenting Enterobacteriaceae (LFE) and *Lactobacillus* spp. for both planktonic and sessile communities (figure 4.3.2.1). All planktonic gut bacterial groups identified and enumerated in the gut model were also present within the biofilm. Populations of planktonic bacteria were higher than those in sessile form (by ~1-1.5 $\log_{10}$cfu/g) although the relative proportions of these planktonic and sessile populations were similar for all bacterial groups. *B. fragilis* group were the least abundant bacterial group present in both planktonic and sessile populations. *Bifidobacterium* spp. populations were not detected in either the planktonic or sessile form at this stage of the experiment.

4.3.2.2 *C. difficile* Populations

C. difficile vegetative cells and spores were present in planktonic (figure 4.3.2.2) and sessile (figure 4.3.2.3) form in all three vessels of the human gut model.

Planktonic populations of *C. difficile* TVC (~6.3, 8.5, 8.4 $\log_{10}$cfu/g for vessels 1, 2 and 3 respectively) were greater than the biofilm populations (~5.2, 6.7, 5.5 $\log_{10}$cfu/g for vessels 1, 2 and 3 respectively) in all three vessels.

Planktonic spore populations were greater than sessile populations in vessels 2 (~5.7 $\log_{10}$cfu/g planktonic: ~4.0 $\log_{10}$cfu/g sessile) and 3 (~ 5.3 $\log_{10}$cfu/g planktonic: ~3.3 $\log_{10}$cfu/g sessile) however, the converse was observed in vessel 1 (~4.3 $\log_{10}$cfu/g sessile: ~3.5 $\log_{10}$cfu/g planktonic). Planktonic and sessile TVC were greater than spore populations (by ≥ 2 $\log_{10}$cfu/g) in vessel 2 and 3, indicating the presence of vegetative cells. Planktonic TVC in vessel 1 were greater than spore populations by ~3 $\log_{10}$cfu/g, whilst corresponding sessile TVC were less than 1 $\log_{10}$cfu/g greater than spore populations.

Cytotoxin was also not detected in vessel 1 of the biofilm whilst it was detected in all other vessels within planktonic culture and biofilm.

4.3.2.3 Antimicrobial Levels within the Planktonic Culture and Biofilm

Clindamycin antimicrobial activity could not be demonstrated within the planktonic culture or biofilm of the human gut model using large plate bioassay.

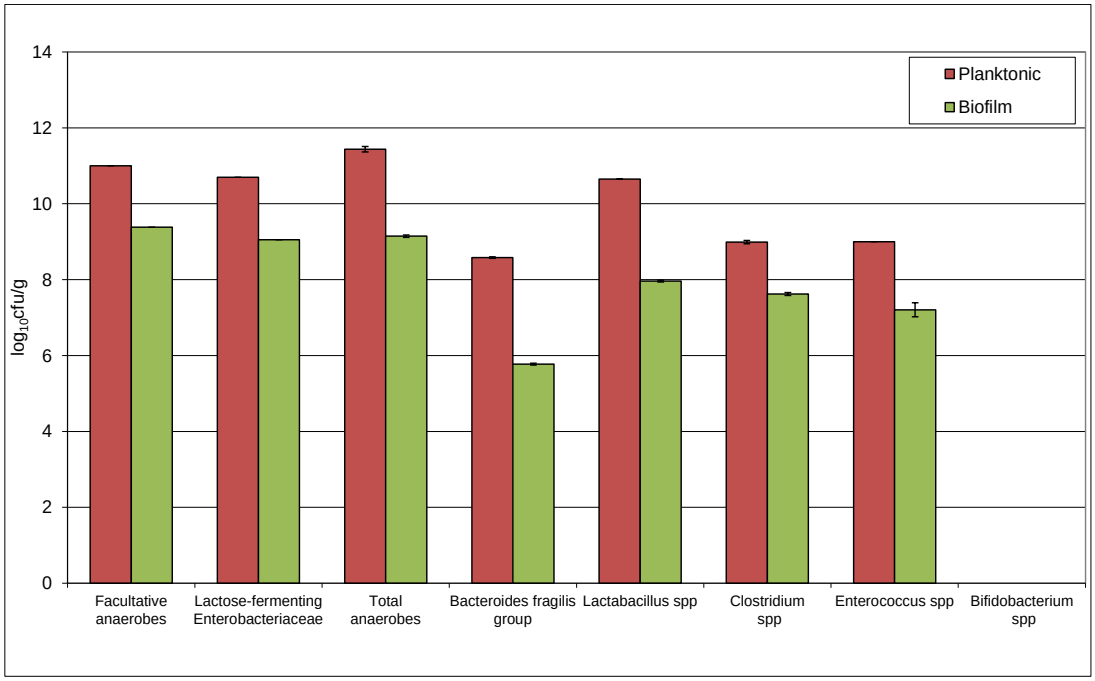

Figure 4.3.2.1: Mean (±SE) planktonic and biofilm populations (log_{10}cfu/g) of indigenous gut microbiota populations present in vessel 3 of the human gut model.

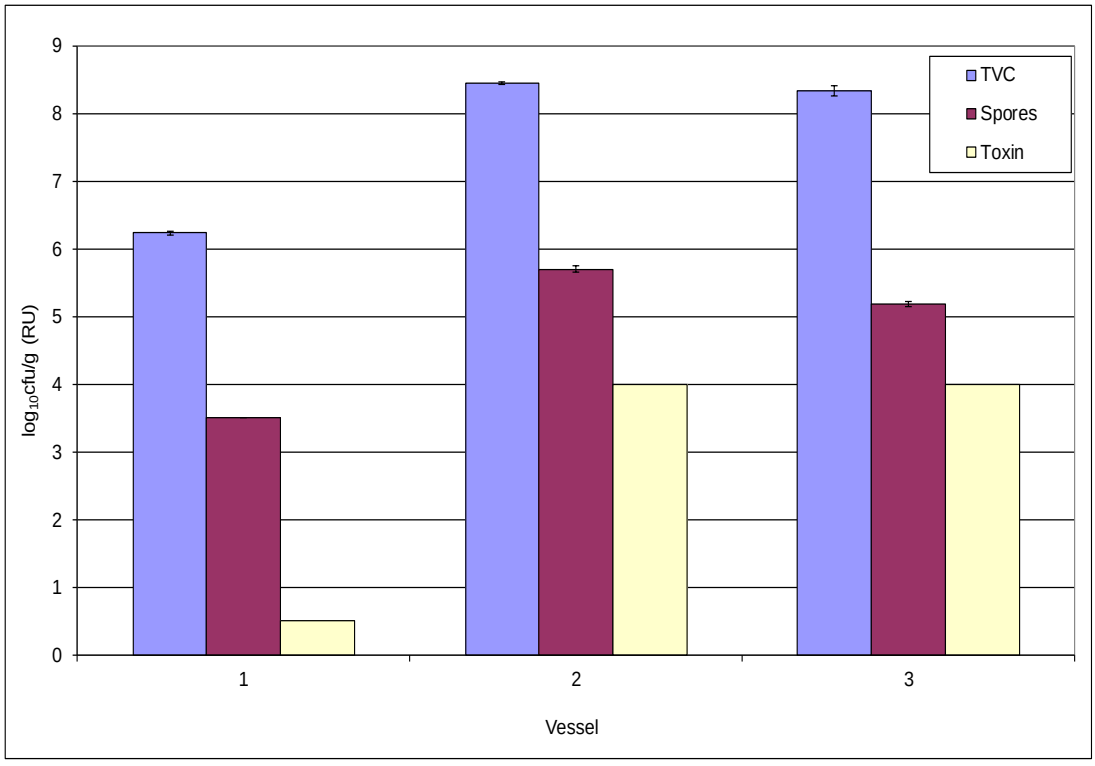

Figure 4.3.2.2: Mean (± SE) planktonic populations (log_{10}cfu/g) of *C. difficile* total viable counts (TVC), spores and cytotoxin (RU) in vessel 1, 2 and 3 of the human gut model.

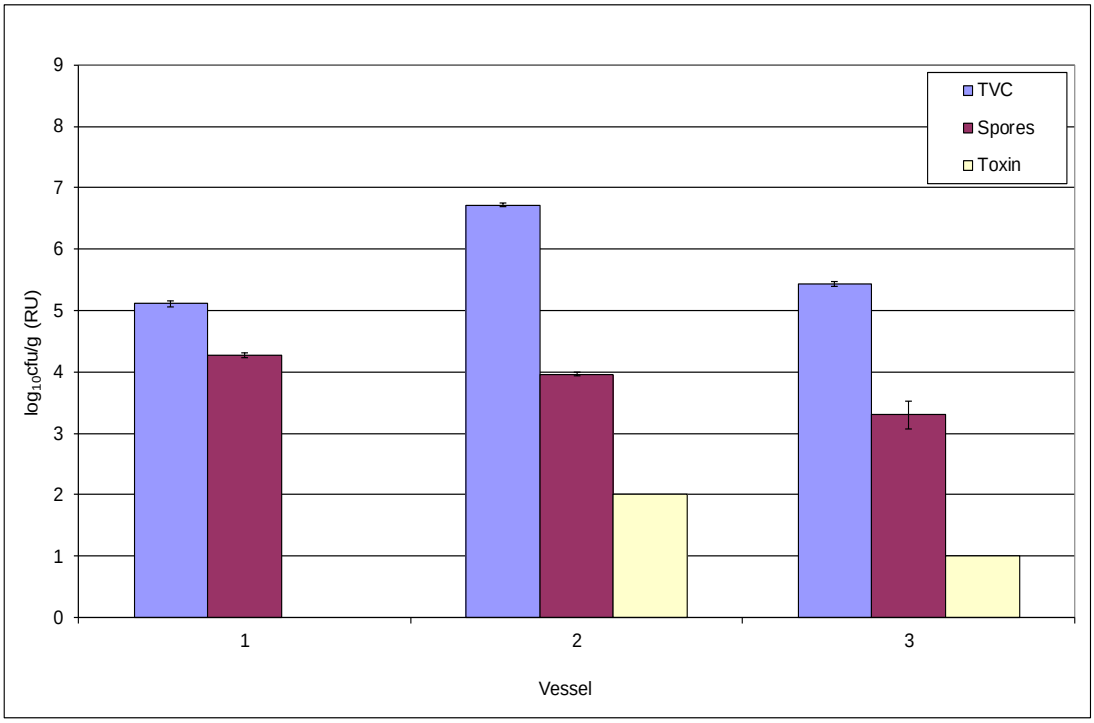

Figure 4.3.2.3: Mean (±SE) biofilm populations (log_{10}cfu/g) of *C. difficile* total viable counts (TVC), spores and cytotoxin (RU) in vessel 1, 2 and 3 of the human gut model.

4.3.3 Discussion

Before biofilm was removed and analysed, the gut model experiment had involved induction of simulated CDI using clindamycin. Germination and proliferation of *C. difficile* occurred 24 days after antimicrobial cessation with subsequent toxin production in all vessels prior to biofilm analysis (figure 4.3.1, vessel 3; vessel 1 and 2, data not shown).

Results from the original gut model demonstrate that all planktonic indigenous gut microbiota groups were present during the steady state period (period A, data not shown). *Bifidobacterium* spp. populations declined from ~8 log_{10}cfu/mL at the beginning of the experiment to ~4 log_{10}cfu/mL at the end (data not shown). The absence of planktonic and sessile *Bifidobacterium* spp. on day 55 (figure 4.3.2.1), suggests that this bacterial group may have continued to decline to below the LOD. This

profound reduction in *Bifidobacterium* spp. populations following clindamycin instillation has been previously observed in gut model experiments[272, 512, 515].

All indigenous gut microbiota populations present within the planktonic mode of growth on day 55 were also present in the sessile mode of growth, indicating that gut model-associated biofilm structures are able to support populations of all bacterial groups enumerated in this study. Populations of sessile bacteria were comparative to their planktonic counterparts, with no obvious differences in their levels or composition. This study does not provide evidence on the composition of these biofilm structures during the early stages of biofilm formation. It remains unknown which bacterial groups provided initial colonisation of the abiotic surface within the gut model, and the relative contributions and time scales with which subsequent maturation of the biofilm occurred. The *in vitro* adherence of several intestinal bacterial species have previously been characterised[446, 447] and demonstrate similar results to this study, although sessile lactobacillus populations were not always detected. The detection of sessile *Lactobacillus* populations in this study is therefore uncommon. The *in vitro* chemostat models used to monitor the sessile mode of growth to date were utilised for a shorter duration than this study. Increased biofilm maturity and complexity, facilitated by an increased time frame, may provide additional resources and conditions necessary for the recruitment of *Lactobacillus* populations into biofilms *in vitro*.

In order to compare planktonic and sessile populations from a single time point, populations from both modes of growth were expressed as $\log_{10}$cfu/g. In general, planktonic indigenous gut microbiota populations were higher than their sessile counterparts. The weight of the pellet from a 1 mL suspension of planktonic culture fluid or re-suspended biofilm is used to determine the cfu per gram of biomass. Planktonic cultures are likely to

contain a high proportion of bacteria within this biomass whilst the biofilm comprises a large amount of extracellular material in addition to the bacterial mass. In general, it is estimated that bacteria account for ≤ 10% of the dry mass of a biofilm, where as the matrix accounts for ≥90 %[378]. This may explain the apparently more numerous planktonic populations compared with sessile populations. Furthermore, Macfarlane *et al* have also reported increased planktonic populations compared with sessile populations[446]. Although Probert and Gibson reported higher populations within the culture fluid from a biofilm fermenter compared with that of a conventional planktonic chemostat[447].

Germination, proliferation and toxin production of planktonic *C. difficile* within the original gut model occurred in all vessels and this remained evident within the planktonic culture at the time of biofilm analysis (day 55). Vegetative and spore forms of *C. difficile* were observed within biofilm structures analysed here, although their presence and populations differ within distinct regions of the model. Only *C. difficile* spores were present within biofilms structures in vessel 1, whilst *C. difficile* spores and vegetative cells were present within biofilm structures in vessels 2 and 3. Toxin was detected in biofilm in vessels 2 and 3 only.

Biofilm formation is dependent on environmental conditions such incubation time, temperature and growth medium[454, 516, 517]. Biofilm structures within different vessels of the human gut model form under a unique set of conditions, differing most notably in nutrient availability and pH. Biofilm biomass of vessel 1 is greater than vessels 2 and 3 (data not shown), correlating with the increased nutrient availability in vessel 1. Increased *in vitro Bacillus cereus* biofilm formation by certain strains in nutrient-rich conditions has been previously demonstrated[518]. The dense biofilm present in vessel 1 may potentially harbour a greater total bacterial population and possess distinct properties from the biofilm in

vessels 2 and 3. Quorum sensing, a bacterial cell-density dependant process is known to regulate transcription of cellular process such as sporulation and virulence factors[391, 394, 519]. The increased bacteria cell density within vessel 1 may potentially activate quorum sensing pathways otherwise redundant in vessel 2 and 3, thus accounting for the heterogeneity of biofilm composition within the gut model.

C. difficile vegetative cells were absent from the biofilm of vessel 1, despite their presence within the planktonic culture fluid. Sessile *C. difficile* vegetative cells and spores were detected within biofilm structures in other vessels, demonstrating the capacity of *C. difficile* to exist within biofilm structures in either form. Therefore, the absence of *C. difficile* vegetative cells within vessel 1 may not due to the inability of vegetative cells to associate with biofilms. In other spore-forming bacteria both vegetative and spores have previously been observed in sessile communities[518, 520].

Cytotoxin was detected within the planktonic fluid of vessel 1 but absent from the biofilms in this vessel correlating with an absence of vegetative cells and suggesting that toxin sequestration is not in occurrence. Within vessels 2 and 3 it is unclear whether toxin detection was due to production by vegetative cells, or sequestration from planktonic fluid. The observation that sequestration was not apparent in vessel 1 suggests that the toxin in vessels 2 and 3 was actively produced by sessile vegetative cells.

Clindamycin was not detected within the planktonic culture or biofilm of any vessel. The absence of clindamycin within the planktonic culture is common within the original gut model, with clindamycin concentrations often declining to below the limits of detection approximately 4 days after the cessation of antimicrobial instillation [515]. The possible persistence of antimicrobial agents within biofilm structures in the model remained unexplored within the original model.

4.4 Biofilm Analysis 2

4.4.1 Experimental Design

The triple stage human gut model experimental design is outlined in figure 4.4.1. Briefly, after inoculation with faecal emulsion, gut microbiota populations were allowed to equilibrate for 14 days (period A), before a single inoculum of *C. difficile* spores were added to vessel 1 of the model on day 14. A second inoculum of *C. difficile* spores were inoculated into the model on day 21. At this point a dosing regimen of clindamycin (33.9 mg/L, QD, 7 days) commenced (period C). Following commencement of clindamycin dosing no further intervention were made until *C. difficile* germination, proliferation and high toxin production was observed (period D). Instillation of oritavancin (64 mg/L, BD, 4 days) commenced on day 49. Following cessation of therapeutic instillation the model was left without intervention for 21 days (period F). Biofilm was sampled on day 74.

Planktonic indigenous gut microbiota (periods A-F, vessels 2 and 3), *C. difficile* TVC, spores, cytotoxin (periods B-F, all vessels) and antimicrobial activity (periods C-F, all vessels) were monitored during the experiment.

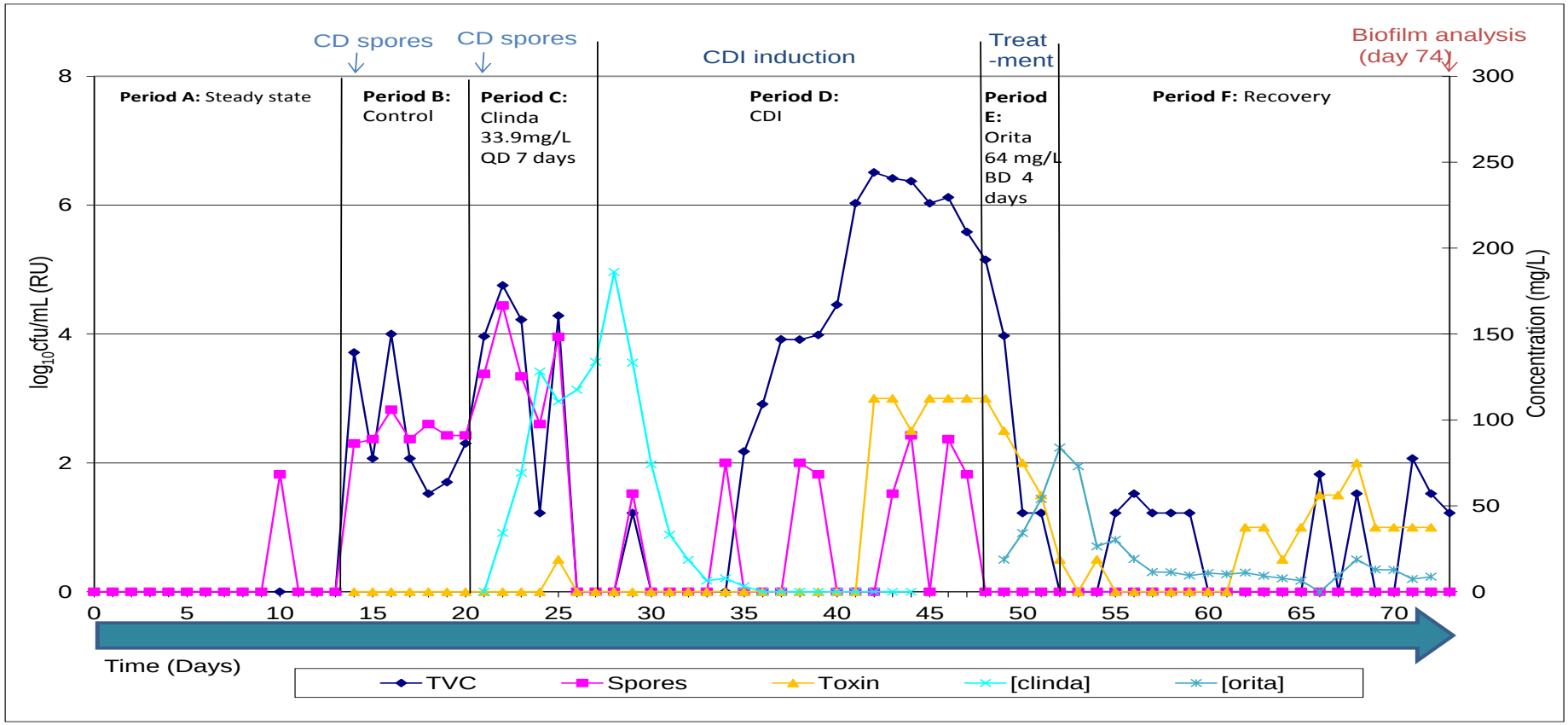

Figure 4.4.1: *C. difficile* results from vessel 3 of the original gut model and experimental design of human gut model prior to biofilm sampling[515]. Vertical line indicates last day of period. (CD: *C. difficile* PCR ribotype 027 (~10^7cfu); Clinda: clindamycin; Orita: oritavancin).

4.4.2 Results

4.4.2.1 Indigenous Gut Microbiota Populations

Bacterial populations within the human gut model were dominated by LFE and *Lactobacillus* spp. for both planktonic and sessile (figure 4.4.2.1) communities. All planktonic gut bacterial groups identified and enumerated in the original gut model were also present within the biofilm. Populations of planktonic bacteria were generally higher than those in sessile form with the exception of *B. fragilis* group, although the relative proportions of these planktonic and sessile populations were similar for all bacterial groups. *Enterococcus* spp. were the least abundant bacterial group present in both planktonic and sessile populations. *Bifidobacterium* spp. populations were not detected in either form at this stage of the experiment.

4.4.2.2 *C. difficile* Populations

C. difficile populations were present in planktonic and biofilm form in all three vessels of the human gut model (figures 4.4.2.2 and 4.4.2.3) and TVCs decreased progressively in number from vessel 1 (~5.5 $\log_{10}$cfu/g planktonic: ~6.8 $\log_{10}$cfu/g sessile) to vessel 3 (~3.3 $\log_{10}$cfu/g planktonic: ~4.6 $\log_{10}$cfu/g sessile). Sessile populations of vegetative cells (~4.6-6.8 $\log_{10}$cfu/g) were greater than their corresponding planktonic populations (~2.0-4.3 $\log_{10}$cfu/g) in all three vessels. Spores were absent from most vessels of the human gut model in either planktonic or sessile form, indicating that *C. difficile* populations are comprised mainly (in vessel 1 planktonic) or completely (all other vessels) of vegetative cells.

Low levels of cytotoxin was detected in vessel 1 only from the planktonic cultures fluid but was present in the biofilm of all 3 vessels.

4.4.2.3 Antimicrobial Levels within the Planktonic Culture and Biofilm

Antimicrobial activity was detected within the biofilm of vessels 2 (57.4 mg/L) and 3 (36.7 mg/L) and within the planktonic cultures fluid within vessel 3 (7.9 mg/L).

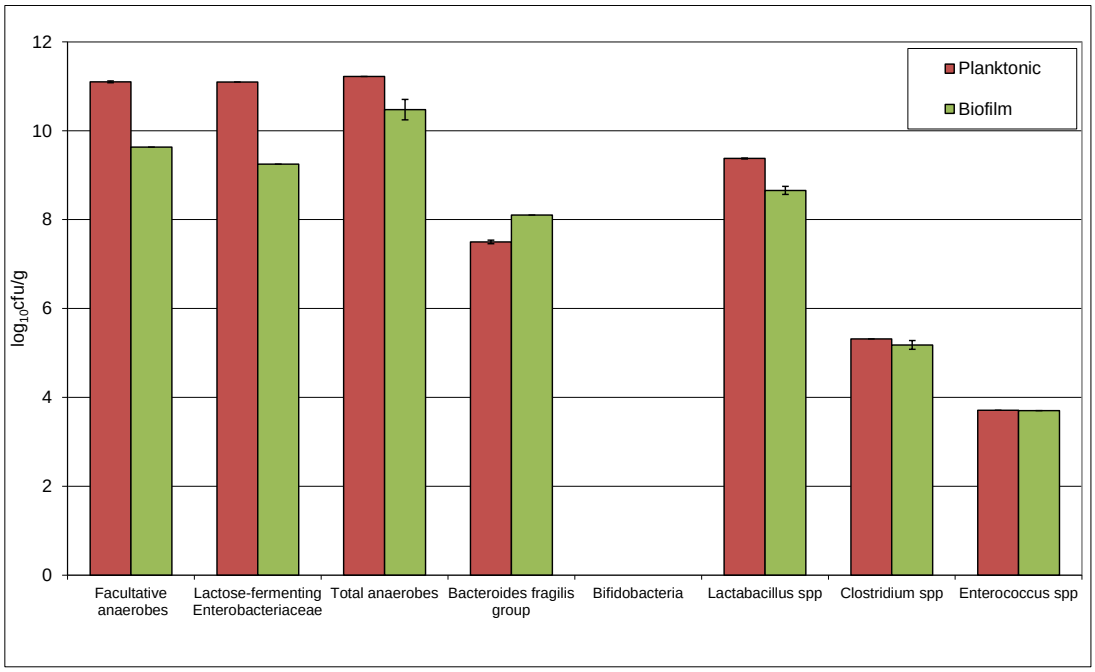

Figure 4.4.2.1: Mean (±SE) planktonic and biofilm populations (log_{10}cfu/g) of indigenous of indigenous gut microbiota populations present in vessel 3 of the human gut model.

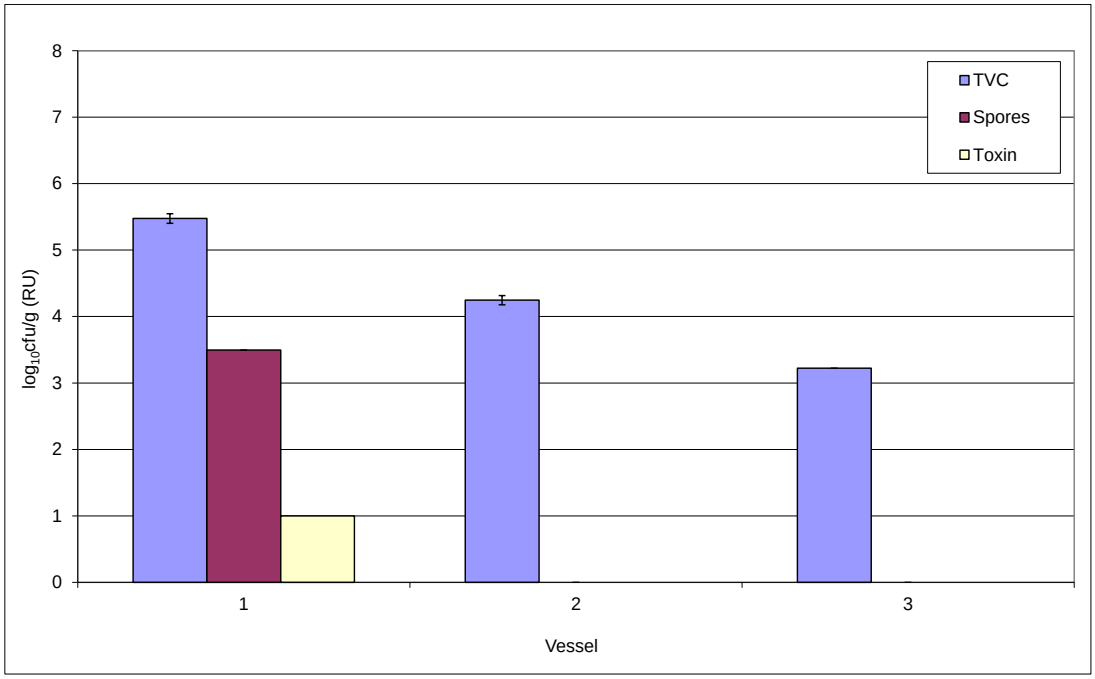

Figure 4.4.2.2: Mean (± SE) planktonic populations (log_{10}cfu/g) of *C. difficile* total viable counts (TVC), spores and cytotoxin (RU) in vessel 1, 2 and 3 of the human gut model.

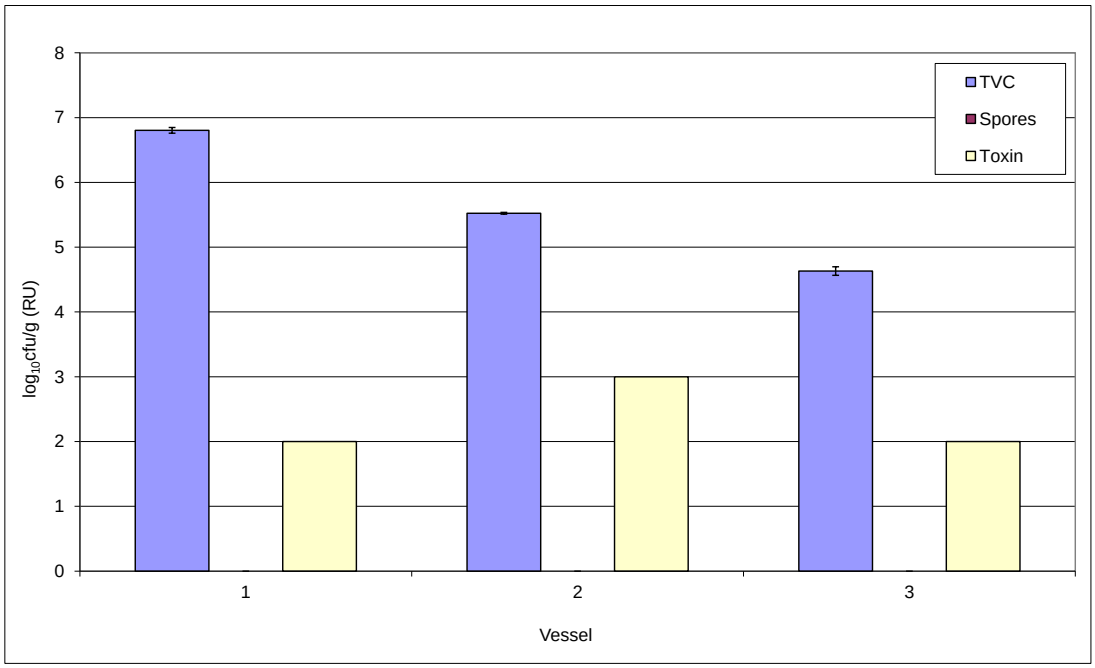

Figure 4.4.2.3: Mean (±SE) biofilm populations (log_{10}cfu/g) of *C. difficile* total viable counts (TVC), spores and cytotoxin (RU) in vessel 1, 2 and 3 of the human gut model.

4.4.3 Discussion

Before biofilm was removed and analysed, the gut model experiment had involved induction of simulated CDI using clindamycin. Germination and proliferation of *C. difficile* occurred after 6-7 days with subsequent toxin production in all vessels (figure 4.4.1, vessel 3; vessel 1 and 2, data not shown). Treatment of simulated CDI commenced with the instillation of oritavancin. Treatment was initially successful with the rapid decrease in *C. difficile* vegetative cells and toxin to below the LOD (figure 4.4.1). However, low levels of vegetative cells and toxin (recurrence) were detected in all vessels before the completion of the experiment. Spores remained undetected from the commencement of oritavancin dosing.

Results from the original gut model demonstrated that all indigenous gut microbiota groups were present during periods A and B, but following clindamycin instillation, *Bifidobacterium* spp. declined to below LOD and remained there for the duration of the experiment, as previously observed within the gut model[512]. This explains the absence of *Bifidobacterium* spp. in planktonic and sessile form at the time of biofilm analysis (day 74).

Upon biofilm sampling (day 74), all bacterial groups present within the planktonic fluid were also present within the biofilm. Again, planktonic bacterial populations were generally higher than their sessile counterparts when expressed as $\log_{10}$cfu/g.

On day 74, planktonic *C. difficile* populations were present in vegetative and spore form, and low level toxin was detected. In vessels 2 and 3 only vegetative cells were detected and toxin was below LOD. Within the biofilm structures, *C. difficile* was only present in vegetative form in all vessels and toxin was detected in all vessels.

The reasons why toxin was present within the biofilm of vessels 2 and 3, but not in planktonic culture fluid, remains unclear. During the original gut

model experiment toxin was detected within vessels 2 (0.5 RU, data not shown) and 3 (1 RU, figure 4.4.1) until the end of the experiment therefore its absence from the planktonic state of the biofilm analysis work is unexpected. Levels of toxin from the original model were very low and may have dropped below the limit of detection during biofilm analysis. This could be due to degradation, or dilution of toxin out of the model. The dilution of vessel contents in the planktonic phase may therefore confer a more timely removal of toxin compared with removal from biofilm structures.

Clindamycin activity was absent from all vessels of the original gut model experiment 5 days after cessation of dosing whilst oritavancin activity persisted within vessel 3 for the remainder of the experiment (figure 4.4.1). Biofilm analysis on day 74 showed that antimicrobial activity remained in vessel 3 in the planktonic culture at a level of 7.9 mg/L. Antimicrobial activity was also detected within the biofilm of vessels 2 and 3 (57.4 and 36.7 mg/L respectively). At the time of biofilm removal and analysis instillation of more than one antimicrobial agent had occurred. The bioassay used in this study can not accurately distinguish between different antimicrobial agents. However, during the original gut model experiment antimicrobial activity is monitored daily therefore identification of antimicrobial agent responsible for inhibition is possible. Oritavancin persisted within the original gut model whilst clindamycin activity was absent 5 days post instillation. It is therefore likely that any antimicrobial activity detected during biofilm analysis work was oritavancin.

Oritavancin is a semi-synthetic lipoglycopeptide analogue of vancomycin currently under investigation for CDI treatment[272, 515, 521]. Oritavancin displays multiple unknown mechanisms of action in addition to the inhibition of peptidoglycan synthesis. The anti-spore activity of oritavancin has been investigated. The apparent adherence of this agent to the surface of spores has previously been observed[522], potentially allowing rapid exertion

of an anti-*C. difficile* activity once spores break dormancy. It is speculated that the highly positive charge of oritavancin confers its ability to adhere to surfaces, potentially providing an increased affinity for components of the biofilm matrix. The subsequent dispersal of biofilm aggregates may confer entry of sequestered oritavancin into the planktonic fluid, possibly explaining the prolonged detection of oritavancin within the planktonic culture fluid and biofilm structures. In addition, the highly adherent nature and apparent anti-spore activity of this agent may explain the absence of detectable spores within the biofilm.

Oritavancin displays rapid bactericidal activity against exponentially growing Gram-positive bacteria[523]. Furthermore, it has also demonstrated concentration-dependant bactericidal activity against stationary phase and biofilm cultures of MRSA[524]. Whether or not oritavancin exerts this bactericidal activity against *C. difficile* vegetative cells within complex biofilm communities remains unknown. The persistence of oritavancin with biofilm structures potentially provides a reservoir of antimicrobial activity, which may act upon any residual *C. difficile*, thus preventing recurrent infection.

4.5 Biofilm Analysis 3

4.5.1 Experimental Design

The triple stage human gut model experimental design is outlined in figure 4.5.1. Briefly, after inoculation with faecal emulsion, gut microbiota populations were allowed to equilibrate for 14 days (period A), before a single inoculum of *C. difficile* spores were added to vessel 1 of the model on day 14. A second inoculum of *C. difficile* spores were inoculated into the model on day 21. At this point a dosing regimen of clindamycin (33.9 mg/L, QD, 7 days) commenced (period C). Following commencement of clindamycin dosing no further intervention were made until *C. difficile* germination, proliferation and high toxin production was observed (period D). Instillation of vancomycin (125 mg/L, QD, 4 days) commenced on day 49. Following cessation of therapeutic instillation the model was left without intervention for 21 days (period F). Biofilm was sampled on day 74.

Planktonic indigenous gut microbiota (periods A-F), *C. difficile* TVC, spores, cytotoxin (periods B-F) and antimicrobial activity (periods C-F) were monitored during the experiment.

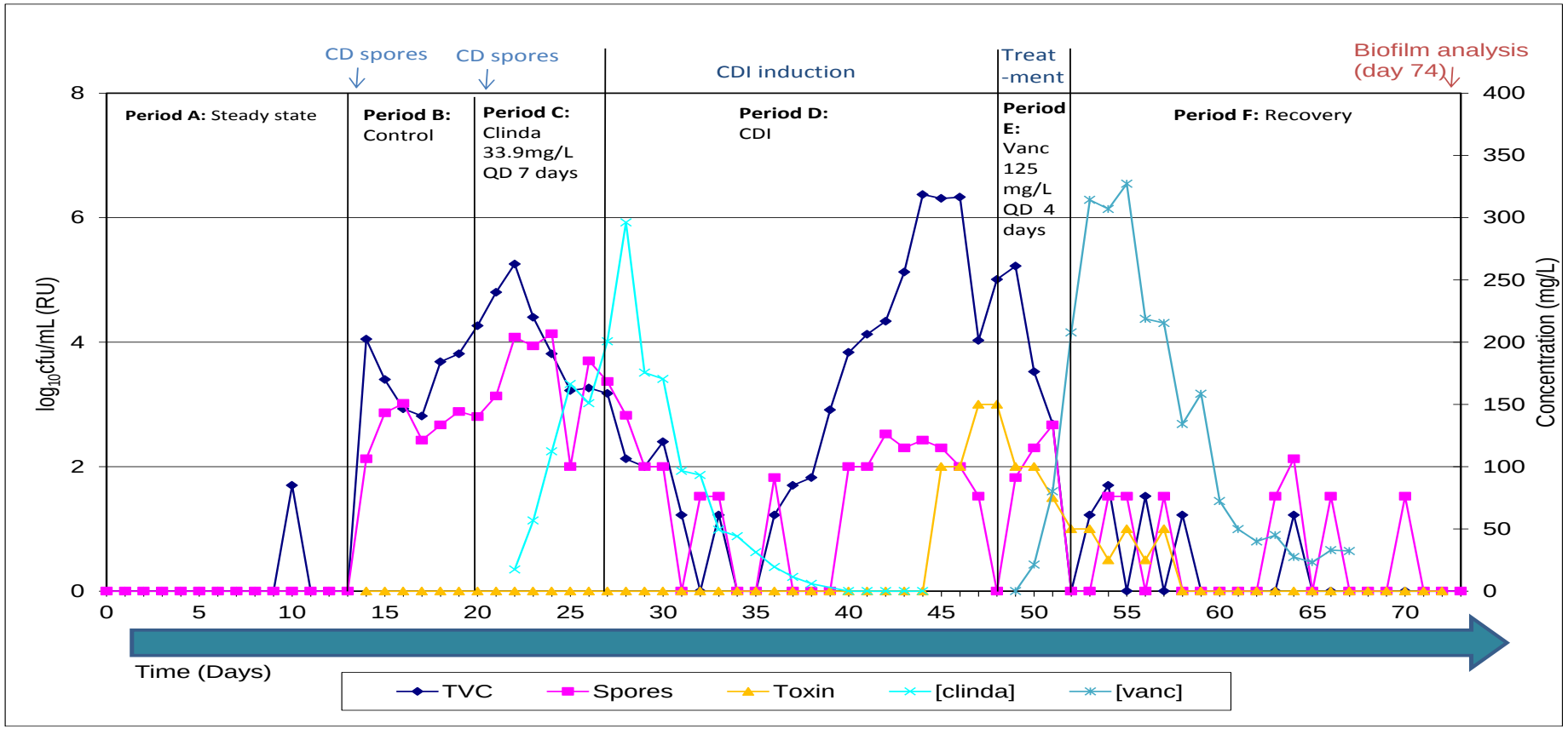

Figure 4.5.1: *C. difficile* results from vessel 3 of the original gut model and experimental design of human gut model prior to biofilm sampling. Vertical line indicates last day of period. (CD: *C. difficile* PCR ribotype 027 (~10^7cfu); Clinda: clindamycin; vanc: vancomycin).

4.5.2 Results

4.5.2.1 Indigenous Gut Microbiota Populations

On day 74, populations of planktonic and sessile indigenous gut microbiota within the human gut model were dominated by facultative anaerobic species such as LFE and *Lactobacillus* spp. (figure 4.5.2.1). All planktonic gut bacterial groups identified and enumerated in the original gut model were also present within the biofilm. *Clostridium* spp. planktonic and sessile communities were the least abundant bacterial group. Planktonic populations were greater than corresponding sessile populations (~1 – 2 $\log_{10}$cfu/g). *Bifidobacterium* spp. populations were not detected in either the planktonic or sessile form at this stage of the experiment.

4.5.2.2 *C. difficile* Populations

Sessile *C. difficile* vegetative cells and spores (figure 4.5.2.3) were present in all three vessels of the human gut model. Planktonic *C. difficile* populations were present as spores in vessels 1 and 3 (figure 4.5.2.2) but absent in either form in vessel 2. Vegetative cells were absent from all vessels in planktonic or sessile form. Sessile *C. difficile* populations (~4.3, 4.1, 3.5 $\log_{10}$cfu/g in vessel 1, 2, 3 respectively) of were greater than the planktonic populations (~3.5, below LOD, 3.4 $\log_{10}$cfu/mL in vessels 1, 2, 3 respectively) in all three vessels (figure 4.5.2.3). Cytotoxin was present in low levels in the planktonic fluid of vessels 2 and 3 but absent from vessel 1 biofilm. Toxin was not detected in biofilm from any vessel.

4.5.2.3 Antimicrobial Levels within the Planktonic Culture and Biofilm

Antimicrobial activity could not be demonstrated within the planktonic culture or biofilm of the human gut model using large plate in house bioassay.

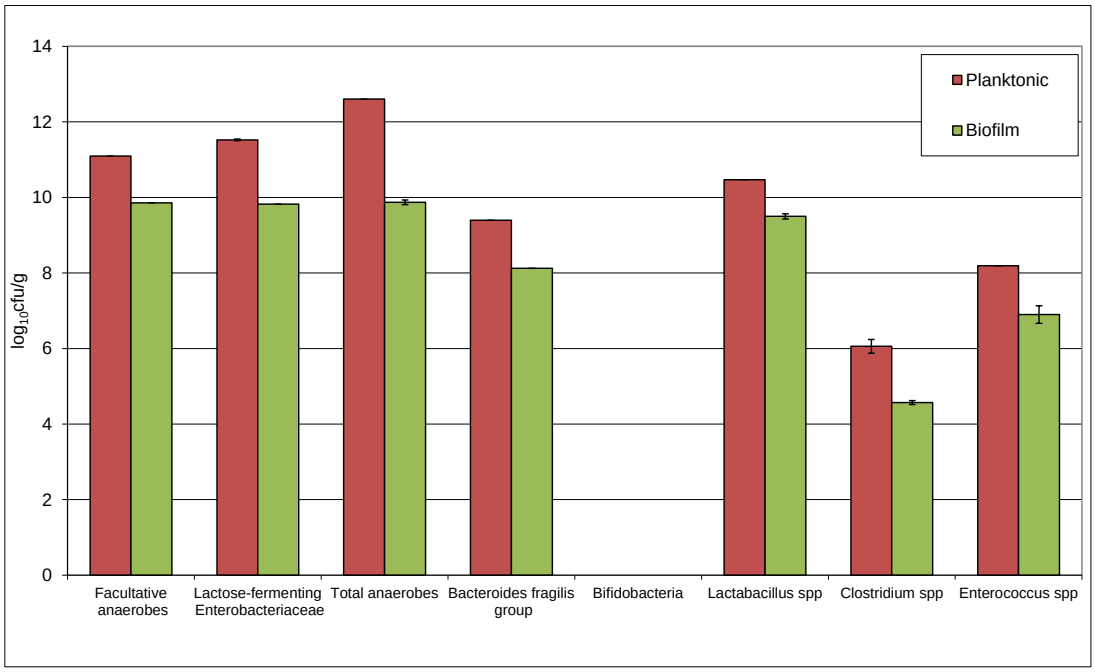

Figure 4.5.2.1: Mean (±SE) planktonic and biofilm populations (log_{10}cfu/g) of indigenous of indigenous gut microbiota populations present in vessel 3 of the human gut model.

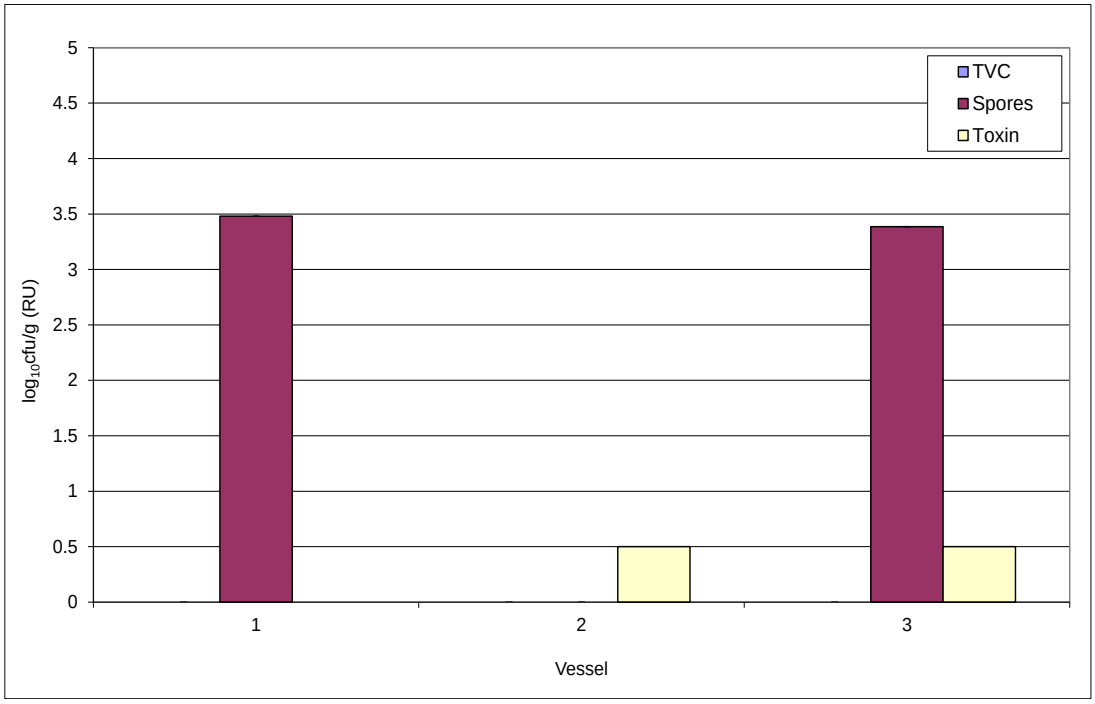

Figure 4.5.2.2: Mean (± SE) planktonic populations (log_{10}cfu/g) of *C. difficile* total viable counts (TVC), spores and cytotoxin (RU) in vessel 1, 2 and 3 of the human gut model.

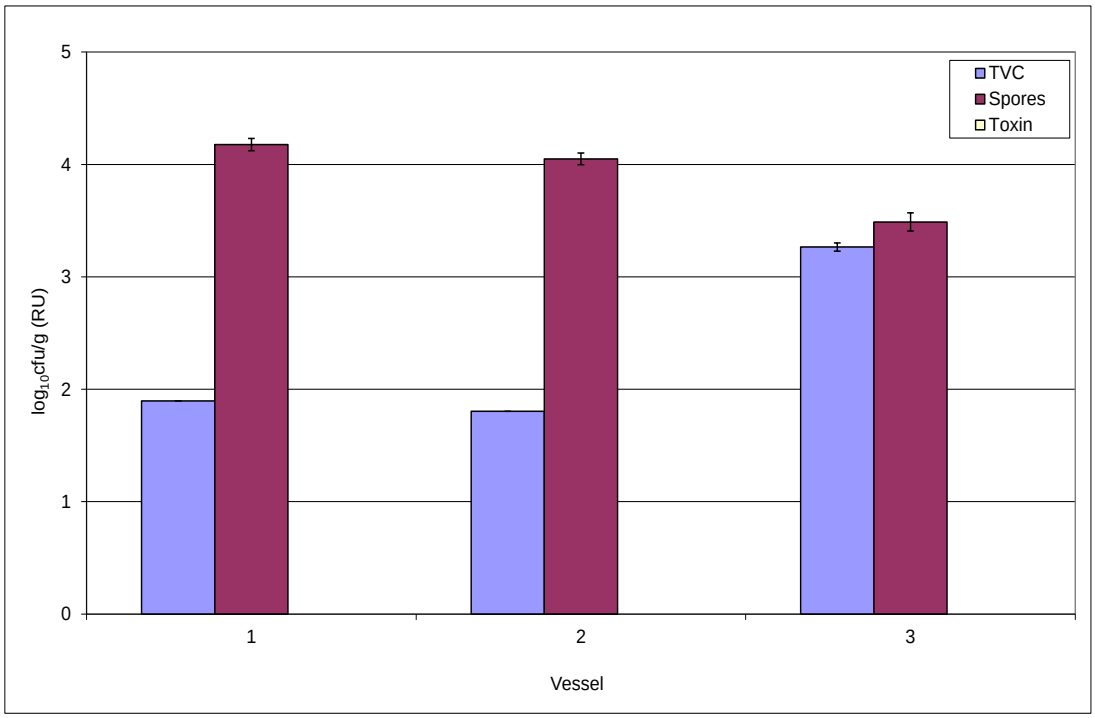

Figure 4.5.2.3: Mean (±SE) biofilm populations (log_{10}cfu/g) of *C. difficile* total viable counts (TVC), spores and cytotoxin (RU) in vessel 1, 2 and 3 of the human gut model.

4.5.3 Discussion

Before biofilm was removed and analysed, the gut model experiment had involved induction of simulated CDI using clindamycin. *C. difficile* germination and proliferation occurred 10 days after cessation of antimicrobial instillation with subsequent toxin production in vessels 2 (data not shown) and 3 (figure 4.5.1). Treatment of simulated CDI commenced with the instillation of vancomycin. Treatment was successful with only spores detected at the LOD at the completion of the experiment with no further vegetative cell or toxin detection.

On day 74, the indigenous microbiota populations present within the planktonic form were also present within the biofilm with the exception of *Bifidobacterium* spp. which were absent in both forms due to the antimicrobial interventions carried out in the original model experiment (data not shown).

On day 74, planktonic *C. difficile* populations were in spore form within vessels 1 and 3 (no *C. difficile* present in vessel 2). Low levels of toxin were detected in vessels 2 and 3. Within biofilm structures *C. difficile* was present in spore form in all vessels, and toxin was not detected. Biofilm analysis experiment 1 demonstrates that toxin is able to exist within a biofilm. The absence of toxin persistence here, despite previous toxin detection within the planktonic fluid of the original model demonstrates that long term biofilm-associated toxin persistence is not always evident.

Simulated CDI treatment within the original model was successful and only spores were detected at the cessation of the experiment (figure 4.5.1). In addition, during sampling of the original gut model toxin was not detected (figure 4.5.1). Upon biofilm removal and analysis vegetative cell growth was not detected in planktonic or sessile form (figures 4.5.2.2-3). Therefore, the low levels of toxin detected within the planktonic culture during biofilm

analysis (figure 4.5.2.2) are unexpected and the reasons for this presence remain unclear.

The absence of spores from the planktonic culture of vessel 2 but presence within the biofilm of this vessel provides further evidence of the persistence of *C. difficile* spores within the protected environment of the biofilm.
See 4.13 for further discussion.

No antimicrobial activity was detected within the planktonic culture fluid or biofilm. Within previous original human gut model experiments, vancomycin [515, 525] (along with clindamycin) activity was diluted out of the culture fluid before completion of the experiment; therefore, the absence of this agent within the planktonic culture fluid is expected. Vancomycin and clindamycin persistence within biofilm structures was not apparent in this experiment.

4.6 Biofilm Analysis 4

4.6.1 Experimental Design

The triple stage human gut model experimental design is outlined in figure 4.6.1. Briefly, after the gut model was inoculated with faecal slurry, no further interventions were made for 26 days to allow the system to equilibrate (period A). On day 26 an inoculum of approximately 10^7 cfu *C. difficile* 027 spores were added to vessel 1 of the gut model (period B). This serves as an internal control period. After 7 days a further inoculum of approximately 10^7 cfu *C. difficile 0*27 spores were added to vessel 1 of the gut model along with a dosing regimen of co-amoxiclav (8 mg/L, 6 hourly, 7 days – period C). Following cessation of co-amoxiclav instillation the model was left without intervention for 22 days (period C). Biofilm was sampled on day 62.

Planktonic indigenous gut microbiota (periods A-D), *C. difficile* TVC, spores, cytotoxin (periods B-D) and antimicrobial activity (periods C-D) were monitored during the experiment.

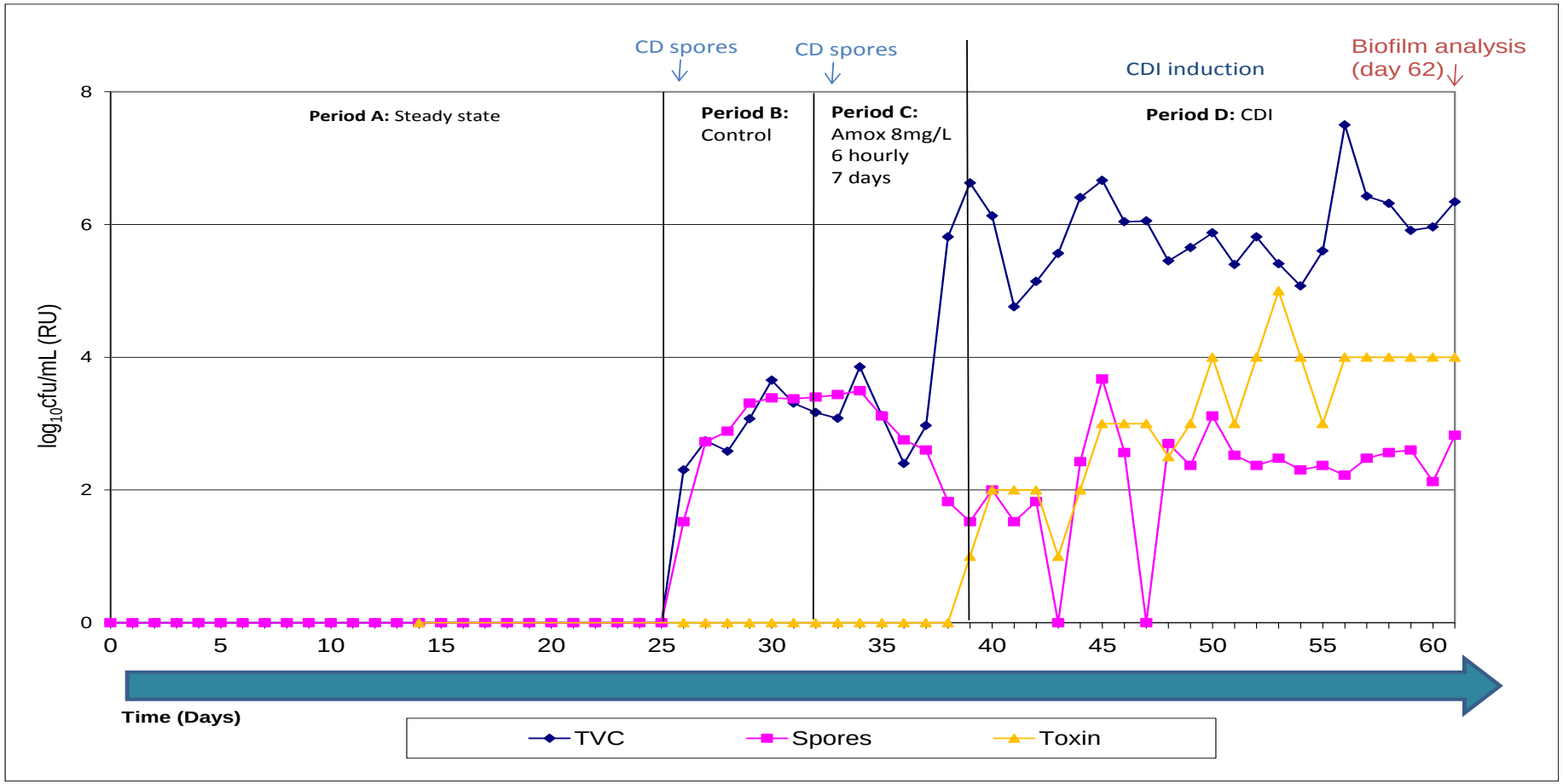

Figure 4.6.1: *C. difficile* results from vessel 3 of the original gut model and experimental design of human gut model prior to biofilm sampling[473]. Vertical line indicates last day of period. (CD: *C. difficile* PCR ribotype 027 (~10^7cfu); Amox: Amoxiclav).

4.6.2 Results

4.6.2.1 Indigenous Gut Microbiota Populations

On day 62, indigenous gut microbiota populations present within planktonic and sessile form within the gut model were dominated by *B. fragilis* group and *Clostridium* spp. (figure 4.6.2.1). All planktonic gut bacterial groups identified and enumerated in the original gut model (data not shown) were also present within the biofilm. Planktonic populations were greater than sessile populations for the anaerobic populations although sessile populations were greater for the facultative aerobes (facultative anaerobes, LFE, *Enterococcus* spp.). *Bifidobacterium* spp. were recovered in the biofilm although no result was obtained for the planktonic populations.

4.6.2.2 *C. difficile* Populations

C. difficile vegetative cells and spores were present in planktonic (figure 4.6.2.2) and sessile (figure 4.6.2.3) form in all three vessels of the human gut model.

Planktonic *C. difficile* TVCs were marginally greater in vessels 2 and 3 compared with their sessile counterparts, although TVCs of sessile *C. difficile* were greater than their planktonic counterparts in vessel 1 (~5.3 $\log_{10}$cfu/mL planktonic: ~7.2 $\log_{10}$cfu/mL sessile).

Vegetative cells were more populous in planktonic rather than sessile form in vessels 2 (~3.7 and 2.4 $\log_{10}$cfu/g for planktonic and sessile populations, respectively) and 3 (~2.7 and 1.3 $\log_{10}$cfu/g for planktonic and sessile populations, respectively) with the converse true in vessel 1 (~ 1 and 1.9 $\log_{10}$cfu/g for planktonic and sessile populations, respectively). Cytotoxin was detected in all 3 vessels in the planktonic culture and within the biofilm.

4.6.2.3 Antimicrobial Levels within the Planktonic Culture and Biofilm

Antimicrobial activity could not be demonstrated within the planktonic culture or biofilm of the human gut model using large plate in house bioassay.

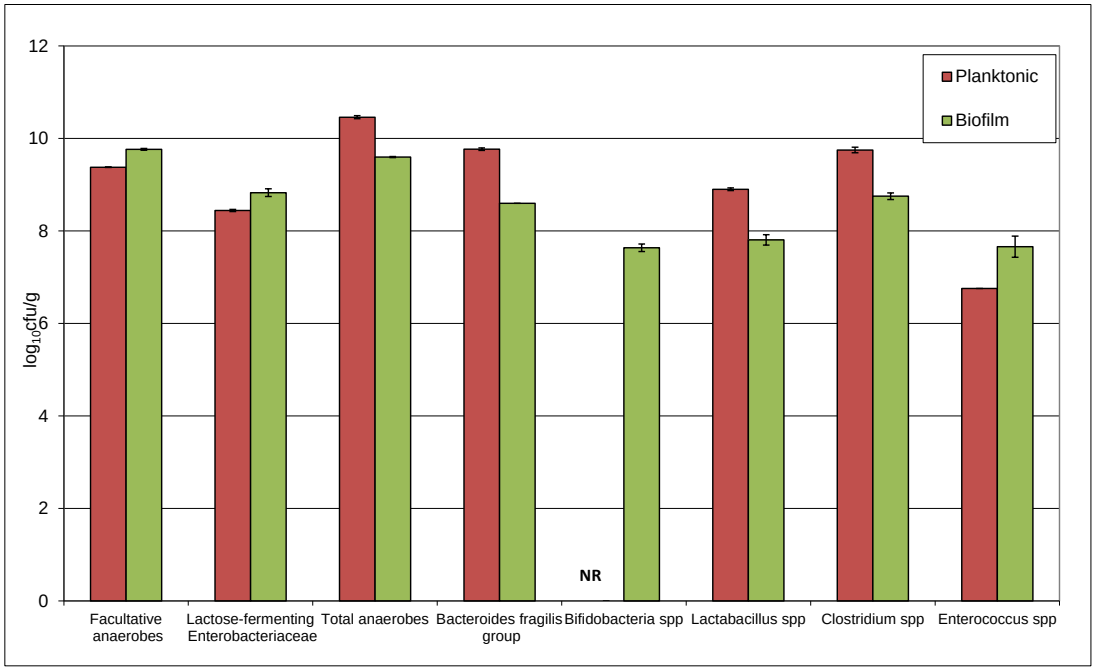

Figure 4.6.2.1: Mean (±SE) planktonic and biofilm populations (log_{10}cfu/g) of indigenous gut microbiota populations present in vessel 3 of the human gut model (NR- no result).

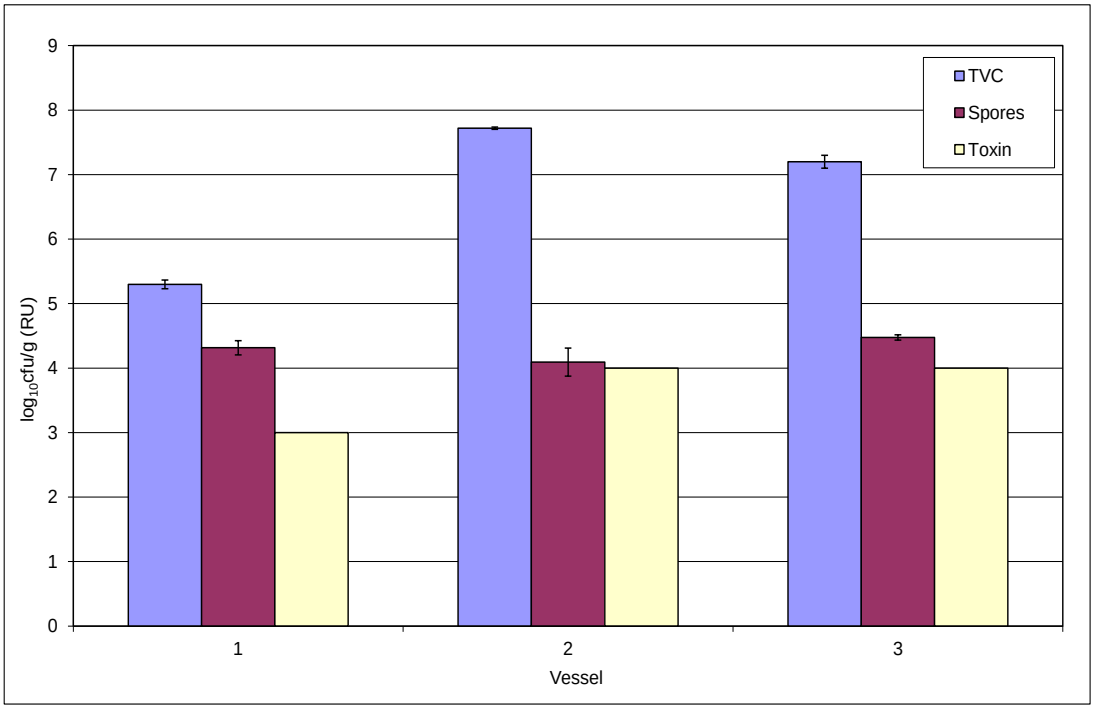

Figure 4.6.2.2: Mean (± SE) planktonic populations (log_{10}cfu/mL) of *C. difficile* total viable counts (TVC), spores and cytotoxin (RU) in vessel 1, 2 and 3 of the human gut model.

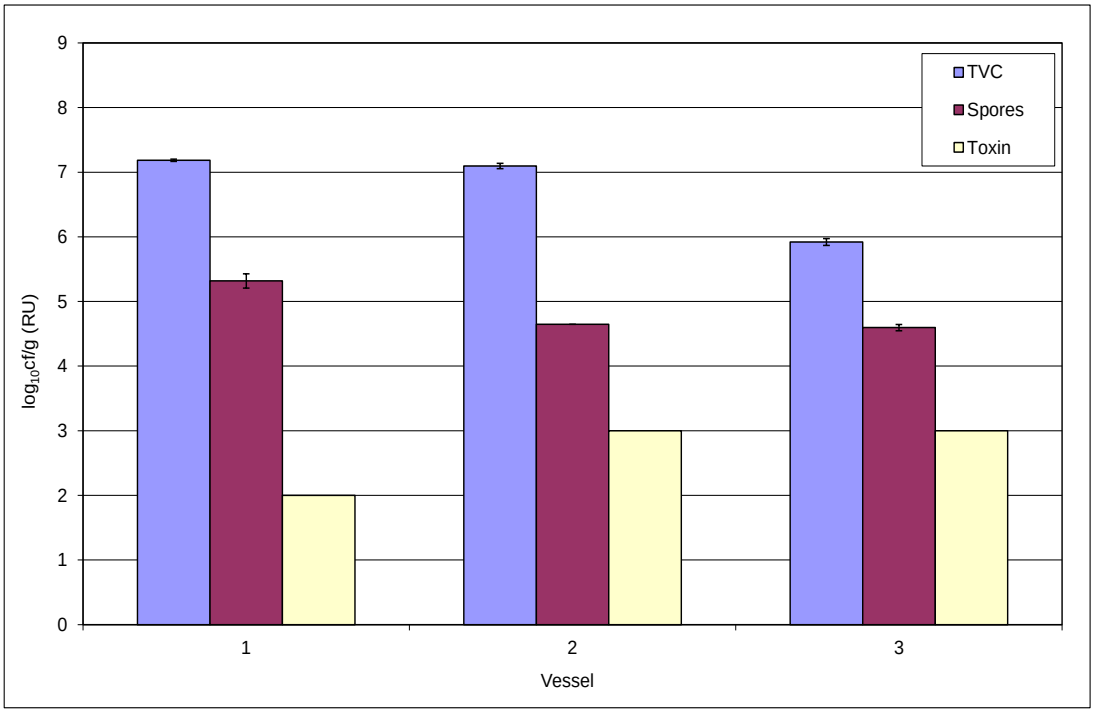

Figure 4.6.2.3: Mean (± SE) biofilm populations (log_{10}cfu/g) of *C. difficile* total viable counts (TVC), spores and cytotoxin (RU) in vessel 1, 2 and 3 of the human gut model.

4.6.3 Discussion

Before biofilm was removed and analysed, the gut model experiment had involved induction of simulated CDI using co-amoxiclav. *C. difficile* germination, proliferation and toxin production occurred in all three vessels. Toxin remained present in all three vessels until the end of the experiment. Vegetative cells and spores were detected within vessel 2 and 3 whilst only spores were present within vessel 1 (data not shown).

All indigenous gut microbiota bacterial groups present in the planktonic form were also present in sessile form. No result was obtained for the planktonic *Bifidobacterium* spp. populations during the biofilm analysis experiment; however results from the original gut model indicate that this bacterial group was present up until the completion of the experiment. It is therefore likely that populations will have also been present at the time of the biofilm analysis experiment but the absence may be due to experimental error, such as poor agar quality.

Within the planktonic culture fluid on day 62, *C. difficile* populations and toxin remained as described above (observations from the original experiment). Within the biofilm *C. difficile* existed in both vegetative and spore form, and toxin was detected in all vessels. The proportions of spores were higher in vessels 2 and 3 when compared with the planktonic form although the converse was true for vessel 1.

No antimicrobial activity was detected within the planktonic culture fluid or biofilm indicating that sequestration of co-amoxiclav into biofilm structures is not apparent.

4.7 Biofilm Analysis 5

4.7.1 Experimental Design

The triple stage human gut model experimental design is outlined in figure 44.7.1. Briefly, after inoculation with faecal emulsion, gut microbiota populations were allowed to equilibrate for 26 days (period A), before a single inoculum of *C. difficile* spores were added to vessel 1 of the model on day 26. A second inoculum of *C. difficile* spores were inoculated into the model on day 33. At this point a dosing regimen of clindamycin (33.9 mg/L, QD, 7 days) commenced (period C). Following commencement of clindamycin dosing no further intervention were made until *C. difficile* germination, proliferation and high toxin production was observed (period D). Instillation of vancomycin (125 mg/L, QD, 4 days) commenced on day 70 (period E). Following cessation of therapeutic instillation the model was left without intervention for 24 days (period F). Biofilm was sampled on day 97.

Planktonic indigenous gut microbiota (periods A-F), *C. difficile* TVC, spores, cytotoxin (periods B-F) and antimicrobial activity (periods C-F) were monitored during the experiment.

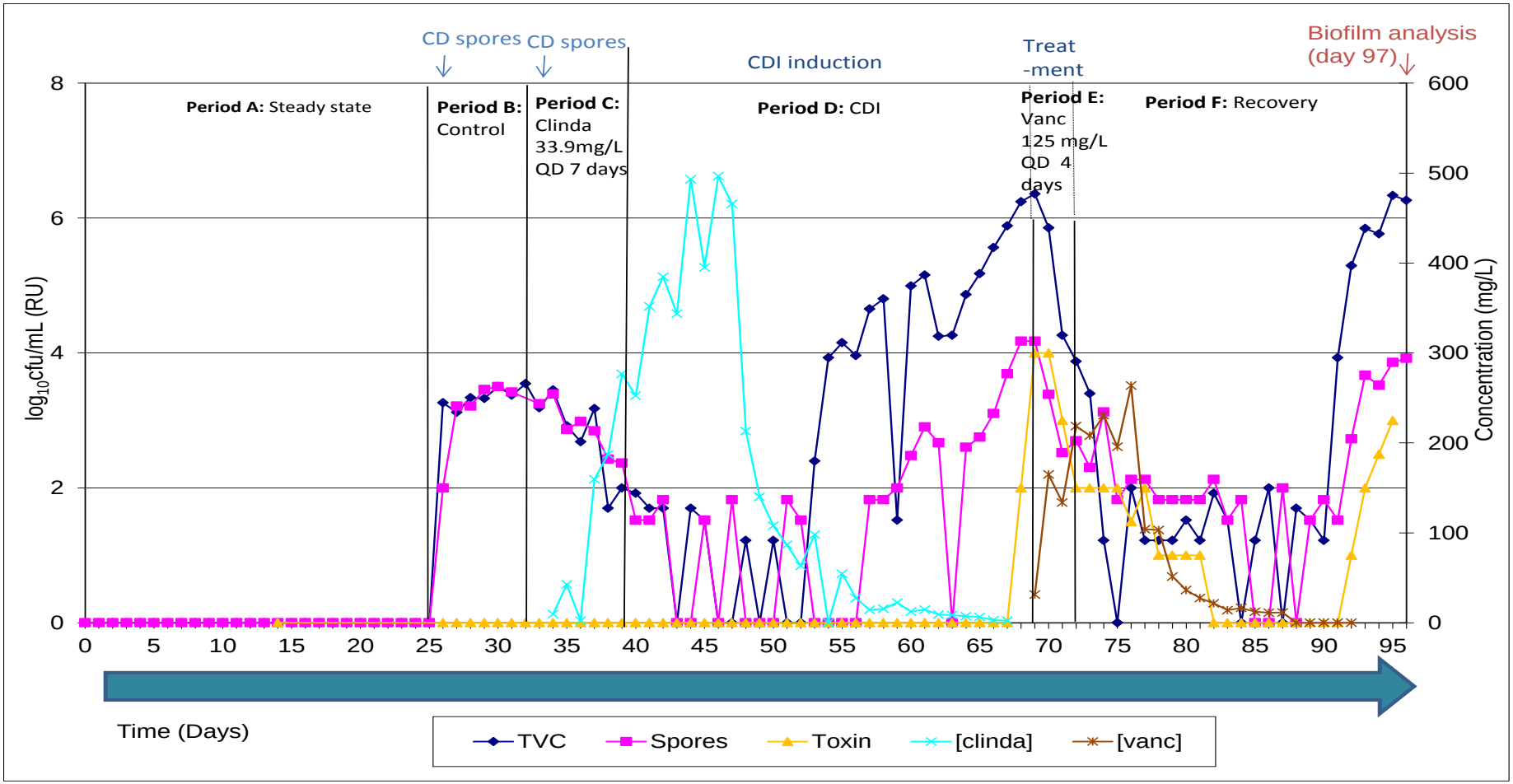

Figure 4.7.1: *C. difficile* results from vessel 3 of the original gut model and experimental design of human gut model prior to biofilm sampling[515]. Vertical line indicates last day of period. (CD: *C. difficile* PCR ribotype 027 (~10^7cfu); Vanc: vancomycin).

4.7.2 Results

4.7.2.1 Indigenous Gut Microbiota Populations

On day 97, indigenous gut microbiota populations present within planktonic form were also recovered at similar levels from the biofilm, and were dominated by *B. fragilis* group, *Lactobacillus* spp. and LFE (figure 4.7.2.1). Planktonic populations were greater than sessile populations for all groups identified (by ~0.5 – 1 $\log_{10}$cfu/g). *Bifidobacterium* spp. were present in both the planktonic and sessile form.

4.7.2.2 *C. difficile* Populations

C. difficile vegetative cells and spores were present in planktonic (figure 4.7.2.2) and sessile (figure 4.7.2.3) form in all three vessels of the human gut model. Planktonic *C. difficile* populations were generally greater than the sessile form (by ~1–2.5 $\log_{10}$cfu/g). Planktonic vegetative cell populations were 1. -2.5 $\log_{10}$cfu/g with spore populations of ~5.5-5.9 $\log_{10}$cfu/g in all vessels. Sessile *C. difficile* spore populations were ~5 $\log_{10}$cfu/g in all three vessels, with vegetative populations of ~2.2 $\log_{10}$cfu/g vessels 1 and ~0.7 $\log_{10}$cfu/g in vessel 2. Cytotoxin was detected in all vessels within the planktonic culture and biofilm with the exception of the biofilm in vessel 1.

4.7.2.3 Antimicrobial Levels within the Planktonic Culture and Biofilm

Antimicrobial activity from the experiment designed to detect clindamycin activity was detected in within the biofilm of vessel 2 (9.9 mg/L) and 3 (10.0 mg/L). Antimicrobial activity from the experiment designed to detect vancomycin activity was present within the biofilm at concentrations

of 70 mg/L and 67.7 mg/L in vessel 2 and 3 respectively. No antimicrobial activity was detected in the planktonic culture fluid from any vessel.

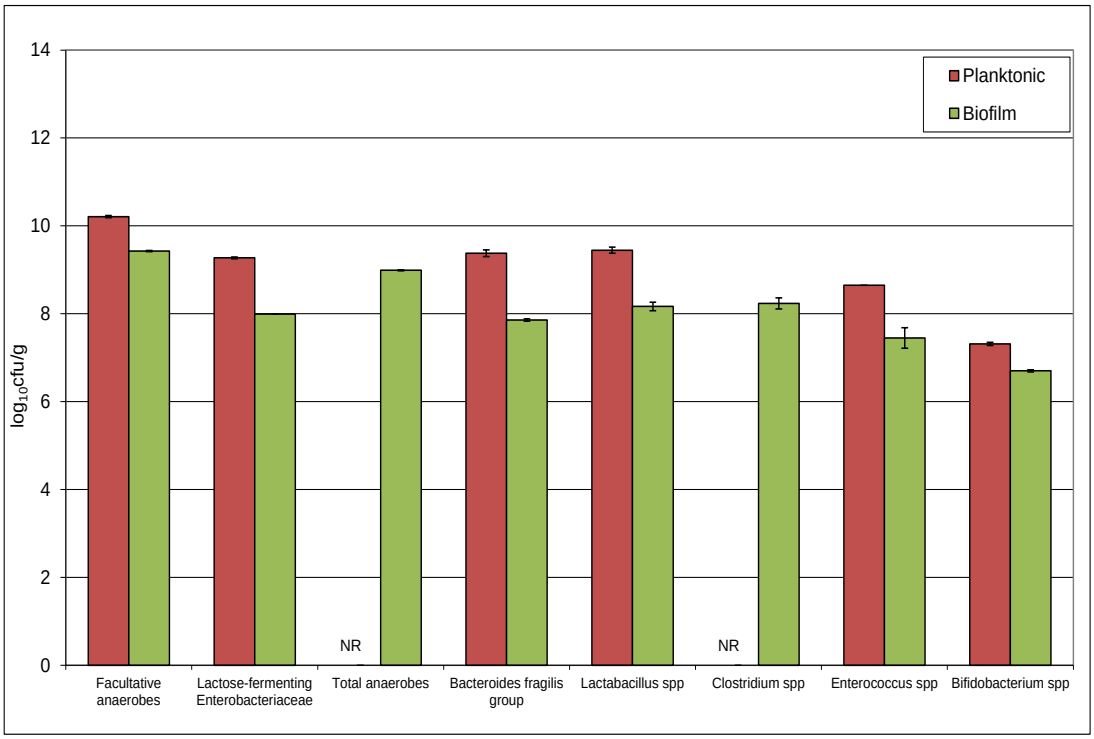

Figure 4.7.2.1: Mean (±SE) planktonic and biofilm populations (log_{10}cfu/g) of indigenous of indigenous gut microbiota populations present in vessel 3 of the human gut model (NR- no result).

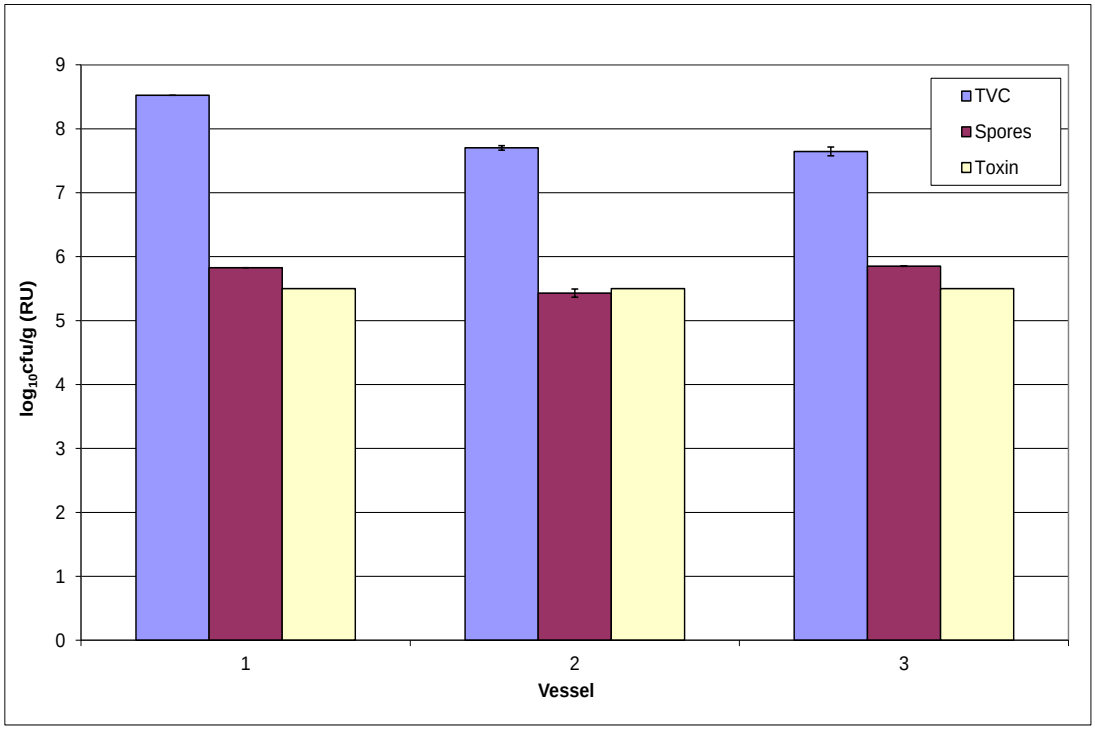

Figure 4.7.2.2: Mean (± SE) planktonic populations (log_{10}cfu/g) of *C. difficile* total viable counts (TVC), spores and cytotoxin (RU) in vessel 1, 2 and 3 of the human gut model.

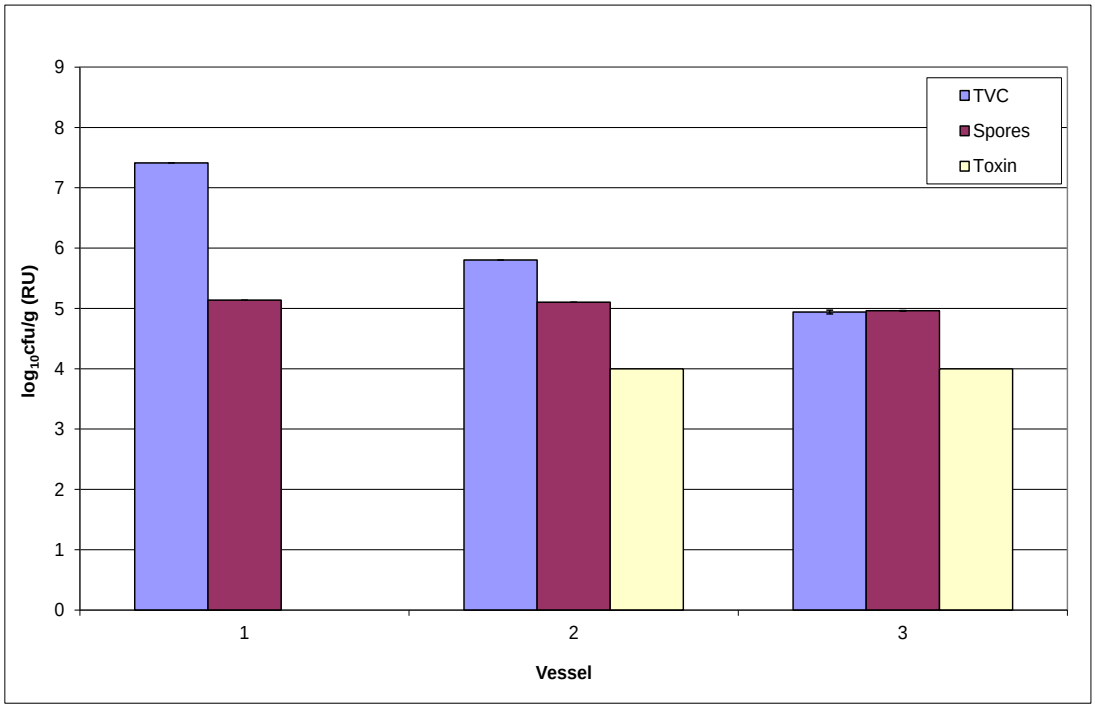

Figure 4.7.2.3: Mean (±SE) biofilm populations (log_{10}cfu/g) of *C. difficile* total viable counts (TVC), spores and cytotoxin (RU) in vessel 1, 2 and 3 of the human gut model.

4.7.3 Discussion

The original gut model experimental design for this experiment involved clindamycin-induced simulated CDI followed by a treatment regimen of a short course of vancomycin. Initial treatment appeared successful; however, in the final 3-6 days of the experiment recurrent CDI occurred with increasing levels of *C. difficile* germination, proliferation and toxin production in all vessels.

Populations of indigenous gut microbiota present in planktonic form on day 97 were also present in sessile form. No results were obtained for sessile total anaerobe and clostridial bacterial groups due to media contamination.

Planktonic *C. difficile* results from the biofilm analysis experiment reported *C. difficile* vegetative cells, spores and cytotoxin in all vessels. *C. difficile* populations within biofilms demonstrated the presence of vegetative cells and spores in vessel 1 although toxin was not detected. Within vessels 2 and 3, *C. difficile* was only present as spores, and toxin was detected.

Antimicrobial activity was detected within the biofilm of vessel 2 and 3 despite its absence in the planktonic culture fluid. Clindamycin and vancomycin were the antimicrobial agents used in the original gut model experiment and the assays designed for the detection of each antimicrobial agent provided positive results. It is therefore difficult to delineate which antimicrobial agent has been detected within the biofilm. Vancomycin is the most likely due to its more recent administration into the original gut model, although neither agent utilised previously in the model and subsequent biofilm analysis experiments has provided positive activity within the biofilm.

4.8 Biofilm Analysis 6

4.8.1 Experimental Design

The triple stage human gut model experimental design is outlined in figure 4.8.1. Briefly, after inoculation with faecal emulsion, gut microbiota populations were allowed to equilibrate for 27 days (period A), before a single inoculum of *C. difficile* PCR ribotype 001 spores (table 3.1) were added to vessel 1 of the model on day 27. A second inoculum of *C. difficile* spores were inoculated into the model on day 34. At this point a dosing regimen of clindamycin (33.9 mg/L, QD, 7 days) commenced (period C). Following commencement of clindamycin dosing no further intervention were made until *C. difficile* germination, proliferation and high toxin production was observed (period D). A novel CDI therapeutic drug was used in this experiment. Data have not yet been published and are confidential; therefore, this agent is referred to here as drug Z. Instillation of drug Z (250 mg/L, BD, 7 days) commenced on day 52 (period E). Following cessation of therapeutic instillation the model was left without intervention for 20 days (period F). Biofilm was sampled on day 79. Planktonic indigenous gut microbiota (periods A-F), *C. difficile* TVC, spores, cytotoxin (periods B-F) and antimicrobial activity (periods C-F) were monitored during the experiment.

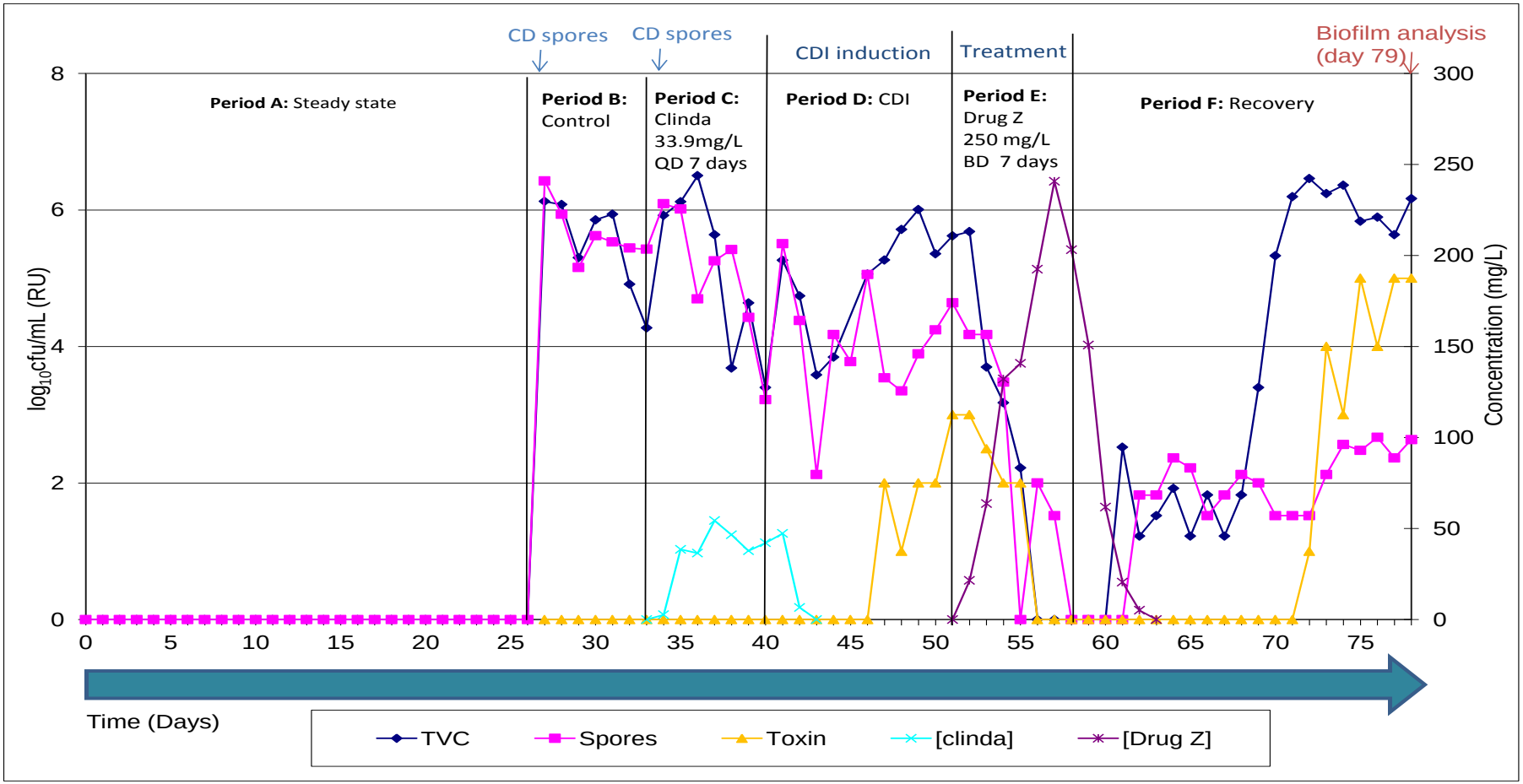

Figure 4.8.1: *C. difficile* results from vessel 3 of the original gut model and experimental design of human gut model prior to biofilm sampling. Vertical line indicates last day of period. (CD: *C. difficile* PCR ribotype 001 (~10^7cfu); Clinda: clindamycin).

4.8.2 Results

4.8.2.1 Indigenous Gut Microbiota Populations

On day 79, *Bifidobacterium* spp. populations were the dominant bacterial group identified and enumerated in the human gut model and planktonic populations were up to ~2 log_{10}cfu/g greater than sessile populations (figure 4.8.2.1). All bacterial groups identified and enumerated from this model were present in both planktonic and sessile form and the relative populations of each bacterial group were similar. Planktonic populations were slightly greater for most bacterial groups other than LFE and *Enterococcus* spp., which presented greater sessile populations compared with the planktonic populations.

4.8.2.2 *C. difficile* Populations

C. difficile vegetative cells and spores were present in planktonic (figure 4.8.2.2) and sessile (figure 4.8.2.3) form in all three vessels of the human gut model; the exception was the absence of planktonic spores in vessel 1. TVCs of planktonic *C. difficile* were ~1 log_{10}cfu/g greater than sessile TVCs in vessels 2 and 3. Sessile TVCs were ~1 log_{10}cfu/g greater than planktonic TVCs. Planktonic *C. difficile* populations comprised solely vegetative cells (~6.2 log_{10}cfu/g) in vessel 1 whilst sessile communities displayed spore and vegetative populations of ~5.5 log_{10}cfu/g and ~2.0 log_{10}cfu/g, respectively. Cytotoxin was detected in all vessels within the planktonic culture and biofilm.

4.8.2.3 Antimicrobial Levels within the Planktonic Culture and Biofilm

No active antimicrobial activity was detected within the gut model at this stage of the experiment.

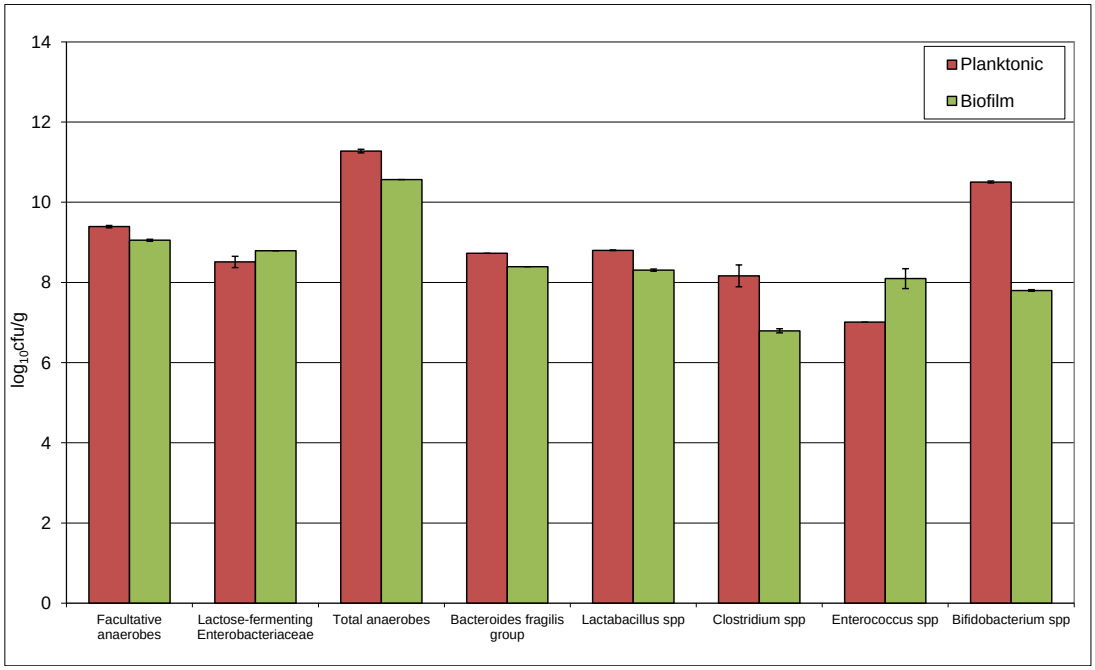

Figure 4.8.2.1: Mean (±SE) planktonic and biofilm populations (log_{10}cfu/g) of indigenous of indigenous gut microbiota populations present in vessel 3 of the human gut model.

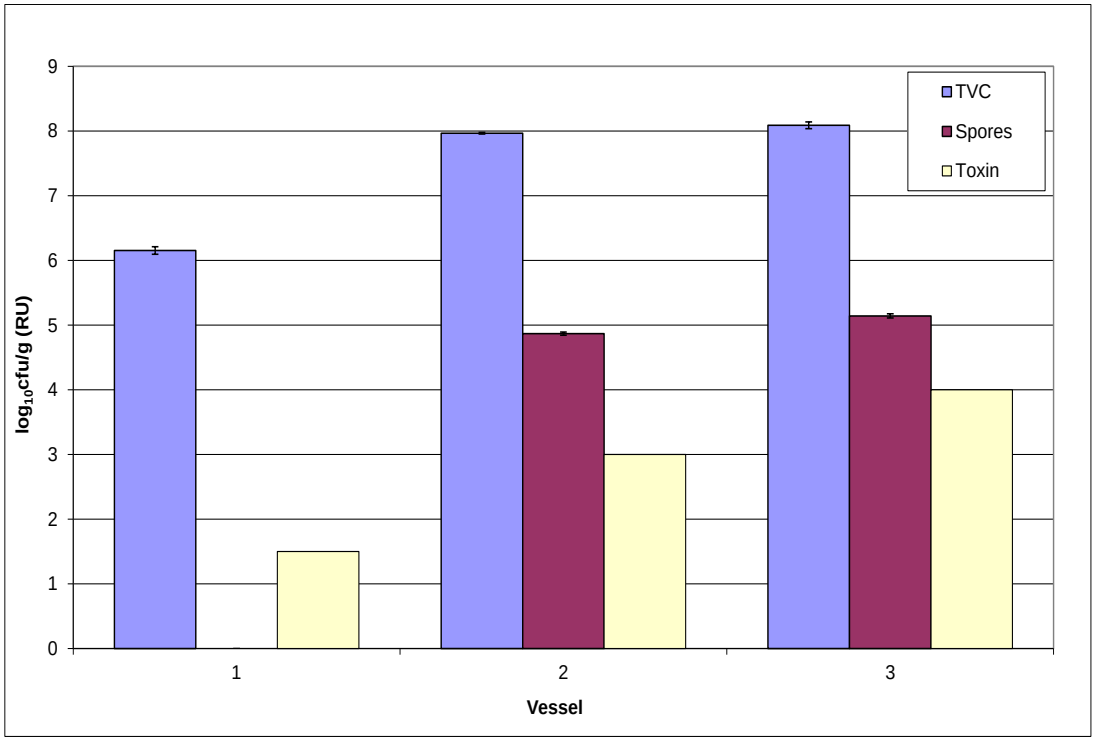

Figure 4.8.2.2: Mean (± SE) planktonic populations (log_{10}cfu/g) of *C. difficile* total viable counts (TVC), spores and cytotoxin (RU) in vessel 1, 2 and 3 of the human gut model.

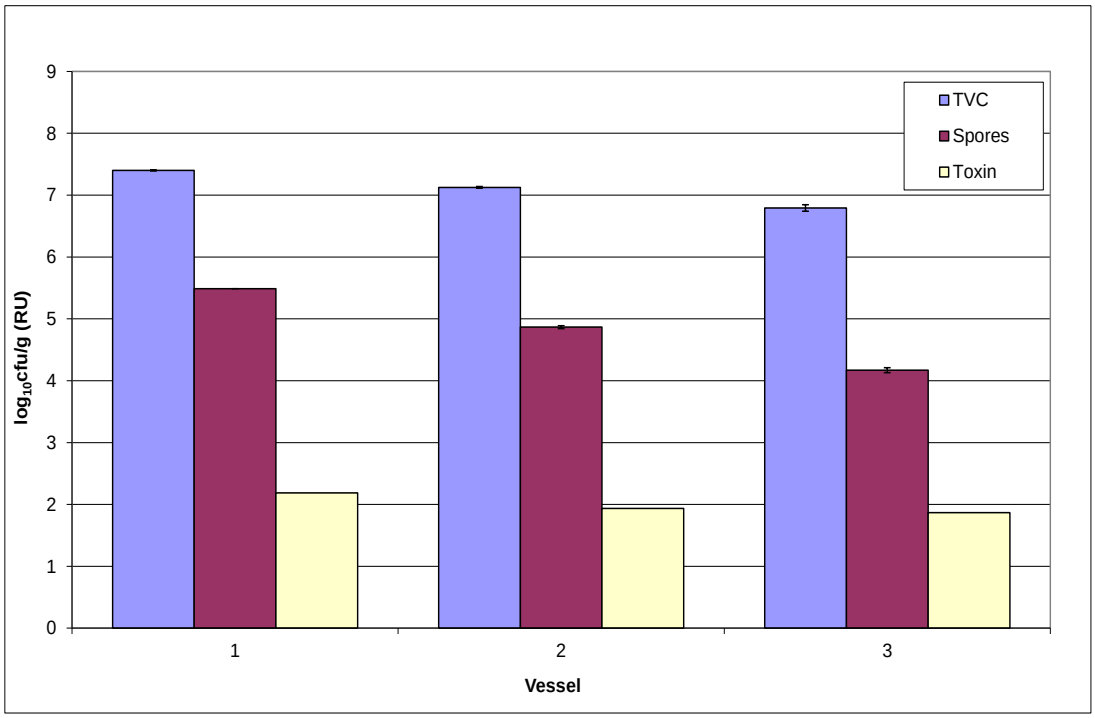

Figure 4.8.2.3: Mean (±SE) biofilm populations (log10cfu/g) of *C. difficile* total viable counts (TVC), spores and cytotoxin (RU) in vessels 1, 2 and 3 of the human gut model.

4.8.3 Discussion

The original gut model experimental design prior to biofilm analysis involved clindamycin induced CDI (PCR ribotype 001 strain) followed by a treatment dosing regimen of drug Z. Treatment was initially successful although recurrence of simulated CDI was evident before the end of the experiment with *C. difficile* germination and proliferation in all vessels and toxin production in vessels 2 (data no shown) and 3 (figure 4.8.1).

Planktonic indigenous microbiota populations were also present in sessile form, and antimicrobial activity was absent from the planktonic culture fluid and biofilm in all vessels. Results from the biofilm analysis experiment shows that planktonic *C. difficile* comprised vegetative cells and spores (vegetative cells only vessel 1), and that toxin was present in all vessels. In the biofilm, vegetative cells, spores and toxin were present in all vessels. The proportion of sessile spores was greater than the planktonic form. This has previously been observed in biofilm analysis 1 and 4 and discussed in 4.13.

4.9 Biofilm Analysis 7

4.9.1 Experimental Design

The triple stage human gut model experimental design is outlined in figure 4.9.1. Briefly, after inoculation with faecal emulsion, gut microbiota populations were allowed to equilibrate for 10 days (period A), before a single inoculum of *C. difficile* PCR ribotype 027 spores (table 3.1) were added to vessel 1 of the model on day 10. A second inoculum of *C. difficile* PCR ribotype 027 spores were inoculated into the model on day 17. At this point a dosing regimen of clindamycin (33.9 mg/L, QD, 7 days) commenced (period C). Following commencement of clindamycin dosing, no further interventions were made until *C. difficile* germination, proliferation and high toxin production was observed (period D). Instillation of drug Z (250 mg/L, BD, 7 days) commenced on day 33 (period E). Following cessation of therapeutic instillation, the model was left without intervention for 20 days (period F). Biofilm was sampled on day 60. Planktonic indigenous gut microbiota (periods A-F), *C. difficile* TVC, spores, cytotoxin (periods B-F) and antimicrobial activity (periods C-F) were monitored during the experiment.

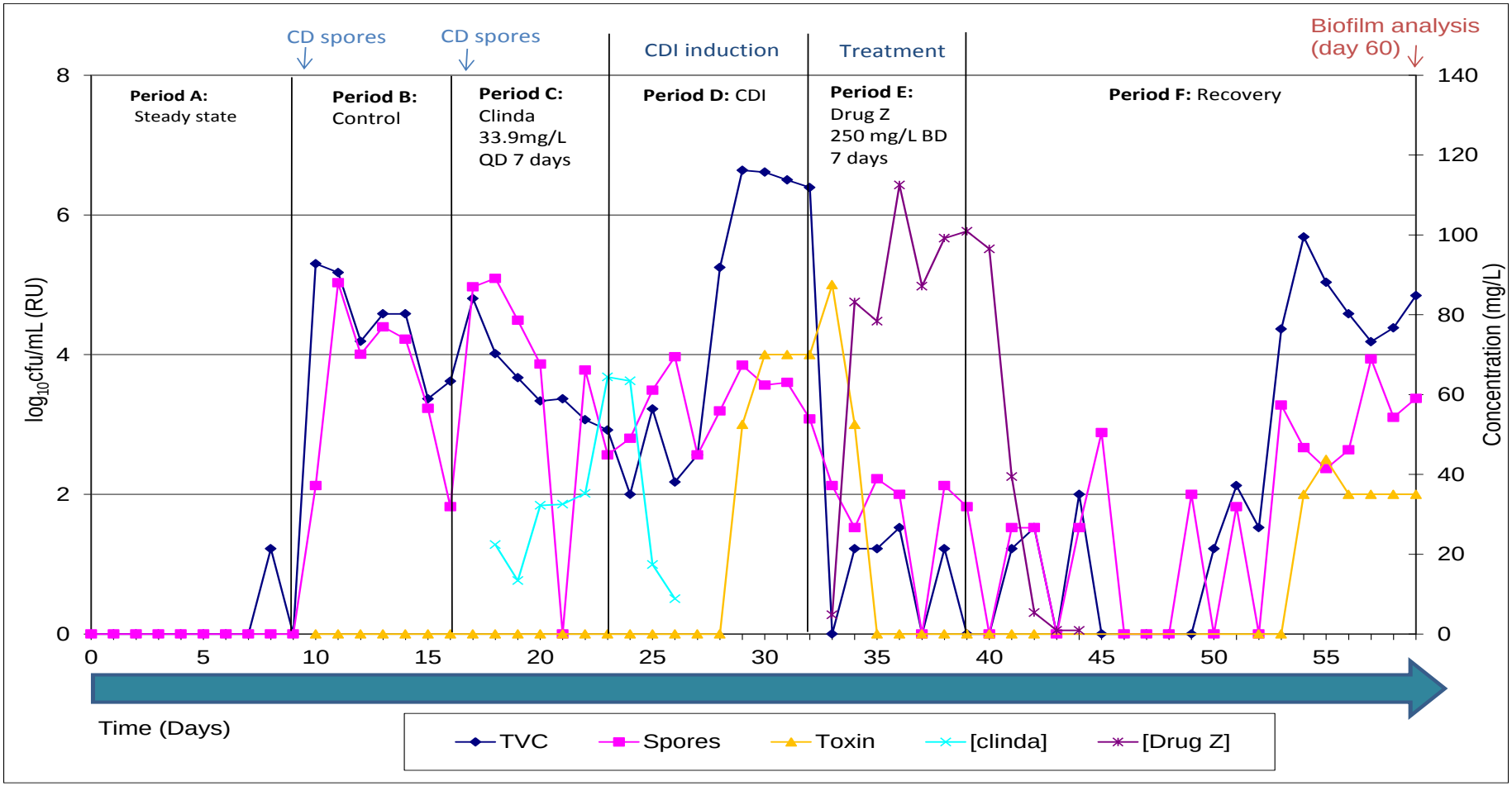

Figure 4.9.1: *C. difficile* results from vessel 3 of the original gut model and experimental design of human gut model prior to biofilm sampling. Vertical line indicates last day of period. (CD: *C. difficile* PCR ribotype 027 (~10^7cfu); Clinda: clindamycin).

4.9.2 Results

4.9.2.1 Indigenous Gut Microbiota Populations

On day 60, all planktonic gut bacterial groups identified and enumerated in the original gut model were also present within the biofilm (figure 4.9.2.1). Populations of anaerobic bacterial populations such as *Clostridium* spp., *Bifidobacterium* spp., and *B. fragilis* group were the most prevalent bacterial groups. All bacterial species which are enumerated aerobically (facultative anaerobes, LFE, *Enterococcus* spp.) displayed greater sessile populations compared with their planktonic counterparts, whilst the converse was true for the anaerobic bacterial populations enumerated.

4.9.2.2 *C. difficile* Populations

Sessile and planktonic spore populations were ~5 $\log_{10}$cfu/g in all vessels (figures 4.9.2.2 and 4.9.2.3). Vegetative *C. difficile* populations of ~2 $\log_{10}$cfu/g were present in all vessels in planktonic form and vessel 1 of the biofilm, with vegetative cells of ≤ 1 $\log_{10}$cfu/g present in vessels 2 and 3 of the biofilm (figures 4.9.2.2 and 4.9.2.3). Cytotoxin was detected in all vessels within the planktonic culture and biofilm.

4.9.2.3 Antimicrobial Levels within the Planktonic Culture and Biofilm

Antimicrobial activity was detected using the clindamycin bioassay method. A concentration of ~19.6 mg/L was detected within the biofilm of vessel 1 only. Antimicrobial activity was absent from the planktonic culture fluid of all vessels of the human gut model. No antimicrobial activity was detected using the drug Z bioassay methodology.

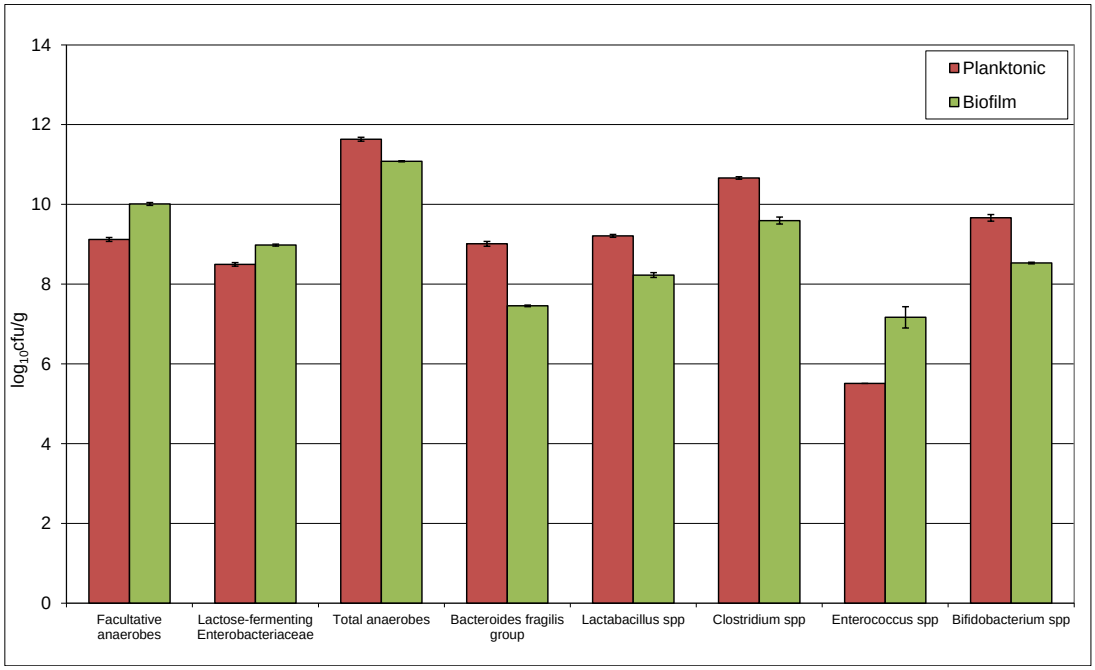

Figure 4.9.2.1: Mean (±SE) planktonic and biofilm populations (log_{10}cfu/g) of indigenous of indigenous gut microbiota populations present in vessel 3 of the human gut model.

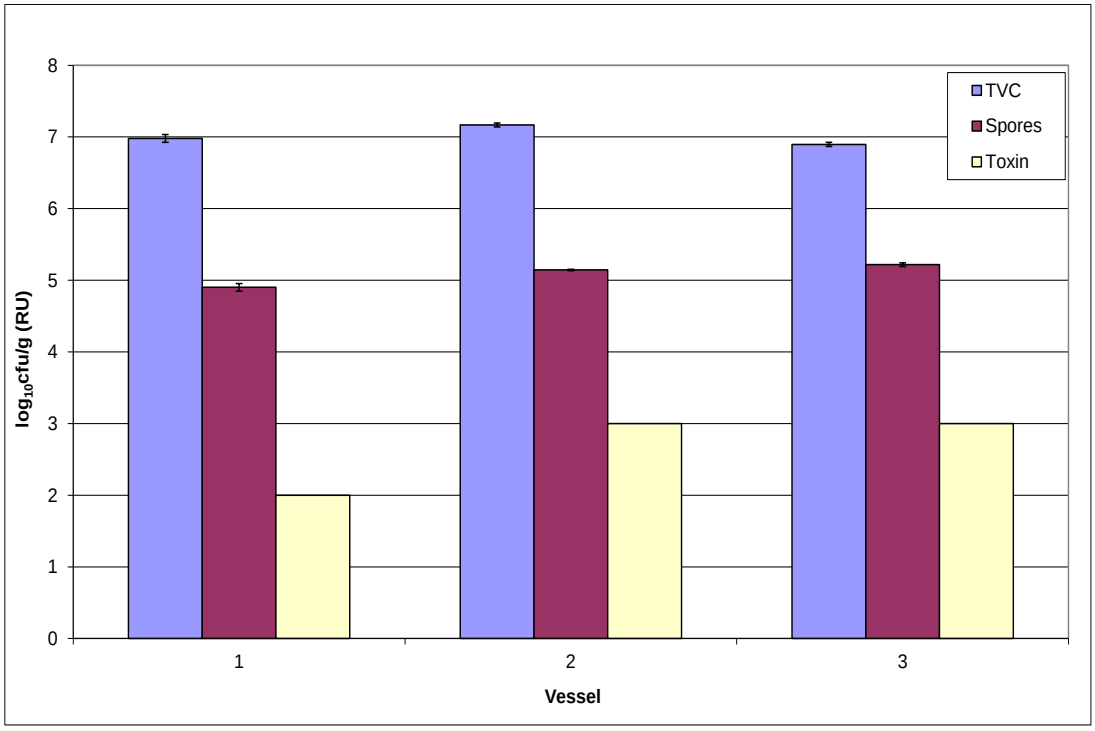

Figure 4.9.2.2: Mean (± SE) planktonic populations (log_{10}cfu/g) of *C. difficile* total viable counts (TVC), spores and cytotoxin (RU) in vessel 1, 2 and 3 of the human gut model.

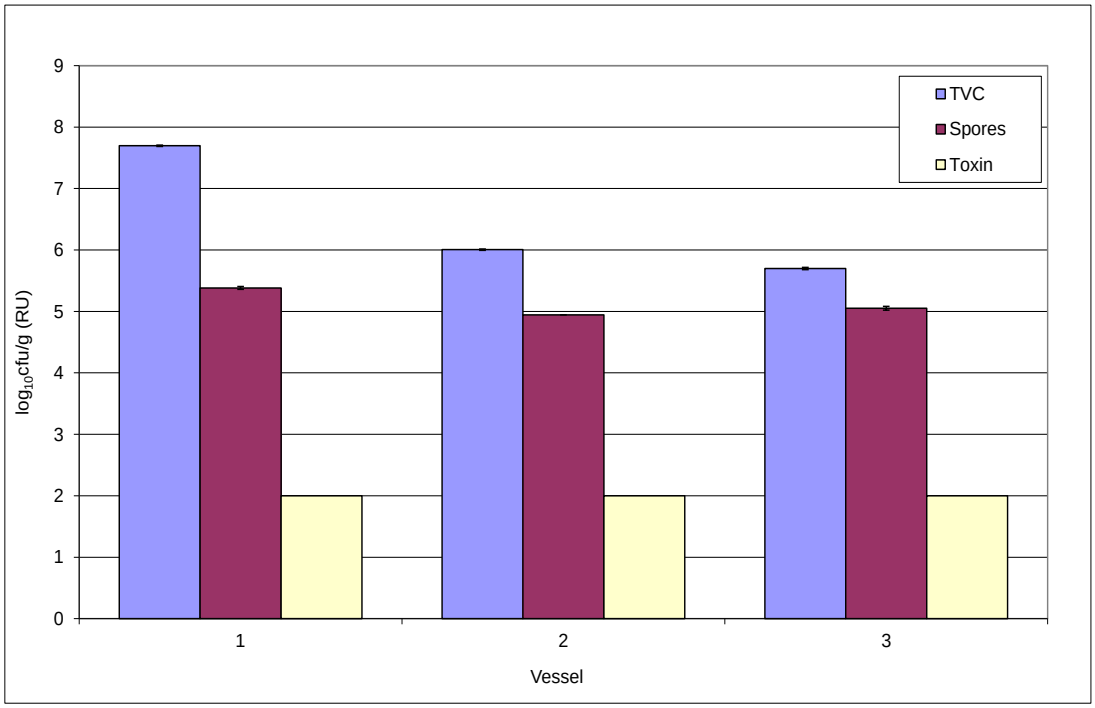

Figure 4.9.2.3: Mean (±SE) biofilm populations (log_{10}cfu/g) of *C. difficile* total viable counts (TVC), spores and cytotoxin (RU) in vessel 1, 2 and 3 of the human gut model.

4.9.3 Discussion

The original gut model experimental design prior to biofilm analysis involved clindamycin-induced CDI (PCR ribotype 027 strain) followed by a treatment dosing regimen of drug Z. Treatment was initially successful although recurrence of infection was evident as described in the previous experiment (biofilm analysis 6).

Results from the biofilm analysis experiment shows that both planktonic and sessile *C. difficile* were comprised of vegetative cells and spores, and that toxin was present in all vessels. Once again the proportion of sessile spores (most notably in vessels 2 and 3) were greater than the planktonic form.

In this experiment, using *C. difficile* PCR ribotype 027, sessile *C. difficile* populations in vessel 2 and 3 are dominated by spores. The same experiment using PCR ribotype 001 strain (biofilm analysis 6) found sessile vegetative cells and spores in vessel 2 and 3. The reduced numbers of ribotype 027 vegetative cells was also evident within the planktonic phase, therefore does not appear to be a unique characteristic of sessile cells. Inter-strain spore coat heterogeneity is thought to exist within *C. difficile*. *C. difficile* spores form exosporial protrusions that can facilitate adherence to surfaces [149]. Different spore coat structures may confer a greater ability to form these extensions, thereby increasing the adherence of certain spore strains. Furthermore, association of *C. difficile* with colonic mucosa was evident within hamsters and appeared to be strain specific[121] and batch culture experiments (chapter 3.0) evaluated the adherence capacity of different *C. difficile* ribotypes, with PCR ribotype 001, displaying reduced capabilities compared with other strains. Moreover, it has been demonstrated that sporulation capacity is strain dependent, with reports highlighting the increased sporulation of 027 spores [144]. These observations may explain differences in sessile and planktonic spore populations of ribotype 027 strains compared with 001.

Antimicrobial activity was not detected 4 days post-clindamycin and 5 days post-drug Z instillation within the original gut model. On day 60, antimicrobial activity was detected in the biofilm of vessel 1 only, indicating sequestration of one of these agents into the biofilm structure. Antimicrobial activity has not been detected within the biofilm in previous clindamycin-exposed biofilm analysis experiments; therefore, it is unlikely that the activity with the biofilm is due to clindamycin.

Drug Z is a novel lipopeptide structurally related to daptomycin. Diffusion of daptomycin into biofilm structures has been previously noted,[526] although to our knowledge there are no data pertaining to the persistence of drug Z within biofilms. The data presented here provide evidence of the possible sequestration and persistence of drug Z in biofilm structures; however, this was not observed in biofilm analysis 6.

4.10 Biofilm Analysis 8

4.10.1 Experimental Design

The triple stage human gut model experimental design is outlined in table 4.10.1. Briefly, after inoculation with faecal emulsion, gut microbiota populations were allowed to equilibrate for 20 days (period A), before a single inoculum of *C. difficile* PCR ribotype 027 spores (table 3.1) were added to vessel 1 of the model on day 20. A second inoculum of *C. difficile* PCR ribotype 027 spores were inoculated into the model on day 27. At this point a dosing regimen of clindamycin (33.9 mg/L, QD, 7 days) commenced (period C). Following commencement of clindamycin dosing no further intervention were made until *C. difficile* germination, proliferation and high toxin production was observed (period D). Instillation of metronidazole (9.6 mg/L, TD, 7 days) commenced on day 54 (period E). Following cessation of therapeutic instillation the model was left without intervention for 8 days (period F) before instillation secondary therapeutic agent, fidaxomicin (125 mg/L, BD, 7 days) commenced on day 69 (period G). Following cessation of secondary therapeutic instillation the model was left without intervention for 23 days (period H). Biofilm was sampled on day 99. Planktonic indigenous gut microbiota (periods A-H), *C. difficile* TVC, spores, cytotoxin (periods B-H) and antimicrobial activity (periods C-H) were monitored during the experiment.

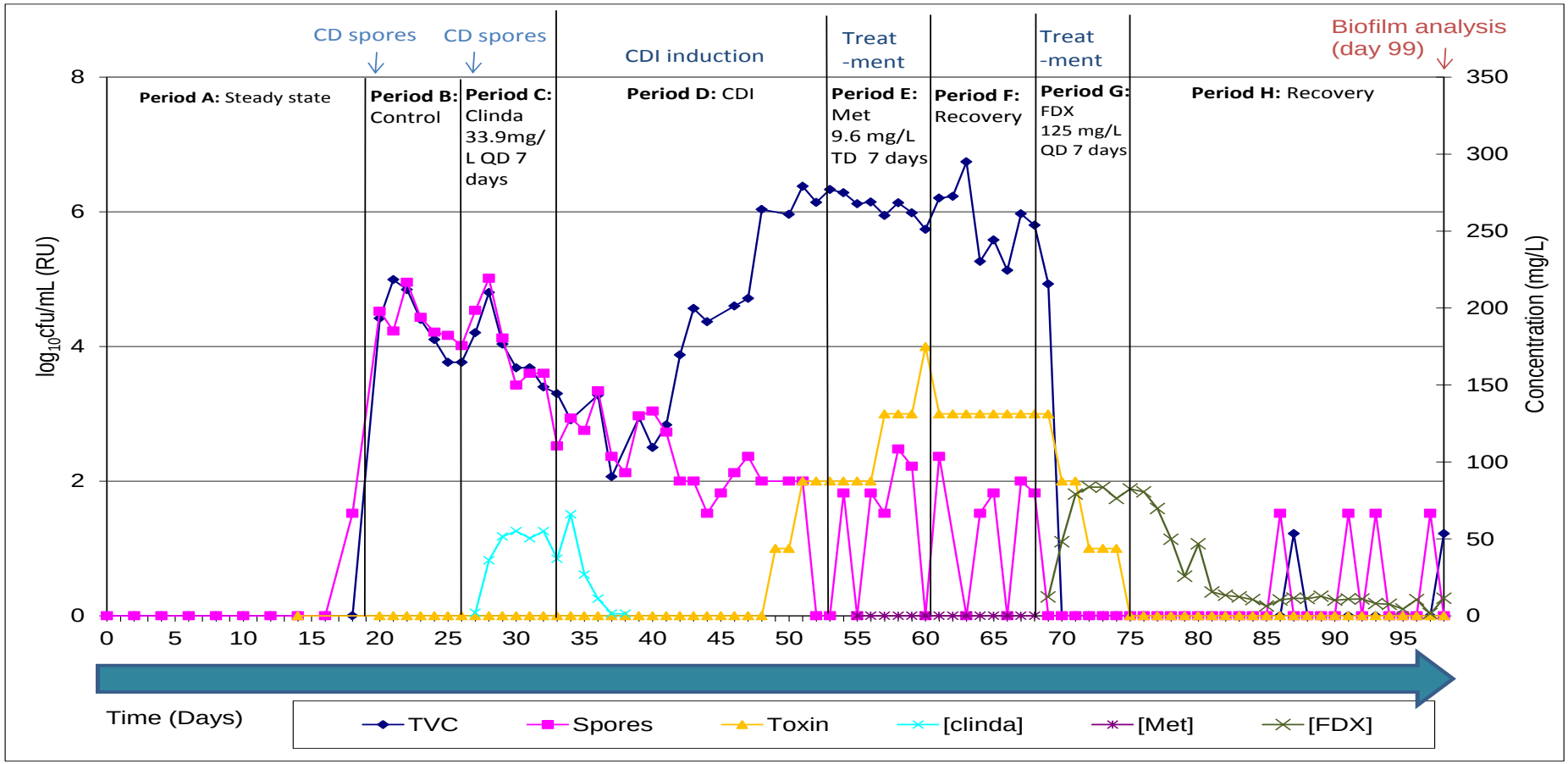

Figure 4.10.1: *C. difficile* results from vessel 3 of the original gut model and experimental design of human gut model prior to biofilm sampling[527]. Vertical line indicates last day of period. (CD: *C. difficile* PCR ribotype 027 (~10^7cfu); Clinda: clindamycin; Met: metronidazole; FDX: fidaxomicin). TVC – total viable count

4.10.2 Results

4.10.2.1 Indigenous Gut Microbiota Populations

All bacterial species identified and enumerated within the planktonic populations were also present within the biofilm and at similar levels (figure 4.10.2.1). *Bifidobacterium* spp. were not recovered in either form in this experiment. Planktonic populations were generally greater than their sessile counterparts, with the greatest difference observed in the *B. fragilis* group, for which planktonic populations outnumbered sessile populations by ~1 $\log_{10}$cfu/g.

4.10.2.2 *C. difficile* Populations

Planktonic *C. difficile* was only detected at a population of ~3 $\log_{10}$cfu/g in vessel 3 (figure 4.10.2.2). Sessile *C. difficile* populations comprised ~3.5 $\log_{10}$cfu/g spores and ~2 $\log_{10}$cfu/g vegetative cells in vessel 2 and ~4.2 $\log_{10}$cfu/g spores and ~0.7 $\log_{10}$cfu/g vegetative cells in vessel 3 (figure 4.10.2.3). *C. difficile* was not recovered from vessel 1 in sessile or planktonic form. Cytotoxin was not detected in any vessel within the planktonic phase or biofilm.

4.10.2.3 Antimicrobial Levels within the Planktonic Culture and Biofilm

The clindamycin bioassay method measured active antimicrobial levels in the planktonic culture fluid of ~1.9 and 5.6 mg/L in vessels 2 and 3 respectively, with no detectable activity in vessel 1. Levels of activity within the biofilm of vessels 1 and 2 are 11.7 and 6.4 mg/L respectively, with no detectable activity in vessel 3. Active antimicrobial concentrations measured using the fidaxomicin methodology states that antimicrobial levels were 2.3 and 7.3 mg/L in planktonic culture fluid in vessels 2 and 3, respectively,

with no detectable activity in vessel 1. Levels of activity within the biofilm of vessels 1, 2 and 3 are 14.3, 7.8 and 10.1 mg/L, respectively. Levels of active antimicrobial measured using the metronidazole methodology were 1.5 and 4.9 mg/L in planktonic samples from vessel 2 and 3, respectively. No activity was detected in the planktonic fluid of vessel 1. Antimicrobial activity was detected at 13.5, 6.7 and 6.8 mg/L, within the biofilm of vessel 1, 2 and 3, respectively.

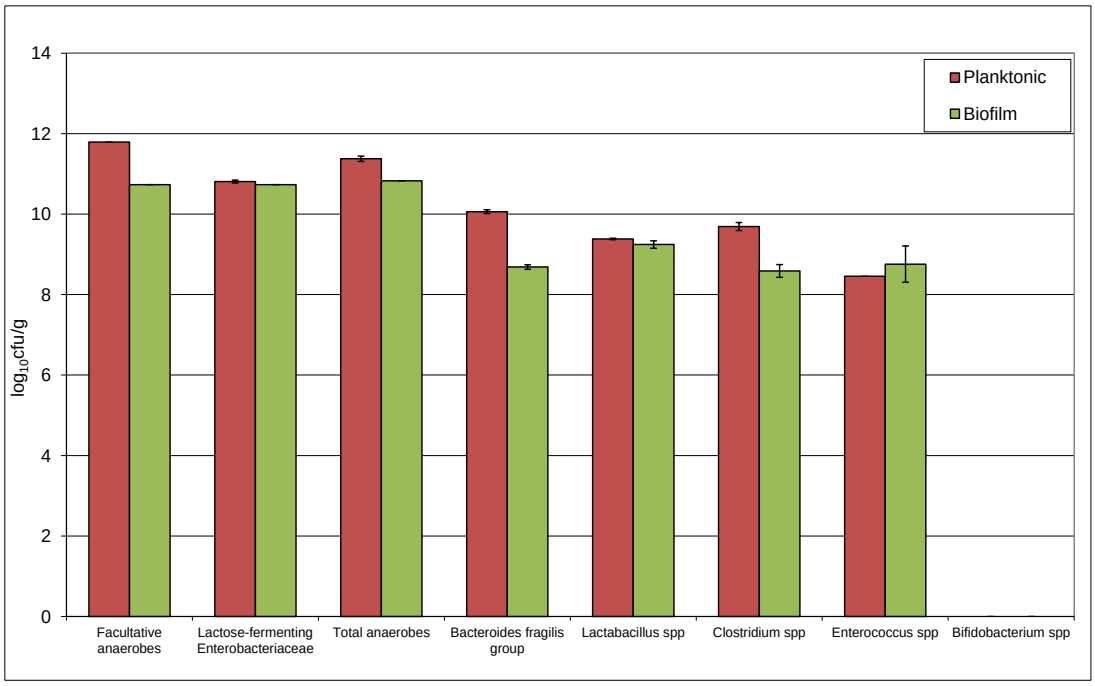

Figure 4.10.2.1: Mean (±SE) planktonic and biofilm populations (log_{10}cfu/g) of indigenous of indigenous gut microbiota populations present in vessel 3 of the human gut model.

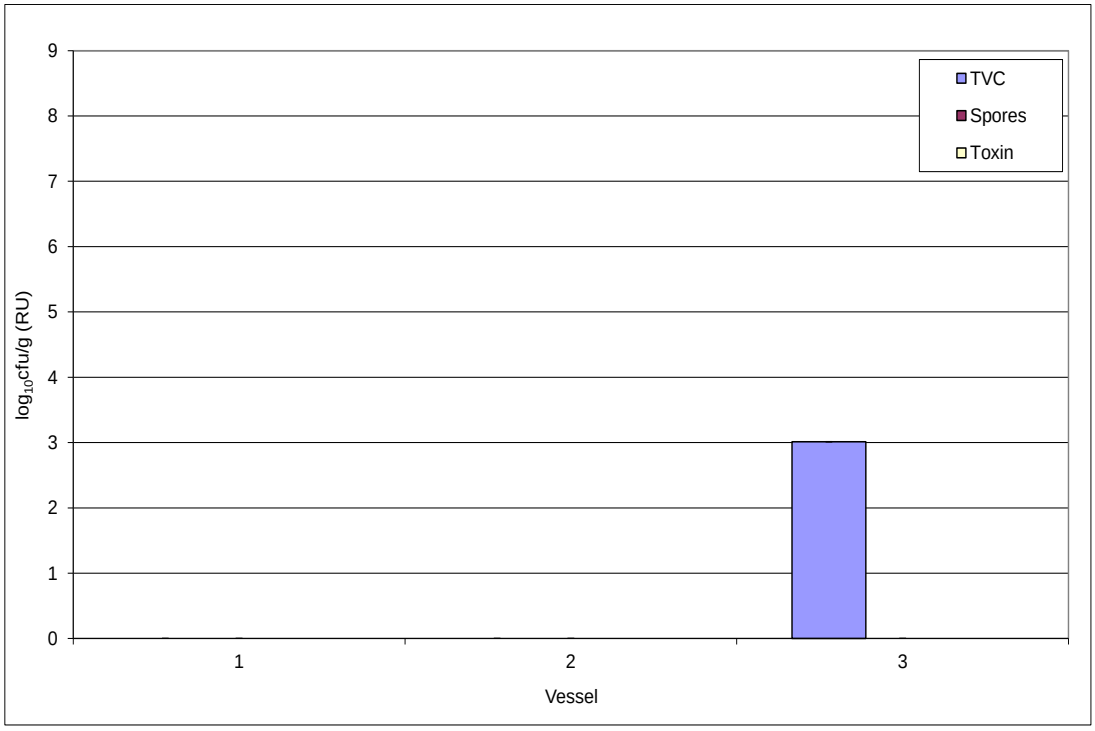

Figure 4.10.2.2: Mean (± SE) planktonic populations (log_{10}cfu/g) of *C. difficile* total viable counts (TVC), spores and cytotoxin (RU) in vessel 1, 2 and 3 of the human gut model.

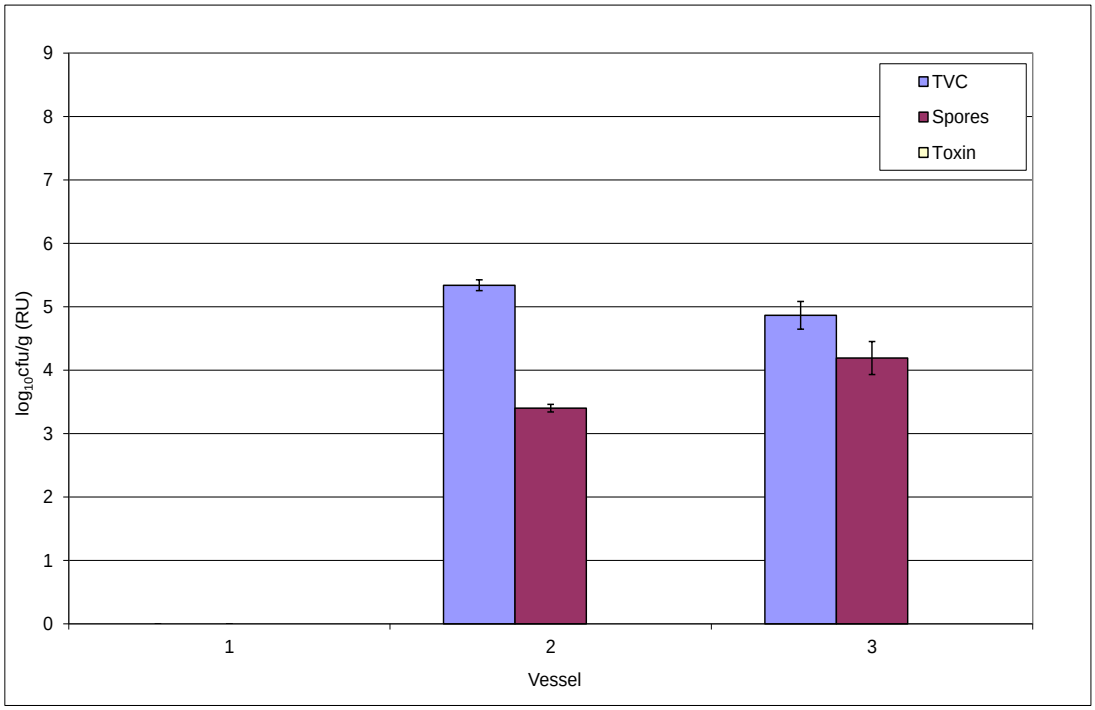

Figure 4.10.2.3: Mean (±SE) biofilm populations (log_{10}cfu/g) of *C. difficile* total viable counts (TVC), spores and cytotoxin (RU) in vessel 1, 2 and 3 of the human gut model.

4.10.3 Discussion

The original gut model experimental design prior to biofilm analysis comprised of the clindamycin induction of CDI followed by a treatment dosing regimen of metronidazole. Metronidazole treatment failed and vegetative cells and toxin remained after cessation of the dosing regimen. Failure of the initial treatment was followed by a second treatment regimen of fidaxomicin. The second treatment course was successful and recurrence was not observed. *C. difficile* was only sporadically recovered in spore form from the commencement of fidaxomicin instillation until the end of the experiment (figure 4.10.1).

On day 99, comparison of planktonic and sessile indigenous gut microbiota results were to those described previously. *Enterococcus* spp. were again slightly higher in sessile than planktonic form.

The only *C. difficile* populations recovered from the planktonic culture fluid of the biofilm analysis experiments were vegetative cells in vessel 3 at the LOD. Within the original model vegetative cells were not recovered for at least 28 days prior to biofilm analysis. Therefore, it is likely that these colonies were, in fact, derived from spores. The value of ~3 $\log_{10}$cfu/g was the LOD of this assay, and therefore only limited interpretation is possible. The units used in these experiments require the weight of the pellet of a millilitre of planktonic culture fluid to be used to determine populations; as a result, the limit of detection increases as a factor of pellet weight.

Sessile *C. difficile* populations were greater than planktonic populations in vessels 2 and 3. Sessile populations were comprised primarily of spores although vegetative cells were present at ~2 and 1 $\log_{10}$cfu/g in vessels 2 and 3, respectively. Vegetative cells were undetected from the planktonic fluid of the original gut model post-fidaxomicin; therefore, the detection of these cells within the biofilm, even at low levels, is unexpected.

Cytotoxin was absent in planktonic samples and biofilm on day 99 of original gut model (due to the successful second treatment course and lack of recurrent CDI). Toxin was present for up to 26 days during earlier periods in the original model. However, absence of toxin within biofilms indicates that prolonged sequestration of toxin is not apparent.

Antimicrobial activity was detected in biofilm from all vessels, and in the planktonic fluid of vessels 2 and 3. The identity of the antimicrobial agent responsible for this activity is unknown. However, fidaxomicin was the final antimicrobial agent used within the original model design, and was shown to persist within the planktonic fluid of the original gut model (figure 4.10.1). It is therefore likely that fidaxomicin was the cause of residual antimicrobial activity. The increased presence of sessile compared with planktonic *C. difficile* provides evidence that the protected environment of the biofilm provides a niche for *C. difficile* persistence.

4.11 Biofilm Analysis 9

4.11.1 Experimental Design

The triple stage human gut model experimental design is outlined in table 4.11.1. Briefly, after inoculation with faecal emulsion, gut microbiota populations were allowed to equilibrate for 20 days (period A), before a single inoculum of *C. difficile* PCR ribotype 027 spores (table 3.1) were added to vessel 1 of the model on day 20. A second inoculum of *C. difficile* PCR ribotype 027 spores were inoculated into the model on day 27. At this point a dosing regimen of clindamycin (33.9 mg/L, QD, 7 days) commenced (period C). Following commencement of clindamycin dosing no further interventions were made until *C. difficile* germination, proliferation and high toxin production was observed (period D). Instillation of vancomycin (125 mg/L, QD, 7 days) commenced on day 43 (period E). Following cessation of therapeutic instillation, the model was left without intervention for 19 days (period F) before instillation of a second therapeutic agent, (fidaxomicin 125 mg/L, BD, 7 days) that commenced on day 69 (period G). Following cessation of the second therapeutic instillation, the model was left without intervention for 23 days (period H). Biofilm was sampled on day 99. Planktonic indigenous gut microbiota (periods A-H), *C. difficile* TVC, spores, cytotoxin (periods B-H) and antimicrobial activity (periods C-H) were monitored during the experiment.

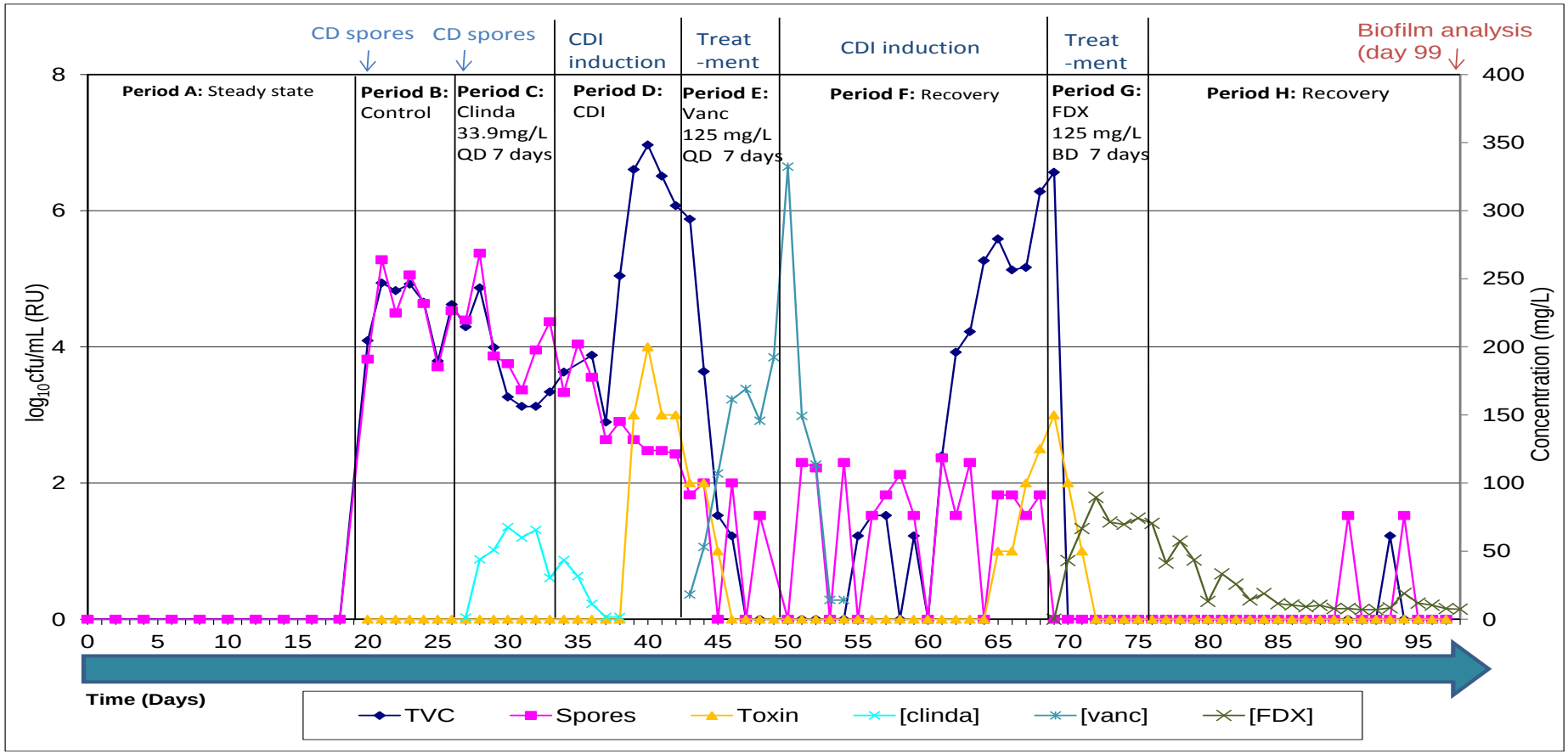

Figure 4.11.1: *C. difficile* results from vessel 3 of the original gut model and experimental design of human gut model prior to biofilm sampling[527]. Vertical line indicates last day of period. (CD: *C. difficile* PCR ribotype 027 (~10^7cfu); Clinda: clindamycin; Vanc: vancomycin; FDX: fidaxomicin).

4.11.2 Results

4.11.2.1 Indigenous Gut Microbiota Populations

The planktonic and sessile bacterial populations within the human gut model were dominated by total anaerobes including *Clostridium* spp. and *B. fragilis* group (figure 4.11.2.1). Planktonic populations were generally greater than sessile populations with the exception of *Enterococcus* spp. *Bifidobacterium* spp. were not detected in either planktonic or sessile form.

4.11.2.2 *C. difficile* Populations

Planktonic *C. difficile* was only detected at a population of ~2.9 $\log_{10}$cfu/g in vessel 1 only (figure 4.11.2.2). Sessile *C. difficile* populations comprised spores only at populations of ~4.2 $\log_{10}$cfu/g and ~5.1 $\log_{10}$cfu/g in vessels 2 and 3, respectively (figure 4.11.2.3). *C. difficile* was not recovered from vessel 1 in sessile or planktonic form. Cytotoxin was not detected in planktonic culture or biofilm from any vessel.

4.11.2.3 Antimicrobial Levels within the Planktonic Culture and Biofilm

Concentrations of active antimicrobial agent utilising the clindamycin bioassay methodology were 1.9, 3.8 and 5.9 mg/L in the planktonic fluid from vessel 1, 2 and 3, respectively. Levels of active antimicrobial using the clindamycin methodology were 56.0, 19.1 mg/L in the biofilm of vessels 1 and 2, respectively; no activity was detected in vessel 3 biofilm. Levels of active antimicrobial agent enumerated using the fidaxomicin methodology were 2.4, 4.9 and 7.0 mg/L in the planktonic fluid fromvessels 1, 2 and 3, respectively. No antimicrobial activity was detected in the biofilm of vessel 3, but was present at levels of 72.6 and 22.3 mg/L in vessels 1 and 2, respectively. No active antimicrobial agent was detected in

the planktonic phase of any vessel using the vancomycin methodology. Antimicrobial activity measured 30.5 mg/L within vessel 1 biofilm only.

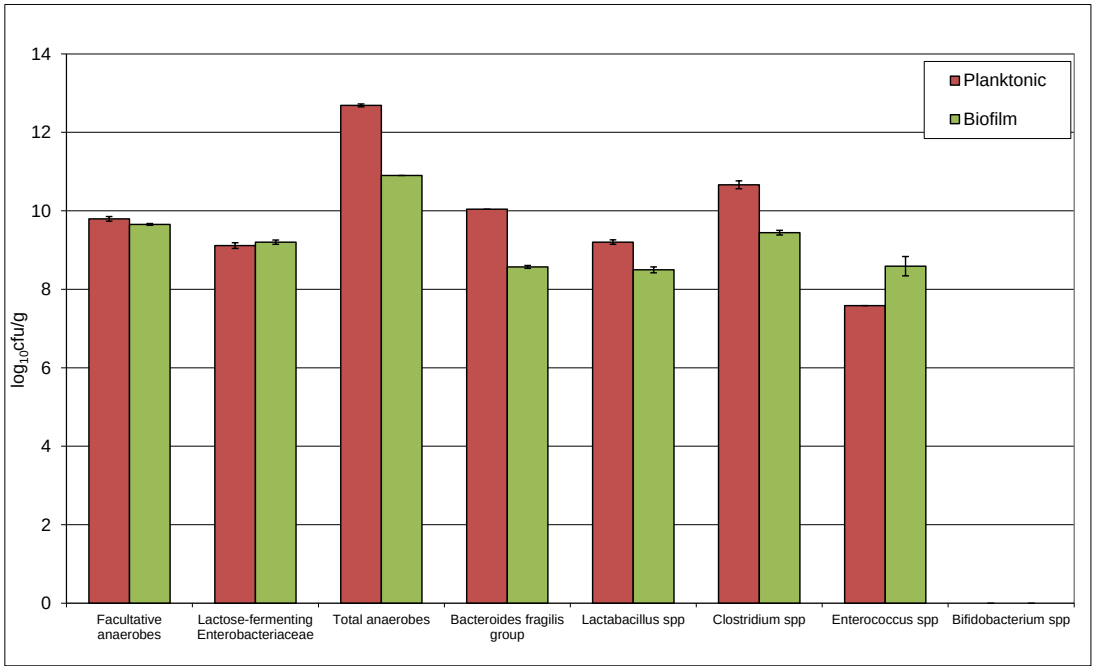

Figure 4.11.2.1: Mean (±SE) planktonic and biofilm populations (log_{10}cfu/g) of indigenous of indigenous gut microbiota populations present in vessel 3 of the human gut model.

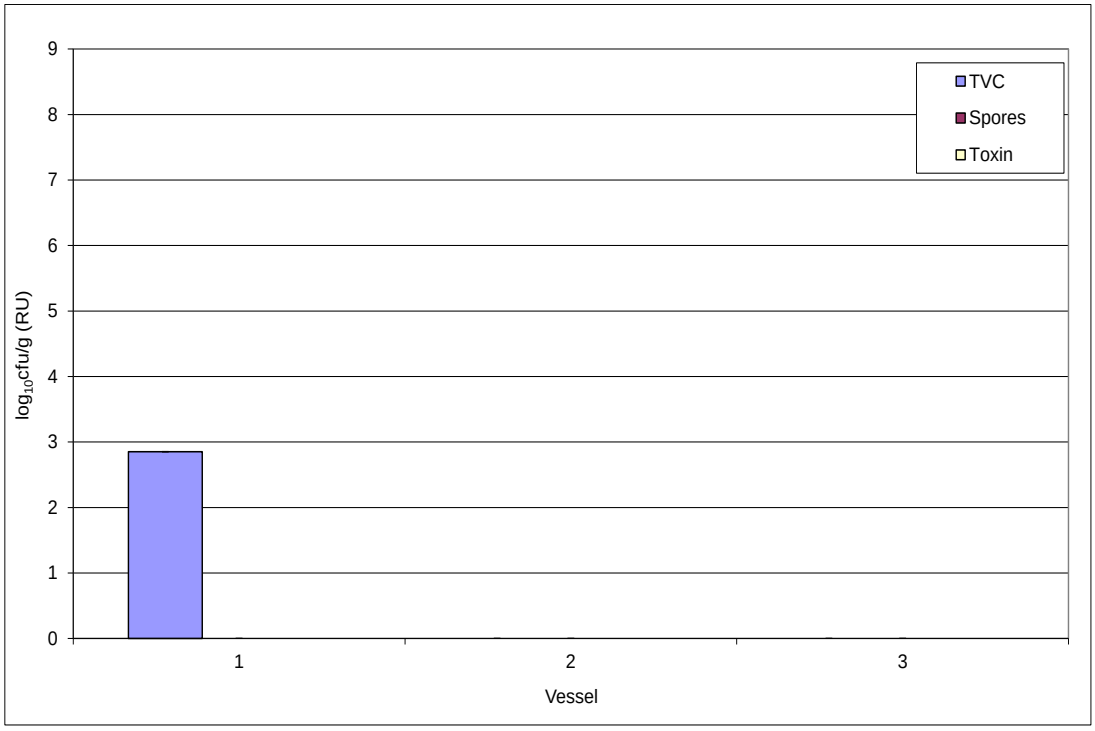

Figure 4.11.2.2: Mean (± SE) planktonic populations (log_{10}cfu/g) of *C. difficile* total viable counts (TVC), spores and cytotoxin (RU) in vessel 1, 2 and 3 of the human gut model.

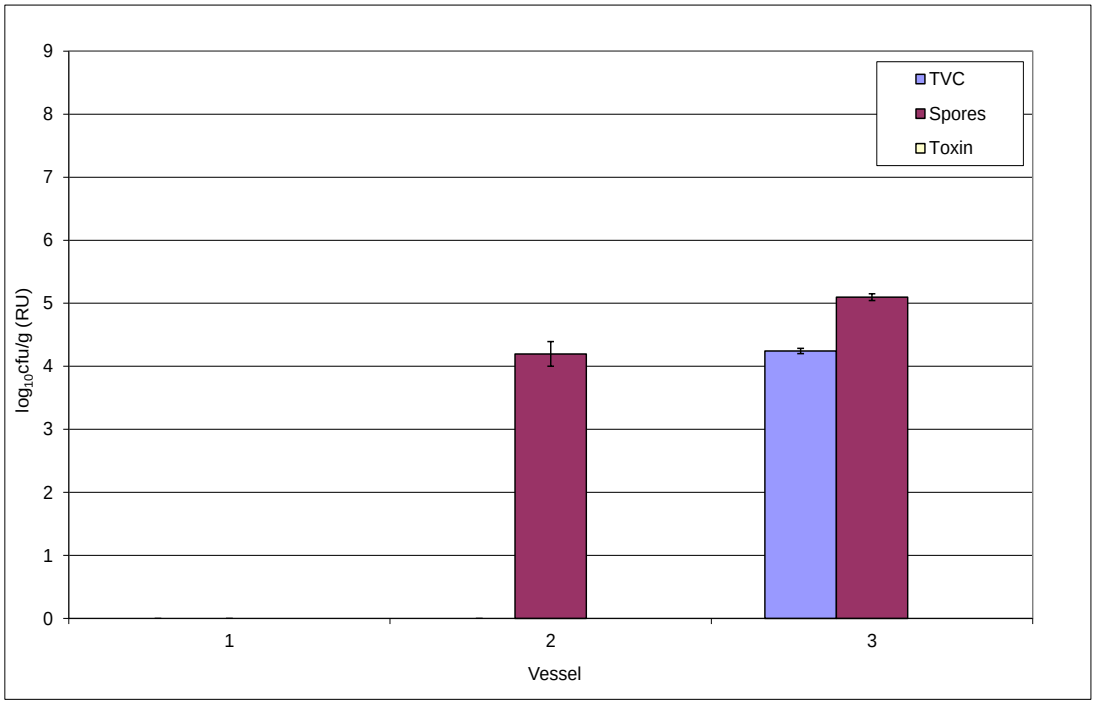

Figure 4.11.2.3: Mean (±SE) biofilm populations (log_{10}cfu/g) of *C. difficile* total viable counts (TVC), spores and cytotoxin (RU) in vessel 1, 2 and 3 of the human gut model.

4.11.3 Discussion

The original gut model experimental design prior to biofilm analysis is described in section 4.10.1, although vancomycin was used as the initial treatment. Treatment was initially successful, however; recurrence of simulated CDI after initial treatment was evident. A second treatment, comprising fidaxomicin, was successful, with only sporadic spore recovery thereafter (figure 4.11.1).

Indigenous gut microbiota results were similar for the previous experiment, again with increased sessile *Enterococcus* spp. populations compared with planktonic populations.

The only *C. difficile* population recovered from the planktonic culture fluid on day 99 were in vegetative form in vessel 1 at the LOD. However, the significance of this recovery should be interpreted with caution due to the lack of vegetative cell recovery in the original model post-fidaxomicin, and the very low level value obtained. In vessels 2 and 3 *C. difficile* spore populations were present within the biofilm; although these levels were low, they were greater than planktonic populations, and thus provide a source of recalcitrant spores for possible subsequent dispersal. Cytotoxin was not detected in the original gut model (due to successful treatment and lack of recurrent CDI) and was also not detected from the biofilm.

Antimicrobial activity was detected the planktonic fluid of all vessels and the biofilm of vessels 1 and 2. As described in section 4.10.3, it is likely that this activity is due to residual fidaxomicin.

4.12 Biofilm Analysis 10

4.12.1 Experimental Design

The triple stage human gut model experimental design is outlined in table 4.12.1. Briefly, after inoculation with faecal emulsion, gut microbiota populations were allowed to equilibrate for 22 days (period A), before a single inoculum of *C. difficile* PCR ribotype 027 spores (table 3.1) were added to vessel 1 of the model on day 22. A second inoculum of *C. difficile* PCR ribotype 027 spores were inoculated into the model on day 29. At this point a dosing regimen of clindamycin (33.9 mg/L, QD, 7 days) commenced (period C). Following commencement of clindamycin dosing, no further intervention were made until *C. difficile* germination, proliferation and high toxin production was observed (period D). Instillation of fidaxomicin (125 mg/L, BD, 7 days) commenced on day 57 (period E). Following cessation of therapeutic instillation, the model was left without intervention for 22 days (period F). Biofilm was sampled on day 86. Planktonic indigenous gut microbiota (periods A-F), *C. difficile* TVC, spores, cytotoxin (periods B-F) and antimicrobial activity (periods C-F) were monitored during the experiment.

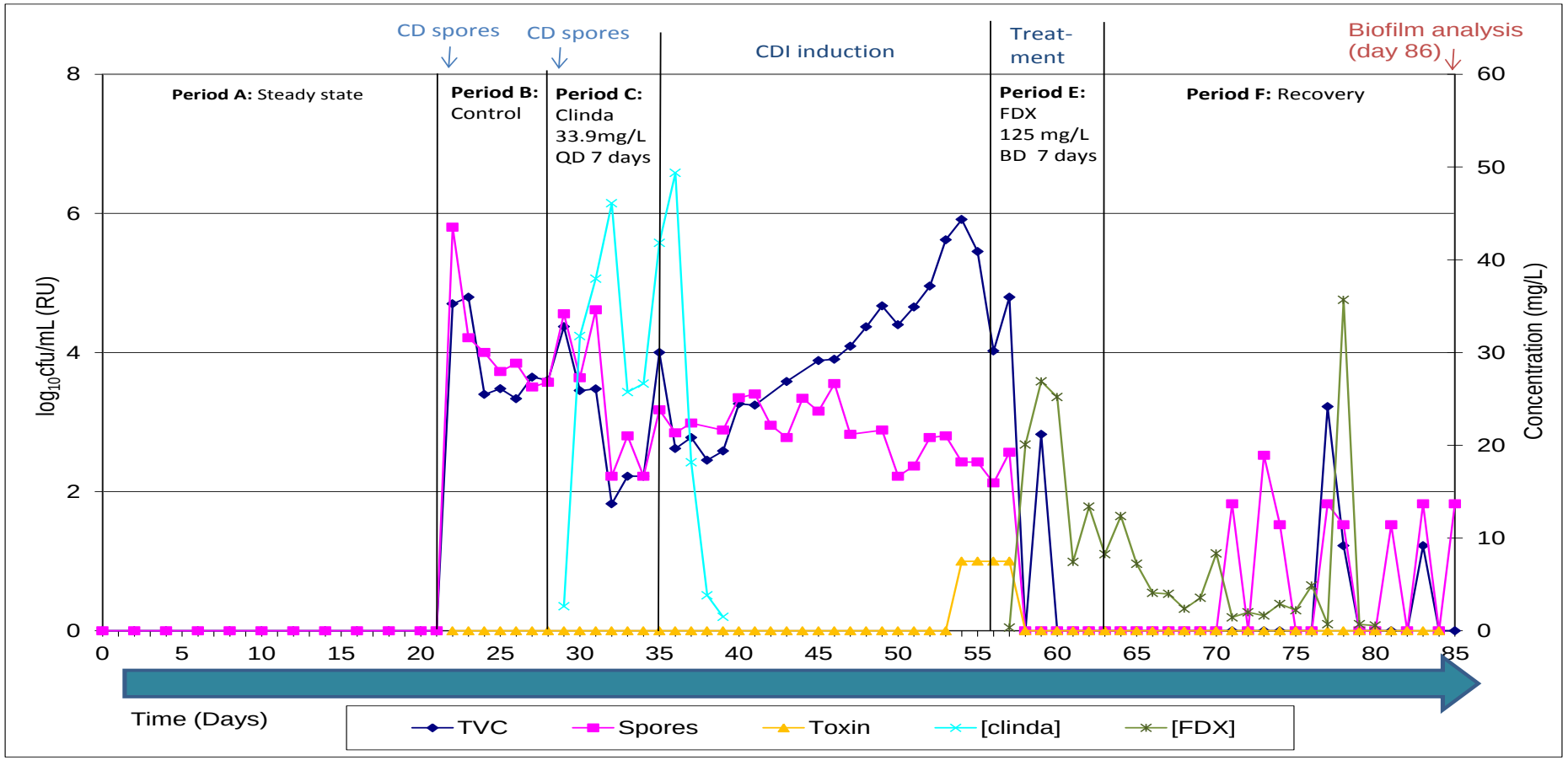

Figure 4.12.1: *C. difficile* results from vessel 3 of the original gut model and experimental design of human gut model prior to biofilm sampling. Vertical line indicates last day of period. (CD: *C. difficile* PCR ribotype 027 (~10^7cfu); Clinda: clindamycin; FDX: fidaxomicin). TVC – total viable count.

4.12.2 Results

4.12.2.1 Indigenous Gut Microbiota Populations

On day 86, bacterial populations within the human gut model were dominated by LFE, *B. fragilis* group and *Clostridium* spp. for both planktonic and sessile communities (figure 4.12.2.1). All planktonic gut bacterial groups identified and enumerated in the gut model were also present within the biofilm. Populations of planktonic bacteria were higher than those in sessile form, although the relative proportions of these planktonic and sessile populations were similar for all bacterial groups. *Bifidobacterium* spp. populations were not detected in neither the planktonic nor sessile form at this stage of the experiment.

4.12.2.2 *C. difficile* Populations

Planktonic *C. difficile* populations were only detected as spores at a population of ~ 1.3 $\log_{10}$cfu/g (LOD) in vessel 1 only (figure 4.12.2.2). Sessile *C. difficile* populations were detected in all 3 vessels (figure 4.12.2.3). Only vegetative cells were present in vessel 1 (~3.5 $\log_{10}$cfu/g) and only spores in vessel 2 (~3.9 $\log_{10}$cf/g) and 3 (~4.8 $\log_{10}$cfu/g). Cytotoxin was not detected in any vessel within the planktonic culture or biofilm.

4.12.2.3 Antimicrobial Levels within the Planktonic Culture and Biofilm

Active antimicrobial levels detected using the clindamycin bioassay methodology were 1.9, 3.8 and 5.9 mg/L the planktonic fluid of vessels 1, 2 and 3, respectively. Activity was not detected in the biofilm of vessel 3, but was present at levels of 65.2 and 4.3 mg/L in vessels 1 and 2, respectively.

Active antimicrobial agent concentration detected using the fidaxomicin methodology was below the LOD (4 mg/L) in the planktonic fluid of all vessels. Activity was detected within the biofilm of vessels 1 (73.9mg/L) and 2 (7.0 mg/L), whilst no activity was detected in vessel 3.

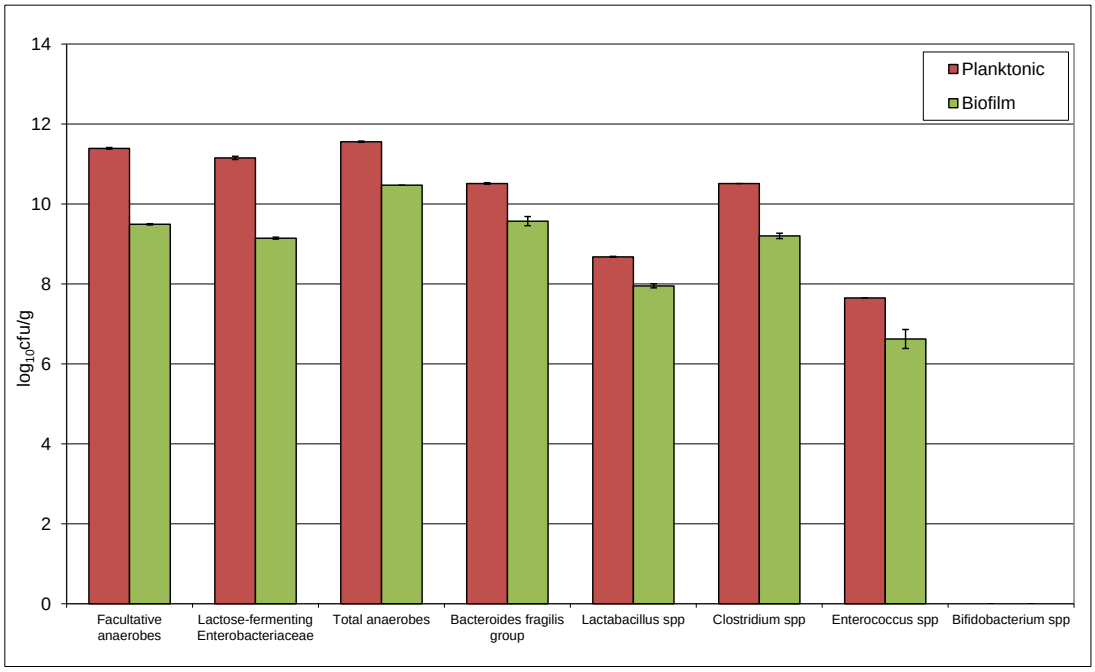

Figure 4.12.2.1: Mean (±SE) planktonic and biofilm populations (log_{10}cfu/g) of indigenous of indigenous gut microbiota populations present in vessel 3 of the human gut model.

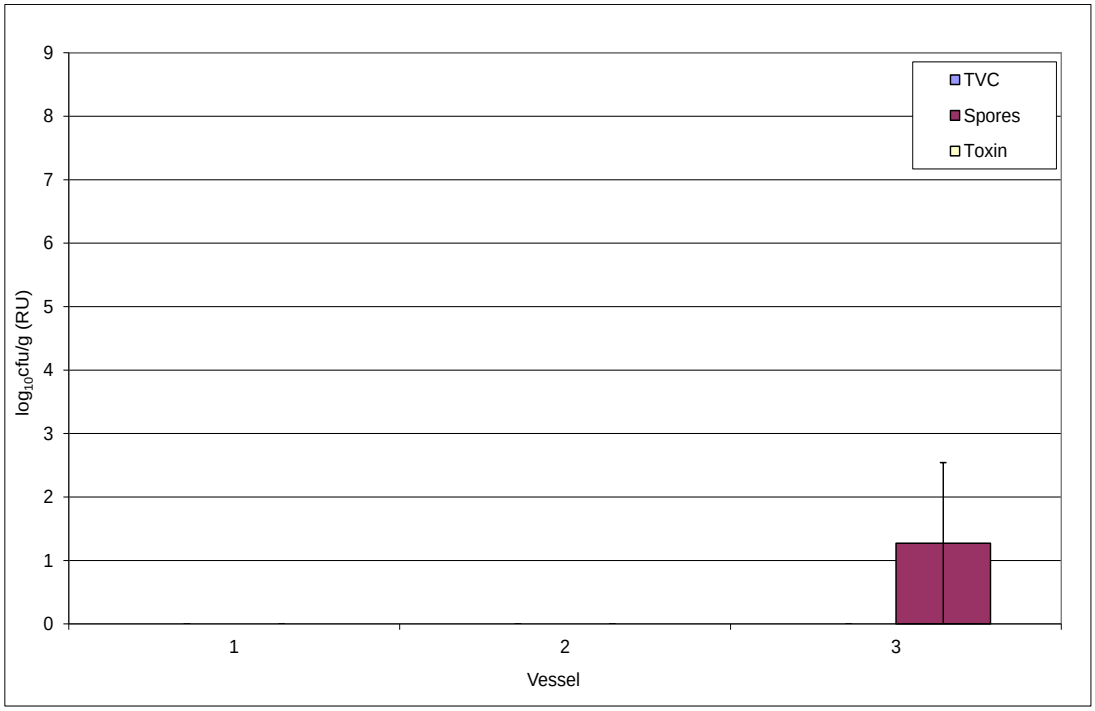

Figure 4.12.2.2: Mean (± SE) planktonic populations (log_{10}cfu/g) of *C. difficile* total viable counts (TVC), spores and cytotoxin (RU) in vessel 1, 2 and 3 of the human gut model.

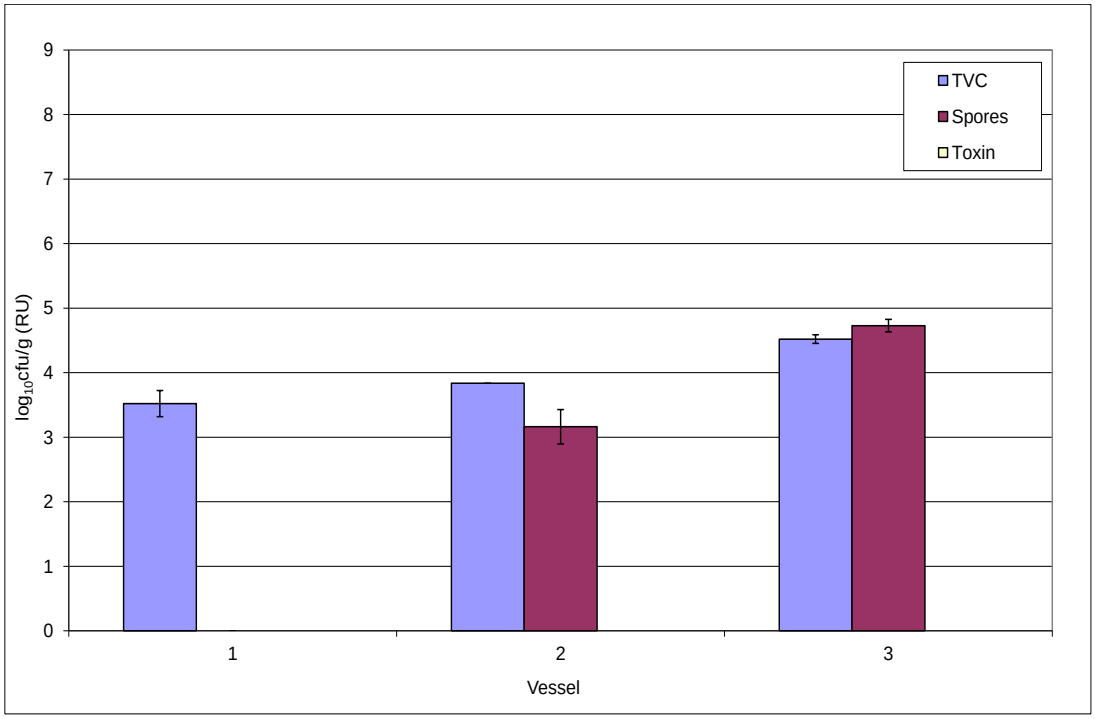

Figure 4.12.2.3: Mean (±SE) biofilm populations (log_{10}cfu/g) of *C. difficile* total viable counts (TVC), spores and cytotoxin (RU) in vessel 1, 2 and 3 of the human gut model.

4.12.3 Discussion

The original gut model experimental design prior to biofilm analysis comprised clindamycin-induced CDI followed by successful fidaxomicin treatment with no recurrence and sporadic spore recovery post-fidaxomicin.

Indigenous gut microbiota population results were as expected and as described previously. Planktonic *C. difficile* populations were represented by the detection of spores in vessel 3 at the limit of detection. *C. difficile* spores were recovered from the biofilm in vessels 2 and 3 and vegetative cells from vessel 1. Again, levels recovered in vessel 1 of the biofilm were very low, and therefore little significance should be assigned to this observation. Spore populations in vessels 2 and 3 were ~0.5-1 $\log_{10}$cfu/g higher than the LOD, but still exhibited reduced sessile populations compared with results from all other biofilm analysis experiments (although only marginally lower than other gut model runs utilising fidaxomicin treatment).

Fidaxomicin is a novel macrocyclic antimicrobial, which inhibits RNA synthesis,recently licensed for the treatment of CDI. Instillation of fidaxomicin during the original gut model experiment elicited rapid reduction of *C. difficile* vegetative cells, with only sporadic spore detection for the duration of the experiment. The presence of this agent within biofilm structures in this study demonstrate that biofilms may act as a reservoir for fidaxomicin persistence, allowing the subsequent slow release of aggregates of biofilm (including fidaxomicin) into the planktonic cultures fluid after cessation of antimicrobial instillation, thus preventing regrowth of *C. difficile* vegetative cells and symptomatic disease. The supra-MIC (MIC 0.25 mg/L) levels of fidaxomicin present within the biofilm confer potential antibacterial ability. There are currently no data pertaining to the action of fidaxomicin against sessile bacteria.

4.13 Conclusions

Preliminary results detailed in this section highlight for the first time the composition of *in vitro* biofilm structures present within the human gut model at a single time point. These structures are mature and persist for up to 13 weeks *in vitro* despite antimicrobial exposure.

One of the most difficult situations facing clinicians in treating CDI is the management of recurrent infection, which occurs in ~20% of patients[243-245]. Several factors are considered as determinants of disease recurrence including *C. difficile* persistence, colonisation resistance and host immune response. Recurrence of simulated *C. difficile* germination, proliferation and toxin production after successful initial treatment within a human gut model has been observed previously[272, 515]. Results presented here detail the persistence of *C. difficile* within biofilm structures in a human gut model. It is postulated that this pool of recalcitrant *C. difficile* may lead to regrowth of *C. difficile* vegetative cells and toxin production, once antimicrobial therapy has ceased.

Indigenous microbiota populations present in planktonic form were also largely present in sessile form. In general, planktonic bacterial counts per unit weight/volume exceeded respective sessile counts. In some experiments counts of sessile facultative anaerobes, particularly *Enterococcus* spp. were notably higher than the planktonic counts. The lower ratio of anaerobes to aerobes at the gut mucosal surface compared with the lumen has been observed *in vivo*[279]. MacFarlane *et al* observed similar trends, with planktonic anaerobe: facultative anaerobe ratios greater than those in the sessile mode of growth[446]. *P. aeruginosa,* a notorious EPS producer, is inconsistently recovered from the gut model. The association of *P. aeruginosa* with *E. faecalis* has previously been noted[528], potentially implying a symbiotic relationship between the two organisms. The presence

of *P. aeruginosa* may lead to recruitment of increased levels of enterococci species into biofilm structures.

In batch culture experiments (chapter 3), *C. difficile* did not consistently form mature biofilm, and intestinal microorganisms did not readily associate with glass. However, in these experiments, mature, mixed-species biofilm were consistently harvested from glass vessel walls. This discrepancy highlights the differences between batch and continuous culture systems. *C. difficile* is able to exist within biofilm structures in the gut model in spore and vegetative forms. However, this may be due to *C. difficile* associating with pre-existing biofilm structures rather than initiating biofilm formation.

The biofilm mode of growth of *C. difficile* is highly variable and complex. Sessile populations within vessel 1 often produce distinct populations from those within vessels 2 and 3. Distinct differences in *C. difficile* composition and toxin presence have also been observed between planktonic and sessile populations. *C. difficile* spores often numerically dominated sessile *C. difficile* populations.

The designs of experiments in which biofilm was analysed were variable. Experiments 1 and 4 induced CDI only, whereas other experiments included therapeutic treatment, although differences in treatment success were evident. Such differences likely affect biofilm composition and may account for the variation in results obtained.

Biofilm formation and sporulation pathways are interconnected and differentially regulated by Spo0A in *B. subtilis*[434]. *C. difficile* possesses a Spo0A orthologue with 56% amino acid homology to that of *B. subtilis*. This orthologue plays a key role in *C. difficile* sporulation and biofilm formation[454, 455]. The *C. difficile* biofilm lifecycle is a complex process, which remains to be fully elucidated. Dawson *et al* demonstrated that 6-day-old batch culture biofilms contained greater numbers of spores compared with 3-day-old

biofilms[455], thus providing evidence of heterogenetic *C. difficile* composition in distinct biofilm lifecycle stages. In addition, Ethapa *et al* demonstrated that *C. difficile* Spo0A mutants were defective for biofilm formation within a batch culture system [454], demonstrating a possible link between biofilm formation and sporulation within *C. difficile.* Similar observations in both *C. difficile* [457] and other spore-forming sessile bacteria[434, 529, 530] have been noted.

The association between increased biofilm maturity and increased spore rather than vegetative forms by other groups provides a possible explanation for the high level of spores often observed within mature biofilm structures within the gut model [455, 457]. However, it should also be noted that conversely, Ethapa *et al* demonstrated extremely low numbers of spores in biofilm and planktonic phases after 3 and 5 days incubation[454].

Whilst the majority of spores within a population initiate rapid germination in response to germinants, a sub-population of spores are refractory to these stimuli and the germination process is slow. This response is termed superdormancy and has been most extensively characterised in *Bacillus* spp.[531-534]. The persistence of a superdormant fraction of *C. difficile* spores after exposure to germinants has been described[535], although our understanding in this area remains basic. Sessile spores may display analogies to superdormant spores and display increased recalcitrance to germination, resulting in high spore populations.

Spore formation in *B. subtilis* occurs in apical areas of biofilms, allowing for optimal spore dispersal to distinct niches. Spatial characterisation of *C. difficile* biofilms is unclear however; correlations in spatial organisation may also exist, possibly providing greater ease of seeding of spores into the planktonic fluid *in vitro,* or into the lumen of the gastrointestinal tract *in vivo*.

It was expected that spores would remain in a dormant state within the non-growing biofilm environment; however, vegetative cells were detected within some biofilm structures. This may be due to germination and proliferation of planktonic *C. difficile,* and subsequent recruitment into biofilm structures or true germination of sessile spores. Lindsey *et al* have previously reported the ability of *B. cereus* spores to attach to surfaces and germinate under favourable and unfavourable nutrient conditions, leading to a biofilm comprised of both spores and vegetative cells[518]. However, vegetative sessile cells may display increased dormancy or a 'persister' status, compared to planktonic cells as reported with other organisms[536, 537].

Sporulation is an energy intensive process. A sub-population of *B. subtilis* delay sporulation by differentiation down a pathway which gives rise to 'cannibals'[435]. In addition to sporulation and biofilm formation, cannibalism is also regulated by Spo0A. Cannibals secrete toxins to which they are resistant; these toxins kill a fraction of siblings in order to overcome nutrient limitation and delay sporulation, and thus some cells remain in vegetative form despite unfavourable conditions. There are currently no data pertaining to the existence of a sub-population of *C. difficile* cells that may possess a survival strategy similar to the *B. subtilis* cannibals. However, the role of Spo0A in *B. subtilis* and *C. difficile* is similar; therefore, it is possible that a sub-population of sessile *C. difficile* differentiate to a pathway distinct from that of sporulation, thus remaining in vegetative rather than spore form.

The presence of both vegetative cells and toxin within biofilm structure suggests that these vegetative cells may be actively producing toxin. Laning[457] utilised Western Blot analysis to identify putative toxin antibodies in toxigenic, but not non-toxigenic *C. difficile* batch culture biofilms, and showed that toxin concentration increased over time from 1 to 6-day-old biofilms. This suggests that toxigenic sessile *C. difficile* are able to produce

toxin actively. However, these results should be interpreted with caution as this group also observed that 6-day-old biofilms comprised only spores, which would not be expected to produce toxin.

Within the present study, the presence of toxin within biofilm structures, despite the absence of cultureable vegetative cells, was observed. An alternative explanation is that biofilms are able to sequester toxin from the culture fluid, or that *C. difficile* within the biofilm were at one time actively producing toxin before converting to their spore form, with residual toxin remaining present.

In vessel 1, vegetative forms of *C. difficile* were sometimes present within the biofilm, although toxin production was absent. *C. difficile* germination, proliferation and toxin production is not always observed within vessel 1 of the human gut model[525, 538]. Reasons for this remain unclear, but may be because of a more acidic pH within this vessel, which is not conducive to spore germination[539]. Spore germination and proliferation, but not toxin production has also previously been observed within this vessel[525]. Repression of toxin production or rapid degradation of toxin may be enhanced by the reduced pH within this vessel. Diminished toxin production has previously been associated with low pH levels[23, 540], although contradictory studies also exist[541].

Toxin is unstable and degrades under certain conditions[542]. Bacterial species may produce extracellular enzymes that degrade toxin within a biofilm structure. Proteolytic cleavage of toxin A and B by *Saccharomyces boulardii* has previously been described[543, 544]. Whilst protease secretion by this organism may not be present within the human gut model, it is possible that the complex sessile microbial communities, but not planktonic fluid, harbour and allow the attainment of protease-producing bacteria in sufficient concentrations to cause toxin degradation. This may in part explain the

absence of toxin from within the biofilm whilst present within the planktonic culture fluid.

Transcription of *tcdA* and *tcdB* is regulated by environmental factors such as temperature and nutrient availability[56, 57,58, 59,60]. Biofilms comprise microenvironments with distinct conditions. Certain areas of biofilms may be favourable for toxin transcription, which is otherwise absent from the planktonic fluid. Furthermore, the sessile mode of growth may possess a distinct phenotype which enables the continued transcription of virulence factors including *tcdA* and *tcdB*, thus accounting for the presence of toxin within biofilms but absence from planktonic phase.

The biofilm matrix may reduce diffusion of toxins as well as antimicrobials into the biofilm structure. Whilst there is some evidence to suggest that reduced susceptibility is elicited by antimicrobial inactivation or reduced penetration, there is also confounding evidence to suggest that this is not the only pathway[422, 545]. Sequestration of antimicrobials may be possible but penetration to all areas (particularly the inner biofilm) may be prevented.

The distinct properties of biofilms from different areas of the gut model may explain the absence of toxin in some biofilms, potentially providing a greater ability to reduce penetration of toxin, degrade toxin or prevent the residence of toxin-producing cells.

Persistence of antimicrobial agents within biofilm structures after cessation of instillation is evident, but not universal, within the human gut model. Certain antimicrobials, notably fidaxomicin, appear to display increased affinity to associate with biofilms than others. Reasons for this persistence may be modulated by antimicrobial specific characteristics. When sessile populations are considered in terms of total biomass, this provides a considerable reservoir of *C. difficile* for potential subsequent dispersal into the planktonic phase. Treatment of CDI with fidaoxomicin in biofilm

analysis experiments 8-10 elicited a reduced *C. difficile* spore reservoir within biofilm structures compared with other biofilm analysis experiments. Fidaxomicin treatment also elicited only sporadic recovery of planktonic spores. Allen *et al* identified that fidaoximicn prevents outgrowth of vegetative cells[546]. Further work from our group indicates that fidaxomicin binds to spore structures despite repeated washing, preventing recovery of spores [547]. This suggests that lack of detection of spores from the planktonic and biofilm components of the gut model are due to fidaxomicin binding to spores, preventing subsequent outgrowth onto agar. This evidence implies that fidaxomicin confers a reduced capacity for regrowth of vegetative cells from spores, mediating reduced rates of recurrence. A pooled analysis of two recent phase III clinical trials showed fidaxomicin was not inferior to vancomycin for clinical cure and superior over vancomycin for recurrence and global cure (p<0.0001)[233]. However, subgroup analysis identified an insignificant benefit of fidaxomicin over vancomycin for treating PCR ribotype 027 infection. Initial trial reports suggested that fidaxomicin therapy was not inferior to vanomcyin for treatment of recurrent 027 infection[548]. Data presented here provides evidence of successful treatment of recurrent CDI and reduced recurrent infection following fidaxomicin therapy with a PCR ribotype 027 *C. difficile* strain.

It is postulated that prolonged persistence within biofilm structures may facilitate subsequent slow release of antimicrobial agent into the planktonic fluid, allowing prolonged exertion of inhibitory activity, potentially preventing regrowth of *C. difficile* vegetative cells and reducing the likelihood of recurrent infection. However, the benefits of persistent activity against *C. difficile* may also cause enhanced perturbation of the gut microbiota. Recovery of indigenous gut microbiota is thought to be necessary in order to reduce the risk of recurrent infection; therefore,

delayed recovery may offset a benefit of persistent antimicrobial activity in reducing risk of CDI recurrence.

These results provide preliminary information on the complex, multifactorial existence of biofilm structures within the human gut model. These experiments are highly variable and lack a controlled environment; thus making reliable conclusions difficult. However, the data provide evidence of the association of *C. difficile* spore, vegetative cells and cytotoxin with biofilm structures, indicating that further investigation is warranted.

5.0 Mucin Alginate Investigational Biofilm Human Gut Model

5.1 Background

The original *in vitro* human gut model was designed to simulate the various stages of CDI; from a healthy state, asymptomatic carriage, induction of CDI, simulation of a diseased state, treatment, and post-treatment observation. The indigenous gut microbiota and *C. difficile* populations vary considerably during these distinct phases within the system. In order fully to elucidate the sessile mode of growth of *C. difficile* and the possible role of intestinal biofilms in recurrent CDI, it is necessary to monitor the composition of biofilm structures within the human gut model longitudinally. Analysis of biofilm from the vessel walls of the gut model is unsuitable for multiple analyses; therefore adaptations to the vessel system are needed to provide an opportunity for multiple sample points.

Biofilm analysis (chapter 4.0) and batch culture experiments (chapter 3.0) have provided preliminary information on the biofilm association abilities of *C. difficile* and the indigenous gut microbiota on a variety of substratum materials, including glass and mucin alginate. Porcine gastric mucin is structurally similar to human epithelial mucin[304]. Alginate is an EPS produced by mucoid strains of *P. aeruginosa*. Alginate and mucin can be combined, along with the addition of calcium, to provide durable beads, which have previously been used as a substratum material within a short term chemostat system[447]. The beads are reflective of conditions *in vivo* and allow multiple biofilm sampling opportunities.

5.2 Materials and Methodology

5.2.1 Single Stage Mucin Alginate Gut Model

5.2.1.1 Single Stage Chemostat Gut Model

The single stage human gut model comprises of a single glass fermentation vessel (280 mL), top fed with a complex growth medium (Appendix A1) at a controlled rate (flow rate = 13.2 mL/h) and connected to a waste outlet system. The vessel was maintained at pH 6.8±0.3 using an automatic fermenter controller (Biosolo 3, Brighton Systems) delivering 0.5M NaOH/HCl. The vessel was heated using a water jacketed system to maintain a temperature of 37° C and continuously sparged with oxygen-free nitrogen to ensure anaerobiosis. Excessive foaming was prevented by the addition of 0.5 mL of polypropylene glycol (VWR) *ad libitum*.

5.2.1.2 Mucin Alginate Bead Preparation

A MA mixture was prepared as previously described (section 3.2.2.4), fed through a peristaltic pump and allowed to fall from a height of 40cm into a 0.3M $CaCl_2$ solution to form beads (mean diameter 2.9 mm).

5.2.1.3 Preparation of Growth Medium

Growth medium was prepared in 2 L volumes (section 4.2.2). The mucin alginate investigational experiments utilised one of two growth media; original gut model growth medium or biofilm model growth medium. Preparation methods of both media are the same although the constituents differ (Appendix A1).

5.2.1.4 Preparation of Gut Model

The single vessel was inoculated with faecal emulsion, obtained from an existing original gut model. The original gut model was inoculated with a faecal emulsion prepared from *C. difficile*-negative faeces donated from healthy elderly volunteers. A total volume of 240 mL of faecal emulsion was removed from vessels 1-3 of the original model and instilled into the single chemostat. Details of the stage of the original model when faecal emulsion was removed as well as the timing of MA bead (50% w/v) instillation into the vessel is detailed for each experiment (table 5.1).

5.2.1.5 *Clostridium difficile* Strains

The strain used throughout the MA investigation experiments was *C. difficile* PCR ribotype 027 (table 3.0), which was isolated during an outbreak of CDI at the Maine Medical Centre, Portland, MA, USA.

5.2.1.6 Sampling Protocol

Approximately 10 mL of planktonic culture fluid/MA bead mixture were removed from the chemostat vessel using a sterile pipette. Planktonic culture fluid was removed from the MA beads and analysed separately.

5.2.1.7 Enumeration of Planktonic Indigenous Gut Microbiota and *C. difficile*

Planktonic bacterial populations were enumerated as described previously (sections 2.1 and 2.2). Populations were expressed as $\log_{10}$cfu/mL.

5.2.1.8 Enumeration of Sessile Indigenous Gut Microbiota and *C. difficile*

Two millilitres of CTAB (0.001%) or saline (table 5.1) were added to the MA beads, vortexed intermittently for 30 mins, and enumerated as described previously (sections 2.1 and 2.2). Populations are expressed as $\log_{10}$cfu/g of beads.

	Inv 1	Inv 2	Inv 3	Inv 4	Inv 5	Triple
Growth medium	Biofilm	Biofilm + 0.4 g/ L glucose	Original	Original	Original	Original
Bacterial dissociation	CTAB	Saline	Saline	Saline	Saline	Saline
MA bead composition	M:A 50:50	M:A 50:50	M:A 50:50	M:A 50:50	M:A 20:80	M:A 50:50
Bead addition	Day 0	Day 0	Day 8	Day 8	Day 7	Day 7
Faecal emulsion	V1-3 (80 mL from each vessel) CD -ve	V1-3 (80 mL from each vessel) CD -ve	V1-3 (80 mL from each vessel) CD +ve	V3 only (240 mL from V3) CD +ve	V1-3 (80 mL from each vessel) CD -ve	Fresh preparation from stool

Table 5.1: Specificities in methodologies used for mucin alginate investigation (inv) experiments 1-5 and triple stage mucin alginate experiment. (CD –ve: *C. difficile* negative; CD +ve: *C. difficile* positive; MA: mucin alginate).

5.3 Investigation 1

5.3.1 Rationale

Batch culture experiments (sections 3.2.2 and 3.2.5) have demonstrated the capacity of *C. difficile* and members of the indigenous gut microbiota to adhere to MA beads. However, these experiments were conducted in short-term batch culture systems. Batch culture conditions are known to vary considerably from a continuous culture system. A series of further investigational experiments were devised to assess the suitability of MA beads for the adaptation of the human gut model.

5.3.2 Experimental Design

The experimental design timeline is highlighted in figure 5.3.2.1. Faecal emulsion along with 120g (50% w/v) MA beads were instilled into the chemostat vessel on day 0. Growth medium was delivered into the model at a controlled rate (flow rate = 13.2 mL/h). No interventions were made for 13 days (period A; figure 5.2.1.1). See table 5.1 for experimental specificities.

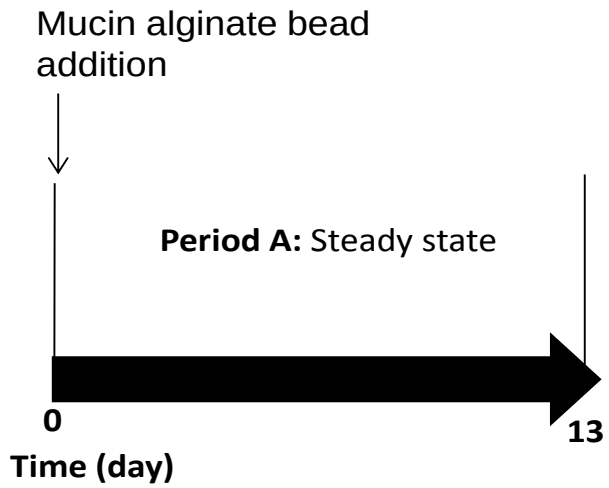

Figure 5.3.2.1: Experimental design of single stage mucin alginate human gut model investigation 1.

5.3.3 Results

5.3.3.1 Experimental Observations

MA bead preparation and instillation into the single stage model was successful. Beads settled towards the base of the vessel and overflow of the beads out of the vessel outlet port was minimal. Initial bead-associated sampling protocol was successful and sessile bacterial populations were obtained on days 1, 3 and 5. Observations from day 5 onwards demonstrated the gradual breakdown and loss of integrity of the MA beads. As a result sampling was increasingly difficult, with separation of the planktonic fluid and beads problematic.

5.3.3.2 Planktonic Indigenous Gut Microbiota Populations

The single stage vessel is able to support planktonic indigenous gut microbiota populations with *Bifidobacterium* spp. (~8-10 $\log_{10}$cfu/g) the most abundant, and *Enterococcus* spp. (~2.5-6 $\log_{10}$cfu/g) the least abundant bacterial groups (figure 5.3.1.1). Bacterial populations remained relatively steady for the duration of the experiment.

5.3.3.3 Sessile Indigenous Gut Microbiota Populations

MA beads within the single stage model were able to facilitate adherence of all bacterial groups also present within the planktonic fluid. *Bifidobacterium* spp. (~7.0 $\log_{10}$cfu/g) were the most, whilst *Enterococcus* spp. (~2.5-5.5 $\log_{10}$cfu/g) and *Clostridium* spp. (2.5-3 $\log_{10}$cfu/g) the least abundant bacterial groups (figure 5.3.1.2). Bead-associated bacterial enumeration commenced on day 1. At this early stage populations were similar to those subsequently obtained on days 3 and 5.

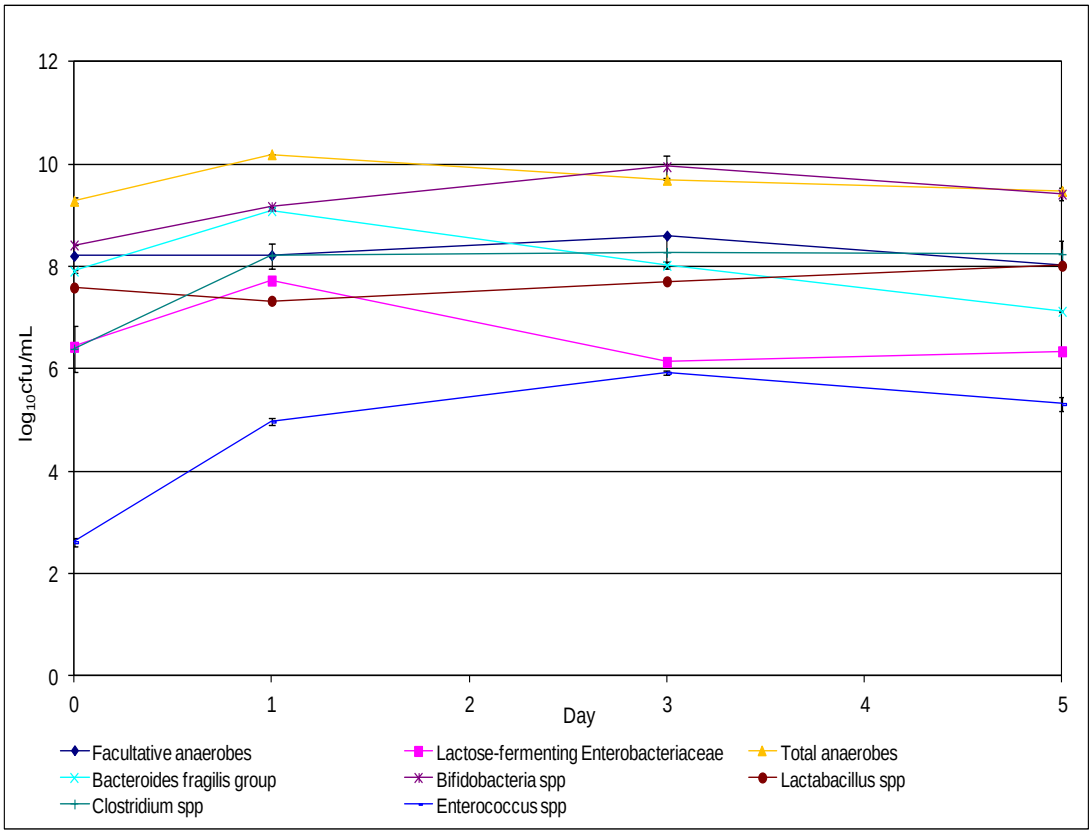

Figure 5.3.1.1: Planktonic populations (log_{10}cfu/mL) (±SE) of indigenous gut microbiota in single stage mucin alginate gut model investigation 1.

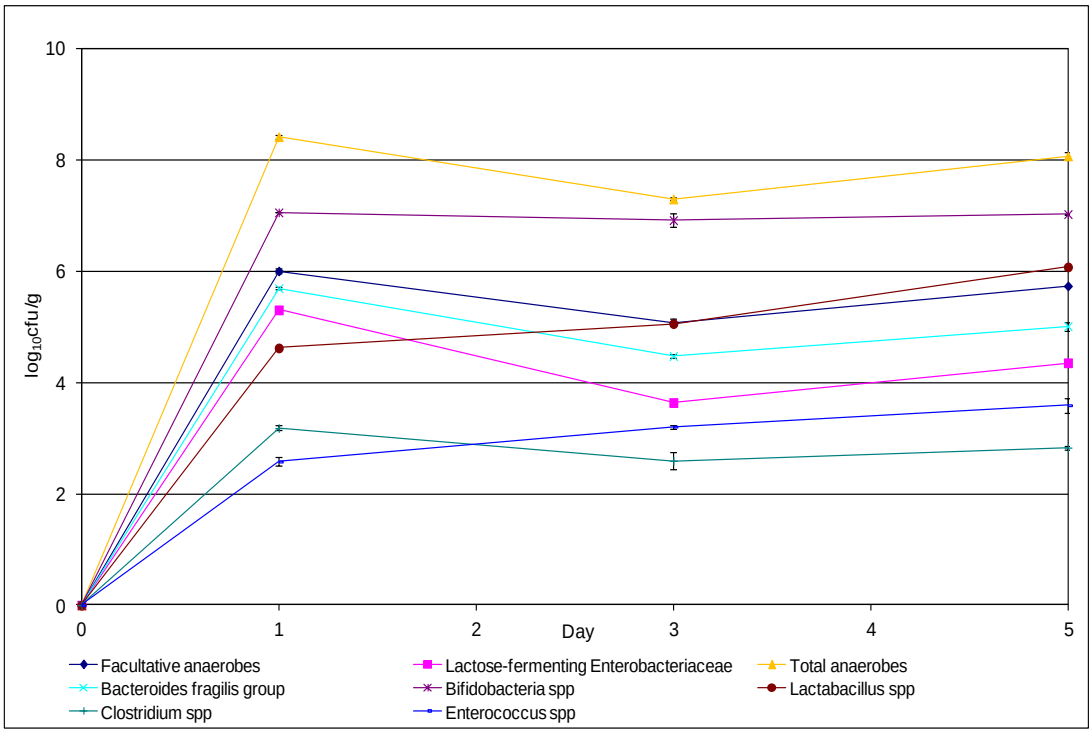

Figure 5.3.1.2: Bead-associated populations (log_{10}cfu/mL) (±SE) of indigenous gut microbiota in single stage mucin alginate gut model investigation 1.

5.3.4 Discussion

Initial bead instillation in investigation 1 proved successful, with the rapid and stable association of gut microbiota populations to the bead surface. Planktonic populations within this system largely reflect those previously observed within gut model experiments[515, 549]. Exposure of these beads to faecal emulsion over 5 days resulted in a loss of structural integrity, which restricted further bead-associated sampling.

5.4 Investigation 2-4

5.4.1 Rationale

Further investigative experiments were conducted in order to extend the lifespan of MA bead structure. Various adaptations to the experimental set up and design were undertaken in investigative experiments 2-4. These include alterations to media, MA bead and faecal emulsion composition, and timing of MA bead introduction (table 5.1).

5.4.2 Experimental Design

The experimental design timelines for investigation experiments 2-4 are highlighted in figures 5.4.2.1-5.4.2.3. See table 5.1 for experimental details.

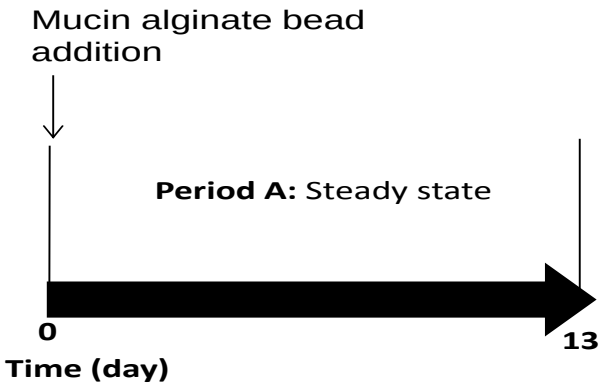

Figure 5.4.2.1: Experimental design of single stage mucin alginate human gut model investigation 2.

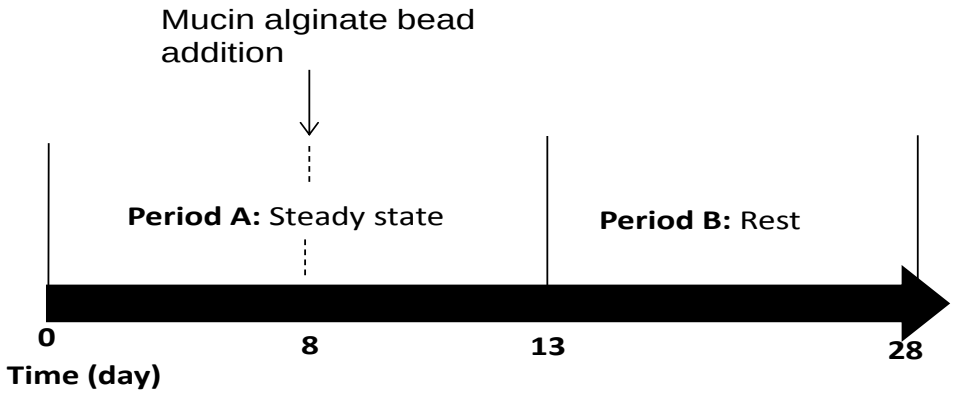

Figure 5.4.2.2: Experimental design of single stage mucin alginate human gut model investigation 3. Vertical line represents the last day of each period.

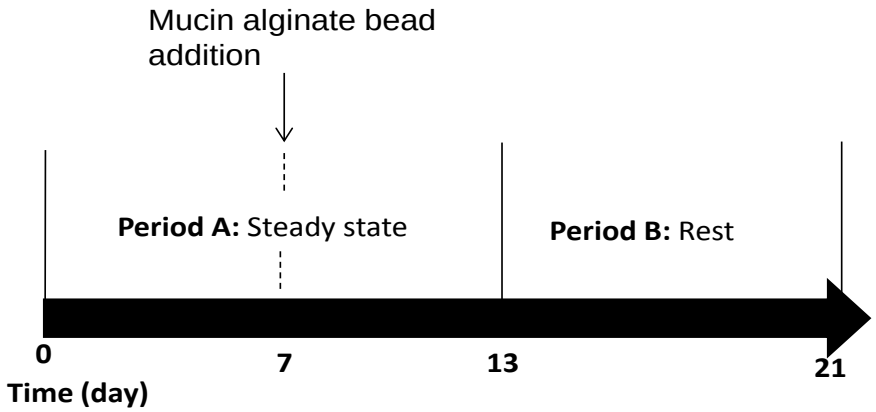

Figure 5.4.2.3: Experimental design of single stage mucin alginate human gut model investigation 4. Vertical line represents the last day of each period.

5.4.3 Results and Discussion

The primary aim of these investigative experiments was to elucidate the suitability of MA beads for study of biofilms within an *in vitro* human gut model, and to prolong the duration of MA bead integrity; thus, bacterial enumeration results are not discussed here.

Investigations 2-4 displayed bead survival times of 3, 13 and 6 days, respectively (table 5.2). Therefore, variation in experimental design failed to prolong the integrity of the MA bead structure for more than 13 days.

Investigation	Growth medium	Faecal emulsion	Bead addition	Bead survival
1	Biofilm	V1-3 CD –ve	Day 0	5 days
2	Biofilm + 0.4 g/L glucose	V1-3 CD –ve	Day 0	3 days
3	Original	V1-3 CD +ve	Day 8	13 days
4	Original	V3 CD +ve	Day 8	6 days

Table 5.2: Summary of alteration to experimental design and effect on bead survival (CD –ve, *C. difficile* negative; CD +ve, *C. difficile* positive; V1-3, faecal emulsion removed from vessels 1 to 3 of original gut model).

Distinct bacterial populations are known to exist within different regions of the colon both *in vivo* and within the human gut model[98, 511, 550]. Removal of faecal emulsion from different vessels of the gut model, as well as during different periods allowed the assessment of these parameters on MA degradation. Investigations 1-2 utilised faecal emulsion from all three vessels of the original gut model obtained during the bacterial equilibrium

period. Investigation 3 also utilised faecal emulsion from all three vessels, although the removal of faecal emulsion was during a *C. difficile* internal control period, once *C. difficile* spores had been added to the faecal slurry. Bead degradation from this investigation was evident after 13 days exposure to faecal emulsion as opposed to 3 and 5 days in other investigation experiments. The use of faecal emulsion from a more advanced stage of a gut model experiment may allow this increased lifespan of the bead structure.

Within a continuous culture *in vitro* model, planktonic bacterial populations must multiply at an adequate rate (*i.e.* above the dilution rate) to maintain colonisation and avoid expulsion from the model. During early stages of a gut model experiment (steady state) bacterial populations compete for fermentable substrate in order to establish a population. Upon equilibration, this bacterial community remains relatively stable in the absence of interventions. During initial stages of an experiment raised levels of competition and fermentation may exist, which may result in increased production of degradative enzymes, including glycosidases. Faecal emulsion from a more advanced stage of a gut model experiment may contain a stable population, resulting in a decrease in fermentation products and enzymes contributing to mucin degradation.

Within investigation 3, biofilm gut model growth medium was replaced with original gut model growth medium. These two media types comprise both conserved and distinct constituents, which may alter production of degradative enzymes within the model. Furthermore, the mucin degradation assay (chapter 3.0) identified that the presence of glucose reduces mucin degradation. Despite inclusion of glucose into the growth medium in investigation experiment 2, degradation of MA beads remained evident.

Vessel 3 of the human gut model represents conditions within the distal colon, the region of most physiological relevance in CDI. These conditions include reduced substrate availability. Investigation 4 was designed to determine whether the bacterial populations resident in the distal colon (vessel 3) exhibited reduced levels of MA-degradative activity, therefore bacterial culture from vessel 3 only (post *C. difficile* PCR ribotype 027 spore inoculation) was inoculated into the chemostat. However, MA bead degradation was evident 6 days after their instillation into the model.

Faecal emulsion utilised in investigation 4 was removed from the original gut model at a similar stage to that used in investigation 3. Despite this similarity, the degradation of MA in investigation 4 was reduced to 6 days, demonstrating the variability of MA degradation within a single stage gut model system.

Despite problems within bead degradation, utilisation of the MA bead material could potentially provide a wealth of information regarding the biofilm mode of growth within an *in vitro* human gut model, reflective of conditions *in vivo*. Therefore, further investigations using this substratum material were carried out.

5.5 Investigation 5

5.5.1 Rationale

Numerous attempts to reduce MA degradation and prolong the lifespan of the bead structure failed. The MA bead material comprises equal proportions of mucin to alginate. Degradation of mucin by faecal bacteria has been well characterised. Incorporation of alginate in addition to mucin decreased degradation of agar as discussed in chapter 3.0. It was therefore hypothesised that increasing the proportion of alginate to mucin may further decrease degradation, allowing the beads to survive longer in the biofilm gut model. The proportion of alginate to mucin was increased to 80:20 for this experiment.

5.5.2 Experimental Design

The experimental design timeline is highlighted in figure 5.5.1. After a steady state period of 13 days (period A; figure 5.5.1.) a single inoculum of *C. difficile* PCR ribotype 027 spores (~10^7 cfu) were inoculated into the vessel on day 14. Days 14-20 serve as an internal control period to demonstrate that spores remain quiescent in the absence of antimicrobial administration (period B; figure 5.5.1.). On day 21 a further inoculum of *C. difficile* spores along with a dosing regimen of ceftriaxone, 150 mg/L, once daily for 7 days was instilled into the model (period C; figure 5.5.1). Thereafter, no further interventions were taken (period D; figure 5.5.1). Planktonic and sessile populations were sampled and enumerated intermittently for the duration of the experiment. See table 5.1 for experimental specifics.

5.5.3 Mucin Alginate Bead Preparation

MA beads (20:80 M:A) were prepared by adding 0.8% (w/v) hog gastric mucin (Sigma) and 3.2 % (w/v) sodium alginate (Sigma) to warm sterile water, stirring continuously until a smooth paste is formed. The MA mixture was fed into peristaltic pump through E1000 tubing as described previously (section 3.2.2.4).

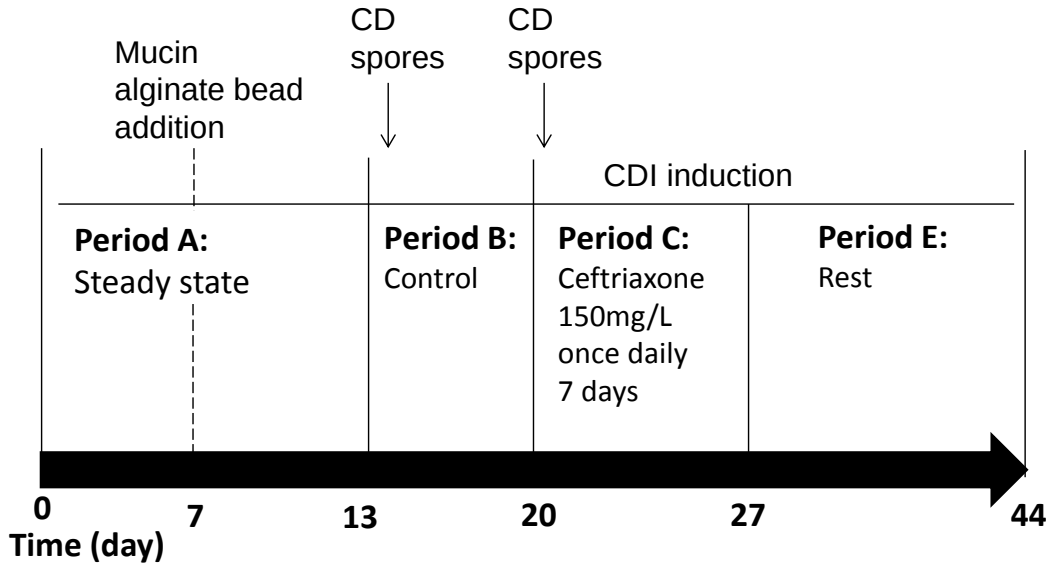

Figure 5.5.1: Experimental design of single stage mucin alginate human gut model investigation 5. Vertical line represents the last day of each period.

5.5.4 Results

5.5.4.1 Experimental Observations

The integrity of 20:80 M:A bead structure was superior to the 50:50 M:A bead type. Beads remained intact for the full 44 day duration (30 days after bead addition) of the experiment. The bead structure was more robust and provided greater sampling ease.

5.5.4.2 Planktonic Indigenous Gut Microbiota Populations

Between days 0 and 7 all bacterial groups in the planktonic phase established a population within the gut model. During steady state period (period A, figure 5.5.1.1a) most bacterial populations remained relatively steady with *B. fragilis* group dominating populations (~9.0 $\log_{10}$cfu/mL) and *Lactobacillus* spp. the least populous bacterial group (~4 – 5 $\log_{10}$cfu/mL). *Lactobacillus* spp. fell to below LOD between days 7 and 23, before recovering to initial population levels (~5.5 $\log_{10}$cfu/mL).

Inoculation of *C. difficile* spores on day 14 did not affect indigenous gut microbiota populations. Instillation of a further inoculum of *C. difficile* spores on day 21 along with a dosing regimen of ceftriaxone (period C, figure 5.5.1.1a) elicited a rapid deleterious effect on most bacterial groups (with the exception of facultative anaerobes) and was most notable in *Clostridium* spp. (decline ~7 $\log_{10}$cfu/mL), *B. fragilis* group (decline ~7 $\log_{10}$cfu/mL) and *Lactobacillus* spp. (decline ~5.5 $\log_{10}$cfu/mL). After initial reductions in populations, most bacterial groups recovered to pre-ceftriaxone levels by the end of period D. *Bifidobacterium* spp. and *Clostridium* spp. remained low or below LOD for the remainder of the experiment.

5.5.4.3 Sessile Indigenous Gut Microbiota Populations

Most bead-associated bacterial populations established and maintained a population within the *C. difficile* internal control period (period B, figure 5.5.1.1b), with *B. fragilis* group (~6-7.5 log_{10}cfu/g) and *Clostridium* spp. (~4 – 5 log_{10}cfu/g) the most and least abundant groups, respectively. *Lactobacillus* spp. failed to associate with the MA interface until day 23/24 where it reached a population of ~4.5 log_{10}cfu/g before once again declining to below the LOD.

Commencement of ceftriaxone instillation on day 21 elicited a rapid decline in all bacterial groups with the exception of *Enterococcus* spp., which maintained a steady population. LFE demonstrated minor reaction to ceftriaxone instillation with an initial population decrease (~2 log_{10}cfu/g) before subsequent recovery to pre-ceftriaxone levels of 6 log_{10}cfu/g with a similar observation for *Bifidobacterium* spp. *Clostridium* spp. and *Lactobacillus* spp. were the only bacterial groups that failed to recover to pre-ceftriaxone populations by the end of the experiment.

5.5.4.4 Planktonic *C. difficile* Populations

After introduction of *C. difficile* spores into the gut model total viable counts (TVC) and spores were approximately equivalent at ~4 log_{10}cfu/mL (figure 5.5.1.2a). An initial decline in populations was evident before the second inoculum of spores was instilled on day 21, which was concurrent with an increase in *C. difficile* TVC (~4 log_{10}cfu/mL) and spores (~1.2 log_{10}cfu/mL). Subsequent declines in both TVC and spores to below the LOD before the cessation of ceftriaxone instillation was evident. Spores remained below the LOD for the remainder of the experiment whilst 7 days after ceftriaxone instillation ceased *C. difficile* TVCs increased to

~6 log_{10}cfu/mL. This increase in TVCs was concurrent with an increase in toxin (2.5 RU).

5.5.4.5 Sessile *C. difficile* Populations

Initial bead-associated *C. difficile* TVCs and spores were approximately equivalent at ~4 log_{10}cfu/g (figure 5.5.1.2b). Six days after the introduction of *C. difficile* spores into the gut model, TVCs and spores were below the LOD of detection, where they remained until TVCs increased to ~3.2 log_{10}cfu/g five days after cessation of ceftriaxone instillation. An increase in toxin to a maximum tire of 2 RU was observed on the final day of the experiment.

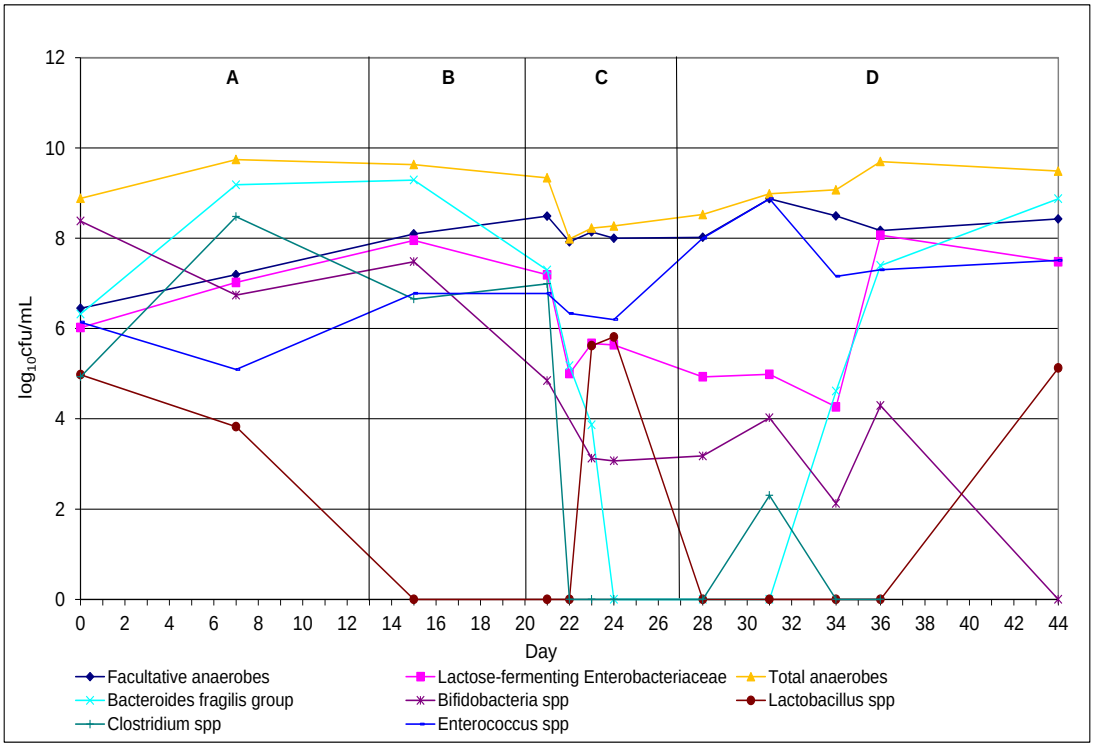

Figure 5.5.1.1a:

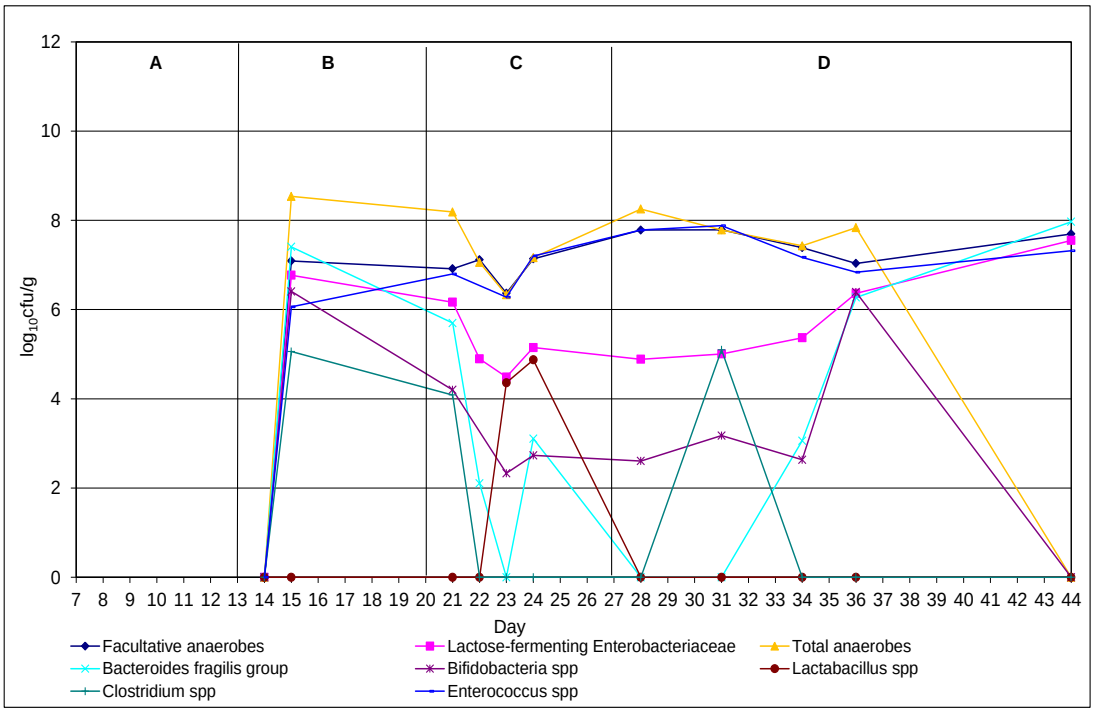

Figure 5.5.1.1b: A, planktonic (log_{10}cfu/mL) and **B,** bead-associated (log_{10}cfu/g) (±SE) populations of indigenous gut microbiota in single stage mucin alginate gut model investigation 5. Vertical line represents the last day of each period. A – steady state; B – internal control; C – ceftriaxone instillation; D – rest.

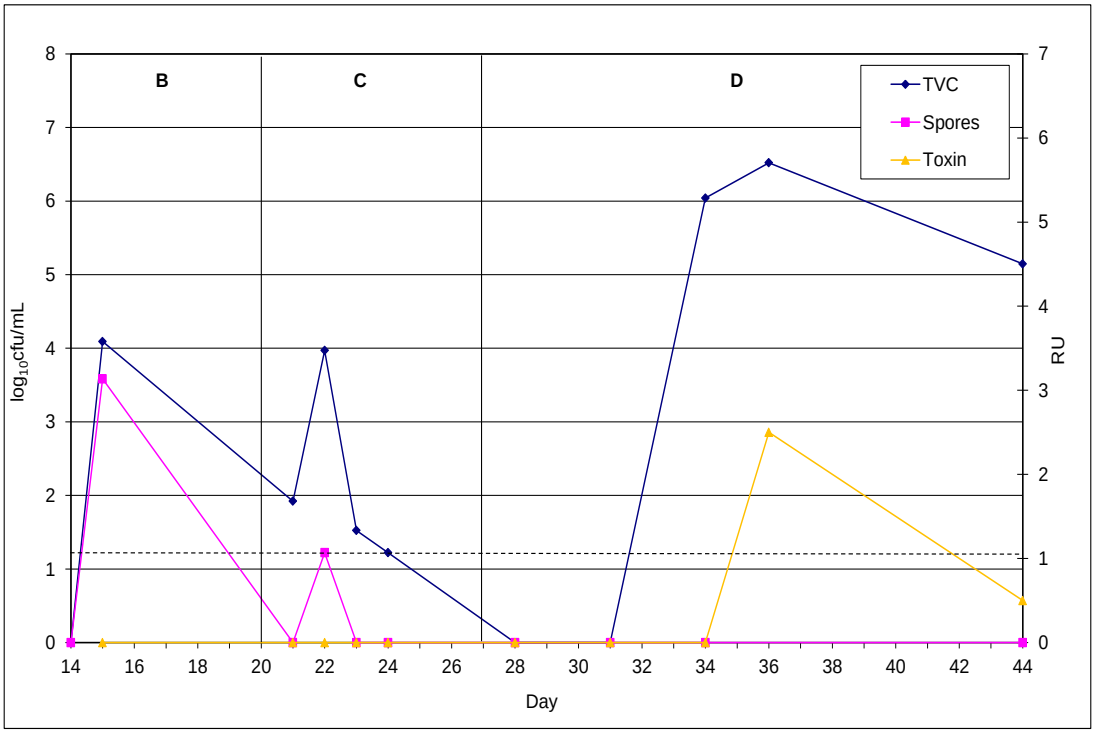

Figure 5.5.1.2a:

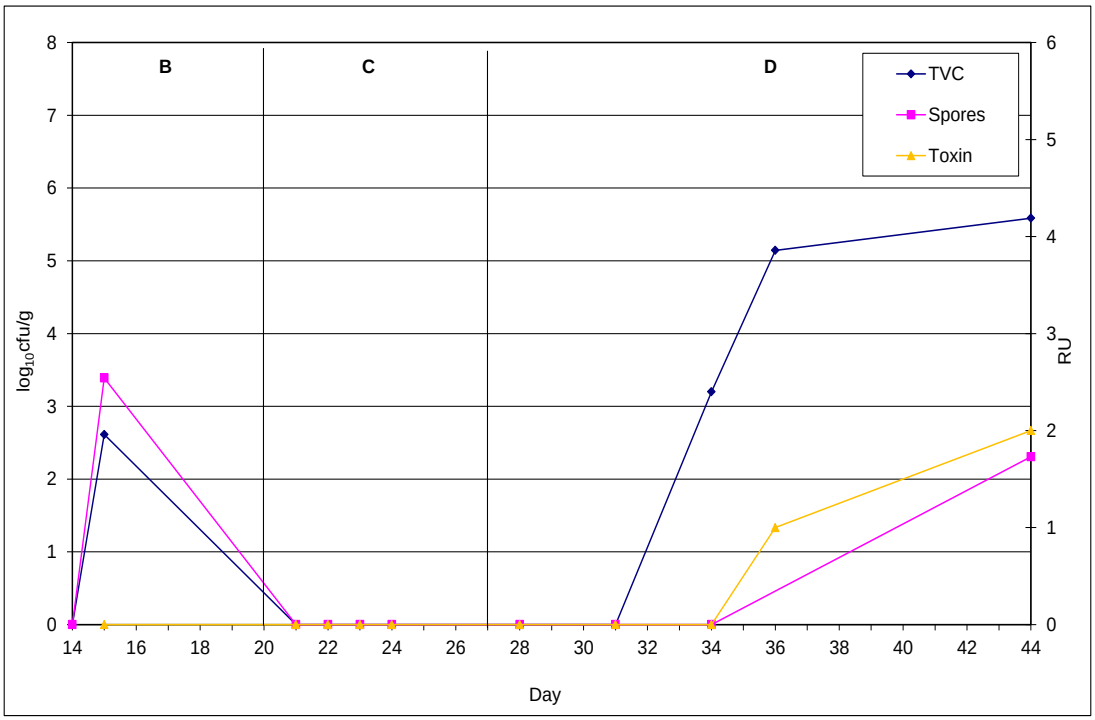

Figure 5.5.1.2b: A, planktonic (log_{10}cfu/mL) and bead-associated populations (log_{10}cfu/g) (±SE) of *C. difficile* in single stage mucin alginate gut model investigation 5. Vertical line represents the last day of each period. B – internal control; C – ceftriaxone instillation; D – rest.

5.5.5 Discussion

Degradation of mucin by a subpopulation of faecal bacteria has been previously characterised[309]. Despite attempts to reduce this degradation the continued loss of bead integrity was evident in single stage gut model experiments. Alginate is a naturally derived hydrogel-forming polysaccharide widely used in tissue engineering[551]. Exposure of alginate to multivalent cations results in the formation of ionic bridges between polymer chains giving rise to a high level of structural integrity. Alginate is sensitive to the action of chelating compounds such as phosphate, citrate and lactate [552] and alginate-degradation enzyme, alginate lyase has been isolated from marine molluscs, bacteria and brown algae[553-556]. Whilst the degradation of alginate has been documented, the increased lifespan of 20:80 M:A compared with 50:50 M:A beads observed within this study suggests that faecal bacteria-associated degradation of alginate is reduced compared with mucin.

Altered MA bead composition did not affect bacterial colonisation within the single stage chemostat, with the rapid and stable association of bacteria to the bead surface. MA (20:80 M:A) bead-associated bacterial gut microbiota populations (figures 5.5.1.1-2) were similar to those observed on the 50:50 M:A surface (figures 5.5.1.1-2). Introduction of beads into the model on day 7 did not affect planktonic populations with the exception of *Lactobacillus* spp. which decreased to below LOD. The introduction of an increased biomass into the model results in a degree of expulsion of culture fluid from the model system, possibly resulting in the decrease of *Lactobacillus* spp. populations.

The tendency for *Lactobacillus* spp. to exist within biofilms has previously been disputed with both *in vitro* and *in vivo* data suggesting that this bacterial group is either absent or present in reduced numbers within intestinal biofilms[446, 447]. The sporadic isolation of sessile *Lactobacillus* spp.

from investigation experiment 5 appears to support this notion. However, planktonic *Lactobacillus* spp. populations were also sporadic; therefore this factor is unlikely to be specific to sessile *Lactobacillus* spp. behaviour.

Investigation 5 utilised a more complex experimental design than previous experiments. The prolonged bead survival allowed for antimicrobial intervention within the experimental run. Ceftriaxone instillation (150 mg/L, once daily, 7 days) commenced concurrent with instillation of a single inoculum of *C. difficile* spores (period C, figure 5.5.1). A rapid decline in both planktonic and sessile populations was evident one day after instillation commenced. Rates of planktonic and sessile C*lostridium* spp., *B. fragilis* group and *Bifidobacterium* spp. population declines were comparable, although a ~2.5 $\log_{10}$cfu/mL LFE reduction was observed in the planktonic phase compared with a ~1 $\log_{10}$cfu/g sessile reduction. Numerous groups have reported that biofilms confer a reduced susceptibility to antimicrobials agents[399, 400]. LFE populations present within the protected environment of the biofilm may be less receptive to the action of ceftriaxone. The reduced susceptibility of sessile *E. coli* to cepholasporins is well documented. The minimum biofilm eradication concentration of cefotaxime, a third generation cephalosporin similar to ceftriaxone, is reported as being 256 mg/L (planktonic MIC 1 mg/L)[399]. However, similar observations have been identified in other indigenous gut microbiota, and the reason this phenomenon was only evident in LFE populations within this study is unclear.

Probert and Gibson utilised a MA bead framework within a chemostat system and reported higher levels of *E. coli* detection in biofilm samples compared with populations within the culture fluid[447], with similar findings evident on mucin gels within a two-stage chemostat culture system[446].

C. difficile spore preparations (~10^7 cfu) were inoculated into the model on days 14 and 21. Planktonic and sessile *C. difficile* spores were detected the day after instillation with planktonic populations ~ 1 $\log_{10}$cfu/mL greater than sessile populations. Both planktonic and sessile spores appeared to be quickly diluted out of the model. The wash out of planktonic spores is sometimes observed within the original gut model, although rarely so rapidly. However, the absence of sessile spores can not be attributed to the dilution factor of the model as MA beads do not exit the model in the same manner as the culture fluid. Low levels of expulsion of the beads from the waste outlet port of the model was observed, possibly explaining the decrease in bead-associated spores. Sampling of planktonic and sessile populations was carried out one day after initial *C. difficile* spore inoculation (day 15) and again one day after the second instillation of spores concurrent with ceftriaxone instillation (day 22). An increase in planktonic populations which coincides with the instillation of a further inoculum of spores was observed a day later (day 22). Sessile *C. difficile* populations were below the LOD between days 21-31; this may be due to an increased timeframe for association to the MA bead. However, planktonic *C. difficile* possessed lower populations than previous single stage (data not shown) and gut model experiments[270, 512] which should be taken into consideration when analysing the absence of bead-associated *C. difficile* during period C. The second inoculum of spores was concurrent with ceftriaxone instillation although it is unlikely that the antimicrobial activity of this agent was responsible for this reduced spore population. Ceftriaxone has not been shown to possess anti-spore activity in previous gut model experiments therefore unlikely to be the cause of this reduction in *C. difficile* populations[525].

5.6 Triple Stage Mucin Alginate Gut Model

5.6.1 Rationale

The design of the triple stage human gut model is reflective of condition *in vivo,* with vessel 1 reflective of the high substrate availability of the proximal colon, and vessel 3 reflective of the low substrate availability of the distal colon. The high nutrient availability in the proximal colon will support the colonisation and proliferation of increased bacterial populations compared with the distal colon, so the levels of mucinolytic enzyme producing bacteria should be lower in the distal colon. Therefore, a triple stage human gut model was set up to investigate whether mucin alginate beads would display increased integrity in the lower substrate environment of vessel 3.

5.6.2 Experimental Design

The triple stage human gut model was set up and prepared as described in section 4.2.1. Following instillation of the faecal emulsion into all three vessels, the model was top fed with a complex growth medium (section 4.2.2) at a controlled rate (flow rate = 13.2 mL/h).

The experimental timeline for this experiment is highlighted in figure 5.6.1. The model was left for a steady state period for 13 days to allow bacterial populations to equilibrate (period A, figure 5.6.1). On day 7 of this period, 50 % (w/v) 50:50 MA beads were instilled into vessel 3.
Days 14-20 serve as an internal control period to demonstrate that spores remain quiescent in the absence of antimicrobial administration (period B; figure 5.61). On day 21 a further inoculum of *C. difficile* spores along with a dosing regimen of clindamycin, 33.9 mg/L, QD for 7 days were instilled into the model (period C; figure 5.6.1). Planktonic and sessile populations were

sampled and enumerated intermittently for the duration of the experiment. See table 5.1 for experimental details.

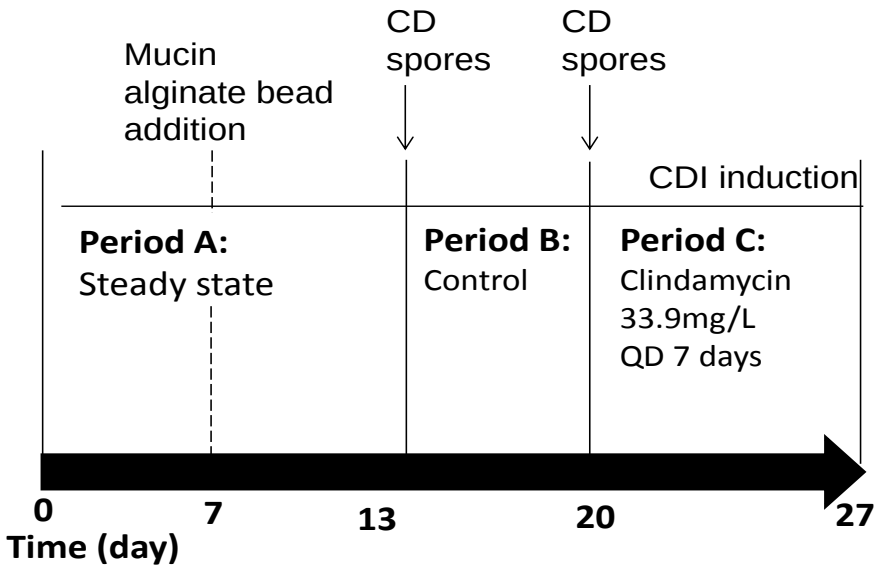

Figure 5.6.1: Experimental design of the triple stage mucin alginate human gut model investigation. Vertical line represents the last day of each period.

5.6.3 Results

5.6.3.1 Experimental Observation

Addition of the 50:50 M:A bead into vessel 3 of a triple stage model extended the bead lifespan from 3-13 days within the single stage model to 14 days in the triple stage model (day 21 of the experiment) but prevented completion of period C. MA beads settled to the base of the vessel and expulsion of beads from the model was minimal. The pH probe protruded into the settlement of MA beads; thus disrupting functionality of the probe.

5.6.3.2 Planktonic Indigenous Gut Microbiota Populations

All bacterial groups established relatively steady planktonic populations in periods A and B (figure 5.6.1.1 and 5.6.1.2) within both vessel 2 and 3.

Bifidobacterium spp. dominated (~8 log_{10}cfu/mL) with *Clostridium* spp. (vessel 2) and also LFE (vessel 3) displaying the least abundant populations by the end of the steady state period (period A).

5.6.3.3 Sessile Indigenous Gut Microbiota Populations

MA beads were introduced into vessel 3 of the gut model on day 7. By day 9 all bacterial groups had associated with the bead surface with populations remaining steady during period B (figure 5.6.1.3). *B. fragilis* group (~6.5 log_{10}cfu/g) and LFE (~3.8 log_{10}cfu/g) were the most and least numerous bacterial populations adherent to MA beads, respectively.

5.6.3.4 Planktonic *C. difficile* Populations

Within all 3 vessels, TVCs were equal to spore populations, and toxin was absent for the duration of the experiment (figures 5.6.1.4-6). *C. difficile* total cell populations in vessels 1, 2 and 3 were ~5 log_{10}cfu/g, ~ 5 log_{10}cfu/g and ~4.5 log_{10}cfu/g, respectively, and these populations were maintained for the duration of the experiment.

5.6.3.5 Sessile *C. difficile* Populations

Bead-associated *C. difficile* TVCs and spores were equivalent for the duration of the experiment, and toxin was absent throughout (figure 5.6.1.7). *C. difficile* populations decreased from ~3 log_{10}cfu/g on day 15 to ~1.7 log_{10}cfu/g on day 21.

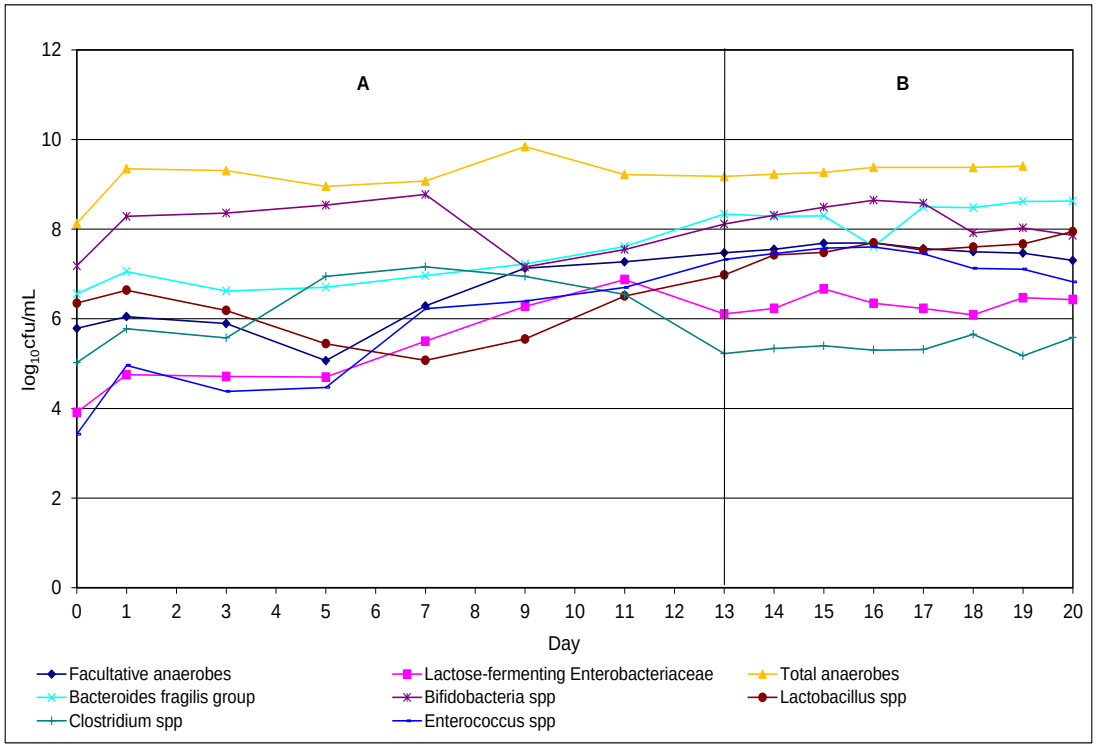

Figure 5.6.1.1: Planktonic populations (log_{10}cfu/mL) (±SE) of indigenous gut microbiota in vessel 2 of the triple stage mucin alginate biofilm gut model investigation. Vertical line represents the last day of each period.

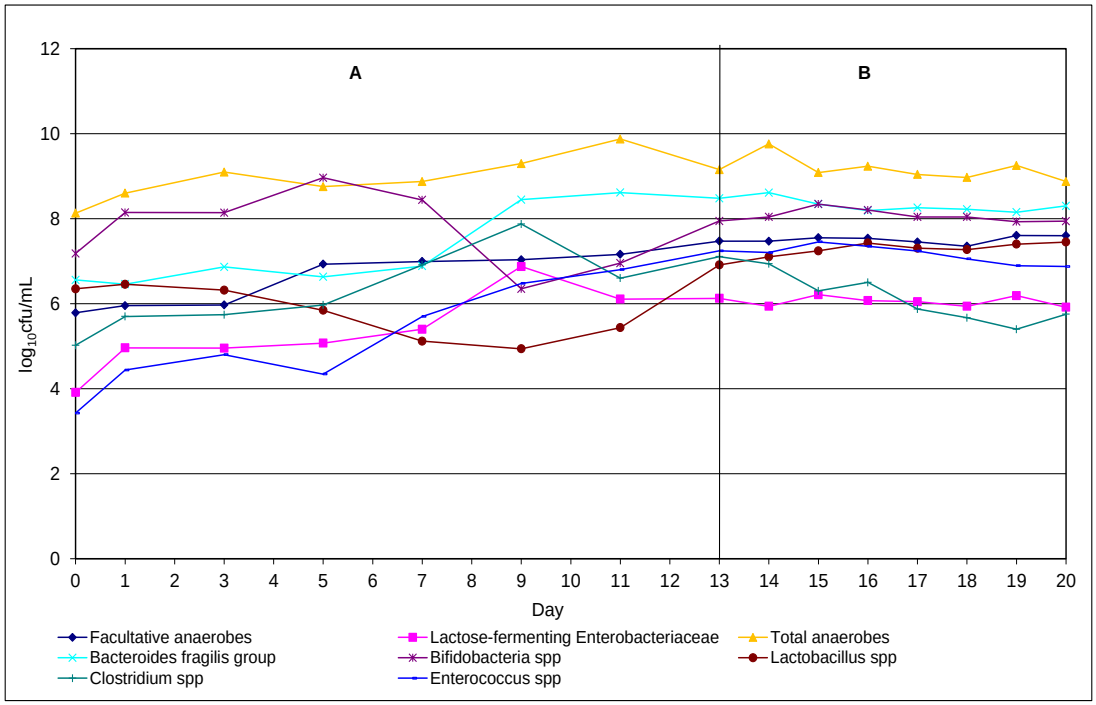

Figure 5.6.1.2: Planktonic populations (log_{10}cfu/mL) (±SE) of indigenous gut microbiota in vessel 3 of the triple stage mucin alginate biofilm gut model investigation. Vertical line represents the last day of each period.

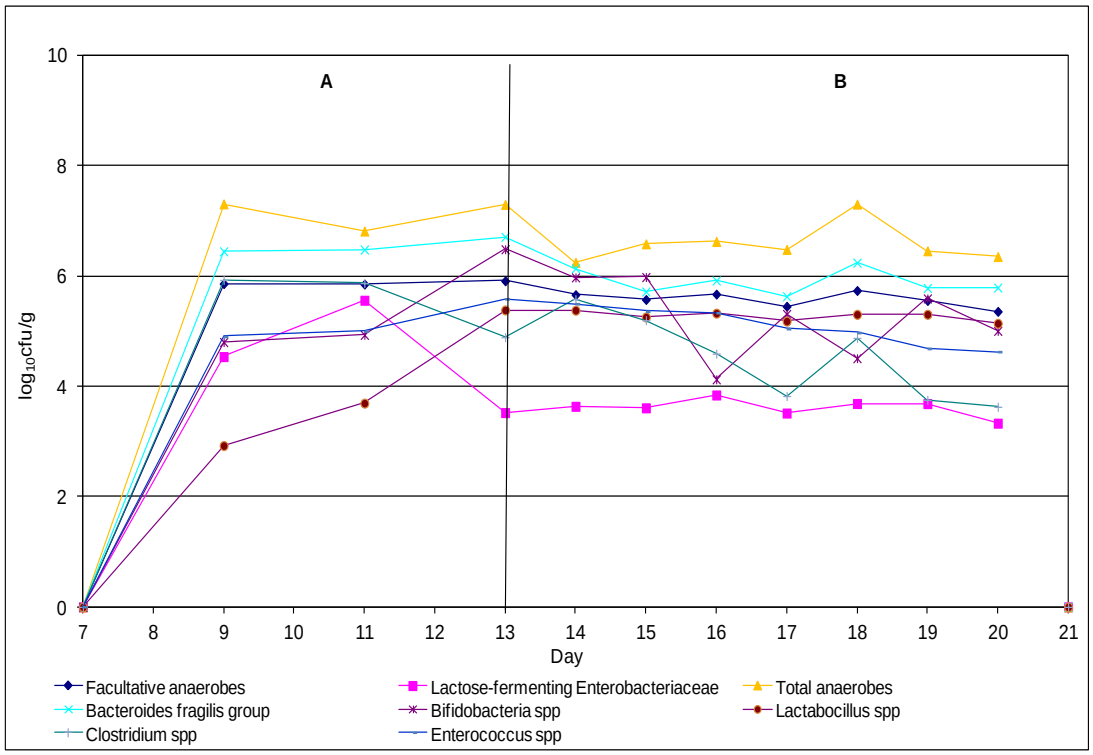

Figure 5.6.1.3: Bead-associated populations (log_{10}cfu/g) (±SE) of indigenous gut microbiota in vessel 3 of the triple stage mucin alginate biofilm gut model investigation. Vertical line represents the last day of each period.

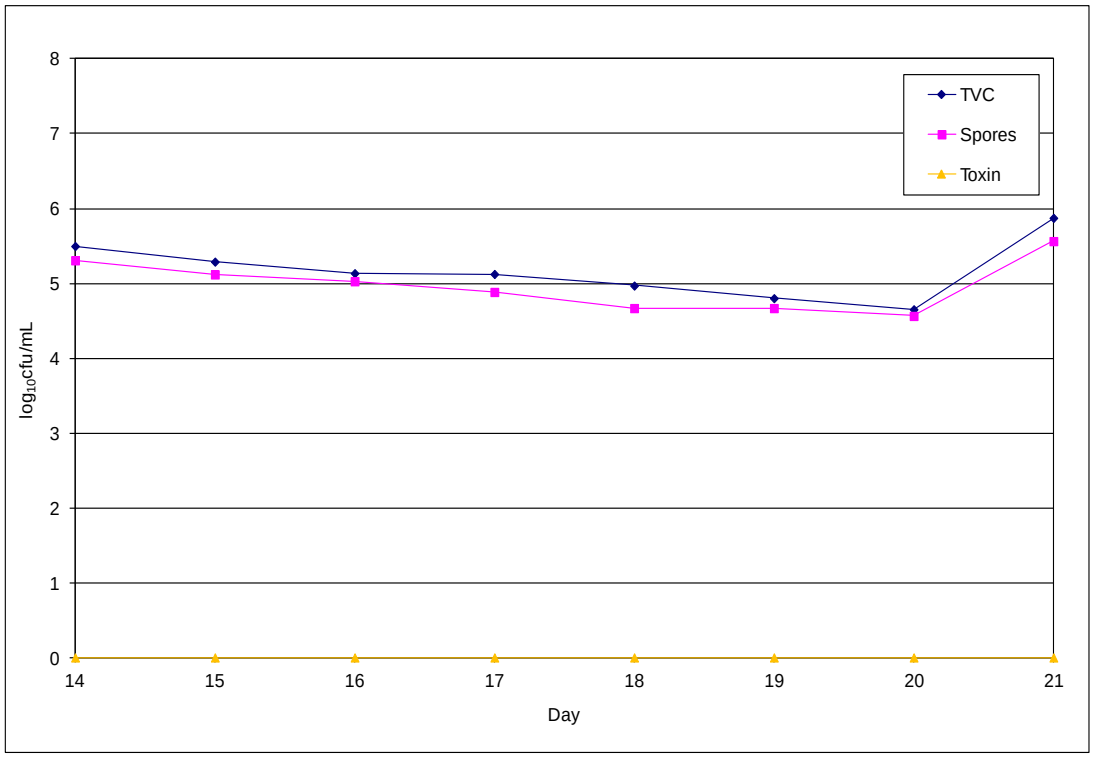

Figure 5.6.1.4: Planktonic populations (log_{10}cfu/mL) (±SE) of *C. difficile* in vessel 1 of the triple stage mucin alginate biofilm gut model investigation.

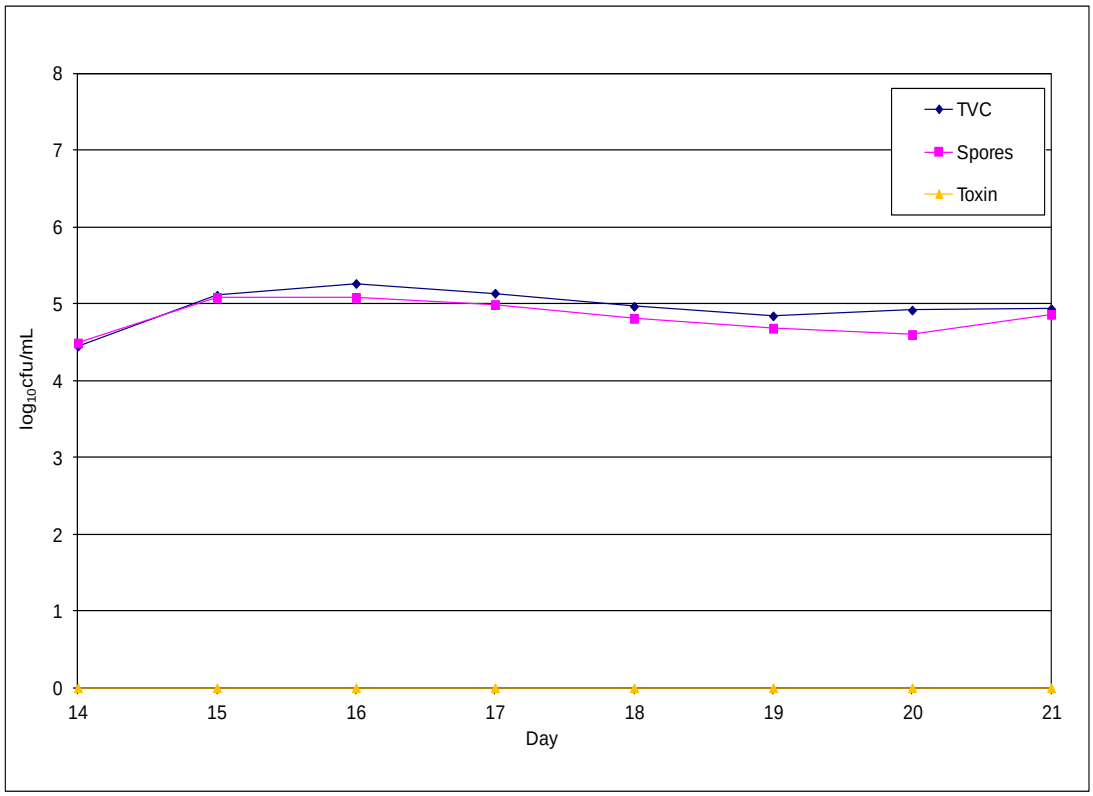

Figure 5.6.1.5: Planktonic populations (log_{10}cfu/mL) (±SE) of *C. difficile* in vessel 2 of the triple stage mucin alginate biofilm gut model investigation.

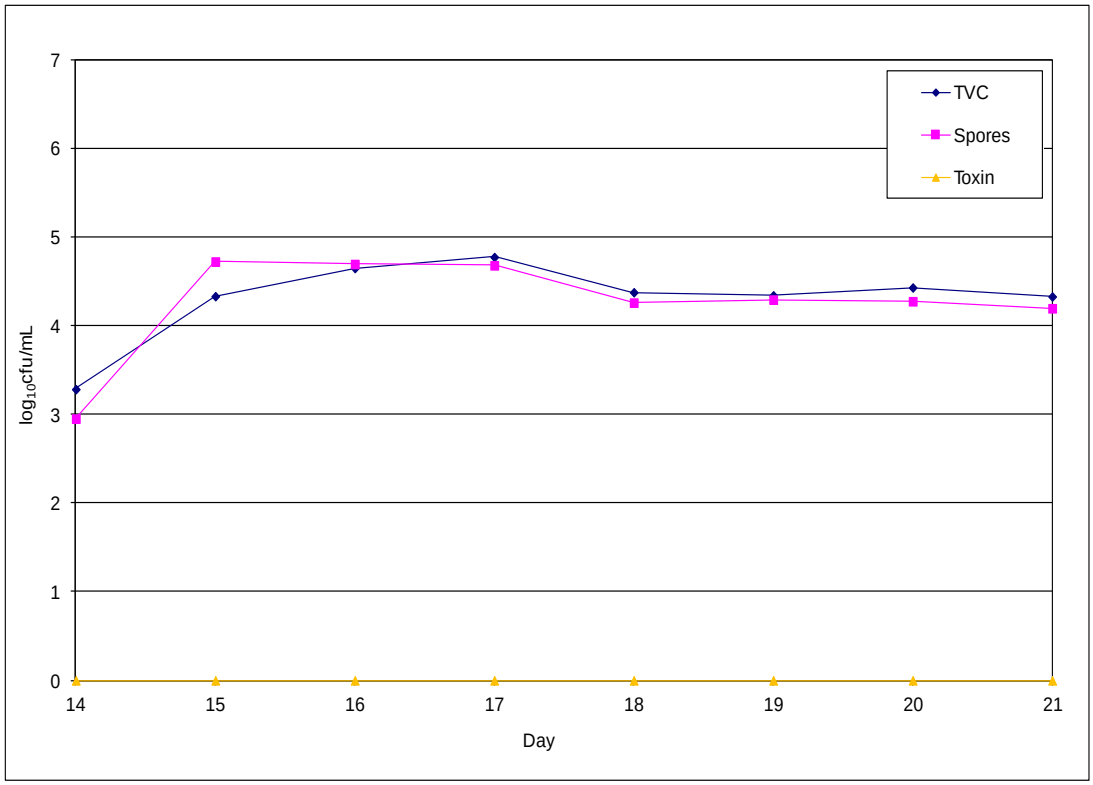

Figure 5.6.1.6: Planktonic populations (log_{10}cfu/mL) (±SE) of *C. difficile* in vessel 3 of the triple stage mucin alginate biofilm gut model investigation.

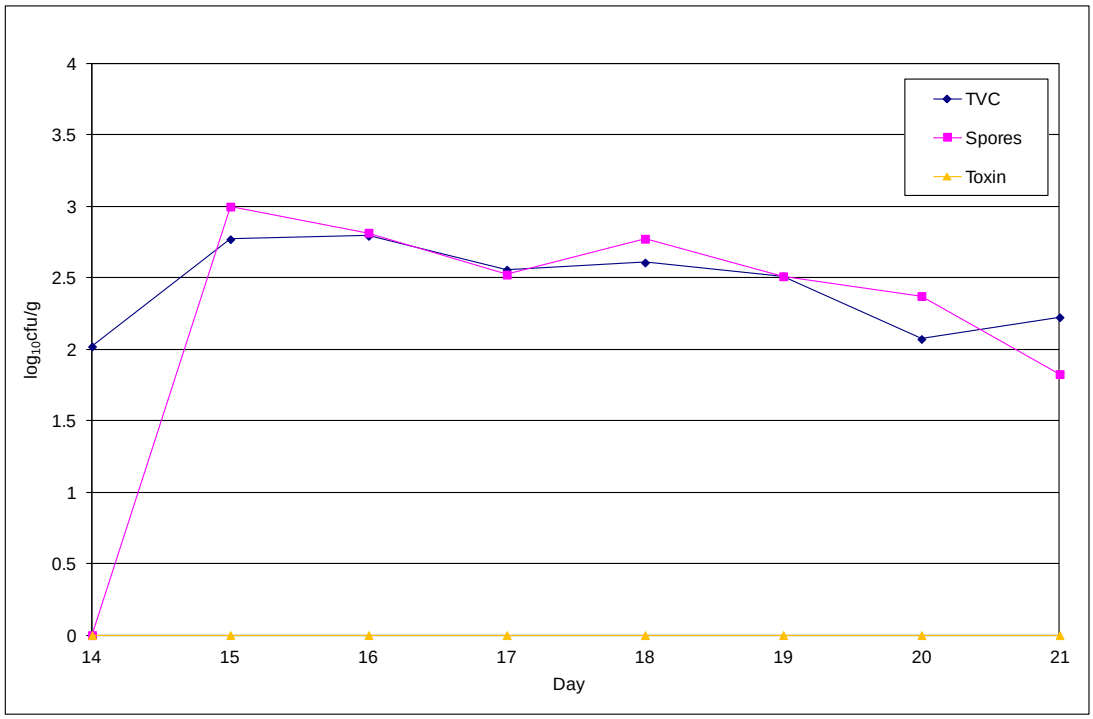

Figure 5.6.1.7: Bead-associated populations (log_{10}cfu/g) (±SE) of *C. difficile* in vessel 3 of the triple stage mucin alginate biofilm gut model investigation.

5.6.4 Discussion

The human gastrointestinal tract comprises distinct regions which confer unique environments. The proximal colon displays increased substrate availability and low pH whilst the converse is true in the distal colon. The physiology and ecology of bacteria growing in the proximal colon is distinct from those in the distal colon. Bacterial metabolism and hydrolytic enzyme production differs between bacterial populations. Environmental conditions and metabolism end products within vessel 3 of the gut model will vary from those in vessel 1. As a result it was hypothesised that the unique conditions within vessel 3 may confer an increased lifespan of MA beads.

MA beads were previously instilled in a high substrate vessel, which elicited the rapid degradation of the beads (3-13 days). MA beads in the triple stage experiment were instilled into vessel 3 (distal colon) and prolonged the lifespan of the beads to 14 days. Whilst this was an improvement of

previous 50:50 M:A bead experiments, 14 days remains insufficient for the aims of this study. Pure and mixed culture studies demonstrate that synthesis of hydrolytic enzymes is catabolite regulated, and is therefore dependent on carbohydrate concentrations. Macfarlane *et al* established that mucin degradation is greatest in substrate-limited environments[446], potentially explaining the continued degradation of mucin within vessel 3 of the triple stage mucin alginate experiment.

MA beads were able to support bacterial adherence of all groups enumerated, including *Lactobacillus* spp. Both planktonic and sessile indigenous gut microbiota populations remained stable in the absence of antimicrobial intervention and showed similarity with investigation 5 results.

Within the triple stage experiment both planktonic and sessile *C. difficile* populations behaved in a similar manor; *C. difficile* existed as spores only and remained detectable for the duration of the experiment. Planktonic *C. difficile* spore populations were ~1.5 $\log_{10}$cfu/mL greater than their biofilm counterparts, an observation commonly encountered during biofilm analysis studies. This is hypothesised to be due to an increased proportion of biofilm pellet weight owing to extracellular material, rather than bacterial mass.

The planktonic mode of growth of *C. difficile* described here mimics observations consistently observed within the original gut model [512]; with *C. difficile* spores remaining quiescent in the absence of antimicrobial pressure. Distinct differences in planktonic compared with sessile bacterial characteristics are well documented[292]. However, within this study the sessile mode of growth largely mirrored the planktonic mode of growth.

5.7 Conclusions

The gastrointestinal tract is lined by a mucosal surface covered largely by mucus. In healthy adults this mucus layer harbours sessile bacterial communities which exist within biofilm structures. These mucins structurally resemble the porcine mucus utilised in this study[304], however the structural integrity of mucus alone is insufficient for immersion within the faecal emulsion of a gut model. The combination of alginate, an EPS produced by *P. aeruginosa,* and mucin has been successfully utilised as an adhesion framework previously[447]. The formation of the bead structure in this experiment is carried out in the presence of 0.3M $CaCl_2$. Ca^{2+} stabilizes the crossbridges between alginate, increasing mechanical stability[557].

A series of experiments were conducted in order to extend the integrity of MA beads within an *in vitro* human gut model. Single stage mucin alginate experiments using 50:50 M:A beads were initially carried out to provide preliminary information. After the continued degradation of beads within a single stage model, a triple stage model was utilised with the aim to reduce degradation. In addition, the composition of the beads was altered to increase the proportion of alginate to mucin (20:80 M:A).

Carbohydrate structures present on mucins provide highly diverse binding sites for microbial adhesion, as well as an energy source. Within this study high levels of gut microbiota were found in association with the MA beads. The degradation of mucin within the highly competitive environment of the gut model has been consistently observed by bacteria that utilise mucin components as a major energy source and establish a population on MA beads, thus providing an ecological advantage of colonisation of mucin structures[308, 499, 558, 559].

Sessile populations within these experiments largely reflect planktonic populations with *B. fragilis* group dominating populations and

Enterococcus spp. and *Clostridium* spp. the least populous groups for both modes of growth. All bacterial groups enumerated during these experiments were detected in association with MA beads. The association of *Bifidobacterium* spp. with mucin within continuous culture systems has only been reported within nutrient-limited conditions[446], a characteristic not observed within MA gut model systems reported here. During batch MA experiments MA bead adherence was not observed for all bacterial groups. This observation is possibly mediated by the difference in conditions between batch and continuous culture systems.

The association of *C. difficile* with mucus has previously been reported[123, 124,117]. Whilst evidence suggests that *C. difficile* is able to colonise mucus the ability of this organism to degrade components of mucins remains to be fully elucidated. *C. difficile* is characteristically able to ferment simple monosaccharide sugars[137] as well as *N*-acetylneuraminic acid and *N*-acetlyglucosamine[560]; both are found in large amounts in the side chains of mucin, however *C. difficile* is unable to cleave the monosaccharides from the oligosaccharide chains. The lack of neuraminidase, a glycoside hydrolase enzyme, has been identified for this pathogen[561, 562]. These data suggest that *C. difficile* is unable to utilise mucin as an energy source, but can associate with mucus in mixed-species communities, possibly utilising simple carbohydrate structures cleaved from mucin structures by other organisms.

C. difficile is able to adhere to MA beads within batch and single and triple stage continuous culture systems, and generally maintains populations for the duration of the experiment.

C. difficile planktonic and sessile behaviour was varied throughout these continuous culture experiments. This may in part be due to the variation in the method of *C. difficile* introduction into the model. Variations in experimental set up, growth media, faecal emulsion, and bead composition

may all play a role in this inconsistent behaviour. The aim of these experiments was to assess the suitability of the MA bead design to adapt the original gut model. The analysis of bacterial behaviour was secondary; therefore, appropriate experimental control necessary for such investigation was absent. Results presented here pertaining to bacterial behaviour should be interpreted within caution and only used as an additional observation.

Submerging the beads within a faecal emulsion results in rapid degradation, which was consistently observed in the MA investigation experiments. Further experiments to elucidate the mechanisms involved in this degradation were carried out and are highlighted in chapter 3.0. Results from the mucin degradation experiment highlight the sequential degradation of mucin glycoproteins by a sub-population of faecal bacteria. This degradation was reduced by the combination of mucin with alginate. Investigative experiment 5 was designed to test this theory.
A 20:80 mucin:alginate mixture was used to form the bead framework. This construction increased the lifespan of the bead for a minimum of 30 days, whilst facilitating the adhesion of indigenous gut microbiota to the bead surface. The increased timeframe of bead survival provided an extended period for biofilm formation; however macroscopic biofilm structures were not evident, despite the presence of visible biofilm on the glass walls of the chemostat vessels.

Whilst the MA investigation experiments were being conducted, analysis of the biofilm from the vessel walls of the original model was on-going (chapter 4.0). Biofilm formation was greatest in vessel 1 (also observed by Macfarlane *et al* [446]) of the triple stage model, with the liquid-air interface facilitating the greatest biofilm biomass. The MA beads were fully submerged within the faecal emulsion, possibly explaining the lack of visible biofilm formation. It is speculated that the adherence of the bacterial populations apparent on the bead structure may represent the immature

stages of biofilm formation (reversible and irreversible adhesion) with maturation processes absent. The liquid-air interface has been shown to provide favoured biofilm formation for *B. cereus*, with the formation of biofilm pellicles[345]. In order to understand the biofilm mode of growth fully it is necessary for the sessile processes to be active. The presence of a mature biofilm with distinct microcolonies encased within a matrix is a fundamental characteristic of a biofilm. Other biofilm traits such as the upregulation of certain phenotypic traits may rely on increased cell density. The bead-associated bacterial populations observed in the presnt experiments may lack these vital attributes.

6.0 Substratum Material Investigation

6.1 Background

Further substratum material investigation is necessary in order to ascertain a suitable design for mature biofilm growth within an *in vitro* human gut model. Information gained in these preliminary MA experiments provides information on the composition of bacterial adherence to this material. This information, along with other published work can be used to ensure adherent populations on other materials closely mimic MA-associated and *in vivo* mucosa-associated populations.

6.2 Single Stage Glass and Magnetic Bead Investigation

6.2.1 Rationale

Alternative substratum materials, which were inert and non-degradable were investigated. Biofilm formation is consistently observed on the glass vessels of the original gut model. Whilst this substratum material is inferior to MA in mimicking conditions *in vivo*, it may facilitate the formation of mature biofilms that could provide valuable biofilm-associated characteristics otherwise absent from the immature biofilm structures present on MA beads. Biofilm composition on the glass vessels of the model have previously been analysed (chapter 4.0) and demonstrate mature biofilm strucutre and bacterial populations similar to those on MA beads and other published work[292, 294, 446, 563]. However, one of the major limitations of this work was the destructive nature of the sampling process, only allowing the biofilm to be analysed at the end of an experiment.

A variety of substratum materials were considered for this investigation including cellulose and polystyrene, but disregarded due to a lack of suitability for this project. Reports of cellulose degradation by anaerobic bacteria were noted[564] and polystyrene was hypothesised to float on the surface of the culture fluid, thus allowing for their expulsion from the vessel through the waste outlet port.

Glass beads were initially investigated as they are inert, non-degradable, readily available and allowed multiple sampling opportunities. MA beads were problematic in that they sometimes floated to the top of the vessel, where they exited through the waste outlet port. Glass beads are sufficiently dense to remain submerged within the model. Magnetic beads, covered in polytetrafluoroethylene (PTFE) material were also investigated as they potentially provided greater ease of sampling.

6.2.2 Materials and Methodology

6.2.2.1 Single Stage Chemostat Gut Model

The single stage gut model comprises of a single glass fermentation vessel (280 mL), top fed with a complex growth medium and was set up as described in section 5.2.1.1.

6.2.2.2 Magnetic and Glass beads

One hundred and twenty grams of glass beads (2 mm diameter) and 1 g of PTFE-covered magnetic beads (2 mm diameter) were introduced into the vessel via the sample port.

6.2.2.3 Sampling Protocol

Planktonic culture samples were removed from the vessel via a sample port secured by a glass stopper on days 0 and 25. Bead-associated bacterial populations were sampled on day 25 only. The chemostat lid system was detached and glass beads removed from the vessel using a sterile scoop and magnetic beads removed using a sterile magnet.

6.2.2.4 Enumeration of Planktonic Indigenous Gut Microbiota

Planktonic bacterial populations were enumerated as described previously (section 2.2) and populations expressed as $\log_{10}$cfu/mL.

6.2.2.5 Enumeration of Sessile Indigenous Gut Microbiota

Glass and magnetic beads were weighed independently (as described in section 3.2.2.9). Glass and magnetic beads were resuspended in 5 mL and 2 mL saline, respectively, and vortexed intermittently for 30 mins. Bacteria were enumerated as described previously (section 2.2) and expressed as $\log_{10}$cfu/g of beads.

6.2.2.6 Experimental Design

The experimental design timeline is highlighted in figure 6.2.1. Faecal emulsion along with 120 g glass and 1 g magnetic beads were instilled into the chemostat vessel via the sample point on day 0 and the media pump started. Original gut model growth medium (section 4.2.2; Appendix A1) was delivered into the model at a controlled rate. No interventions were made for 25 days (period A; figure 6.2.1). Vessel contents were not magnetically stirred for this experiment.

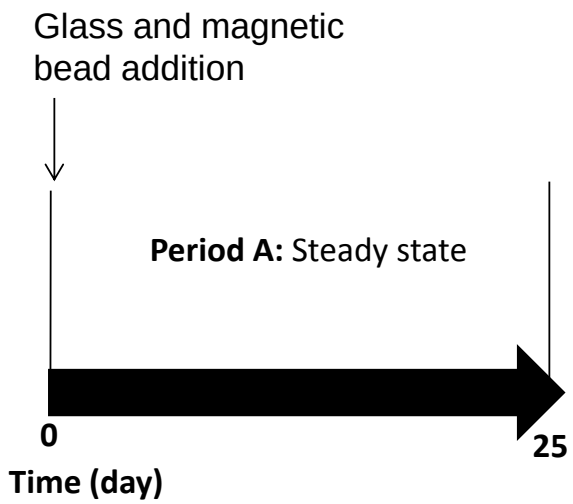

Figure 6.2.1: Experimental design of single stage glass and magnetic bead substratum investigation.

6.2.3 Results

6.2.3.1 Experimental Observations

Both glass and magnetic beads immediately sank to the base of the vessel where they remained for the duration of the experiment. Magnetic stirring of the vessel contents was not in operation in this experiment in order to prevent localisation of the magnetic beads. The natural stirring effect of the gas flow was insufficient to mobilise the beads, and sedimentation of particulate matter within the culture fluid was evident within the vessel and concentrated within the vicinity of the beads.

Upon removal of the beads from the vessel, macroscopic biofilm formation was not evident. Due to the density of the bead materials sampling at numerous time points was not possible; removal of the beads was only conceivable upon disruption of the vessel structure.

6.2.3.2 Planktonic Indigenous Gut Microbiota Populations

Planktonic indigenous gut microbiota populations were enumerated on day 0 and 25. Planktonic populations on day 25 were generally equivalent to or greater than corresponding populations on day 0, with the exception of *B. fragilis* group and *Lactobacillus* spp. (figure 6.2.3.1). Notably, *Enterococcus* spp. populations were ~3.5 $\log_{10}$cfu/mL greater on day 25 compared with day 0.

On day 0, *B. fragilis* group (~8.4 $\log_{10}$cfu/mL) and *Lactobacillus* spp. (~7.7 $\log_{10}$cfu/mL) were the dominant bacterial groups with *Enterococcus* spp. (~4.4 $\log_{10}$cfu/mL) and *Clostridium* spp. (~5.9 $\log_{10}$cfu/mL) the least populous.

On day 25 LFE (~8.7 $\log_{10}$cfu/mL) and *Enterococcus* spp. (~7.9 $\log_{10}$cfu/mL) dominated bacterial populations with *Lactobacillus* spp. (~5.9 $\log_{10}$cfu/mL) and *Clostridium* spp. (~5.8 $\log_{10}$cfu/mL) displaying the lowest populations.

6.2.3.3 Sessile Indigenous Gut Microbiota Populations

Sessile gut microbiota populations adherent to magnetic beads within the single stage chemostat vessel outnumbered those adherent to glass beads for all bacterial groups by ~0.5 – 1.5 $\log_{10}$cfu/g (figure 6.2.3.2). LFE and *Enterococcus* spp. were the prevalent and *B. fragilis* group, *Lactobacillus* spp. and *Clostridium* spp. the least common bacterial groups adherent to both glass and magnetic beads. Relative sessile bacterial populations were comparable with those of the planktonic bacterial populations on day 25 (figure 6.2.3.2), although sessile populations were ~0.5 - 1 $\log_{10}$cfu/g and ~0.5 – 2.5 $\log_{10}$cfu/g lower on magnetic and glass beads, respectively.

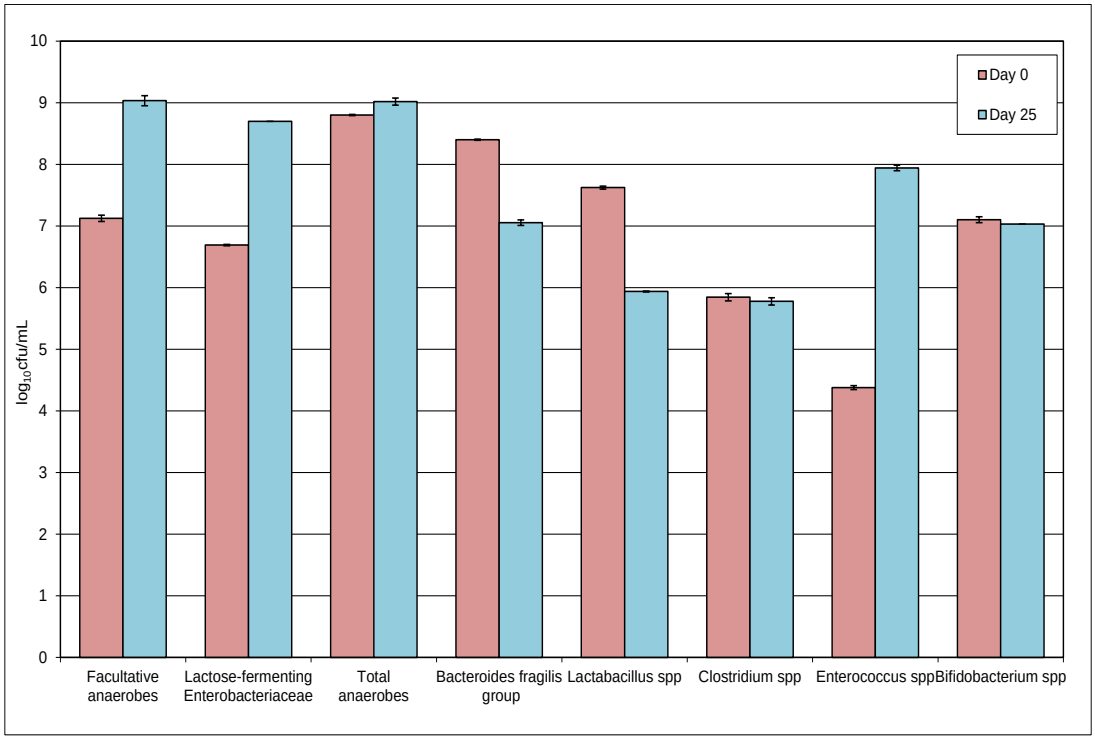

Figure 6.2.3.1: Mean (±SE) planktonic populations (log_{10}cfu/mL) of indigenous gut microbiota on days 0 and 25 of the single stage substratum material investigation.

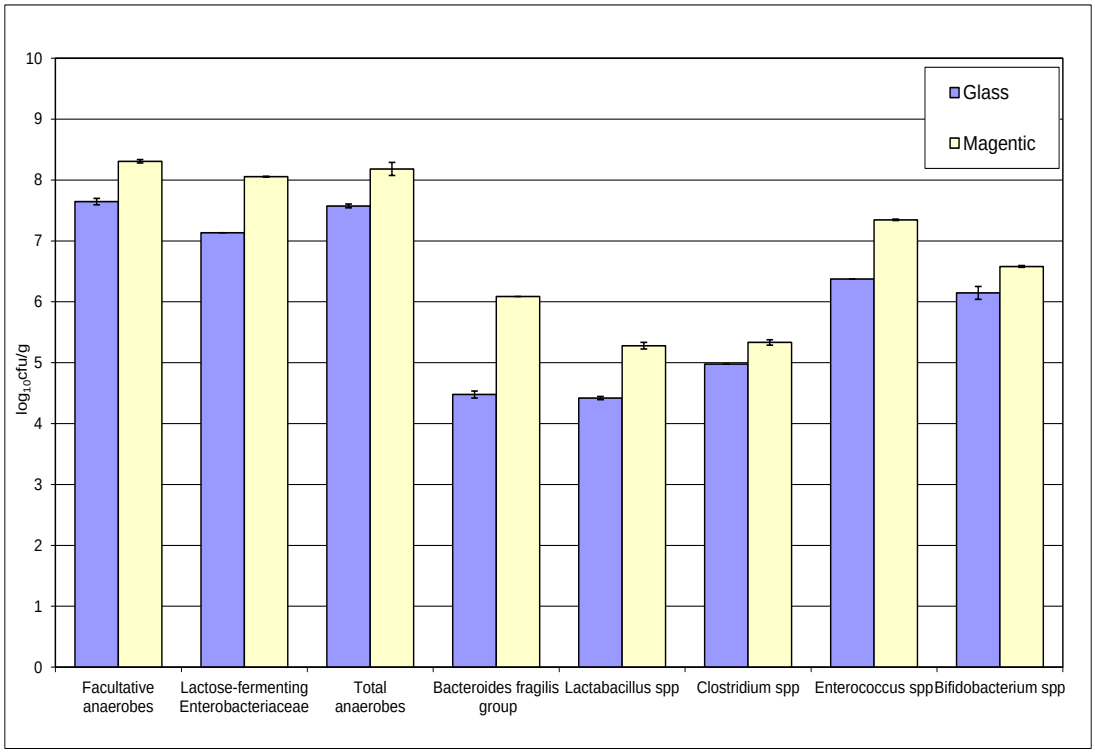

Figure 6.2.3.2: Mean (±SE) sessile populations (log10cfu/g) of indigenous gut microbiota on glass and magnetic beads on day 25 of the single stage substratum material investigation.

6.3 Single Stage Liquid/Air Interface Investigation

6.3.1 Rationale

The substratum materials investigated to date proved unsuitable for this study. Upon close observation of biofilm formation on the glass walls and attachments of the original gut model, it was noted that maximum biofilm formation was present on solid surfaces at the liquid/air interface. Since minimal biofilm was observed on the substratum materials investigated to date, all of which were submerged below the level of the liquid, substratum materials which extend across the liquid/air interface were investigated. Mature biofilm formation has consistently been observed on glass objects within the original gut model therefore this material was investigated in this experiment.

6.3.2 Materials and Methodology

6.3.2.1 Single Stage Chemostat Gut Model

The single human gut model comprises of a single glass fermentation vessel (280 mL), top fed with a complex growth medium and was set up as described in section 5.2.1.1.

6.3.2.2 Glass Rod

Prior to sterilisation and faecal emulsion inoculation, two glass pipettes were inserted into the chemostat vessel. These items extended across the liquid/air interface.

6.3.2.3 Sampling Protocol

Planktonic bacterial populations were sampled regularly for the duration of the experiment (as described in section 4.2.5). Glass rod-associated bacterial populations were sampled on days 41 and 55. One glass pipette per biofilm sample point was removed from the sampling port using sterilised tweezers.

6.3.2.4 Enumeration of Planktonic Indigenous Gut Microbiota and *C. difficile*

Planktonic bacterial populations were enumerated as described previously (sections 2.1 and 2.2). Populations were expressed as $\log_{10}$cfu/mL.

6.3.2.5 Enumeration of Sessile Indigenous Gut Microbiota and *C. difficile*

The glass pipette was transferred into a 15 mL centrifuge tube containing 10 mL of pre-reduced sterile saline. The tube was vortexed thoroughly until the pipette was devoid of macroscopic biofilm. The pipette was removed and discarded and bacteria enumerated as described previously (sections 2.1 and 2.2) and expressed as $\log_{10}$cfu/g.

6.3.2.6 Experimental Design

Substratum materials were present within the model upon instillation of the faecal emulsion on day 0. The experimental design is highlighted in figure 6.3.1. Briefly, after inoculation with faecal emulsion, gut microbiota populations were allowed to equilibrate for 25 days (period A), before a single inoculum of *C. difficile* spores were added to vessel 1 of the model on day 25. A second inoculum of *C. difficile* spores were inoculated into the model on day 32. At this point a dosing regimen of ceftriaxone (150 mg/L, once daily, 7 days) commenced (period C). Following commencement of

ceftriaxone dosing no further interventions were made until *C. difficile* germination, proliferation and high toxin production was observed (period D). Instillation of metronidazole (9.6 mg/L, TD, 7 days) commenced on day 44. Following cessation of therapeutic instillation the model was left without intervention for 13 days (period F). Biofilm was sampled on days 41 and 55.

Planktonic indigenous gut microbiota (periods A-F, vessels 2 and 3), *C. difficile* TVC, spores, cytotoxin (periods B-F, all vessels) and antimicrobial activity (periods C-F, all vessels) were monitored during the experiment.

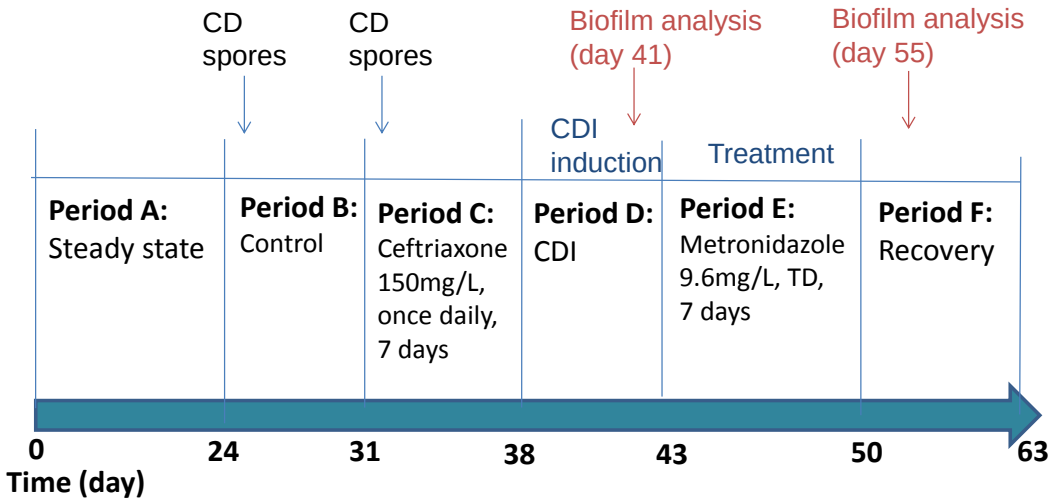

Figure 6.3.1: Experimental design of single stage liquid/air interface investigation. Vertical line represents the last day of each period.

6.3.3 Results

6.3.3.1 Experimental Observations

Insertion of glass pipettes into the chemostat vessel did not interfere with the working system. Macroscopic biofilm formation was visible at the liquid-air interface upon removal of the pipettes on day 41 and 55. The removal of macroscopic biofilm structures from the surface of the pipettes was successful.

6.3.3.2 Planktonic Indigenous Gut Microbiota Populations

All indigenous gut microbiota populations were present from the onset of the experiment with a steady increase in most populations within period A (figure 6.3.3.1). *Bifidobacterium* spp. predominated populations with *Enterococcus* spp. the least numerous by the end of period A. Most bacterial groups maintained a steady population during *C. difficile* spores instillation (period B), with the exception of *B. fragilis* group, *Bifidobacterium* spp. and *Clostridium* spp. which decreased by ~1-2 $\log_{10}$cfu/mL.

Instillation of a second inoculum of *C. difficile* spores on day 32, concurrent with the commencement of ceftriaxone dosing regimen (period C) elicited a rapid deleterious effect on LFE and *Clostridium* spp. (~4 $\log_{10}$cfu/mL and ~3 $\log_{10}$cfu/mL LFE and *Clostridium* spp. respectively), with minor declines in *Bifidobacterium* spp. and *Lactobacillus* spp. In contrast, *Enterococcus* spp. increased markedly (~4 $\log_{10}$cfu/mL) during period C, peaking at ~9 $\log_{10}$cfu/mL. Following ceftriaxone cessation, all bacterial groups recovered to pre-dosing levels by the end of period D, although *Enterococcus* spp. levels remained elevated.

Metronidazole instillation commenced on day 44 (period E). This resulted in minor fluctuations in bacterial populations, although *Enterococcus* spp. declined by ~3.5 log10cfu/mL by the end of period D, before rapidly recovering 6 days after metronidazole instillation ceased.

6.3.3.3 Sessile Indigenous Gut Microbiota Populations

Sessile indigenous gut microbiota populations were enumerated on days 41 (awaiting *C. difficile* germination and toxin production, period D, figure 6.3.1) and 55 (recovery after metronidazole treatment, period F, figure 6.3.1) only. Sessile populations of all bacterial groups were evident at both time points, with the exception of *Clostridium* spp. when no result was

obtained on day 41 (figure 6.3.3.2). Planktonic populations were generally higher than their sessile counterparts on days 41 and 55, although the converse was true for facultative anaerobes and *Enterococcus* spp. on day 41. Marked differences between planktonic and sessile populations were evident in *B. fragilis* group, *Bifidobacterium* spp. and *Lactobacillus* spp. with maximum variances of 1.76, 1.45 and 1.23 $\log_{10}$cfu, respectively.

6.3.3.4 Planktonic *C. difficile* Populations

C. difficile remained primarily as spores during internal control period (period B, figure 6.3.3.3). Following commencement of ceftriaxone instillation (period C), *C. difficile* spores declined to below LOD, one day after dosing cessation. A similar decrease in TVCs was evident, declining to ~1.7 $\log_{10}$cfu/mL, 3 days after dosing cessation. Thereafter, *C. difficile* germination was detected. *C. difficile* populations increased sharply to peak viable counts of ~6.5 $\log_{10}$cfu/mL, with cytotoxin production evident on day 40 and peaking at 5 RU on day 44. *C. difficile* spores were detected sporadically at around the LOD during periods D and E. On day 5 of metronidazole instillation (period E), TVCs were equal to spore counts with subsequent decrease in toxin levels to 0.5 RU, 2 days after cessation of metronidazole instillation. Regrowth of *C. difficile* vegetative cells proceeded the day after metronidazole cessation, increasing to and remaining at ~6.5 $\log_{10}$cfu/mL for the duration of the experiment. A similar increase in spores and toxin was noted with spore populations and toxin levels peaking and persisting at ~4.5 $\log_{10}$cfu/mL and 3 RU, respectively.

6.3.2.5 Sessile *C. difficile* Populations

Sessile *C. difficile* population enumeration was carried out on days 41 and 55 of this experiment. Within planktonic populations *C. difficile*

germination and toxin production was evident at both time points (figure 6.3.3.3). Sessile *C. difficile* germination and toxin production was apparent on day 41, with TVCs of ~6.5 log_{10}cfu/g and spore levels below the LOD (figure 6.3.3.4). On day 55, once again *C. difficile* germination and toxin production was evident, although to a lesser degree than day 41, with TVCs and spore levels of ~6.7 and ~4 log_{10}cfu/g, respectively. Toxin was detected within the biofilm on days 41 and 55 at levels of 2 and 1.5 RU, respectively.

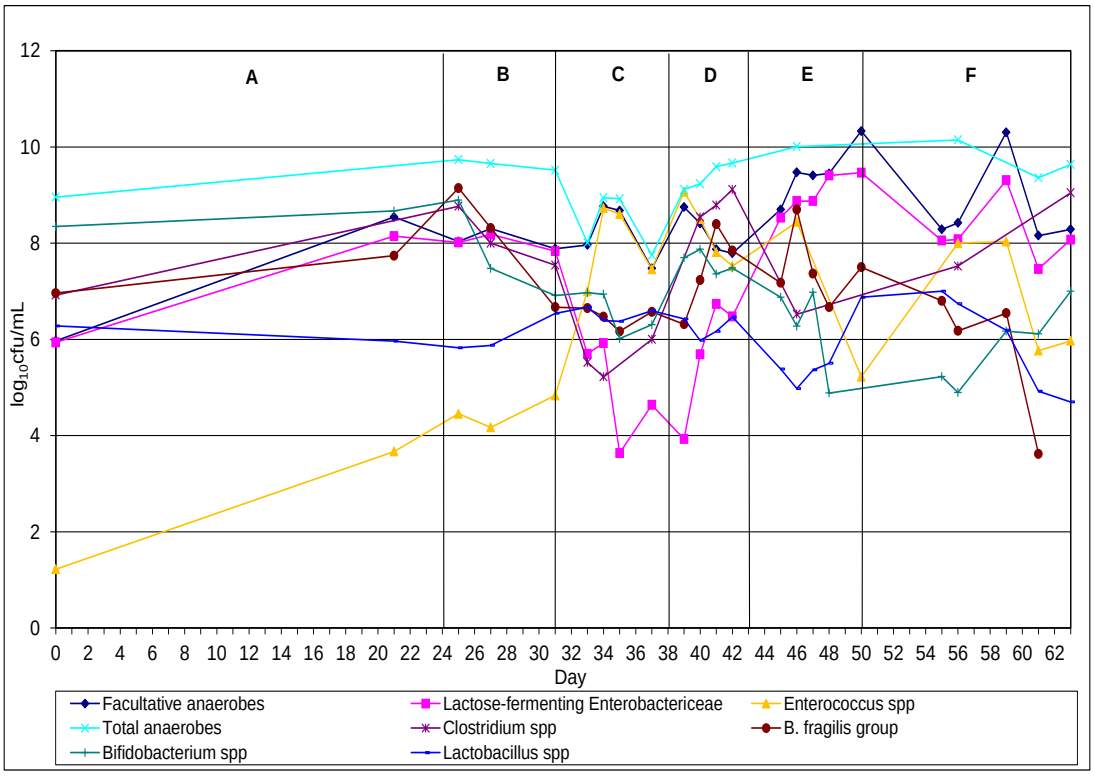

Figure 6.3.3.1: Planktonic populations (log_{10}cfu/mL) (±SE) of indigenous gut microbiota in the single stage liquid/air interface investigation. Vertical line indicates the last day of each period. B – internal control, C – ceftriaxone instillation, D – CDI induction, E – metronidazole instillation, F – rest.

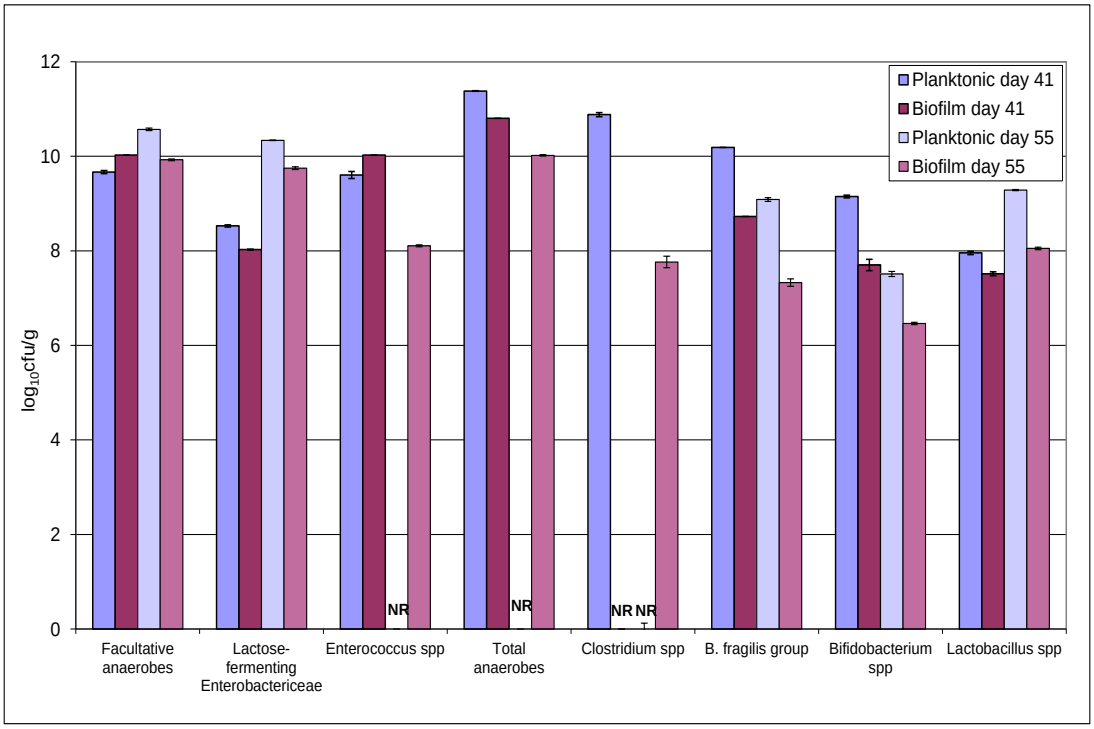

Figure 6.3.3.2: Sessile populations (log_{10}cfu/g) (±SE) of indigenous gut microbiota in the single stage liquid/air interface investigation. NR – no result

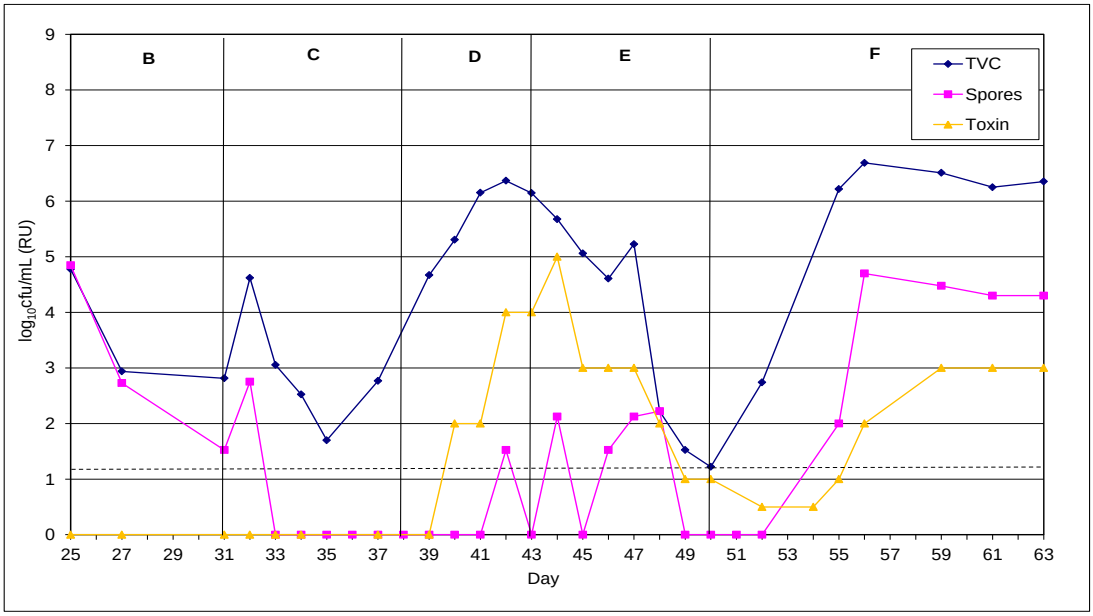

Figure 6.3.3.3: Planktonic *C. difficile* TVC and spore populations (log_{10}cfu/g) and toxin (RU) in the single stage liquid/air interface investigation. Vertical line indicates the last day of each period. Dashed line indicates the approximate LOD. B – internal control, C – ceftriaxone instillation, D – CDI induction, E – metronidazole instillation, F – rest.

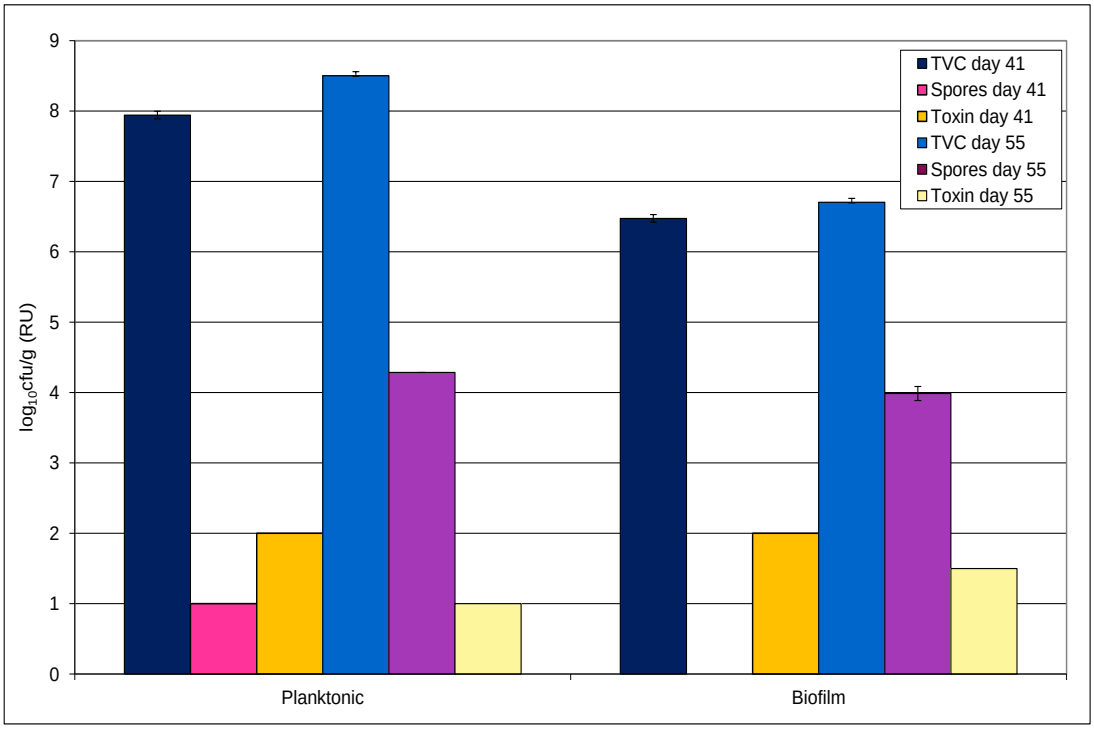

Figure 6.3.3.4: Mean (±SE) planktonic and biofilm *C. difficile* TVC and spore populations (log_{10}cfu/g) and toxin (RU) in the single stage liquid/air interface investigation.

6.4 Discussion

Many factors govern the ability of bacteria to adhere to surfaces, including substratum material physicochemical properties, fluid hydrodynamics and aqueous medium characteristics. The process of biofilm growth is dependant on the initial colonisation/attachment rate of organisms, the subsequent growth and further recruitment of organisms, and the level and rate of detachment of sessile populations. This process can be described using the following formula:

accumulation rate = attachment rate + growth rate – detachment rate [565].

Biofilm growth rate increases as a factor of flow rate as a greater cellular mass will come into contact with the surface, although efficient adherence of these cells may be reduced and mass detachment increased due to higher

shear forces. The extent of biofilm accumulation increases at low fluid velocities [566-568], whilst biofilm detachment increases as a factor of biofilm mass and increased flow velocity [566]. Furthermore, biofilm accumulation is positively influenced by increased surface roughness[569, 570], due to the diminished shear forces and increased surface area associated with rough surfaces.

Stoodley *et al*[340] demonstrated that laminar flow conditions elicit arrival at maximal surface coverage sooner than those growing under turbulent conditions with maximal coverage of biofilm grown under laminar conditions less than those grown when turbulent flow was present. The authors postulated that this reduced maturation may be due to decreased nutrient and cellular supply.

The present study demonstrates the formation of mature mixed-species biofilms on glass surfaces. A macroscopic thin, plaque-like biofilm forms on the submerged portion of the glass materials with a dense biofilm structure evident at the liquid/air interface. Within the milieu of the chemostat vessel, bacterial cells are potentially attracted to organic nutrients which concentrate on solids surfaces[571]. The original vessel design is magnetically stirred, thus creating a shear force within the vessel with potentially increased shear forces on the outer edges of the vessel (vessel wall). In addition, each vessel is continuously sparged with nitrogen gas, causing increased levels of fluid turbidity at the air-liquid interface.

Other properties such as the pH [341], nutrient level[340], ionic strength[342] and temperature[343] may also play a role in colonisation. Nutrient level and pH variation exist within different vessels of the gut model, with increased substrate availability and low pH in vessel 1, and low substrate availability and high pH in vessel 3. Within the original gut model, greatest biofilm biomass is observed within vessel 1. Stoodley *et al* utilised a biofilm reactor system to generate mixed-species biofilms with glucose as the limiting

nutrient. Under high glucose concentrations biofilm biomass increased rapidly. Stanley *et al*[341] demonstrated that attachment of motile and non-motile *P. aeruginosa* cells to stainless steel coupons increased from pH 4.8 to 7. Observations within the human gut model suggest that high nutrient availability is more conducive to increased biofilm biomass than the potential negative influence of decreased pH associated with vessel 1. These factors may potentially lead to increased biofilm accumulation rates observed at the liquid/air interface at the vessel wall.

Dexter *et al* first outlined the role of surface wettability, or hydrophobicity on upon bacterial adhesion[572]. Hydrophobic and non-polar surfaces (such as Teflon) have been shown to facilitate more rapid attachment of bacteria than hydrophilic materials (such as glass),[335-337 573] although contradictory data is also evident[572, 574, 575]. PTFE/Teflon is a high molecular weight synthetic polymer with a low coefficient of friction, widely utilised in industry due to its 'non-stick' properties. Reports of increased bacterial adhesion to this material are unexpected, suggesting that microbial adherence is regulated by factors in addition to substratum physicochemical properties. Submergence of materials within liquid environments, such as the faecal culture fluid within the gut model, may elicit the rapid conditioning of these surfaces. This conditioning film may mask the properties of the underlying material. In addition, the hydrophobicity and charge of adherent bacteria plays a role in the rate of adherence to material types. Together, these factors may explain the increased bacterial adhesion to PTFE compared with glass surfaces observed within this study and by others.

The populations of glass-adherent bacterial groups (figure 6.3.3.2 & 4) appear comparable to MA-associated populations (figures 5.5.1.2 & 4), indicating that glass-adherent biofilms posses characteristics similar to those on an *in vivo* realistic material (MA). These results indicate that the substratum material (glass) and system design (rod/pipette) highlighted in

this section provides a means to facilitate the formation of a mature mixed-species biofilm which reflects sessile populations observed previously[446, 447]. This system design can be modified to adapt the original gut model for the study of both the planktonic and biofilm modes of growth of *C. difficile* and the indigenous gut microbiota.

7.0 Biofilm Gut Model Redesign Reproducibility Experiments

7.1 Background

The human gut model successfully simulates the different stages of CDI. *In vitro* biofilm composition must be analysed at each stage of infection in order to elucidate the role that biofilms may play in these stages of simulated CDI fully. Removal of biofilm from the original gut model vessel walls (chapter 4.0) only permits biofilm sampling at the end stage of the infection process. Therefore, in order to maximise the number and frequency of biofilm sample points, adaptation of the human gut model vessel design was necessary.

Results and observations from previous gut model experiments have highlighted greatest biofilm formation at the liquid/air interface, and analysis of different substratum materials indicated that glass was conducive to mature biofilm formation. In order to maximise biofilm formation/maturation and number of sampling points, a rod system was implemented. This allowed independent formation and analysis of 18 different rod-associated biofilms. However, in order to compare biofilm composition at different time points, it was necessary to determine the reproducibility of the model in terms of consist biofilm formation and composition across all rods, regardless of position within the vessel.

7.2 Biofilm Gut Model Vessel Design

A schematic representation of the redesigned vessel system is depicted in figures 7.2.1 and 7.2.2 with photographic visualisation in figure 7.2.3. Vessel system dimensions were altered to maximise the inclusion of rods. The diameter was increased to 98 mm and working depth reduced to 40 mm. This ensured the vessel volume was maintained at 300mL.

Ground/'roughened' or smooth glass rods were inserted into the vessel through the lid and positioned to ensure the sampling portion of the rod extended across the liquid/air interface. Rods were screwed into the lid system and anaerobic atmosphere maintained by the delivery of nitrogen gas to the vessel via a circular pipe, with drilled holes interspersed on the surface to encourage even distribution of gas flow across the rods. Upon removal of rods, replacement screw caps were placed onto the lid to maintain the integrity of the system. The blue circles represent the glass rods and their distribution throughout the vessel system (figure 7.2.1). The positions of other necessary ports are also highlighted.

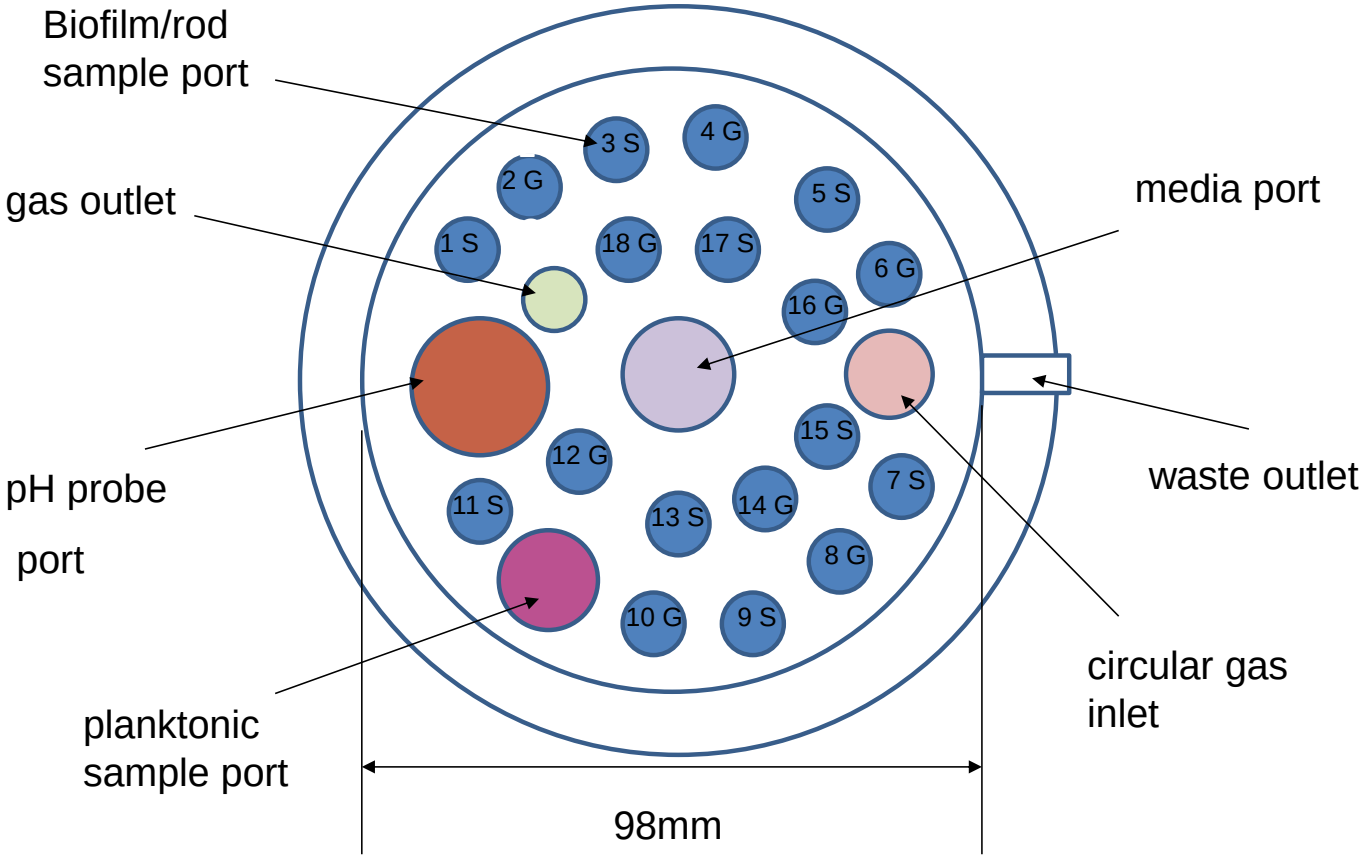

Figure 7.2.1: Schematic diagram of the redesigned biofilm human gut model from a bird's eye view. S: smooth glass rod; G: ground/'roughened glass rod

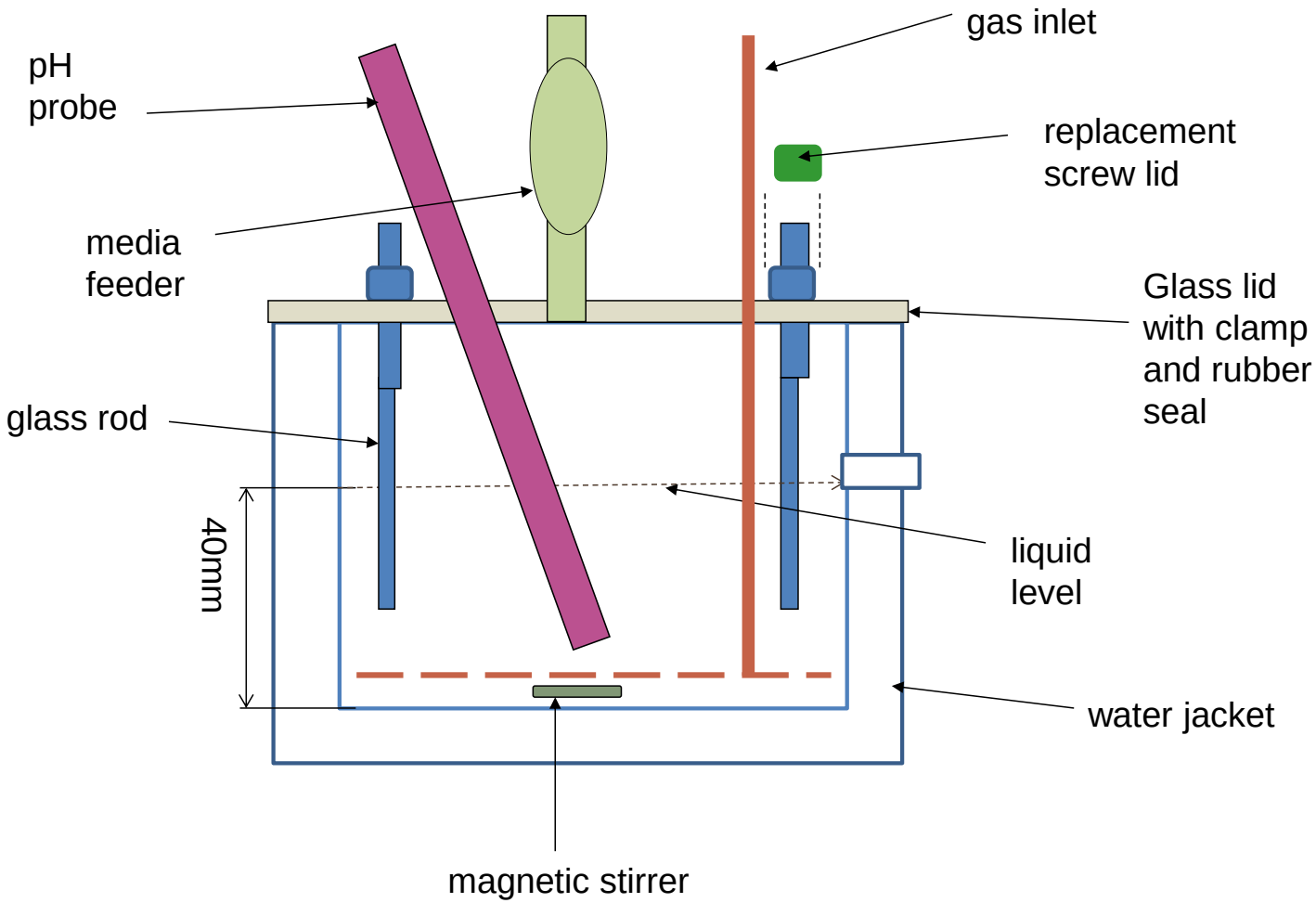

Figure 7.2.2: Schematic diagram of the redesigned biofilm human gut model vessel from a side-on view.

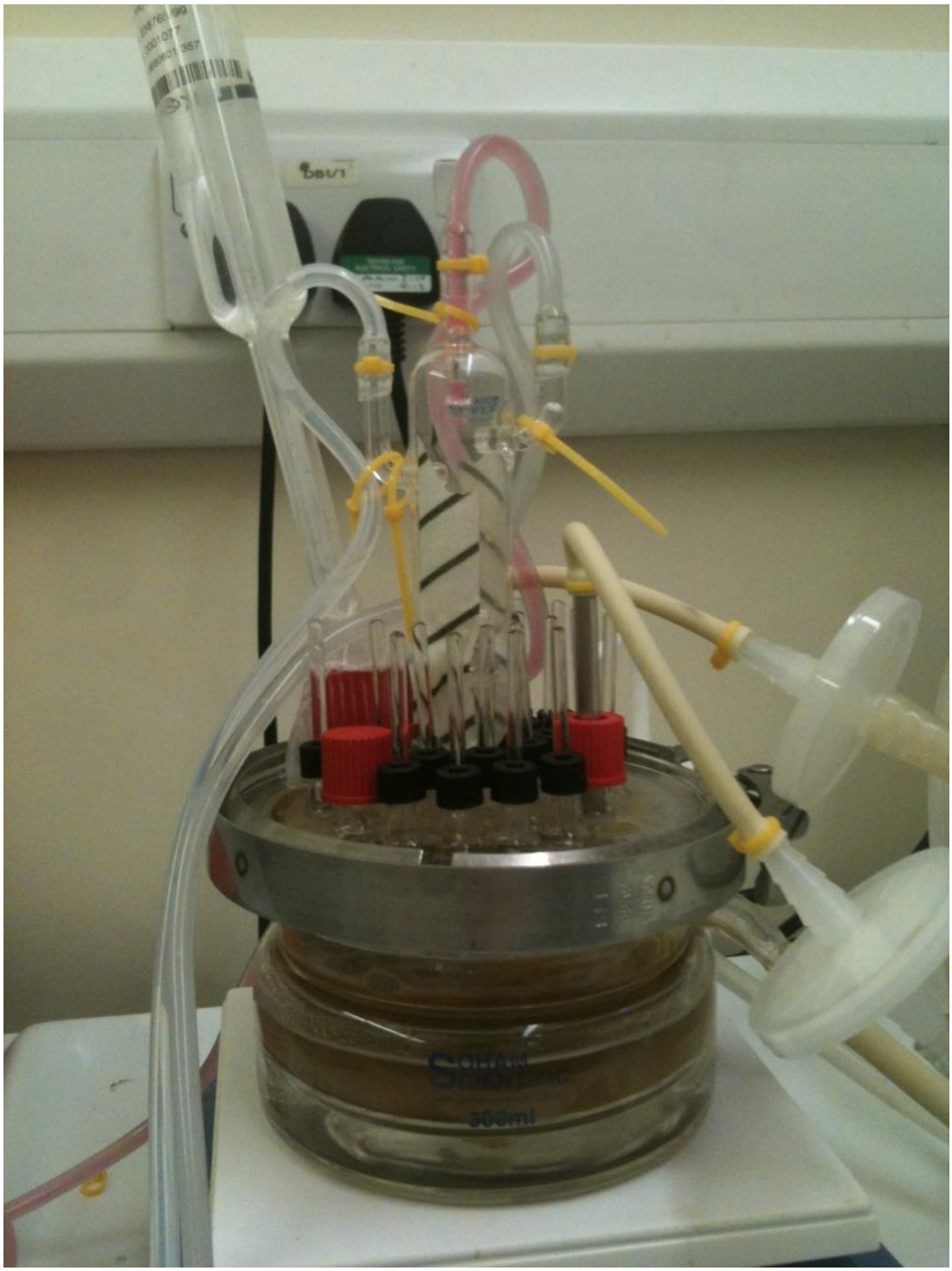

Figure 7.2.3: Photograph of the redesigned biofilm human gut model vessel.

7.3 Single Stage Biofilm Gut Model Reproducibility Experiments

7.3.1 Materials and Methodology

7.3.1.1 Experiments 1 and 2

7.3.1.1.1 Single Stage Chemostat Biofilm Gut Model

The biofilm redesign model was assembled as a single stage model as described previously 5.2.1.1. Alterations to certain conditions were made: the vessel was maintained at pH 5.5 and 1 % (v/v) PEG introduced to the growth medium to reduce foaming. The experimental design is outlined in figure 7.3.1. Briefly, eighteen rods were positioned within the vessel, nine consisted of smooth glass rods, and nine consisted of ground glass rods. Their relative positions within the vessel are highlighted in figure 7.2.1. Preparation of gut model growth medium is highlighted in 4.2.2.

7.3.1.1.2 Planktonic Sampling and Enumeration Protocol

Planktonic culture fluid was removed from the planktonic sample port on the biofilm vessel into a Wasserman tube and transferred to an anaerobic cabinet. Planktonic indigenous gut microbiota, *C. difficile* TVCs and spores and cytotoxin titres were measured throughout the experiment as described in sections 2.1, 2.2 and 2.4 and expressed as $\log_{10}$cfu/mL (or $\log_{10}$cfu/g when analysed alongside sessile populations).

7.3.1.1.3 Sessile Sampling Protocol

Loosely-adherent planktonic bacteria and true biofilm bacterial populations were determined independently. Following careful removal from the vessel, rods were gently rinsed by pipetting 5 mL pre-reduced sterile saline along

the length of the rod and run-off collected in a sterile Wasserman tube. This solution was enumerated as a loosely-adherent population. The rod was then transferred into a separate Wasserman's tube containing 5 mL pre-reduced sterile saline. The bacterial communities remaining on the rod were removed from the glass rods by vortexing intermittently for approximately two minutes, and enumerated as true biofilm populations. Biofilm was fully removed from the glass rod and suspended in saline; the rod was removed and discarded.

7.3.1.1.4 Sessile Enumeration Protocol

Samples of loosely-adherent and true biofilm samples (1 mL) were taken for each rod and centrifuged in a pre-weighed eppendorf at 16000 *g* for 10 mins. The supernatant was stored at 4˚C for cytotoxin assay (section 4.2.7) and the weight of the remaining pellet determined. Loosely adherent and true biofilm indigenous gut microbiota, *C. difficile* TVCs and spores were enumerated as described in section 2.1 and 2.2 and converted to $\log_{10}$cfu/g of pellet. Cytotoxin quantification was performed as described in sections 2.4.

7.3.1.1.5 Experimental Design

Pooled human faecal emulsion (sections 2.5-2.7) was added to the single vessel, media pump was started and the system was left without intervention to until bacterial populations were in steady state (period A, figure 7.3.1). On day 31 a single inoculum of *C. difficile* PCR ribotype 027 spores were added to the vessel (period B). The model was left without interventions until day 46 when all 18 rods were removed from the model for analysis. Planktonic bacterial populations were determined at regular intervals for the duration of the experiment.

This experiment was repeated using a distinct faecal donation pool and results from each experiment were analysed separately due to inter-individual differences in faecal bacterial composition. The only alteration to experiment 2 was the continuous sparging of the growth medium with oxygen free nitrogen to limit the growth of *P. aeruginosa* observed in the initial experiment (experiment 1).

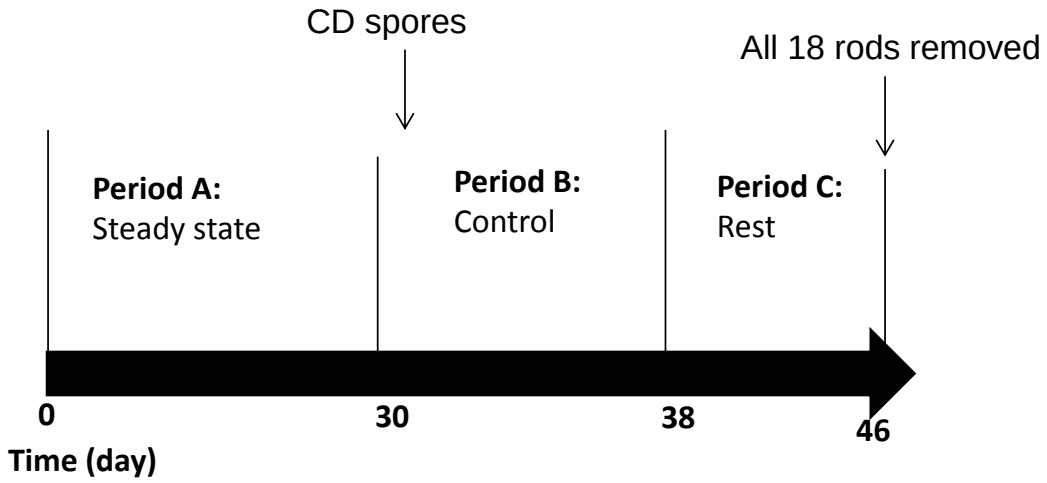

Figure 7.3.1: Experimental design of single stage biofilm gut model experiments 1 and 2. Vertical line represents last day of each period.

7.3.2 Results

7.3.2.1 Experiment 1

7.3.2.1.1 Experimental Observations

Biofilm formation was observed at the liquid-air interface on all rods (figure 7.3.2.1.1). Minimal biofilm formed on the area of the rods submerged under the liquid level within the vessel. Due to the fragile nature of the glass rods, one was broken during the experiment; therefore, only 17 rods were analysed. Variation in biofilm biomass was observed between rods with total pellet weight from 1 mL of re-suspended biofilm ranging from 0.034 to 0.122 g with an average (±SE) weight of 0.068±0.007 g (figure 7.3.2.1.5).

Smooth rods were utilised in rod positions 1,3,5,7,9,11,13,15,17 (figure 7.2.1) and 'roughned'/ground rods were used for the remaining rods. No discernible difference in the amount (figure 7.3.2.1.5) or composition (figure 7.3.2.1.4) of biofilm removed from the two rod materials was noted.

7.3.2.1.2 Planktonic Indigenous Gut Microbiota Populations

Gut microbiota populations remained relatively steady within the steady state period of the experiment (period A, figure 7.3.2.1.2), although *Enterococcus* spp., LFE and *Clostridium* spp. populations fluctuated slightly. *B. fragilis* group. populations were below LOD from day 18 onwards.

The addition of *C. difficile* spores on day 32 did not greatly affect gut microbiota populations, although there was a temporary decline in the populations of *Clostridium* spp., which may have been attributable to a pH disturbance on day 33 (period B, figure 7.3.2.1.2). *Clostridium* spp. quickly recovered to pre-*C. difficile* inoculation populations. All other populations remained relatively steady for the duration of the experiment.

7.3.2.1.3 Sessile Indigenous Gut Microbiota Populations

Populations of bacterial groups present on each rod are highlighted in figure 7.3.2.1.4. Each point represents the populations present on a single rod. Sessile communities of all enumerated bacterial groups, except *B. fragilis group* were present on the glass rods. Variation of sessile bacterial populations across all 17 rods were minimal (table 7.1), with standard errors of variation of most bacterial groups ≤ 0.18 log_{10}cfu/g. *Enterococcus* spp. demonstrated greatest variation, with a population standard error across 17 rods of 0.3 log_{10}cfu/g (table 7.2). *Enterococcus* spp. population variation between rods 1-12 (SE ±0.05 log_{10}cfu/g) appears minimal and comparable to that of other bacterial groups. However, increased variation was evident on rods 13-17 (SE ±0.57 log_{10}cfu/g), a trend not observed for other bacterial groups on these particular rods. *Lactobacillus* spp. dominated biofilm populations (mean 9.88 log_{10}cfu/g) with *Enterococcus* spp. (mean 5.03 log_{10}cfu/g) the least abundant bacterial group.

7.3.2.1.4 Planktonic *C. difficile* Populations

C. difficile TVCs were equal to spore levels for the duration of the experiment, indicating the absence of vegetative cells (figure 7.3.2.1.3). *C. difficile* TVCs reduced from ~5 log_{10}cfu/mL on day 31 to sporadic detection at around the LOD from day 43. Cytotoxin was not detected for the duration of the experiment.

7.3.2.1.5 Sessile *C. difficile* Populations

Rod-associated *C. difficile* populations comprised primarily spores on all 17 rods. *C. difficile* TVCs ranged from 2.54 to 5.14 log_{10}cfu/g, with a mean and standard error of 3.76±0.17 log_{10}cfu/g. *C. difficile* spores ranged

from 3.44 to 5.25 log_{10}cfu/g, with a mean and standard error of 4.18±0.11 log_{10}cfu/g (figure 7.3.2.1.4).

Figure 7.3.2.1.1: Mature biofilm structure on a single rod taken from the biofilm gut model on day 46.

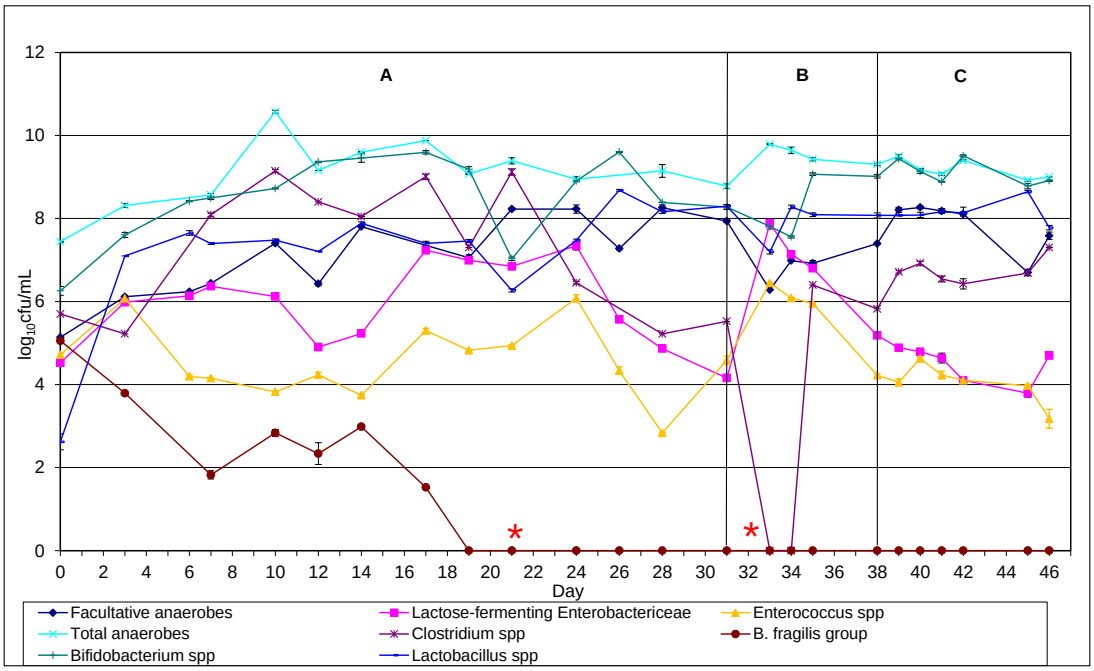

Figure 7.3.2.1.2: Planktonic populations (log_{10}cfu/mL) of indigenous gut microbiota in experiment 1 of the single stage biofilm redesign gut model experiment. Vertical line represents the last day of each period. * pH disturbance.

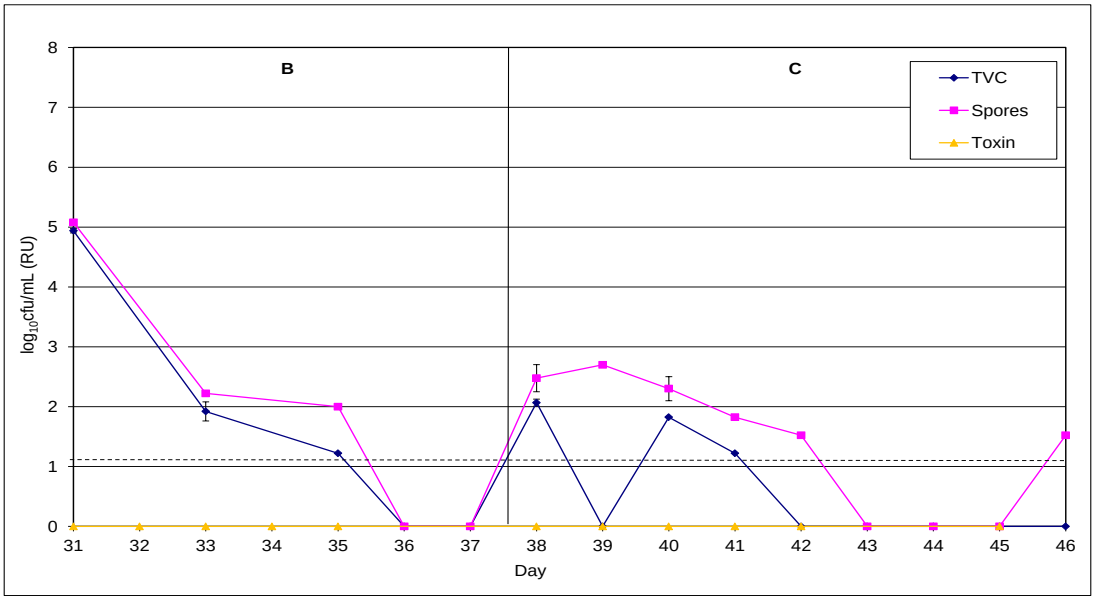

Figure 7.3.2.1.3: Planktonic populations (log_{10}cfu/mL) of *C. difficile* in experiment 1 of the single stage biofilm redesign gut model experiment. Vertical line represents the last day of each period. Dashed line: ~ limit of detection.

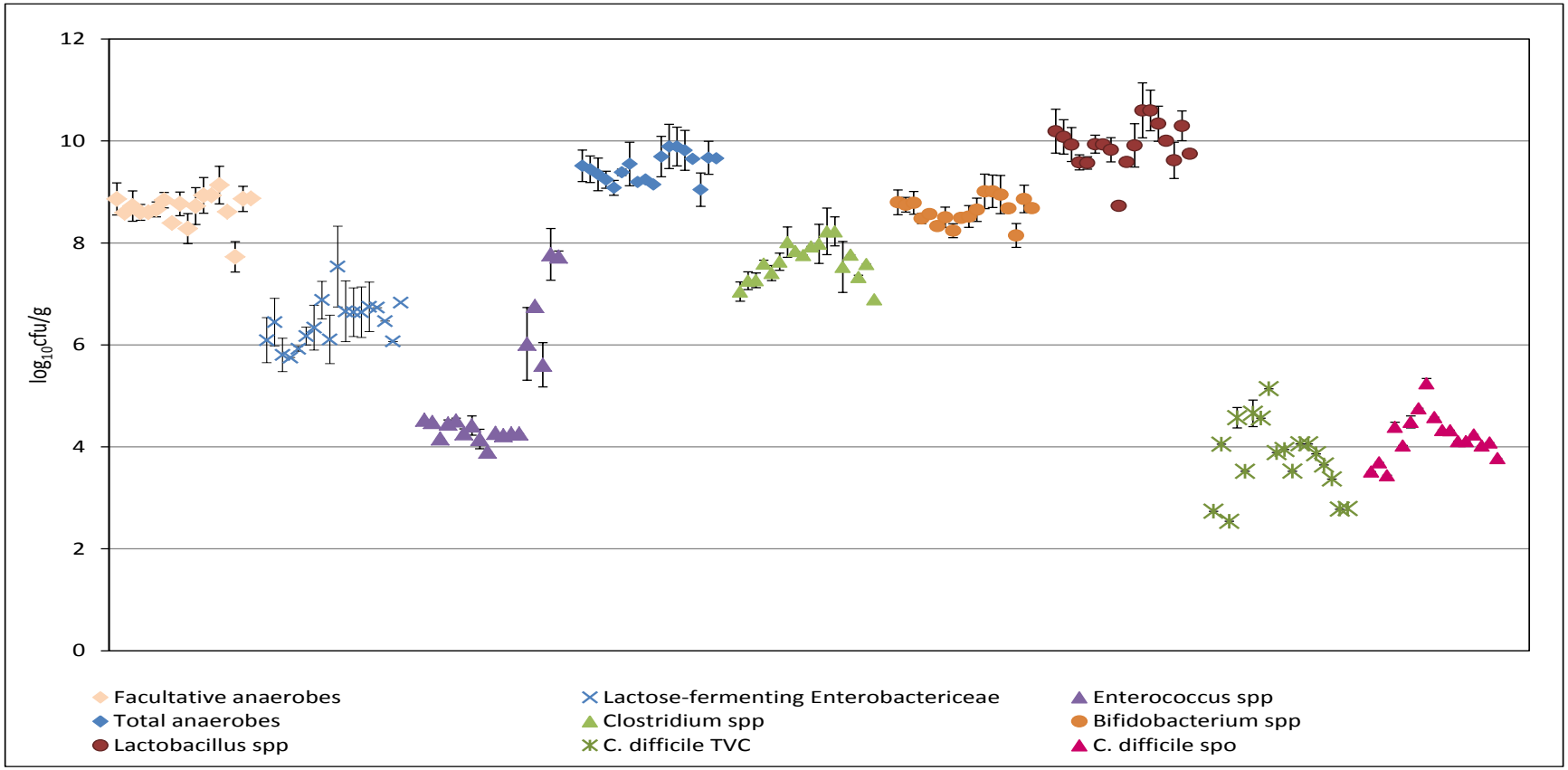

Figure 7.3.2.1.4: Sessile populations (log_{10}cfu/g) of indigenous gut microbiota on rods 1-17 within the single stage redesign biofilm gut model experiment 1. Standard errors (± log_{10}cfu/g) for populations on each rod displayed. Each point represents populations present on each rod. *B. fragilis* group – no result.

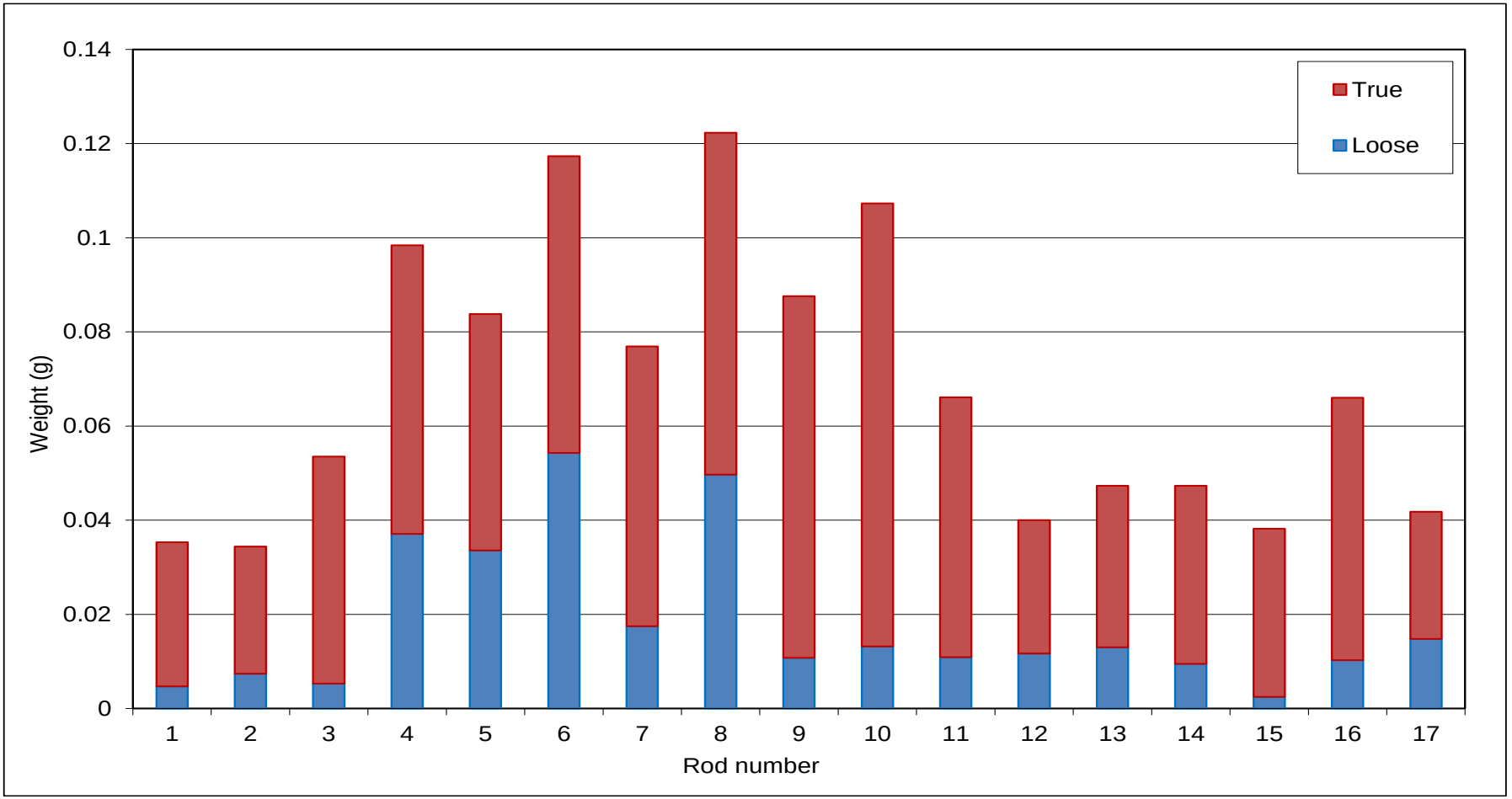

Figure 7.3.2.1.5: Pellet weights (g) of 1 mL culture of re-suspended loose, true and total biofilm from rods within the single stage biofilm human gut model experiment 1.

Bacterial group	Mean (log_{10}cfu/g)	Range (log_{10}cfu/g)	Standard error (log_{10}cfu/g)
Facultative anaerobes	8.66	1.41	0.07
Lactose-fermenting Enterobacteriaceae	6.42	1.78	0.11
Enterococcus spp.	5.03	3.87	0.30
Total anaerobes	9.44	0.85	0.06
Clostridium spp.	7.59	1.33	0.09
Bifidobacterium spp.	8.61	0.87	0.06
Bacteroides fragilis group	NR	NR	NR
Lactobacillus spp.	9.88	1.61	0.10
C. difficile TVC	3.74	2.60	0.18
C. difficile spores	4.19	1.80	0.11

Table 7.1: Mean, range and standard error (log_{10}cfu/g) of populations of indigenous gut microbiota and *C. difficile* on rods 1-17 in the single stage biofilm redesign gut model experiment 1. TVC – total viable counts; NR – no result.

Rods	Mean (log_{10}cfu/g)	Range (log_{10}cfu/g)	Standard error (log_{10}cfu/g)
1-17	5.03	3.87	0.3
1-12	4.3	0.62	0.05
13-17	6.78	2.167	0.57

Table 7.2: Mean, range and standard error of populations of *Enterococcus* spp. on rods within the single stage biofilm redesign gut model experiment 1.

7.3.2.2 Experiment 2

7.3.2.2.1 Experimental observations

No major problems were encountered during the experimental run and the system performed as previously (experiment 1). On day 46 of the experiment glass rods were removed from the vessel. All 18 rods facilitated the growth of biofilm as observed in the first reproducibility experiment. The macroscopic biofilm mass differed amongst rods with total pellet weight ranging from 0.021 to 0.082 g with an average (±SE) weight of 0.046±0.004 g (figure 7.3.2.2.4).

No correlation between biofilm biomass levels on different rods were evident between experiments 1 and 2, indicating that differences in biofilm biomass are not a result of their position within the vessel.

7.3.2.2.2 Planktonic Indigenous Gut Microbiota Populations

Gut microbiota populations remained relatively stable within the steady state period (period A), with the exception of *B. fragilis* group which fluctuated at levels around the LOD (figure 7.3.2.2.1). *Bifidobacterium* spp. dominated the bacterial community.

Instillation of *C. difficile* spores on day 32 did not greatly affect gut microbiota populations, although *Enterococcus* spp. populations gradually declined from ~5 $\log_{10}$fu/mL to ~2 $\log_{10}$cfu/ml before recovering to ~4 $\log_{10}$cfu/mL before the cessation of the experiment. All other populations remained steady for the further duration of the experiment.

7.3.2.2.3 Sessile Indigenous Gut Microbiota Populations

Glass rods supported sessile growth of all bacterial groups enumerated in this study with the exception of *B. fragilis* group (figure 7.3.2.2.3).

Bifidobacterium spp. were the dominant bacterial group (mean 9.18 log_{10}cfu/g) and *Enterococcus* spp. the least populous group (mean 5.16 log_{10}cfu/g – table 7.3). All enumerated populations were constant across all 18 rods (figure 7.3.2.2.5), with standard errors of ≤ 0.16 log_{10}cfu/g.

7.3.2.2.4 Planktonic *C. difficile* Populations

Planktonic *C. difficile* TVCs were equivalent to spore counts throughout the duration of the experiment, demonstrating the absence of vegetative cells. *C. difficile* TVCs declined from an initial population of 5.3 log_{10}cfu/mL to around the LOD from day 43 onwards (figure 7.3.2.2.2).

7.3.2.2.5 Sessile *C. difficile* Populations

Rod-associated *C. difficile* TVCs were equal to or less than spore counts on all 18 rods, with minimal variation between rods (figure 7.3.2.2.3). TVCs and spores ranged from 3.58 to 5.78 log_{10}cfu/g (± SE 0.14 log_{10}cfu/g) and 5.22 to 6.91 log_{10}cfu/g (± SE 0.11 log_{10}cfu/g), respectively).

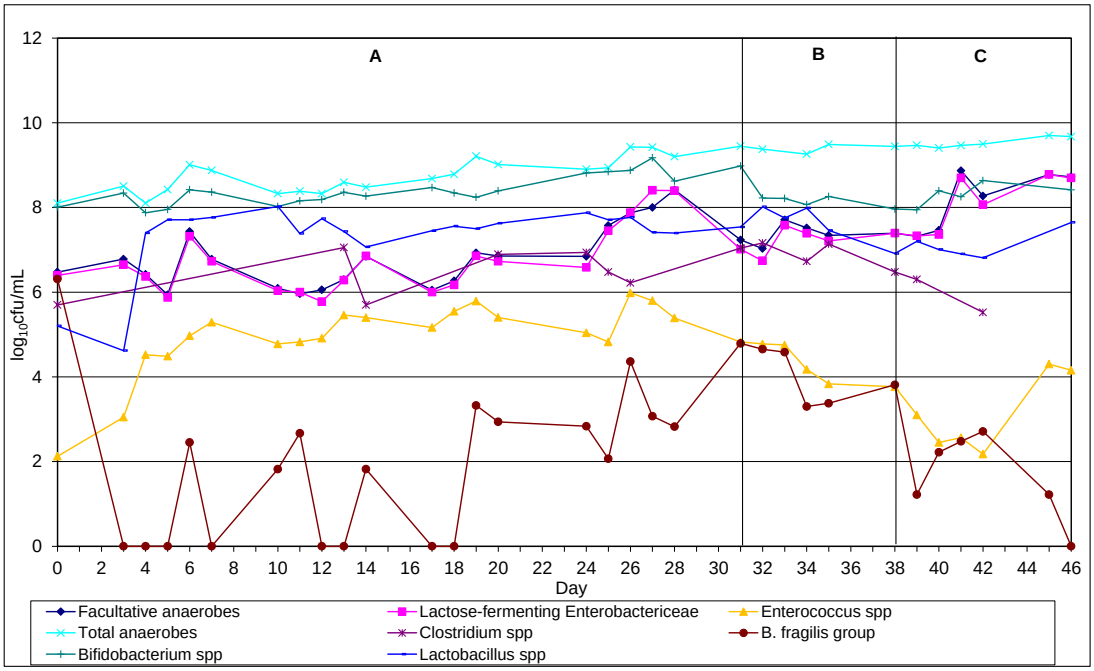

Figure 7.3.2.2.1: Planktonic populations (log_{10}cfu/mL) of indigenous gut microbiota of the single stage biofilm redesign gut model experiment 2. Vertical line represents the last day of each period.

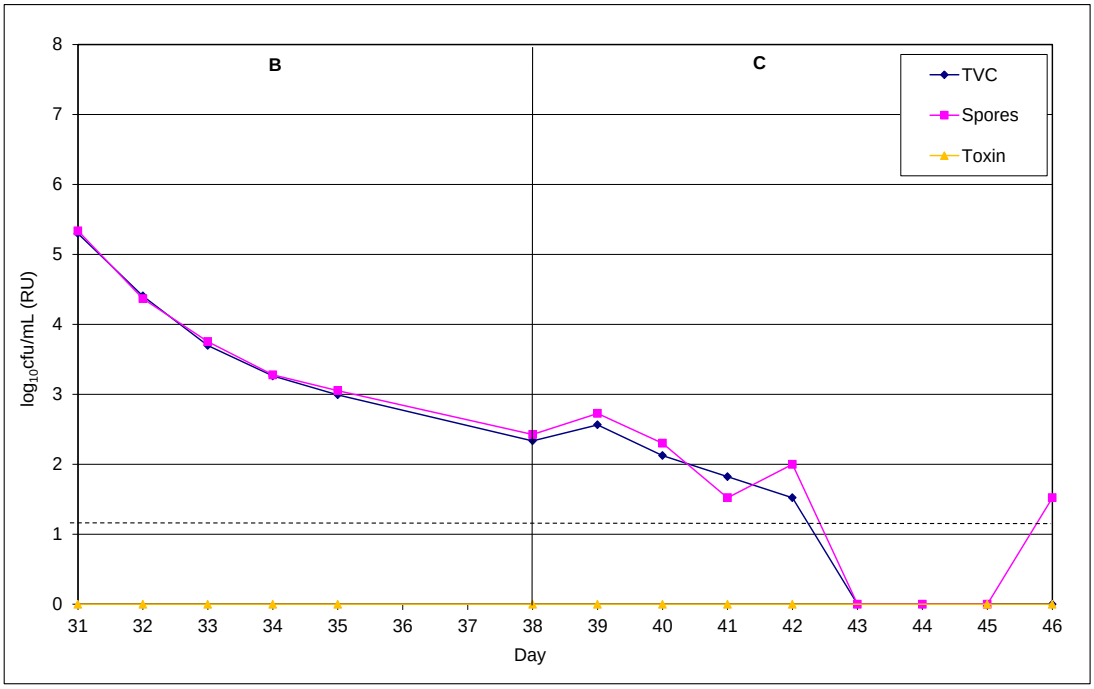

Figure 7.3.2.2.2: Planktonic populations (log_{10}cfu/mL) of *C. difficile* of the single stage biofilm redesign gut model experiment 2. Vertical line represents the last day of each period.

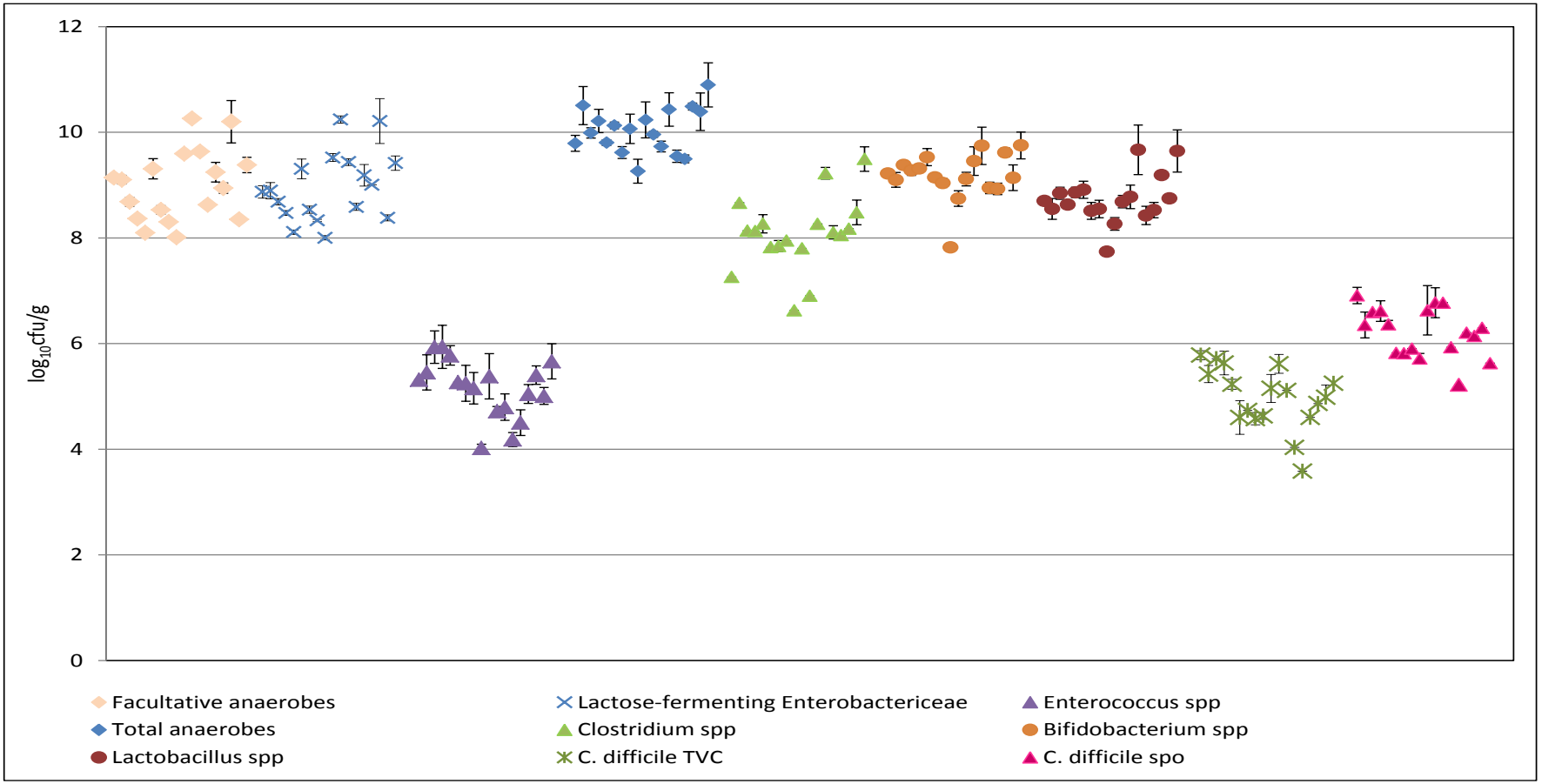

Figure 7.3.2.2.3: Sessile populations (±SE) (log_{10}cfu/g) of indigenous gut microbiota on rods 1-17 within the single stage redesign biofilm gut model experiment 2. Standard errors (± log_{10}cfu/g) for populations on each rod displayed. Each point represents populations present on each rod. *B. fragilis* group – no result.

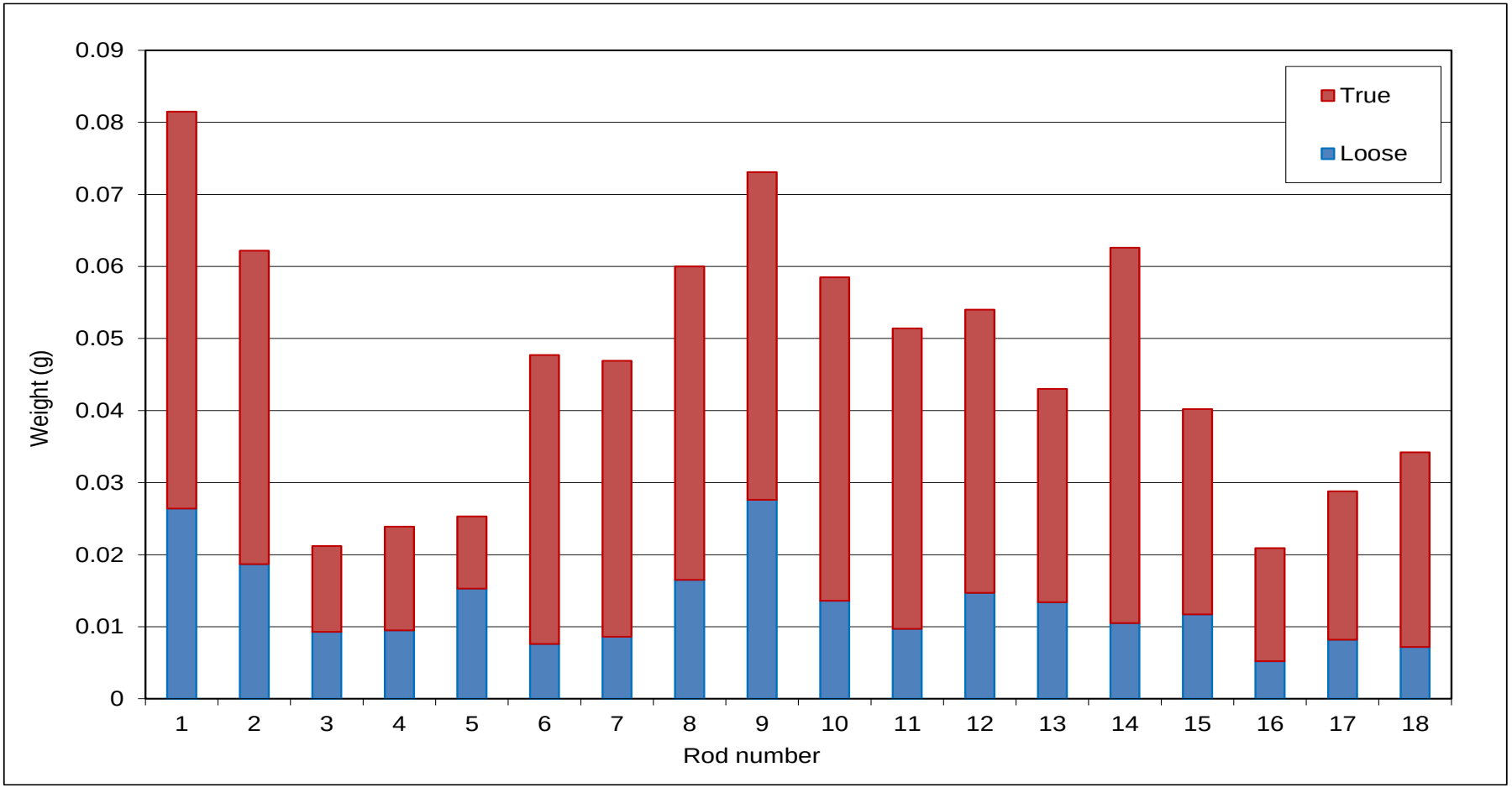

Figure 7.3.2.2.4: Pellet weights (g) of 1mL culture of re-suspended loose, true and total biofilm from rods within the single stage biofilm human gut model experiment 2.

Bacterial group	Mean (log_{10}cfu/g)	Range (log_{10}cfu/g)	Standard error (log_{10}cfu/g)
Facultative anaerobes	8.99	2.25	0.02
Lactose-fermenting Enterobacteriaceae	8.96	2.24	0.15
Enterococcus spp.	5.16	1.91	0.13
Total anaerobes	10.03	1.63	0.10
Clostridium spp.	8.07	2.59	0.16
Bifidobacterium spp.	9.18	1.93	0.10
Bacteroides fragilis group	NR	NR	NR
Lactobacillus spp.	8.73	1.928	0.11
C. difficile TVC	4.97	2.20	0.14
C. difficile spores	6.20	1.69	0.11

Table 7.3: Mean, range and standard error (log_{10}cfu/g) of populations of indigenous gut microbiota on rods 1-18 in the single stage biofilm redesign gut model experiment 2. TVC – total viable counts; NR – no result.

7.3.3 Discussion

The redesigned single stage biofilm gut model provided a successful system in which to study the growth of mixed-species biofilm. Maximal biofilm formation was macroscopically evident at the liquid/air interface on each rod. Despite the minimum solid-liquid-air surface area of the glass rod system utilised within the biofilm model system, biomass of mature biofilm structures was sufficient for analysis. Although attempts were made to ensure a homogenous environment for biofilm formation, variation in biofilm biomass was evident across the 18 rods, although no relationship between rod position and biofilm biomass was evident between experiments 1 and 2. Microenvironments within the model were evident, with variations in gas flow turbidity. Shear forces and turbidity levels within culture fluids control biofilm formation, with turbid environments eliciting increased biofilm formation[340], potentially explaining the variation observed within this study.

Both smooth and 'roughened' rods were incorporated within the system. Increased surface roughness has been reported as conducive to increased cellular adhesion[570]. Whilst initial adherence rate is uncharacterised within this study; biofilm biomass in experiment 1 and 32 (figures 7.3.2.1.5 and 7.3.2.2.4) demonstrates weak evidence to support this theory, particularly amongst rods 3 – 13 within experiment 1 (figure 7.3.2.1.5). In future experiments only rough rods will be used.

Although biomass variation was evident amongst rods, counts of bacterial groups (per g of biofilm) were consistent. Therefore, any variation between rod populations at different time points are likely caused by distinct differences in biofilm composition due to outside pressure rather than part of any inherent variation in biofilm populations amongst different rods within the model.

Previous gut model investigations were maintained at pH 6.8, reflecting conditions of the distal colon *in vivo.* However, single stage chemostat models represent a high substrate availability environment more analogous to that of the proximal colon. In order to maintain an environment fully reflective of the proximal colon the pH was maintained at 5.5 in this experiment. As a result, conditions, and therefore bacterial populations are distinct from previous experiments.

Slight variation (average, 0.8 $\log_{10}$cfu/g; maximum < 2.5 $\log_{10}$cfu/g) in indigenous gut microbiota populations was evident between experiments 1 and 2. Differences between faecal bacterial compositions between individuals are well documented[279]. Donor pools used in the two experiments varied, which likely contribute to the differences observed in populations in the two experiments.

Decreased number and stability of *B. fragilis* group populations within vessel 1 of the gut model compared with vessels 2 and 3 have previously been noted[98]. Furthermore, detection of *Bacteroides* spp. within distinct regions of the colon of sudden death victims are variable [294]. Reasons behind these differences are unclear but may be mediated by the reduced pH, increased substrate availability and resulting unique fermentation profile within different regions of the model[511]. Variation of behaviour of other bacterial groups, notably *C. difficile* germination and toxin production within vessel 1, compared with vessels 2 and 3 has previously been observed within the gut model[525, 538, 576].

Biofilm structures harbour heterogeneous microenvironments. Bacteria existing in outer areas often possess distinct characteristics from inner structure populations[434]. Biofilm detachment, particularly swarming/seeding processes, results in the existence of biofilm-associated bacteria in the processes of detachment. These organisms may display planktonic rather than sessile attributes. In addition, planktonic bacteria may form a weak

association with biofilm structures without possessing sessile traits. These bacterial populations may contribute to sessile populations enumerated in this study, whilst not comprising a true biofilm state. Categorisation of loose and strongly adherent biofilm populations was performed to differentiate between characteristics of these two populations. However, differences with these two groups (data not shown) were inconsistent.

During the rinsing procedure to isolate loose bacterial populations, large clumps of biofilm often became detached from the rod, thereby skewing the loose biofilm-associated results. The fragile nature of some biofilm structures prevented the reliable characterisation of these two groups. As a result, this procedure was abandoned for future reproducibility experiments and all rod-associated bacterial populations enumerated together.

An increased level of variation in *Enterococcus* spp. populations was observed within experiment 1. *P. aeruginosa* is an opportunistic pathogen isolated from the lungs of cystic fibrosis sufferers and often persists despite long-term antimicrobial therapy, owing to the formation of biofilm structures. The bacterium is aerobic although it can survive in anaerobic environments where nitrate is available as a terminal electron acceptor in the electron transport chain. Within the gut model, sections of biofilm often display a green pigment, presumptively due to pseudomonal growth. Within the single stage gut model, green pigmentation was observed in biofilms on rods associated with increased *Enterococcus* spp. variation (rods 13-17, figure 7.3.2.1.4). The association of *Enterococcus* spp. with *P. aeruginosa* has previously been noted within triple stage analysis experiments (chapter 4.0) and within other groups[528]. It is postulated that this may elicit increased *Enterococcus* spp. recruitment into these biofilm structures. Such variation rod-associated bacterial groups (experiment 1 and 2) or in *Enterococcus* spp. (experiment 2) within the biofilm vessel have not been observed therefore are unlikely to have occurred in experiment 1.

However, the recruitment of pseudomonas due to increased *Enterococcus* spp. on these particular rods cannot be ruled out.

Initial reproducibility validation of the rod system indicates the suitability of this design for biofilm analysis. Glass rods reliably facilitated biofilm formation in all areas of the vessel. Rods could be removed and analysed with ease and bacterial populations across all rods were very consistent.

7.4 Triple Stage Biofilm Gut Model

7.4.1 Materials and Methodology

7.4.2.1 Experiments 1 and 2

7.4.2.1.1 Background

Once the suitability of the redesigned biofilm gut model was determined further reproducibilty experiments were designed. CDI affects the distal colon and vessel 3 of the gut model is analogous to this region, therefore the redesigned vessel system was placed in this position. The biofilm vessel design was maintained from that of the initial single stage reproducibility experiments; however, a more complex experimental design was incorporated into this experimental process, allowing for longitudinal monitoring of biofilm formation. Biofilm detachment protocols were evaluated within this study to determine the most efficient procedure for removal of biofilm from ground glass rods.

7.4.2.1.2 Triple Stage Biofilm Gut Model

The biofilm redesign model was set up as a triple stage model as described previously 4.2.1, however, vessel 3 was replaced with the redesigned biofilm vessel (figure 7.4.2.2). Alterations to certain conditions were made: 1% PEG was added to the growth medium to reduce foaming in vessel 1. The experimental design is outlined in figure 7.4.2.1. Briefly, eighteen ground glass rods were positioned within the vessel and their relative positions are shown in figure 7.2.1. Preparation of gut model growth medium is described in 4.2.2. In order to ensure maximal biofilm recovery from the rods, the use of sonication and vortexing were investigated in experiment 1 to determine which method provided greatest biofilm removal from the surface of the rod.

7.4.2.1.3 Planktonic Sampling and Enumeration Protocol

Planktonic indigenous gut microbiota, *C. difficile* TVCs and spores, and cytotoxin were enumerated as described in 7.3.1.1.2. At biofilm sampling time points planktonic populations were also expressed as log_{10}cfu/g.

7.4.2.1.4 Sessile Sampling and Enumeration Protocol

Rods were submerged with 5 mL of pre-reduced sterile saline, vortexed (experiment 1 and 2) or sonicated (experiment 1 only) thoroughly for ~ 5 mins and rod removed and discarded. Sessile gut microbiota, *C. difficile* TVCs, spores and cytotoxin were enumerated from all 18 rods (at three separate time points, figure 7.4.2.1) within vessel 3 of the triple stage gut model as described in sections 2.1 and 2.2.

7.4.2.1.5 Experimental Design

The biofilm model was left to allow bacterial populations to equilibrate for 19 days (figure 7.4.1, period A). On day 20, rods 1-6 (sample point Z) were selected as representative of all areas of the vessel and removed and bacterial populations enumerated. A single inoculum of *C. difficile* PCR ribotype 027 spores were added to vessel 1 of the model on day 21 and the system was left without further interventions until rods 7-12 (sample point W) were sampled on day 27. The remaining rods were sampled on day 42 (sample point W). Planktonic indigenous gut microbiota (periods A-C, vessels 2 and 3), *C. difficile* total viable counts, spores and cytotoxin (periods B and C, vessels 1-3) were monitored during the experiment.

This experiment was repeated using a distinct faecal donation pool and results from each experiment were analysed separately due to inter-individual differences in faecal bacterial composition.

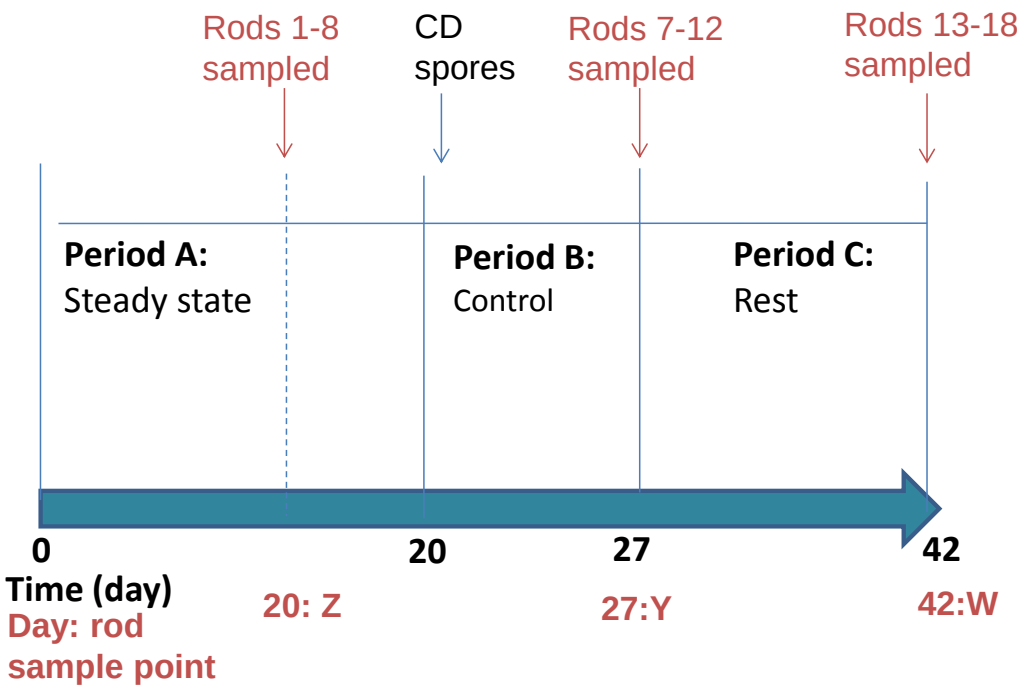

Figure 7.4.2.1: Experimental design of triple stage biofilm gut model. Vertical line represents last day of each period.

Figure 7.4.2.2: Photograph of the triple stage biofilm gut model. Vessel 3 represents the desgined biofilm vessel.

7.4.2 Results

7.4.2.1 Experiment 1

7.4.2.1.1 Planktonic Indigenous Gut Microbiota Populations

Planktonic indigenous gut microbiota populations rapidly established a stable population within vessel 3, and remained predominantly steady for the duration of the experiment (figure 7.4.2.1.1). Gut microbiota populations were dominated by *Bifidobacterium* spp. and *Clostridium* spp., whereas *Enterococcus* spp. and LFE were less numerous.

7.4.2.1.2 Sessile Indigenous Gut Microbiota Populations

Indigenous gut microbiota populations adherent to rods at time points Z-U are graphically depicted in figures 7.4.2.1.5 & 7.4.2.1.6. Planktonic populations (log_{10}cfu/g) for each bacterial group at time points Z-X are also depicted. Bacterial group populations across the 6 rods at each time point displayed minimal variation, with standard errors of ≤ 0.31 log_{10}cfu/g at all time points (table 7.4). LFE dominated gut microbiota populations, and *Bifidobacterium* spp. were the most numerous obligate anaerobe. Standard error variation of bacterial groups generally increased from time points Z-X. No result was obtained for time point X due to failure of selective agar for this bacterial genera.

7.4.2.1.3 Planktonic *C. difficile* Populations

C. difficile populations initially remained quiescent in all vessels of the gut model (figures 7.4.2.1.2-7.4.2.1.2.4). However, 5 days after *C. difficile* spore instillation, TVCs began to increase by ~1 log_{10}cfu/mL relative to spore populations and maintained this level for the duration of the experiment. *C. difficile* spore populations decreased from peak levels

of 5.2, 5.2 and 4.6 log_{10}cfu/mL in vessels 1, 2 and 3, respectively to ~3 log_{10}cfu/mL by the end of the experiment. Cytotoxin was not detected throughout the experiment in any vessel.

7.4.2.1.4 Sessile *C. difficile* Populations

Sessile sampling timepoint Z occurred one day prior to *C. difficile* spores instillation, therefore *C. difficile* populations were absent. *C. difficile* spores were present with biofilm structures (mean TVCs 6.2 log_{10}cfu/g), six days after spore introduction into the model (time point Y, figure 7.4.2.1.7). *C. difficile* populations existed in spore form only, with little variation amongst rods (standard error: TVCs and spores 0.13 and 0.19 log_{10}cfu/g, respectively).

On the final day of the experiment (day 46, time point X), mean sessile *C. difficile* TVCs had declined to 4.4 log_{10}cfu/g (time point X, figure 7.4.2.1.7). *C. difficile* populations remained as spores. Variation of *C. difficile* populations amongst rods at time point X was greater than other bacterial groups with TVC and spore standard errors of 0.4 and 0.28 log_{10}cfu/g, respectively.

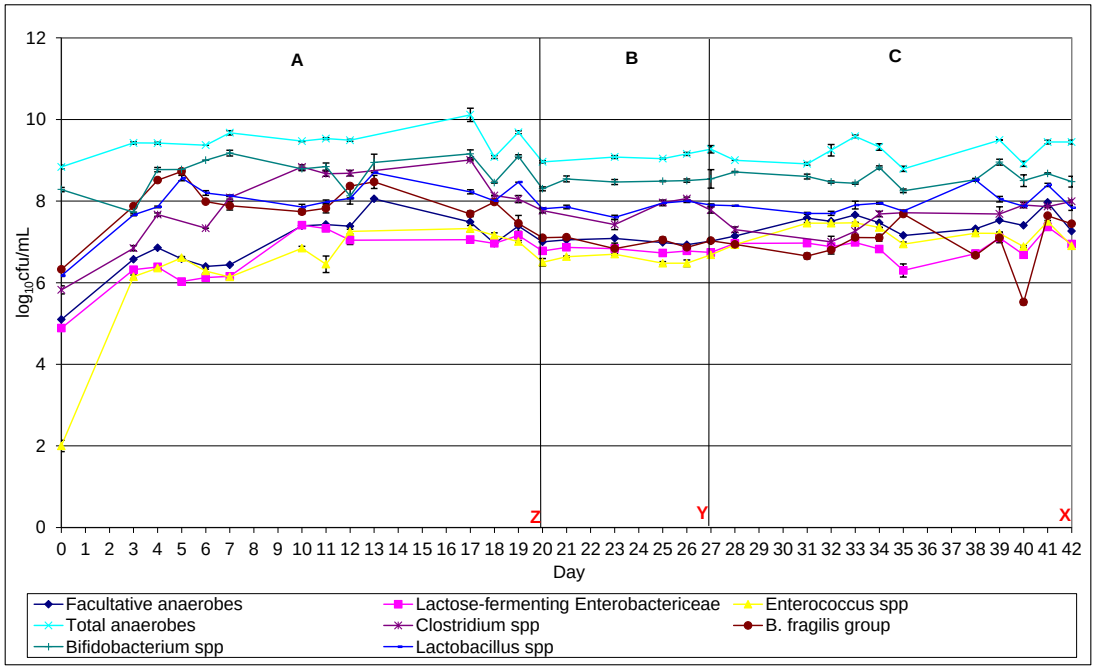

Figure 7.4.2.1.1: Planktonic (log_{10}cfu/mL) ± SE populations of indigenous gut microbiota in vessel 3 of the redesigned triple stage biofilm gut model experiment 1. Z-U biofilm/rod sampling points. Vertical line represents the last day of each period.

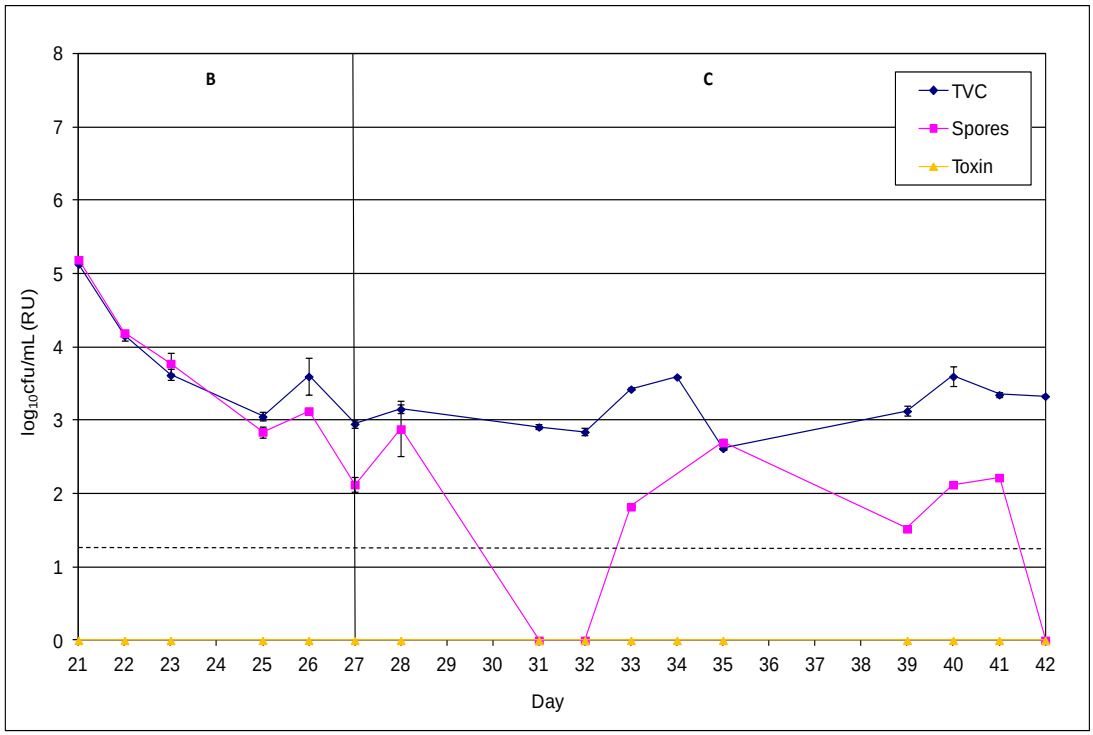

Figure 7.4.2.1.2: Planktonic (log_{10}cfu/mL) ± SE *C. difficile* populations in vessel 1 of the redesigned triple stage biofilm gut model experiment 1. Vertical line represents the last day of each period.

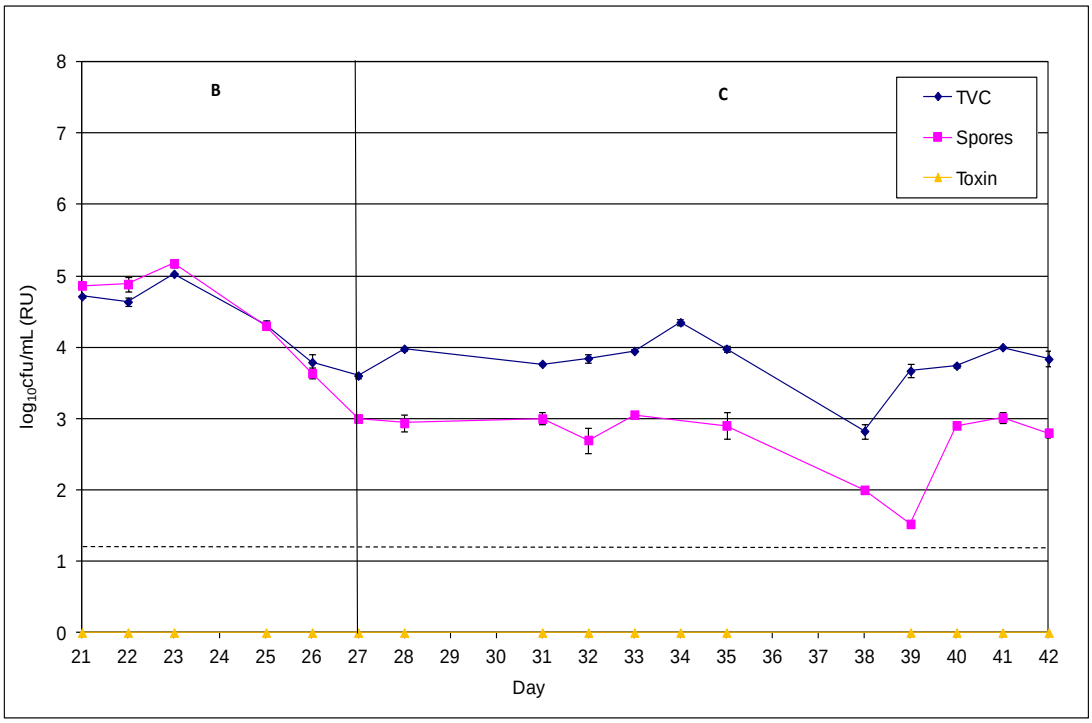

Figure 7.4.2.1.3: Planktonic (log_{10}cfu/mL) ± SE *C. difficile* populations in vessel 2 of the redesigned triple stage biofilm gut model experiment 1. Vertical line represents the last day of each period.

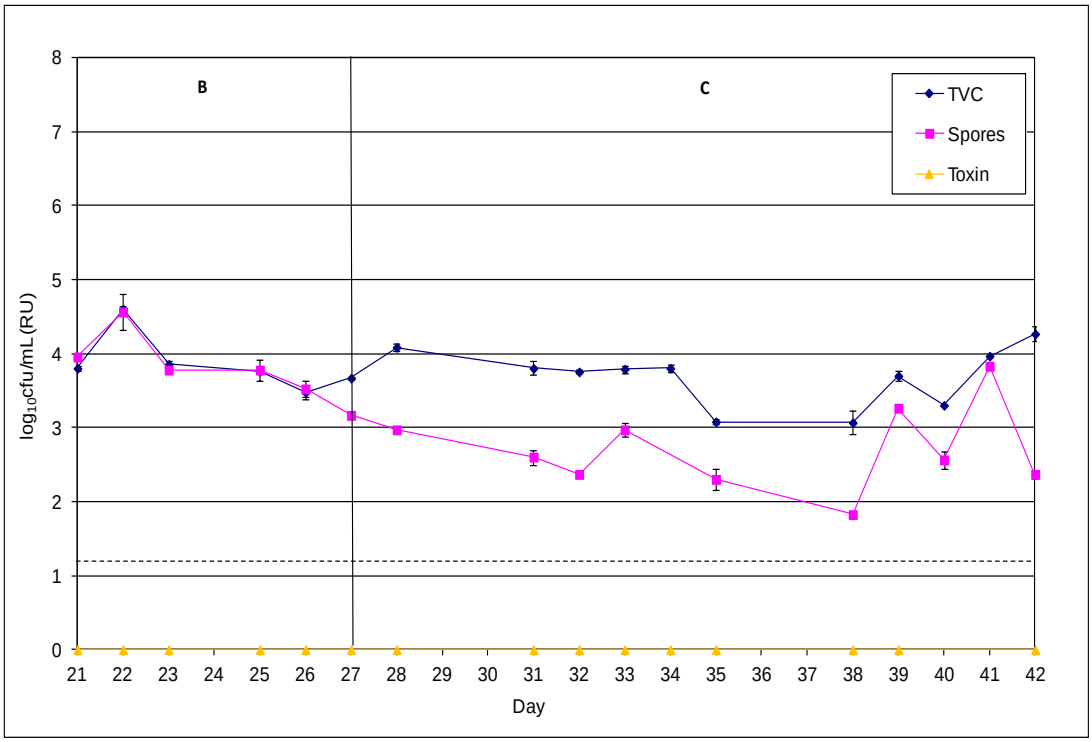

Figure 7.4.2.1.4: Planktonic (log_{10}cfu/mL) ± SE *C. difficile* populations in vessel 3 of the redesigned triple stage biofilm gut model experiment 1. Vertical line represents the last day of each period.

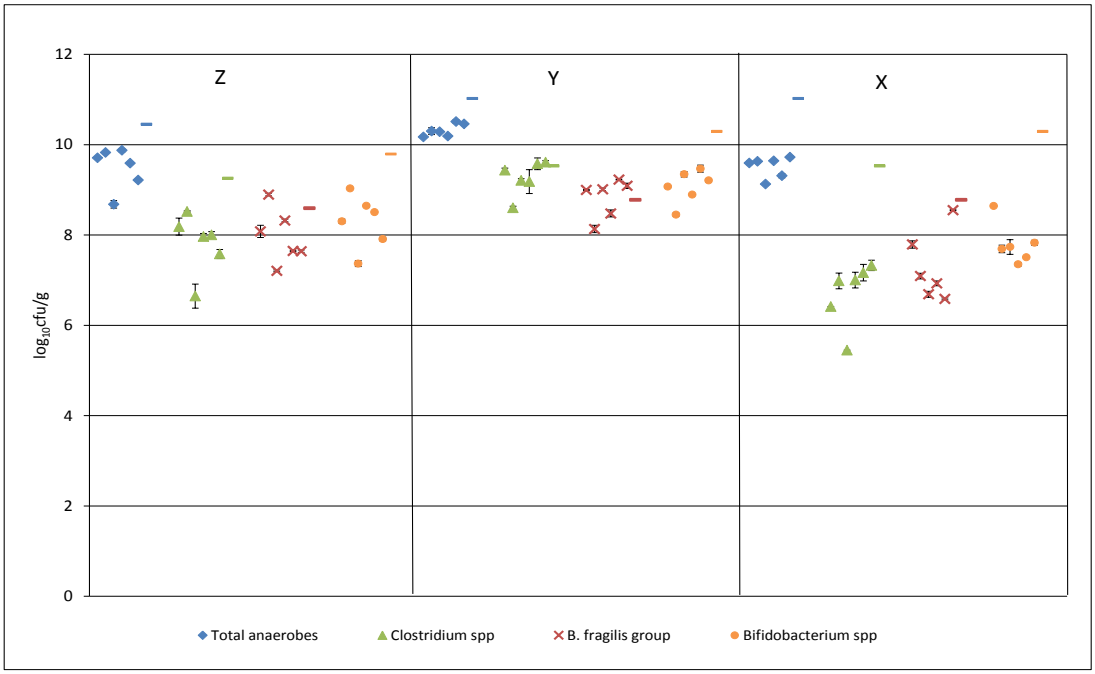

Figure 7.4.2.1.5: Populations (log_{10}cfu/g) ± SE of obligate anaerobes on rods within the triple stage biofilm gut model experiment 1 at time points Z-X. Planktonic populations of each bacterial group (log_{10}cfu/g) present at each time point are represented by a line in the appropriate colour.

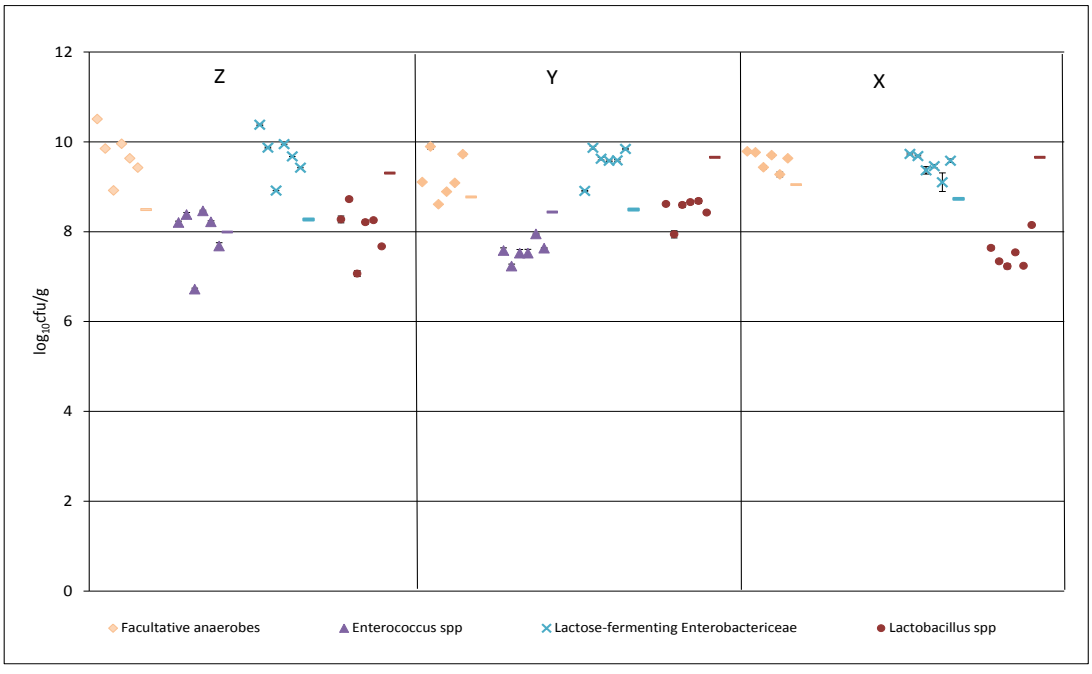

Figure 7.4.2.1.6: Populations (log_{10}cfu/g) ± SE of facultative anaerobes on rods within the triple stage biofilm gut model experiment 1 at time points Z- X. Planktonic populations of each bacterial groups (log_{10}cfu/g) present at each time point are represented by a line in the appropriate colour.

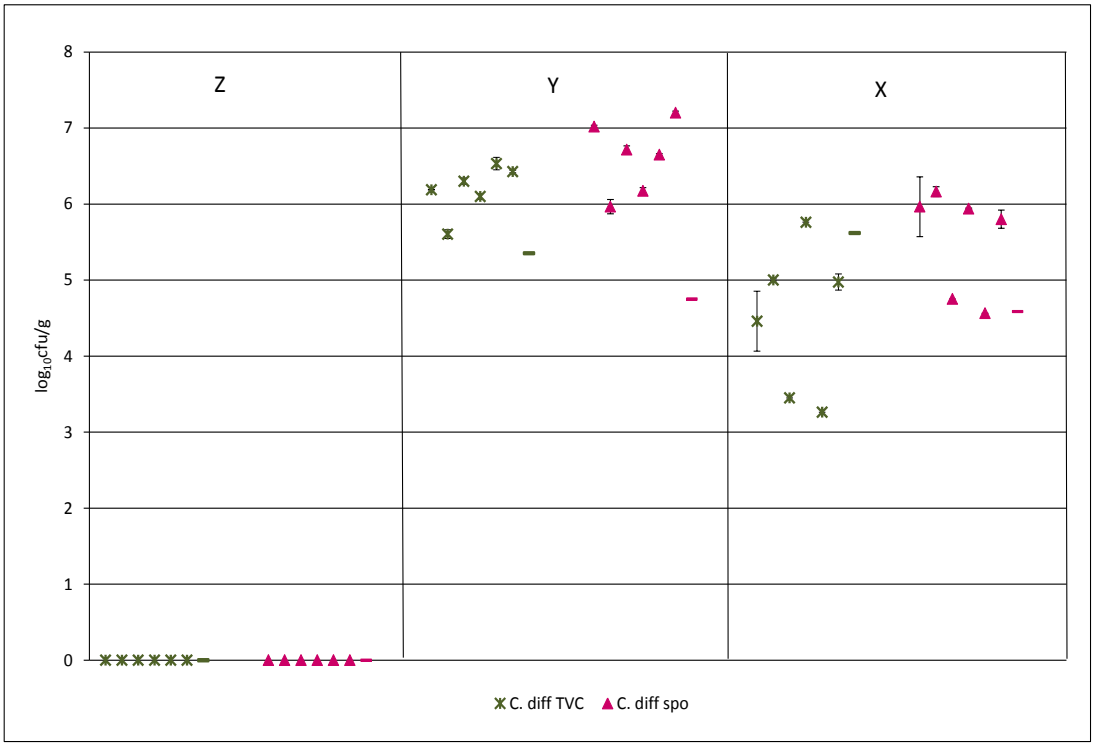

Figure 7.4.2.1.7: Populations (log_{10}cfu/g) ± SE of *C. difficile* on rods within the triple stage biofilm gut model experiment 1 at time points Z- X. Planktonic populations of each bacterial groups (log_{10}cfu/g) present at each time point are represented by a line in the appropriate colour.

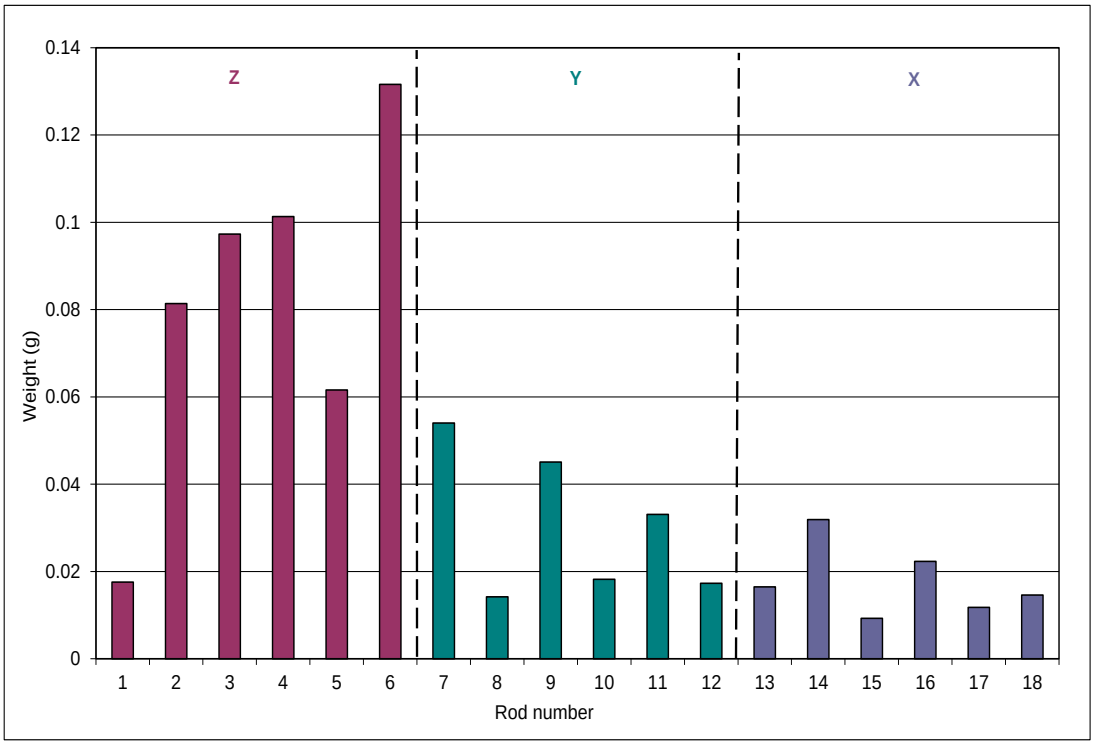

Figure 7.4.2.1.8: Pellet weight of 1 mL of re-suspended biofilm within the triple stage biofilm human gut model experiment 1 at time points Z-X.

Bacterial group	Mean 1-6	SE 1-6	Mean 7-12	SE 7-12	Mean 13-18	SE 13-18
Facultative anaerobes	9.71	0.07	9.22	0.20	9.60	0.08
Lactose-fermenting Enterobacteriaceae	9.70	0.11	9.57	0.14	9.49	0.09
Enterococcus spp.	7.94	0.30	7.57	0.09	NR	NR
Total anaerobes	9.48	0.06	10.32	0.06	9.51	0.10
Clostridium spp.	7.82	0.09	9.27	0.15	6.72	0.28
Bifidobacterium spp.	8.29	0.06	9.07	0.15	7.79	0.18
Bacteroides fragilis group.	7.97	0.24	8.82	0.17	7.27	0.31
Lactobacillus spp.	8.03	0.10	8.49	0.12	7.52	0.14
C. difficile TVC	NR	NR	6.19	0.13	4.49	0.40
C. difficile spores	NR	NR	6.62	0.19	5.53	0.28

Table 7.4: Mean (log_{10}cfu/g) and standard error (SE) of populations of indigenous gut microbiota on rods 1-6 (sample point Z), 7-12 (sample point Y) and 13-18 (sample point X) in the triple stage biofilm redesign gut model experiment 1. NR – no result

7.4.2.2 Experiment 2

7.4.2.2.1 Planktonic Indigenous Gut Microbiota Populations

Indigenous gut microbiota populations within vessel 3 of the gut model remained steady during period A. Instillation of *C. difficile* spores (day 21, period B) did not substantially affect microbiota populations (figure 7.4.2.2.1).

7.4.2.2.2 Sessile Indigenous Gut Microbiota Populations

Sessile viable counts of enumerated bacterial groups on rods 1-6 (sample point Z), 7-12 (sample point Y) and 13-18 (sample point X) were consistent, with a maximum standard error of 0.35 log_{10}cfu/g between *Enterococcus* spp. (figure 7.4.2.2.6 and table 7.5). Biofilm communities were dominated by LFE, with *Enterococcus* spp. the least numerous bacterial group for all time points. Rod-associated populations for each bacterial group remained largely steady across the 3 time points, although *Clostridium* spp., *B. fragilis* group and *Bifidobacterium* spp. populations reduced slightly at time point X (~1-2 log_{10}cfu/g decline). Variations (SE) of sessile populations at time point X were generally more pronounced compared with previous time points. Only two results for *Clostridium* spp. were obtained at time point X due to contamination of media.

7.4.2.2.3 Planktonic *C. difficile* Populations

Upon instillation of *C. difficile* spores into the gut model, populations remained as spores for ~5 days before TVCs and spores diverged, indicating the presence of low level vegetative cells in addition to spores (figures 7.4.2.2.2-4). *C. difficile* spore populations declined from peak levels of 5.7, 4.9 and 4.2 log_{10}cfu/mL in vessels 1, 2 and 3 respectively to

~ 3 log_{10}cfu/mL by the end of the experiment. Cytotoxin was detected on the penultimate day of the experiment at a level of 2 RU in vessels 2 and 3.

7.4.2.2.4 Sessile *C. difficile* Populations

Following *C. difficile* spore instillation (day 21; post time point Z), *C. difficile* populations existed solely as spores, with no indication of vegetative cell presence within all rod-associated biofilm structures at time points X and Y (figure 7.4.2.2.7). Variation between populations present on each rod was minimal (max standard error 0.14 log_{10}cfu/g). *C. difficile* decreased from a mean population of 5.4 to 4.8 log_{10}cfu/g at time points Y and X, respectively.

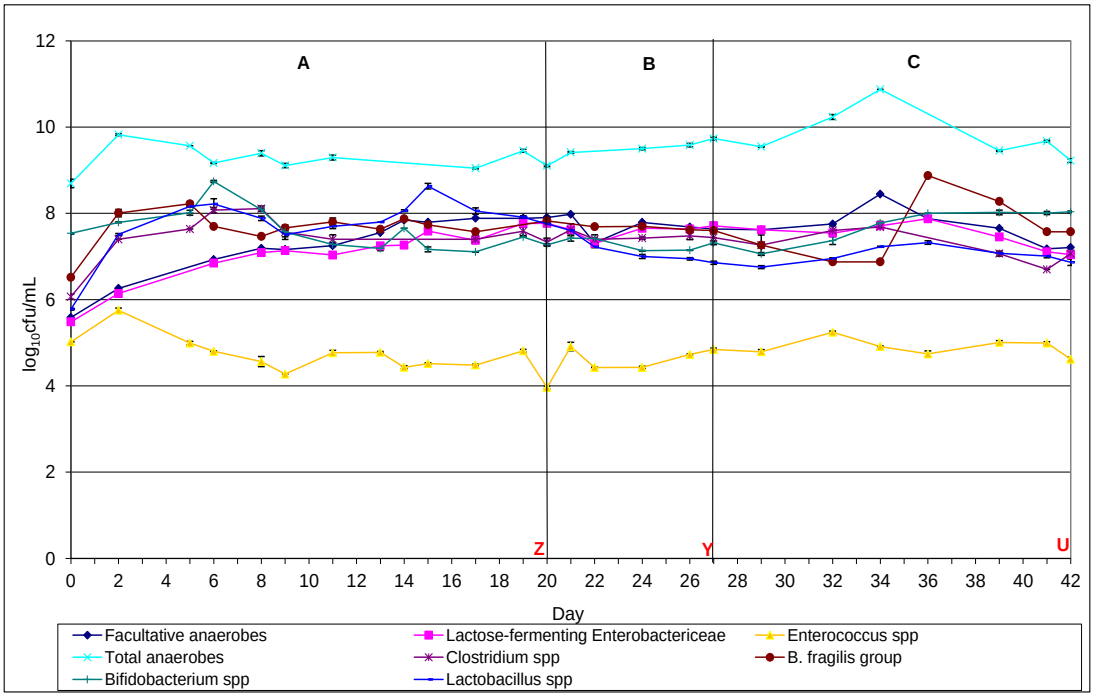

Figure 7.4.2.2.1: Planktonic (log_{10}cfu/mL) ± SE populations of indigenous gut microbiota in vessel 3 of the redesigned triple stage biofilm gut model experiment 2. Z-U rod/biofilm sampling points. Vertical line represents the last day of each period.

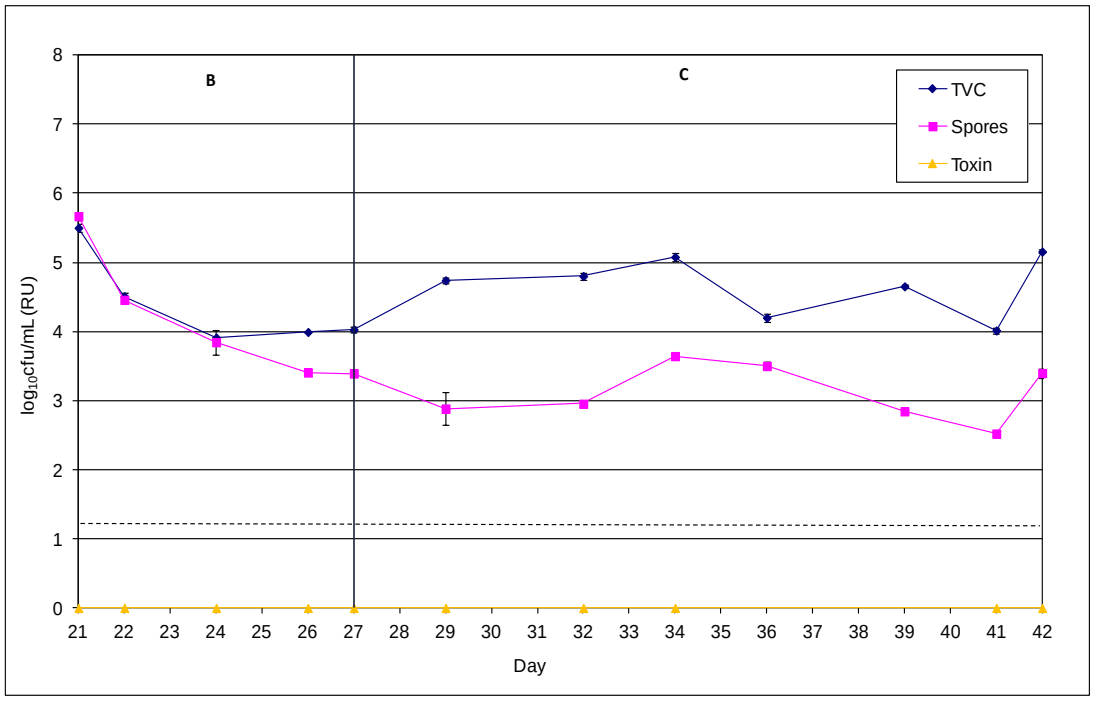

Figure 7.4.2.2.2: Planktonic (log_{10}cfu/mL) ± SE populations of *C. difficile* in vessel 1 of the redesigned triple stage biofilm gut model experiment 2. Vertical line represents the last day of each period.

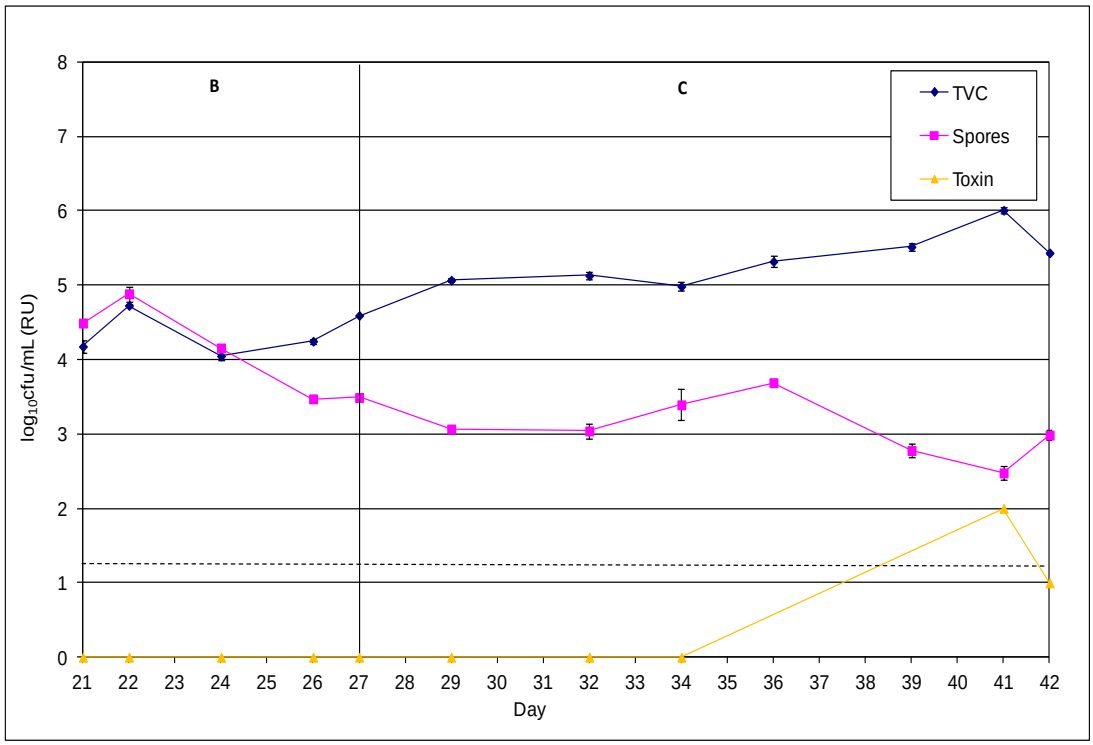

Figure 7.4.2.2.3: Planktonic (log_{10}cfu/mL) ± SE populations of *C. difficile* in vessel 2 of the redesigned triple stage biofilm gut model experiment 2. Vertical line represents the last day of each period.

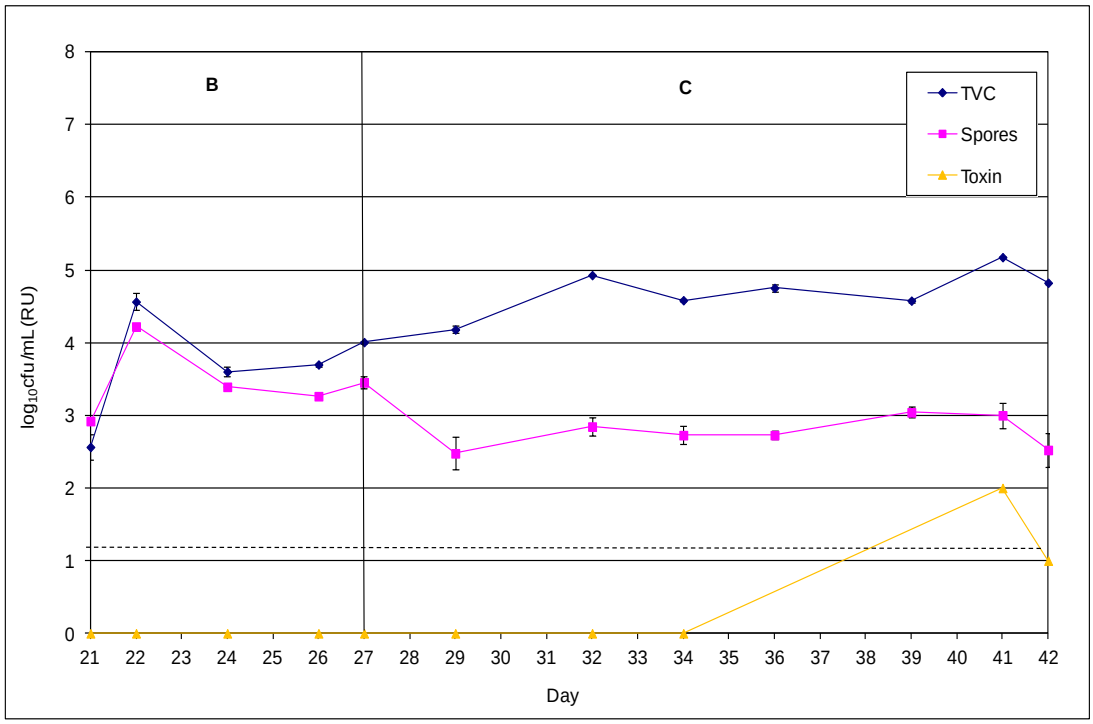

Figure 7.4.2.2.4: Planktonic (log_{10}cfu/mL) ± SE populations of *C. difficile* in vessel 3 of the redesigned triple stage biofilm gut model experiment 2. Vertical line represents the last day of each period.

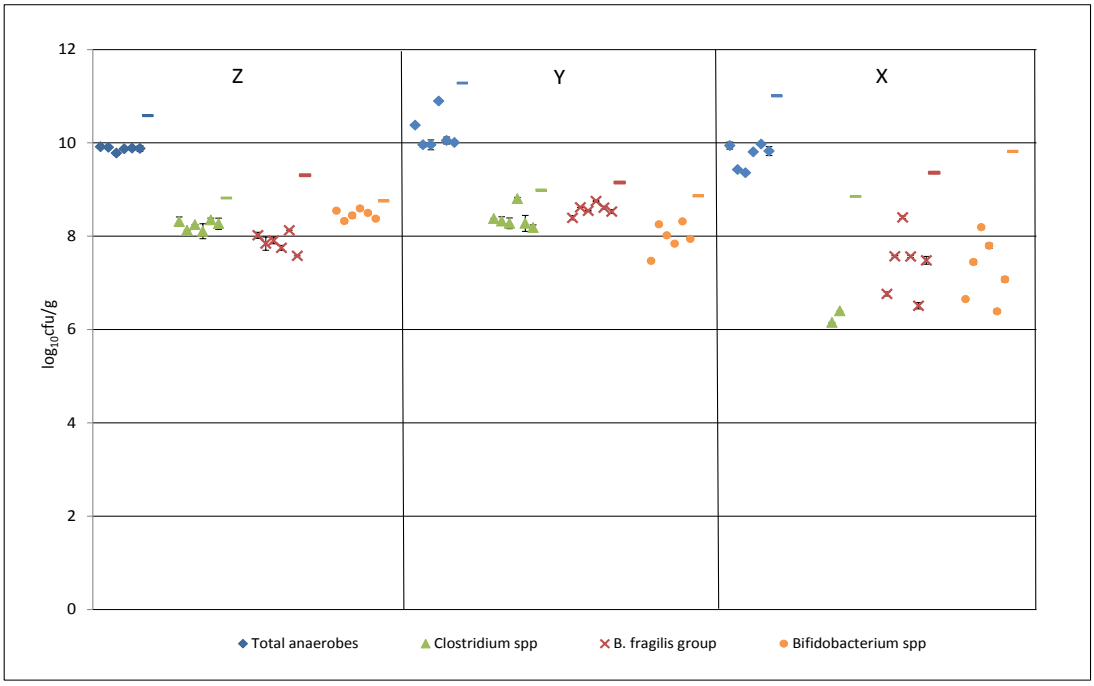

Figure 7.4.2.2.5: Populations (log_{10}cfu/g) ± SE of obligate anaerobes on rods within the triple stage biofilm gut model experiment 2 at time points Z-X. Planktonic populations of each bacterial groups (log_{10}cfu/g) present at each time point are represented by a line in the appropriate colour.

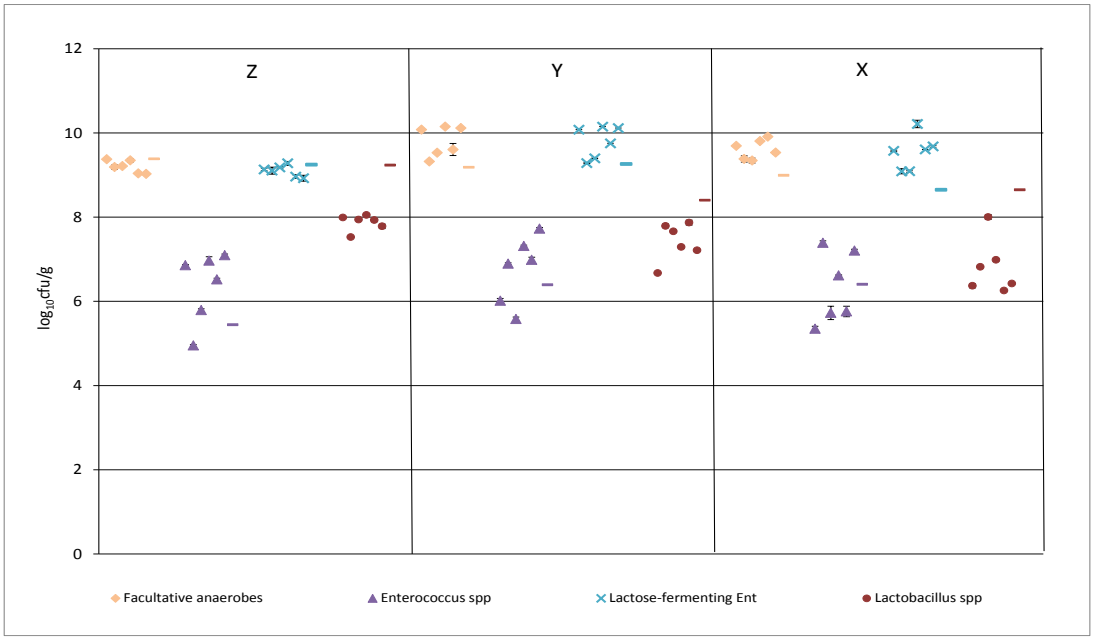

Figure 7.4.2.2.6: Populations (log_{10}cfu/g) ± SE of facultative anaerobes on rods within the triple stage biofilm gut model experiment 2 at time points Z-X. planktonic populations of each bacterial groups (log_{10}cfu/g) present at each time point are represented by a line in the appropriate colour.

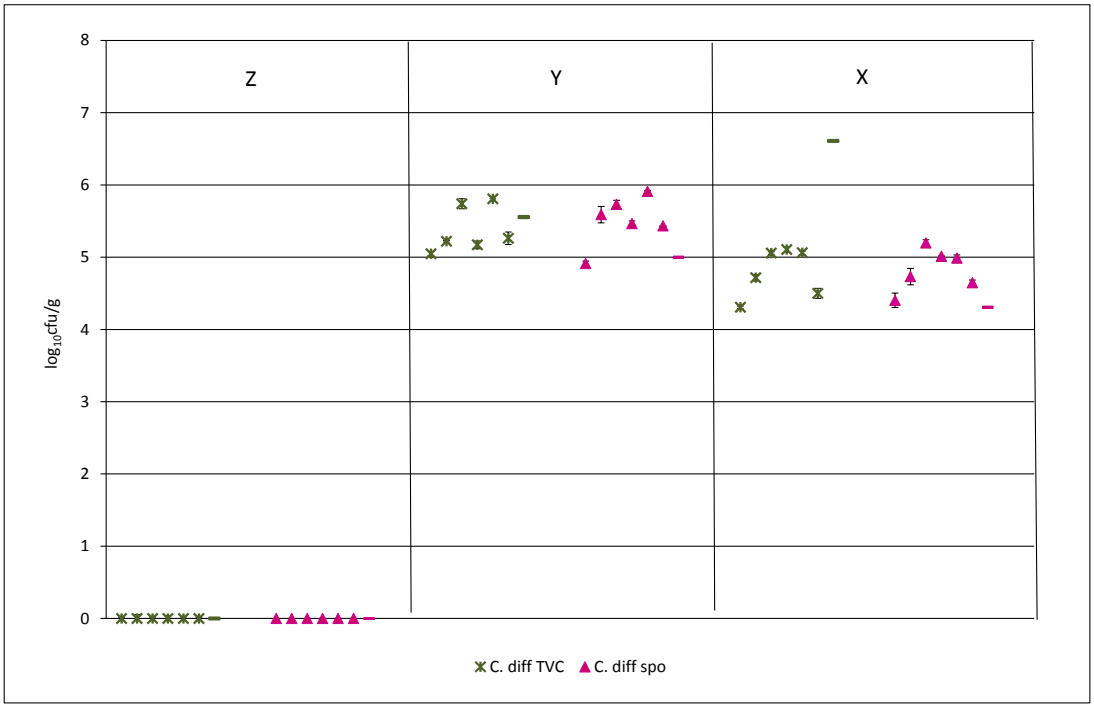

Figure 7.4.2.2.7: Populations (log_{10}cfu/g) ± SE of obligate anaerobes on rods within the triple stage biofilm gut model experiment 2 at time points Z - X. Planktonic populations of each bacterial groups (log_{10}cfu/g) present at each time point are represented by a line in the appropriate colour.

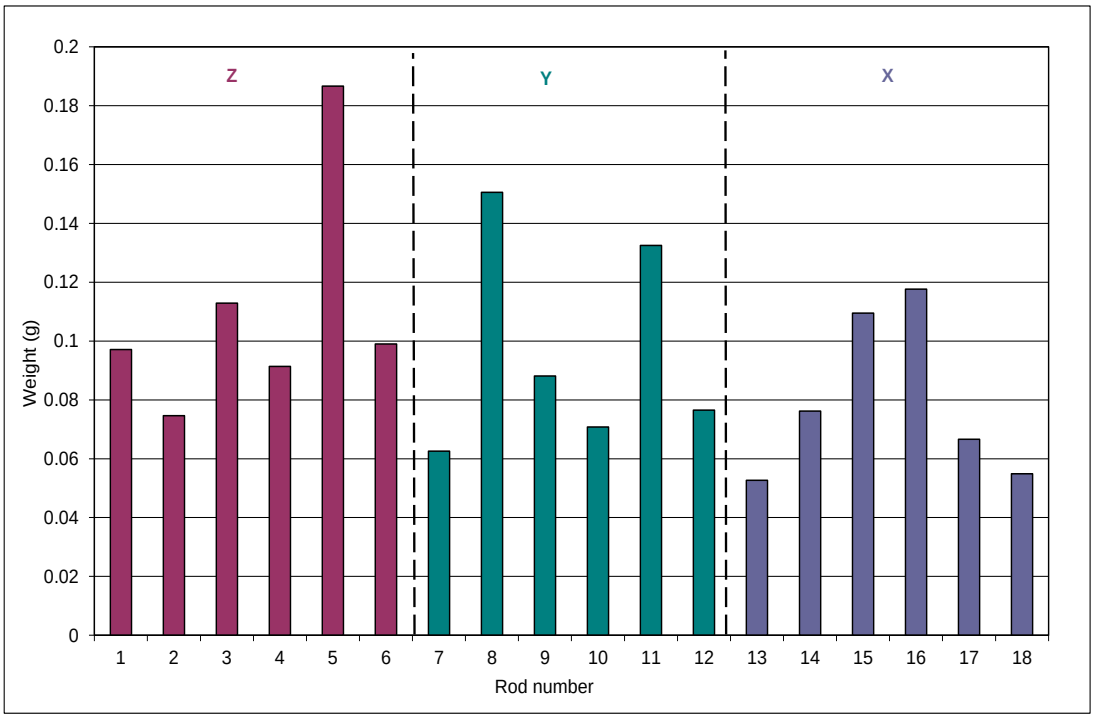

Figure 7.4.2.2.8: Pellet weight of 1mL of re-suspended biofilm within the triple stage biofilm human gut model experiment 2 at time points Z-X.

Bacterial group	Mean 1-6	SE 1-6	Mean 7-12	SE 7-12	Mean 13-18	SE 13-18
Facultative anaerobes	9.22	0.06	9.80	0.15	9.61	0.09
Lactose-fermenting Enterobacteriaceae	9.10	0.05	9.80	0.15	9.54	0.17
Enterococcus spp.	6.36	0.34	6.75	0.33	6.34	0.35
Total anaerobes	9.87	0.02	10.21	0.15	9.72	0.11
Clostridium spp.	8.24	0.09	8.37	0.09	6.24	0.07
Bifidobacterium spp.	8.46	0.04	7.97	0.13	7.26	0.30
Bacteroides fragilis group.	7.87	0.08	8.58	0.05	7.38	0.28
Lactobacillus spp.	7.87	0.08	7.42	0.18	6.81	0.26
C. difficile TVC	NR	NR	5.38	0.13	4.79	0.14
C. difficile spores	NR	NR	5.51	0.14	4.83	0.12

Table 7.5: Mean and standard error (SE) (log_{10}cfu/g) of populations of indigenous gut microbiota on rods 1-6 (sample point Z), 7-12 (sample point Y) and 13-18 (sample point X) in the triple stage biofilm redesign gut model experiment 2.

7.4.3 Discussion

The triple stage human gut model is designed to reflect the changing conditions of the proximal to distal human colon. In addition to microbiological and metabolic differences, it is also evident that biofilm structures vary within different vessel environments of the gut model. Vessel wall-associated biofilm biomass is greater in the high substrate environment of vessel 1 and reduced sequentially from vessel 1 to 3. However, rod-associated biofilm biomass within the single stage compared with triple stage redesigned biofilm gut model did not show such variation.

As noted in the single stage vessel, biofilm biomass was variable, although bacterial group populations (log_{10}cfu/g) remained consistent across rods. The triple stage experimental design allowed the investigation of sessile communities at three distinct time points. The biofilm lifecycle is a dynamic process. Stages of the biofilm lifecycle varied between structures on individual rods, resulting in differences in biofilm biomass. The final stage of biofilm development is dispersal of attached cells into the surrounding environment, mediating bacterial survival and disease transmission. Within this study, rod-associated biofilm biomass generally decreased as the experiment progressed (figures 7.4.2.1.8 and 7.4.2.2.8). Biofilm detachment is regulated by factors such as pH, nutrient availability and sheer forces[362, 364, 577], therefore decreased biofilm mass may be due to biofilm communities reaching increased structural stability and optimal biomass.

Maximal biofilm removal is desirable for this study. Hence, investigations were carried out to determine the optimal and most suitable biofilm removal techniques from glass rods. Previous investigations identified vortexing as providing maximal recovery of *C. difficile* populations from MA beads (chapter 3.0). Within this investigation there appeared to be no obvious difference in the use of vortex or sonication to remove mixed-species

biofilms from ground glass rods. The vortex technique proved greatest ease of use, therefore will be utilised in future experiments.

Within the original gut model an internal control period was designed to demonstrate the quiescent nature of *C. difficile* spores within the triple stage gut model in the absence of antimicrobial intervention. During this period, *C. difficile* spores were instilled into the model, *C. difficile* TVCs were equivalent to spore counts, indicating that only spores were present. Within this investigation, planktonic *C. difficile* TVCs increased above spore levels by ~1-2 $\log_{10}$cfu/mL in all vessels, 4-5 days after spore instillation, demonstrating the presence of low levels (~1-2 $\log_{10}$cfu/mL) of planktonic *C. difficile* vegetative/active cells within the model. Whilst germination of *C. difficile* spores appeared evident, proliferation of vegetative cells remained restricted, particularly in experiment 1.

Persistence of *C. difficile* spores (without washout of the continuous model system) has previously been observed within the original gut model (during the post-treatment period). However, increased TVCs compared within spores, as observed in this experiment, were less pronounced within the original gut model[515, 578]. Planktonic *C. difficile* populations may be maintained by the continued seeding of *C. difficile* spores from biofilm structures. It is possible that low level turnover (germination and outgrowth but minimum proliferation) of *C. difficile* spores is present, preventing washout of this population, allowing maintenance of a community, explaining the presence of low levels of vegetative cells.

Reasons for the inconsistent behaviour of *C. difficile* remain unclear. Within the redesign reproducibility experiments, following *C. difficile* instillation, no further interventions were made for the duration of the experiment, whilst within the original gut model, the internal *C. difficile* control period is limited to 7 days before clindamycin instillation commences. *C. difficile* vegetative

cells are susceptible to clindamycin (PCR ribotype 027 MIC = 0.5 mg/L), therefore active clindamycin prevents proliferation of these cells. Low level *C. difficile* spore turnover may potentially be a natural process in the presence of certain environmental stimuli, explaining observations within this study.

Whilst the presence of increased TVCs compared with spores was evident within planktonic *C. difficile* communities, there was no evidence of this trait within biofilm populations (figures 7.4.2.1.7 and 7.4.2.2.7), although it is possible that within the biofilm, sporulation of these vegetative cells may be occurring, thus preventing their detection. Sessile bacteria possess distinct metabolic and phenotypic characteristics from their planktonic counterparts, including reduced growth rate. The recruitment of quiescent spores into a dormancy-inducing biofilm structure enhances the likelihood of spores remaining inactive.

C. difficile spores germinate in response to external stimuli such as pH, heat and nutrients such as glycine and taurocholate[32, 170, 539]. Conditions within planktonic fluid of the human gut model may vary markedly from the protected environment of biofilms, potentially eliciting the diverse behaviour of *C. difficile* between the two phases.

Furthermore, sessile *C. difficile* spore populations maintained increased population levels compared with planktonic populations. These sessile spores may be shed as part of the natural lifecycle of biofilms, seeding spores into the planktonic environment. The persistence of *C. difficile* in spore form may mediate increased transmission of *C. difficile.*

Low level cytotoxin production was evident within the planktonic fluid of vessels 2 and 3 in experiment 2, but absent from biofilm structures. Active vegetative cells, were present within the planktonic phase, whilst absent from biofilm structures. Despite the presence of toxin within the planktonic

fluid surrounding the biofilms, sequestration of this toxin into biofilm structures was not evident. Reduced penetration of antimicrobial agents and biocides into biofilms has been previously reported [406, 579], although conflicting evidence also exists[545]. Similar mechanisms which confer reduced penetration of antimicrobials potentially reduce penetration or deactivation of toxin (or germinants) from the planktonic fluid, preventing detection of toxin (or vegetative cells) within biofilms as observed in this experiment.

Decreased populations of sessile compared within planktonic samples were observed for many bacterial groups, particularly at more advanced time points. Increased sessile populations compared within planktonic counterparts have previously been observed here and by others[446], particularly amongst facultative anaerobes such as *Enterococcus* spp.

No result was obtained for *Enterococcus* spp. at time point X in experiment 1 due to failure of selective media for this genera. However, full results for *Enterococcus* spp. were obtained in experiment 2. This highlights the importance of experimental repetition.

7.5 Conclusions

Baines *et al* evaluated and validated the triple stage chemostat gut model to study CDI [98]. Whilst biofilm structures are evident within the gut model, analysis of this parameter within the original model design is not feasible. Glass rods that create a solid-air-liquid interface for biofilm formation were incorporated into a chemostat vessel. Biofilm structures present on glass rods provided a means to sample and analyse distinct biofilm structures independently. Despite reduced levels of biofilm biomass from vessel 1 to 3 within the triple stage gut model, biofilm structures on glass rods within vessel 3 proved sufficient for analysis within this study. Biofilm consistently formed macroscopic structures on all glass rods over extended periods. Whilst variation in biofilm biomass was evident between rods, populations of bacterial groups (log_{10}cfu/g of biofilm) remained relatively consistent between rods at each sampling point. Despite design intervention within vessel 3 of the gut model, the planktonic mode of growth of *C. difficile* and the indigenous gut microbiota reflected observations within the original gut model. Furthermore, rod-associated sessile *C. difficile* and gut microbiota populations were comparable to those observed within previous investigations (chapters 4.0-6.0).

The redesigned biofilm chemostat model has been validated for reproducible and consistent formation of mixed-species intestinal biofilms. Optimal biofilm formation and removal techniques have been determined. This model can be utilised for the analysis of sessile mixed-species communities longitudinally, potentially providing information of the role of biofilms in CDI.

8.0 Triple Stage Biofilm Human Gut Model of Simulated *Clostridium difficile* Infection

8.1 Background

The original gut model system has proven a successful *in vitro* model of CDI; however, it is unable to reflect the extensive and complex bacterial communities that colonise intestinal mucosal surfaces in biofilm structures accurately. The triple stage biofilm human gut model has been developed to facilitate the formation and analysis of biofilm communities *in vitro*, allowing the investigation of the biofilm mode of growth of *C. difficile* and the indigenous gut microbiota in CDI. Therefore, this biofilm model can now be used to investigate the effects of CDI induction and treatment on sessile, as well as planktonic, bacterial populations.

8.2 Materials and Methodology

8.2.1 Triple Stage Biofilm Gut Model Set Up

The biofilm redesign model was set up as a triple stage model as described previously (sections 4.2.1 and 7.4.2.1.2). The experimental design is outlined in figure 8.2.1. Briefly, eighteen 'roughened' glass rods were positioned within the vessel (relative positions are highlighted in figure 7.2.1). Preparation of gut model growth medium is described in section 4.2.2.

8.2.2 Planktonic Sampling and Enumeration Protocol

Planktonic indigenous gut microbiota, *C. difficile* TVCs and spores and cytotoxin were enumerated as described in section 7.3.1.1.2. At biofilm

sampling points planktonic populations are also expressed as log_{10}cfu/g. Antimicrobial activity was enumerated as described in section 4.2.8.

8.2.3 Sessile Sampling and Enumeration Protocol

Sessile gut microbiota, *C. difficile* TVCs and spores and cytotoxin were enumerated from all 18 rods (at six separate time points, figure 8.2.1) within vessel 3 of the triple stage gut model. Rods were submerged in 5 mL of pre-reduced sterile saline, vortexed thoroughly for ~2 mins and rod removed and discarded. The biofilm suspension was centrifuged at 3000 g for 10 mins, supernatant discarded and pellet resuspended in 2mL pre-reduced sterile saline. Rod-associated parameters were enumerated as described in sections 2.1, 2.2 and 2.4. Antimicrobial activity was enumerated as described in 4.2.8.

8.2.4 Experimental Design

Once the biofilm model was set up and the media pump started the system was left to allow bacterial populations to equilibrate for 20 days (figure 8.2.4 period A). During period A, planktonic gut microbiota populations were monitored every 2 days. A single inoculum of *C. difficile* PCR ribotype 027 spores (~10^7 cfu) were inoculated into vessel 1 of the model on day 21 (period B). From this point onwards planktonic gut microbiota, *C. difficile* TVCs, spores and cytotoxin were monitored daily. The system was left without further intervention until rods 1-3 were sampled on day 27 (27:time point Z). Sessile gut microbiota, *C. difficile* TVCs, spores and cytotoxin were quantified. On day 28 a further inoculum of *C. difficile 0*27 spores (10^7 cfu) were instilled to vessel 1 of the gut model along with a dosing regimen of clindamycin (33.9mg/L QD 7 days – period C). Antimicrobial activity was monitored from this point onwards.

Clindamycin (33.9 mg/L, QD, 7 days) was instilled to reflect the concentration in faeces of patients and volunteers[514]. Rods 4-6 and 7-9 were sampled on days 35 (35:time point Y) and 41 (41:time point X), respectively. In addition to enumerated parameters at time point Z, antimicrobial activity was also monitored in sessile communities from hereon. Once high level cytotoxin titre (≥4RU) was observed within the planktonic fluid (period D), instillation of vancomycin commenced (125 mg/L, QD, 7 days – period E). Following cessation of vancomycin instillation, gut microbiota, *C. difficile* TVCs, spores populations, cytotoxin titres and antimicrobial activity were monitored for a further 24 days (period F). A further three rods were sampled at each time point; W, V and U, on days 52, 59 and 73, respectively. Planktonic indigenous gut microbiota (periods A-F, vessels 2 and 3), *C. difficile* total viable counts, spores and cytotoxin (periods B-F, vessels 1-3) and antimicrobial agents (periods C-F, vessel 1-3) were monitored during the experiment.

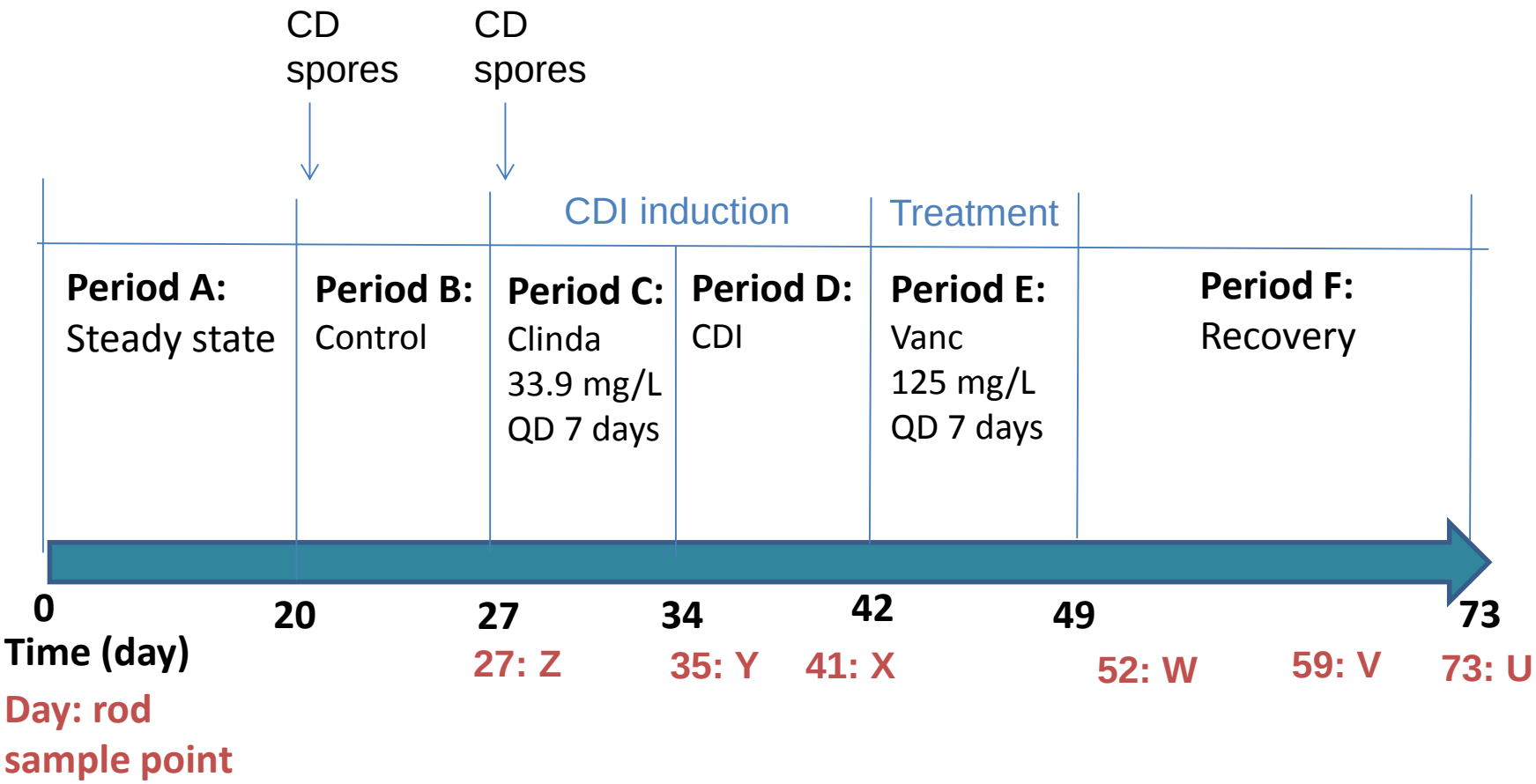

Figure 8.2.1: Experimental design of triple stage biofilm gut model of simulated CDI. Vertical lines represent the last day of each period. Vertical line represents the last day of each period.

8.3 Results

8.3.1 Planktonic Indigenous Gut Microbiota Populations

Indigenous gut microbiota bacterial groups reached steady state by the end of period A in vessels 2 and 3 (figures 8.3.1 and 8.3.2). *Bifidobacterium* spp. were the most abundant bacterial group with *Enterococcus* spp. the least abundant during period A.

The instillation of *C. difficile* spores on day 21 (period B) did not appear to affect gut microbiota populations with levels remaining steady. Clindamycin instillation (period C) elicited a precipitous decline in *Bifidobacterium* spp. in both vessel 2 and 3 (~8 $\log_{10}$cfu/mL decline), with populations declining to below LOD, 4 days after instillation commenced. A less marked decline was evident in *B. fragilis* group (vessel 2, ~2.5 $\log_{10}$cfu/mL; vessel 3, ~1 $\log_{10}$cfu/ml), *Clostridium* spp. (vessel 2, ~2.5 $\log_{10}$cfu/mL; vessel 3, ~2 $\log_{10}$cfu/ml) and *Lactobacillus* spp. (vessel 2, ~2 $\log_{10}$cfu/mL; vessel 3, ~1.5 $\log_{10}$cfu/ml). Viable counts of bacterial groups began to recover by the end of period C, with the exception of *Bifidobacterium* spp., with viable counts increasing by the end of period D. Vancomycin instillation (period E) commenced eight days after clindamycin cessation, resulting in profound decreases in *B. fragilis* group (~6-6.5 $\log_{10}$cfu/mL) and *Bifidobacterium* spp. (~6 $\log_{10}$cfu/mL) viable counts in vessels 2 and 3. Smaller declines in *Enterococcus* spp., LFE and *Clostridium* spp. were evident, although *Lactobacillus* spp. populations increased (~1-1.5 $\log_{10}$cfu/mL). Most bacterial groups recovered to, or exceeded pre-vancomycin levels ~9 days after dosing cessation, except *Bifidobacterium* spp. which recovered after 18-21 days (period F).

8.3.2 Sessile Indigenous Gut Microbiota Populations

Rod-associated bacterial populations were monitored at six different time points (Z-U, figure 8.2.4). Time point Z was the final day of period B, pre-clindamycin instillation; Y, one day after clindamycin dosing ceased; X, during planktonic simulated CDI; W, after completion of vancomycin dosing; V, during the recovery period; U, during recurrent planktonic disease. Sessile gut microbiota figures (figures 8.3.6 and 8.3.7) also present planktonic (log_{10}cfu/g) populations obtained at that time point and will be referred to here. Bacterial group populations on each rod at time point Z display little variation (figures 8.3.6 and 8.3.7). LFE (average 9.2 log_{10}cfu/g) dominated sessile bacterial populations, with *B. fragilis* group (average 8.1 log_{10}cfu/g) the least populous group.

Clindamycin instillation commenced eight days prior to time point Y and elicited a deleterious effect on gut planktonic microbiota, most notably *Bifidobacterium* spp. which declined below LOD, three days previous to biofilm sampling, Y. However, sessile *Bifidobacterium* spp. populations, whilst declining (~5 log_{10}cfu/g), maintained an average population of 3.9 log_{10}cfu/g. More modest decreases in sessile *Lactobacillus* spp. (~1.5 log_{10}cfu/g), *Clostridium* spp. (~1 log_{10}cfu/g), *Enterococcus* spp. (~1 log_{10}cfu/g) and *B. fragilis* group (~1 log_{10}cfu/g) were also noted. Sessile populations at time point X, remained at similar levels to time point Y, although *Bifidobacterium* spp. increases by ~1.5 log_{10}cfu/g. Vancomycin instillation commenced ten days before biofilm sampling point W, resulting in a marked decline in sessile *B. fragilis* group and *Bifidobacterium* spp. to below the LOD, whilst *Lactobacillus* spp. increased by ~2.5 log_{10}cfu/g. Similar trends were also noted for planktonic populations, although planktonic *Clostridium* spp. also declined to below LOD, whilst sessile populations remained at 7.9 log_{10}cfu/g. Planktonic and sessile *Bifidobacterium* spp. population remained below LOD at time point V. *B. fragilis* group began to

recover with sessile and planktonic populations increasing to 5.1 log_{10}cfu/g and 8.9 log_{10}cfu/g, respectively. All bacterial groups established sessile populations by the completion of the experiment; counts of facultative anaerobic groups and *B. fragilis* group, and *Clostridium* spp. populations remained marginally lower than initial (Z) levels.

8.3.3 Planktonic *C. difficile* Populations

C. difficile was not isolated during the steady state period (period A). *C. difficile* populations were comprised primarily of spores during the internal control period (period B) in all vessels, declining from ~5-5.5 to ~3 log_{10}cfu/mL as vessel contents were diluted (figures 8.3.3-5). Cytotoxin was not detected (period B). A second inoculum of *C. difficile* spores concurrent with the start of clindamycin instillation (period C) was instilled on day 28. *C. difficile* population initially comprised spores primarily until a marked increase in TVCs relative to spore counts was observed in vessels 2 and 3, five days after instillation cessation. TVCs peaked at ~6.5 log_{10}cfu/mL, one day previous to peak cytotoxin titre of 4RU in vessel 3. Vancomycin instillation elicited a rapid decline in TVCs in vessels 2 and 3, with only spores remaining after two days (~2 log_{10}cfu/mL decline in vessels 2 and 3). Cytotoxin decreased to below LOD, 5 days after the start of vancomycin instillation within vessel 3. Vancomycin did not demonstrate an effect on *C. difficile* spore populations within vessel 1, which remained as spores for the remainder of the experiment in vessel 1, although TVCs increased relative to spores ~14-16 days after vancomycin cessation within vessels 2 and 3. Subsequent increase in cytotoxin was observed, reaching peak titres of 4 RU in vessels 2 and 3.

8.3.4 Sessile *C. difficile* Populations

Sessile *C. difficile* data (figure 8.3.8) also presents planktonic (log_{10}cfu/g) populations obtained at that time point. Rod-associated *C. difficile* populations remained primarily as spores for the duration of the experiment. At time point Z, *C. difficile* rod-associated populations demonstrated consistent populations across the three rods, with populations comprising spores primarily (~5.8 log_{10}cfu/g). Cytotoxin was not detected with biofilm structures. Instillation of a second inoculum of *C. difficile* spores, alongside a dosing regimen of clindamycin, did not greatly affect sessile *C. difficile* populations, although slightly increased variation amongst rods was noted (SE time point Z, 0.05-0.09 log_{10}cfu/g; SE time point Y, 0.36-0.37 log_{10}cfu/g). Cytotoxin was not detected.

During simulated planktonic CDI, sessile *C. difficile* maintained a consistent population, comprising primarily of spores (~5.5 log_{10}cfu/g). Cytotoxin was detected at low levels (1 RU) within 1 of the 3 rods. During time points W and V, *C. difficile* populations remained as spores at ~5.5 log_{10}cfu/g with no toxin detected. During recurrent planktonic infection (time point U), sessile *C. difficile* populations remained in spore form, although levels dropped by ~0.5 log_{10}cfu/g. Cytotoxin was detected in 1 of the 3 rods at low levels (2 RU).

8.3.5 Antimicrobial activity

Clindamycin was detected within the planktonic phase of all three vessels of the gut model, peaking at a concentration of 64.9, 50.7 and 50.8 mg/L in vessel 1, 2 and 3, respectively (figure 8.3.9). Detection of clindamycin activity continued 1, 2 and 3 days after dosing cessation in vessels 1, 2 and 3, respectively. Rods from time point Y (day 35) were sampled and analysed,

one day after dosing cessation. Clindamycin activity could not be detected within rod-associated biofilm structures.

Vancomycin activity was detected within the planktonic fluid throughout period E and continued to be detected for three days after dosing cessation in all three vessels (figure 8.3.10). Concentrations peaked on the final day of instillation (day 49) at concentrations of 330.2, 317.8 and 270.3 mg/L in vessels 1, 2 and 3, respectively. Vancomycin activity within biofilm structures per rod (time point W, day 52) ranged from 38.7 to 43.4 mg/L (figure 8.3.11). Planktonic antimicrobial activity on day 52 within vessel 3 was 6.05 mg/L.

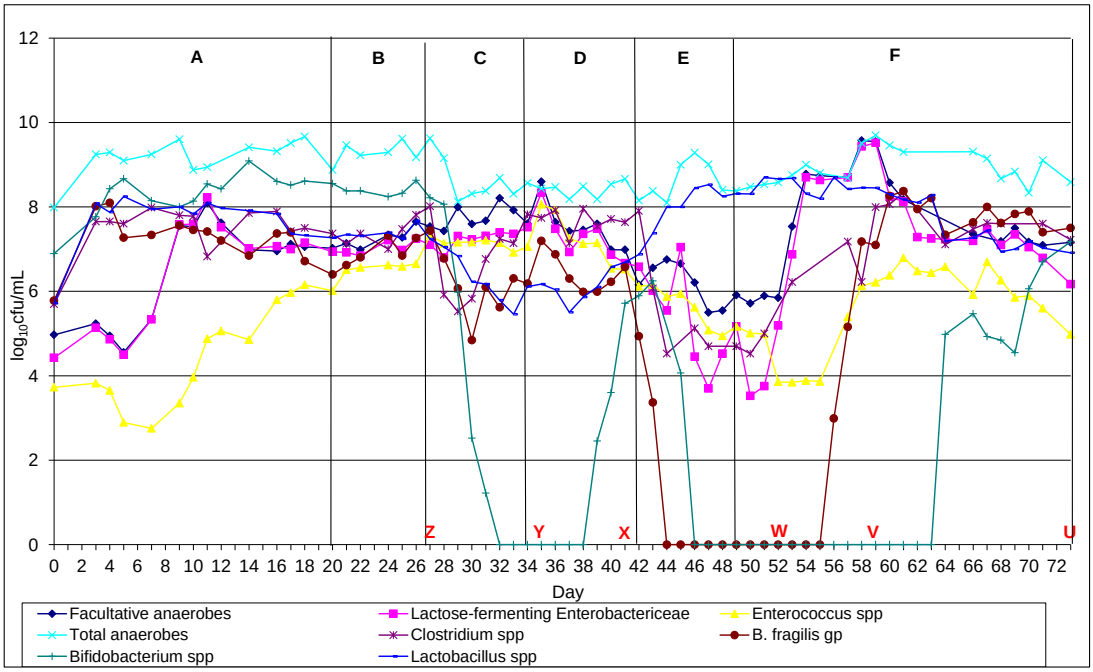

Figure 8.3.1: Planktonic populations (log_{10}cfu/mL, ±SE) of indigenous gut microbiota in vessel 2 of the triple stage biofilm gut model. Vertical line represents the last day of each period. A – steady state, B – internal control, C – clindamycin instillation, E – simulated CDI, F - rest

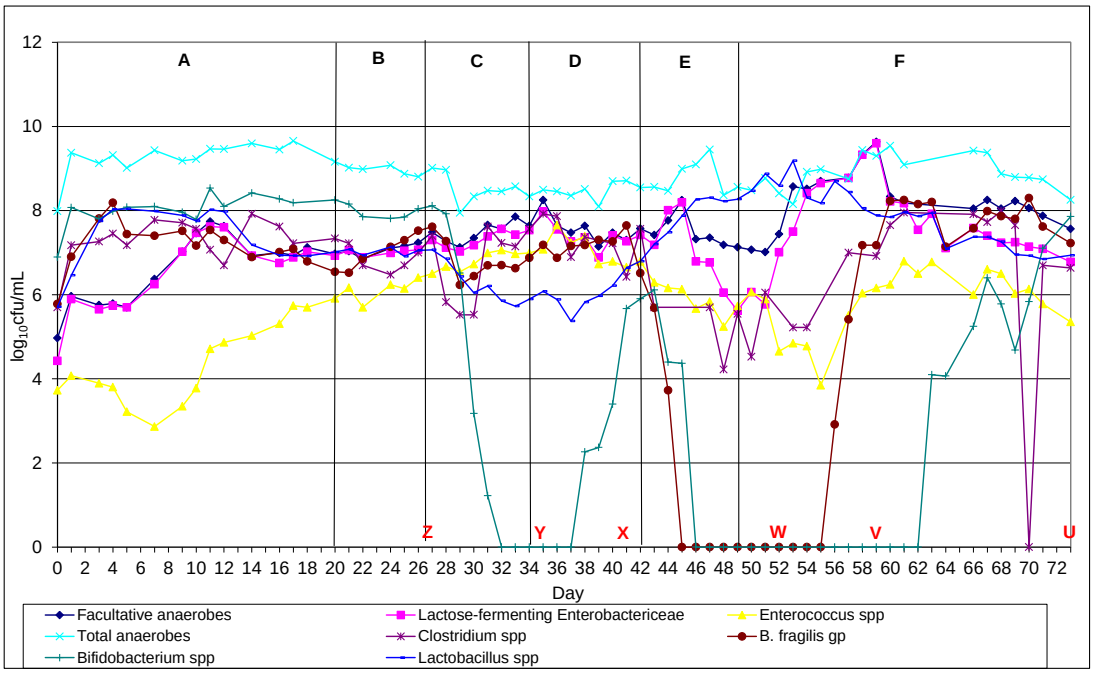

Figure 8.3.2: Planktonic populations (log_{10}cfu/mL, ±SE) of indigenous gut microbiota in vessel 3 of the triple stage biofilm gut model. Vertical line represents the last day of each period. A – steady state, B – internal control, C – clindamycin instillation, E – simulated CDI, F - rest

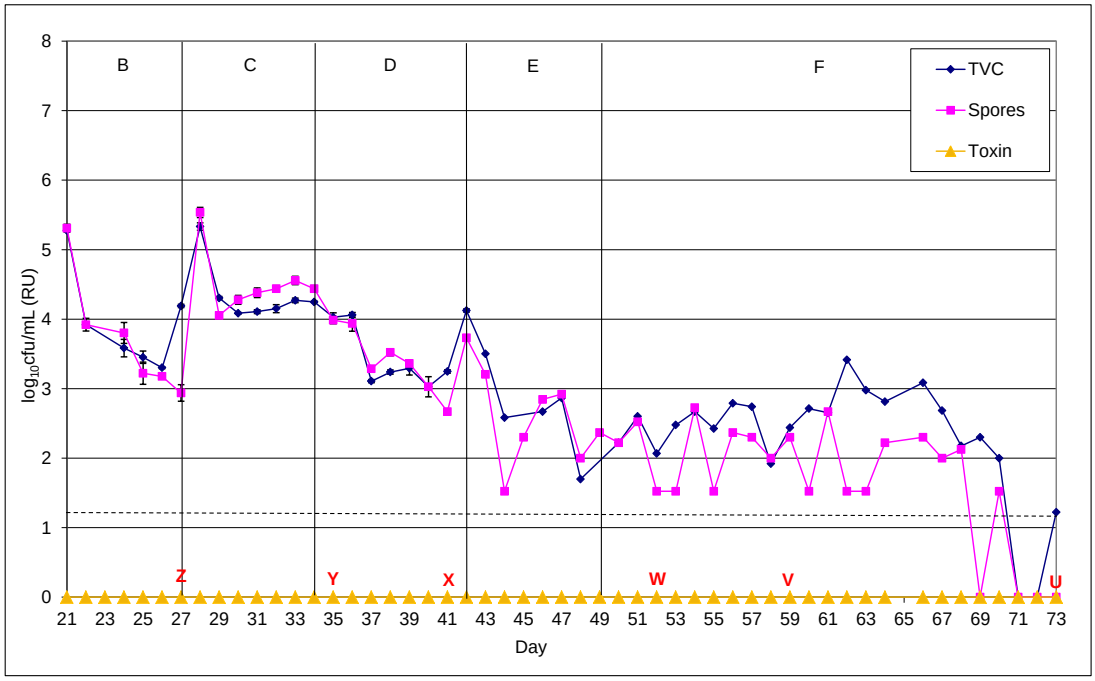

Figure 8.3.3: Planktonic populations (log_{10}cfu/mL, ±SE) of *C. difficile* within vessel 1 of the triple stage biofilm gut model. Vertical line represents the last day of each period. B – internal control, C – clindamycin instillation, E – simulated CDI, F – rest. Dashed line - ~LOD

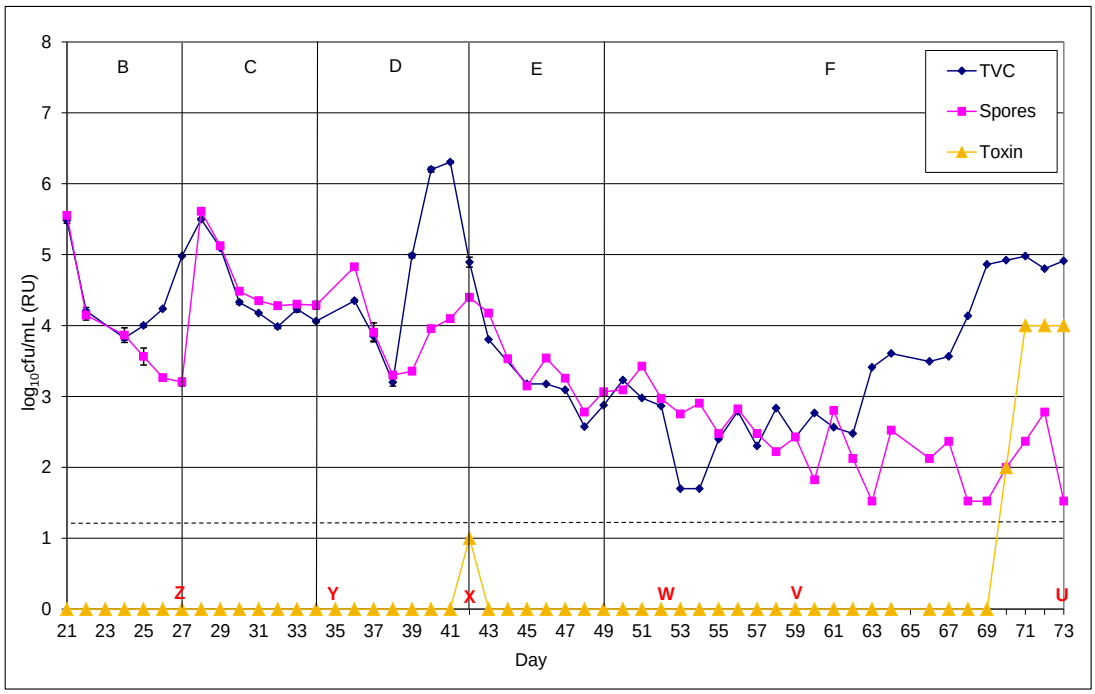

Figure 8.3.4: Planktonic populations (log_{10}cfu/mL, ±SE) of *C. difficile* within vessel 2 of the triple stage biofilm gut model. Vertical line represents the last day of each period. B – internal control, C – clindamycin instillation, E – simulated CDI, F – rest. Dashed line - ~LOD

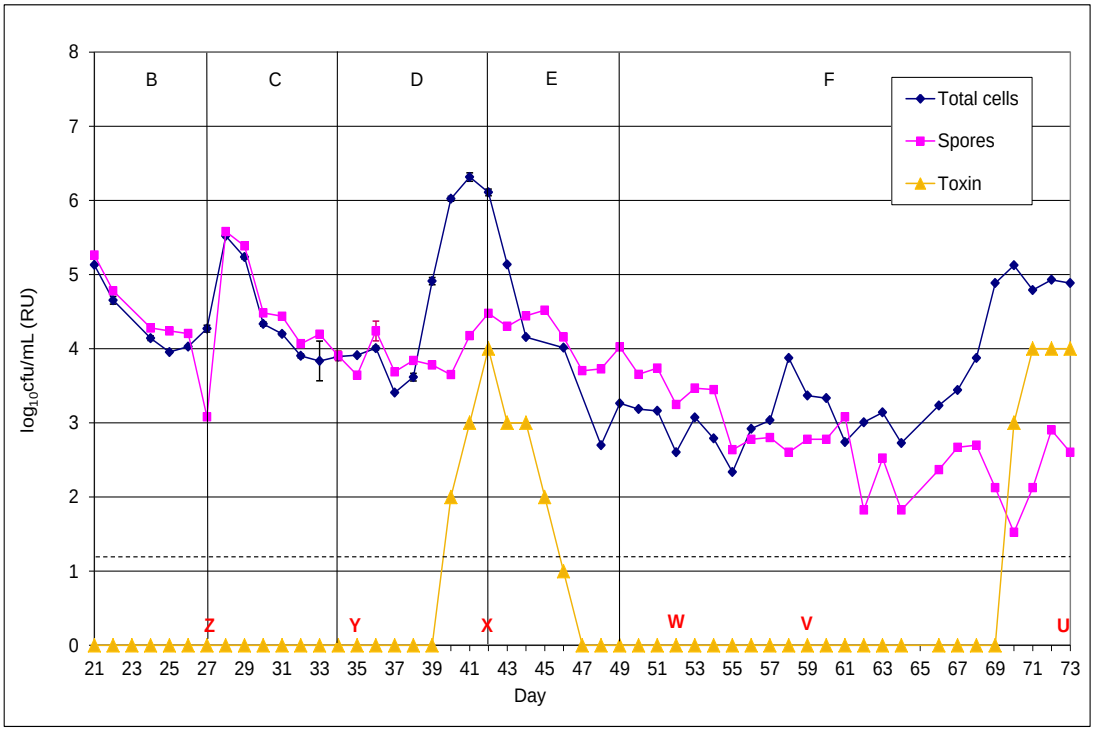

Figure 8.3.5: Planktonic populations (log_{10}cfu/mL, ±SE) of *C. difficile* within vessel 3 of the triple stage biofilm gut model. Vertical line represents the last day of each period. B – internal control, C – clindamycin instillation, E – simulated CDI, F – rest. Dashed line - ~LOD.

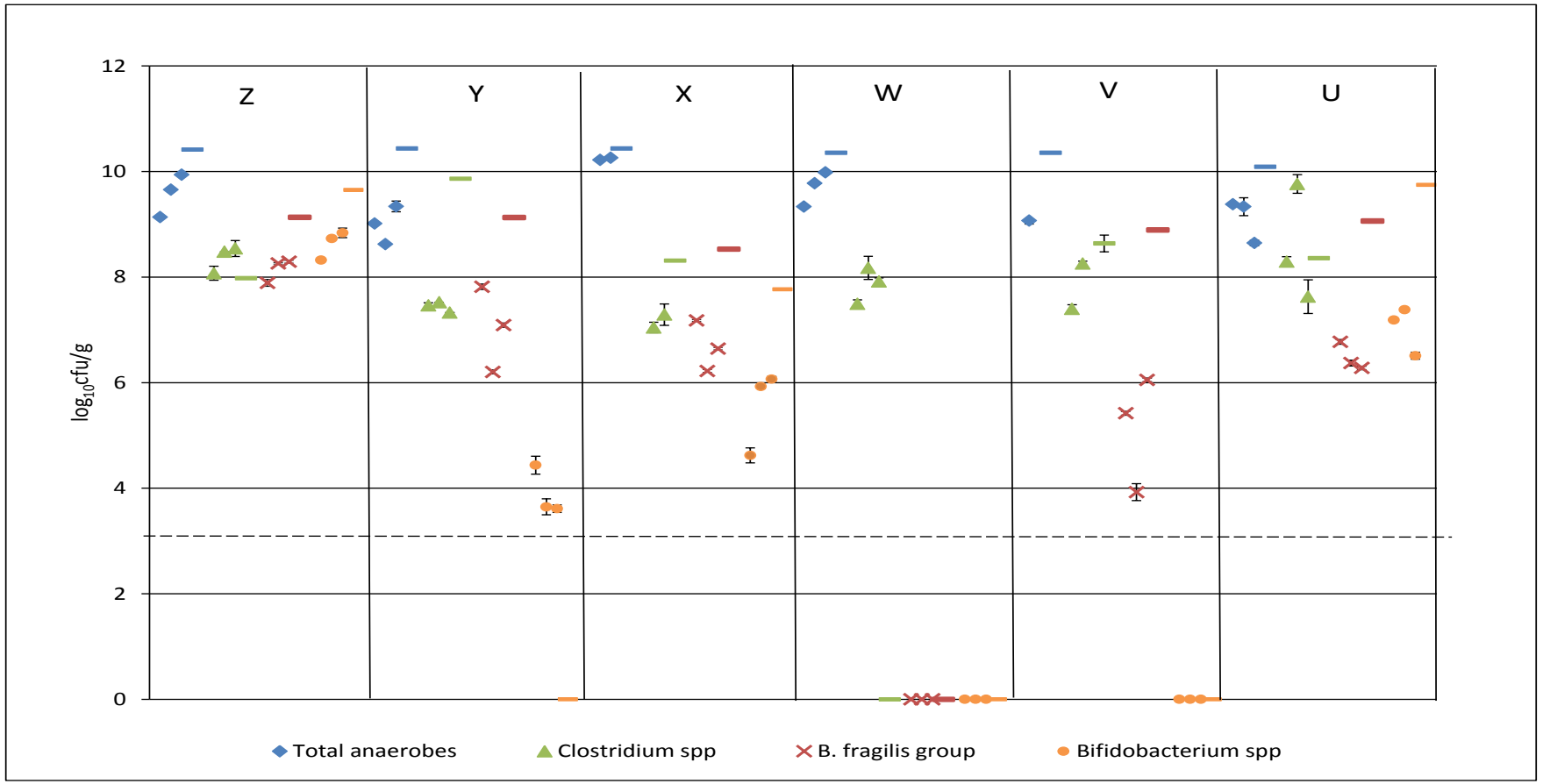

Figure 8.3.6: Sessile obligate anaerobic microbiota populations (±SE) from rod/biofilm sampling points Z-U within the triple biofilm human gut model. Planktonic populations of each bacterial groups (log_{10}cfu/g) present at each time point are represented by a line in the appropriate colour; dashed line, approximate limit of detection.

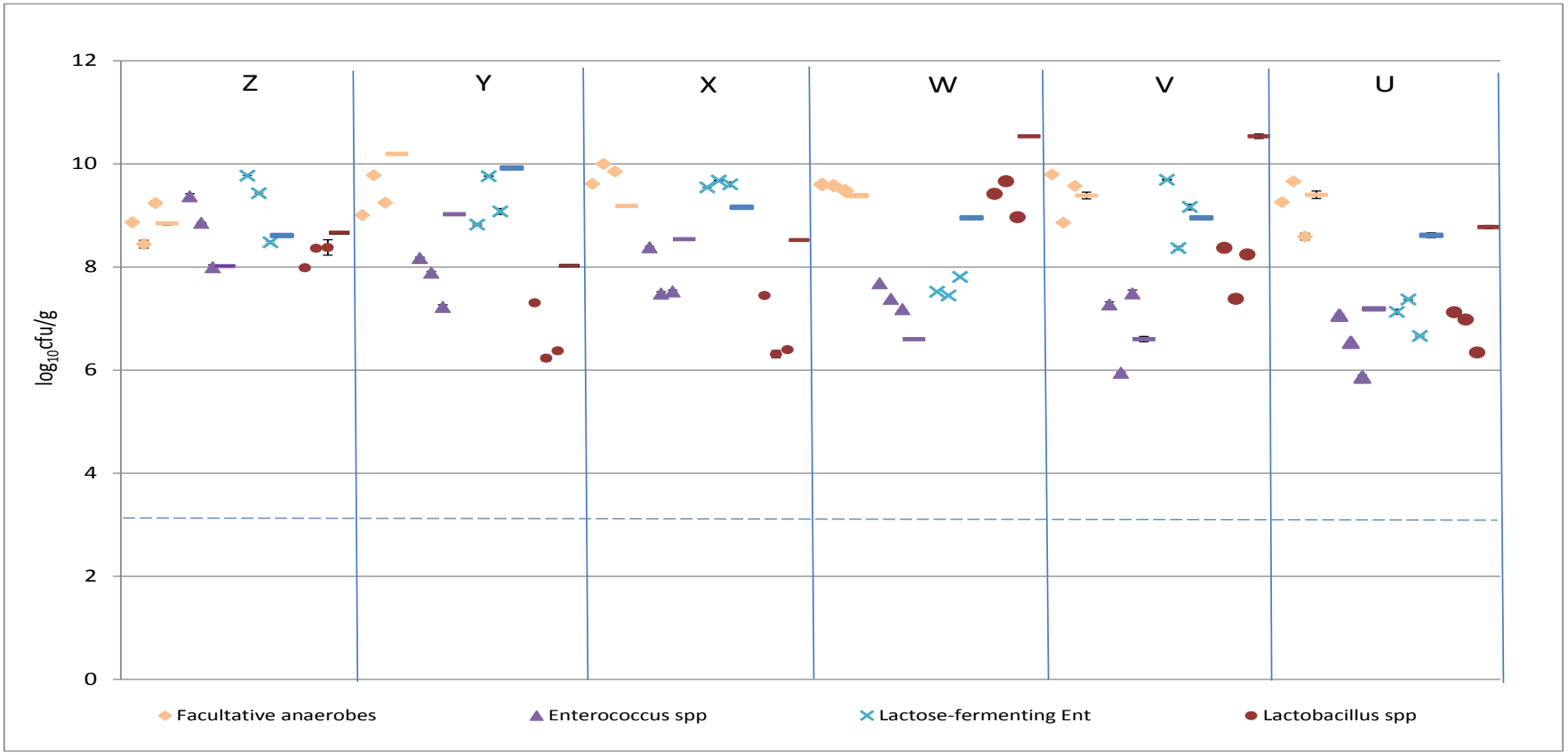

Figure 8.3.7: Sessile (and planktonic) facultative anaerobic microbiota populations (±SE) from rod/sampling points Z-U. Planktonic populations of each bacterial groups (log_{10}cfu/g) present at each time point are represented by a line in the appropriate colour; dashed line, approximate limit of detection.

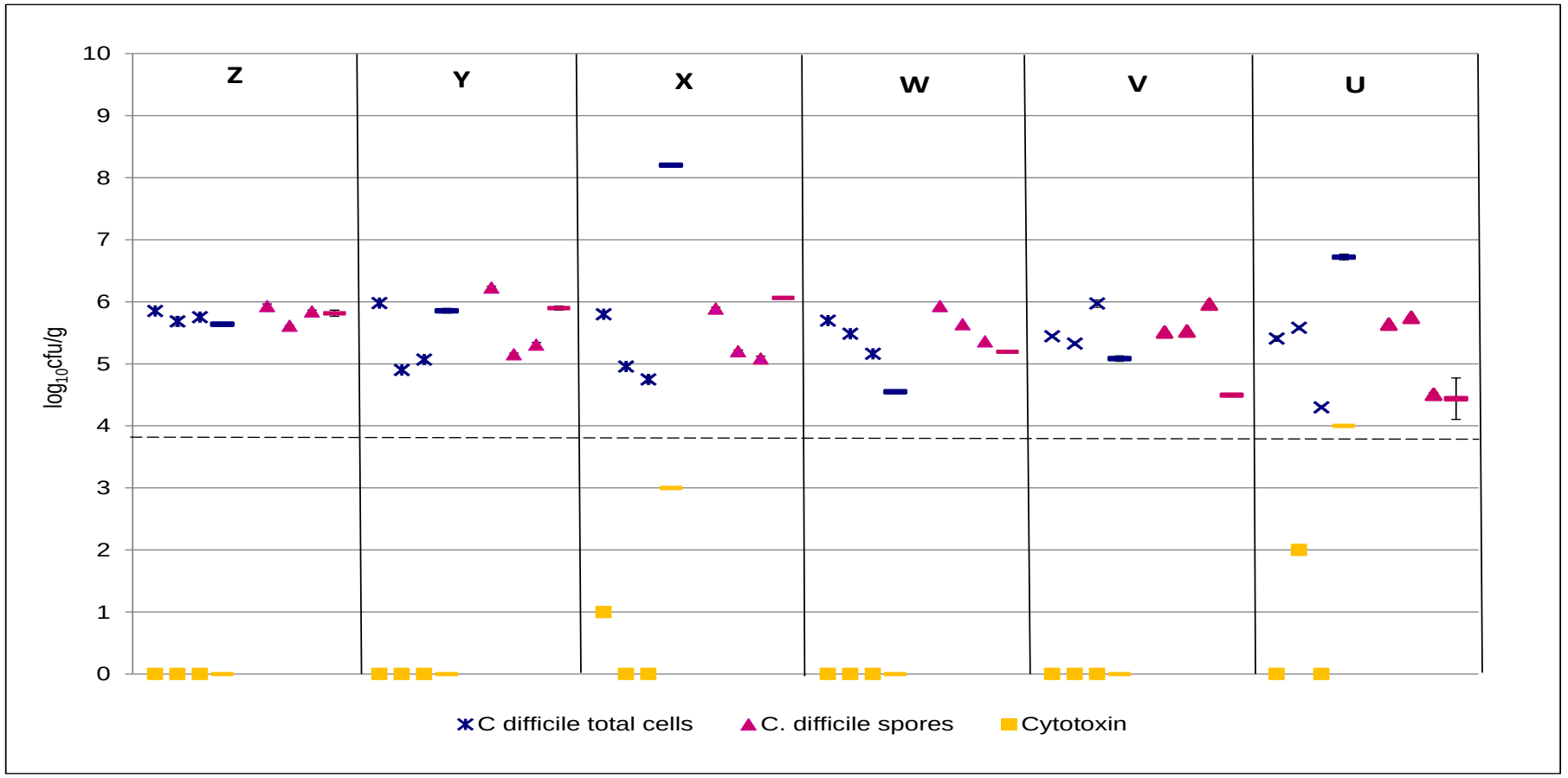

Figure 8.3.8: Sessile *C. difficile* populations (±SE) from rod/biofilm sampling points Z-U within the triple biofilm human gut model. Planktonic populations of each bacterial groups (log_{10}cfu/g) present at each time point are represented by a line in the appropriate colour.

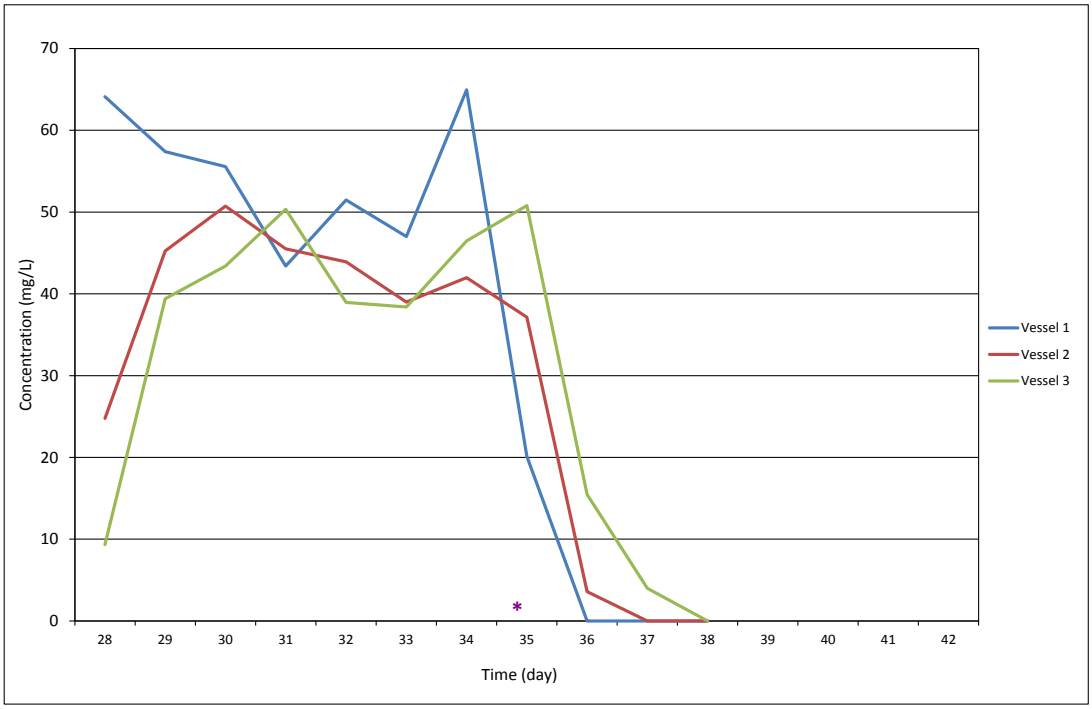

Figure 8.3.9: Concentration (mg/L) of clindamycin within the planktonic culture fluid of the biofilm gut model. * Sessile clindamycin antimicrobial activity not detected.

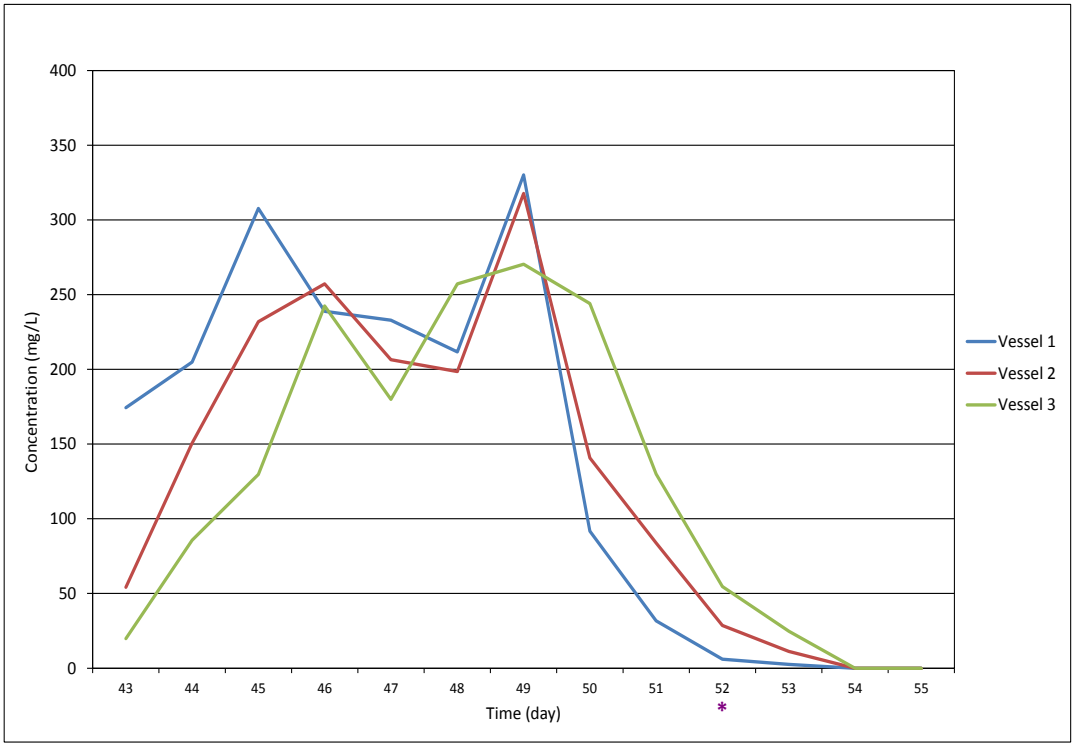

Figure 8.3.10: Concentration (mg/L) of vancomycin within the planktonic culture fluid of the biofilm gut model. * Sessile vancomycin concentration data also available (figure 8.3.11).

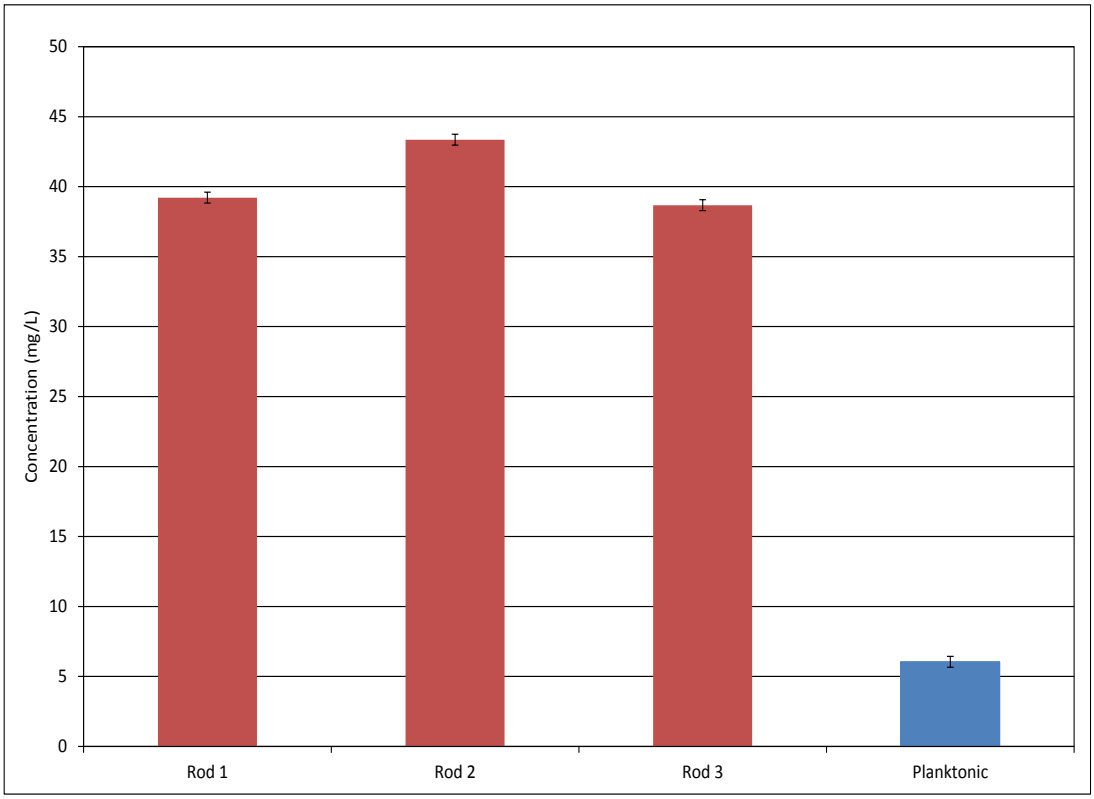

Figure 8.3.11: Concentration (mg/L) of vancomycin (±SE) within biofilm structures on 3 rods at time point W (day 52).

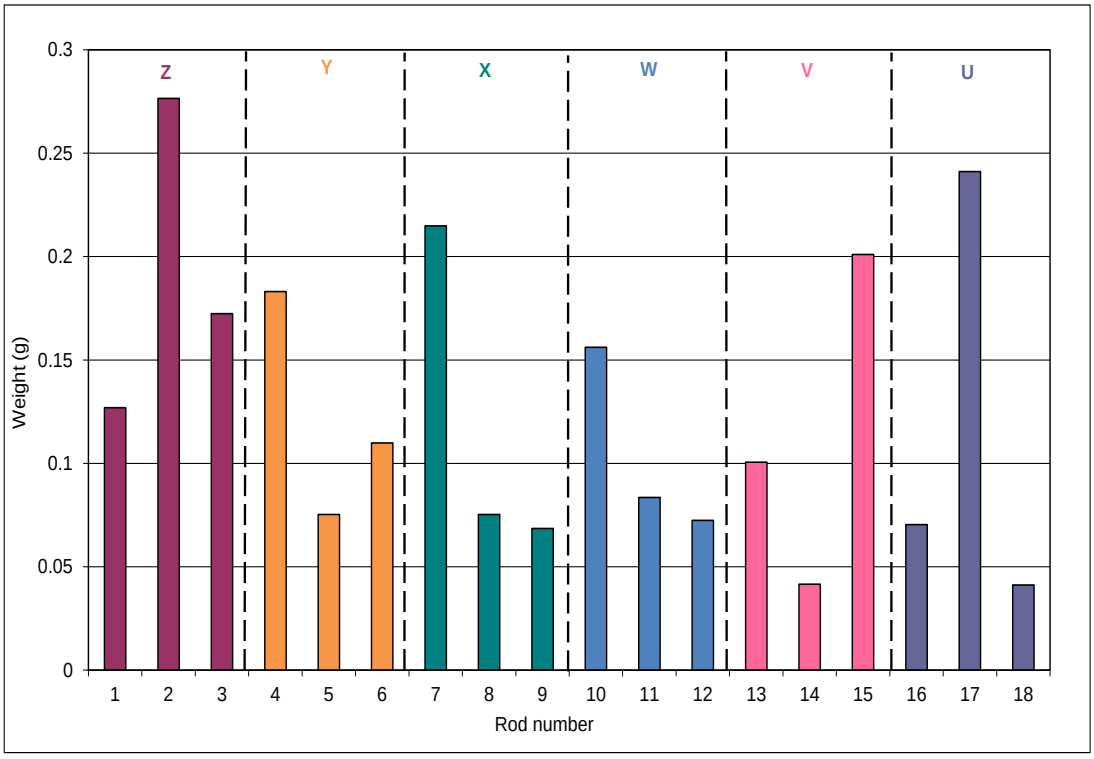

Figure 8.3.12: Pellet weight of 1mL of re-suspended biofilm within the triple stage biofilm human gut model at time points Z-U.

8.4 Discussion

Recurrence of simulated CDI after initial successful vancomycin treatment has previously been observed within the original gut model. Biofilm communities are known to play a role within other chronic infections, such as chronic otitis media [429] and periodontitis [580]. It was therefore hypothesised that biofilm structures within the gut model may play a role in the recurrence of symptomatic CDI.

The original gut model utilises a well established experimental design which has been maintained for this study. In addition, biofilm sampling points were introduced at key times. Due to the finite number of rods within the vessel and precautions taken to minimise sessile population bias, a maximum of six biofilm time points were included. Rod sample point Z was taken after the initial *C. difficile* spore inoculation (day 27, period B) to demonstrate recruitment of *C. difficile* into biofilm structures. Previous vreproducibility experiments (chapter 7.0), highlighted the mature nature of rod-associated biofilms after 21 days, therefore providing a well established biofilm to facilitate *C. difficile* recruitment. Rod sample point Y was chosen after completion of a clindamycin dosing regimen to provide information on the effect of administration of this antimicrobial on sessile gut microbiota populations. A third rod sample point, X was chosen during simulated planktonic CDI to determine the behaviour of sessile *C. difficile* during this key period of disease. Upon successful treatment (elicited by vancomycin, period F), rod sampling (W) was carried out to determine whether successful treatment was also evident within biofilms. Sample points V and U were designed to provide information on the possible recurrence of CDI.

Continuous culture systems, such as the one described here, operate under a controlled flow rate (f=13.2mL/hr, in this study), thus allowing bacterial growth to be maintained at a steady state. Within the gut model

experiments described here period A is designed to allow populations to reach this steady state, after which interventions may be made. Differences in bacterial growth phase (*i.e.* exponential versus stationary) will affect the dynamics of the culture vessel. Whilst all efforts are taken to ensure that bacterial populations reach steady state, slight fluctuations (≤ 1 log_{10}cfu/mL) were evident within period A of this experiment (figures 8.3.1 and 8.3.2). This may be due to inherent variation in the bacterial enumeration protocol.

In the absence of antimicrobial intervention (period B), sessile and planktonic gut microbiota and *C. difficile* behaved in a similar manner. Planktonic populations of obligate species were marginally greater than sessile populations, whilst sessile facultative populations were greater than planktonic facultative species. A similar trend has previously been observed within the biofilm gut model (chapter 7.0) and biofilm analysis (chapter 4.0) experiments. This is possibly mediated by experimental methods and increased aerobic handling time required to process samples for this experiment. Alternatively, the presence of these rods increases the surface area of rod-adherent bacteria exposed to the liquid-air interface. It is possible that this area of the vessel is less anaerobic than submerged areas, possibly eliciting the increased adherence of facultative species. However, similar observations have been noted by other groups[279, 446].

Planktonic gut microbiota populations within the model behaved in response to clindamycin as observed previously[272, 515, 525], with a notable deleterious effect on *Bifidobacterium* spp. and more modest declines in *B. fragilis* group and *Clostridium* spp. Similar declines in these groups were also evident in sessile communities. However, although planktonic *Bifidobacterium* spp. were below the LOD, sessile communities were still detected at 3.9 log_{10}cfu/g. At biofilm sampling point Y (period D), planktonic *B. fragilis* group and *Clostridium* spp. had recovered to pre-clindamycin levels. However, sessile populations of these groups

remained at reduced levels. These differences in behaviour of sessile and planktonic gut microbiota populations suggests that clindamycin elicits a similar effect on both communities, although the effect and recovery of sessile populations may be delayed compared with planktonic populations. Reduced susceptibility of biofilms to antimicrobial agents is a well defined characteristic of sessile communities[399, 581]. To date, little work exists investigating the exposure of mixed-species intestinal biofilms to antimicrobial agents, with the majority of groups focussing on simple single species biofilms[399].

Clindamycin successfully induced planktonic *C. difficile* germination, proliferation and toxin production. Simulated planktonic CDI was evident, five days after cessation of clindamycin dosing, whilst gut microbiota remained perturbed. Clindamycin demonstrates an *in vitro* activity against vegetative *C. difficile* (PCR ribotype 027 planktonic MIC 1 mg/L), potentially preventing germination until sub-MIC levels remained within the system. This was achieved four days after dosing cessation within vessel 3.

Behaviour of *C. difficile* within planktonic communities was as previously observed[272, 525]. However, distinct differences between the planktonic and biofilm modes of growth were evident, with sessile *C. difficile* communities remaining in spore form, a characteristic observed previously in biofilm gut model reproducibility experiments (chapter 7.0) and biofilm analysis (chapter 4.0) experiments. Mechanisms and conditions necessary to induce CDI remain to be fully elucidated. CDI is frequently associated with the use of antimicrobial agents, leading to the assumption that the disruption of the gut microbiota may play a role in the pathogenesis of *C. difficile*. Clindamycin-induced perturbation of planktonic gut microbiota is evident within the gut model. Instillation of spores concurrent with administration of antimicrobial agents leads to CDI, whilst this is not the case in the absence of antimicrobial administration. This gut microbiota disruption was also

evident within sessile communities but did not elicit germination and proliferation of sessile spores. At biofilm sample point W (day 52), clindamycin was detected within planktonic fluid at a level of 50.8 mg/L. However, within biofilm structures no clindamycin activity was detected. Despite the absence of detectable clindamycin within the biofilm, antimicrobial disruption of sessile communities appears evident.

Studies on exposure of *S. aureus*[582] and *Propionibacterium acnes*[583] biofilms to clindamycin highlight the planktonic MIC/sessile MBEC values as 0.25/>128 mg/L and 0.125/512 mg/L, respectively, indicating the increased resistance of sessile organisms to antimicrobial administration compared with planktonic populations. Another study reported biofilm-associated cell survival after clindamycin exposure as 20-99 %[584]. This highlights the complex nature of the biofilm mode of growth.

Numerous microenvironments exist within biofilms that differ with respect to pH, oxygen concentration, nutrient availability, and cell density. This results in heterogeneity in metabolic and reproductive activity among cells located in different parts of the biofilm. Initial treatment often effectively kills bacteria on the outer margins of the biofilm, whilst metabolically inactive cells located in the interior of the biofilm may be resistant to the actions of antimicrobial agents that target actively growing cells[415]. *Bifidobacterium* spp. and *B. fragilis* group, which demonstrated a susceptibility to antimicrobial administration, may localise on the outer margins of the biofilm, leaving them susceptible to clindamycin action. *C. difficile* spores, which did not demonstrate a response to clindamycin instillation or perturbation of gut microbiota, may reside within a heavily protected portion of the biofilm. Furthermore, the release and detection of germinants that are required for efficient germination may have been prevented from accessing the spores.

Following planktonic *C. difficile* germination, proliferation and toxin production, planktonic *Bifidobacterium* spp. populations began to recover to pre-clindamycin levels, although this was at a greater rate than sessile recovery, providing further evidence for the delayed reaction of sessile compared with planktonic communities. This is potentially due to the delayed action of antimicrobial agents on sessile communities. The increase in biofilm populations is likely mediated by recruitment of planktonic cells into these structures rather than the active proliferation of sessile populations due to the inherent dormant, slow-growing nature of these communities. Recruitment of planktonic cells requires the planktonic population to increase in number to then facilitate transfer to the biofilm mode of growth.

Vancomycin is a first line option for CDI treatment, and has been utilised as a treatment option on numerous occasions within the original gut model, therefore is the most useful agent to use in this study. Planktonic *C. difficile* viable counts declined rapidly and re-converged with spore counts 2 days after vancomycin instillation, with cytotoxin reduced to undetectable levels after five days. Sessile *C. difficile,* which remained as spores, were not affected by vancomycin instillation, potentially due to the absence of anti-spore activity of vancomycin. Vancomycin instillation elicited a marked deleterious effect on planktonic *B. fragilis* group and *Bifidobacterium* spp. and an increase in *Lactobacillus* spp., as previously observed within the gut model[272, 525]. *Clostridium* spp. levels were sporadic, a trend often observed with this bacteria group. Similar declines and increases in sessile communities were also observed during periods W and V, demonstrating the proficient effect of vancomycin upon sessile populations. Delay in the response of sessile communities to vancomycin instillation was not evident at time point W. This may be caused by the increased length of time of biofilm analysis following vancomycin cessation (+ 3 days), whereas time

point Y was one day after clindamycin instillation ceased. Alternatively, it has been reported that vancomycin displays a more profound action against sessile communities compared with clindamycin. Vancomycin and clindamycin displayed an 81 and 64% kill rate against sessile *S. aureus*, respectively[584].

Vancomycin activity within the rod-associated biofilm structures at time point W averaged at ~40 mg/L, demonstrating the penetration of this agent within the biofilm structures. This level is approximate to the *in vitro* MIC (16-32 mg/L) of vancomycin to *B. fragilis* group, providing the potential of antimicrobial activity of vancomycin on sessile *B. fragilis* organisms, as observed within this experiment. Successful penetration of vancomycin into biofilm structures has previously been reported. Exposure of *S. epidermidis* biofilms to increasing concentrations of vancomycin elicited increased vancomycin detection within biofilms[585]. As concentration of vancomycin within biofilms increased, the number of viable sessile bacteria decreased. Furthermore, an increased concentration of vancomycin was detected within biofilms compared to the surrounding incubating medium. The authors postulated that this is potentially mediated by the biofilm matrix trapping and concentrating vancomycin molecules in a manner similar to that used to trap and concentrate nutrients. Within this study, increased levels of vancomycin were also evident within biofilm structures compared with planktonic fluid.

Vancomycin treatment of planktonic simulated CDI was initially successful with *C. difficile* populations remaining as spores post-treatment. Recurrence of disease was evident 14-16 days after vancomycin cessation, with an increase in *C. difficile* viable counts and toxin. Sessile *C. difficile* populations remained in spore form. Sessile population levels were maintained at ~5 $\log_{10}$cfu/g from time point Z through to U, despite fluctuations in planktonic populations, demonstrating the highly stable nature of sessile

C. difficile populations. Recurrence following vancomycin instillation within the original gut model has previously been observed[515, 586], but not always[474, 512, 525].

Sub-inhibitory levels of vancomycin promote increased *S. epidermidis* biofilm density [587,588]. It is postulated that exposure of low concentrations of vancomycin may affect expression of genes involved in biofilm production, providing a means by which bacteria protect themselves from antimicrobials. Studies involving *C. difficile* biofilms demonstrate that exposure to supra-MIC levels (and to lesser extent sub-MIC levels) of vancomycin over three days induced biofilms formation [454]. However, biofilm pellet weights (figure 8.3.12) post-vancomycin exposure (time point W) did not display increased biomass compared within other time points.

Early signs of recurrence were evident between days 63 - 68. However, at this point most gut microbiota populations had recovered to pre-dosing levels. *Bifidobacterium* spp. levels began to recover, reaching populations of 4 - 4.5 $\log_{10}$cfu/g between days 63 - 64 in vessels 2 and 3 respectively. Despite recovery of gut microbiota, CDI recurrence was evident, suggesting recurrence is a complex process not only reliant on colonisation resistance of the gut microbiota.

Biofilm dispersal mechanisms are important factors for microbial survival, allowing single organisms or biofilm aggregates to colonise new niches[371, 372]. Many factors are thought to mediate this dispersal including regulatory systems (*e.g.* quorum sensing)[364], active dispersal mechanisms (*e.g.* matrix degrading enzymes)[577] and changes in nutrient levels[589]. Various dispersal mechanisms are in continued operation within the biofilm lifecycle. The persistence of a stable population of *C. difficile* spores within biofilms was observed in this study. Within *B. subtilis,* gene expression is described as a dynamic process during biofilm development. Cells expressing certain genes localised at distinct regions of a biofilm, with spores located at upper

aerial structures[434]. This provides an ideal nidus for *B. subtilis* spores and their seeding into the surrounding environment. *B. subtilis* and *C. difficile* sporulation (and potentially biofilm formation) are regulated by Spo0A, of which they share 56% amino acid homology. *C. difficile* may potentially display similar cellular expression pathways and spatial biofilm architecture.

Deakin et al[163] demonstrated that Spo0A is required for recurrence of CDI within a murine model. Vancomycin-treated mice, after initial treatment success, suffered multiple episodes of recurrent infection in those mice infected with wild-type strains but not those with *spo0A* mutations, indicating that spores are a persistence and transmission factor. Interestingly, wild type *C. difficile* was not detected in the intestinal tract of mice receiving vancomycin therapy, but was detected within environmental sites. Clearly this study is in contrast to the persistence of *C. difficile* spores outlined within the *in vitro* biofilm gut model. Differences between the two model systems exist, in particular pertaining to gut microbiota composition, highlighting the complexity of recurrent infection and the need to investigate the process further.

9.0 Conclusions

Recurrent CDI is a major problem in healthcare facilities worldwide and gaining a greater understanding of the reasons behind treatment failure and recurrent disease is invaluable in reducing this burden[249]. Biofilms have been identified as causing chronic infections[430] and our knowledge of the existence of multispecies biofilms on mucosal surfaces, including the gastrointestinal tract[294] provide evidence that the existence of these structures may play a role in recurrent CDI. Analysis and evaluation of mucosal biofilms *in vivo* is difficult due to the physical inaccessibility of this area in healthy patients. Therefore, this project was designed to develop and characterise an *in vitro* model of the planktonic and biofilm communities of the human colon, providing an opportunity to study the role that biofilms may play in recurrent CDI.

Various *in vitro* model designs were evaluated in this study. The reliable formation of biofilms which could be sampled for extended periods was a key aim of this project. The use of MA beads proved unsuccessful due to bacterial-mediated degradation of this substratum material. Glass beads provided the longevity required for the project, although the formation of mature biofilms was absent. Observation of increased biofilm biomass at the solid/liquid/air interface lead to the incorporation of glass rods into the vessel design. This model design was validated for the reliable formation and consistent populations of bacterial groups across all rods.

The original human gut model was initially validated against the intestinal contents of sudden death victims and subsequently evaluated to study CDI[98]. The redesigned biofilm model maintains this basic model design, providing validated information on the planktonic communities within the model. The redesigned model provides preliminary validation work on the

biofilm structures within the system; however, validation against the mucosal biofilm communities of intestinal contents from sudden death victims was not feasible during this study. Separate studies investigating the intestinal mucosal biopsy samples display similarities between sessile communities present within the biofilm gut model[292, 294, 563], proving a degree of confidence in the results obtained in the present study. Limitations in the model system are acknowledged; the system is unable to reflect the immunological and secretory processes observed *in vivo*. Also, the 18 rods facilitating biofilm formation are unable to reflect the large surface area of the mucosal surface of the human colon accurately.

Intestinal planktonic populations within the redesigned gut model were also present in sessile form during steady state periods, with planktonic populations displaying increased obligate anaerobic populations compared with sessile populations and the converse true for facultative anaerobes. Instillation of antimicrobial agents elicited a rapid effect on planktonic gut microbiota populations. A deleterious effect was also observed against sessile populations, although they demonstrated delayed reaction to, and recovery from, antimicrobial administration. This was potentially mediated by reduced antimicrobial penetration through the biofilm matrix or reduced efficacy against the slow growing sessile mode of growth[409, 411].

The reduced susceptibility of sessile bacteria to antimicrobial agents has previously been reported[358, 399], although many conflicting reports exist[400, 590]. Many researchers use simple CBD experiments to determine this effect, exposing sessile and planktonic communities to antimicrobial agents separately at a single time point. Results from this project indicate that sessile communities display delayed response to antimicrobial exposure. Appropriately designed CBD experiments using multiple time points may demonstrate a similar observation, possibly explaining the conflicting results obtained by researchers to date.

Simple batch culture microtiter tray-associated *C. difficile* biofilm formation is highly variable and inconsistent and appears to be dependent on incubation time. Characterisation of complex mixed-species biofilms within the continous original gut model system provided useful preliminary information on the existence of *C. difficile* vegetative cells, spores and cytotoxin within mature biofilm structures. The behaviour of *C. difficile* within this continuous system was variable, potentially mediated by previous and current planktonic behaviours which differ due to differences in complex experimental designs.

Attempts to screen the pure culture biofilm forming abilities of a panel of *C. difficile* isolates on abiotic surfaces provided inconsistent results. Positive biofilm formation was obtained, although the degree of biofilm biomass varied between repeat experiments under the same conditions. Furthermore, incubation time and media appeared to affect results, as observed by other groups[454].

Differing conditions within the original gut model appeared to affect behaviour of sessile *C. difficile,* with differences observed in sessile properties between vessels 1, and 2 and 3. This behaviour does not appear to be restricted to sessile populations, with planktonic *C. difficile* demonstrating variable behaviours, particularly in vessel 1 of the model. Vessel 1 is a high substrate environment with a low pH and elicits greatest biofilm formation. Nutrient level and composition, bacterial population density and pH may mediate the variable behaviour of both planktonic and sessile *C. difficile.* In addition, gut microbiota populations, notably planktonic *B. fragilis* group demonstrate distinct population differences in vessel 1 compared with vessels 2 and 3.

Sessile *C. difficile* often possess increased populations of spores compared with planktonic populations within the same vessel, an observation noted

during analysis of vessel wall- and rod-adherent biofilms within the gut model, as well as by other groups[455, 457]. Vegetative forms have been observed within mature mixed-species biofilms structures in this study and pure culture structures by other researchers[355, 454]. It is postulated that both biofilm formation and sporulation pathways of *C. difficile* are regulated by Spo0A, as observed in *B subtilis*[529, 591], possibly mediating this observation.

Use of the redesigned biofilm gut model allows the biofilm mode of growth of *C. difficile* to be monitored at distinct phases of CDI, with sessile *C. difficile* remaining in dormant spore form for the duration of the experimental design. Biofilm analysis work (chapter 4.0) analysed biofilm structures at only a single time point. However, experimental designs of each of these experiments were diverse, providing information on the sessile mode of growth of *C. difficile* after successful treatment, during recurrence, after and during initial CDI simulation. Collectively the information obtained in these biofilm analysis experiments provides information on the biofilm mode of growth of *C. difficile* at these distinct time points. Whilst increased levels of spores were often observed within biofilm compared with planktonic phases in these experiments, this behaviour was more consistent within the biofilm redesign model.

Sessile *C. difficile* are known to exist in both spore and vegetative form. The work presented here does not provide information on whether sessile spores demonstrate and ability to germinate into vegetative form or whether vegetative cells from the planktonic fluid were recruited into the biofilm.

The maintenance of a dormant *C. difficile* spore state within the redesigned biofilm model, but presence of low levels of biofilm-associated toxin, and high levels of planktonic toxin, indicates the active sequestration of planktonic-associated toxin into the biofilm. Mucosal biofilms potentially cover toxin receptors; therefore the presence of toxin within these structures possibly mediates the localisation of toxin in close proximity to receptors.

However, persistence of biofilm-associated toxin was not prolonged and at low levels, suggesting a minimal impact on contribution to disease. However, the presence of pseudomembranous legions on the mucosal surface *in vivo* suggests that the action of toxins is evident at this site. It is possible that disruption of the mucosal biofilm, possibly by antimicrobial therapy, allows access of toxins to the mucosal epithelial and their receptors. Alternatively, extensive mucosal biofilms *in vivo* may facilitate the sequestration of toxin at concentrations greater than those obsesrved in this study.

Removal of mature biofilms from the *in vitro* gut model demonstrated a profound persistence of some antimicrobial agents (fidaxomicin and oritavancin), but not others (clindamycin and co-amoxiclav). Mechanisms of persistence were not determined from this study, but indicate variations in structure and properties of antimicrobial agents. Interestingly, fidaxomicin and oritavancin both displayed an apparent anti-spore activity, demonstrated by sporadic detection of spores within the original gut model and adherence of these agents to spores, which is postulated to prevent the outgrowth of vegetative cells[515, 522, 527, 547]. Persistence of these agents for prolonged periods within biofilms, in close proximity to spores, may elicit an advantageous pharmacodynamic property, thus preventing germination of these spores into vegetative form. Such properties may be of focus for development of novel treatment options. Persistence of *C. difficile* spores within biofilm structures in the redesigned gut model may have implications *in vivo.* Detachment processes associated with the biofilm lifecycle may possibly mediate the seeding of these spores into the colonic lumen. Once antimicrobial therapy has ceased, if conditions are favourable, these spores may germinate into their vegetative form, proliferate and release toxin, leading to recurrence of symptomatic disease.

The biofilm human gut model identifies the presence and characterises the behaviour of *C. difficile* during different disease stages, indicating the importance of biofilms in CDI. The biofilm mode of growth of *C. difficile* is a complex, multifactorial lifestyle, which remains to be fully elucidated. Data presented in this study and by other[355, 454, 457, 592] provide preliminary information within this field. Recurrent CDI is a major problem for healthcare facilities worldwide, with rates of recurrence of ~20%[243]. This project identifies the potential role of biofilms in recurrence of CDI, necessitating the need for further work to understand the role that these biofilm structures may play in CDI and recurrent infection fully, potentially proving the opportunity to analyse the efficacy of novel CDI treatment therapies on sessile, in addition to planktonic communities. Furthermore, utilisation of this model system to investigate other parameters of intestinal biofilms is possible. Additional validation in the form of a comparative study on biofilm communities in healthy human subjects with biofilm populations within the biofilm gut model would provide a further level of confidence in previous and future results.

List of References

1. Hall IC, O'Toole E. Intestinal flora in new-borin infants - With a description of a new pathogenic anaerobe, *Bacillus difficilis*. *American Journal of Diseases of Children* 1935; **49**: 390-402.
2. Snyder ML. Further studies on *Bacillus difficilis* (Hall and O'Toole). *Journal of Infectious Diseases* 1937; **60**: 223-31.
3. Finney JMT. Gastroenterostomy for cicatrizing ulcer of the pylorus. *John Hopkins Hospital Bulletin* 1893; **4**: 53-5.
4. Bartlett JG, Chang, T.W., Gurwith, M., Gorbach, S.L., and Onderdonk, A.B. Antibiotic-associated pseudomembranous colitis due to toxin-producing clostridia. *New England Journal of Medicine* 1978; **298**: 531-4.
5. Bartlett JG, Onderdonk, A.B., Cisneros, R.L. and Kasper, D.L. Clindamycin-associated colitis due to a toxin-producing species of *Clostridium* in hamsters. *Journal of Infectious Diseases* 1977; **136**: 701-5.
6. Larson HE, Parry JV, Price AB et al. Undescribed toxin in pseudomembranous colitis. *British Medical Journal* 1977; **1**: 1246-8.
7. Larson HE, Price AB. Pseudomembranous colitis: Presence of clostridial toxin. *Lancet* 1977; **2**: 1312-4.
8. Rifkin GD, Fekety FR, Silva J, Jr. Antibiotic-induced colitis implication of a toxin neutralised by *Clostridium sordellii* antitoxin. *Lancet* 1977; **2**: 1103-6.
9. George RH, Symonds JM, Dimock F *et a*l. Identification of *Clostridium difficile* as a cause of pseudomembranous colitis. *British Medical Journal* 1978; **1**: 695.
10. George WL, Sutter VL, Goldstein EJ *et al*. Aetiology of antimicrobial-agent-associated colitis. *Lancet* 1978; **1**: 802-3.
11. Bartlett JG, Chang T, Taylor NS et al. Colitis induced by *Clostridium difficile. Reviews of Infectious Diseases* 1979; **1**: 370-8.
12. Guerrero DM, Nerandzic MM, Jury LA *et al.* Acquisition of spores on gloved hands after contact with the skin of patients with *Clostridium difficile* infection and with environmental surfaces in their rooms. *American Journal of Infection Control* 2012; **40**: 556-8.
13. Riggs MM, Sethi AK, Zabarsky TF *et al.* Asymptomatic carriers are a potential source for transmission of epidemic and nonepidemic *Clostridium difficile* strains among long-term care facility residents. *Clinical Infectious Diseases* 2007; **45**: 992-8.
14. Kim KH, Fekety R, Batts DH *et a*l. Isolation of *Clostridium difficile* from the environment and contacts of patients with antibiotic-associated colitis. *Journal of Infectious Diseases* 1981; **143**: 42-50.
15. Hurley BW, Nguyen CC. The spectrum of pseudomembranous enterocolitis and antibiotic-associated diarrhea. *Archives of Internal Medicine* 2002; **162**: 2177-84.
16. Bouza E, Munoz P, Alonso R. Clinical manifestations, treatment and control of infections caused by *Clostridium difficile. Clinical Microbiology and Infection* 2005; **11 Suppl 4**: 57-64.
17. Bolton RP, Tait SK, Dear PR *et al*. Asymptomatic neonatal colonisation by *Clostridium difficile*. *Archives of Disease in Childhood* 1984; **59**: 466-72.

18. Bartlett JG. Management of *Clostridium difficile* infection and other antibiotic-associated diarrhoeas. *European Journal of Gastroenterology & Hepatology* 1996; **8**: 1054-61.
19. Olson MM, Shanholtzer CJ, Lee JT, Jr. *et al*. Ten years of prospective *Clostridium difficile*-associated disease surveillance and treatment at the Minneapolis VA Medical Center, 1982-1991. *Infection Control and Hospital Epidemiology* 1994; **15**: 371-81.
20. Bartlett JG. Leukocytosis and *Clostridium difficile*-associated diarrhea. *American Journal of Gastroenterology* 2000; **95**: 3023-4.
21. Johnson S, Kent SA, O'Leary KJ *et al*. Fatal pseudomembranous colitis associated with a variant *clostridium difficile* strain not detected by toxin A immunoassay. *Annals of Internal Medicine* 2001; **135**: 434-8.
22. Sayedy L, Kothari D, Richards RJ. Toxic megacolon associated *Clostridium difficile* colitis. *World Journal of Gastrointestinal Endoscopy* 2010; **2**: 293-7.
23. Borriello SP, Barclay FE. An in-vitro model of colonisation resistance to *Clostridium difficile* infection. *Journal of MedicalMmicrobiology* 1986; **21**: 299-309.
24. Kyne L, Warny M, Qamar A *et al*. Asymptomatic carriage of *Clostridium difficile* and serum levels of IgG antibody against toxin A. *The New England Journal of Medicine* 2000; **342**: 390-7.
25. Jangi S, Lamont JT. Asymptomatic colonization by *Clostridium difficile* in infants: implications for disease in later life. *Journal of Pediatric Gastroenterology and Nutrition* 2010; **51**: 2-7.
26. Rousseau C, Lemee L, Le Monnier A *et al*. Prevalence and diversity of *Clostridium difficile* strains in infants. *Journal of Medical Microbiology* 2011; **60**: 1112-8.
27. Niyogi SK, Dutta D, Bhattacharya MK *et al*. Frequency of isolation of toxigenic *Clostridium difficile* from healthy adults. *The Indian Journal of Medical Research* 1997; **106**: 497-9.
28. Janezic S, Ocepek M, Zidaric V *et al*. *Clostridium difficile* genotypes other than ribotype 078 that are prevalent among human, animal and environmental isolates. *BMC Microbiology* 2012; **12**: 48.
29. Kyne L, Warny M, Qamar A *et al.* Asymptomatic carriage of *Clostridium difficile* and serum levels of IgG antibody against toxin A. *New England Journal of Medicine* 2000; **342**: 390-7.
30. Bobulsky GS, Al-Nassir WN, Riggs MM *et al*. *Clostridium difficile* skin contamination in patients with C. difficile-associated disease. *Clinical infectious diseases : an official publication of the Infectious Diseases Society of America* 2008; **46**: 447-50.
31. Riggs MM, Sethi AK, Zabarsky TF *et al.* Asymptomatic carriers are a potential source for transmission of epidemic and nonepidemic *Clostridium difficile* strains among long-term care facility residents. *Clinical infectious diseases : an official publication of the Infectious Diseases Society of America* 2007; **45**: 992-8.
32. Sorg JA, Sonenshein AL. Bile salts and glycine as cogerminants for *Clostridium difficile* spores. *Journal of Bacteriology* 2008; **190**: 2505-12.
33. Grant CCR, Konkel ME, Cieplak W *et al*. Role of Flagella in Adherence, internalization, and translocation of *Campylobacter jejuni* in

nonpolarized and polarized epithelial-cell cultures. *Infecttion and Immunity* 1993; **61**: 1764-71.
34. Vollaard EJ, Clasener HAL. Colonization Resistance. *Antimicrobial Agents and Chemotherapy* 1994; **38**: 409-14.
35. Hecht G, Pothoulakis C, Lamont JT *et al. Clostridium-difficile* toxin-a perturbs cytoskeletal structure and tight junction permeability of cultured human intestinal epithelial monolayers. *Journal of Clinical Investigation* 1988; **82**: 1516-24.
36. Shen A. *Clostridium difficile* toxins: mediators of inflammation. *Journalof Innate Immuninty* 2012; **4**: 149-58.
37. Larson HE, Price AB, Borriello SP. Epidemiology of experimental enterocecitis due to *Clostridium difficile*. *The Journal of Infectious Diseases* 1980; **142**: 408-13.
38. de Vries-Hospers HG, Welling GW, Swabb EA *et al*. Selective decontamination of the digestive tract with aztreonam: a study of 10 healthy volunteers. *Journal of Infectious Diseases* 1984; **150**: 636-42.
39. Hazenberg MP, Pennock-Schroder AM, Van den Boom M *et al.* Binding to and antibacterial effect of ampicillin, neomycin and polymyxin B on human faeces. The *Journal of Hygiene (London)* 1984; **93**: 27-34.
40. Rao A, Jump RL, Pultz NJ *et al*. In vitro killing of nosocomial pathogens by acid and acidified nitrite. *Antimicrobial Agents Chemother* 2006; **50**: 3901-4.
41. Owens RC, Jr., Donskey CJ, Gaynes RP *et al*. Antimicrobial-associated risk factors for *Clostridium difficile* infection. *Clinical infectious diseases : an official publication of the Infectious Diseases Society of America* 2008; **46 Suppl 1**: S19-31.
42. de Lalla F, Privitera G, Ortisi G *et al*. Third generation cephalosporins as a risk factor for *Clostridium difficile*-associated disease: a four-year survey in a general hospital. *The Journal of Antimicrobial Chemotherapy* 1989; **23**: 623-31.
43. Spencer RC. The role of antimicrobial agents in the aetiology of *Clostridium difficile*-associated disease. *The Journal of Antimicrobial Chemotherapy* 1998; **41 Suppl C**: 21-7.
44. Pepin J, Saheb N, Coulombe MA *et al*. Emergence of fluoroquinolones as the predominant risk factor for *Clostridium difficile*-associated diarrhea: a cohort study during an epidemic in Quebec. *Clinical infectious diseases : an official publication of the Infectious Diseases Society of America* 2005; **41**: 1254-60.
45. HPA. *Clostridium difficile* ribotyping network (CDRN) for England and Northern Ireland 2009/10 report. *http://wwwhpaorguk/web/HPAwebFile/HPAweb_C/1296681523205*. (7 August 2013, date last accessed).
46. McFarland LV, Surawicz CM, Rubin M *et al*. Recurrent *Clostridium difficile* disease: epidemiology and clinical characteristics. *Infection Control and Hospital Epidemiology* 1999; **20**: 43-50.
47. Cunningham R, Dale B, Undy B *et al.* Proton pump inhibitors as a risk factor for *Clostridium difficile* diarrhoea. *Jourmal of Hospital Infection* 2003; **54**: 243-5.

48. Brown E, Talbot GH, Axelrod P *et al.* Risk factors for *Clostridium difficile* toxin-associated diarrhea. *Infection Control and Hospital Epidemiology* 1990; **11**: 283-90.
49. Bignardi GE. Risk factors for *Clostridium difficile* infection. *Journal of Hospital Infection* 1998; **40**: 1-15.
50. Klingler PJ, Metzger PP, Seelig MH *et al. Clostridium difficile* infection: risk factors, medical and surgical management. *Digestive Diseases* 2000; **18**: 147-60.
51. Kyne L, Sougioultzis S, McFarland LV *et al*. Underlying disease severity as a major risk factor for nosocomial *Clostridium difficile* diarrhea. *Infection Control and Hospital Epidemiology* 2002; **23**: 653-9.
52. Vesteinsdottir I, Gudlaugsdottir S, Einarsdottir R *et al.* Risk factors for *Clostridium difficile* toxin-positive diarrhea: a population-based prospective case-control study. *European Journal of Clinical Microbiology and Infectious Diseases* 2012; **31**: 2601-10.
53. Sullivan NM, Pellett S, Wilkins TD. Purification and characterization of toxins A and B of *Clostridium difficile*. *Infection and Immunity* 1982; **35**: 1032-40.
54. Pothoulakis C, Barone LM, Ely R *et al*. Purification and properties of *Clostridium difficile* cytotoxin B. *Journal of Biological Chemistry* 1986; **261**: 1316-21.
55. Voneichelstreiber C, Laufenbergfeldmann R, Sartingen S *et al.* Comparative sequence-analysis of the *Clostridium-difficile* toxin-A and toxin-B. *Molecular & General Genetics* 1992; **233**: 260-8.
56. Honda T, Hernadez I, Katoh T et al. Stimulation of enterotoxin production of *Clostridium difficile* ny antibiotics. *Lancet* 1983; **1**: 655.
57. Nakamura S, Mikawa M, Tanabe N *et al*. Effect of clindamycin on cytotoxin production by *Clostridium difficile. Microbiology and Immunology* 1982; **26**: 985-92.
58. Karlsson S, Lindberg A, Norin E *et al*. Toxins, butyric acid, and other short-chain fatty acids are coordinately expressed and down-regulated by cysteine in *Clostridium difficile*. *Infection and Immunity* 2000; **68**: 5881-8.
59. Karlsson S, Dupuy B, Mukherjee K *et al.* Expression of *Clostridium difficile* toxins A and B and their sigma factor TcdD is controlled by temperature. *Infection and Immunity* 2003; **71**: 1784-93.
60. Yamakawa K, Karasawa T, Ohta T *et al*. Inhibition of enhanced toxin production by *Clostridium difficile* in biotin-limited conditions. *Journal of Medical Microbiology* 1998; **47**: 767-71.
61. von Eichel-Streiber C, Meyer zu Heringdorf D, Habermann E *et al.* Closing in on the toxic domain through analysis of a variant *Clostridium difficile* cytotoxin B. *Molecular Microbiology* 1995; **17**: 313-21.
62. von Eichel-Streiber C, Boquet P, Sauerborn M *et al*. Large clostridial cytotoxins--a family of glycosyltransferases modifying small GTP-binding proteins. *Trends in Microbiology* 1996; **4**: 375-82.
63. Voth DE, Ballard JD. *Clostridium difficile* toxins: mechanism of action and role in disease. *Clinical Microbiology Review* 2005; **18**: 247-63.
64. Jank T, Aktories K. Structure and mode of action of clostridial glucosylating toxins: the ABCD model. *Trends in Microbiology* 2008; **16**: 222-9.

65. Popoff MR, Geny B. Multifaceted role of Rho, Rac, Cdc42 and Ras in intercellular junctions, lessons from toxins. *Biochimica et biophysica acta* 2009; **1788**: 797-812.
66. Aktories K, Just I. Monoglucosylation of low-molecular-mass GTP-binding Rho proteins by clostridial cytotoxins. *Trends in Cell Biology* 1995; **5**: 441-3.
67. Just I, Selzer J, Wilm M *et al.* Glucosylation of Rho proteins by *Clostridium difficile* toxin B. *Nature* 1995; **375**: 500-3.
68. Best EL, Freeman J, Wilcox MH. Models for the study of *Clostridium difficile* infection. *Gut Microbes* 2012; **3**: 145-67.
69. Lyerly DM, Saum KE, MacDonald DK *et al*. Effects of *Clostridium difficile* toxins given intragastrically to animals. *Infection and Immunity* 1985; **47**: 349-52.
70. Fiorentini C, Fabbri A, Falzano L *et al*. *Clostridium difficile* toxin B induces apoptosis in intestinal cultured cells. *Infection and Immunity* 1998; **66**: 2660-5.
71. Borriello SP, Wren BW, Hyde S *et al*. Molecular, immunological, and biological characterization of a toxin A-negative, toxin B-positive strain of *Clostridium difficile*. *Infection and Immunity* 1992; **60**: 4192-9.
72. Alfa MJ, Kabani A, Lyerly D *et al*. Characterization of a toxin A-negative, toxin B-positive strain of *Clostridium difficile* responsible for a nosocomial outbreak of *Clostridium difficile*-associated diarrhea. *Journal of Clinical Microbiology* 2000; **38**: 2706-14.
73. al-Barrak A, Embil J, Dyck B *et al*. An outbreak of toxin A negative, toxin B positive *Clostridium difficile*-associated diarrhea in a Canadian tertiary-care hospital. *Cananian Communicable Disease Report* 1999; **25**: 65-9.
74. Barbut F, Lalande V, Burghoffer B *et al*. Prevalence and genetic characterization of toxin A variant strains of *Clostridium difficile* among adults and children with diarrhea in France. *Journal of Clinical Microbiology* 2002; **40**: 2079-83.
75. Pituch H, van den Braak N, van Leeuwen W *et al.* Clonal dissemination of a toxin-A-negative/toxin-B-positive *Clostridium difficile* strain from patients with antibiotic-associated diarrhea in Poland. *Clinical Microbiology and Infection* 2001; **7**: 442-6.
76. Geric B, Rupnik M, Gerding DN *et al.* Distribution of *Clostridium difficile* variant toxinotypes and strains with binary toxin genes among clinical isolates in an American hospital. *Journal of Medical Microbiology* 2004; **53**: 887-94.
77. Lyras D, O'Connor JR, Howarth PM *et al*. Toxin B is essential for virulence of *Clostridium difficile. Nature* 2009; **458**: 1176-9.
78. Steele J, Mukherjee J, Parry N *et al*. Antibody against TcdB, but not TcdA, orevents development of gastrointestinal and systemic *Clostridium difficile* disease. *Journal of Infectious Diseases* 2012.
79. Krivan HC, Clark GF, Smith DF *et al.* Cell surface binding site for *Clostridium difficile* enterotoxin: evidence for a glycoconjugate containing the sequence Gal alpha 1-3Gal beta 1-4GlcNAc. *Infection and Immunity* 1986; **53**: 573-81.
80. Galili U, Shohet SB, Kobrin E *et al.* Man, apes, and Old World monkeys differ from other mammals in the expression of alpha-galactosyl

epitopes on nucleated cells. *Journal of Biological Chemistry* 1988; **263**: 17755-62.
81. Tucker KD, Wilkins TD. Toxin A of *Clostridium difficile* binds to the human carbohydrate antigens I, X, and Y. *Infection and Immunity* 1991; **59**: 73-8.
82. Lyerly DM, Krivan HC, Wilkins TD. *Clostridium difficile*: its disease and toxins. *Clinical Microbiology Reviews* 1988; **1**: 1-18.
83. Hammond GA, Johnson JL. The toxigenic element of *Clostridium difficile* strain VPI 10463. *Microbial Pathogenesis* 1995; **19**: 203-13.
84. Braun V, Hundsberger T, Leukel P *et al*. Definition of the single integration site of the pathogenicity locus in *Clostridium difficile. Gene* 1996; **181**: 29-38.
85. Rupnik M, Dupuy B, Fairweather NF *et al.* Revised nomenclature of *Clostridium difficile* toxins and associated genes. *Journal of Medical Microbiology* 2005; **54**: 113-7.
86. Mani N, Lyras D, Barroso L *et al.* Environmental response and autoregulation of *Clostridium difficile* TxeR, a sigma factor for toxin gene expression. *Journal of Bacteriology* 2002; **184**: 5971-8.
87. Mani N, Dupuy B. Regulation of toxin synthesis in *Clostridium difficile* by an alternative RNA polymerase sigma factor. *Proceeding of the National Acadamy of Sciences of the United States of America* 2001; **98**: 5844-9.
88. Hundsberger T, Braun V, Weidmann M *et al*. Transcription analysis of the genes tcdA-E of the pathogenicity locus of *Clostridium difficile*. *European Journal of Biochemistry* 1997; **244**: 735-42.
89. Matamouros S, England P, Dupuy B. *Clostridium difficile* toxin expression is inhibited by the novel regulator TcdC. *Molecular Microbiology* 2007; **64**: 1274-88.
90. Bakker D, Smits WK, Kuijper EJ *et al*. TcdC does not significantly repress toxin expression in *Clostridium difficile* 630DeltaErm. *PLoS One* 2012; **7**: e43247.
91. Dupuy B, Govind R, Antunes A *et al. Clostridium difficile* toxin synthesis is negatively regulated by TcdC. *Journal of Medical Microbiology* 2008; **57**: 685-9.
92. Cartman ST, Kelly ML, Heeg D *et al*. Precise manipulation of the *Clostridium difficile* chromosome reveals a lack of association between the tcdC genotype and toxin production. *Applied Environmental Microbiology* 2012; **78**: 4683-90.
93. Carter GP, Douce GR, Govind R *et al*. The anti-sigma factor TcdC modulates hypervirulence in an epidemic BI/NAP1/027 clinical isolate of *Clostridium difficile*. *Plos Pathogens* 2011; **7**.
94. Tan KS, Wee BY, Song KP. Evidence for holin function of tcdE gene in the pathogenicity of *Clostridium difficile*. *Journal of Medical Microbiology* 2001; **50**: 613-9.
95. Govind R, Dupuy B. Secretion of *Clostridium difficile* toxins A and B requires the holin-like protein TcdE. *PLoS Pathogens* 2012; **8**: e1002727.
96. Pepin J, Valiquette L, Alary ME *et al. Clostridium difficile*-associated diarrhea in a region of Quebec from 1991 to 2003: a changing pattern of disease severity. *Canadian Medical Association Journal* 2004; **171**: 466-72.

97. Warny M, Pepin J, Fang A *et al*. Toxin production by an emerging strain of *Clostridium difficile* associated with outbreaks of severe disease in North America and Europe. *Lancet* 2005; **366**: 1079-84.
98. Baines SD. Use of a triple-stage chemostat model of the human gut to investigate the effects of antimicrobial administration on bacterial flora and *Clostridium difficile* proliferation and toxin production. *Institute of Molecular and Cellular Biology*. Univeristy of Leeds: University of Leeds, 2006.
99. Stubbs S, Rupnik M, Gibert M *et al*. Production of actin-specific ADP-ribosyltransferase (binary toxin) by strains of *Clostridium difficile*. *FEMS Microbiology Letters* 2000; **186**: 307-12.
100. Goncalves C, Decre D, Barbut F *et al.* Prevalence and characterization of a binary toxin (actin-specific ADP-ribosyltransferase) from *Clostridium difficile*. *Journal of Clinical Microbiology* 2004; **42**: 1933-9.
101. Carter GP, Lyras D, Allen DL *et al*. Binary toxin production in *Clostridium difficile* is regulated by CdtR, a LytTR family response regulator. *Journal of Bacteriology* 2007; **189**: 7290-301.
102. Aktories K, Barmann M, Ohishi I *et al*. Botulinum C2 toxin ADP-ribosylates actin. *Nature* 1986; **322**: 390-2.
103. Schwan C, Stecher B, Tzivelekidis T *et al*. *Clostridium difficile* toxin CDT induces formation of microtubule-based protrusions and increases adherence of bacteria. *PLoS Pathogens* 2009; **5**: e1000626.
104. Barbut F, Decre D, Lalande V *et al*. Clinical features of *Clostridium difficile*-associated diarrhoea due to binary toxin (actin-specific ADP-ribosyltransferase)-producing strains. *Journal of medical microbiology* 2005; **54**: 181-5.
105. Geric B, Carman RJ, Rupnik M *et al*. Binary toxin-producing, large clostridial toxin-negative *Clostridium difficile* strains are enterotoxic but do not cause disease in hamsters. *Journal of Infectious Diseases* 2006; **193**: 1143-50.
106. Bacci S, Molbak K, Kjeldsen MK *et al*. Binary toxin and death after *Clostridium difficile* infection. *Emerging Infectious Diseases* 2011; **17**: 976-82.
107. Geric B, Johnson S, Gerding DN *et al.* Frequency of binary toxin genes among *Clostridium difficile* strains that do not produce large clostridial toxins. *Journal of clinical microbiology* 2003; **41**: 5227-32.
108. Seddon SV, Hemingway I, Borriello SP. Hydrolytic enzyme production by *Clostridium difficile* and its relationship to toxin production and virulence in the hamster model. *Journal of medical microbiology* 1990; **31**: 169-74.
109. Steffen EK, Hentges DJ. Hydrolytic enzymes of anaerobic-bacteria isolated from human infections. *Journal of clinical microbiology* 1981; **14**: 153-6.
110. Seddon SV, Borriello SP. Proteolytic activity of *Clostridium-difficile*. *Journal of medical microbiology* 1992; **36**: 307-11.
111. Borriello SP. Pathogenesis of *Clostridium difficile* infection. *Journal of Antimicrobial Chemotherapy* 1998; **41**: 13-9.
112. Shapiro L. The bacterial flagellum: from genetic network to complex architecture. *Cell* 1995; **80**: 525-7.

113. Feldman M, Bryan R, Rajan S *et al*. Role of flagella in pathogenesis of *Pseudomonas aeruginosa* pulmonary infection. *Infection and Immunity* 1998; **66**: 43-51.
114. Yao R, Burr DH, Doig P *et al.* Isolation of motile and non-motile insertional mutants of *Campylobacter jejuni*: the role of motility in adherence and invasion of eukaryotic cells. *Molecular Microbiology* 1994; **14**: 883-93.
115. Richardson K. Roles of motility and flagellar structure in pathogenicity of *Vibrio cholerae*: analysis of motility mutants in three animal models. *Infection and Immunity* 1991; **59**: 2727-36.
116. Pituch H, Obuch-Woszczatynski P, van den Braak N *et al*. Variable flagella expression among clonal toxin A-/B+*Clostridium difficile* strains with highly homogeneous flagellin genes. *Clinical Microbiology and Infection* 2002; **8**: 187-8.
117. Borriello SP, Bratt, R. Chemotaxis by *Clostridium difficile*: *Science Reviews Ltd, Middlesex,* 1995.
118. Tasteyre A, Barc MC, Collignon A *et al.* Role of FliC and FliD flagellar proteins of *Clostridium difficile* in adherence and gut colonization. *Infection and Immunity* 2001; **69**: 7937-40.
119. Dingle TC, Mulvey GL, Armstrong GD. Mutagenic analysis of the *Clostridium difficile* flagellar proteins, FliC and FliD, and their contribution to virulence in hamsters. *Infection and Immunity* 2011; **79**: 4061-7.
120. Borriello SP. *Clostridium difficile* and its toxin in the gastrointestinal tract in health and disease. *Research and clincal forums* 1979; **1**: 33-5.
121. Borriello SP, Welch AR, Barclay FE *et al.* Mucosal association by *Clostridium difficile* in the hamster gastrointestinal tract. *Journal of medical microbiology* 1988; **25**: 191-6.
122. Waligora AJ, Barc MC, Bourlioux P *et al. Clostridium difficile* cell attachment is modified by environmental factors. *Applied Environmental Microbiology* 1999; **65**: 4234-8.
123. Eveillard M, Fourel V, Barc MC *et al.* Identification and characterization of adhesive factors of *Clostridium-difficile* involved in adhesion to human colonic enterocyte-like Caco-2 and mucus-secreting Ht29 cells in culture. *Molecular Microbiology* 1993; **7**: 371-81.
124. Karjalainen T, Barc MC, Collignon A *et al*. Cloning of a genetic determinant from *Clostridium difficile* involved in adherence to tissue culture cells and mucus. *Infection and Immunity* 1994; **62**: 4347-55.
125. Cerquetti M, Serafino A, Sebastianelli A *et al.* Binding of *Clostridium difficile* to Caco-2 epithelial cell line and to extracellular matrix proteins. *FEMS Immunology and Medical Microbiology* 2002; **32**: 211-8.
126. Waligora AJ, Hennequin C, Mullany P *et al.* Characterization of a cell surface protein of *Clostridium difficile* with adhesive properties. *Infection and Immunity* 2001; **69**: 2144-53.
127. Mauri PL, Pietta PG, Maggioni A *et al.* Characterization of surface layer proteins from *Clostridium difficile* by liquid chromatography electrospray ionization mass spectrometry. *Rapid Communications in Mass Spectrometry* 1999; **13**: 695-703.
128. Calabi E, Ward S, Wren B *et al*. Molecular characterization of the surface layer proteins from *Clostridium difficile*. *Molecular Microbiology* 2001; **40**: 1187-99.

129. Calabi E, Calabi F, Phillips AD *et al*. Binding of *Clostridium difficile* surface layer proteins to gastrointestinal tissues. *Infection and Immunity* 2002; **70**: 5770-8.
130. Karjalainen T, Waligora-Dupriet AJ, Cerquetti M *et al.* Molecular and genomic analysis of genes encoding surface-anchored proteins from *Clostridium difficile*. *Infection and Immunity* 2001; **69**: 3442-6.
131. Hennequin C, Porcheray F, Waligora-Dupriet AJ *et al*. GroEL (Hsp60) of *Clostridium difficile* is involved in cell adherence. *Microbiology-Uk* 2001; **147**: 87-96.
132. Hennequin C, Janoir C, Barc MC *et al*. Identification and characterization of a fibronectin-binding protein from *Clostridium difficile.* *Microbiology-Sgm* 2003; **149**: 2779-87.
133. Panessa-Warren BJ, Tortora GT, Warren JB. High resolution FESEM and TEM reveal bacterial spore attachment. *Microscopy and Microanalysis* 2007; **13**: 251-66.
134. Paredes-Sabja D, Sarker MR. Adherence of *Clostridium difficile* spores to Caco-2 cells in culture. *Journal of medical microbiology* 2012; **61**: 1208-18.
135. Dailey DC, Kaiser A, Schloemer RH. Factors influencing the phagocytosis of *Clostridium-difficile* by human polymorphonuclear leukocytes. *Infection and Immunity* 1987; **55**: 1541-6.
136. Davies HA, Borriello SP. Detection of capsule in strains of *Clostridium-difficile* of varying virulence and toxigenicity. *Microbial Pathogenesis* 1990; **9**: 141-6.
137. Hafiz S, Oakley CL. *Clostridium difficile*: isolation and characteristics. *Journal of medical microbiology* 1976; **9**: 129-36.
138. Dawson LF, Donahue EH, Cartman ST et al. The analysis of para-cresol production and tolerance in *Clostridium difficile* 027 and 012 strains. *BMC microbiology* 2011; **11**.
139. Aronson AI, Fitzjames P. Structure and morphogenesis of bacterial spore coat. *Bacteriological Reviews* 1976; **40**: 360-402.
140. Kamiya S, Yamakawa K, Ogura H *et al*. Recovery of spores of *Clostridium difficile* altered by heat or alkali. *Journal of medical microbiology* 1989; **28**: 217-21.
141. Roberts K, Smith CF, Snelling AM *et al*. Aerial dissemination of *Clostridium difficile* spores. *BMC Infectious Disease* 2008; **8**: 7.
142. Martirosian G. Recovery of *Clostridium difficile* from hospital environments. *Journal of clinical microbiology* 2006; **44**: 1202-3.
143. Sethi AK, Al-Nassir WN, Nerandzic MM *et al.* Persistence of Skin Contamination and Environmental Shedding of *Clostridium difficile* during and after Treatment of C-difficile Infection. *Infection Control and Hospital Epidemiology* 2010; **31**: 21-7.
144. Wilcox MH, Fawley WN. Hospital disinfectants and spore formation by *Clostridium difficile*. *Lancet* 2000; **356**: 1324-.
145. Wilcox MH, Fawley WN, Wigglesworth N *et al*. Comparison of the effect of detergent versus hypochlorite cleaning on environmental contamination and incidence of *Clostridium difficile* infection. *Journal of Hospital Infection* 2003; **54**: 109-14.

146. Merrigan M, Venugopal A, Mallozzi M *et al*. Human hypervirulent *Clostridium difficile* strains exhibit increased sporulation as well as robust toxin production. *Journal of Bacteriology* 2010; **192**: 4904-11.
147. Akerlund T, Persson I, Unemo M *et al*. Increased sporulation rate of epidemic *clostridium difficile* type 027/NAP1. *Journal of Clinical Microbiology* 2008; **46**: 1530-3.
148. Burns DA, Heeg D, Cartman ST *et al.* Reconsidering the sporulation characteristics of hypervirulent *Clostridium difficile* BI/NAP1/027. *PLoS One* 2011; **6**: e24894.
149. Panessa-Warren BJ, Tortora GT, Warren JB. Exosporial membrane plasticity of *Clostridium sporogenes* and *Clostridium difficile*. *Tissue Cell* 1997; **29**: 449-61.
150. Setlow P. Spores of *Bacillus subtilis*: their resistance to and killing by radiation, heat and chemicals. *Journal of Applied Microbiology* 2006; **101**: 514-25.
151. Setlow P. I will survive: DNA protection in bacterial spores. *Trends in Microbiology* 2007; **15**: 172-80.
152. Permpoonpattana P, Tolls EH, Nadem R *et al*. Surface layers of *Clostridium difficile* endospores. *Journal of Bacteriology* 2011; **193**: 6461-70.
153. Lawley TD, Croucher NJ, Yu L *et al.* Proteomic and genomic characterization of highly infectious *Clostridium difficile* 630 spores. *Journal of Bacteriology* 2009; **191**: 5377-86.
154. Driks A. *Bacillus subtilis* spore coat. *Microbiology and Molecular Biology Reviews* 1999; **63**: 1-20.
155. Driks A. The dynamic spore. *Proceedings of the National Academy Science of United States of America* 2003; **100**: 3007-9.
156. Errington J. Regulation of endospore formation in *Bacillus subtilis*. *Nature Reviews: Microbiology* 2003; **1**: 117-26.
157. Stragier P, Losick R. Molecular genetics of sporulation in *Bacillus subtilis*. *Annual Reviews of Genetics* 1996; **30**: 297-41.
158. Moir A, Smith DA. The genetics of bacterial spore germination. *Annual Review of Microbiology* 1990; **44**: 531-53.
159. Burbulys D, Trach KA, Hoch JA. Initiation of sporulation in *B. subtilis* is controlled by a multicomponent phosphorelay. *Cell* 1991; **64**: 545-52.
160. Jiang M, Shao W, Perego M *et al*. Multiple histidine kinases regulate entry into stationary phase and sporulation in *Bacillus subtilis*. *Molecular Microbiology* 2000; **38**: 535-42.
161. Strauch M, Webb V, Spiegelman G *et al.* The SpoOA protein of *Bacillus subtilis* is a repressor of the abrB gene. *Proceedings of the Nationall Acadamy of Science of the United States of America* 1990; **87**: 1801-5.
162. Bird TH, Grimsley JK, Hoch JA *et al.* The *Bacillus subtilis* response regulator SpoOA stimulates transcription of the spoIIG operon through modification of RNA polymerase promoter complexes. *Journal of Molecular of Biology* 1996; **256**: 436-48.
163. Deakin LJ, Clare S, Fagan RP *et al*. The *Clostridium difficile* spo0A gene is a persistence and transmission factor. *Infection and Immunity* 2012; **80**: 2704-11.
164. Kamiya S, Ogura H, Meng XQ *et al*. Correlation between cytotoxin production and sporulation in *Clostridium difficile*. *Journal of Medical Microbiology* 1992; **37**: 206-10.

165. Dupuy B, Sonenshein AL. Regulated transcription of *Clostridium difficile* toxin genes. *Molecular Microbiology* 1998; **27**: 107-20.
166. Underwood S, Guan S, Vijayasubhash V *et al*. Characterization of the sporulation initiation pathway of *Clostridium difficile* and its role in toxin production. *Journal of Bacteriology* 2009; **191**: 7296-305.
167. Rosenbusch KE, Bakker D, Kuijper EJ *et al. C. difficile* 630deltaerm Spo0A regulates sporulation, but does not contribute to toxin production, by direct high-affinity binding to target DNA. *PLoS One* 2012; **7**: e48608.
168. Setlow P. Spore germination. *Current Opinions in Microbiology* 2003; **6**: 550-6.
169. Sorg JA, Sonenshein AL. Chenodeoxycholate is an inhibitor of *Clostridium difficile* spore germination. *Journal of Bacteriology* 2009; **191**: 1115-7.
170. Heeg D, Burns DA, Cartman ST *et al*. Spores of *Clostridium difficile* clinical isolates display a diverse germination response to bile salts. *PLoS One* 2012; **7**: e32381.
171. Health Protection Agency. Results from the mandatory *Clostridium difficile* reporting scheme. Table 5a. *http://wwwhpaorguk/web/HPAweb&HPAwebStandard/HPAweb_C/1195733750761*. (7 August 2013, date last accessed).
172. Health Protection Agency. Voluntary surveillance of *Clostridium difficile* in England, Wales and Northern Ireland. *http://wwwhpaorguk/webc/HPAwebFile/HPAweb_C/1254510474808*. (7 August 2013, date last accessed).
173. Office of National Statistics Death Involving *Clostridium difficile*: England and Wales, 2011. *http://wwwonsgovuk/ons/rel/subnational-health2/deaths-involving-clostridium-difficile/2011/stb-deaths-involving-clostridium-difficile-2011html*. (7 August 2013, date last accessed).
174. European Centre for Disease Prevention and Control. *Clostridium difficile.* *http://ecdceuropaeu/EN/HEALTHTOPICS/CLOSTRIDIUM_DIFFICILE_INFECTION/BASIC_FACTS/Pages/basic_factsaspx*. (7 August 2013, date last accessed).
175. Wiegand PN, Nathwani D, Wilcox MH *et al*. Clinical and economic burden of *Clostridium difficile* infection in Europe: a systematic review of healthcare-facility-acquired infection. *Journal of Hospital Infection* 2012; **81**: 1-14.
176. Health Protecton Agency. Results from the mandatory *Clostridium difficile* reporting scheme. Archive calender year table. *http://wwwhpaorguk/web/HPAweb&HPAwebStandard/HPAweb_C/1195733750761*. (7 August 2013, date last accessed).
177. Cohen SH, Gerding DN, Johnson S *et al*. Clinical practice guidelines for *Clostridium difficile* infection in adults: 2010 update by the society for healthcare epidemiology of America (SHEA) and the infectious diseases society of America (IDSA). *Infection Control and Hospital Epidemiology* 2010; **31**: 431-55.
178. Hirschhorn LR, Trnka Y, Onderdonk A *et al*. Epidemiology of community-acquired *Clostridium difficile*-associated diarrhea. *The Journal of Infectious Diseases* 1994; **169**: 127-33.

179. Pituch H. *Clostridium difficile* is no longer just a nosocomial infection or an infection of adults. *International Journal of Antimicrobial Agents* 2009; **33 Suppl 1**: S42-5.
180. Noren T, Akerlund T, Back E *et al.* Molecular epidemiology of hospital-associated and community-acquired *Clostridium difficile* infection in a Swedish county. *Journal of Clinical Microbiology* 2004; **42**: 3635-43.
181. Dial S, Delaney JA, Barkun AN *et al.* Use of gastric acid-suppressive agents and the risk of community-acquired *Clostridium difficile*-associated disease. *Journal of the Aerican Medical Association* 2005; **294**: 2989-95.
182. Khanna S, Pardi DS, Aronson SL *et al.* The epidemiology of community-acquired *Clostridium difficile* infection: a population-based study. *Am ericanJournal of Gastroenterology* 2012; **107**: 89-95.
183. Dumyati G, Stevens V, Hannett GE *et al.* Community-associated *Clostridium difficile* infections, Monroe County, New York, USA. *Emerging Infectious Diseases* 2012; **18**: 392-400.
184. Fellmeth G, Yarlagadda S, Lyer S. Epidemiology of community-onset *Clostridium difficile* infection in a community in the South of England. *Journal of Infection and Public Health* 2010; **3**: 118-23.
185. Bauer MP, Goorhuis A, Koster T *et al*. Community-onset *Clostridium difficile*-associated diarrhoea not associated with antibiotic usage--two case reports with review of the changing epidemiology of *Clostridium difficile*-associated diarrhoea. *Netherlands Journal of Medicine* 2008; **66**: 207-11.
186. Alvarez-Perez S, Blanco JL, Bouza E *et al*. Prevalence of *Clostridium difficile* in diarrhoeic and non-diarrhoeic piglets. *Veterinary Microbiology* 2009; **137**: 302-5.
187. Koene MG, Mevius D, Wagenaar JA *et al. Clostridium difficile* in Dutch animals: their presence, characteristics and similarities with human isolates. *Clinical Microbiology and Infecition* 2012; **18**: 778-84.
188. Avbersek J, Janezic S, Pate M *et al*. Diversity of *Clostridium difficile* in pigs and other animals in Slovenia. *Anaerobe* 2009; **15**: 252-5.
189. Knight DR, Thean S, Putsathit P *et al*. Cross-sectional study reveals high prevalence of *Clostridium difficile n*on-PCR ribotype 078 strains in australian veal calves at slaughter. *Applied Environmental Microbiology* 2013; **79**: 2630-5.
190. Rodriguez-Palacios A, Staempfli HR, Duffield T *et al*. *Clostridium difficile* in retail ground meat, Canada. *Emerging Infectious Diseases* 2007; **13**: 485-7.
191. de Boer E, Zwartkruis-Nahuis A, Heuvelink AE *et al.* Prevalence of *Clostridium difficile* in retailed meat in the Netherlands. *International Journal of Food Microbiology* 2011; **144**: 561-4.
192. Keel K, Brazier JS, Post KW *et al.* Prevalence of PCR ribotypes among *Clostridium difficile* isolates from pigs, calves, and other species. *Journal of Clinical Microbiology* 2007; **45**: 1963-4.
193. Goorhuis A, Debast SB, van Leengoed LA *et al*. *Clostridium difficile* PCR ribotype 078: an emerging strain in humans and in pigs? *Journal of Clinical Microbiology* 2008; **46**: 1157; author reply 8.
194. Rodriguez-Palacios A, Stampfli HR, Duffield T *et al*. *Clostridium difficile* PCR ribotypes in calves, Canada. *Emerging Infectious Diseases* 2006; **12**: 1730-6.

195. Houser BA, Soehnlen MK, Wolfgang DR *et al.* Prevalence of *Clostridium difficile* toxin genes in the feces of veal calves and incidence of ground veal contamination. *Foodborne Pathogens in Disease* 2012; **9**: 32-6.
196. Hoffer E, Haechler H, Frei R *et al.* Low occurrence of *Clostridium difficile* in fecal samples of healthy calves and pigs at slaughter and in minced meat in Switzerland. *Journal of Food Protection* 2010; **73**: 973-5.
197. Loo VG, Poirier L, Miller MA *et al.* A predominantly clonal multi-institutional outbreak of *Clostridium difficile*-associated diarrhea with high morbidity and mortality. *The New England Journal of Medicine* 2005; **353**: 2442-9.
198. Institut National de Santa Publique du Quebec. Surveillance de diarrhees associees a *Clostridium difficie* au Quebec. Results from 22, 2004-Mar 31, 2005.
199. The Healthcare Commission. Investigation into outbreaks of *Clostridium difficile* at Stoke Mandeville Hospital, Buckinghamshire Hospital NHS trust. London: Commission for Healthcare Audit and Inspection, 2006.
200. McDonald LC, Killgore GE, Thompson A *et al*. An epidemic, toxin gene-variant strain of *Clostridium difficile*. *The New EnglandJjournal of Medicine* 2005; **353**: 2433-41.
201. Kuijper EJ, Coignard B, Tull P. Emergence of *Clostridium difficile*-associated disease in North America and Europe. *Clinical Microbiology and Infection* 2006; **12 Suppl 6**: 2-18.
202. Stubbs SL, Brazier JS, O'Neill GL *et al*. PCR targeted to the 16S-23S rRNA gene intergenic spacer region of *Clostridium difficile* and construction of a library consisting of 116 different PCR ribotypes. *Journal of Clinical Microbiology* 1999; **37**: 461-3.
203. Brazier JS, Patel B, Pearson A. Distribution of *Clostridium difficile* PCR ribotype 027 in British hospitals. *European Surveillance* 2007; **12**: E070426 2.
204. Health Protection Agency. *Clostridium difficile* Ribotyping Network (CDRN) for England and Northern Ireland 2010/11 Annual report. *http://wwwhpaorguk/webw/HPAweb&HPAwebStandard/HPAweb_C/1317133397204*. (7 August 2013, date last accessed).
205. Health Protection Agency. *Clostridium difficile* ribotyping network (CDRN) for England and Northern Ireland 2010/11 annual report. *http://wwwhpaorguk/webc/HPAwebFile/HPAweb_C/1317133396963*. (7 August 2013, date last accessed).
206. Health Protection Agency. Antimicrobial resistance in England, Wales and Northern Ireland 2006 report. *http://wwwhpaorguk/web/HPAwebFile/HPAweb_C/1204100435389*. (1 August 2013, date last accessed).
207. Pelaez T, Alcala L, Alonso R *et al.* Reassessment of *Clostridium difficile* susceptibility to metronidazole and vancomycin. *Antimicrobial Agents and Chemotherrapy* 2002; **46**: 1647-50.
208. Health Protection Agency. *Clostridium difficile* ribotyping network for England and Northern Ireland 2008/09 report. *http://wwwhpaorguk/webc/HPAwebFile/HPAweb_C/1258560554236*. (7 August 2013, date last accessed).
209. Moura I, Spigaglia P, Barbanti F *et al*. Analysis of metronidazole susceptibility in different *Clostridium difficile* PCR ribotypes. *The Journal of Antimicrobial Chemotherapy* 2013; **68**: 362-5.

210. Chilton CH, Crowther, GS *et al*. Reduced susceptibility of *Clostridium difficile* to metronidazole detected by agar incorporation but not Etest. *23 rd European Congress of Clinical Microbiology and Infectious Diseases*. Berlin, Germany, 2013; 138.
211. Arabi Y, Dimock F, Burdon DW *et al.* Influence of neomycin and metronidazole on colonic microflora of volunteers. *The Journal of antimicrobial chemotherapy* 1979; **5**: 531-7.
212. Krook A, Jarnerot G, Danielsson D. Clinical effect of metronidazole and sulfasalazine on Crohn's disease in relation to changes in the fecal flora. *Scandanavian Journal of Gastroenterology* 1981; **16**: 569-75.
213. Bolton RP, Culshaw MA. Faecal metronidazole concentrations during oral and intravenous therapy for antibiotic associated colitis due to Clostridium difficile. *Gut* 1986; **27**: 1169-72.
214. Young GP, Ward PB, Bayley N *et al*. Antibiotic-associated colitis due to *Clostridium difficile*: double-blind comparison of vancomycin with bacitracin. *Gastroenterology* 1985; **89**: 1038-45.
215. Kelly CP, Pothoulakis C, LaMont JT. *Clostridium difficile* colitis. *The New England Journal of Medicine* 1994; **330**: 257-62.
216. Musher DM, Manhas A, Jain P *et al*. Detection of *Clostridium difficile* toxin: comparison of enzyme immunoassay results with results obtained by cytotoxicity assay. *Journal of Clinical Microbiology* 2007; **45**: 2737-9.
217. Knetsch CW, Bakker D, de Boer RF *et al*. Comparison of real-time PCR techniques to cytotoxigenic culture methods for diagnosing *Clostridium difficile* infection. *Journal of ClinicalMmicrobiology* 2011; **49**: 227-31.
218. Eastwood K, Else P, Charlett A *et al*. Comparison of nine commercially available *Clostridium difficile* toxin detection assays, a real-time PCR assay for *C. difficile* tcdB, and a glutamate dehydrogenase detection assay to cytotoxin testing and cytotoxigenic culture methods. *Journal of Clinical Microbiology* 2009; **47**: 3211-7.
219. Goldenberg SD, French GL. Diagnostic testing for *Clostridium difficile*: a comprehensive survey of laboratories in England. *Journal of Hospital Infection* 2011; **79**: 4-7.
220. Sloan LM, Duresko BJ, Gustafson DR *et al.* Comparison of real-time PCR for detection of the tcdC gene with four toxin immunoassays and culture in diagnosis of *Clostridium difficile* infection. *Journal of Clinical Microbiology* 2008; **46**: 1996-2001.
221. Sharp SE, Ruden LO, Pohl JC *C*Evaluation of the C.Diff Quik Chek Complete Assay, a new glutamate dehydrogenase and A/B toxin combination lateral flow assay for use in rapid, simple diagnosis of *clostridium difficile* disease. *Journal of Clinical Microbiology* 2010; **48**: 2082-6.
222. Fenner L, Widmer AF, Goy G *et al*. Rapid and reliable diagnostic algorithm for detection of *Clostridium difficile*. *Journal of Clinical Microbiology* 2008; **46**: 328-30.
223. Planche T, Aghaizu A, Holliman R et al. Diagnosis of *Clostridium difficile* infection by toxin detection kits: a systematic review. *Lancet Infect Dis* 2008; **8**: 777-84.
224. Peterson LR, Manson RU, Paule SM *et al.* Detection of toxigenic *Clostridium difficile* in stool samples by real-time polymerase chain reaction for the diagnosis of *C. difficile*-associated diarrhea. *Clinical Infectious*

Diseases : an official publication of the Infectious Diseases Society of America 2007; **45**: 1152-60.
225. Stamper PD, Alcabasa R, Aird D *et al*. Comparison of a commercial real-time PCR assay for tcdB detection to a cell culture cytotoxicity assay and toxigenic culture for direct detection of toxin-producing *Clostridium difficile* in clinical samples. *Journal of Clinical Microbiology* 2009; **47**: 373-8.
226. O'Connor D, Hynes P, Cormican M *et al*. Evaluation of methods for detection of toxins in specimens of feces submitted for diagnosis of *Clostridium difficile*-associated diarrhea. *Journal of Clinical Microbiology* 2001; **39**: 2846-9.
227. Shetty N, Wren MW, Coen PG. The role of glutamate dehydrogenase for the detection of *Clostridium difficile* in faecal samples: a meta-analysis. *Journal of Hospital Infection* 2011; **77**: 1-6.
228. Crobach MJ, Dekkers OM, Wilcox MH *et al*. European Society of Clinical Microbiology and Infectious Diseases (ESCMID): data review and recommendations for diagnosing *Clostridium difficile*-infection (CDI). *Clinical Microbiology and Infection* 2009; **15**: 1053-66.
229. Department of Health. Updated guidance on the diagnosis and reporting of *Clostridium difficile*. *http://wwwdhgovuk/prod_consum_dh/groups/dh_digitalassets/@dh/@en/documents/digitalasset/dh_133016pdf*. (13 August 2013), 2012.
230. Kim YS, Lee JK, Kim SE *et al*. Comparative value of sigmoidoscopy and stool cytotoxin-A assay for diagnosis of Pseudomembranous colitis. *Gastrointestinal Endoscopy* 2006; **63**: Ab200-Ab.
231. Teasley DG, Gerding DN, Olson MM *et al.* Prospective randomised trial of metronidazole versus vancomycin for *Clostridium-difficile*-associated diarrhoea and colitis. *Lancet* 1983; **2**: 1043-6.
232. Zar FA, Bakkanagari SR, Moorthi KM *et al.* A comparison of vancomycin and metronidazole for the treatment of *Clostridium difficile*-associated diarrhea, stratified by disease severity. *Clinical infectious diseases : an official publication of the Infectious Diseases Society of America* 2007; **45**: 302-7.
233. Crook DW, Walker AS, Kean Y *et al.* Fidaxomicin Versus Vancomycin for *Clostridium difficile* Infection: Meta-analysis of Pivotal Randomized Controlled Trials. *Clinical Infectious Diseases* 2012; **55**: S93-S103.
234. Mattila E, Arkkila P, Mattila PS *et al*. Rifaximin in the treatment of recurrent *Clostridium difficile* infection. *Alimentary Pharmacology and Therapeutics* 2012.
235. Musher DM, Logan N, Hamill RJ *et al.* Nitazoxanide for the treatment of *Clostridium difficile* colitis. *Clinical Infectious Diseases : an official publication of the Infectious Diseases Society of America* 2006; **43**: 421-7.
236. Patino H SC, Louie T, Bernardo P, Vetticaden S, Friedland I. Efficacy and 470 safety of the lipopeptide CB-183,315 for the treatment of *Clostridium difficile* infection. *Interscience conference of antimicrobial agents and chemotherapy; 2011; Chicgo, IL, USA Abstract K-205a*.
237. Mascio CT, Mortin LI, Howland KT *et al*. In vitro and in vivo characterization of CB-183,315, a novel lipopeptide antibiotic for treatment of *Clostridium difficile. Antimicrob Agents Chemotherapy* 2012; **56**: 5023-30.

238. Foglia G, Shah S, Luxemburger C *et al. Clostridium difficile*: development of a novel candidate vaccine. *Vaccine* 2012; **30**: 4307-9.
239. Sougioultzis S, Kyne L, Drudy D et al. *Clostridium difficile* toxoid vaccine in recurrent *C. difficile*-associated diarrhea. *Gastroenterology* 2005; **128**: 764-70.
240. Marozsan AJ, Ma D, Nagashima KA *et al*. Protection against *Clostridium difficile* infection with broadly neutralizing antitoxin monoclonal antibodies. *Journal of Infectious Diseases* 2012; **206**: 706-13.
241. Gough E, Shaikh H, Manges AR. Systematic review of intestinal microbiota transplantation (fecal bacteriotherapy) for recurrent *Clostridium difficile* infection. *Clinical Infectious Diseases : an official publication of the Infectious Diseases Society of America* 2011; **53**: 994-1002.
242. Friedman G. The role of probiotics in the prevention and treatment of antibiotic-associated diarrhea and *clostridium difficile* colitis. *Gastroenterology Clinics of North America* 2012; **41**: 763-79.
243. Barbut F, Richard A, Hamadi K *et al*. Epidemiology of recurrences or reinfections of *Clostridium difficile*-associated diarrhea. *Journal of Clinical Microbiology* 2000; **38**: 2386-8.
244. Young GP, Bayley N, Ward P *et al.* Antibiotic-associated colitis caused by *Clostridium difficile*: relapse and risk factors. *Medical Journal of Australia* 1986; **144**: 303-6.
245. Lowy I, Molrine DC, Leav BA *et al.* Treatment with monoclonal antibodies against *Clostridium difficile* toxins. *The New England Journal of Medicine* 2010; **362**: 197-205.
246. Pepin J, Alary ME, Valiquette L *et al.* Increasing risk of relapse after treatment of *Clostridium difficile* colitis in Quebec, Canada. *Clinical infectious diseases : an official publication of the Infectious Diseases Society of America* 2005; **40**: 1591-7.
247. Petrella LA, Sambol SP, Cheknis A *et al.* Decreased cure and increased recurrence rates for *Clostridium difficile* infection caused by the epidemic C. difficile BI strain. *Clinical Infectious Diseases : an official publication of the Infectious Diseases Society of America* 2012; **55**: 351-7.
248. Kyne L, Warny M, Qamar A et al. Association between antibody response to toxin A and protection against recurrent *Clostridium difficile* diarrhoea. *Lancet* 2001; **357**: 189-93.
249. Bauer MP, Kuijper EJ, van Dissel JT. European Society of Clinical Microbiology and Infectious Diseases (ESCMID): treatment guidance document for *Clostridium difficile* infection (CDI). *Clinical Microbiology and Infection* 2009; **15**: 1067-79.
250. Figueroa I, Johnson S, Sambol SP *et al*. Relapse versus reinfection: recurrent *Clostridium difficile i*nfection following treatment with fidaxomicin or vancomycin. *Clinical infectious diseases : an official publication of the Infectious Diseases Society of America* 2012; **55 Suppl 2**: S104-9.
251. Hall-Stoodley L, Stoodley P. Evolving concepts in biofilm infections. *Cell Microbiology* 2009; **11**: 1034-43.
252. Chang JY, Antonopoulos DA, Kalra A *et al*. Decreased diversity of the fecal microbiome in recurrent *Clostridium difficile*-associated diarrhea. *Journal of Infectious Diseases* 2008; **197**: 435-8.
253. Wilcox MH, Spencer RC. *Clostridium difficile* infection: responses, relapses and re-infections. *Journal of Hospital Infection* 1992; **22**: 85-92.

254. Postigo R, Kim JH. Colonoscopic versus nasogastric fecal transplantation for the treatment of *Clostridium difficile* infection: a review and pooled analysis. *Infection* 2012; **40**: 643-8.
255. Czuprynski CJ, Johnson WJ, Balish E *et al*. Pseudo-membranous colitis in *Clostridium-difficile*-monoassociated rats. *Infection and Immunology* 1983; **39**: 1368-76.
256. Fekety R, Silva J, Toshniwal R *et al*. Antibiotic-associated colitis - effects of antibiotics on *Clostridium-difficile* and the disease in hamsters. *Reviews of Infectious Diseases* 1979; **1**: 386-97.
257. Knoop FC. Clindamycin-associated enterocolitis in guinea-pigs - evidence for a bacterial toxin. *Infection and Immunology* 1979; **23**: 31-3.
258. Kelly CP, Becker S, Linevsky JK *et al*. Neutrophil recruitment in *Clostridium-difficile* toxin-a enteritis in the rabbit. *Journal of Clinical Investigation* 1994; **93**: 1257-65.
259. Douce G, Goulding D. Refinement of the hamster model of *Clostridium difficile* disease. *Clostridium Difficile: Methods and Protocols* 2010; **646**: 215-27.
260. Buckley AM, Spencer J, Maclellan LM *et al*. Susceptibility of hamsters to *Clostridium difficile* isolates of differing toxinotype. *Plos One* 2013; **8**: e64121.
261. Chen X, Katchar K, Goldsmith JD *et al.* A mouse model of *Clostridium difficile*-associated disease. *Gastroenterology* 2008; **135**: 1984-92.
262. Corthier G, Dubos F, Raibaud P. Modulation of cytotoxin production by *Clostridium difficile* in the intestinal tracts of gnotobiotic mice inoculated with various human intestinal bacteria. *Applied Environmental Microbiology* 1985; **49**: 250-2.
263. Giel JL, Sorg JA, Sonenshein AL *et al*. Metabolism of bile salts in mice influences spore germination in *Clostridium difficile*. *Plos One* 2010; **5**: e8740.
264. Onderdonk AB, Cisneros RL, Bartlett JG. *Clostridium difficile* in gnotobiotic mice. *Infection and Immunology* 1980; **28**: 277-82.
265. Lawley TD, Clare S, Walker AW *et al.* Antibiotic treatment of *clostridium difficile* carrier mice triggers a supershedder state, spore-mediated transmission, and severe disease in immunocompromised hosts. *Infection and Immunology* 2009; **77**: 3661-9.
266. Lawley TD, Clare S, Walker AW *et al*. Targeted restoration of the intestinal microbiota with a simple, defined bacteriotherapy resolves relapsing *Clostridium difficile* disease in mice. *Plos Pathogens* 2012; **8**: e1002995.
267. Borriello SP, Ketley JM, Mitchell TJ *et al*. *Clostridium difficile*--a spectrum of virulence and analysis of putative virulence determinants in the hamster model of antibiotic-associated colitis. *Journal of Medical Microbiology* 1987; **24**: 53-64.
268. Levett PN. Time-dependent killing of *Clostridium difficile* by metronidazole and vancomycin. *The Journal of Antimicrobial Chemotherapy* 1991; **27**: 55-62.
269. Macfarlane GT, Macfarlane S, Gibson GR. Validation of a three-stage compound continuous culture system for investigating the effect of retention

time on the ecology and metabolism of bacteria in the human colon. *Microbial Ecology* 1998; **35**: 180-7.
270. Baines SD, Freeman J, Wilcox MH. Effects of piperacillin/tazobactam on *Clostridium difficile* growth and toxin production in a human gut model. *The Journal of Antimicrobial Chemotherapy* 2005; **55**: 974-82.
271. Saxton K, Baines SD, Freeman J *et al.* Effects of exposure of *Clostridium difficile* PCR ribotypes 027 and 001 to fluoroquinolones in a human gut model. *Antimicrobial Agents and Chemotherapy* 2009; **53**: 412-20.
272. Baines SD, O'Connor R, Saxton K *et al*. Comparison of oritavancin versus vancomycin as treatments for clindamycin-induced *Clostridium difficile* PCR ribotype 027 infection in a human gut model. *The Journal of Antimicrobial Chemotherapy* 2008; **62**: 1078-85.
273. Baines SD, O'Connor R, Huscroft G *et al.* Mecillinam: a low-risk antimicrobial agent for induction of *Clostridium difficile* infection in an in vitro human gut model. *The Journal of Antimicrobial Chemotherapy* 2009; **63**: 838-9.
274. Guarner F, Malagelada JR. Gut flora in health and disease. *Lancet* 2003; **361**: 512-9.
275. Brook I, Barrett CT, Brinkman CR *et al*. Aerobic and anaerobic bacterial flora of the maternal cervix and newborn gastric fluid and conjunctiva: a prospective study. *Pediatrics* 1979; **63**: 451-5.
276. Dominguez-Bello MG, Costello EK, Contreras M *et al*. Delivery mode shapes the acquisition and structure of the initial microbiota across multiple body habitats in newborns. *Proceedings of the Nationall Acadamy of Science of the United States of America* 2010; **107**: 11971-5.
277. Rotimi VO, Duerden BI. The development of the bacterial flora in normal neonates. *Journal of Medical Microbiology* 1981; **14**: 51-62.
278. Qin J, Li R, Raes J *et al.* A human gut microbial gene catalogue established by metagenomic sequencing. *Nature* 2010; **464**: 59-65.
279. Eckburg PB, Bik EM, Bernstein CN *et al*. Diversity of the human intestinal microbial flora. *Science* 2005; **308**: 1635-8.
280. Gill SR, Pop M, Deboy RT *et al*. Metagenomic analysis of the human distal gut microbiome. *Science* 2006; **312**: 1355-9.
281. Hong PY, Croix JA, Greenberg E *et al*. Pyrosequencing-based analysis of the mucosal microbiota in healthy individuals reveals ubiquitous bacterial groups and micro-heterogeneity. *PLoS One* 2011; **6**: e25042.
282. Simon GL, Gorbach SL. Intestinal flora in health and disease. *Gastroenterology* 1984; **86**: 174-93.
283. Suau A, Bonnet R, Sutren M *et al*. Direct analysis of genes encoding 16S rRNA from complex communities reveals many novel molecular species within the human gut. *Applied Environmental Microbiology* 1999; **65**: 4799-807.
284. Wilson KH, Blitchington RB. Human colonic biota studied by ribosomal DNA sequence analysis. *Applied Environmental Microbiology* 1996; **62**: 2273-8.
285. Blaut M, Collins MD, Welling GW *et al*. Molecular biological methods for studying the gut microbiota: the EU human gut flora project. *British Journal of Nutrition* 2002; **87 Suppl 2**: S203-11.

286. Buffie CG, Jarchum I, Equinda M *et al.* Profound alterations of intestinal microbiota following a single dose of clindamycin results in sustained susceptibility to *Clostridium difficile*-induced colitis. *Infection and Immunity* 2012; **80**: 62-73.
287. Turroni F, Peano C, Pass DA *et al.* Diversity of bifidobacteria within the infant gut microbiota. *PLoS One* 2012; **7**: e36957.
288. Ross EM, Moate PJ, Bath CR *et al*. High throughput whole rumen metagenome profiling using untargeted massively parallel sequencing. *BMC Genetics* 2012; **13**: 53.
289. Gloor GB, Hummelen R, Macklaim JM *et al*. Microbiome profiling by illumina sequencing of combinatorial sequence-tagged PCR products. *PLoS One* 2010; **5**: e15406.
290. Metzker ML. Sequencing technologies - the next generation. *National Reviews: Genetics* 2010; **11**: 31-46.
291. Gillevet P, Sikaroodi M, Keshavarzian A et al. Quantitative assessment of the human gut microbiome using multitag pyrosequencing. *Chemistry and Biodiversity* 2010; **7**: 1065-75.
292. Zoetendal EG, von Wright A, Vilpponen-Salmela T *et al*. Mucosa-associated bacteria in the human gastrointestinal tract are uniformly distributed along the colon and differ from the community recovered from feces. *Applied Environmental Microbiology* 2002; **68**: 3401-7.
293. Edmiston CE, Jr., Avant GR, Wilson FA. Anaerobic bacterial populations on normal and diseased human biopsy tissue obtained at colonoscopy. *Applied Environmental Microbiology* 1982; **43**: 1173-81.
294. Croucher SC, Houston AP, Bayliss CE *et al*. Bacterial populations associated with different regions of the human colon wall. *Applied Environmental Microbiology* 1983; **45**: 1025-33.
295. Falk PG, Hooper LV, Midtvedt T *et al*. Creating and maintaining the gastrointestinal ecosystem: what we know and need to know from gnotobiology. *Microbiology and Molecular Biology Reviews* 1998; **62**: 1157-70.
296. McCormick DA, Horton LW, Mee AS. Mucin depletion in inflammatory bowel disease. *Journal of Clinical Pathology* 1990; **43**: 143-6.
297. Swidsinski A, Loening-Baucke V, Theissig F et al. Comparative study of the intestinal mucus barrier in normal and inflamed colon. *Gut* 2007; **56**: 343-50.
298. Wesley A, Mantle M, Man D *et al*. Neutral and acidic species of human intestinal mucin. Evidence for different core peptides. *Journal of Biology and Chemistry* 1985; **260**: 7955-9.
299. Sheahan DG, Jervis HR. Comparative histochemistry of gastrointestinal mucosubstances. *American Journal of Anatomy* 1976; **146**: 103-31.
300. Robertson AM, Wright DP. Bacterial glycosulphatases and sulphomucin degradation. *Canadian Journal of Gastroenterology* 1997; **11**: 361-6.
301. Fontaine N, Meslin JC, Lory S *et al*. Intestinal mucin distribution in the germ-free rat and in the heteroxenic rat harbouring a human bacterial flora: effect of inulin in the diet. *British Journal of Nutrition* 1996; **75**: 881-92.
302. Creeth JM. Constituents of mucus and their separation. *British Medical Bulletin* 1978; **34**: 17-24.

303. Sellars LA, Allen, A., Morris, E.R. and Ross-Murphy, S.B. Mucus glycoprotein gels. Role of glycoprotein polymeric structure and carbohydrate side-chains in gel-formation. *Carbohydrate Research* 1988; **178**: 93-110.
304. Allen A. Structure of gastrointestinal mucus glycoproteins and the viscous and gel-forming properties of mucus. *British Medical Bulletin* 1978; **34**: 28-33.
305. Allen A, Bell A, Mantle M *et al.* The structure and physiology of gastrointestinal mucus. *Advances in Experimental Medicine and Niology* 1982; **144**: 115-33.
306. Forstner JF OM, Sylvester FA. Production, structure, and biologic relevance of gastrointestinal mucins. *In: Blaser MJ, Smith PD, Ravdin JI, Greenberg HB, Guerrant RL, eds Infections of the gastrointestinal tract New York: Raven Press* 1995: 71-88.
307. Podolsky DK, Isselbacher KJ. Composition of human colonic mucin. Selective alteration in inflammatory bowel disease. *Journal of Clinical Investigation* 1983; **72**: 142-53.
308. Corfield AP, Wagner SA, Clamp JR *et al.* Mucin degradation in the human colon: production of sialidase, sialate O-acetylesterase, N-acetylneuraminate lyase, arylesterase, and glycosulfatase activities by strains of fecal bacteria. *Infection and Immunity* 1992; **60**: 3971-8.
309. Hoskins LC, Boulding ET. Mucin degradation in human colon ecosystems. Evidence for the existence and role of bacterial subpopulations producing glycosidases as extracellular enzymes. *Journal of Clinical Investigation* 1981; **67**: 163-72.
310. Miller RS, Hoskins LC. Mucin degradation in human colon ecosystems. Fecal population densities of mucin-degrading bacteria estimated by a "most probable number" method. *Gastroenterology* 1981; **81**: 759-65.
311. Johansson ME, Phillipson M, Petersson J *et al.* The inner of the two Muc2 mucin-dependent mucus layers in colon is devoid of bacteria. *Proceedings of National Academy of Sciences of the United States of America* 2008; **105**: 15064-9.
312. Matsuo K, Ota H, Akamatsu T *et al*. Histochemistry of the surface mucous gel layer of the human colon. *Gut* 1997; **40**: 782-9.
313. van der Waaij LA, Harmsen HJ, Madjipour M *et al.* Bacterial population analysis of human colon and terminal ileum biopsies with 16S rRNA-based fluorescent probes: commensal bacteria live in suspension and have no direct contact with epithelial cells. *Inflammatory Bowel Disease* 2005; **11**: 865-71.
314. Neutra MR, O'Malley LJ, Specian RD. Regulation of intestinal goblet cell secretion. II. A survey of potential secretagogues. *American Journal of Physiology* 1982; **242**: G380-7.
315. McCool DJ, Marcon MA, Forstner JF *et al.* The T84 human colonic adenocarcinoma cell line produces mucin in culture and releases it in response to various secretagogues. *The Biochemical Journal* 1990; **267**: 491-500.
316. Epple HJ, Kreusel KM, Hanski C *et al*. Differential stimulation of intestinal mucin secretion by cholera toxin and carbachol. *Pflugers Archive: European Journal of Physiology* 1997; **433**: 638-47.

317. Derrien M, Vaughan EE, Plugge CM *et al. Akkermansia muciniphila* gen. nov., sp. nov., a human intestinal mucin-degrading bacterium. *Internal Journal of Systematic and Evolutionary Microbiology* 2004; **54**: 1469-76.
318. Sansonetti PJ. War and peace at mucosal surfaces. *Nature Reviews Immunology* 2004; **4**: 953-64.
319. Ouellette AJ. Paneth cell alpha-defensins: peptide mediators of innate immunity in the small intestine. *Springer Seminars In Immunopathology* 2005; **27**: 133-46.
320. Macpherson AJ, Geuking MB, McCoy KD. Immune responses that adapt the intestinal mucosa to commensal intestinal bacteria. *Immunology* 2005; **115**: 153-62.
321. Suzuki K, Meek B, Doi Y *et al.* Aberrant expansion of segmented filamentous bacteria in IgA-deficient gut. *Proceedings of National Acadamy of Sciences of the United States of America* 2004; **101**: 1981-6.
322. Macpherson AJ, Uhr T. Induction of protective IgA by intestinal dendritic cells carrying commensal bacteria. *Science* 2004; **303**: 1662-5.
323. Zobell CE. The Effect of Solid Surfaces upon Bacterial Activity. *Journal of Bacteriology* 1943; **46**: 39-56.
324. Cloete TE, Jacobs L, Brozel VS. The chemical control of biofouling in industrial water systems. *Biodegradation* 1998; **9**: 23-37.
325. Dutta D, Cole N, Willcox M. Factors influencing bacterial adhesion to contact lenses. *Molecular Vision* 2012; **18**: 14-21.
326. Elliott TS, Moss HA, Tebbs SE *et al.* Novel approach to investigate a source of microbial contamination of central venous catheters. *European Journal of Clinical Microbiology and Infectious Disease* 1997; **16**: 210-3.
327. Marsh PD. Dental plaque as a biofilm and a microbial community - implications for health and disease. *BMC Oral Health* 2006; **6 Suppl 1**: S14.
328. Brablcova L, Buriankova I, Badurova P *et al.* The phylogenetic structure of microbial biofilms and free-living bacteria in a small stream. *Folia Microbiologica (Praha)* 2012.
329. Archibald LK, Gaynes RP. Hospital-acquired infections in the United States - The importance of interhospital comparisons. *Infectious Disease Clinics of North America* 1997; **11**: 245-&.
330. Costerton JW, Lewandowski Z, Caldwell DE *et al*. Microbial Biofilms. *Annual Reviews: Microbiology* 1995; **49**: 711-45.
331. Emtiazi F, Schwartz T, Marten SM *et al*. Investigation of natural biofilms formed during the production of drinking water from surface water embankment filtration. *Water Research* 2004; **38**: 1197-206.
332. Schultz MP, Bendick JA, Holm ER *et al.* Economic impact of biofouling on a naval surface ship. *Biofouling* 2011; **27**: 87-98.
333. Gomez-Alvarez V, Revetta RP, Domingo JWS. Metagenome analyses of corroded concrete wastewater pipe biofilms reveal a complex microbial system. *BMC microbiology* 2012; **12**.
334. Characklis WG MG, Marshall KC. Physiological ecology in biofilm systems. *In: Characklis WG, Marshall KC, editors Biofilms New York: John Wiley & Sons* 1990: 341-94.
335. Fletcher M, Loeb GI. Influence of substratum characteristics on the attachment of a marine pseudomonad to solid surfaces. *Applied Environmental Microbiology* 1979; **37**: 67-72.

336. Pringle JH, Fletcher M. Influence of substratum wettability on attachment of freshwater bacteria to solid surfaces. *Applied Environmental Microbiology* 1983; **45**: 811-7.
337. Bendinger B, Rijnaarts HH, Altendorf K *et al.* Physicochemical cell surface and adhesive properties of coryneform bacteria related to the presence and chain length of mycolic acids. *Applied Environmental Microbiology* 1993; **59**: 3973-7.
338. Mittleman MW. Adhesion to biomaterials. *In: Fletcher, M editor Bacterial adheson: molecular and ecological diversity New York; Wiley-Liss, Inc* 1996: 89-127.
339. Al-Hashimi I, Levine MJ. Characterization of in vivo salivary-derived enamel pellicle. *Arcihives of Oral Biology* 1989; **34**: 289-95.
340. Stoodley P, Dodds I, Boyle JD *et al.* Influence of hydrodynamics and nutrients on biofilm structure. *Journal of Applied Microbiology* 1999; **85**: 19s-28s.
341. Stanley PM. Factors Affecting the irreversible attachment of *Pseudomonas-aeruginosa* to stainless-steel. *Canadian Journal of Microbiology* 1983; **29**: 1493-9.
342. Jucker BA, Harms H, Zehnder AJB. Adhesion of the positively charged bacterium *Stenotrophomonas (Xanthomonas) maltophilia* 70401 to glass and teflon. *Journal of Bacteriology* 1996; **178**: 5472-9.
343. Cappello S, Guglielmino SPP. Effects of growth temperature on the adhesion of *Pseudomonas aeruginosa* ATCC 27853 to polystyrene. *Annals of Microbiology* 2006; **56**: 383-5.
344. Kobayashi K. *Bacillus subtilis* pellicle formation proceeds through genetically defined morphological changes. *Journal of Bacteriology* 2007; **189**: 4920-31.
345. Wijman JG, de Leeuw PP, Moezelaar R *et al.* Air-liquid interface biofilms of *Bacillus cereus*: formation, sporulation, and dispersion. *Applied Environmental Microbiology* 2007; **73**: 1481-8.
346. Varga JJ, Therit B, Melville SB. Type IV pili and the CcpA protein are needed for maximal biofilm formation by the gram-positive anaerobic pathogen *Clostridium perfringens*. *Infection and Immunity* 2008; **76**: 4944-51.
347. Pratt LA, Kolter R. Genetic analysis of *Escherichia coli* biofilm formation: roles of flagella, motility, chemotaxis and type I pili. *Molecular Microbiology* 1998; **30**: 285-93.
348. Di Bonaventura G, Piccolomini R, Paludi D *et al.* Influence of temperature on biofilm formation by *Listeria monocytogenes* on various food-contact surfaces: relationship with motility and cell surface hydrophobicity. *Journal of Applied Microbiology* 2008; **104**: 1552-61.
349. Whitchurch CB, Erova TE, Emery JA *et al*. Phosphorylation of the *Pseudomonas aeruginosa* response regulator AlgR is essential for type IV fimbria-mediated twitching motility. *Journal of Bacteriology* 2002; **184**: 4544-54.
350. O'Toole GA, Kolter R. Flagellar and twitching motility are necessary for *Pseudomonas aeruginosa* biofilm development. *Molecular Microbiology* 1998; **30**: 295-304.
351. O'Toole G, Kaplan HB, Kolter R. Biofilm formation as microbial development. *Annual Reviews: Microbiology* 2000; **54**: 49-79.

352. Kolenbrander PE. Oral microbial communities: biofilms, interactions, and genetic systems. *Annual Reviews: Microbiology* 2000; **54**: 413-37.
353. Al-Ahmad A, Wunder A, Auschill TM *et al.* The in vivo dynamics of *Streptococcus* spp., *Actinomyces naeslundii*, *Fusobacterium nucleatum* and *Veillonella* spp. in dental plaque biofilm as analysed by five-colour multiplex fluorescence in situ hybridization. *Journal of Medical Microbiology* 2007; **56**: 681-7.
354. Palmer RJ, Jr., Gordon SM, Cisar JO *et al.* Coaggregation-mediated interactions of streptococci and actinomyces detected in initial human dental plaque. *Journal of Bacteriology* 2003; **185**: 3400-9.
355. Donelli G, Vuotto C, Cardines R *et al.* Biofilm-growing intestinal anaerobic bacteria. *FEMS Immunology and Medical Microbiology* 2012; **65**: 318-25.
356. Ledder RG, Timperley AS, Friswell MK *et al.* Coaggregation between and among human intestinal and oral bacteria. *Fems Microbiology Ecology* 2008; **66**: 630-6.
357. Debeer D, Stoodley P, Lewandowski Z. Liquid flow in heterogeneous biofilms. *Biotechnology and Bioengineering* 1994; **44**: 636-41.
358. Ito A, Taniuchi A, May T *et al*. Increased antibiotic resistance of *Escherichia coli* in mature biofilms. *Applied Environmental Microbiology* 2009; **75**: 4093-100.
359. Dunne WM, Jr. Bacterial adhesion: seen any good biofilms lately? *Clinical Microbiology Reviews* 2002; **15**: 155-66.
360. Davies DG, Parsek MR, Pearson JP *et al.* The involvement of cell-to-cell signals in the development of a bacterial biofilm. *Science* 1998; **280**: 295-8.
361. Stoodley P, Wilson S, Hall-Stoodley L *et al.* Growth and detachment of cell clusters from mature mixed-species biofilms. *Applied Environmental Microbiology* 2001; **67**: 5608-13.
362. Stoodley P, Hall-Stoodley L, Lappin-Scott HM. Detachment, surface migration, and other dynamic behavior in bacterial biofilms revealed by digital time-lapse imaging. *Methods in Enzymology* 2001; **337**: 306-19.
363. Hunt SM, Werner EM, Huang B *et al*. Hypothesis for the role of nutrient starvation in biofilm detachment. *Applied Environmental Microbiology* 2004; **70**: 7418-25.
364. Rice SA, Koh KS, Queck SY *et al*. Biofilm formation and sloughing in *Serratia marcescens* are controlled by quorum sensing and nutrient cues. *Journal of Bacteriology* 2005; **187**: 3477-85.
365. Boyd A, Chakrabarty AM. Role of alginate lyase in cell detachment of *Pseudomonas aeruginosa*. *Applied Environmental Microbiology* 1994; **60**: 2355-9.
366. Pecharki D, Petersen FC, Scheie AA. Role of hyaluronidase in *Streptococcus intermedius* biofilm. *Microbiology* 2008; **154**: 932-8.
367. Baty AM, 3rd, Eastburn CC, Techkarnjanaruk S *et al.* Spatial and temporal variations in chitinolytic gene expression and bacterial biomass production during chitin degradation. *Applied Environmental Microbiology* 2000; **66**: 3574-85.
368. Kaplan JB, Ragunath C, Ramasubbu N et al. Detachment of *Actinobacillus actinomycetemcomitans* biofilm cells by an endogenous beta-hexosaminidase activity. *Journal of Bacteriology* 2003; **185**: 4693-8.

369. Kaplan JB, Fine DH. Biofilm dispersal of *Neisseria subflava* and other phylogenetically diverse oral bacteria. *Applied Environmental Microbiology* 2002; **68**: 4943-50.
370. Tolker-Nielsen T, Brinch UC, Ragas PC *et al*. Development and dynamics of *Pseudomonas* sp. biofilms. *Journal of Bacteriology* 2000; **182**: 6482-9.
371. Sauer K, Camper AK, Ehrlich GD *et al*. *Pseudomonas aeruginosa* displays multiple phenotypes during development as a biofilm. *Journal of Bacteriology* 2002; **184**: 1140-54.
372. Hall-Stoodley L, Costerton JW, Stoodley P. Bacterial biofilms: from the natural environment to infectious diseases. *Nature Reviews: Microbiology* 2004; **2**: 95-108.
373. Mattick JS. Type IV pili and twitching motility. *Annual Reviews: Microbiology* 2002; **56**: 289-314.
374. Inglis TJ. Evidence for dynamic phenomena in residual tracheal tube biofilm. *British Journal of Anaesthesia* 1993; **70**: 22-4.
375. Tolker-Nielsen T, Molin S. Spatial organization of microbial biofilm communities. *Microbial Ecology* 2000; **40**: 75-84.
376. Lawrence JR, Swerhone GDW, Kuhlicke U *et al*. In situ evidence for microdomains in the polymer matrix of bacterial microcolonies. *Canadian Journal of Microbiology* 2007; **53**: 450-8.
377. Klausen M, Aaes-Jorgensen A, Molin S *et al*. Involvement of bacterial migration in the development of complex multicellular structures in *Pseudomonas aeruginosa* biofilms. *Molecular Microbiology* 2003; **50**: 61-8.
378. Flemming HC, Wingender J. The biofilm matrix. *Nature Reviews: Microbiology* 2010; **8**: 623-33.
379. Zhang XQ, Bishop PL, Kupferle MJ. Measurement of polysaccharides and proteins in biofilm extracellular polymers. *Water Science and Technology* 1998; **37**: 345-8.
380. Wingender J, Strathmann M, Rode A *et al.* Isolation and biochemical characterization of extracellular polymeric substances from *Pseudomonas aeruginosa*. *Microbial Growth in Biofilms, Pt A* 2001; **336**: 302-14.
381. Conrad A, Kontro M, Keinanen MM *et al.* Fatty acids of lipid fractions in extracellular polymeric substances of activated sludge flocs. *Lipids* 2003; **38**: 1093-105.
382. Davies DG, Geesey GG. Regulation of the alginate biosynthesis gene *algC* in *Pseudomonas aeruginosa* during biofilm development in continuous culture. *Applied Environmental Microbiology* 1995; **61**: 860-7.
383. Izano EA, Amarante MA, Kher WB *et al*. Differential roles of poly-N-acetylglucosamine surface polysaccharide and extracellular DNA in *Staphylococcus aureus* and *Staphylococcus epidermidis* biofilms. *Applied Environmental Microbiology* 2008; **74**: 470-6.
384. Sutherland I. Biofilm exopolysaccharides: a strong and sticky framework. *Microbiology* 2001; **147**: 3-9.
385. Danese PN, Pratt LA, Kolter R. Exopolysaccharide production is required for development of *Escherichia coli* K-12 biofilm architecture. *Journal of Bacteriology* 2000; **182**: 3593-6.
386. Hentzer M, Teitzel GM, Balzer GJ *et al.* Alginate overproduction affects *Pseudomonas aeruginosa* biofilm structure and function. *Journal of Bacteriology* 2001; **183**: 5395-401.

387. Watnick PI, Kolter R. Steps in the development of a *Vibrio cholerae* El Tor biofilm. *Molecular Microbiology* 1999; **34**: 586-95.
388. McKenney D, Hubner J, Muller E et al. The ica locus of *Staphylococcus epidermidis* encodes production of the capsular polysaccharide/adhesin. *Infection and Immunity* 1998; **66**: 4711-20.
389. Winson MK, Camara M, Latifi A *et al.* Multiple N-acyl-L-homoserine lactone signal molecules regulate production of virulence determinants and secondary metabolites in *Pseudomonas aeruginosa*. *Proceedings of National Academy of Sciences of the United States of America* 1995; **92**: 9427-31.
390. Pesci EC, Iglewski BH. The chain of command in Pseudomonas quorum sensing. *Trends Microbiol* 1997; **5**: 132-4; discussion 4-5.
391. Passador L, Cook JM, Gambello MJ *et al.* Expression of *Pseudomonas aeruginosa* virulence genes requires cell-to-cell communication. *Science* 1993; **260**: 1127-30.
392. Hoang HH, Gurich N, Gonzalez JE. Regulation of motility by the ExpR/Sin quorum-sensing system in *Sinorhizobium meliloti*. *Journal of Bacteriology* 2008; **190**: 861-71.
393. Skindersoe ME, Alhede M, Phipps R *et al.* Effects of antibiotics on quorum sensing in *Pseudomonas aeruginosa*. *Antimicrobial Agents Chemotherapy* 2008; **52**: 3648-63.
394. Li J, Chen J, Vidal JE *et al.* The Agr-like quorum-sensing system regulates sporulation and production of enterotoxin and beta2 toxin by *Clostridium perfringens* type A non-food-borne human gastrointestinal disease strain F5603. *Infection and Immunity* 2011; **79**: 2451-9.
395. Hammer BK, Bassler BL. Quorum sensing controls biofilm formation in *Vibrio cholerae*. *Molecular Microbiology* 2003; **50**: 101-4.
396. Meluleni GJ, Grout M, Evans DJ *et al.* Mucoid *Pseudomonas aeruginosa* growing in a biofilm in vitro are killed by opsonic antibodies to the mucoid exopolysaccharide capsule but not by antibodies produced during chronic lung infection in cystic fibrosis patients. *Journal of Immunology* 1995; **155**: 2029-38.
397. Moran FJ, Garcia C, Perez-Giraldo C *et al*. Phagocytosis and killing of slime-producing *Staphylococcus epidermidis* bypolymorphonuclear leukocytes. Effects of sparfloxacin. *Revista Espanola de Quimioterapia* 1998; **11**: 52-7.
398. Jensen ET, Kharazmi A, Garred P *et al.* Complement activation by *Pseudomonas aeruginosa* biofilms. *MicrobialPathogens* 1993; **15**: 377-88.
399. Ceri H, Olson ME, Stremick C *et al.* The Calgary Biofilm Device: new technology for rapid determination of antibiotic susceptibilities of bacterial biofilms. *Journal of Clinical Microbiology* 1999; **37**: 1771-6.
400. Olson ME, Ceri H, Morck DW *et al.* Biofilm bacteria: formation and comparative susceptibility to antibiotics. *Canadian Journal of Veterniary Research* 2002; **66**: 86-92.
401. Sepandj F, Ceri H, Gibb AP *et al.* Biofilm infections in peritoneal dialysis-related peritonitis: comparison of standard MIC and MBEC in evaluation of antibiotic sensitivity of coagulase-negative staphylococci. *Peritoneal Dialysis International* 2003; **23**: 77-9.
402. Post JC. Direct evidence of bacterial biofilms in otitis media. *Laryngoscope* 2001; **111**: 2083-94.

403. Post JC, Aul JJ, White GJ *et al.* PCR-based detection of bacterial DNA after antimicrobial treatment is indicative of persistent, viable bacteria in the chinchilla model of otitis media. *American Journal of Otolaryngology* 1996; **17**: 106-11.
404. Costerton W, Veeh R, Shirtliff M *et al*. The application of biofilm science to the study and control of chronic bacterial infections. *Journal of Clinical Investigation* 2003; **112**: 1466-77.
405. Griffith DP, Klein, A.S. Infection-induced urinary stones. In: Lippincott WW, ed. *Stones: Clinical management of urolithiasis*. New York, 1983.
406. Hatch RA, Schiller NL. Alginate lyase promotes diffusion of aminoglycosides through the extracellular polysaccharide of mucoid *Pseudomonas aeruginosa*. *Antimicrobial Agents and Chemotherapy* 1998; **42**: 974-7.
407. Shigeta M, Tanaka G, Komatsuzawa H *et al.* Permeation of antimicrobial agents through *Pseudomonas aeruginosa* biofilms: a simple method. *Chemotherapy* 1997; **43**: 340-5.
408. Baltimore RS, Cross AS, Dobek AS. The inhibitory effect of sodium alginate on antibiotic activity against mucoid and non-mucoid strains of *Pseudomonas aeruginosa*. *The Journal of Antimicrobial Chemotherapy* 1987; **20**: 815-23.
409. Anderl JN, Franklin MJ, Stewart PS. Role of antibiotic penetration limitation in *Klebsiella pneumoniae* biofilm resistance to ampicillin and ciprofloxacin. *Antimicrobial Agents and Chemotherapy* 2000; **44**: 1818-24.
410. Leid JG, Willson CJ, Shirtliff ME *et al.* The exopolysaccharide alginate protects *Pseudomonas aeruginosa* biofilm bacteria from IFN-gamma-mediated macrophage killing. *Journal of Immunology* 2005; **175**: 7512-8.
411. de Beer D, Stoodley P, Roe F *et al.* Effects of biofilm structures on oxygen distribution and mass transport. *Biotechnology and Bioengineering* 1994; **43**: 1131-8.
412. Ashby MJ, Neale JE, Knott SJ *et al.* Effect of antibiotics on non-growing planktonic cells and biofilms of *Escherichia coli*. *The Journal of Antimicrobial Chemotherapy* 1994; **33**: 443-52.
413. Tanaka G, Shigeta M, Komatsuzawa H *et al.* Effect of the growth rate of *Pseudomonas aeruginosa* biofilms on the susceptibility to antimicrobial agents: beta-lactams and fluoroquinolones. *Chemotherapy* 1999; **45**: 28-36.
414. Shigeta M, Komatsuzawa H, Sugai M *et al*. Effect of the growth rate of *Pseudomonas aeruginosa* biofilms on the susceptibility to antimicrobial agents. *Chemotherapy* 1997; **43**: 137-41.
415. Wentland EJ, Stewart PS, Huang CT *et al*. Spatial variations in growth rate within *Klebsiella pneumoniae* colonies and biofilm. *Biotechnology Progress* 1996; **12**: 316-21.
416. Jeffrey WH, Paul JH. Activity of an attached and free-living *Vibrio* sp. as measured by thymidine incorporation, p-iodonitrotetrazolium reduction, and ATP/DNA ratios. *Applied Environmental Microbiology* 1986; **51**: 150-6.
417. Davies DG, McFeters GA. Growth and comparative physiology of *Klebsiella oxytoca* attached to granular activated carbon particles and in liquid media. *Microbial Ecology* 1988; **15**: 165-75.

418. Booth SC, Workentine ML, Wen J *et al.* Differences in metabolism between the biofilm and planktonic response to metal stress. *Journal of Proteome Research* 2011; **10**: 3190-9.
419. Sauer K, Camper AK. Characterization of phenotypic changes in *Pseudomonas putida* in response to surface-associated growth. *Journal of Bacteriology* 2001; **183**: 6579-89.
420. Stanley NR, Britton RA, Grossman AD *et al*. Identification of catabolite repression as a physiological regulator of biofilm formation by *Bacillus subtilis* by use of DNA microarrays. *Journal of Bacteriology* 2003; **185**: 1951-7.
421. Whiteley M, Bangera MG, Bumgarner RE *et al.* Gene expression in *Pseudomonas aeruginosa* biofilms. *Nature* 2001; **413**: 860-4.
422. Huang CT, Yu FP, McFeters GA *et al.* Nonuniform spatial patterns of respiratory activity within biofilms during disinfection. *Applied Environmental Microbiology* 1995; **61**: 2252-6.
423. Brown MR, Barker J. Unexplored reservoirs of pathogenic bacteria: protozoa and biofilms. *Trends in Microbiology* 1999; **7**: 46-50.
424. Liu X, Ng C, Ferenci T. Global adaptations resulting from high population densities in *Escherichia coli* cultures. *Journal of Bacteriology* 2000; **182**: 4158-64.
425. Hengge-Aronis R. Recent insights into the general stress response regulatory network in *Escherichia coli*. *Journal of Molecular Microbiology and Biotechnology* 2002; **4**: 341-6.
426. King T, Ishihama A, Kori A *et al*. A regulatory trade-off as a source of strain variation in the species *Escherichia coli. Journal of Bacteriology* 2004; **186**: 5614-20.
427. van Hoek AH, Aarts HJ, Bouw E *et al.* The role of rpoS in *Escherichia coli* O157 manure-amended soil survival and distribution of allelic variations among bovine, food and clinical isolates. *FEMS Microbiology Letters* 2012.
428. Donlan RM. Biofilms and device-associated infections. *Emerging Infectious Diseases* 2001; **7**: 277-81.
429. Hall-Stoodley L, Hu FZ, Gieseke A *et al.* Direct detection of bacterial biofilms on the middle-ear mucosa of children with chronic otitis media. *Journal of American Medical Association* 2006; **296**: 202-11.
430. Singh PK, Schaefer AL, Parsek MR *et al*. Quorum-sensing signals indicate that cystic fibrosis lungs are infected with bacterial biofilms. *Nature* 2000; **407**: 762-4.
431. Parsek MR, Singh PK. Bacterial biofilms: an emerging link to disease pathogenesis. *Annual Reviews: Microbiology* 2003; **57**: 677-701.
432. Beloin C, Roux A, Ghigo JM. *Escherichia coli* biofilms. *Current Topice in Microbiology and Immunology* 2008; **322**: 249-89.
433. Tzipori S, Montanaro J, Robins-Browne RM *et al.* Studies with enteroaggregative *Escherichia coli* in the gnotobiotic piglet gastroenteritis model. *Infection and Immunity* 1992; **60**: 5302-6.
434. Vlamakis H, Aguilar C, Losick R *et al*. Control of cell fate by the formation of an architecturally complex bacterial community. *Genes and Development* 2008; **22**: 945-53.
435. Lopez D, Vlamakis H, Losick R et al. Cannibalism enhances biofilm development in *Bacillus subtilis. Molecular Microbiology* 2009; **74**: 609-18.

436. Fujita M, Gonzalez-Pastor JE, Losick R. High- and low-threshold genes in the Spo0A regulon of *Bacillus subtilis*. *Journal of Bacteriology* 2005; **187**: 1357-68.
437. Linton CJ, Sherriff A, Millar MR. Use of a modified Robbins device to directly compare the adhesion of *Staphylococcus epidermidis* RP62A to surfaces. *Journal of Applied Microbiology* 1999; **86**: 194-202.
438. Honraet K, Goetghebeur E, Nelis HJ. Comparison of three assays for the quantification of Candida biomass in suspension and CDC reactor grown biofilms. *Journal of Microbiology Methods* 2005; **63**: 287-95.
439. Parra-Ruiz J, Vidaillac C, Rose WE *et al.* Activities of high-dose daptomycin, vancomycin, and moxifloxacin alone or in combination with clarithromycin or rifampin in a novel in vitro model of *Staphylococcus aureus* biofilm. *Antimicrobial Agents and Chemotherapy* 2010; **54**: 4329-34.
440. Kinniment SL, Wimpenny JW, Adams D *et al.* Development of a steady-state oral microbial biofilm community using the constant-depth film fermenter. *Microbiology* 1996; **142 (Pt 3)**: 631-8.
441. Keevil CW, Bradshaw DJ, Dowsett AB *et al*. Microbial film formation: dental plaque deposition on acrylic tiles using continuous culture techniques. *Journal of Applied Bacteriology* 1987; **62**: 129-38.
442. Gilbert P, Allison DG, Evans DJ *et al.* Growth rate control of adherent bacterial populations. *Applied Environmental Microbiology* 1989; **55**: 1308-11.
443. Hodgson AE, Nelson SM, Brown MR *et al.* A simple in vitro model for growth control of bacterial biofilms. *Journal of Applied Bacteriology* 1995; **79**: 87-93.
444. Li YH, Bowden GH. Characteristics of accumulation of oral gram-positive bacteria on mucin-conditioned glass surfaces in a model system. *Oral Microbiology and Immunology* 1994; **9**: 1-11.
445. Muli F, Struthers JK. Use of a continuous-culture biofilm system to study the antimicrobial susceptibilities of *Gardnerella vaginalis* and *Lactobacillus acidophilus*. *Antimicrobial Agents and Chemotherapy* 1998; **42**: 1428-32.
446. Macfarlane S, Woodmansey EJ, Macfarlane GT. Colonization of mucin by human intestinal bacteria and establishment of biofilm communities in a two-stage continuous culture system. *Applied Environmental Microbiology* 2005; **71**: 7483-92.
447. Gibson GR, Probert, HM. Development of a fermentation system to model sessile bacterial populations in the human colon. *Biofilms* 2004; **1**: 13-9.
448. Schaller M, Zakikhany K, Naglik JR *et al.* Models of oral and vaginal candidiasis based on in vitro reconstituted human epithelia. *Nature Protocols* 2006; **1**: 2767-73.
449. Grubb SEW, Murdoch C, Sudbery PE *et al*. Adhesion of *Candida albicans* to endothelial cells under physiological conditions of flow. *Infectection and Immunity* 2009; **77**: 3872-8.
450. Kim J, Hegde M, Jayaraman A. Microfluidic co-culture of epithelial cells and bacteria for investigating soluble signal-mediated interactions. *Journal of Visualized Experiments* 2010.
451. Macfarlane S, Dillon JF. Microbial biofilms in the human gastrointestinal tract. *Journal of Applied Microbiology* 2007; **102**: 1187-96.

452. Macfarlane S, Furrie E, Cummings JH *et al*. Chemotaxonomic analysis of bacterial populations colonizing the rectal mucosa in patients with ulcerative colitis. *Clinical infectious diseases : an official publication of the Infectious Diseases Society of America* 2004; **38**: 1690-9.
453. Gomez-Trevino M BH, Karjalainen T, Bourlioux P. *Clostridium difficile* adherence to mucus: results of an in vivo and ex vivo assay. *Microbial Ecology in Health and Disease* 1996; **9**: 329-34.
454. Ethapa T, Leuzzi R, Ng YK *et al.* Multiple factors modulate biofilm formation by the anaerobic pathogen *Clostridium difficile*. *Journal of Bacteriology* 2012.
455. Dawson LF, Valiente E, Faulds-Pain A *et al.* Characterisation of *Clostridium difficile* biofilm formation, a role for Spo0A. *PLoS One* 2012; **7**.
456. Mishra NN, Prasad T, Sharma N *et al*. Pathogenicity and drug resistance in *Candida albicans* and other yeast species. A review. *Acta Microbiologica et Immunologica Hungarica* 2007; **54**: 201-35.
457. Laning ML. Characterization of the *Clostridium difficile* biofilm. *Program in Infectious Disease and Immunology*: Loyola University Chicago, 2012.
458. Hickman JW, Tifrea DF, Harwood CS. A chemosensory system that regulates biofilm formation through modulation of cyclic diguanylate levels. *Proceedings of the National Academy of Sciences of the United States of America* 2005; **102**: 14422-7.
459. Newell PD, Monds RD, O'Toole GA. LapD is a bis-(3',5')-cyclic dimeric GMP-binding protein that regulates surface attachment by *Pseudomonas fluorescens* Pf0-1. *Proceedings of th National Academy of Sciences of the United States of America* 2009; **106**: 3461-6.
460. Tischler AD, Camilli A. Cyclic diguanylate (c-di-GMP) regulates *Vibrio cholerae* biofilm formation. *Molecular Microbiology* 2004; **53**: 857-69.
461. Mendez-Ortiz MM, Hyodo M, Hayakawa Y *et al.* Genome-wide transcriptional profile of *Escherichia coli* in response to high levels of the second messenger 3',5'-cyclic diguanylic acid. *Journal of Biology and Chemistry* 2006; **281**: 8090-9.
462. Albert-Weissenberger C, Sahr T, Sismeiro O *et al.* Control of flagellar gene regulation in *Legionella pneumophila* and its relation to growth phase. *Journal of Bacteriology* 2010; **192**: 446-55.
463. Huang B, Whitchurch CB, Mattick JS. FimX, a multidomain protein connecting environmental signals to twitching motility in *Pseudomonas aeruginosa*. *Journal of Bacteriology* 2003; **185**: 7068-76.
464. Kazmierczak BI, Lebron MB, Murray TS. Analysis of FimX, a phosphodiesterase that governs twitching motility in *Pseudomonas aeruginosa*. *Molecular Microbiology* 2006; **60**: 1026-43.
465. Sommerfeldt N, Possling A, Becker G *et al.* Gene expression patterns and differential input into curli fimbriae regulation of all GGDEF/EAL domain proteins in *Escherichia coli*. *Microbiology* 2009; **155**: 1318-31.
466. Kulasakara H, Lee V, Brencic A *et al.* Analysis of *Pseudomonas aeruginosa* diguanylate cyclases and phosphodiesterases reveals a role for bis-(3'-5')-cyclic-GMP in virulence. *Proceedings of the National Academy of Sciences of the United States of America* 2006; **103**: 2839-44.
467. Tischler AD, Camilli A. Cyclic diguanylate regulates *Vibrio cholerae* virulence gene expression. *Infection and Immunity* 2005; **73**: 5873-82.

468. Malone JG, Jaeger T, Spangler C *et al*. YfiBNR mediates cyclic di-GMP dependent small colony variant formation and persistence in *Pseudomonas aeruginosa*. *PLoS Pathogens* 2010; **6**: e1000804.
469. Hisert KB, MacCoss M, Shiloh MU *et al*. A glutamate-alanine-leucine (EAL) domain protein of Salmonella controls bacterial survival in mice, antioxidant defence and killing of macrophages: role of cyclic diGMP. *Molecular Microbiology* 2005; **56**: 1234-45.
470. Sebaihia M, Wren BW, Mullany P *et al*. The multidrug-resistant human pathogen *Clostridium difficile* has a highly mobile, mosaic genome. *Nature Genetics* 2006; **38**: 779-86.
471. Purcell EB, McKee RW, McBride SM *et al*. Cyclic diguanylate inversely regulates motility and aggregation in *Clostridium difficile*. *Journal of Bacteriology* 2012; **194**: 3307-16.
472. Brazier JS, Borriello SP. Microbiology, epidemiology and diagnosis of *Clostridium difficile* infection. *Current Topics in Microbiology Immunology* 2000; **250**: 1-33.
473. Chilton CH, Freeman J, Crowther GS *et al*. Co-amoxiclav induces proliferation and cytotoxin production of *Clostridium difficile* ribotype 027 in a human gut model. *The Journal of Antimicrobial Chemotherapy* 2012; **67**: 951-4.
474. Freeman J, Baines SD, Jabes D *et al*. Comparison of the efficacy of ramoplanin and vancomycin in both in vitro and in vivo models of clindamycin-induced *Clostridium difficile* infection. *The Journal of Antimicrobial Chemotherapy* 2005; **56**: 717-25.
475. Heginbothom M, Fitzgerald TC, Wade WG. Comparison of solid media for cultivation of anaerobes. *Journal of Clinical Pathology* 1990; **43**: 253-6.
476. Hartemink R, Domenech, VR, Rombouts, FM. LAMVAB - A new selective medium for theisolation of lactobacilli from faeces. *Journal of microbiological methods* 1997; **29**: 77-84.
477. Beerens H. Detection of Bifidobacteria by using propionic acid as a selective agent. *American Society for Microbiology* 1991; **57**: 2418-9.
478. Freeman J. Antibiotic related virulence factors in *Clostridium difficile*. *School of Biochemistry and Molecular Biology*. Leeds: University of Leeds, 2001.
479. Drummond LJ, Smith DG, Poxton IR. Effects of sub-MIC concentrations of antibiotics on growth of and toxin production by *Clostridium difficile*. *Journal of Medical Microbiology* 2003; **52**: 1033-8.
480. Borriello SP. 12th C. L. Oakley lecture. Pathogenesis of *Clostridium difficile* infection of the gut. *Journal of Medical Microbiology* 1990; **33**: 207-15.
481. Larson HE, Borriello SP. Quantitative study of antibiotic-induced susceptibility to *Clostridium difficile* enterocecitis in hamsters. *Antimicrobial Agents and Chemotherapy* 1990; **34**: 1348-53.
482. Zmantar T, Kouidhi B, Miladi H *et al*. A microtiter plate assay for *Staphylococcus aureus* biofilm quantification at various pH levels and hydrogen peroxide supplementation. *New Microbiologica* 2010; **33**: 137-45.
483. Djordjevic D, Wiedmann M, McLandsborough LA. Microtiter plate assay for assessment of Listeria monocytogenes biofilm formation. *Appl Environmental Microbiology* 2002; **68**: 2950-8.

484. Bridier A, Le Coq D, Dubois-Brissonnet F et al. The spatial architecture of *Bacillus subtilis* biofilms deciphered using a surface-associated model and in situ imaging. *PLoS One* 2011; **6**: e16177.
485. Caiazza NC, O'Toole GA. SadB is required for the transition from reversible to irreversible attachment during biofilm formation by *Pseudomonas aeruginosa* PA14. *Journal of Bacteriology* 2004; **186**: 4476-85.
486. Kennedy CA, O'Gara JP. Contribution of culture media and chemical properties of polystyrene tissue culture plates to biofilm development by *Staphylococcus aureus*. *Journal of Medical Microbiology* 2004; **53**: 1171-3.
487. Salton MRJ. The adsorption of cetyltrimethylammonium bromide by bacteria, its action in releasing cellular constituents and its bactericidal effects. *Journal of General Microbiology* 1951; **5**: 391-404.
488. Manzo N, D'Apuzzo E, Coutinho PM *et al.* Carbohydrate-active enzymes from pigmented Bacilli: a genomic approach to assess carbohydrate utilization and degradation. *BMC microbiology* 2011; **11**.
489. Ruseler-van Embden JG, van Lieshout LM, Gosselink MJ et al. Inability of *Lactobacillus casei* strain GG, *L. acidophilus*, and *Bifidobacterium bifidum t*o degrade intestinal mucus glycoproteins. *Scandinavian journal of gastroenterology* 1995; **30**: 675-80.
490. Zhou JS, Gopal PK, Gill HS. Potential probiotic lactic acid bacteria *Lactobacillus rhamnosus* (HN001), *Lactobacillus acidophilus* (HN017) and *Bifidobacterium lactis* (HN019) do not degrade gastric mucin in vitro. *International Journal of Food Microbiology* 2001; **63**: 81-90.
491. Doolittle MM, Cooney JJ, Caldwell DE. Lytic Infection of *Escherichia-coli b*iofilms by bacteriophage-T4. *Canadian Journal of Microbiology* 1995; **41**: 12-8.
492. Anwar H, Strap JL, Costerton JW. Eradication of biofilm cells of *Staphylococcus-aureus* with tobramycin and cephalexin. *Canadian Journal of Microbiology* 1992; **38**: 618-25.
493. Bloomfield SF, Arthur M, Begun K *et al.* Comparative testing of disinfectants using proposed European surface test methods. *Letters in Applied Microbiology* 1993; **17**: 119-25.
494. Jeong DK, Frank JF. Growth of *Listeria-monocytogenes* at 10-degrees-C in biofilms with microorganisms isolated from meat and dairy processing environments. *Journal of Food Protection* 1994; **57**: 576-86.
495. GomezTrevino M, Boureau H, Karjalainen T *et al. Clostridium difficile* adherence to mucus: Results of an in vivo and ex vivo assay. *Microbial Ecology in Health and Disease* 1996; **9**: 329-34.
496. Freter R, O'Brien PC, Macsai MS. Role of chemotaxis in the association of motile bacteria with intestinal mucosa: in vivo studies. *Infection and Immunity* 1981; **34**: 234-40.
497. Freter R, Allweiss B, O'Brien PC *et al*. Role of chemotaxis in the association of motile bacteria with intestinal mucosa: in vitro studies. *Infection and Immunity* 1981; **34**: 241-9.
498. Joshi LT, Phillips DS, Williams CF *et al.* Contribution of spores to the ability of *Clostridium difficile* to adhere to surfaces. *Applied Environmental Microbiology* 2012; **78**: 7671-9.
499. Macfarlane GT, Hay S, Gibson GR. Influence of mucin on glycosidase, protease and arylamidase activities of human gut bacteria

grown in a 3-stage continuous culture system. *Journal of Applied Bacteriology* 1989; **66**: 407-17.
500. Deplancke B, Gaskins HR. Microbial modulation of innate defense: goblet cells and the intestinal mucus layer. *American Journal of Clinical Nutrition* 2001; **73**: 1131S-41S.
501. Prizont R, Konigsberg N. Identification of bacterial glycosidases in rat cecal contents. *Digestive Diseases and Science* 1981; **26**: 773-7.
502. Katayama T, Fujita K, Yamamoto K. Novel bifidobacterial glycosidases acting on sugar chains of mucin glycoproteins. *Journal of Bioscienc and Bioengineering* 2005; **99**: 457-65.
503. Aminoff D, Furukawa K. Enzymes that destroy blood group specificity. I. Purification and properties of alpha-L-fucosidase from *Clostridium perfringens*. *Journal of Biology and Chemistry* 1970; **245**: 1659-69.
504. Boureau H, Decre D, Carlier JP *et al.* Identification of a *Clostridium cocleatum* strain involved in an anti-*Clostridium difficile* barrier effect and determination of its mucin-degrading enzymes. *Research in Microbiology* 1993; **144**: 405-10.
505. Stanley RA. Degradation and utilization of mucins by anaerobic bacteria from the colon. *Biochemistry*. Auckland: University of Auckland, 1982.
506. Rafay AM, Homer KA, Beighton D. Effect of mucin and glucose on proteolytic and glycosidic activities of *Streptococcus oralis*. *Journal of Medical Microbiology* 1996; **44**: 409-17.
507. Wright DP, Rosendale DI, Roberton AM. Prevotella enzymes involved in mucin oligosaccharide degradation and evidence for a small operon of genes expressed during growth on mucin. *FEMS Microbiology Letters* 2000; **190**: 73-9.
508. Abe F, Muto M, Yaeshima T et al. Safety evaluation of probiotic bifidobacteria by analysis of mucin degradation activity and translocation ability. *Anaerobe* 2010; **16**: 131-6.
509. Stanley RA, Ram SP, Wilkinson RK et al. Degradation of pig gastric and colonic mucins by bacteria isolated from the pig colon. *Applied Environmental Microbiology* 1986; **51**: 1104-9.
510. Kindon H, Pothoulakis C, Thim L *et al*. Trefoil peptide protection of intestinal epithelial barrier function: cooperative interaction with mucin glycoprotein. *Gastroenterology* 1995; **109**: 516-23.
511. Macfarlane GT, Macfarlane S, Gibson GR. Validation of a three-stage compound continuous culture system for investigating the effect of retention time on the ecology and metabolism of bacteria in the human colon. *Microbial Ecology* 1998; **35**: 180-7.
512. Baines SD, O'Connor R, Saxton K *et al*. Activity of vancomycin against epidemic *Clostridium difficile* strains in a human gut model. *Journal of Antimicrobial Chemotherapy* 2009; **63**: 520-5.
513. Gerding DN, Olson MM, Peterson LR *et al. Clostridium difficile*-associated diarrhea and colitis in adults. A prospective case-controlled epidemiologic study. *Archive of Internal Medicine* 1986; **146**: 95-100.
514. Brown RB, Martyak SN, Barza M *et al.* Penetration of clindamycin phosphate into the abnormal human biliary tract. *Annals of Internal Medicine* 1976; **84**: 168-70.

515. Chilton CH, Freeman J, Crowther GS *et al.* Effectiveness of a short (4 day) course of oritavancin in the treatment of simulated *Clostridium difficile* infection using a human gut model. *The Journal of Antimicrobial Chemotherapy* 2012; **67**: 2434-7.
516. Hancock V, Witso IL, Klemm P. Biofilm formation as a function of adhesin, growth medium, substratum and strain type. *International Journal of Medical Microbiology* 2011; **301**: 570-6.
517. Giaouris E, Chorianopoulos N, Nychas GJ. Effect of temperature, pH, and water activity on biofilm formation by *Salmonella enterica* enteritidis PT4 on stainless steel surfaces as indicated by the bead vortexing method and conductance measurements. *Journal of Food Protection* 2005; **68**: 2149-54.
518. Lindsay D, Brozel VS, Von Holy A. Biofilm-spore response in *Bacillus cereus* and *Bacillus subtilis* during nutrient limitation. *Journal of Food Protection* 2006; **69**: 1168-72.
519. Fuqua WC, Winans SC, Greenberg EP. Quorum sensing in bacteria: the LuxR-LuxI family of cell density-responsive transcriptional regulators. *Journal of Bacteriology* 1994; **176**: 269-75.
520. Sebastian AP, Keerthi TR. Adhesion and cellsurface properties of wild species of spore formers against enteric pathogens. *Asian Pacific Journal of Tropical Medicine* 2013; **6**: 110-4.
521. Freeman J, Marquis M, Crowther GS *et al.* Oritavancin does not induce *Clostridium difficile* germination and toxin production in hamsters or a human gut model. *The Journal of Antimicrobial Chemotherapy* 2012; **67**: 2919-26.
522. Chilton CH, Freeman J, Baines SD *et al*. Evaluation of the effect of oritavancin on *Clostridium difficile* spore germination, outgrowth and recovery. *The Journal of Antimicrobial Chemotherapy* 2013.
523. McKay GA, Beaulieu S, Arhin FF *et al*. Time-kill kinetics of oritavancin and comparator agents against *Staphylococcus aureus*, *Enterococcus faecalis* and *Enterococcus faecium*. *The Journal of Antimicrobial Chemotherapy* 2009; **63**: 1191-9.
524. Belley A, Neesham-Grenon E, McKay G *et al*. Oritavancin kills stationary-phase and biofilm *Staphylococcus aureus* cells in vitro. *Antimicrobial Agents and Chemotherapy* 2009; **53**: 918-25.
525. Crowther GS, Baines SD, Todhunter SL *et al.* Evaluation of NVB302 versus vancomycin activity in an in vitro human gut model of *Clostridium difficile* infection. *The Journal of Antimicrobial Chemotherapy* 2013; **68**: 168-76.
526. Stewart PS, Davison WM, Steenbergen JN. Daptomycin rapidly penetrates a *Staphylococcus epidermidis* biofilm. *Antimicrobial Agents and Chemotherapy* 2009; **53**: 3505-7.
527. Chilton CH, Crowther G, Freeman J *et al.*. Successful Treatment of Simulated *Clostridium difficile* Infection in a Human Gut Model by Fidaxomycin After Vancomycin or Metrondazole Failure. *52nd Interscience Conference on Antimicrobial Agents and Chemotherapy*. San Francisco, 2012; 105.
528. van der Waal SV, van der Sluis LW, Ozok AR *et al.* The effects of hyperosmosis or high pH on a dual-species biofilm of *Enterococcus faecalis* and *Pseudomonas aeruginosa*: an in vitro study. *International Endodontic Journal* 2011; **44**: 1110-7.

529. Hamon MA, Lazazzera BA. The sporulation transcription factor Spo0A is required for biofilm development in *Bacillus subtilis*. *Molecular Microbiology* 2001; **42**: 1199-209.
530. Veening JW, Kuipers OP, Brul S *et al*. Effects of phosphorelay perturbations on architecture, sporulation, and spore resistance in biofilms of *Bacillus subtilis*. *Journal of Bacteriology* 2006; **188**: 3099-109.
531. Ghosh S, Zhang P, Li YQ *et al*. Superdormant spores of *Bacillus* species have elevated wet-heat resistance and temperature requirements for heat activation. *Journal of Bacteriology* 2009; **191**: 5584-91.
532. Wei J, Shah IM, Ghosh S *et al*. Superdormant spores of bacillus species germinate normally with high pressure, peptidoglycan fragments, and bryostatin. *Journal of Bacteriology* 2010; **192**: 1455-8.
533. Ghosh S, Scotland M, Setlow P. Levels of germination proteins in dormant and superdormant spores of *Bacillus subtilis*. *Journal of Bacteriology* 2012; **194**: 2221-7.
534. Perez-Valdespino A, Ghosh S, Cammett EP *et al.* Isolation and characterization of *Bacillus subtilis* spores that are superdormant for germination with dodecylamine or Ca(2+) -dipicolinic acid. *Journal of Applied Microbiology* 2013; **114**: 1109-19.
535. Nerandzic MM, Donskey CJ. Triggering germination represents a novel strategy to enhance killing of *Clostridium difficile* spores. *PLoS One* 2010; **5**: e12285.
536. Sternberg C, Christensen BB, Johansen T *et al.* Distribution of bacterial growth activity in flow-chamber biofilms. *Applied Environmental Microbiology* 1999; **65**: 4108-17.
537. Lewis K. Persister cells and the riddle of biofilm survival. *Biochemistry-Moscow* 2005; **70**: 267-+.
538. Baines SD, Crowther GS, Todhunter SL *et al.* Mixed infection by *Clostridium difficile* in an in vitro model of the human gut. *The Journal of Antimicrobial Chemotherapy* 2013; **68**: 1139-43.
539. Wheeldon LJ, Worthington T, Hilton AC *et al*. Physical and chemical factors influencing the germination of *Clostridium difficile* spores. *Journal of Applied Microbiology* 2008; **105**: 2223-30.
540. Onderdonk AB, Lowe BR, Bartlett JG. Effect of environmental stress on *Clostridium difficile* toxin levels during continuous cultivation. *Applied Environmental Microbiology* 1979; **38**: 637-41.
541. Qa'Dan M, Spyres LM, Ballard JD. pH-induced conformational changes in *Clostridium difficile* toxin B. *Infection and Immunity* 2000; **68**: 2470-4.
542. Freeman J, Wilcox MH. The effects of storage conditions on viability of *Clostridium difficile* vegetative cells and spores and toxin activity in human faeces. *Journal of Clinical Pathology* 2003; **56**: 126-8.
543. Castagliuolo I, Riegler MF, Valenick L *et al. Saccharomyces boulardii* protease inhibits the effects of *Clostridium difficile* toxins A and B in human colonic mucosa. *Infection and Immunity* 1999; **67**: 302-7.
544. Castagliuolo I, LaMont JT, Nikulasson ST *et al*. *Saccharomyces boulardii* protease inhibits *Clostridium difficile* toxin A effects in the rat ileum. *Infection and Immunity* 1996; **64**: 5225-32.

545. Dunne WM, Jr., Mason EO, Jr., Kaplan SL. Diffusion of rifampin and vancomycin through a *Staphylococcus epidermidis* biofilm. *Antimicrobial Agents and Chemotherapy* 1993; **37**: 2522-6.
546. Allen CA, Babakhani F, Sears P *et al.* Both fidaxomicin and vancomycin inhibit outgrowth of *Clostridium difficile* spores. *Antimicrobial Agents and Chemotherapy* 2013; **57**: 664-7.
547. Chilton CH, Crowther GS, *et al* . Fidaxomicin persistence in an in vitro human gut model, and adherence to *Clostridium difficile* spores. *23 rd European Society of Clinical Microbiology and Infectious Diseases*. Berlin, Germany, 2013; 109.
548. Louie TJ, Miller MA, Mullane KM *et al*. Fidaxomicin versus Vancomycin for *Clostridium difficile* Infection. *New England Journal of Medicine* 2011; **364**: 422-31.
549. Baines SD, Chilton CH, Crowther GS *et al.* Evaluation of antimicrobial activity of ceftaroline against *Clostridium difficile* and propensity to induce C. difficile infection in an in vitro human gut model. *The Journal of Antimicrobial Chemotherapy* 2013.
550. Ahmed S, Macfarlane GT, Fite A *et al.* Mucosa-associated bacterial diversity in relation to human terminal ileum and colonic biopsy samples. *Applied and Environmental Microbiology* 2007; **73**: 7435-42.
551. Boontheekul T, Kong HJ, Mooney DJ. Controlling alginate gel degradation utilizing partial oxidation and bimodal molecular weight distribution. *Biomaterials* 2005; **26**: 2455-65.
552. Smidsrod O, Skjak-Braek G. Alginate as immobilization matrix for cells. *Trends Biotechnol* 1990; **8**: 71-8.
553. Boyd J, Turvey JR. Isolation of poly-alpha-L-guluronate lyase from Klebsiella aerogenes. *Carbohydrate Research* 1977; **57**: 163-71.
554. Linker A, Evans LR. Isolation and characterization of an alginase from mucoid strains of *Pseudomonas aeruginosa. Journal of Bacteriology* 1984; **159**: 958-64.
555. Kitamikado M, Tseng CH, Yamaguchi K *et al.* Two types of bacterial alginate lyases. *Applied Environmental Microbiology* 1992; **58**: 2474-8.
556. Davidson IW, Sutherland IW, Lawson CJ. Purification and properties of an alginate lyase from a marine bacterium. *The Biochemistry Journal* 1976; **159**: 707-13.
557. Fuongfuchat A, Jamieson AM, Blackwell J *et al.* Rheological studies of the interaction of mucins with alginate and polyacrylate. *Carbohydrate Research* 1996; **284**: 85-99.
558. Cohen PS, Rossoll R, Cabelli VJ *et al.* Relationship between the mouse colonizing ability of a human fecal *Escherichia coli* strain and its ability to bind a specific mouse colonic mucous gel protein. *Infection and Immunity* 1983; **40**: 62-9.
559. Macfarlane GT, Gibson GR. Formation of glycoprotein degrading enzymes by *Bacteroides fragilis*. *FEMS Microbiology Letters* 1991; **61**: 289-93.
560. Scheline RR. Metabolism of phenolic acids by the rat intestinal microflora. *Acta Pharmacologica Toxicologica (Copenh)* 1968; **26**: 189-205.
561. Wilson KH, Perini F. Role of competition for nutrients in suppression of *Clostridium difficile* by the colonic microflora. *Infection and Immunity* 1988; **56**: 2610-4.

562. Popoff MR, Dodin A. Survey of neuraminidase production by *Clostridium butyricum, Clostridium beijerinckii,* and *Clostridium difficile* strains from clinical and nonclinical sources. *Journal of clinical microbiology* 1985; **22**: 873-6.
563. Probert HM, Gibson GR. Bacterial biofilms in the human gastrointestinal tract. *Current Issues in Intestestinal Microbiology* 2002; **3**: 23-7.
564. Schwarz WH. The cellulosome and cellulose degradation by anaerobic bacteria. *Applied Microbiology Biotechnology* 2001; **56**: 634-49.
565. Bryers J, Characklis W. Early fouling biofilm formation in a turbulent-flow system - overall kinetics. *Water Research* 1981; **15**: 483-91.
566. Trulear MGaC, W.G. Dynamics of biofilm processes. *Journal (Water Pollutions Control Federation)* 1982; **54**: 1288-301.
567. Duddridge JE, Kent CA, Laws JF. Effect of surface shear-stress on the attachment of *Pseudomonas-fluorescens* to stainless-steel under defined flow conditions. *Biotechnology Bioengineering* 1982; **24**: 153-64.
568. Lau YL, Liu D. Effect of Flow-rate on biofilm accumulation in open channels. *Water Research* 1993; **27**: 355-60.
569. Heijnen JJ, Vanloosdrecht MCM, Mulder A *et al*. Formation of biofilms in a biofilm airlift suspension reactor. *Water Science Technology* 1992; **26**: 647-54.
570. Gjaltema A, vander Marel N, vanLoosdrecht MCM Adhesion and biofilm development on suspended carriers in airlift reactors: Hydrodynamic conditions versus surface characteristics. *Biotechnology and Bioengineering* 1997; **55**: 880-9.
571. Costerton JW, Lewandowski Z, Caldwell DE *et al.* Microbial biofilms. *Annual Review of Microbiology* 1995; **49**: 711-45.
572. Dexter SC, Sullivan JD, Williams J et al. Influence of substrate wettability on the attachment of marine bacteria to various surfaces. *Applied Microbiology* 1975; **30**: 298-308.
573. Oliveira R, Azeredo J, Teixeira P *et al*. The role of hydrophobicity in bacterial adhesion. In: Gilbert P, Allison, D., Brading, M., Verran, J. and Walker, J., ed. *Biofilm Community and Interactions: Chance or Necessity?* Bioline, Cardiff, 2001.
574. van Dijk J, Herkstroter F, Busscher H *et al.* Surface-free energy and bacterial adhesion. An in vivo study in beagle dogs. *Journal of Clinical Periodontology* 1987; **14**: 300-4.
575. Chavant P, Martinie B, Meylheuc T *et al. Listeria monocytogenes* LO28: surface physicochemical properties and ability to form biofilms at different temperatures and growth phases. *Applied and Environmental Microbiology* 2002; **68**: 728-37.
576. Baines SD, Noel AR, Huscroft GS *et al*. Evaluation of linezolid for the treatment of *Clostridium difficile* infection caused by epidemic strains using an in vitro human gut model. *The Journal of Antimicrobial Chemotherapy* 2011; **66**: 1537-46.
577. Lee SF, Li YH, Bowden GH. Detachment of *Streptococcus mutans* biofilm cells by an endogenous enzymatic activity. *Infection and Immunity* 1996; **64**: 1035-8.
578. Baines SD, Saxton K, Freeman J *et al*. Tigecycline does not induce proliferation or cytotoxin production by epidemic *Clostridium difficile* strains

in a human gut model. *The Journal of Antimicrobial Chemotherapy* 2006; **58**: 1062-5.
579. De Beer D, Srinivasan R, Stewart PS. Direct measurement of chlorine penetration into biofilms during disinfection. *Applied Environmental Microbiology* 1994; **60**: 4339-44.
580. Zijnge V, van Leeuwen MB, Degener JE *et al.* Oral biofilm architecture on natural teeth. *Plos One* 2010; **5**: e9321.
581. Davies D. Understanding biofilm resistance to antibacterial agents. *Nature Reviews Drug Discovery* 2003; **2**: 114-22.
582. Cha JO, Park YK, Lee YS *et al.* In vitro biofilm formation and bactericidal activities of methicillin-resistant *Staphylococcus aureus* clones prevalent in Korea. *Diagnostic Microbiology and Infectious Disease* 2011; **70**: 112-8.
583. Furustrand Tafin U, Corvec S, Betrisey B *et al*. Role of rifampin against *Propionibacterium acnes* biofilm *in vitro* and in an experimental foreign-body infection model. *Antimicrobial Agents and Chemotherapy* 2012; **56**: 1885-91.
584. Smith K, Perez A, Ramage G *et al.* Comparison of biofilm-associated cell survival following in vitro exposure of meticillin-resistant *Staphylococcus aureus* biofilms to the antibiotics clindamycin, daptomycin, linezolid, tigecycline and vancomycin. *International Journal of Antimicrobial Agents* 2009; **33**: 374-8.
585. Darouiche RO, Dhir A, Miller AJ *et al.* Vancomycin penetration into biofilm covering infected prostheses and effect on bacteria. *Journal of Infectious Diseases* 1994; **170**: 720-3.
586. Chilton CH, Crowther GS, Freeman J *et al*. Successful treatment of simulated *Clostridium difficile* infection in a human gut model by fidaxomicin first line and after vancomycin or metronidazole failure. *The Journal of Antimicrobial Chemotherapy* 2013.
587. Cargill JS, Upton M. Low concentrations of vancomycin stimulate biofilm formation in some clinical isolates of *Staphylococcus epidermidis. Journal of Clinical Pathology* 2009; **62**: 1112-6.
588. Kaplan JB. Antibiotic-induced biofilm formation. *International Journal of Artificial Organs* 2011; **34**: 737-51.
589. Gjermansen M, Ragas P, Sternberg C *et al.* Characterization of starvation-induced dispersion in *Pseudomonas putida* biofilms. *Environmental Microbiology* 2005; **7**: 894-906.
590. Spoering AL, Lewis K. Biofilms and planktonic cells of *Pseudomonas aeruginosa* have similar resistance to killing by antimicrobials. *Journal of Bacteriology* 2001; **183**: 6746-51.
591. Sonenshein AL. Control of sporulation initiation in *Bacillus subtilis*. *Current Opinions in Microbiology* 2000; **3**: 561-6.
592. Dawson LF, Valiente E, *et al* Production of biofilms by *Clostridium difficile* is affected by Spo0A. *4th International Clostridium Difficile Sympsium* 2012; **Abstract P12**: 88.

List of Abbreviations

Abbreviation	Full text
ADP	Adenosine diphosphate
AHL	Acyl-homoserine lactone
Amox	Co-amoxiclav
ATCC	American Type Culture Collection
BD	Twice daily
BHI	Brain heart infusion
BSAC	British Society for Antimicrobial Chemotherapy
CBD	Calgary biofilm device
CC	Cytotoxigenic culture
CCEYL	Cycloserine cefoxitin egg yolk lysozyme agar
CCEYLM	Cycloserine cefoxitin egg yolk lysozyme moxifolxacin agar
CD	*Clostridium difficile*
CDAD	*Clostridium difficile*-associated diarrhoea
c-di-GMP	3′, 5′-cyclic diguanylic acid
CDI	*Clostridium difficile* infection
CDRN	*Clostridium difficile* ribotyping network
CDT	*Clostridium difficile* transferase
CFU	Colony forming units
Clinda	Clindamycin
CLSM	Confocal laser scanning microscopy
CTA	Cytotoxin assay
CTAB	Cetyltrimethylammonium bromide
DMEM	Dulbecco's Modified Eagle Medium
DNA	Deoxyribonucleic acid

Abbreviation	Full text
ELISA	Enzyme-linked immunosorbent assay
EPS	Extra polymeric substance
ESMID	European Society of Clinical Microbiology and Infectious Diseases
FBA	Columbia blood agar
FDX	Fidaxomicin
F*i*SH	Fluorescent *in situ* hybridisation
GDH	Glutamate dehydrogenase
GM	Geometric mean
HBSS-EDTA	Hanks balanced salt solution- containing 0.25 g/L trypsin-EDTA
HIV	Human immunodeficiency virus
IgA, IgM, IgG	Immunoglobulins A, M and G
LFE	Lactose-fermenting Enterobacteriaceae
LGI	Leeds General Infirmary
LOD	Limit of detection
MA	Mucin alginate
Met	Metronidazole
MBEC	Minimum biofilm eradication concentration
MIC	Minimum inhibitory concentration
MLST	Multilocus sequence typing
MLVA	Multilocus variant analysis
MRD	Modified Robbin's device
NA	North American Pulsotype
NAAT	Nucleic acid amplification test
NAP1	North American pulsotype
NCCLS	National Committee for Clinical Laboratory Standards.
NCTC	National Collection of Type Cultures
NR	No result

Abbreviation	Full text
PAGE	Polyacrylamide gel electrophoresis
PaLoc	Pathogenicity locus
PBS	Phosphate buffered saline
PCR	Polymerase chain reaction
PEG	Polyethyl glycol
PFGE	Pulsed-field gel electrophoresis
PHE	Public Health England
PMC	Pseudomembranous colitis
PMN	Polymorphonuclear leukocytes
PPMO	Potentially pathogenic microorganism
PTFE	Polytetrafluroethylene
QD	Four times daily
RCM	Robinson's cooked meat
REA	Restriction endonuclease
RNA	Ribonucleic acid
RR	Risk ratio
rRNA	Ribosomal RNA
RU	Relative unit
SCFA	Short chain fatty acid
SE	Standard error
TD	Three times daily
TSB	Tryptone soy broth
TVC	Total viable counts
Vanc	Vancomycin

Appendix A

Bacteriological Culture Medium Used For This Project

Media were autoclaved at 123° C for 15 minutes after which resazurin (Sigma; 0.005 g/L) and where required, glucose (Sigma; 0.4 g/L) were filter-sterilised and added to the medium through 0.22 μm syringe filters.

A.1 Gut model growth medium

Original Gut Model Growth Medium

Constituent	g/L	Product code	Supplier
Starch (potato)	3.0	5/7960/53	Fisher
Pectin	2.0	416862500	Oxoid
Yeast extract	2.0	LP0021	Oxoid
Peptone water	2.0	CM0009	Oxoid
Sodium hydrogen carbonate, ($NaHCO_3$)	2.0	71631	Sigma
Arabinogalactan	1.0	10830	Sigma
Bile salts no. 3	0.5	B8756	Sigma
Cysteine HCl	0.5	C1276	Sigma
Tween 80	2.0 mL/L	P1754	Sigma
Vitamin K	10 μL/L	V3501	Sigma
Sodium chloride	0.1	S7653	Sigma
Potassium dihydrogen phosphate (KH_2PO_4)	0.04	EC23183245	Fisher
di-potassium monohydrogen phosphate (K_2HPO_4)	0.04	10203	AnalR
Magnesium sulphate, ($MgSO_4.6H_20$)	0.01	M1880	Sigma
Calcium chloride, ($CaCl_2$)	0.01	C3881	Sigma
Haemin	0.005	51280	Sigma
Glucose	0.4	G8270	Sigma

Biofilm Gut Model Growth Medium

Constituent	g/L	Product code	Supplier
Starch	5.0	5/7960/53	Merck
Peptone water	5.0	CM0009	Oxoid
Tryptone	5.0	LP0042	Oxoid
Yeast extract	4.5	LP0021	Oxoid
Sodium chloride (NaCl)	4.5	S7653	Sigma
Potassium chloride, (KCl)	4.5	P9333	Sigma
Casein	3	C7078	Sigma
Pectin	2	416862500	Acros organics
Xylan	2	X0505	Sigma
Arabinogalactan	2	W325406	Sigma
Sodium hydrogen carbonate, ($NaHCO_3$)	1.5	71631	Sigma
Magnesium sulphate, ($MgSO_4.6H_20$)	1.25	M1880	Sigma
Guar gum	1	G4129	Sigma
Inulin	1	57614	Fluka
Cysteine HCl	0.8	C1276	Sigma
Potassium dihydrogen phosphate (KH_2PO_4)	0.5	EC23183245	Fisher
di-potassium monohydrogen phosphate (K_2HPO_4)	0.5	10203	AnalR
Bile salts no. 3	0.4	B8756	Sigma
Calcium chloride, ($CaCl_2$)	0.15	C3881	Sigma
Iron (II) sulphate ($FeSO_4.7H_20$)	0.005	21,549-2	Sigma
Haemin	0.05	51280	Sigma
Vitamin K	10 µL/L	V3501	Sigma
Tween 80	1.0 µL/L	P1754	Sigma

A.2 Liquid Culture Medium, Diluents and Buffers

Unless otherwise stated, all media were autoclaved at 123° C (15 mins) prior to use.

Brain Heart Infusion Broth

Brain Heart Infusion broths (CM225, Oxoid) were prepared according to the manufacturer's instructions.

Formulation	g/L
Calf brain infusion solids	12.5
Beef heart infusion solids	5.0
Proteose peptone	10.0
Glucose	2.0
Sodium chloride	5.0
Di-sodium phosphate	2.5

Cetylmethylammonium Bromide (CTAB)

Haxadecyltrimethylammonium bromide (H9151, Sigma) was prepared to a concentration of 0.001% w/v.

Cooked Meat Medium

Cooked meat medium (CM0081, Oxoid) was prepared according to the manufacturer's instructions.

Peptone Water

Peptone water (CM0009, Oxoid) was prepared according to the manufacturer's instructions.

Formulation	g/L
Peptone	10.0
NaCl	5.0

Phosphate Buffered Saline

Phosphate buffered saline (PBS) (P4417, Sigma) was prepared according to the manufacturer's instructions.

Saline

Saline (S7653, Sigma) was prepared according to the manufacturer's instructions.

Schaedler's Anaerobic Broth

Schaedler's anaerobic broth (CM496, Oxoid) was prepared according to the manufacturer's instructions.

Formulation	g/L
Tryptone soya broth	10.0
Special peptone	5.0
Yeast extract powder	5.0
Glucose	5.0
Cysteine HCl	0.4
Haemin	0.01
Tris buffer	0.75

Tryptic Soy Broth

Tryptic soy broth (T8907, Oxoid) was prepared according to the manufacturer's instructions.

Formulation	g/L
Casein	17.0
Soya peptone	3.0
Sodium chloride	5.0
Dipotassium phosphate	2.5
Dextrose	2.5

A.3 Solid Media Used For Gut Microbiota Identification and Enumeration

Unless otherwise stated, all solid media were autoclaved at 123° C (15 minutes), cooled to 50°C prior to the addition of supplements and distributed into 90 mm triple vented Petri dishes (Sarstedt)

Nutrient Agar

Nutrient agar (CM0003, Oxoid) was prepared according to the manufacturer's instructions. Inoculated plates incubated aerobically.

Formulation	g/L
Lab-Lemco powder	1.0
Yeast extract	2.0
Peptone	5.0
Sodium chloride	5.0
Agar	15.0

MacConkey Agar

MacConkey Agar No. 3 (CM115, Oxoid) was prepared according to the manufacturer's instructions. Inoculated plates incubated aerobically.

Formulation	g/L
Peptone	20.0
Lactose	10.0
Bile salts No.3	1.5
Sodium chloride	5.0
Neutral red	0.03
Crystal violet	0.001
Agar	15.0

Kanamycin Aesulin Azide Agar

Kanamycin Aesculin Azide Agar (CM0591, Oxoid) was prepared according to the manufacturer's instructions and supplemented with 20 mg/L kanamycin (K4000, Sigma) and 10 mg/L aztreonam (150415, MP Biomedicals) following autoclaving. Inoculated plates incubated aerobically.

Formulation	g/L
Tryptone	20.0
Yeast Extract	5.0
Sodium Chloride	5.0
Sodium Citrate	1.0
Aesculin	1.0
Ferric Ammonium Citrate	0.5
Sodium Azide	0.15
Agar	10.0

Fastidious Anaerobe Agar

Fastidious anaerobe agar (LAB090, LabM) was prepared following the manufacturer's instructions. Following cooling to 50° C 10% sterile horse blood (BHB400, E & O) was added. Inoculated plates incubated anaerobically.

Formulation	g/L
Peptone mix	23.0
Sodium chloride	5.0
Sodium bicarbonate	0.4
L-cysteine HCl	0.4
Starch	1.0
Glucose	1.0
Sodium pyruvate	1.0
Arginine	1.0
Sodium succinate	0.5
Ferric pyrophosphate	0.3
Haemin	0.005
Vitamin K	0.004
Bacteriological agar	12.0

Bile Aesulin Agar

Bile Aesculin Agar base (CM888, Oxoid) was prepared according to the manufacturer's instructions and supplemented with 5 µg/mL haemin (H5533, Sigma) and 20 µL/L vitamin K_1 (V3501, Sigma) prior to autoclaving. Following cooling to 50° C, 7.5 mg/L vancomycin (V2002, Sigma), 1 mg/L penicillin G (13752, Fluka) and 75 mg/L kanamycin (K4000, Sigma) were added to the molten agar. Inoculated plates incubated anaerobically.

Formulation	g/L
Peptone	8.0
Bile salts	20.0
Ferric citrate	0.5
Aesculin	1.0
Agar	15.0

LAMVAB agar

LAMVAB was prepared as described by Hartemink *et al.* (1997). Briefly, the medium consisted of three solutions (A, B, and C).

Solution A (500mL) was prepared with 104.4 g/L MRS Broth (CM359, Oxoid), supplemented with 0.5 g/L cysteine hydrochloride (C1276, Sigma) prior to autoclaving.

MRS Broth

Formulation	g/L
Peptone	10.0
Lab-Lemco powder	8.0
Yeast extract	4.0
Glucose	20.0
Sorbitan mono-oleate	1 mL
Dipotassium hydrogen phosphate	2.0
Sodium acetate $3H_20$	5.0
Triammonium citrate	2.0
Magnesium sulphate $7H_20$	0.2
Magnesium sulphate $4H_20$	0.05

Solution B consisted of 40g/L Agar Technical N° 3 (LP0013, Sigma) prepared in a 500 mL volume. Both Solutions A and B were sterilised by autoclaving at 121° C for 15 minutes.

Following cooling, solutions A and B were mixed, 1mL vancomycin (V2002, Sigma) was added to the molten agar and the solution adjusted to pH 5.0+/- 0.1 using 4 M HCl (Sigma). Inoculated plates incubated anaerobically.

Beerens Agar

Beerens Agar was made by adding 42.5 g/L Columbia Agar base (CM331, Oxoid); 5 g Agar Technical No.3) (LP0013, Oxoid); 5 g/L glucose (G7528, Sigma); 0.5 g/L cysteine HCl (C1276, Sigma) to sterile distilled water. The mixture was heated to 100° C and then cooled to 55-60° C before the addition of 5 mL/L propionic acid (P1386, Sigma) and adjustment to pH 5. Inoculated plates incubated anaerobically.

Columbia Agar base

Formulation	g/L
Special peptone	23.0
Starch	1.0
Sodium chloride	5.0
Agar	10.0

Brazier's Agar (CCEYL(M))

Brazier's CCEY agar base (LAB 160, LabM) was supplemented with 8 mg/L cefoxitin and 250 mg/L cycloserine, supplied as lyophilised vials (X093, LabM, 2% lysed horse blood (BHB400, E and O) and 5 mg/L lysozyme (L6876, Sigma), with 2 mg/L moxifloxacin (Bayer) for CCEYLM, following autoclaving and cooling to 50° C. Agar plates were prepared according to the manufacturer's instructions. Inoculated plates incubated anaerobically.

Formulation	g/L
Peptone mix	23.0
Sodium chloride	5.0
Soluble starch	1.0
Agar	12.0
Sodium bicarbonate	0.4
Glucose	1.0
Sodium pyruvate	1.0
Cysteine HCl	0.5
Haemin	0.01
Vitamin K	0.001
L-arginine	1.0
Soluble pyrophosphate	0.25
Sodium succinate	0.5
Cholic acid	1.0
p-hydroxyphenylacetic acid	1.0

A.4 Solid Media Used in Antimicrobial Bioassays

Wilkins Chalgren

Wilkins-Chalgren anaerobe agar (CM619, Oxoid) was prepared according to the manufacturer's instructions.

Formulation	g/L
Tryptone	10.0
Gelatin peptone	10.0
Yeast extract	5.0
Glucose	1.0
Sodium chloride	5.0
L-arginine	1.0
Sodium pyruvate	1.0
Menadione	0.0005
Haemin	0.005
Agar	10.0

Mueller Hinton Agar

Mueller Hinton agar (CM0337, Oxoid) was prepared according to the manufacturer's instructions.

Formulation	g/L
Beef, dehydrated infusion	300.0
Casein hydrolysate	17.5
Starch	1.5
Agar	17.0

Antibiotic Medium Number 1

Antibiotic medium number 1 agar (CM619, Oxoid) was prepared according to the manufacturer's instructions.

Formulation	g/L
Beef, dehydrated infusion	300.0
Casein hydrolysate	17.5
Starch	1.5
Agar	17.0

Appendix B
Media, Solutions and Additives Used in the Culture of Vero Cells

Dubecco's Modified Eagle's Medium (DMEM) (D6546, Sigma) was supplied in sterile 500 mL bottles and stored at 4°C.

Formulation	g/L		Formulation	g/L
Calcium chloride	0.265		L-lysine HCl	0.146
Iron (III) nitrate	0.0001		L-methionine	0.03
Potassium chloride	0.4		L-phenylalanine	0.066
Magnesium sulphate	0.09767		L-serine	0.042
Sodium chloride	6.4		L-threonine	0.095
Sodium hydrogen carbonate	3.7		L-tryptophan	0.016
Sodium dihydrogen phosphate	0.109		L-tyrosine	0.10379
Phenol Red Na	0.015		L-valine	0.094
Pyruvate Na	0.11		D-pantothenate 1/2 Ca	4
D-glucose	4.5		Choline chloride	0.004
L-arginine HCl	0.084		Folic acid	0.004
L-cysteine	0.0626		myo-inositol	0.0072
L-glutamine	0.584		Niacinamide	0.004
Glycine	0.03		Pyridoxine HCl	0.004
L-histidine HCl.H_2O	0.042		Riboflavin	0.0004
L-isoleucine	0.105		Thiamine HCl	0.004
L-leucine	0.105			

Media Additives

Newborn calf serum (N4637, Sigma) was collected from animals up to 10 days old and was tested to ensure that free from viruses and

mycoplasmas. This additive was stored at –20°C in 25 mL volumes to give a 10% concentration when added to 500 mL DMEM.

Antibiotic/antimycotic solution (A5955, penicillin 100 U/mL, streptomycin 100 mg/L , amphotericin B 0.25 mg/L) was supplied as 100X liquid solution. This mixture was stored at –20° C in 5 mL volumes to give an appropriate concentration when added to 500 mL DMEM.

L-Glutamine (G7513, Sigma) was supplied as a 200 mM liquid solution. This was stored at -20° C in separate volumes and diluted 1:100 in 500 mL supplemented DMEM.

Solutions

Hank's Balanced Salts Solution (H9394, Sigma) was supplied in sterile 500 mL bottles.

Formulation	g/L
Potassium chloride (KCl)	0.4
Potassium hydrogen phosphate (KH_2PO_4)	0.06
Sodium chloride (NaCl)	8
Sodium hydrogen carbonate ($NaHCO_3$)	0.35
Sodium hydrogen phosphate (Na_2HPO_4)	0.04788
D-glucose	1
Phenol Red	0.011

Trypsin (T4174, Sigma) was supplied as 10x liquid solution containing 5.0 g porcine trypsin and 2 g EDTA • 4Na per liter of 0.9% sodium chloride. This was stored at –20° C in and diluted 1:10 in HBSS to yield a 1X solution.

Appendix C

Addresses of Suppliers of Chemicals, Reagents and Equipment

Supplier	Address
Acros Organics	Thermo Fisher Scientific UK, Bishop Meadow Road, Loughborough, Leicestershire, LE11 5RG, UK
Bayer	Bayer plc. Pharmaceutical Division, Bayer House, Strawberry Hill, Newbury, Berkshire, RG14 1JA UK
Beckton Dickinson	Beckton Dickinson, The Danby Building, Edmund Halley Road, Oxford Science Park, Oxford, OX4 4DQ UK
Bigger Trading Ltd	Bigger Trading Ltd. 34A Station Road, Cuffley, Hertfordshire, EN6 4HE UK
Bioconnections	Bioconnections, Thorp Arch Estate, Wetherby, Leeds, LS23 7BJ, UK

Supplier	Address
Brighton Systems	Brighton Systems Ltd. 44 Meeching Road, Newhaven, East Sussex, BN9 9RH UK
Don Whitely Scientific, Ltd.	Don Whitely Scientific, Ltd. 14 Otley Rd, Shipley, West Yorkshire, BD17 7SE, UK
E and O Laboratories	E and O Laboratories, Burnhouse, Bonnybridge, FK4 2HH, Scotland
Gibco	Life Technologies , 3 Fountain Drive, Inchinnan Business Park, Paisley, PA4 9RF UK
Grant Instruments	Grant Instruments, Sherpreth, Cambridgeshire, SG8 6GB, UK
Fisher Scientific	Thermo Fisher Scientific UK, Bishop Meadow Road, Loughborough, Leicestershire, LE11 5RG, UK
Fluka	Sigma-Aldrich Co. Ltd. Fancy Road, Poole, Dorset, UK, BH12 4QH.

Supplier	Address
LabM	Topley House, 52 Wash Lane, Bury, Lancs, BL9 6AS
Life Technologies	Life Technologies Ltd. 3 Fountain Drive, Inchinnan Business Park, Paisley, Scotland PA4 9RF
Merck	Merck KgaA, 64271 Darmstadt, Germany.
Millepore Corporation	Millepore Corporation 290 Concord Road, Billerica, MA, USA
Molecular Devices	Molecular Devices, 660-665, Winnersh Triangle, Winnersh, Berkshire, RG41 5TS UK
Nunc	Thermo Scientific NUNC™ and NALGENE® 75 Panorama Creek, Rochester, New York 14625 USA
Oxoid	Oxoid Ltd., Basingstoke, Hampshire, RG24 8PW UK

Supplier	Address
Priorclave Ltd	Priorclave Ltd, 129-131 Nathan Way, West Thamesmead Business Park, London, SE28 0AB, UK
Pro-lab Diagnostics	Pro-lab Diagnostics, 7 Westwood Court, Neston, CH64 3UJ UK
Sigma	Sigma-Aldrich Co. Ltd., Fancy Road, Poole, Dorset, UK, BH12 4QH.
Soham Scientific	Soham Scientific, Muncey's Mill, 37 Mildenhall Road, Fordham, Ely, Cambridgeshire, CB7 5NP UK
VWR International	VWR International Ltd. Hunter Boulevard, Magna Park, Lutterworth, Leicestershire, LE17 4XN UK

Appendix D

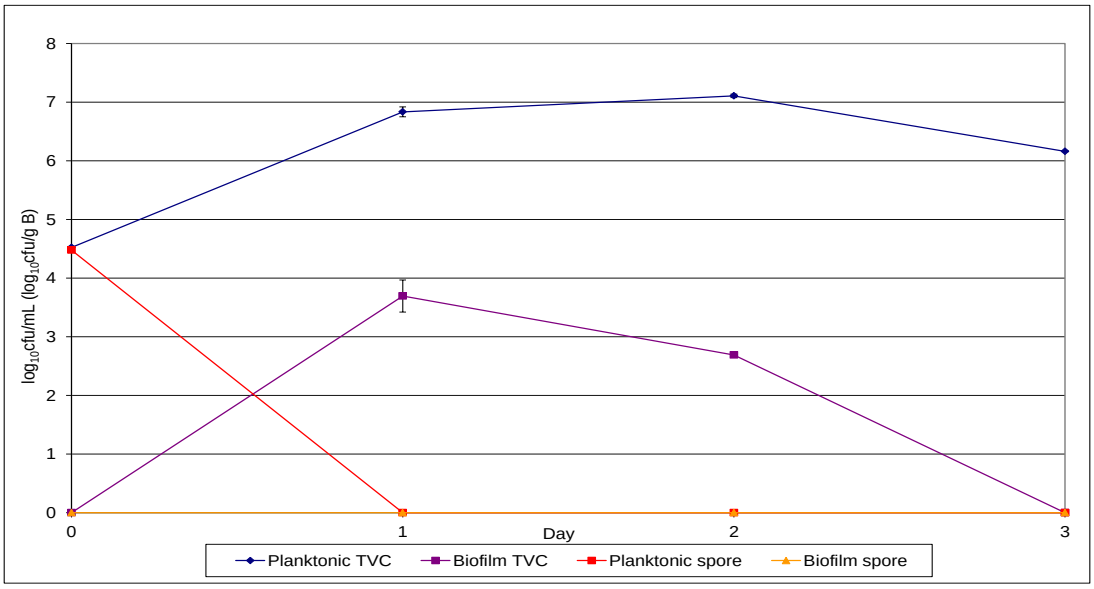

Appendix D1: Mean populations (± SE) of *C. difficile* PCR ribotype 078 in planktonic (log_{10}cfu/mL) and biofilm (log_{10}cfu/g) form when grown in biofilm gut model growth medium. (TVC, total viable counts; LOD, ~ 2 log_{10}cfu/g, ~ 1.5 log_{10}cfu/mL).

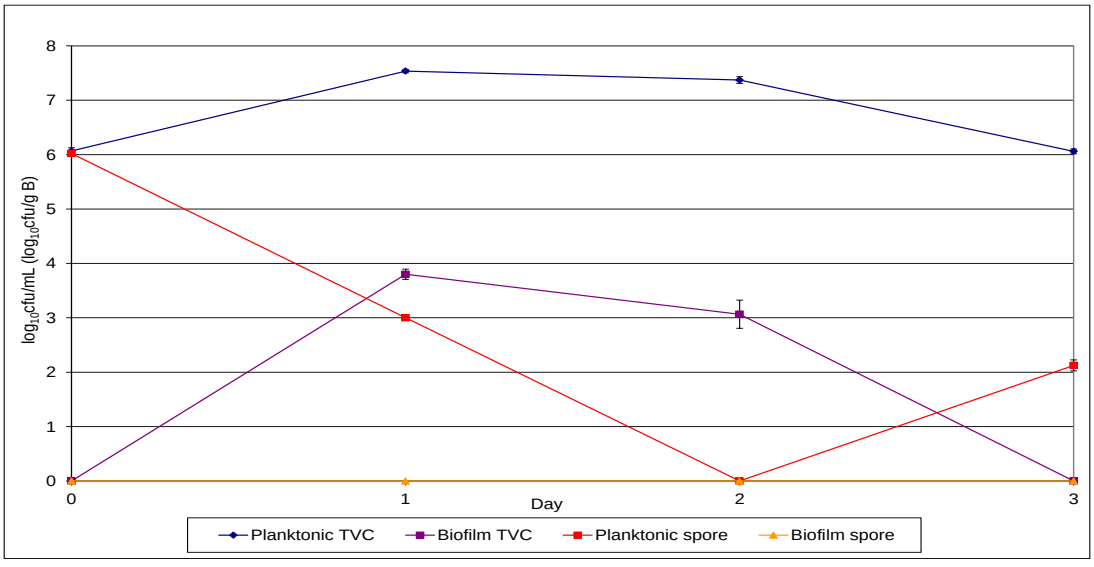

Appendix D2: Mean populations (± SE) of *C. difficile* PCR ribotype 106 in planktonic (log_{10}cfu/mL) and biofilm (log_{10}cfu/g) form when grown in biofilm gut model growth medium. (TVC, total viable counts; LOD, ~ 2 log_{10}cfu/g, ~ 1.5 log_{10}cfu/mL).

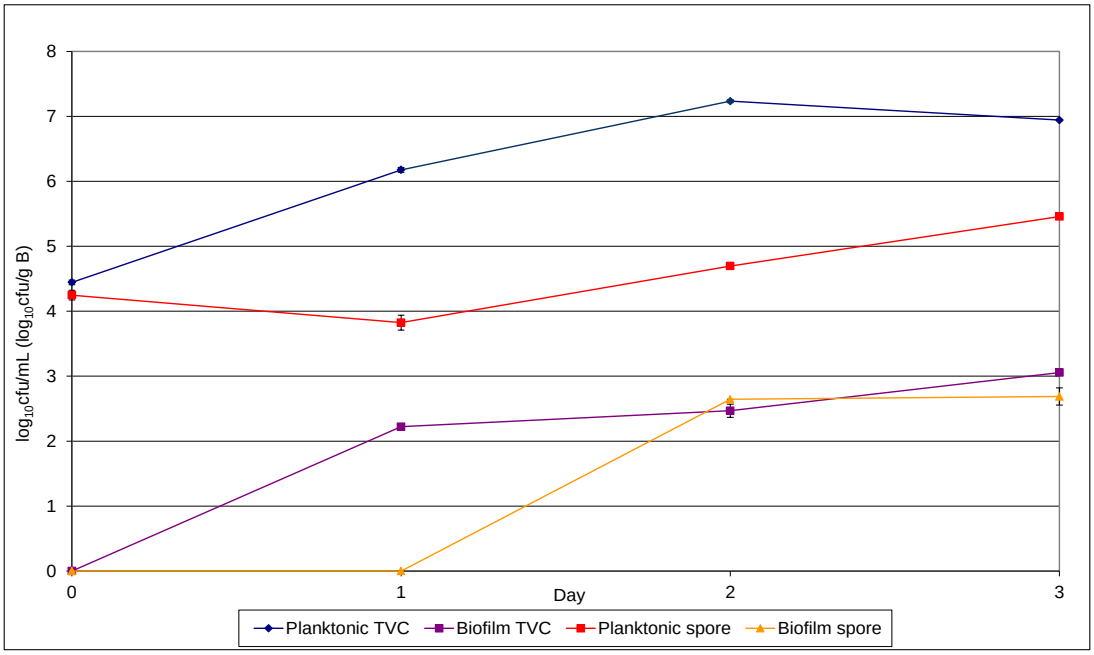

Appendix D3: Mean populations (± SE) of *C. difficile* PCR ribotype 078 in planktonic (log_{10}cfu/mL) and biofilm (log_{10}cfu/g) form when grown in brain heart infusion broth. (TVC, total viable counts; LOD, ~ 2 log_{10}cfu/g, ~ 1.5 log_{10}cfu/mL).

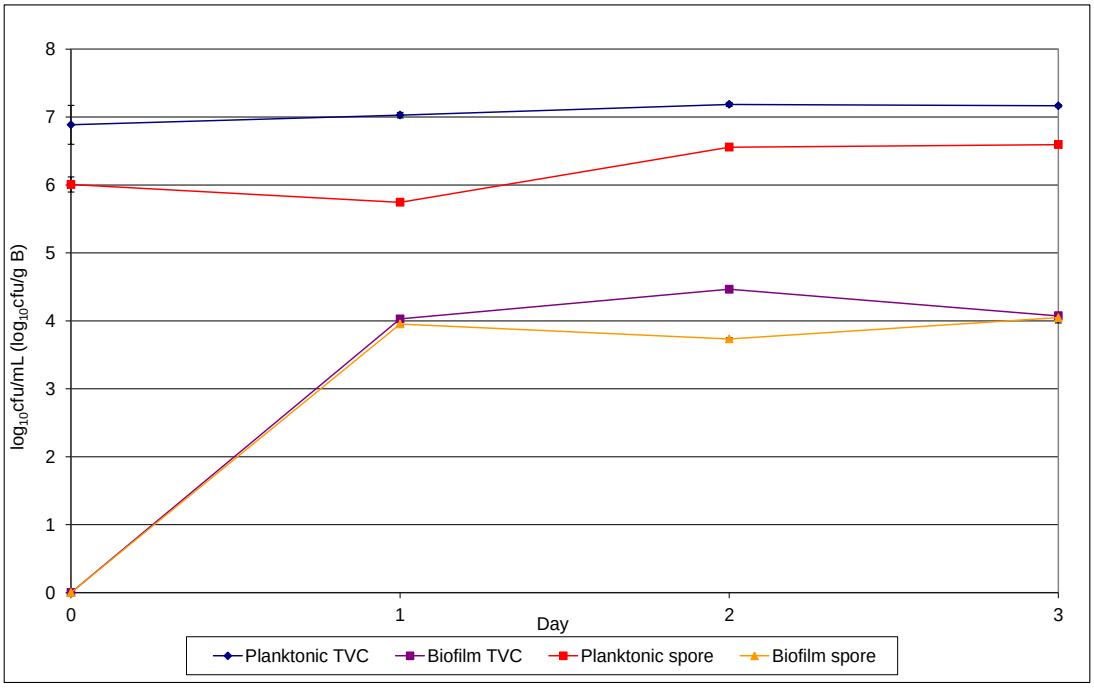

Appendix D4: Mean populations (± SE) of *C. difficile* PCR ribotype 106 in planktonic (log_{10}cfu/mL) and biofilm (log_{10}cfu/g) form when grown in BHI (TVC, total viable counts; LOD, ~ 2 log_{10}cfu/g, ~ 1.5 log_{10}cfu/mL).

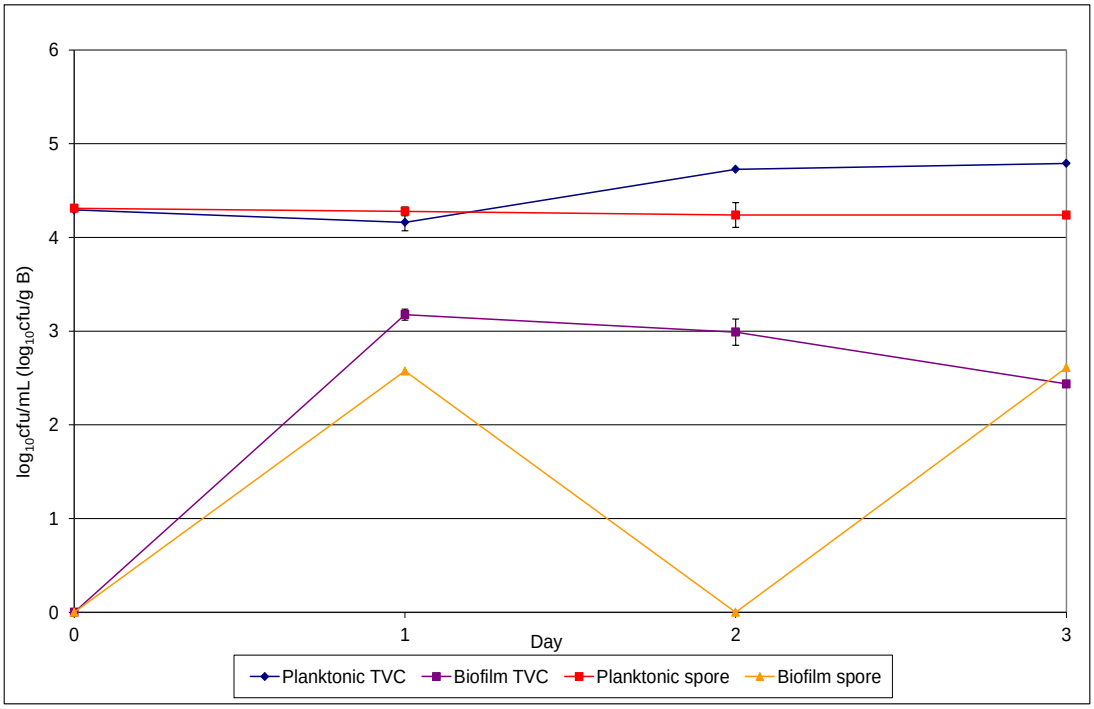

Appendix D5: Mean populations (± SE) of *C. difficile* PCR ribotype 078 in planktonic (log_{10}cfu/mL) and biofilm (log_{10}cfu/g) form when grown in saline. (TVC, total viable counts; LOD, ~ 2 log_{10}cfu/g, ~ 1.5 log_{10}cfu/mL).

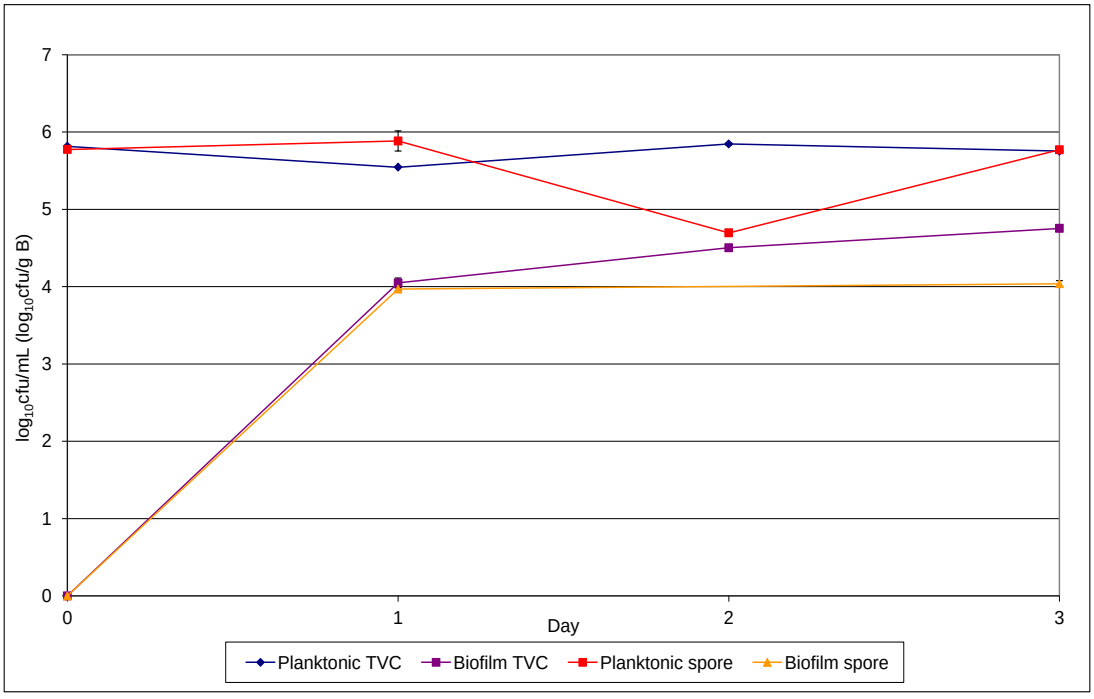

Appendix D6: Mean populations (± SE) of *C. difficile* PCR ribotype 106 in planktonic (log_{10}cfu/mL) and biofilm (log_{10}cfu/g) form when grown in saline. (TVC, total viable counts; LOD, ~ 2 log_{10}cfu/g, ~ 1.5 log_{10}cfu/mL).